Neuromethods 110

Springer Protocols

Rafael Luján
Francisco Ciruela *Editors*

Receptor and Ion Channel Detection in the Brain

Methods and Protocols

Humana Press

NEUROMETHODS

Series Editor
Wolfgang Walz
University of Saskatchewan
Saskatoon, SK, Canada

For further volumes:
http://www.springer.com/series/7657

Receptor and Ion Channel Detection in the Brain

Methods and Protocols

Edited by

Rafael Luján

Research Institute on Neurological Disabilities (IDINE), Department of Medical Sciences, School of Medicine, University of Castilla-La Mancha, Albacete, Spain

Francisco Ciruela

Pharmacology Unit, Department of Pathology and Experimental Therapeutics, School of Medicine, IDIBELL, University of Barcelona, Barcelona, Spain

Humana Press

Editors
Rafael Luján
Research Institute on Neurological Disabilities (IDINE), Department of Medical Sciences, School of Medicine
University of Castilla-La Mancha
Albacete, Spain

Francisco Ciruela
Pharmacology Unit, Department of Pathology and Experimental Therapeutics, School of Medicine, IDIBELL
University of Barcelona
Barcelona, Spain

ISSN 0893-2336 ISSN 1940-6045 (electronic)
Neuromethods
ISBN 978-1-4939-3063-0 ISBN 978-1-4939-3064-7 (eBook)
DOI 10.1007/978-1-4939-3064-7

Library of Congress Control Number: 2015958769

Springer New York Heidelberg Dordrecht London

Printed on acid-free paper

Humana Press is a brand of Springer
Springer Science+Business Media LLC New York is part of Springer Science+Business Media (www.springer.com)

Series Preface

Experimental life sciences have two basic foundations: concepts and tools. The *Neuromethods* series focuses on the tools and techniques unique to the investigation of the nervous system and excitable cells. It will not, however, shortchange the concept side of things as care has been taken to integrate these tools within the context of the concepts and questions under investigation. In this way, the series is unique in that it not only collects protocols but also includes theoretical background information and critiques which led to the methods and their development. Thus it gives the reader a better understanding of the origin of the techniques and their potential future development. The *Neuromethods* publishing program strikes a balance between recent and exciting developments like those concerning new animal models of disease, imaging, in vivo methods, and more established techniques, including, for example, immunocytochemistry and electrophysiological technologies. New trainees in neurosciences still need a sound footing in these older methods in order to apply a critical approach to their results.

Under the guidance of its founders, Alan Boulton and Glen Baker, the *Neuromethods* series has been a success since its first volume published through Humana Press in 1985. The series continues to flourish through many changes over the years. It is now published under the umbrella of Springer Protocols. While methods involving brain research have changed a lot since the series started, the publishing environment and technology have changed even more radically. Neuromethods has the distinct layout and style of the Springer Protocols program, designed specifically for readability and ease of reference in a laboratory setting.

The careful application of methods is potentially the most important step in the process of scientific inquiry. In the past, new methodologies led the way in developing new disciplines in the biological and medical sciences. For example, Physiology emerged out of Anatomy in the nineteenth century by harnessing new methods based on the newly discovered phenomenon of electricity. Nowadays, the relationships between disciplines and methods are more complex. Methods are now widely shared between disciplines and research areas. New developments in electronic publishing make it possible for scientists that encounter new methods to quickly find sources of information electronically. The design of individual volumes and chapters in this series takes this new access technology into account. Springer Protocols makes it possible to download single protocols separately. In addition, Springer makes its print-on-demand technology available globally. A print copy can therefore be acquired quickly and for a competitive price anywhere in the world.

Wolfgang Walz

Preface

The scientific world allows us to be very effective when facing the complexity of any aspect of nature, describing such complexity and comparing it with other realities. To do that, science uses its own specific method, known as the scientific method, which offers people a unique accessibility to the real world. It is that understandable that the methodological rigour is one of the key aspects when determining the credibility of a scientific work. A work badly designed, poorly analysed or with quantification errors is not a rigorous scientific work. One of the virtues of the scientific work is its capacity to facilitate the interpretation of the same fact by different people. The experimental data generated rigorously in a scientific work should be reproduced by any scientist, regardless of the working place and the moment when experiments are performed. This is only possible using the same methodology. Although there is also a small margin for subjective interpretation of the same fact, science has a number of mechanisms for self-correction of any statement. These mechanisms are based in methodological resources that help reduce the relative weight of subjectivity. The mechanisms use predictions, experimental verification and validations and, hence, the emphasis that the methodology has in any research work. That is exactly why every scientific publication always includes a section on material and methods, which describes the techniques that have been employed so that it is easy to know how the data was generated. Among the most important challenges in biological and biomedical research are the improvements of the understanding, the accessibility and the efficient reproduction of experimental techniques between different laboratories. We must improve and work harder in the transparency and reproducibility of experimental work and somehow lighten the sacrifice required to learn each new experimental technique. Every scientist knows very well that optimising, improving and applying a new experimental technique can take weeks and even months. Actually, a huge amount of the time expended in a laboratory goes by learning and optimising new techniques. This can be a very demanding process because of the relevant innovative technologies continuously appearing.

Research on neurotransmitter receptors and ion channels has exploded in the last couple of decades, increasing our understanding of the brain. It is now clear that they play essential roles in cell biology and physiology, with their dysfunction being the cause of many neurological diseases. The development and application of new experimental approaches has led to a boom in the investigation of neurotransmitter receptors and ion channels, placing scientists in the unique position of being able to directly study their structural, biochemical and functional parameters. We certainly believe that recently developed technologies useful to study neurotransmitter receptors and ion channels should be readily available to any interested scientist. Thus, the purpose of *Receptor and Ion Channel Detection in the Brain: Methods and Protocols* is to provide state-of-the-art and up-to-date representative methodological information on molecular, neuroanatomical and functional techniques that are currently used to study neurotransmitter receptors and ion channels in the brain. This book joins the effort of a worldwide recognised bunch of neuroscientists which explains in an easy and detailed way well-established and tested protocols embracing molecular, cellular, neuro-

anatomical and electrophysiological aspects of the brain. We feel that our book is both comprehensive and practical, and, therefore, the detailed methods and notes will facilitate choosing the best method for the neurotransmitter receptor and/or ion channel under study.

We write *Receptor and Ion Channel Detection in the Brain: Methods and Protocols* with the hopes that it will summarise the most commonly used techniques in neuroscience to study neurotransmitter receptor and/or ion channel, but also major methodological improvements of established methods are presented. When obtaining information on those methods, it is common to turn to several scattered sources, and sometimes protocols offer conflicting advice. To date there are no books putting up together all these methodologies in a single volume. We pursue presenting the basic aspects of the different methodologies to any scientist or student from many disciplines, as well as neurologists who are requested to understand how new technologies might impact their day-to-day work. Everyone knows the technical approaches most commonly used in their respective research field, but it is not so common that they also know the ones used in other disciplines, and thus we aim to fill this gap. In addition, we also aim to bring closer these techniques to all those people introduced for the first time to the field of neurotransmitter receptors and ion channels who frequently ask for detailed protocols in neuroscience.

The book is structured in three sections. Beginning with the topic of molecular techniques, the first part of the book embraces all these molecular, immunological and pharmacological aspects related to the detection of receptors and ion channels in the brain. Thus, Chap. 1 by Masahiko Watanabe provides a detailed description of the generation of high-quality antibodies against receptors and ion channels. The use of these antibodies in co-immunoprecipitation experiments performed in brain membrane extracts is further discussed in Chap. 2 by Xavier Morató and collaborators. The biochemical fractionation of membrane extracts to separate presynaptic, postsynaptic and extrasynaptic fraction is analysed by Paula M. Canas in Chap. 3. Next, in Chap. 4 Elek Molnar describes how to detect cell surface receptors and ion channels in native conditions by using a biotinylation approach in brain slices. The way how these membrane proteins diffuse within the cell surface of neurons is discussed by Juan Varela and collaborators in Chap. 5. Subsequently, in Chap. 6 of Fuencisla Pilar-Cuéllar and collaborators, the pharmacological properties of receptors in brain membranes are assessed by describing classical radioligand-binding experiment. The ectopic in vitro, in situ and in vivo expression of receptors and ion channels by means of infectious but replication-deficient Semliki Forest virus is discussed in Chap. 7 by Markus U. Ehrengruber and Kenneth Lundstrom. Next, in Chap. 8 Víctor Fernández-Dueñas and collaborators describe the novel methodological approach (i.e. time-resolved fluorescence resonance energy transfer using fluorescent ligands) employed to reveal receptor-receptor interactions in brain tissue. Part I ends with Chap. 9 in which Dasiel Borroto-Escuela and collaborators describe another experimental approach (i.e. proximity ligation assay, PLA) to detect receptor-receptor interactions in native tissue (i.e. brain).

Next, the book moves into the neuroanatomical techniques devoted to localise receptors and ion channels within the central nervous system. In Chap. 10, by Miwako Yamasaki and Masahiko Watanabe, a description of in situ hybridisation applied to detection of receptors and ion channels is presented. In Chap. 11 Rebeca Vidal and collaborators expose how autoradiographic methods allow visualising G protein-coupled receptors in the brain. Next in Chap. 12 Elek Molnar presents the histoblot technique to study the expression of receptor and ion channels in the brain. Next, several tips for improving antibody detection of receptors, ion channels and interacting proteins by immunohistochemistry are provided by

Kohtarou Konno and Masahiko Watanabe in Chap. 13. Subsequently, Gil-Perotin and collaborators in Chap. 14 explain how GFP-tagged proteins could be detected at the electron microscopic level. Furthermore, the basis of the pre- and post-embedding methods for electron microscopy detection of receptors and ion channels in the brain is described by Rafael Luján in Chaps. 15 and 16, respectively. Indeed, the high-resolution localisation of these membrane proteins by SDS-digested freeze-fracture replica labelling (SDS-FRL) is examined by Harumi Harada and Ryuichi Shigemoto in Chap. 17. Then, the use of viral vectors to trace neuronal circuits and single neuron synaptic connections at the light and electron microscopic level is considered in Chaps. 18 and 19 by Hiroyuki Hioki and Takahiro Furata. Finally, this second section of the book ends with Chap. 20 by Yoshiyuki Kubota dealing with the morphological and neurochemical characterisation of electrophysiologically identified neurons.

Once the neuroanatomical approaches were analysed, the volume moves on to revising these functional approaches devoted to ascertain the receptor's and ion channel's functionality in the brain. Accordingly, several chapters focus on the assessment of functionality by means of electrophysiological techniques both in single neurons and in behaving animal. Thus, Chap. 21 by David Soto and collaborators provides a general overview of basic electrophysiology in primary neuronal cultures. Next, Chap. 22 by Norbert Weiss and Michel De Waard presents a step-by-step illustration of the two main analytical methods in patch-clamp experiments that can be used to extract and describe the main parameters of "ON" and "OFF" G protein landmarks. The electrophysiological assessment and voltammetry measurements in behaving animal are exposed in Chaps. 24 and 25 by Agnès Gruart and Kendra D. Bunner, respectively. In addition, the description of the microdialysis methodology to measure in vivo extracellular levels of monoamines in different brain regions is shown in Chap. 25 by Jorge E. Ortega and collaborators. Next, Rhiannon M. Meredith and Martine R. Groen in Chap. 26 describe how to determine calcium transients in single dendrites and spines of pyramidal neurons. Also, the recording of neuronal membrane potential changes by means of FRET-based voltage biosensors is explored in Chap. 27 by Víctor Fernández-Dueñas and collaborators. Finally, Part III ends with Chaps. 28 and 29 by Jaume Taura and Maricel Gómez-Soler, respectively, and these two chapters describe how to determine second messengers (i.e. cAMP and ERKs) in native tissue (i.e. brain).

Overall, we hope that readers will not only enjoy the reading but also benefit from the collective methods to provide new opportunities for everybody's research. To this end, our gratitude most especially goes out to our collaborators, students and fellows for their insights and encouragement. Last, we would like to thank those who supported us financially in our undertaking: The European Union (HBP – Project Ref. 604102), Ministerio de Economía y Competitividad/Instituto de Salud Carlos III, Institució Catalana de Recerca i Estudis Avançats and Agentschap voor Innovatie door Wetenschap en Technologie.

Albacete, Spain — *Rafael Luján*
Barcelona, Spain — *Francisco Ciruela*
May 2015

Contents

Contributors

Patrizia Ambrogini • *Department of Earth, Life and Environmental Sciences, Section of Physiology, Campus Scientifico Enrico Mattei, Urbino, Italy*

Josep Amigó • *Instituto de Biomedicina y Biotecnología de Cantabria (IBBTEC) (UC-CSIC-SODERCAN), Santander, Spain; Departamento de Fisiología y Farmacología, Universidad de Cantabria, Santander, Spain; CIBERSAM, Instituto de Salud Carlos III, Madrid, Spain*

Dasiel O. Borroto-Escuela • *Department of Neuroscience, Karolinska Institutet, Stockholm, Sweden*

Kendra D. Bunner • *Program in Neuroscience, Department of Psychological and Brain Sciences, Indiana University, Bloomington, USA*

Luis F. Callado • *Department of Pharmacology, University of the Basque Country UPV/EHU and CIBERSAM, Leioa Bizkaia, Spain*

Paula M. Canas • *CNC-Center for Neurosciences and Cell Biology and Faculty of Medicine, University of Coimbra, Coimbra, Portugal*

María Josefa Castillo • *Instituto de Biomedicina y Biotecnología de Cantabria (IBBTEC) (UC-CSIC-SODERCAN), Santander, Spain*

Elena Castro • *Instituto de Biomedicina y Biotecnología de Cantabria (IBBTEC) (UC-CSIC-SODERCAN), Santander, Spain; Departamento de Fisiología y Farmacología, Universidad de Cantabria, Santander, Spain; CIBERSAM, Instituto de Salud Carlos III, Madrid, Spain*

A. Cebrián-Silla • *Laboratorio de Neurobiología Comparada, Instituto Cavanilles, Universidad de Valencia, CIBERNED, Valencia, Spain*

Francisco Ciruela • *Pharmacology Unit, Department of Pathology and Experimental Therapeutics, School of Medicine, IDIBELL, University of Barcelona, Barcelona, Spain*

Ian D. Coombs • *Department of Neuroscience, Physiology and Pharmacology, University College London, London, UK*

Rodrigo A. Cunha • *CNC-Center for Neurosciences and Cell Biology and Faculty of Medicine, University of Coimbra, Coimbra, Portugal*

Riccardo Cuppini • *Department of Earth, Life and Environmental Sciences, Section of Physiology, Campus Scientifico Enrico Mattei, Urbino, Italy*

Michel De Waard • *Grenoble Institute of Neuroscience, University Joseph Fourier, Grenoble, France*

José M. Delgado-García • *Division of Neurosciences, Pablo de Olavide University, Seville, Spain*

Michael Di Palma • *Department of Earth, Life and Environmental Sciences, Section of Physiology, Campus Scientifico Enrico Mattei, Urbino, Italy*

Alvaro Díaz • *Instituto de Biomedicina y Biotecnología de Cantabria (IBBTEC) (UC-CSIC-SODERCAN), Santander, Spain; Departamento de Fisiología y Farmacología, Universidad de Cantabria, Santander, Spain; CIBERSAM, Instituto de Salud Carlos III, Madrid, Spain*

Julien Dupuis • *Interdisciplinary Institute for Neuroscience, University of Bordeaux, Bordeaux, France*
Thierry Durroux • *Institut de Génomique Fonctionnelle, CNRS, UMR5203, Montpellier, France; INSERM, U.661, Montpellier and Université Montpellier 1,2, Montpellier, France*
Markus U. Ehrengruber • *Department of Biology, Kantonsschule Hohe Promenade, Zurich, Switzerland*
Kristin Feltmann • *Department of Clinical Neuroscience, Karolinska Institutet, Stockholm, Sweden*
Víctor Fernández-Dueñas • *Unitat de Farmacologia, Departament Patologia i Terapèutica Experimental, Facultat de Medicina, Universitat de Barcelona, IDIBELL, L'Hospitalet de Llobregat, Barcelona, Spain; Pharmacology Unit, Department of Pathology and Experimental Therapeutics, School of Medicine, IDIBELL, University of Barcelona, Barcelona, Spain*
M. Fil • *Laboratorio de Neurobiología Comparada, Instituto Cavanilles, Universidad de Valencia, CIBERNED, Valencia, Spain*
Takahiro Furuta • *Department of Morphological Brain Science, Graduate School of Medicine, Kyoto University, Kyoto, Japan*
Kjell Fuxe • *Department of Neuroscience, Karolinska Institutet, Stockholm, Sweden*
P. García-Belda • *Laboratorio de Neurobiología Comparada, Instituto Cavanilles, Universidad de Valencia, CIBERNED, Valencia, Spain; Unidad Mixta de Esclerosis Múltiple y Neurorregeneración, IIS Hospital La Fe, Valencia, Spain*
José Manuel García-Verdugo • *Laboratorio de Neurobiología Comparada, Instituto Cavanilles, Universidad de Valencia, CIBERNED, Valencia, Spain; Unidad Mixta de Esclerosis Múltiple y Neurorregeneración, IIS Hospital La Fe, Valencia, Spain*
Emilio Garro-Martínez • *Instituto de Biomedicina y Biotecnología de Cantabria (IBBTEC) (UC-CSIC-SODERCAN), Santander, Spain; CIBERSAM, Instituto de Salud Carlos III, Madrid, Spain*
S. Gil-García • *Laboratorio de Neurobiología Comparada, Instituto Cavanilles, Universidad de Valencia, CIBERNED, Valencia, Spain; Unidad Mixta de Esclerosis Múltiple y Neurorregeneración, IIS Hospital La Fe, Valencia, Spain*
Sara Gil-Perotin • *Laboratorio de Neurobiología Comparada, Instituto Cavanilles, Universidad de Valencia, CIBERNED, Valencia, Spain; Unidad Mixta de Esclerosis Múltiple y Neurorregeneración, IIS Hospital La Fe, Valencia, Spain*
Maricel Gómez-Soler • *Unitat de Farmacologia, Departament Patologia i Terapèutica Experimental, Facultat de Medicina, Universitat de Barcelona, IDIBELL, L'Hospitalet de Llobregat, Barcelona, Spain*
Laurent Groc • *Interdisciplinary Institute for Neuroscience, University of Bordeaux, Bordeaux, France*
Martine R. Groen • *Department of Neuroscience, Wolfson Institute for Biomedical Research, University College London, London, UK*
Agnès Gruart • *Division of Neurosciences, Pablo de Olavide University, Seville, Spain*
Beth Hagman • *Department of Neuroscience, Karolinska Institutet, Stockholm, Sweden*
Harumi Harada • *Institute of Science and Technology Austria (IST Austria), Klosterneuburg, Austria*

V. Herranz-Pérez • *Laboratorio de Neurobiología Comparada, Instituto Cavanilles, Universidad de Valencia, CIBERNED, Valencia, Spain; Unidad Mixta de Esclerosis Múltiple y Neurorregeneración, IIS Hospital La Fe, Valencia, Spain*

Hiroyuki Hioki • *Department of Morphological Brain Science, Graduate School of Medicine, Kyoto University, Kyoto, Japan*

Antonio Jiménez-Beristain • *Department of Neuroscience, Karolinska Institutet, Stockholm, Sweden*

Thomas Knöpfel • *RIKEN Brain Science Institute, Wako City, Japan; Division of Brain Sciences, Imperial College London, London, UK*

Kohtarou Konno • *Department of Anatomy, Hokkaido University Graduate, School of Medicine, Sapporo, Japan*

Yoshiyuki Kubota • *Division of Cerebral Circuitry, National Institute for Physiological Sciences, Okazaki, Aichi, Japan; Department of Physiological Sciences, The Graduate University for Advanced Studies (SOKENDAI), Okazaki, Aichi, Japan*

J.S. Lee • *Department of Molecular and Cellular Physiology, Stanford University School of Medicine, Stanford, CA, USA*

Raquel Linge • *Instituto de Biomedicina y Biotecnología de Cantabria (IBBTEC) (UC-CSIC-SODERCAN), Santander, Spain; Departamento de Fisiología y Farmacología, Universidad de Cantabria, Santander, Spain; CIBERSAM, Instituto de Salud Carlos III, Madrid, Spain*

Rafael Luján • *Research Institute on Neurological Disabilities (IDINE), Department of Medical Sciences, School of Medicine, University of Castilla-La Mancha, Albacete, Spain*

Kenneth Lundstrom • *PanTherapeutics, Lutry, Switzerland*

Alicia Martín • *Instituto de Biomedicina y Biotecnología de Cantabria (IBBTEC) (UC-CSIC-SODERCAN), Santander, Spain; Departamento de Fisiología y Farmacología, Universidad de Cantabria, Santander, Spain*

J. Javier Meana • *Department of Pharmacology, University of the Basque Country UPV/EHU and CIBERSAM, Leioa Bizkaia, Spain*

Rhiannon M. Meredith • *Department of Integrative Neurophysiology, Center for Neurogenomics and Cognitive Research, VU University Amsterdam, Amsterdam, The Netherlands*

Elek Molnár • *School of Physiology and Pharmacology, University of Bristol, Bristol, UK*

Xavier Moratò • *Unitat de Farmacologia, Department Patologia i Terapèutica Experimental, Facultat de Medicina, Universitat de Barcelona, IDIBELL, L'Hospitalet de Llobregat, Barcelona, Spain; Pharmacology Unit, Department of Pathology and Experimental Therapeutics, School of Medicine, IDIBELL, University of Barcelona, Barcelona, Spain*

M.V. Nachury • *Department of Molecular and Cellular Physiology, Stanford University School of Medicine, Stanford, CA, USA*

Hisashi Nakamura • *Department of Morphological Brain Science, Graduate School of Medicine, Kyoto University, Kyoto, Japan*

Manuel Narvaez • *Department of Physiology, School of Medicine, University of Málaga, Málaga, Spain*

Julia Oflijan • *Department of Neuroscience, Karolinska Institutet, Stockholm, Sweden*

Keiko Okamoto-Furuta • *Division of Electron Microscopic Study, Center for Anatomical Studies, Graduate School of Medicine, Kyoto University, Kyoto, Japan*

Jorge E. Ortega • *Department of Pharmacology, University of the Basque Country UPV/EHU and CIBERSAM, Leioa Bizkaia, Spain*
Fuencisla Pilar-Cuéllar • *Instituto de Biomedicina y Biotecnología de Cantabria (IBBTEC) (UC-CSIC-SODERCAN), Santander, Spain; Departamento de Fisiología y Farmacología, Universidad de Cantabria, Santander, Spain; CIBERSAM, Instituto de Salud Carlos III, Madrid, Spain*
Luca Pinton • *Department of Neuroscience, Karolinska Institutet, Stockholm, Sweden*
George V. Rebec • *Program in Neuroscience, Department of Psychological and Brain Sciences, Indiana University, Bloomington, USA*
Beatriz Romero • *Instituto de Biomedicina y Biotecnología de Cantabria (IBBTEC) (UC-CSIC-SODERCAN), Santander, Spain; Departamento de Fisiología y Farmacología, Universidad de Cantabria, Santander, Spain*
Stfano Sartini • *Department of Earth, Life and Environmental Sciences, Section of Physiology, Campus Scientifico Enrico Mattei, Urbino, Italy*
Ryuichi Shigemoto • *Institute of Science and Technology Austria (IST Austria), Klosterneuburg, Austria*
David Soto • *Laboratory of Neurobiology, Bellvitge Biomedical Research Institute, L'Hospitalet de Llobregat, Spain*
Jaume Taura • *Pharmacology Unit, Department of Pathology and Experimental Therapeutics, School of Medicine, IDIBELL, University of Barcelona, Barcelona, Spain*
Elsa M. Valdizán • *Instituto de Biomedicina y Biotecnología de Cantabria (IBBTEC) (UC-CSIC-SODERCAN), Santander, Spain; Departamento de Fisiología y Farmacología, Universidad de Cantabria, Santander, Spain; CIBERSAM, Instituto de Salud Carlos III, Madrid, Spain*
Juan Varela • *Interdisciplinary Institute for Neuroscience, University of Bordeaux, Bordeaux, France*
Rebeca Vidal • *Instituto de Biomedicina y Biotecnología de Cantabria (IBBTEC) (UC-CSIC-SODERCAN), Santander, Spain; Departamento de Fisiología y Farmacología, Universidad de Cantabria, Santander, Spain; CIBERSAM, Instituto de Salud Carlos III, Madrid, Spain; Departamento de Farmacología, Facultad de Medicina, Universidad Complutense de Madrid, Madrid, Spain*
Masahiko Watanabe • *Department of Anatomy, Hokkaido University Graduate, School of Medicine, Sapporo, Japan*
Norbert Weiss • *Institute of Organic Chemistry and Biochemistry, Academy of Sciences of the Czech Republic, v.v.i., Prague, Czech Republic*
Miles Woolfenden • *Department of Neuroscience, Karolinska Institutet, Stockholm, Sweden*
Miwako Yamasaki • *Department of Anatomy, Hokkaido University Graduate, School of Medicine, Sapporo, Japan*

Part I

Molecular Techniques

Chapter 1

Production of High-Quality Antibodies for the Study of Receptors and Ion Channels

Masahiko Watanabe

Abstract

High-quality antibodies must have high specificities and titres. The development and application of high-quality antibodies have greatly contributed to our current understanding of the life sciences, including neuroscience. However, it is often difficult to develop high-quality antibodies for neural proteins with complex and highly ordered structures and compositions, such as receptors and ion channels. As a researcher who has tackled the production of polyclonal antibodies, this chapter introduces the procedures for antigen peptide preparation, immunisation, serum preparation, affinity purification and specificity tests that I have adopted and modified over two decades. I believe that the two key points in high-quality antibody production are the *whole-or-short* strategy in which the full length or short peptides are preferable to the incomplete length as immunising peptides and the *gold-dust-fishing* strategy by which useful antibodies are purified using affinity peptides designed to be shorter than, or displaced from, immunising peptides.

Key words Polyclonal antibody, Bacterial fusion protein, Synthetic peptide, Immunisation, Serum preparation, Affinitypurification, Specificity test

1 Introduction

Immunochemistry and immunohistochemistry, which use antibodies as biological reagents to detect antigen–antibody interactions, provide universal and powerful strategies to identify and characterise the expression and distribution of proteins in tissues and cells. The development and application of specific antibodies have greatly contributed to the cultivation of our understanding of cellular functions and molecular mechanisms. In particular, antibodies have had an inestimable impact on neuroscience, which deals with the brain and other neural tissues that have extensive anatomical, electrophysiological and pharmacological diversity and complexity. However, it is also true that neuroscientists confront substantial difficulties in developing and/or finding specific antibodies for neural proteins, particularly for receptors and ion channels, which are key molecules that confer neuronal diversity and complexity.

Rafael Luján and Francisco Ciruela (eds.), *Receptor and Ion Channel Detection in the Brain: Methods and Protocols*, Neuromethods, vol. 110, DOI 10.1007/978-1-4939-3064-7_1,

This arises mainly from the complex and highly ordered structures and compositions of endogenous proteins, whose steric conformations may not be reproduced faithfully by short synthetic or expressed peptides used for immunisation.

In support of this notion, the most frequent outcome of immunisation is the production of antibodies that bind the immunising peptides, but not the endogenous proteins, i.e. useless antibodies. The second most frequent outcome is a failure to produce any antibodies. This occurs when immunising peptides fail to elicit effective immune responses in host animals because of their low antigenicity. The least frequent outcome is the production of antibodies that bind both the immunising peptides and endogenous proteins, i.e. useful antibodies. In my experience, the success rate of antibody production, which is the proportion of useful antibodies produced relative to the total number of antigenic peptides used in immunisation, is less than 5 %, although the success rate is highly variable, as it depends on the class of proteins. When the full sequences of small cytosolic proteins, such as Ca^{2+}-binding proteins and fluorescent proteins, are used as immunogens, even if they are expressed and purified from bacteria, the success rate rises to nearly 100 %. In contrast, it falls to nearly 0 % for some classes of receptors and ion channels.

The production of polyclonal antibodies consists of the preparation of peptide antigens, immunisation, serum preparation, affinity purification and a specificity test. This chapter summarises the protocols for polyclonal antibody production that I have adopted and modified over two decades [1–7].

2 Materials

2.1 Preparation of Peptides for Immunisation and Affinity Purification

2.1.1 Preparation of cDNA Fragments

1. cDNA library. Total RNA is isolated from fresh brains by the acid–phenol method using Isogen (Nippon Gene, Toyama, Japan). Briefly, 1 g of fresh brain tissue is homogenised in a 50-mL plastic tube in 10 mL of Isogen using a Polytron homogeniser. Then, 2 mL of chloroform is added and shaken vigorously for 3 min. Following centrifugation at 2000 × *g* for 15 min at 4 °C in a swinging bucket rotor, the aqueous phase is transferred to a new plastic tube and mixed with 5 mL of isopropanol. After incubation at room temperature for 10 min, total RNA is precipitated by centrifugation at 2000 × *g* for 15 min at 4 °C, washed with 70 % ethanol and dissolved in TE buffer (10 mM Tris–HCl, pH 8.0/1 mM EDTA, pH 8.0). The OD_{260} of the total RNA is measured to calculate the concentration (1.0 OD_{260} is equivalent to 40 μg/mL of RNA). A cDNA library is constructed using the total RNA and the First-Strand cDNA Synthesis Kit according to the manufacturer's instructions (GE Healthcare, Uppsala, Sweden).

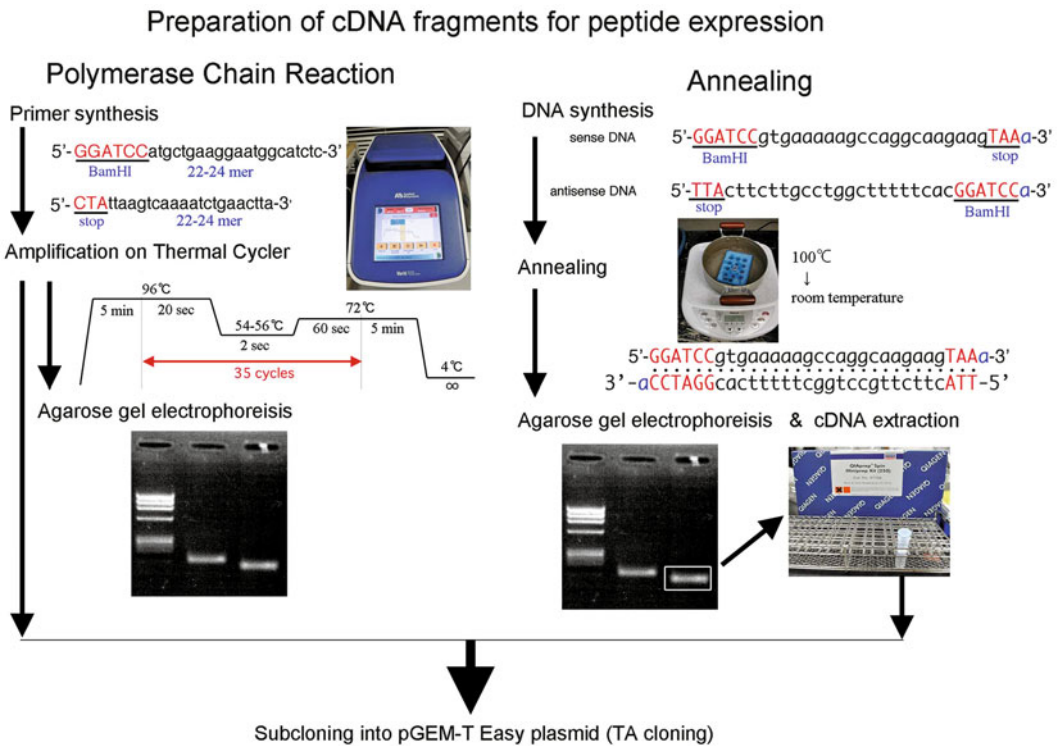

Fig. 1 Procedures for the preparation of cDNA fragments for peptide expression. cDNA fragments can be obtained via amplification by PCR (*left*) and annealing of DNAs (*right*). For subcloning into the pGEM-T Easy plasmid, annealed cDNA should be purified from agarose gel bands, while this purification step is not necessary for the use of PCR-amplified cDNAs

2. PCR primers. A BamHI recognition site (GGATCC) and a stop codon (TAA, TGA or TAG) are introduced in the forward and reverse primers, respectively, followed by 22–24 bases of the sense or antisense sequences, respectively, of the target cDNAs (Fig. 1, left). Primer sequences for peptide expression must be designed to be in frame when ligated into the cloning site of the plasmids used for expression, e.g. pGEX4T that is used in this protocol. If a BamHI site is present in the cDNAs used for peptide expression, other restriction enzyme sites, such as EcoRI, should be selected.
3. Synthetic DNAs for annealing. In cases where PCR amplification is unsuccessful, sense and antisense DNAs are synthesised so that after annealing, the cDNA fragments contain a BamHI recognition site and a stop codon in frame, with a protruding adenine (A) base at the 3′-end of both the sense and antisense DNAs for subsequent TA cloning (Fig. 1, right).
4. Phosphate-buffered saline (PBS). 10 mM sodium phosphate buffer (pH7.2)/150 mM NaCl.

5. PrimeSTAR HS DNA polymerase (Takara, Kyoto, Japan).
6. SeaPlaque GTG Agarose (Lonza, Rockland, ME, USA)
7. QIAquick Gel Extraction Kit (Qiagen, Hilden, German).

2.1.2 Plasmid Construction

1. pGEM-T Easy Vector System I (Promega, Madison, WI, USA). A BamHI site and stop codon are introduced in the PCR primers, and an EcoRI site is positioned on both sides of the TA cloning site in the pGEM-T Easy plasmid. Therefore, restriction enzyme digestion of recombinant plasmids by BamHI and EcoRI liberates in-frame cDNA fragments, followed by a stop codon, for protein expression.
2. pGEX4T plasmid vector (GE Healthcare). This vector allows the aforementioned cDNA fragments to be fused in frame with glutathione S-transferase (GST), thereby enabling their purification via glutathione-affinity chromatography.
3. BamHI (10 units/μL, Takara).
4. EcoRI (10 units/μL, Takara).
5. Alkaline phosphatase (0.5 units/μL, *Escherichia coli* C75, Takara).
6. T4 DNA ligase (Thermo Fisher Scientific, Waltham, MA, USA).

2.1.3 GST Fusion Proteins and GST-Free Peptides

1. *Escherichia coli* DH5α-competent cells (Takara).
2. L-broth. In a 5-L flask, the components below are mixed and autoclaved (121 °C, 20 min). Prior to culturing, 150 μg of ampicillin (Sigma-Aldrich, St. Louis, MO, USA) is added to the medium.

Bacto Tryptone (BD, Sparks, MD, USA)	30 g
Bacto Yeast Extract (BD)	15 g
NaCl	30 g
H_2O	3 L

3. Isopropyl β-D-1-thiogalactopyranoside (IPTG; Wako Pure Chemicals, Osaka, Japan).
4. Lysis buffer.

0.5 M sodium phosphate buffer (pH 7.2)	20 mL
0.5 M EDTA (pH 8.0, Wako)	20 mL
EGTA (Wako)	3.8 g
Phenylmethylsulfonyl fluoride (Wako) (10 mg/mL in isopropanol)	4 mL
2-mercaptoethanol (Sigma-Aldrich)	0.7 mL/L

5. Glutathione Sepharose 4B (GE Healthcare). Before use, spin down to pellet the Sepharose 4B gel.
6. Econo-Column (737–1006, 1.0×5 cm; Bio-Rad, Hercules, CA, USA). Using the appropriate fittings (Bio-Rad; 731–8221 for the adaptor, 732–8102 for the two-way stopcock), silicone tubes (1.5-mm inner diameter/3.0-mm outer diameter) are connected to the top and bottom of the Econo-Column to wash the GST fusion protein-bound glutathione Sepharose 4B. For elution of the GST fusion proteins, the cap is released from the Econo-Column and an 18-G needle is attached to the two-way stopcock at the bottom of the column.
7. Elution buffer. Dissolve 150 mg of glutathione (Wako) in 50 mL of 50 mM Tris–HCl (pH9.5).
8. Dialysis. Pooled eluates are packed into a hydrated cellulose tube for dialysis (UC20-32-100; Viskase, Darien, IL, USA) and sealed with polypropylene closures (Spectrum, Rancho Dominguez, CA, USA). The eluates are dialysed against PBS three to five times until the smell of glutathione is gone.
9. Digestion buffer. Dissolve 4.76 g of HEPES and 8.76 g of NaCl in 1 L of distilled water and adjust the pH to 8.0 with 5 M NaOH.
10. Thrombin (Wako). Bovine plasma thrombin (10,000 units) is dissolved in 5 mL of PBS and 5 mL of glycerol and kept in a freezer (−30 °C) until use.

2.1.4 Synthetic Peptides

1. Keyhole limpet hemocyanin (KLH; Sigma-Aldrich).
2. Carrier conjugation. If peptides for chemical synthesis contain no cysteine residues, this residue is added to the *N*- or *C-terminus* of the peptides (*N*-terminal conjugation is recommended) by the m-maleimidobenzoyl-*N*-hydroxysuccinimide ester (MBS) method. If cysteine is present, carrier conjugation is performed using the 1-ethyl-3-(3-dimethylaminopropyl) carbodiimide hydrochloride (EDC) or quick chemistry method. When peptides are synthesised for affinity purification only, neither the introduction of a cysteine residue nor carrier conjugation is necessary.

2.1.5 Other Methods worth Trying

1. SDS-PAGE gels. SDS-PAGE gels are constructed using 14-cm glass plates, spacers, a comb to make a single large well and a tube of silicone. Between the glass plates, pour 12 mL of the resolving gel solution (*1) and overlay 2 mL of distilled water on the gel solution. After polymerisation, the water is discarded, and 5 mL of the stacking gel solution (*2) is layered over the resolving gel until it polymerises. Two millilitres of GST fusion protein is mixed with an equal volume of 2×SDS sampling buffer (*3) and boiled for 5 min. After running the

samples at a constant current of 20 mA for several hours, an interface of refraction can be seen 1–2 cm above the bromophenol blue marker and a 1-cm-wide gel band just above the refraction interface is excised. In a 50-mL plastic tube, the gel band is homogenised in 10 mL of PBS using a Polytron homogeniser.

*1. Resolving gel solution. Solution A:Solution B:H_2O = 5:6:1.

*2. Stacking gel solution. Solution A:Solution C = 0.75:4.25.

Solution A: 29 % acrylamide and 1 % bis-acrylamide.

Solution B: 75 mL 1 M Tris–HCl (pH 8.8), 2 mL 10 % SDS and 23 mL H_2O.

Solution C: 25 mL 1 M Tris–HCl (pH 6.8), 2 mL 10 % SDS and 153 mL H_2O.

*3. 2 × SDS sampling buffer.

1 M Tris–HCl (pH 6.8)	6.25 mL
10 % SDS	40 mL
50 % glycerol	40 mL
0.1 % bromophenol blue	1 mL
2-mercaptoethanol	5 mL
H_2O	47.75 mL/total volume 100 mL

2.2 Immunisation

1. Freund's complete adjuvant (BD).
2. Freund's incomplete adjuvant (BD).
3. Luer-lock glass syringes (5 mL) and a connecting metal tube.
4. Host animals for immunisation. I have used New Zealand White rabbits, Hartley guinea pigs and goats as host animals for immunisations.

2.3 Serum Preparation

1. 18-G butterfly needle.
2. 50-mL plastic tubes.
3. Water bath.
4. Centrifuge with a swinging bucket rotor.

2.4 Affinity Purification

1. CNBr-activated Sepharose 4B (GE Healthcare).
2. Glass filter flask for suction filtration. This kit consists of a glass filter (Buchner type with a maximal pore size of 20–30 or 40–50 μm), a silicone stopper and a 500- or 1000-mL flask with an adaptor sleeve for vacuum tubing and an aspirator or low-pressure vacuum pump.
3. 1 mM HCl. Eighty-five microlitres of concentrated hydrochloric acid (12 N) is diluted with distilled water to make 1 L.

4. PBS.
5. Neutralising buffer. 1 M Tris–HCl (pH 7.6) and 5 M NaCl are added at a 1:2 ratio for neutralisation and protein stability.
6. 10 % sodium azide stock solution.

3 Methods

3.1 Preparation of Peptides for Immunisation and Affinity Purification

Because useful and useless antibodies are often produced simultaneously in a single host animal, identifying good peptide regions for immunisation and affinity purification is a key factor in developing high-quality antibodies that have sufficient specificities and titres for experimental purposes. Although there are no golden rules for producing high-quality antibodies, high-quality antibodies are produced most often against the *N*- and *C*-terminal regions of proteins. This empirical knowledge suggests that the extremities of many endogenous proteins are prone to adopting confirmations similar to those formed by short peptide antigens. Therefore, *N*- and *C*-terminal sequences should be considered as primary candidates for immunogens.

3.1.1 Preparation of cDNA Fragments

For peptide antigens, cDNAs encoding 20–50 amino acid residues (**Note 4.1**) are amplified by PCR using a pair of forward and reverse primers that carry a BamHI site or stop codon, respectively (Fig. 1). A series of 35 cycles, each consisting of 96 °C for 20 s, 56 °C for 2 s and 72 °C for 60 s, is run on a thermal cycler (Veriti, Applied Biosystems, Waltham, MA, USA), using a high-fidelity proofreading polymerase. When PCR amplification does not work, double-stranded cDNA fragments that carry a BamHI site and stop codon are prepared by annealing synthetic sense and antisense DNAs (Fig. 1). Annealing is completed by gradual cooling after boiling in PBS. Annealed cDNA fragments are purified by 1 % agarose gel electrophoresis, followed by extraction from the agarose gel bands.

3.1.2 Plasmid Construction

cDNA fragments obtained from PCR or DNA annealing (Fig. 1) are first subcloned into the pGEM-T Easy plasmid using TA cloning (*1). BamHI/EcoRI fragments are excised by digesting recombinant pGEM-T Easy plasmids (*2), followed by 1 % agarose gel electrophoresis and gel extraction. The pGEX4T plasmid for the expression of GST fusion proteins is digested by BamHI and EcoRI, dephosphorylated and purified by 1 % agarose gel electrophoresis and gel extraction (*3). BamHI/EcoRI fragments are ligated to pGEX4T (*4). The nucleotide sequences of the cDNA inserts must be checked after obtaining mini-preparations of the recombinant pGEM-T Easy and pGEX4T plasmids.

*1. TA cloning into pGEM-T Easy.

pGEM-T Easy plasmid	0.25 μL
cDNA fragment	1 μL
2 × buffer	2.5 μL
H_2O	1 μL
T4 DNA ligase	0.25 μL/total volume 5 μL, 12 °C, 1 h overnight

*2. Restriction enzyme digestion of pGEM-T Easy.

pGEM-T Easy plasmid	10 μL (3–5 μg)
10 × buffer	10 μL
H_2O	76 μL
BamHI	2 μL
EcoRI	2 μL/total volume 100 μL, 37 °C, 1–2 h

BamHI/EcoRI fragments are purified by 1 % agarose gel electrophoresis and gel extraction.

*3. Restriction enzyme digestion and dephosphorylation of pGEX4T.

pGEX4T-2 plasmid (1 μg/μL)	10 μL
10 × buffer	20 μL
EcoRI	2 μL
BamHI	2 μL
H_2O	166 μL/total volume 200 μL, 37°C, 2 h
Digested pGEX4T-2 plasmid	200 μL
10 × alkaline phosphatase buffer	20 μL
Alkaline phosphatase	2 μL/total volume 222 μL, 50 °C, 30 min

pGEX4T-2 is finally purified by 1 % agarose gel electrophoresis and gel extraction.

*4. Subcloning into pGEX4T.

pGEX4T-2 plasmid (25 ng/μL)	0.5 μL
cDNA fragment	1 μL
5 × ligation buffer	1 μL
H_2O	2 μL
T4 DNA ligase	0.5 μL/total volume 5 μL, 12 °C, 1 h

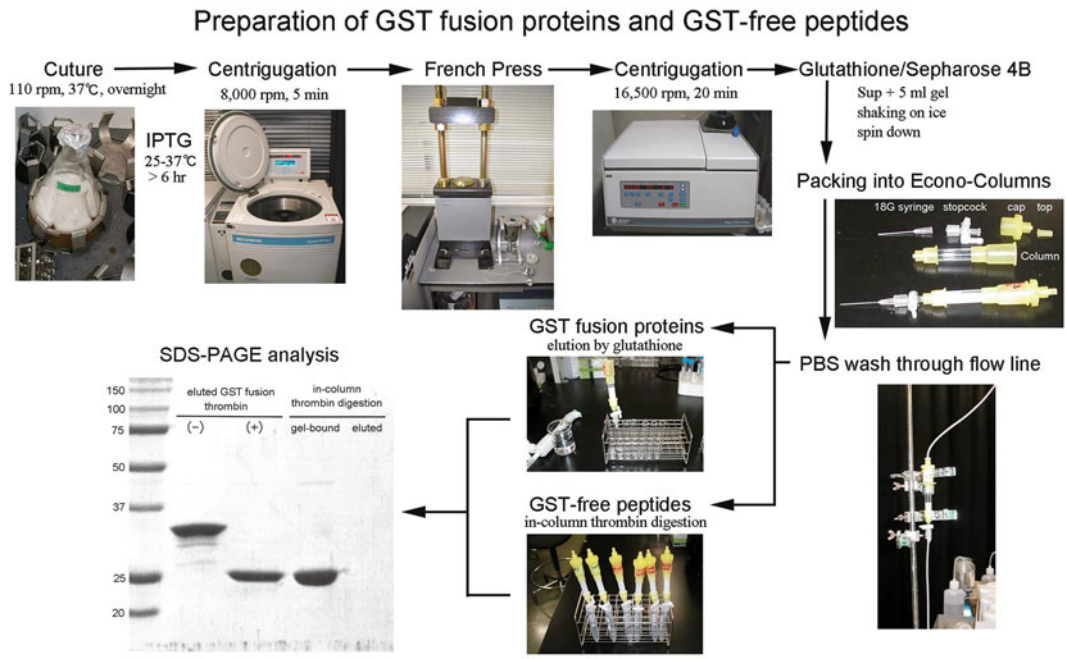

Fig. 2 Procedures for the preparation of glutathione S-transferase (GST) fusion proteins and GST-free peptides

3.1.3 GST Fusion Proteins and GST-Free Peptides (Fig. 2)

DH5α *E. coli* cells are transformed with recombinant pGEX4T plasmids and cultured overnight in 3 L of L-broth on a shaking incubator (110 rpm, 37 °C). Then, 215 mg of IPTG (final concentration 0.3 mM) is added to induce protein expression. After culturing for 6 h to overnight at 25–37 °C, cells are pelleted by centrifugation at 11,900 × *g* for 5 min (Avanti HP-20I centrifuge with a JLA10.500 rotor, Beckman Coulter, Indianapolis IN, USA) and suspended in 30 mL of lysis buffer. Cells are lysed by a single passage through a French press (model 5501-M, Ohtake Works, Tokyo, Japan). After centrifugation at 29,220 × *g* for 20 min (Allegra 64R centrifuge with a F0850 rotor, Beckman Coulter), supernatants are transferred to a 50-mL plastic tube and mixed with 5 mL of glutathione Sepharose 4B. After 1 h shaking on ice, Sepharose 4B is collected and packed into two Econo-Columns, one for GST fusion proteins (antigen) and another for GST-free peptides (affinity purification). Using silicone tubes and fittings, a flow line is attached to the Econo-Columns and each column is washed with 100 mL of PBS.

To recover GST fusion proteins, 2 mL of elution buffer is successively poured onto the top of the Sepharose 4B gel and collected into five borosilicate glass tubes (13 × 100 mm). The OD_{280} is measured to determine the protein concentration (1.0 OD_{280} is equivalent to 1.0 mg/mL of protein), and fractions with high protein concentrations are pooled. Glutathione bound to GST fusion

proteins is removed by repeated dialysis against PBS. Dialysed GST fusion proteins are dispensed into six aliquots (0.7 mL each) for immunisation, and kept in the freezer (−30 °C) until use. The remainder is stored for future use in the antigen absorption test.

To prepare GST-free peptides, 10 mL of the digestion buffer is passed through a glutathione Sepharose 4B column. By closing the top and bottom of the Econo-Column, the Sepharose 4B gel is suspended in 3 mL of digestion buffer containing 50 μL of 1 unit/μL thrombin. After overnight in-column digestion at room temperature, the digestion buffer containing GST-free peptides is eluted. Residual GST-free peptides are eluted by an additional 3 mL of the digestion buffer. The GST-free peptide solution (6 mL in total) is kept in the freezer (−30 °C) until the preparation of affinity purification media. The reduced molecular masses of protein bands after thrombin digestion should be confirmed by SDS-PAGE-->. Usually, GST-free peptides are not visible directly because of their small masses.

3.1.4 Synthetic Peptides

For chemical synthesis, 5 mg of 8–30 amino acid peptides is synthesised: 3 mg for carrier conjugation (immunisation), 1 mg for affinity media preparation (purification) and 1 mg for the pre-absorption test (specificity test).

Because of high sequence homology to other proteins or experimental constraints, peptide regions for immunisation must sometimes be shorter than 20 amino acid residues. On such occasions, it is convenient to use commercial services for the synthesis of peptides and their conjugation to carrier proteins, although this costs much more than bacterially expressed fusion proteins. The hydrophilicity (**Note 4.2**) and purity (>70 % or more) of the synthetic peptides are prerequisites for the production of high-quality antibodies. In general, the conjugation of synthetic peptides to carrier proteins, such as KLH, increases the immunogenicity and stability of synthetic peptides in host animals. Moreover, by wisely using synthetic peptides for affinity purification, one can increase the quality of antibodies (**Note 4.3**).

3.1.5 Other Methods worth Trying

If the antibodies raised against GST fusion proteins do recognise the proteins of interest, but are not satisfactory in terms of their specificities and titres, the use of SDS-PAGE-purified antigens is worth undertaking. If this occurs for antibodies raised against synthetic peptides conjugated to carrier proteins, immunisation with free synthetic peptides may yield good results on occasion. The notion learned from my experience is that any procedures and manipulations that preserve the steric conformation of peptide antigens in a manner that approximates that of endogenous proteins will aid in the development of high-quality antibodies.

3.2 Immunisation

Peptide antigens are emulsified in Freund's adjuvant, a mineral oil used as an immunopotentiator or booster. Complete Freund's adjuvant contains inactivated and dried mycobacteria (usually *Mycobacterium tuberculosis*) and is used in the initial immunisation, whereas incomplete Freund's adjuvant, which lacks mycobacteria, is used in the subsequent immunisations. It is important to thoroughly mix the water-in-oil emulsion, as peptide antigens in this state remain longer in subcutaneous injection sites, thereby potentiating cell-mediated immunity for long term.

To this end, two Luer-lock glass syringes, each containing either Freund's adjuvant (1 mL) or antigen solution/gel (0.7 mL), are interconnected by a metal tube ending with adaptors for the Luer-lock syringe. Mix the solutions vigorously by alternatingly pushing the plungers. Emulsified peptide antigens are injected through a 25-G needle into many subcutaneous sites on the back and extremities of host animals every 2–3 weeks.

3.3 Serum Preparation

One to two weeks after the sixth injection, blood is taken only once by inserting an 18-G butterfly needle into the heart of guinea pigs and the common carotid artery of goats under pentobarbital anaesthesia. In comparison, blood is sampled several times (every 3–4 days) by inserting an 18-G butterfly needle into the central ear artery of rabbits. Clot formation and retraction are facilitated by warming the blood to 37 °C in a water bath for 1 h, followed by overnight cooling in a refrigerator. The serum is separated from the clot by centrifugation at $2000 \times g$ for 10 min in a swinging bucket rotor.

3.4 Affinity Purification

Affinity medium is prepared by coupling GST-free or synthetic peptides to CNBr-activated Sepharose 4B. For each coupling, 1.0 g of CNBr-activated Sepharose 4B is placed on a glass filter and activated by the passage of 200 mL of 1 mM HCl and then 100 mL of PBS by aspiration. Immediately, activated gels are transferred to a 15-mL plastic tube, suspended in 5 mL of PBS and mixed with GST-free peptide solution (6 mL) or 1 mg of synthetic peptides dissolved in 3 mL of PBS. The coupling reaction is completed in 1 h at room temperature or 3 h in the refrigerator on a rotator. To block residual functional groups, 1 mL of 1 M Tris–HCl (pH 8.0) is mixed and rotated for an additional 1 h.

The affinity medium is packed into Econo-Columns, and a flow line is attached using silicone tubes and fittings, as is the case for GST fusion protein purification. After washing with 100 mL of 1 mM HCl and then with 100 mL of PBS, serum is applied to the affinity column. After washing with 100 mL of PBS, the cap of the Econo-Column is released and an 18-G needle is attached to a two-way stopcock at the bottom of the column. To elute immunoglobulins bound to the affinity medium, 3-mL volumes of 1 mM HCl are successively poured on top of the affinity medium and

collected into 5–10 borosilicate glass tubes (13 × 100 mm), each containing 200 μL of neutralising buffer. The OD_{280} is measured to determine the protein concentration (1.0 OD_{280} is equivalent to 1.0 mg/mL of immunoglobulins), and fractions with high concentrations of immunoglobulins are pooled. After dialysis in PBS, denatured debris is removed by centrifugation at 2000 × *g* for 10 min in a swinging bucket rotor. The final concentration of purified antibodies is determined by an OD_{280} measurement. When purifying sera from different host species injected with the same antigens, affinity media must be packed into separate columns, with each column only being used for a single species. Otherwise, antibodies of one species that remain from the previous purification are eluted with those of other species in a subsequent purification. Such contaminated antibodies cannot be used for multiple immunohistochemical labelling because of cross-reactions with secondary antibodies.

Purified antibodies are added to 1/100 volume of 10 % sodium azide as a preservative and aliquoted into 1.5-mL plastic tubes. As immunoglobulins are stable, working antibodies kept in the refrigerator can be used for several years or more. For long-term storage, it is better to store antibodies in the deep freezer (–80 °C).

3.5 Specificity Tests

There are several tests that assess the quality and specificity of antibodies. Antibodies applicable to immunochemical techniques, such as immunoblotting and immunoprecipitation, are not always specific when used for immunohistochemistry and vice versa. Therefore, researchers should try multiple specificity tests, including immunochemical and/or immunohistochemical methods, for their own experiments.

3.5.1 Normal Tissue Samples

Using normal tissue samples, the apparent molecular mass of protein bands by immunoblotting, as well as characteristic immunohistochemical patterns, provides basic information regarding the recognition of antibodies. These basic tests become particularly important when combined with the loss or reduction of immunolabelling signals in knockdown and knockout tissues or in the preabsorption test.

3.5.2 Mammalian Cell Transfection

The specificity of antibodies can be tested by immunochemical and immunocytochemical techniques using cell lines (such as COS or HEK293T cells) transfected by mammalian expression plasmids and viral vectors carrying the cDNAs of interest. This test is widely applicable. However, because of different post-translational modifications in cell lines, the apparent masses of the proteins of interest often shift compared with those in tissue samples. Moreover, even low-specificity and low-titre antibodies can yield strong signals in cell lines overexpressing the proteins of interest.

3.5.3 Knockdown Cells and Tissues

Using the RNA interference (RNAi) technique, the expression of proteins of interest can be downregulated. Knockdown by RNAi is performed by transfecting cells and tissues with short interfering RNAs or with mammalian vectors encoding short hairpin RNAs or microRNAs. The specificity of antibodies is validated by the reduction of immunohistochemical, immunocytochemical or immunoblot signals in knockdown samples. However, it is necessary to consider the efficacy and specificity of knockdowns by RNAi.

3.5.4 Preabsorption Test

The preabsorption test is conducted by pre-incubation of primary antibodies with (controls) or without (experiments) peptide antigens, which are applied to all immunochemical and immunohistochemical incubations under the same condition. The loss of immunosignals in controls compared with those in experiments indicates the specificity of the signals, while the remaining signals in the controls represent the background. The preabsorption of antibodies by antigens is usually performed by mixing an antibody, diluted to a final concentration of, e.g. 1–2 μg/mL for affinity-purified antibodies or a 1:1000–5000 dilution of antisera, with an excess amount of antigen or equivalent volume of PBS.

Preabsorption by GST fusion proteins:

	Control	Experiment
Antibody (200 μg/mL)	5 μL	5 μL
GST fusion protein (1 mg/mL)	20 μL	0 μL
PBS	975 μL	995 μL

Preabsorption by synthetic peptide:

	Control	Experiment
Antibody (200 μg/mL)	5 μL	5 μL
Synthetic peptide (1 mg/mL)	2 μL	0 μL
PBS	993 μL	995 μL

This mixture yields final antibody, GST fusion protein and synthetic peptide concentrations of 1 μg/mL, 20 μg/mL and 2 μg/mL, respectively. Considering the molecular weights of immunoglobulins (160 kDa), the GST fusion protein (26 kDa for GST plus 2.4–6.0 kDa for 20–50 amino acid peptides) and synthetic peptides (900–3600 Da for 8–30 amino acid peptides), the molar ratio of antibody to antigen is around 1:100 for preabsorption by GST fusion proteins and 1:100–350 for synthetic peptides.

If cross-reaction of antibodies to homologous proteins is an issue, the preabsorption test using peptide antigens or the corresponding regions of homologous proteins will ameliorate this problem.

3.5.5 Comparison with In Situ Hybridisation

If the proteins of interest have characteristic regional and cellular expression patterns, a comparison of immunohistochemical staining patterns with those by *in situ* hybridisation offers supporting information regarding the specificity of antibodies and immunohistochemical signals. This test is not suited for housekeeping genes that are widely expressed in many cell types and tissues.

3.5.6 Gene Knockout Animals

Gene knockout mice or their tissues are the best tools to verify the specificity of antibodies used in immunoblotting, immunoprecipitation and immunohistochemistry, at both the light and electron microscopic levels.

4 Notes

4.1 Length of Peptide Antigens

Researchers and students who do not have much experience with antibody production prefer longer (>100 amino acid residues) antigens in their initial attempts. However, the expression of proteins larger than 5 kDa in bacteria results in low yields and premature stoppage of translation. This stoppage of translation, rather than the degradation of translated products, is responsible for ladders of purified fusion proteins. Moreover, as the length of a peptide antigen increases, the chance of producing useless or poor antibodies also increases. In contrast, as described in the introduction, small cytosolic proteins 100–300 amino acids in length, such as Ca^{2+}-binding proteins (e.g. calbindin and parvalbumin) and fluorescent proteins (green fluorescent protein and DsRed), are often fully translated in bacteria and they serve as good immunogens. I believe that '*the whole-or-short*' strategy in immunisation is superior to the incomplete length of peptide antigens.

4.2 Hydrophilicity of Peptide Antigens

Hydrophilicity is an important factor to be considered when designing peptide antigens. If their solubility is low, a substantial fraction of bacterially expressed fusion proteins and synthetic peptides becomes resistant to purification, enzymatic digestion, coupling to affinity media, conjugation to carrier proteins and affinity purification. Moreover, hydrophilic sequences are expected to be surface exposed, and, therefore, antibodies can readily access their epitope sites. Of the 20 amino acids, hydrophilicity is high for charged amino acids, such as arginine, aspartate, glutamate and lysine, and low for alanine, isoleucine, leucine, phenylalanine, tryptophan, tyrosine and valine. The amino acid composition needs to be considered before the preparation of peptide antigens.

4.3 Use of Short or Displaced Peptides for Affinity Purification

As stated in the introduction, high specificity and titre are the two key factors of high-quality antibodies. However, useless antibodies are often produced together with useful ones in the same host animals. This is partly because of different steric conformations

between endogenous proteins and peptide antigens. Moreover, it should be kept in mind that the use of partial or truncated peptide antigens yields antibodies against peptide conformations that do not exist in endogenous proteins. Affinitypurification using the same peptides as used for immunisation could collect antibodies that produce non-specific signals, such as those recognizing artificial N- or C-termini of peptide antigens used. To avoid this, synthetic peptides, which are designed to be shorter than, or displaced from, peptide antigens, could concentrate useful antibodies and eliminate useless ones. Of practical importance, this strategy for affinity purification (I refer this as '*the gold-dust-fishing*' strategy) can be applied at any time after serum preparation to increase the likelihood of obtaining satisfactory outcomes.

When unique sequences available for immunisation are limited because of high sequence homology to other related proteins, long peptides cavering unique sequences (either GST fusion proteins or synthetic peptides) are used for immunisation, while short peptides corresponding to the unique sequence (usually, synthetic peptides) are used for affinity purification. For example, if the last six amino acids of the C-terminus are conserved in a protein family, I recommend that the C-terminal portion, including the last six amino acids, is used as an immunogen, while a C-terminal peptide lacking the last 4–5 amino acids is used for affinity purification. This is also true for cases where unique sequences are only found in the middle of proteins.

Acknowledgements

I appreciate all my colleagues who have used my antibodies in their splendid anatomical experiments.

References

1. Watanabe M, Fukaya M, Sakimura K, Manabe T, Mishina M, Inoue Y (1998) Selective scarcity of NMDA receptor channel subunits in the stratum lucidum (mossy fiber-recipient layer) of the hippocampal CA3 subfield. Eur J Neurosci 10:478–487
2. Fukaya M, Watanabe M (2000) Improved immunohistochemical detection of postsynaptically-located PSD-95/SAP90 protein family by protease section pretreatment. A study in the adult mouse brain. J Comp Neurol 426: 572–586
3. Yoshida T, Fukaya M, Uchigashima M, Kamiya H, Kano M, Watanabe M (2006) Localization of diacylglycerol lipase-α around postsynaptic spine suggests close proximity between production site of an endocannabinoid, 2-arachidonoyl-glycerol, and presynaptic cannabinoid CB1 receptor. J Neurosci 26: 4740–4751
4. Miyazaki T, Yamasaki M, Hashimoto K, Yamazaki M, Abe M, Usui H, Kano M, Sakimura K, Watanabe M (2011) Cav2.1 in cerebellar Purkinje cells regulates competitive excitatory synaptic wiring, cell survival, and cerebellar biochemical compartmentalization. J Neurosci 32:1311–1328
5. Uchigashima M, Yamazaki M, Yamasaki M, Tanimura A, Sakimura K, Kano M, Watanabe M (2011) Molecular and morphological

configuration for 2-arachidonoylglycerol-mediated retrograde signaling at mossy cell-granule cell synapses in the dentate gyrus. J Neurosci 31:7700–7714

6. Yamasaki M, Okada R, Takasaki C, Toki S, Fukaya M, Natsume R, Sakimura K, Mishina M, Shirakawa T, Watanabe M (2014) Opposing role of NMDA receptor GluN2B and GluN2D in somatosensory development and maturation. J Neurosci 34:11534–11548
7. Konno K, Matsuda K, Nakamoto C, Uchigashima M, Miyazaki T, Yamasaki M, Sakimura K, Yuzaki M, Watanabe M (2014) Enriched expression of GluD1 in higher brain regions and its involvement in parallel fiber-interneuron synapse formation in the cerebellum. J Neurosci 34:7412–7424

Chapter 2

Co-immunoprecipitation from Brain

Xavier Morató, Dasiel O. Borroto-Escuela, Kjell Fuxe, Víctor Fernández-Dueñas, and Francisco Ciruela

Abstract

Co-immunoprecipitation (Co-IP) is one of the most broadly used methodologies to identify, validate and characterize protein–protein interactions (PPIs) in native conditions. In brief, this technique consists of immunocapturing a protein of interest from a tissue lysate using a specific antibody. Subsequently, the immunocomplex containing the antibody, the antigen of interest and the antigen-associated proteins is precipitated by means of a Proteins A/G conjugated resin and analysed by immunoblot. Of note, since PPIs are extremely dynamic and/or labile, the Co-IP method has to be optimized for each specific PPI. Remarkably, it is mandatory paying special attention to the specificity of antibodies used in the immunoprecipitation and the lysis buffer employed. Finally, it is important to point out that, by means of this approach, it is difficult to differentiate physiological (real) interactors from non-specific binders, thus an additional tool is recommended to validate the results. Here, we describe the methodology to Co-IP two plasma membrane receptors from different brain areas (i.e. hippocampus and raphe nucleus) using the same set of antibodies.

Key words Protein–protein interaction, Immunoprecipitation, Antibody, Co-immunoprecipitation

1 Introduction

In the brain, nearly all functions require the existence of multiprotein complexes, thus the identification and characterization of protein–protein interactions (PPIs) constitute an essential step to understand its functioning [1]. Interestingly, brain proteins may be expressed in different cell types and also in a temporally and spatially different manner, thus making difficult the study of these PPIs. Consequently, PPI discovery and characterization in different types of brain cells may provide useful information to understand the complexity of brain.

Several methods can be applied for discovery, validation and characterization of PPI processes [2, 3]. Importantly, before implementing any PPI method, two fundamental notions have to be kept in mind: (i) sensitivity and (ii) specificity. In such way, if the

Rafael Luján and Francisco Ciruela (eds.), *Receptor and Ion Channel Detection in the Brain: Methods and Protocols*, Neuromethods, vol. 110, DOI 10.1007/978-1-4939-3064-7_2,

objective is to detect as many as possible life-occurring PPIs, a high-sensitivity screen methodology is needed. However, if the goal is to achieve a high PPI validation rate, a high specificity method should be chosen, thus ensuring that most of the interactions detected by the screen method will occur in life. Accordingly, since all PPI methods have its own strengths and weaknesses, a balance between sensitivity and specificity should be accomplished when choosing a concrete PPI method.

PPI methods can be classified into two main categories, namely, biochemical approaches and biophysical (including theoretical) technologies. Within the biochemical methods, the co-immunoprecipitation (Co-IP) is considered the gold standard PPI assay [4], especially when endogenous PPIs (i.e. not overexpressed and not tagged proteins) are assessed. Co-IP is a simple but effective PPI method that relies on target-specific antibodies. A general overview of the Co-IP process is shown in Fig. 1. In brief, a soluble extract (i.e. lysate) from the brain area of interest is initially prepared upon relatively mild conditions to retain PPI integrity. To this end, a lysis buffer containing detergent(s) is used to solubilize proteins from the brain tissue. Normally, non-ionic detergents (e.g. NP-40, Triton X-100) are employed, but some integral membrane proteins (e.g. resident postsynaptic density proteins) may require harsh solubilizing conditions and thus ionic detergents may be incorporated into the lysis buffer. Overall, a suitable lysis buffer should allow high-protein yield while retaining PPI integrity. Once the soluble extract is prepared, the protein of interest is immunocaptured by incubating with specific antibodies (Fig. 1). Then, the resulting immunocomplexes including the antibody, the protein of interest (i.e. antigen) and the antigen-associated proteins can be precipitated by means of a resin (e.g. agarose, sepharose) containing IgG-binding Proteins A/G conjugated to its surface (Fig. 1). After extensive washes to remove non-specific interactors, the specifically bound (i.e. immunoprecipitated) proteins are eluted from the immunoaffinity resin by treatment with SDS-PAGE buffer (Fig. 1) and subsequently analysed by immunoblot.

Importantly, the Co-IP methodology typically requires a great deal of optimization and troubleshooting. In most cases, the critical factor is the antibody, while in others, the lysis buffer and the primary tissue sample are the problems to solve. Nevertheless, a major drawback that is needed to remark is the difficulty from differentiating physiological (real) interactors from non-specific binders, thus a complementary technique is usually used to validate the PPI. In the present chapter, we focus on describing the methodology used to Co-IP two plasma membrane receptors from different brain areas (i.e. hippocampus and raphe nucleus) using the same set of antibodies.

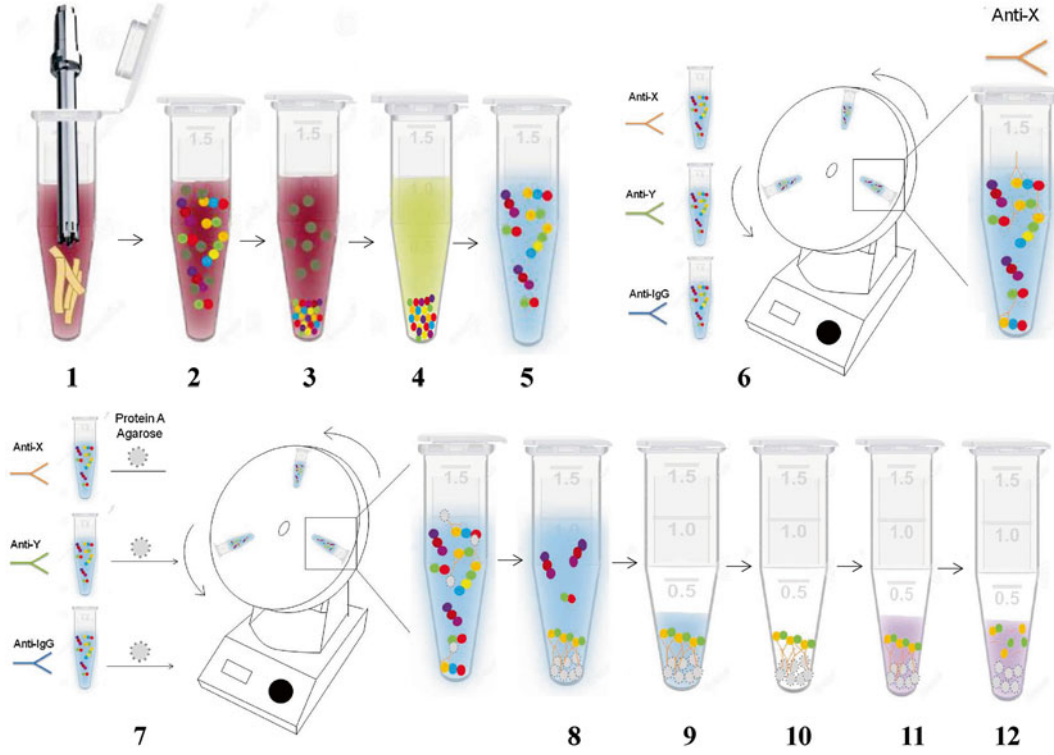

Fig. 1 Scheme of the co-immunoprecipitation procedure. Brain tissue is homogenized with the aid of the polytron (***Step 1***). The crude extract (***Step 2***) is then centrifuged at low rpm to eliminate nucleus from the total membrane extract. The supernatant is collected in a new eppendorf and centrifuged at high speed to pellet total membrane proteins (***Step 3***). Supernatant, containing cytosolic proteins, is discarded (***Step 4***) and pellet is resuspended in ice-cold Tris 50 mM. At this point, the protein concentration is determined using the BCA assay. Total membrane extracts are aliquoted (1–2 mg) according to the number of experimental conditions, centrifuged and the pellet resuspended in 1 mL of RIPA to solubilize total membrane proteins (***Step 5***). Then, samples are centrifuged at high rpm and the corresponding supernatant incubated with the indicated antibody overnight with constant rotation at 4 °C (***Step 6***). Next, 50 μL of either Protein A or TrueBlot resin is added to each tube and further incubated for 2 h at 4 °C with constant rotation (***Step 7***). The resin is washed with ice-cold RIPA by centrifuging at 10.000 rpm for 1 min (***Step 8***) and the supernatant discarded (***Step 9***). Finally, the supernatant is aspirated to dryness (***Step 10***). The resin is resuspended in SDS-PAGE or urea sample buffer (***Step 11***) and heated before loading into the polyacrylamide gel (***Step 12***)

2 Materials

2.1 Animals

1. Sprague–Dawley rats (Charles River Laboratories, L'Arbresle, France).

2.2 Buffers and Reagents

1. *Tris 50 mM buffer*: 50 mM Tris Base, pH 7.4.
2. *Radioimmunoprecipitation assay (RIPA) buffer*: 50 mM Tris–HCl, pH 7.4, 100 mM NaCl, 1 % Triton-X100, 0.5 % sodium deoxycholate, 0.2 % SDS, and 1 mM EDTA.

3. *Sodium dodecyl sulphate polyacrylamide gel electrophoresis (SDS-PAGE-->) sample buffer*: 125 mM Tris–HCl, pH 6.8, 4 % SDS, 20 % glycerol, 0.004 % bromophenol blue, and freshly prepared 50 mM dithiothreitol (DTT).
4. *Urea sample buffer:* 375 mM Tris–HCl, pH 6.8, 8 M urea, 50 mM DTT, 2 % SDS, 0.004 % bromophenol blue.
5. *Separating gel buffer*: 1.5 M Tris Base, pH 8.8
6. *Stacking gel buffer*: 25 mM Tris Base, pH 6.8.
7. *Electrophoresis buffer:* 25 mM Tris Base, pH 8.0, 180 mM glycine, 0.1 % SDS.
8. *Anode buffer:* 300 mM Tris Base, 20 % methanol.
9. *Cathode buffer:* 40 mM 6-aminocaproic acid, 20 % methanol.
10. *Phosphate-buffered saline (PBS)*: 137 mM NaCl, 2.7 mM KCl, 1.4 mM KH_2PO_4, 17 mM Na_2HPO_4, pH 7.2.
11. *Immunoblot(IB) washing solution*: PBS containing 0.05 % Tween 20.
12. *IB blocking solution*: PBS containing 0.05 % Tween 20 and 5 % (w/v) of nonfat dry milk.
13. *Reagents:* protein A-immobilized agarose fast flow, 50 % (v/v) (Sigma-Aldrich, St. Louis, MO, USA), TrueBlot™ anti-mouse IgG IP resin (eBioscience, San Diego, CA, USA), Protease Inhibitor Cocktail Set III (Millipore, Temecula, CA, USA), acrylamide/bis-acrylamide (30 %/0.8 % w/v) (Bio-Rad Laboratories, Hercules, CA, USA), ammonium persulfate (APS) (Sigma-Aldrich),tetramethylethylenediamine(TEMED)(Sigma-Aldrich), methanol 99.8 % (Pancreac Química SL, Barcelona, Spain), precision plus protein standards (Bio-Rad), Tween 20 (Sigma-Aldrich), nonfat dry milk, SuperSignal west pico chemiluminescent substrate (Thermo Fisher Scientific Inc., Waltham, MA, USA), BCA protein assay kit (Pierce Biotechnology, Rockford, IL, USA).
14. *Primary antibodies*: rabbit anti-$mGlu_5$ receptor antibody (Millipore), rabbit anti-5-HT_{1A} receptor (Abcam, Cambridge, UK), mouse anti-FGFR1 (clone M2F12, Abcam), control mouse IgG (GenScript, Piscataway, NJ, USA).
15. *Secondary antibodies*: horseradish-peroxidase (HRP)-conjugated goat anti-rabbit IgG (Thermo Fisher Scientific), HRP-conjugated anti-mouse IgG TrueBlot™ (eBioscience).

2.3 Instrumentation, Equipment and Software

1. Tweezers (style 5; Dumont, Montignez, Switzerland).
2. Carbon steel surgical blade (No. 20; Swann-Morton Limited, Sheffield, UK).
3. Polytron (VDI 12 Adaptable Homogenizer; VWR, Radnor, PA, USA).

4. Microfuge (Heraeus Fresco 21; Thermo Fisher Scientific Inc.).
5. Rotator "Orbit" (12 r.p.m. rotation speed; Selecta, Abrera, Spain).
6. Needles (Microlance-3 30G; Becton, Dickinson and Company, Franklin Lakes, NJ, USA).
7. Mini-PROTEAN casting frame (Bio-Rad).
8. Immobilon-P Transfer Membrane (pore 0.45 μm; Millipore).
9. Extra thick blot paper, filter paper (Bio-Rad)
10. Trans-Blot Turbo Transfer System (Bio-Rad).
11. Rocker 25 (Labnet, Woodbridge, NJ, USA)
12. Amersham Imager 600 (GE Healthcare Europe GmbH, Barcelona, Spain).

3 Methods

3.1 Preparation of Total Brain Membranes

1. Sacrifice rats weighting 200–250 g by decapitation and carefully dissect the brain area of interest (e.g. hippocampus and raphe nucleus). Keep the sample in a chilled eppendorf (*see* **Note 1**).
2. Add 1 mL of ice-cold Tris 50 mM buffer containing the Protease Inhibitor Cocktail to each brain tissue sample.
3. Homogenize with the polytron for three periods of 10 s each (*see* **Notes 2** and **3**) (Fig. 1, **step 1**).
4. Spin the homogenate for 10 min at 1000 × *g* at 4 °C to remove the nucleus and tissue debris.
5. Recover the supernatant containing the membrane extracts in a new eppendorf and centrifuge for 30 min at 12,000 × *g* at 4 °C (Fig. 1, **step 2**).
6. Discard the supernatant containing the cytosolic proteins and resuspend the pellet containing the membrane extracts in 1 mL of Tris 50 mM with Protease Inhibitor Cocktail (*see* **Note 4**) (Fig. 1, **steps 3** and **4**).
7. Determine the protein content of each membrane extract by means of the BCA Protein Assay Kit. Adjust all membrane extracts to the same final concentration, normally between 1 and 2 mg/mL in Tris 50 mM containing the Protease Inhibitor Cocktail.
8. Use the freshly obtained membrane extracts immediately. Alternately, they can be frozen down in liquid nitrogen and stored at −80 °C until use.

3.2 Co-immunoprecipitation

A general scheme for the co-immunoprecipitation procedure is provided in Fig. 1.

1. Take 1 mL of the brain membrane extract (e.g. hippocampus and/or raphe nucleus) for each antibody to be tested in the experiment.
2. Centrifuge during 30 min at 12,000 × *g* at 4 °C.
3. Resuspend pellet in 1 mL of RIPA buffer containing the Protease Inhibitor Cocktail and homogenize using the polytron (*see* 3.1.3.) (Fig. 1, **step 5**).
4. Incubate during 30 min in constant rotation at 4 °C.
5. Centrifuge for 30 min at 12,000 × *g* at 4 °C.
6. Collect each supernatant in a new eppendorf (*see* **Note 5**), add 1–4 μg of the indicated primary antibody and incubate overnight in constant rotation at 4 °C to allow the formation of the immune complexes (Fig. 1, **step 6**).
7. Add 50 μL of either a suspension of protein A-immobilized agarose or TrueBlot anti-mouse Ig IP resin slurry (Fig. 1, **step 7**) (*see* **Note 6** and **7**).
8. Incubate the mixture in constant rotation for 2 h at 4 °C to allow the antibody to bind to the protein complexes.
9. Wash the resin three times by centrifuging at 10,000 × *g* for 1 min at 4 °C. Carefully discard the supernatant and resuspend the resin in 1 mL of ice-cold RIPA buffer. In the last wash, aspirate the supernatant to dryness with a 28-gauge needle.
10. Resuspend the resin and the acetone-precipitated extract (*see* **Note 5**) with either SDS-PAGE sample buffer or urea sample buffer (*see* **Note 8**).

3.3 SDS-PAGE

The percentage of polyacrylamide in the gel, ranging from 6 % to 15 %, depends on the size of the protein under study. The gels contain two different polyacrylamide phases (i.e. stacking or concentrating and separating).

1. Clamp two glass plates in the casting frames.
2. Set the casting frames on the casting stands.
3. Prepare the polyacrylamide separating gel solution by mixing (for 7.5 %) 2.5 mL of acrylamide/bis-acrylamide, 2.5 mL distilled H_2O and 2.5 mL separating gel buffer.
4. Add 100 μL of 10 % SDS, 30 μL of 10 % of APS and 10 μL of TEMED to facilitate gel polymerization (*see* **Note 9**).
5. Pipet the appropriate amount of separating gel solution into the gap between the glass plates. Make a flat surface separating gel by adding some isopropanol on top. Wait for 20–30 min to allow acrylamide/bis-acrylamide polymerization.

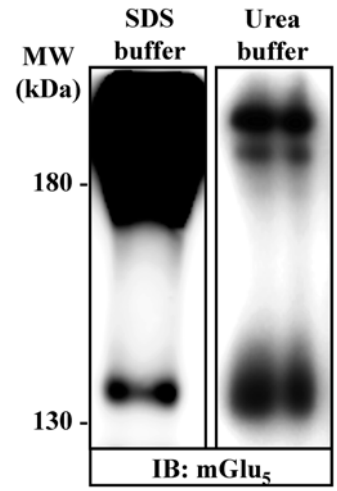

Fig. 2 Comparison of SDS-PAGE and urea sample buffer. Immunoblot showing $mGlu_5$ receptor expression in hippocampal membranes treated with two different PAGE denaturalization buffers: SDS-PAGE (*left*) and urea sample buffer (*right*). Hippocampal membranes were analysed by SDS-PAGE and immunoblotted using a rabbit anti-$mGlu_5$ receptor antibody (1 μg/mL; IB: $mGlu_5$). A HRP-conjugated goat anti-rabbit IgG (1/30.000) was used to detect the primary rabbit antibody. The immunoreactive bands were visualized by chemiluminescence. (Xavier Morató, 2014)

6. Prepare the polyacrylamide stacking gel solution by mixing 1 mL of acrylamide/bis-acrylamide, 6.3 mL of H_2O and 2.5 mL of stacking gel buffer in a beaker (*see* **Note 9**). Add 100 μL of 10 %SDS, 100 μL of a 10 % of APS solution and 10 μL of TEMED to polymerize the gel. Remove the isopropanol and pour the stacking gel solution on top of the polymerized separating gel until it overflows. Insert a 10 well-forming comb without trapping air under the teeth and wait for 20–30 min to allow polymerization. Meanwhile, prepare samples for SDS-PAGE (*see* **Note 8**, Fig. 2).
7. Load the Mini-PROTEAN Tetra Cell with electrophoresis buffer.
8. Load protein marker and samples into the gel wells (see **Note 10**).
9. Run the gels at 75 V until samples reach the separating gel and then increase voltage until 150 V. Stop SDS-PAGE running when the downmost band of the protein marker reaches the foot line of the glass plate.

3.4 Immunoblotting

1. Cut Immobilon-P transfer membranes in 9 cm x 6 cm sheets. Completely soak membranes in methanol for 3 s to activate them and finally equilibrate in anode buffer (see **Note 11**). To avoid membrane contamination, always use tweezers with no teeth or gloves when handling them.

2. Cut two immunoblot thick filter papers in 6.25 × 9.25 cm sheet. Soak one of them in anode buffer and the other in cathode buffer.
3. Following electrophoresis, separate glass plates, recover the gel and equilibrate it in anode buffer for 5 min.
4. Place the anode buffer pre-soaked sheet of filter paper onto the anode cassette.
5. Place the anode buffer pre-wetted transfer membrane on top of the filter paper.
6. Carefully place the anode buffer equilibrated gel on top of the transfer membrane, aligning the gel on the center of the membrane.
7. Place the other cathode buffer pre-soaked extra thick filter paper on top of the gel.
8. Roll a plastic pipet over the surface of the filter paper in both directions to eliminate air bubbles and to ensure complete contact between polyacrylamide gel and the transfer membrane.
9. Carefully place the cathode top onto the cassette.
10. Turn on the power and transfer mini gels for 30 min at 25 V.
11. Following transfer, turn off the power supply and discard filter papers and polyacrylamide gel.
12. Block transfer membrane in IB blocking solution for 45 min at room temperature with continuous shacking.
13. Incubate the membrane overnight at 4 °C with the indicated primary antibody diluted in IB blocking solution with continuous shaking (*see* **Note 12**).
14. Make three washes of 10 min with IB washing solution to eliminate unbound primary antibody.
15. Incubate with the indicated secondary antibody for 90 min at room temperature in continuous shaking.
16. Make three washes of 10 min with IB washing solution to eliminate unbound secondary antibody.
17. Incubate membrane with SuperSignal west pico chemiluminescent substrate (prepare the mix following the proportion 1:1 of solution A and B provided by the manufacturer in dark conditions).
18. Develop membrane in an Amersham Imager 600. An example is shown in Fig. 3.

4 Notes

1. Animals are housed and tested in compliance with the guidelines described in the Guide for the Care and Use of Laboratory Animals [5] and following the European Community, law

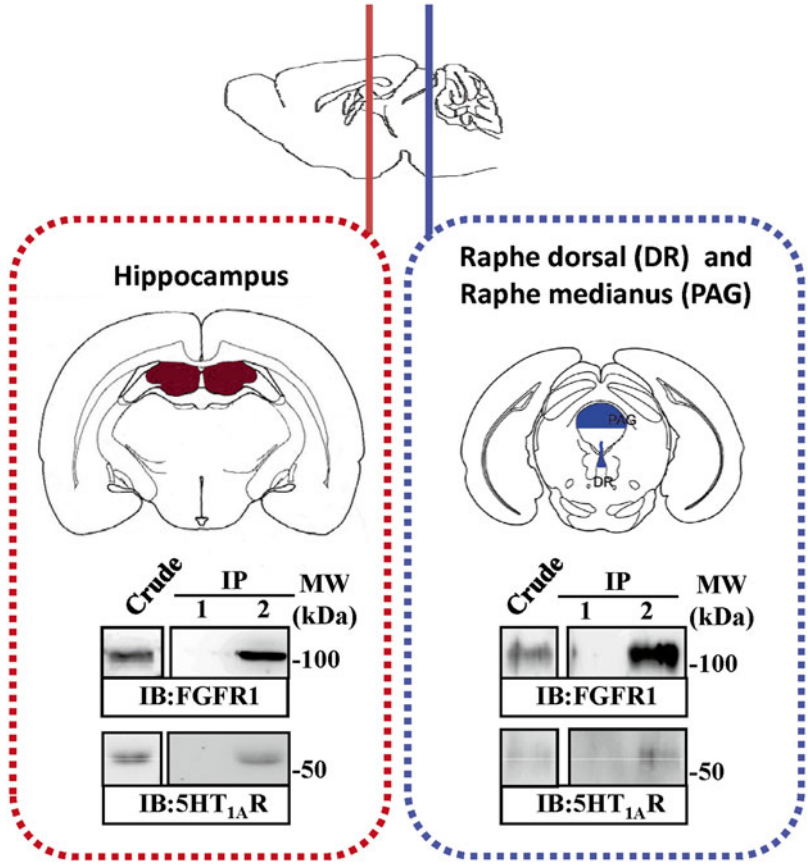

Fig. 3 Examples of co-immunoprecipitation from brain. RIPA-solubilized extracts from rat hippocampus (*left*) and raphe nuclei (*right*) were subjected to immunoprecipitation analysis using a control mouse IgG (2 μg/mL; lane 1) and a mouse anti-FGFR1 antibody (2 μg/mL; lane 2). Extracts (crude) and immunoprecipitates (IP) were analysed by SDS-PAGE and immunoblotted using a mouse anti-FGFR1 antibody (1 μg/mL; IB: FGFR1) and a rabbit anti-$5HT_{1A}R$ (1 μg/mL; IB: $5HT_{1A}R$). An HRP-conjugated anti-mouse IgG TrueBlot™ (1/1000) was used as a secondary antibody in order to avoid IgG cross-reactivity in the mouse anti-FGFR1 antibody immunoblot. Also, an HRP-conjugated goat anti-rabbit IgG (1/30.000) was used to detect the primary rabbit anti-$5HT_{1A}R$ antibody. The immunoreactive bands were visualized by chemiluminescence. Fibroblast growth factor receptor 1 (FGFR1); 5-hydroxytryptamine 1A (5-HT_{1A}) receptor; immunoblot (IB); immunoprecipitation (IP). The Co-IP data from hippocampus is adapted from [6] and the result from raphe nuclei is Xavier Morató, 2014, unpublished data

86/609/CCE, FELASA and ARRIVE guidelines. Moreover, the experiments were approved by the regional animal ethics committee. Thus, animals are housed in standard cages with ad libitum access to food and water and maintained under controlled standard conditions (12 h dark/light cycle starting at 7:30 AM, 22 °C temperature and 66 % humidity).

2. An initial manual homogenization of the sample can be performed by means of a glass Dounce homogenizer. Thus, both the tissue grinder tube and pestle should be prechilled in a beaker of ice before homogenization.

3. Polytron is usually set at position six. It is recommended to perform homogenization in an ice bath to preclude sample warming.
4. If the pellet is still too bloody, wash the pellet by resuspending it in 1 mL of Tris 50 mM with Protease Inhibitor Cocktail and repeat **steps 4** and **5**.
5. Before adding any primary antibody, take 100 μL of each RIPA-solubilized extract, keep in a separate eppendorf and add 1 mL of chilled (−20 °C) acetone. Incubate overnight at −20 °C to allow the precipitation of the whole protein content present in the 100 μL RIPA-soluble extract. The next day, centrifuge during 30 min at 12,000 × *g* at 4 °C to recover proteins, air-dry to remove any acetone trace and process for SDS-PAGE in parallel with the immunoprecipitates. The epitope immunodetected in each acetone sample will represent the 10 % of the total present in each RIPA-soluble extract used, thus an estimate of the efficacy of the immunoprecipitation process can be assessed.
6. Both protein A and TrueBlot resin should be washed 3 times with ice-cold RIPA buffer before being added to the RIPA-soluble extracts containing the primary antibodies.
7. If the antibody used for the immunoprecipitation process is the same than the one for the immunoblotting detection or the same host specie IgG, the TrueBlot system (http://www.rockland-inc.com/TrueBlot-IP-Western-Blotting-Main.aspx) can be used to avoid immunoblot cross-detection of the heavy (~55 kDa) and light (~23 kDa) chains of the immunoglobulins used in the immunoprecipitation.
8. For SDS-PAGE sample buffer, add freshly prepared DTT to a final concentration of 50 mM and heat the sample at 90 °C for 10 min before loading into the gel. Alternatively, the use of urea sample buffer is recommended to diminish protein aggregation in the SDS-PAGE process and subsequently in the immunoblot detection (Fig. 2). Importantly, the samples treated with the urea sample buffer should be incubated at 37 °C for 1–2 h before electrophoresis.
9. Since oxygen interferes with acrylamide/bis-acrylamide polymerization, first degas both the separating and the stacking gel solutions by sonication during 5 min. The optimal temperature for gel polymerization is 23 °C–25 °C. Low temperature will lead to turbid, porous and inelastic gels.
10. Make sure buffer covers the gel completely, and remove the comb carefully.
11. Use only high-grade methanol. Contaminated methanol can result in increased transfer buffer conductivity, as well as poor transfer of macromolecules.
12. Optimal concentration of the antibody should be empirically determined.

Acknowledgements

This work was supported by Ministerio de Economía y Competitividad/Instituto de Salud Carlos III (SAF2014-55700-P, PCIN-2013-019-C03-03 and PIE14/00034), Institució Catalana de Recerca i Estudis Avançats (ICREA Academia-2010) and Agentschap voor Innovatie door Wetenschap en Technologie (SBO-140028) to FC. Also, F.C., X.M. and V.F.-D. belong to the "Neuropharmacology and Pain" accredited research group (Generalitat de Catalunya, 2014 SGR 1251).

References

1. Suzuki H (2006) Protein-protein interactions in the mammalian brain. J Physiol 575:373–377. doi:10.1113/jphysiol.2006.115717
2. Yao Z, Petschnigg J, Ketteler R, Stagljar I (2015) Application guide for omics approaches to cell signaling. Nat Chem Biol 11:387–397. doi:10.1038/nchembio.1809
3. Berggård T, Linse S, James P (2007) Methods for the detection and analysis of protein-protein interactions. Proteomics 7:2833–2842. doi:10.1002/pmic.200700131
4. Markham K, Bai Y, Schmitt-Ulms G (2007) Co-immunoprecipitations revisited: an update on experimental concepts and their implementation for sensitive interactome investigations of endogenous proteins. Anal Bioanal Chem 389:461–473. doi:10.1007/s00216-007-1385-x
5. Clark JD, Gebhart GF, Gonder JC et al (1997) Special report: the 1996 guide for the care and use of laboratory animals. ILAR J 38:41–48
6. Borroto-Escuela DO, Romero-Fernandez W, Mudó G et al (2012) Fibroblast growth factor receptor 1–5-hydroxytryptamine 1A heteroreceptor complexes and their enhancement of hippocampal plasticity. Biol Psychiatry 71:84–91. doi:10.1016/j.biopsych.2011.09.012

Chapter 3

Subsynaptic Membrane Fractionation

Paula M. Canas and Rodrigo A. Cunha

Abstract

We here describe the methodology to carry out a fractionation procedure that separates presynaptic, postsynaptic, and extrasynaptic fraction, allowing to access the localization of proteins within synapses, which we exemplify in rodent and human brain tissue. The procedure begins with the fractionation of synaptosomes (synaptic compartments) and then combines light solubilization with mild detergents together with alterations of pH to allow a separation by gradient and isopycnic centrifugations of the different subsynaptic compartments. The subsequent use of these fractions in Western blot analysis allows the required validation with markers of each synaptic compartment and enables a direct identification of the localization of any particular synaptic receptor. Although it does not allow the detailed mapping achieved by electron microscopy, the possibility of concentrating the samples allows a greater sensitivity.

Key words Fractionation, pH, Detergent, Presynaptic, Postsynaptic and extrasynaptic, Western blot

1 Introduction

Understanding the localization of the different receptors in synapses is essential to elucidate their function in this critical compartment involved in information flow in the brain. In view of the size of synapses, the golden approach to survey the localization of synaptic receptors is still electron microscopy involving pre-embedding and post-embedding immunogold and pre-embedding immunoperoxidase techniques. One obvious great advantage of these electron microscopy approaches is that they largely preserve the structure of the synapse, but this is also their major drawback, since the dense mesh of proteins in the synapse constitutes a major hurdle for the accessibility to the epitopes of large molecules such as antibodies, thus potentially hampering their detection. We will now describe an alternative approach, which takes advantage of fractionation techniques to separate the presynaptic, the postsynaptic, and an extrasynaptic fraction that allows the immunological detection of solubilized membrane proteins by a subsequent Western blot analysis. This method, first described by Philips et al. [3], largely eliminates problems related with the accessibility of antibodies

Rafael Luján and Francisco Ciruela (eds.), *Receptor and Ion Channel Detection in the Brain: Methods and Protocols*, Neuromethods, vol. 110, DOI 10.1007/978-1-4939-3064-7_3,

in situ and further allows concentrating the proteins of interest, thus increasing the sensitivity for their detection, obviously at the cost of their detailed geographical localization in synapses.

The core idea of this fractionation method is to take advantage of a pH shift, which exploits the isoelectric point of most transmembrane proteins, to decrease their interaction thus weakening the ligation of the presynaptic and postsynaptic components. In the presence of mild detergents at pH 6.0, the interaction of the extracellular matrix proteins holding the active zone and the postsynaptic density is maintained, but the extrasynaptic fraction is solubilized and can be separated from synaptic contacts; then the exposure of the synaptic contacts to a change of pH from 6.0 to 8.0 in the presence of mild detergents allows the separation of the extracellular matrix that maintain the presynaptic active zone tightly bound to the postsynaptic density; the presence of mild detergents during this pH shift allows the solubilization of the active zone and its separation from the postsynaptic density, which is basically preserved because the concentration of detergent is not sufficient for its solubilization [3]. The efficiency of separation (over 90 % efficiency) is demonstrated by the ability to segregate the immunoreactivity for the different markers in the three subsynaptic fractions, namely, synaptosomal-associated protein 25 (SNAP-25) or syntaxin in the presynaptic active zone, postsynaptic density protein 95 (PSD-95) or N-methyl-D-aspartate receptor (NMDAR) 1 subunit in the postsynaptic density, and synaptophysin (vesicle protein not tightly linked to the synaptic scaffold) in the synaptosomes outside the active zone (extrasynaptic fraction) ([4]; *see* Fig. 1).

We have repeatedly used this subsynaptic fractionation technique to map in different brain regions (hippocampus, cortex, striatum) the subsynaptic localization of different receptors such as presynaptic alpha-amino-3-hydroxy-5-methyl-4-isoxazolepropionic acid receptors (AMPA receptors) [4], adenosine A_1 receptor (A1R) [6], adenosine A_{2A} receptor (A2AR) [5], ATP (P2) receptors [8], Ret (rearranged during transfection) and GFRα1 (GDNF family receptor alpha 1) [2], interleukin (IL)-1β type receptor [9], nicotinic acetylcholine receptor subunits [1], and amyloid-β protein precursor (APP) [7]. However, there are some limitations to this technique, namely, the amount of tissue necessary to perform the fractionation, the low yield, and the mandatory requirement to validate the efficiency of each separation before performing the actual experiment.

2 Materials

2.1 Make Fresh Solutions Every Time Before Performing the Isolation

Isolation buffer (IB) for a final volume 50 mL: weight 5.48 g of sucrose (0.32 M); add calcium chloride (0.1 mM–5 μL of $CaCl_2$ 1 M available commercially), magnesium chloride (1 mM–50 μL of $MgCl_2$ 1 M available commercially), and

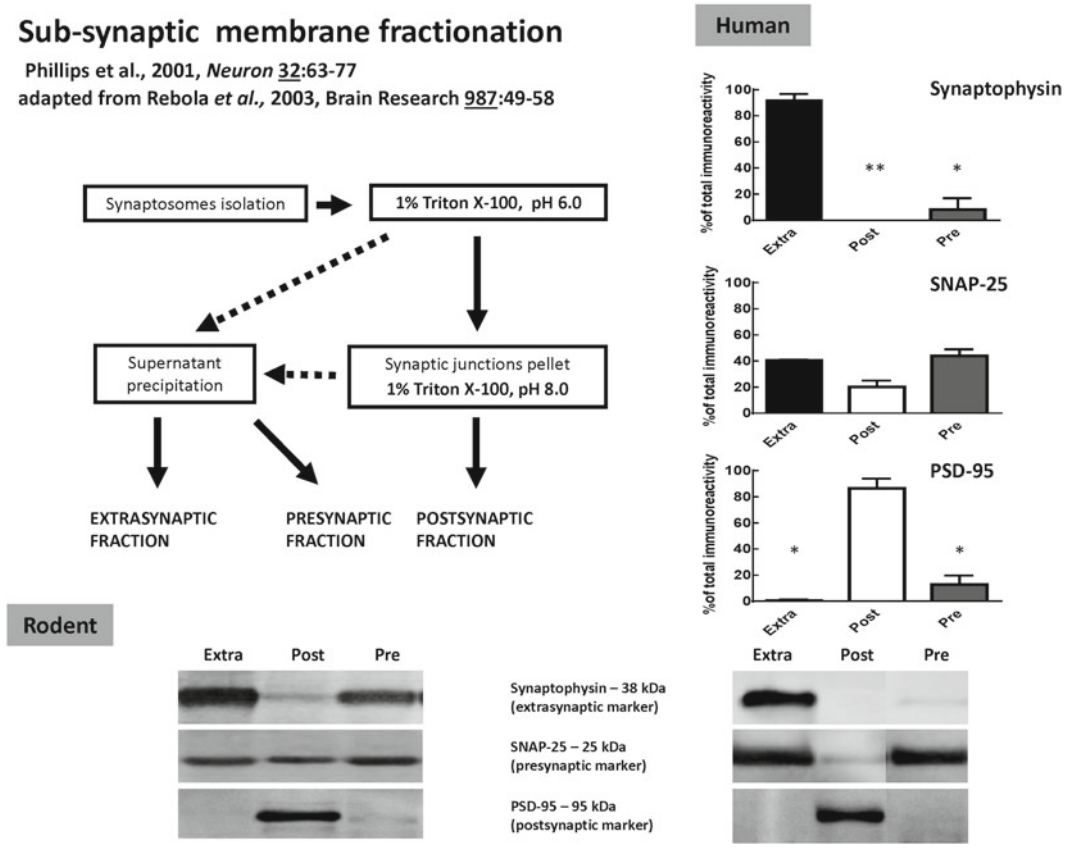

Fig. 1 Schematic representation of the subsynaptic fractionation method. Representative Western blot images for a rodent and human tissue fractionation. Quantification of the efficiency of the fractionation in human tissue was performed by measuring the relative immunoreactivity concerning the total immunoreactivity for the different fractions when using different markers. * $p \leq 0.05$, or ** $p \leq 0.001$, repeated measures one-way ANOVA followed by a post hoc Newman-Keuls (Adapted from Phillips et al. [3] and Rebola et al. [6])

phenylmethylsulfonyl fluoride (PMSF) (1 mM–250 µL from a stock solution of 200 mM PMSF); and add one tablet from and a cocktail of inhibitor of proteases (Roche). Keep the solution at 4 °C until use.

Sucrose 2 M – weight 27.38 g of sucrose, dilute it in 8 to 9 mL of distilled water, and add PMSF (1 mM–200 µL from a 200 mM stock solution) and then complete the volume to 40 mL.

Sucrose 1 M/ $CaCl_2$ 0.1 mM – weight 6.85 g of sucrose, dilute it in 8–9 mL of distilled water, add $CaCl_2$ (0.01 mM–2 µL of a 1 M stock) and PMSF (1 mM–100 µL from a 200 mM stock solution), and complete the volume to 20 mL.

$CaCl_2$ 0.1 mM – add 2 µL of $CaCl_2$ 1 M–20 mL of double-distilled water.

Solubilization buffer 2x pH 6.0 (adjust pH at 4 °C, in the day of the experiment) – for a final volume 50 mL, weight 0.242 g of

Trizma Base (40 mM – Sigma-Aldrich) and add 1 mL of Triton X-100 (2 % – available commercially).

Solubilization buffer 1x pH 6.0 (adjust pH at 4 °C, in the day of the experiment) – for a final volume 50 mL, weight 0.121 g of Trizma Base 20 mM (Sigma-Aldrich) and add 0.5 mL of Triton X-100 (1 % – available commercially).

Solubilization buffer pH 8.0 (adjust pH at 4 °C, in the day of the experiment) – for a final volume 50 mL, weight 0.121 g of Trizma Base 20 mM (Sigma-Aldrich) and add 0.5 mL of Triton X-100 (1 %, available commercially).

3 Pre-, Post-, and Extrasynaptic Isolation

For the separation and purification of the synaptosomal fraction, use a discontinuous sucrose gradient followed by an ultracentrifugation.

1. Isolate the tissue at 4 °C or use frozen tissue (*see* **Note 1**).
2. Add 2 mL of isolation buffer (IB; 4 °C) to the tissue in a Potter-Elvehjem glass tube.
3. Homogenize the tissue at 4 °C (10 *strokes* a 700–900 rotations per min) and wash the potter pestle and tube with 500 μL of IB.
4. Place the homogenized tissue in a 50 mL conical tube and add 12 mL of sucrose 2 M and 5 mL of $CaCl_2$ 0.1 mM (4 °C). Resuspend slowly with a glass pipette.

   "Calcium addition is important to maintain the structure of the different *'densities'*, since it is critical for protein interaction involved in robust cell-cell adhesion."
5. Divide the solution and place equal amounts in two Ultra-Clear centrifuge tubes.
6. Add 2.5 mL of sucrose 1 M/$CaCl_2$ 0.1 mM on top of each tube, very slowly, to form the sucrose gradient. To make it easier to visualize the interface, label the location of the interface in the tube using a marker.
7. Weight and equilibrate the tubes with IB solution within their steel supports and with their closing lids. Use an Ultra-Swinging Bucket rotor and note that the rotor should be completely filled with tubes (even empty if required).
8. Centrifuge for 3 h at 100,000 *g* at 4 °C.
9. Take out IB solution and the first layer (myelin) and collect the layer between the 1.25 M and 1 M sucrose interphase (synaptosomes). The pellet is composed of non-homogenized tissue and extrasynaptosomal mitochondria.

10. Dilute the synaptosome fraction with nine times its volume with IB.
11. Centrifuge the fraction for 30 min at 15,000*g* (4 °C).
12. Remove the supernatant and resuspend the pellet with 1 mL of IB solution. Collect 100 μL, centrifuge this sample at 11,000*g* for 11 min at 4 °C, resuspend the resulting pellet in 5 % sodium dodecyl sulfate (SDS), and store this sample at -80 °C, which corresponds to total synaptosome fraction (to use later on as an internal control).
13. Dilute ten times the pellets and resuspended in 1 mL of IB solution with $CaCl_2$ 0.1 mM (1 mL to 9 mL of $CaCl_2$). This step must be done slowly.
14. Add same volume (10 mL) of solubilization buffer 2x pH 6.0 and incubate for 30 min in ice, under slow agitation.
15. Centrifuge at 40,000*g* for 30 min at 4 °C. The supernatant represents the extrasynaptic fraction. The pellet corresponds to the synaptic junction pellet. Keep the supernatant in conical tubes in ice to precipitate later with acetone (*see* **step 21**).

    "Triton X-100 1 % at pH 6.0 causes the solubilization of practically all plasma membrane, but preserves the insoluble pellet of paired pre- and postsynaptic structures [3]."
16. Carefully wash the pellet with solubilization buffer 1x pH 6.0, without disrupting it.
17. Resuspend the pellet with 2 mL of solubilization buffer 1x pH 8.0 (*see* **Note 2**) and then add more 3 mL of the same solution.

    "Triton X-100 1 % at pH 8.0 causes the solubilization of the presynaptic specialization, while preserving the insoluble post-synaptic density [3]."
18. Incubate the suspension for 30 min in ice with slow agitation.
19. Centrifuge the solution at 40,000*g* for 30 min at 4 °C. The resulting pellet is the postsynaptic fraction and supernatant is the presynaptic fraction. Keep the supernatant in conical tubes in ice to precipitate later with acetone (*see* **step 21**).
20. Resuspend the pellet with 5 % SDS.
21. To precipitate both the extrasynaptic fraction and the presynaptic fraction, use three volumes of precooled acetone (−20 °C) and mix it with each of these two fractions overnight (the tubes should be kept in horizontal position for at least 18 h).
22. In the following day, precool the centrifuge and centrifuge the extrasynaptic and presynaptic fractions at 18,000*g* for 30 min (−15 °C). After centrifugation, mark the pellet with a marker and discard the acetone in a fume hood to a liquid waste disposal. Leave the pellet to dry and make sure that there are no residues of acetone.

23. Resuspend the pellet in 5 % SDS (use a maximum volume of 200–300 μL, according to the size of the pellet – *see* **Note 3**) and sonicate the pellets if required.

To validate the fractionation, it is necessary to perform a Western blot analysis for different markers:

1. After determining the amount of protein using the bicinchoninic acid protein assay (Pierce), each fraction can be diluted with five volumes of SDS-PAGE buffer containing 30 % (v/v) glycerol, 0.6 M dithiothreitol, 10 % (w/v) SDS, and 375 mM Tris-HCl pH 6.8 and heated at 70 °C for 20 min.
2. These diluted samples (10 μg) and the pre-stained molecular weight markers (from BioRad) are separated by SDS-PAGE (10 % with a 4 % concentrating gel) under reducing conditions and electro-transferred to PVDF membranes (from Amersham).
3. After blocking for 1 h at room temperature with 5 % milk in Tris-buffered saline, pH 7.6 containing 0.1 % Tween 20 (TBS-T), incubate the membranes overnight at 4 °C either with anti-SNAP-25, anti-PSD-95, or anti-synaptophysin (1:20,000, from Sigma-Aldrich).
4. Wash three times for 10 min with TBS-T containing 0.5 % milk.
5. Incubate the membranes with alkaline phosphatase-conjugated goat anti-mouse secondary antibody (1:120,000, from GE Healthcare) in TBS-T containing 1 % milk during 120 min at room temperature.
6. After washing three times for 10 min with TBS-T with 0.5 % milk, the membranes are incubated with ECF substrate (from GE Healthcare) and then analyzed using a chemifluorescent detection equipment.

4 Notes

1. In order to perform the fractionation, use around 1–1.2 g of tissue or else the yield will be very low to perform the validation as well as the localization of your synaptic protein of interest. If the tissue is used in excess, the separation (**step 8–9**) will not occur in optimal conditions.
2. The pellet resuspension requires patience and resilience. In this step, to help dissolving the pellet, use a P1000 and a P200 micropipette.
3. When resuspending the pellet, part of the liquid will turn into bubbles. To avoid waste and increase yield, collect the liquid and bubbles to a chilled 2 mL conical tube. During the collection, leave the tube in ice.

Acknowledgments

We would like to thank Anna Pliássova and Ana Xavier for contributing to the figure and Paula Agostinho, who helped reviewing the protocol. This work was supported by the Defense Advanced Research Projects Agency (DARPA, grants 09-68-ESR-FP-010 and W911NF-10-1- 0059), the Portuguese Foundation for Science and Technology (FCT, PEst-C/SAU/LA0001/2013–2014), and Quadro de Referência Estratégica Nacional (QREN, CENTRO-07-ST24-FEDER-002006).

References

1. Garção P, Oliveira CR, Cunha RA, Agostinho P (2014) Subsynaptic localization of nicotinic acetylcholine receptor subunits: a comparative study in the mouse and rat striatum. Neurosci Lett 566:106–110
2. Gomes CA, Simões PF, Canas PM, Quiroz C, Sebastião AM, Ferré S, Cunha RA, Ribeiro JA (2009) GDNF control of the glutamatergic cortico-striatal pathway requires tonic activation of adenosine A_{2A} receptors. J Neurochem 108: 1208–1219
3. Phillips GR, Huang JK, Wang Y, Tanaka H, Shapiro L, Zhang W, Shan WS, Arndt K, Frank M, Gordon RE, Gawinowicz MA, Zhao Y, Colman DR (2001) The presynaptic particle web: ultrastructure, composition, dissolution, and reconstitution. Neuron 32:63–77
4. Pinheiro PS, Rodrigues RJ, Silva AP, Cunha RA, Oliveira CR, Malva JO (2003) Solubilization and immunological identification of presynaptic α-amino-3-hydroxy-5-methyl-4-isoxazolepropionic acid receptors in the rat hippocampus. Neurosci Lett 336:97–100
5. Rebola N, Canas PM, Oliveira CR, Cunha RA (2005) Different synaptic and subsynaptic localization of adenosine A_{2A} receptors in the hippocampus and striatum of the rat. Neuroscience 132:893–903
6. Rebola N, Pinheiro PC, Oliveira CR, Malva JO, Cunha RA (2003) Subcellular localization of adenosine A_1 receptors in nerve terminals and synapses of the rat hippocampus. Brain Res 987:49–58
7. Rodrigues DI, Gutierres J, Pliassova A, Oliveira CR, Cunha RA, Agostinho P (2014) Synaptic and sub-synaptic localization of amyloid-beta protein precursor in the rat hippocampus. J Alz Dis 40:981–992
8. Rodrigues RJ, Almeida T, Richardson PJ, Oliveira CR, Cunha RA (2005) Dual presynaptic control by ATP of glutamate release via facilitatory P2X1, P2X2/3, and P2X3 and inhibitory P2Y1, P2Y2, and/or P2Y4 receptors in the rat hippocampus. J Neurosci 25:6286–6295
9. Simões AP, Duarte JA, Agasse F, Canas PM, Tomé AR, Agostinho P, Cunha RA (2012) Blockade of adenosine A_{2A} receptors prevents interleukin-1β -induced exacerbation of neuronal toxicity through a p38 mitogen-activated protein kinase pathway. J Neuroinflammation 9:204

Chapter 4

Investigation of Neurotransmitter Receptors in Brain Slices Using Cell Surface Biotinylation

Elek Molnár

Abstract

Cell surface trafficking and endocytosis of neurotransmitter receptors are important regulatory mechanisms of neurotransmission. Biotinylation of plasma membrane proteins in brain slices allows their separation from those present in intracellular organelles. Membrane-impermeable, thiol-cleavable and amine-reactive biotinylation reagents (e.g. EZ-link sulfo-NHS-SS-biotin) form a stable covalent linkage with primary amino groups of surface-exposed proteins. Following homogenisation of brain slices and solubilisation of membranes, biotin-labelled proteins can be isolated with avidin or streptavidin linked to agarose beads. Bound biotinylated proteins are released from avidin or streptavidin in the presence of reducing agents (e.g. glutathione or β-mercaptoethanol). Quantitative differences in the molecular composition of biotin-labelled (surface) and unlabelled (intracellular) protein fractions can be analysed using immunoblotting with target protein-specific antibodies. While many variations of this procedure exist in the literature, in this chapter we describe the biotinylation protocol that we have applied for the investigation of quantitative changes in the cell surface expression and internalisation of ionotropic glutamate receptors in acute brain slices.

Key words Antibodies, Avidin, Biotinylation, Cell surface expression, Endocytosis, Internalisation, Targeting, Trafficking

1 Introduction

Dynamic changes in cell surface expression and internalisation of neurotransmitter receptors are associated with synaptic plasticity. These processes are extensively investigated, and various approaches have been developed for the selective investigation of cell-surface-expressed neurotransmitter receptors, mainly in dissociated neuronal cultures and transfected cells. These techniques include (i) immunofluorescent labelling (e.g. [1, 2]), (ii) cell ELISA analysis of non-permeabilised cells using extracellular domain-specific antibodies (e.g. [1, 2]), (iii) radioligand binding to intact cells, (iv) covalent cross-linking of receptor complexes (e.g. [3, 4]), (v) enzymatic cleavage of surface-expressed proteins using proteases and (vi) cell surface biotinylation (e.g. [3, 5–9]). While it is a more

Rafael Luján and Francisco Ciruela (eds.), *Receptor and Ion Channel Detection in the Brain: Methods and Protocols*, Neuromethods, vol. 110, DOI 10.1007/978-1-4939-3064-7_4, © Springer Science+Business Media New York 2016

indirect approach, (vii) EndoH sensitivity and resistance of glycosylated receptor proteins also show good correlation with their intracellular retention and surface expression, respectively (e.g. [3, 9]). Dissociated neuronal cultures grow as a monolayer, and the surface-expressed neurotransmitter receptors are therefore readily accessible for both immunocytochemical and biochemical analysis. Studies performed on low-density primary neuronal cultures were instrumental in the investigation of surface trafficking and endocytosis of neurotransmitter receptors and the correlation of these changes to different forms of synaptic plasticity (reviewed in [10, 11]). However, cultured neurons lack important cellular interactions (e.g. with glial cells), and their use for the investigation of complex neuronal networks is limited.

Acute or organotypic brain slices are routinely used for electrophysiological studies of various neuronal circuits. While these preparations allow the functional investigation of neurons in situ, molecular analysis of surface-expressed receptors is more challenging in the native tissue. This is due to the fact that cells and synapses are densely packed in the brain and only small molecules can penetrate into the relatively thick (300–400 μm) brain slices.

Biotin is a vitamin that binds with high affinity to avidin and streptavidin proteins. Due to its small size (244 Da), biotin can be conjugated to many proteins without altering their biological activity. *N*-hydroxysuccinimide (NHS) esters of biotin are the most widely used biotinylation reagents. The EZ-link sulfo-NHS-SS-biotin (sulfosuccinimidyl-2-[biotinamido] ethyl-1,3-dithiopropionate) is a thiol-cleavable version, which can be removed from labelled proteins by glutathione. NHS-activated biotins react effectively with primary amino groups ($-NH_2$) in pH 7–9 buffers to form stable amine bounds. The majority of membrane proteins have several primary amines in the side chain (ε-amine) of lysine (K) residues and the N-terminus of each polypeptide that are available as targets for labelling with NHS-activated biotin reagents. However, N-terminal α-amine groups are rarely accessible for conjugation. Biotinylated proteins can be easily separated from unlabelled proteins using immobilised streptavidin or avidin and analysed using immunoblots.

Biotinylation proved to be a useful tool for the covalent labelling and separation of cell-surface-expressed proteins in brain slices (e.g. [12–18]). This chapter describes the protocol that we have successfully used for the analysis of α-amino-3-hydroxy-5-methylisoxazole-4-propionate (AMPA) receptor surface expression and endocytosis in metabotropic glutamate receptor (mGluR)-dependent long-term depression (LTD) in rodent hippocampal slices [19]. The principles and methodology described here are also applicable to other cell-surface-expressed proteins.

2 Materials

2.1 Buffers

1. Artificial cerebrospinal fluid (ACSF): 124 mM NaCl, 3 mM KCl, 10 mM d-glucose, 2 mM $CaCl_2$, 1 mM $MgSO_4$, 26 mM $NaHCO_3$ and 1.25 mM NaH_2PO_4 (pH7.4). To prepare 1000 mL of ACSF buffer, dissolve 7.25 g NaCl, 0.22 g KCl, 1.8 g D-glucose, 0.22 g $CaCl_2$, 0.25 g $MgSO_4$ $7{\times}H_2O$ (or 0.12 g anhydrous $MgSO_4$), 2.18 g $NaHCO_3$ and 0.15 g NaH_2PO_4. Equilibrate solution with 95 % O_2 and 5 % CO_2 on ice for at least 30 min prior to use and confirm that pH is 7.4.
2. 0.5 mg/mL (82 μM) EZ-link sulfo-NHS-SS-biotin (Thermo Scientific/Pierce Biotechnology, Rockford, IL, USA) in ACSF. Prepare this solution immediately before use.
3. 50 mM NH_4Cl in ACSF: Dissolve 1.34 g NH_4Cl in 500 mL ACSF and confirm that pH is 7.4.
4. Biotin stripping buffer: 50 mM glutathione, 75 mM NaOH, 75 mM NaCl, 1 mM ethylenediaminetetraacetic acid (EDTA) and 0.5 % BSA (pH9.0). To prepare 500 mL of biotin stripping buffer, dissolve 7.68 g glutathione, 1.5 g NaOH, 2.19 g NaCl, 0.15 g EDTA and 2.5 g bovine serum albumin (BSA), confirm pH, and adjust volume to 500 mL.
5. HEPES buffered saline (HBS) buffer: 20 mM HEPES, 5 mM KCl, 137 mM NaCl, 2.3 mM $CaCl_2$, 0.5 mM $MgCl_2$ and 10 mM Na_2HPO_4 (pH7.4). To prepare 1000 mL of HBS buffer, dissolve 4.77 g HEPES, 0.37 g KCl, 8.01 g NaCl, 0.26 g $CaCl_2$, 0.05 g $MgCl_2$ and 1.42 g Na_2HPO_4. Confirm pH and adjust volume to 1000 mL.
6. 10 mM iodoacetamide in HBS buffer (pH7.4): Dissolve 0.92 g iodoacetamide in 500 mL HBS buffer and confirm pH.
7. Homogenisation buffer: 320 mM sucrose and 10 mM HEPES-NaOH (pH7.2), supplemented with a mixture of 'complete' protease inhibitors (Roche Diagnostics, Lewes, UK). To prepare 500 mL homogenisation buffer, dissolve 54 g sucrose, 1.19 g HEPES and appropriate amount of protease inhibitor mixture according to the manufacturer's recommendation. Adjust pH to 7.2 before volume is adjusted to 500 mL.
8. Solubilisation buffer: 1 % (v/v) Triton X-100, 0.1 (w/v) sodium dodecyl sulphate (SDS), 150 mM NaCl, 20 mM HEPES and 2 mM EDTA, supplemented with a mixture of 'complete' protease inhibitors (Roche Diagnostics, Lewes, UK) (pH7.4). To prepare 500 mL of solubilisation buffer, dissolve 2.5 mL Triton X-100, 0.5 g SDS, 4.38 g NaCl, 2.38 g HEPES, 0.29 g EDTA and appropriate amount of protease inhibitor mixture according to the manufacturer's recommendation. Adjust pH to 7.4 before volume is adjusted to 500 mL.

9. 5 × SDS polyacrylamide gel electrophoresis (PAGE) sample buffer: 5 % (w/v) SDS, 125 mM Tris-HCl (pH 6.8), 25 % (v/v) glycerol, 12.5 % (v/v) β-mercaptoethanol and 0.05 % (w/v) bromophenol blue. To prepare 100 mL of 5 × SDS-PAGE sample buffer, dissolve 5 g SDS, 1.51 g Trizma base, 25 mL glycerol and 12.5 mL β-mercaptoethanol. Adjust pH to 6.8 using HCl and add 50 mg bromophenol blue before volume is adjusted to 100 mL.
10. 2 × SDS-PAGE sample buffer: 2 % (w/v) SDS, 50 mM Tris-HCl (pH 6.8), 10 % (v/v) glycerol, 5 % β-mercaptoethanol and 0.02 % (w/v) bromophenol blue. To prepare 100 mL of 2 × SDS-PAGE sample buffer, dissolve 2 g SDS, 0.60 g Trizma base, 10 mL glycerol and 5 mL β-mercaptoethanol. Adjust pH to 6.8 using HCl and add 20 mg bromophenol blue before volume is adjusted to 100 mL.

3 Methods

3.1 Preparation of Brain Slices

The procedure used for the preparation of brain slices for cell surface biotinylation experiments is essentially the same to what is widely used for electrophysiological recordings. Therefore, it is possible to perform correlated electrophysiological and molecular studies.

1. Anaesthesia: Follow national and international guidelines for the care and handling of animals. Use approved protocols for anaesthesia and killing of animals appropriate for the species used for the study.
2. Quickly remove brains and immerse them into ice-cold ACSF bubbled with 95 % O_2 and 5 % CO_2.
3. Separate hemispheres and cut 400 μm thick slices using a vibratome (e.g. VT1000 S, Leica Microsystems Ltd, Milton Keynes, Buckinghamshire, UK) or a McIlwain tissue chopper (e.g. Mickle Laboratory Engineering Company, Guildford, UK). Isolate region of interest (e.g. hippocampus) from surrounding tissue using chilled scalpel.
4. Place slices onto a supporting nylon mesh (e.g. Falcon™, BD Biosciences) and immerse them into ACSF perfused with 95 % O_2 and 5 % CO_2 in a 6-well cell culture plate (or small Petri dish) at room temperature (~20 °C). Allow brain slices to recover for at least 1 h prior to use.

3.2 Treatment of Brain Slices

Various pharmacological and electrophysiological induction protocols can be used to manipulate the activity of neuronal networks in brain slices (e.g. [10, 11, 19]). This part of the protocol is project specific and needs to be tailored to the study. Using 4–5 slices (e.g. from rodent hippocampal region) per condition provides enough material for immunoblot analysis.

3.3 Cell Surface Biotinylation

This protocol can be used to study changes in cell surface expression of proteins.

1. Following treatment (Sect. 3.2), wash 'induced' and 'control' (sham treated) slices in ice-cold ACSF twice for 5 min.
2. Add 0.5 mg/mL EZ-link sulfo-NHS-SS-biotin in ACSF and incubate for 30 min at 4 °C with gentle shaking. Due to the rapid hydrolysis of the NHS ester moiety, the EZ-link sulfo-NHS-SS-biotin solution should be prepared just before it is needed otherwise it may become non-reactive.
3. Following cell surface biotinylation, wash slices twice with 50 mM NH_4Cl in ACSF and twice in ACSF for 5 min each at 4 °C to quench and remove unbound EZ-link sulfo-NHS-SS-biotin.

Proceed to Sect. 3.5 if the aim of the study is to compare the surface expression of proteins in 'induced' and 'control' brain slices. Proceed to Sect. 3.4 if the study also requires the analysis of receptor endocytosis.

3.4 Investigation of Receptor Internalisation from the Cell Surface

These additional steps performed on a subset of biotinylated brain slices allow the monitoring of the endocytosis of biotin-labelled proteins from the cell surface in response to various stimuli (e.g. the internalisation of AMPA receptors (AMPARs) following the stimulation of metabotropic glutamate 5 (mGlu5) or *N*-methyl-D-aspartate (NMDA) receptors (NMDARs; 19)). Because endocytosis is significantly reduced at room temperature [19], the stimulation of cell surface biotinylated slices (after **step 3** of Sect. 3.3) needs to be performed at 37 °C. The induction protocol for receptor internalisation is project specific and needs to be tailored to the study. Use 4–5 slices per condition.

1. After the induction of receptor internalisation, incubate some of the brain slices in ice-cold 50 mM glutathione containing biotin stripping buffer for 15 min. Repeat this incubation twice with fresh biotin stripping buffer. Glutathione will remove conjugated biotin from the cell surface, and only internalised proteins will remain biotinylated after this step.
2. Incubate slices in ice-cold 10 mM iodoacetamide in HBS buffer (pH 7.4) for 2 × 10 min to quench and remove excess glutathione.
3. Wash slices in ice-cold ACSF for 2 × 5 min.

3.5 Homogenisation of Slices and Solubilisation of Membrane Proteins

1. Transfer slices into Eppendorf tubes (Eppendorf Scientific, Westbury, NY, USA) and add ice-cold homogenisation buffer with protease inhibitors to prevent the degradation of proteins. Homogenise slices using a pellet pestle.
2. Remove tissue debris by centrifugation at 1000 × *g* for 15 min at 4 °C.

3. Spin supernatant at 100,000 × *g* for 1 h at 4 °C. (The obtained pellets can be stored at −80 °C if required.)
4. Solubilise membrane proteins in 0.5 mL solubilisation buffer. Use a pellet pestle and short bursts of sonication on ice and rotate samples for 1 h at 4 °C.
5. Remove any insoluble material by centrifugation at 100,000 × *g* for 30 min at 4 °C.
6. Measure protein concentration (e.g. by using BCA™ protein assay reagent according to the manufacturer's instructions; Pierce, Northumberland, UK).

3.6 Separation of Biotinylated and Non-biotinylated Proteins

1. Keep an aliquot (100 μg protein) of the lysate, and it will be used as a whole input (total) reference sample. Add appropriate amount (1/4 of the aliquot's volume) of 5 × SDS-PAGE sample buffer.
2. Wash 40 μL of streptavidin beads (8 μL/brain slice) four times in solubilisation buffer by centrifugation (500 × *g*, 4 °C). Cut off the narrow end of the plastic pipette tip before the aliquoting of the streptavidin beads into Eppendorf tubes.
3. Incubate 100 μg solubilised proteins with washed streptavidin beads for 3 h at 4 °C on shaker.
4. Recover beads by centrifugation (500 × *g*, 1 min, 4 °C). Transfer supernatant to clean Eppendorf tube and measure its volume. Add 5 × SDS-PAGE sample buffer (1/4 of the supernatant's volume). Mix tubes and keep samples on ice.
5. Wash beads four times with solubilisation buffer by centrifugation (500 × *g*, 1 min, 4 °C).
6. Remove solubilisation buffer and add 2 × SDS-PAGE sample buffer to elute biotinylated proteins from streptavidin-coated beads. To allow direct comparisons, the final volumes of eluted proteins, corresponding whole input (from **step 1**) and supernatant (from **step 4**), need to be equal.
7. Incubate all the samples [*i*, whole inputs (from **step 1**); *ii*, supernatants with non-biotinylated proteins (from **step 4**) and *iii*, streptavidin-coated beads with biotinylated proteins (from **step 6**)] at 95 °C for 10 min.
8. Separate the stripped beads by centrifugation (500 × *g*, 5 min, 20 °C) and transfer supernatant to clean Eppendorf tubes. (If required, samples can be stored at −20 °C after this step.)
9. Use standard SDS-PAGE procedures for the separation of equal volumes of protein samples, followed by electrophoretic transfer onto Immobilon™ polyvinylidene difluoride (PVDF, 0.45 μm, Millipore, Durham, UK) membranes for immunoblotting.
10. Immunostaining conditions need to be optimised for each primary and secondary antibody and specificity of the labelling

verified using appropriate controls [20]. The linear sensitivity range of the detection method (e.g. enhanced chemiluminescence in combination with horseradish peroxidase-conjugated secondary antibodies) should be confirmed by using different dilutions of the whole input (total) reference sample (from **step 1** of Sect. 3.6). In addition to using target protein-specific antibodies, probe samples with anti-β-actin or anti-tubulin (or other intracellular protein-specific) antibodies. The absence of β-actin and tubulin in the biotinylated protein fraction confirms that only cell surface proteins were labelled. The labelling of β-actin or tubulin can also be used as internal loading control for the comparison of 'whole input' samples.

11. Use an appropriate imaging system or scan exposed and developed films using a flatbed scanner to capture greyscale images of immunoreactive bands.
12. Quantitative comparisons of immunoreactivities can be performed using Adobe® Photoshop® (Adobe Systems, San Jose, CA, USA), Image J (NIH Image, Bethesda, MD, USA; http://imagej.nih.gov/ij) or similar image analysis softwares.

4 Notes

1. While 400 μm acute brain slices are appropriate for most cell surface biotinylation experiments, 300 μm slices prepared from mouse brains [19] and organotypic slice cultures [16, 17] are also suitable.
2. Cell surface biotinylation may not be suitable for the detection of localised changes if only a relatively few neurons or a subset of synapses are altered (e.g. following electrophysiological stimulation of specific neurons). Therefore, chemical or pharmacological induction protocols that affect a large proportion of neurons and synapses are preferable. For example, long-term potentiation (LTP) can be induced in brain slices by brief transient depolarisation using high K^+ (3 × 1 s application of 90 mM KCl) or by increasing cAMP levels by the application of the adenylyl cyclase activator forskolin (50 μM) and the phosphodiesterase inhibitor rolipram (0.1 μM) in Mg^{2+} and 2-Cl-adenosine-free ACSF for 16 min (reviewed in [11]). LTD of synaptic activity can be induced by the activation of NMDA receptors (20 μM NMDA, 3 min) or group I metabotropic glutamate receptors (100 μM (RS)-3,5-DHPG, 10 min) [10, 19].
3. The protocol described above has been extensively tested for neurotransmitter receptors. However, it is possible that the biotinylation approach is less suitable for the labelling and isolation of some other (smaller) cell surface proteins due to the lack of primary amines or steric hindrance in the exposed regions.

4. Avoid buffers containing primary amines (e.g. glycine or Tris) as these will react with EZ-link sulfo-NHS-SS-biotin and could hinder the labelling of proteins. Use amine-free buffers such as phosphate-buffered saline.
5. Variants of the radioimmunoprecipitation assay (RIPA) buffer (1 % (v/v) Triton X-100, 0.1–1 % (w/v) SDS, 0.4–0.5 % (w/v) sodium deoxycholate, 1–2 mM EDTA, 150 mM NaCl, 50 mM Tris-HCl (pH7.4) in the presence of protease and phosphatase inhibitors) can also be used as an alternative for direct homogenisation of brain slices and extraction of membrane proteins (*see* Sect. 3.5) [12, 18, 19].
6. After the solubilisation of membrane proteins (*see* Sect. 3.5), cell surface biotinylation can be combined with immunoprecipitation for the investigation of potential differences in the subunit composition [14, 15] or phosphorylation states [19] of cell-surface-expressed and intracellular receptor populations. If the aim is to study receptor phosphorylation, include 100 μM genistein, 1 mM orthovanadate and phosphatase inhibitor mixture 1 (Sigma-Aldrich, St. Louis, MO, USA) to the homogenisation and solubilisation buffers to prevent dephosphorylation of samples [19].
7. For correct interpretation of the results, it is essential to probe the biotinylated protein fraction for the presence of intracellular proteins (e.g. β-actin or tubulin) in each experiment. As long as cells in brain slices remain intact, only proteins exposed on the cell surface will be biotinylated. Positive reaction with intracellular proteins indicates that the integrity of the plasma membrane was compromised during the experiment and the obtained results cannot be attributed to surface proteins only.
8. Biotinylation reaction can be influenced by the temperature, pH and incubation time. While NHS reactions occur more rapidly at higher pH (e.g. pH 8.0), it is often necessary to maintain slices at neutral pH under more physiological conditions. This is particularly important for subsequent endocytosis experiments (*see* Sect. 3.4). It has been confirmed that all layers of a 400 μm thick slice can be labelled by biotin without significant labelling of intracellular proteins under conditions described above [12, 14, 19].
9. Antibodies that react with intracellular domains are more suitable for the analysis of biotinylated proteins. Avoid using antibodies with extracellular binding sites, particularly if the epitope region contains lysine (K), arginine (R), asparagine (N) and glutamine (Q). Biotinylation of these amino acid residues can interfere with the immunochemical identification of the target proteins.

Acknowledgements

I would like to thank Dr Clare M. Galdding for adapting the cell surface biotinylation technique for the investigation of tyrosine dephosphorylation of AMPA receptors in mGluR-LTD and NMDAR-LTD using hippocampal slices (Gladding et al., 2009). This research was supported by Grant from the Biotechnology and Biological Sciences Research Council, UK (Grant BB/J015938/1).

References

1. Pickard L, Noël J, Henley JM, Collingridge GL, Molnár E (2000) Developmental changes in synaptic AMPA and NMDA receptor distribution and AMPA receptor subunit composition in living hippocampal neurons. J Neurosci 20:7922–7931
2. Pickard L, Noel J, Duckworth JK, Fitzjohn SM, Henley JM, Collingridge GL, Molnár E (2001) Transient synaptic activation of NMDA receptors leads to the insertion of native AMPA receptors into hippocampal neuronal plasma membrane. Neuropharmacology 41:700–713
3. Ball SM, Atlason PT, Shittu-Balogun OO, Molnár E (2010) Assembly and intracellular distribution of kainate receptors is determined by RNA editing and subunit composition. J Neurochem 114:1805–1818
4. Boudreau AC, Milovanovic M, Conrad KL, Nelson C, Ferrario CR, Wolf ME (2012) A protein cross-linking assay for measuring cell surface expression of glutamate receptor subunits in the rodent brain after in vivo treatments. Curr Protoc Neurosci, Chapter 5:Unit 5.30.1–19
5. McIlhinney RAJ, Molnár E (1996) Characterization, cell-surface expression and ligand-binding properties of different truncated N-terminal extracellular domains of the ionotropic glutamate receptor subunit GluR1. Biochem J 315:217–225
6. McIlhinney RAJ, Molnár E, Atack JR, Whiting PJ (1996) Cell surface expression of the human N-methyl-D-aspartate receptor subunit 1[a] requires the co-expression of the NR2A subunit in transfected cells. Neuroscience 70:989–997
7. McIlhinney RAJ, Le Bourdellès B, Molnár E, Tricaud N, Streit P, Whiting PJ (1998) Assembly intracellular targeting and cell surface expression of the human *N*-methyl-D-aspartate receptor subunits NR1a and NR2A in transfected cells. Neuropharmacology 37: 1355–1367
8. Gallyas F, Ball SM, Molnár E (2003) Assembly and cell surface expression of KA-2 subunit-containing kainate receptors. J Neurochem 86:1414–1427
9. Atlason PT, Scholefield CL, Eaves RJ, Mayo-Martin B, Jane DE, Molnár E (2010) Mapping the ligand binding sites of kainate receptors: molecular determinants of subunit-selective binding of the antagonist [3H]UBP310. Mol Pharmacol 78:1036–1045
10. Gladding CM, Fitzjohn SM, Molnár E (2009) Metabotropic glutamate receptor-mediated long-term depression: molecular mechanisms. Pharmacol Rev 61:395–412
11. Molnár E (2011) Long-term potentiation in cultured hippocampal neurons. Semin Cell Dev Biol 22:506–513
12. Thomas-Crusells J, Vieira A, Saarma M, Rivera C (2003) A novel method for monitoring surface membrane trafficking on hippocampal acute slice preparation. J Neurosci Methods 125:159–166
13. Rial Verde EM, Lee-Osbourne J, Worley PF, Malinow R, Cline HT (2006) Increased expression of immediate-early gene Arc/Arg3.1 reduces AMPA receptor-mediated synaptic transmission. Neuron 52:461–474
14. Holman D, Henley JM (2007) A novel method for monitoring the cell surface expression of heteromeric protein complexes in dispersed neurons and acute hippocampal slices. J Neurosci Methods 160:302–308
15. Holman D, Feligioni M, Henley JM (2007) Differential redistribution of native AMPA receptor complexes following LTD induction in acute hippocampal slices. Neuropharmacology 52:92–99

16. Joshi S, Kapur J (2009) Slow intracellular accumulation of GABAA receptor δ subunit is modulated by brain-derived neurotrophic factor. Neuroscience 164:507–519
17. Soares C, Lee KFH, Nassrallah W, Béïque J (2013) Differential subcellular targeting of glutamate receptor subtypes during homeostatic plasticity. J Neurosci 33: 13547–13559
18. Whitehead G, Jo J, Hogg EL, Piers T, Kim D-H, Seaton G, Seok H, Bru-Mercier G, Son GH, Regan P, Hildebrandt L, Waite E, Kim B-C, Kerrigan TL, Kim K, Whitcomb DJ, Collingridge GL, Lightman SL, Cho K (2013) Brain 136:3753–3765
19. Gladding CM, Collett VJ, Jia Z, Bashir ZI, Collingridge GL, Molnár E (2009) Tyrosine dephosphorylation regulates AMPAR internalisation in mGluR-LTD. Mol Cell Neurosci 40:267–279
20. Molnár E (2013) Production of antibodies. In: Langton PD (ed) Essential guide to reading biomedical papers: recognising and interpreting best practice. Wiley-Blackwell, Chichester, West Sussex, UK, pp 105–116. ISBN 978-1-1199-5996-0

Chapter 5

Single Nanoparticle Tracking of Surface Ion Channels and Receptors in Brain Cells

Juan Varela, Julien Dupuis, and Laurent Groc

Abstract

Neuronal communication requires a constant adjustment of the number and subtype of neurotransmitter receptors and ion channels at the plasma membrane. Although classical fluorescence ensemble approaches have provided valuable insights into cellular and molecular pathways, their inherent limitations (e.g., average behaviors, spatial resolution) have prompted neuroscientists to use and adapt other imaging approaches. Among these, single nanoparticle tracking offers a remarkable mean to explore, at the single neurotransmitter receptor and ion channel level, the behavior of these molecular actors in living brain cells. In this chapter, we describe the procedure and experimental steps necessary to perform single nanoparticle tracking of membrane neurotransmitter receptors and ion channels in living brain cells.

Key words Single-molecule detection, Nanoparticle, Quantum dot, Neurons

1 Introduction

One important feature of neuronal connections is to adapt their strength in response to network stimuli. One way of adapting is to dynamically regulate the number and subtype of neurotransmitter receptors and ion channels at the pre- and postsynaptic levels. Over the last decade, numerous studies have explored the molecular mechanisms shaping fast and sustained changes in synaptic transmissions. The current view is that neurotransmitter receptors and ion channels cycle to and from the plasma membrane through exocytosis and endocytosis processes, respectively, and once inserted at the membrane, they diffuse at the surface of brain cells and even within the synapse through lateral diffusion. These major discoveries have been possible thanks to the development of high-resolution imaging approaches that revolutionized the cellular biology field (2014 Nobel Laureates in Chemistry). Indeed, classical fluorescence approaches using, for instance, green fluorescent protein and its variants can only provide information on the average behavior of rather large receptor clusters with diffraction-limited spatial

Rafael Luján and Francisco Ciruela (eds.), *Receptor and Ion Channel Detection in the Brain: Methods and Protocols*, Neuromethods, vol. 110, DOI 10.1007/978-1-4939-3064-7_5,

resolutions (few hundreds of nanometers). In contrast, single nanoparticle/molecule tracking techniques allow to directly measure the movements of individual surface neurotransmitter receptors and ion channels with nanometer resolutions [4]. Movements of neurotransmitter receptors and ion channels at the neuronal surface have initially been recorded by tracking submicron-sized latex particles manipulated with optical tweezers. The size of the particles however precluded access to confined compartments, such as synapses. This drawback has been overcome by replacing the bead with individual nanometer-sized fluorescent objects such as semiconductor nanocrystals (e.g., "quantum dots"), which are less bulky objects (~10–20 nm) with characteristic blinking behavior and strong photoresistance (allowing minute-long recordings). The method is based on the labeling of surface neurotransmitter receptors and ion channels with low concentrations of nanoparticle complexes through a ligand (typically an antibody) binding to an extracellular domain of the receptor/channel or to a genetically engineered tag. Single nanoparticle tracking provides an important advantage over ensemble measurements, namely, the possibility to track molecules with a position accuracy only limited by the signal-to-noise ratio at which the molecules are detected, typically below 30 nm in live cells. By removing the averaging inherent to ensemble measurements, single nanoparticle tracking yields a measure of the full mobility distribution of neurotransmitter receptors and ion channels within various cellular compartments (e.g., inside and outside synapses). This new approach and its application to the neurobiology field revealed, for instance, that neurotransmitter receptors and ion channels exchange rapidly by lateral diffusion between submicron neighboring compartments such as the synaptic, peri-, and extrasynaptic spaces. Thus, the single-molecule/nanoparticle tracking offers a unique possibility to explore, at the single neurotransmitter receptor and ion channel level, the behavior of these molecular actors in living brain cells. The following chapter specifically describes the procedure and experimental steps necessary to perform single nanoparticle tracking of membrane neurotransmitter receptor and ion channel in living brain cells.

2 Materials

2.1 Media and Buffers

The most commonly used medium for single-particle tracking applications on neurons is complete Neurobasal medium. Phosphate buffer saline (PBS) is also often used to dilute antibodies or quantum dots, or as a solvent for drugs applied in the bath.

1. Complete Neurobasal medium. To prepare complete recording medium, supplement 500 mL of Neurobasal medium (Gibco, Life Technologies, Thermo Fisher Scientific Inc., USA)

with 10 mL of 50X B-27 serum-free supplement (Gibco, Life Technologies, Thermo Fisher Scientific Inc., USA) and glutamine (Sigma-Aldrich, St Louis, USA) at a final concentration of 2 mM. Complete Neurobasal medium can be stored at 4 °C for several weeks under sterile conditions. To avoid unspecific binding of antibodies, complete Neurobasal medium is pre-heated at 37 °C on the day of experiment and supplemented with casein or bovine serum albumin (BSA; Sigma-Aldrich, St Louis, USA) at a final concentration of 1 % before use.

2. Phosphate buffer saline (PBS). When required, quantum dot-coupled secondary antibodies can be pre-diluted in PBS 1X. To obtain 1 L of PBS 1X, dilute 100 mL of PBS solution 10X (Euromedex, France) in 900 mL of ultrapure water. Filter before use and store at 4 °C.

2.2 Dissociated Neuronal Cultures

Although the procedures described here apply to any neuronal preparation, we will deliberately focus on primary hippocampal cultures which are the most commonly used in vitro model by the neuroscience community. Briefly, cultures of hippocampal neurons are prepared from embryonic (day 18) Sprague-Dawley rats as follows (for details, *see* [5]):

1. Hippocampi of embryonic day 18 Sprague-Dawley rats are dissected and transferred to a 15 mL Falcon tube filled with pre-heated HBSS medium (Gibco, Life Technologies, Thermo Fisher Scientific Inc., USA).
2. To initiate dissociation, the HBSS medium is then replaced by 5 mL of pre-heated trypsin/EDTA solution (Gibco, Life Technologies, Thermo Fisher Scientific Inc., USA) for 15 min incubation at 37 °C. Trypsin/EDTA is then removed and washed twice with 10 mL of pre-heated HBSS medium. Hippocampi are transferred in 2 mL of pre-heated HBSS, and the tissue is dissociated by gently pipetting several times.
3. Cells are plated on polylysine-precoated glass coverslips in Ø60 mm petri dishes (Falcon, Corning Inc., USA) at a density of 350×10^3 cells per dish. Coverslips are maintained at 37 °C/5 % CO_2 for 72 h in 5 mL of a 3 % horse serum-supplemented Neurobasal medium. This medium is then replaced by pre-heated and equilibrated serum-free Neurobasal medium, and cultures can be maintained at 37 °C/5 % CO_2 for up to 20 days.
4. For imaging experiments requiring the tracking of recombinant membrane proteins, neurons can be transfected with plasmids of interest at 7–14 days in vitro using the Effectene transfection kit (Qiagen, Germany) according to the manufacturer's instructions.

Warning: all procedures are performed in sterile conditions under a hood.

2.3 Quantum Dot Labeling

Single-particle tracking on neurons requires highly specific monoclonal or polyclonal antibodies targeting extracellular epitopes of the receptor or channel of interest, as well as photostable nanoparticles functionalized with secondary antibodies of which quantum dots (QDs) are the most commonly used. Bright and coated QDs are commercially available, with fluorescence emission at several different wavelengths.

1. Cell culture incubator set at 37 °C/5 % CO_2
2. Twelve-well culture plate
3. 50 mL of BSA-supplemented (1 %) Neurobasal medium
4. 1 mL of PBS 1X
5. Appropriate primary antibody and QD-coupled secondary antibody
6. 1000 μL, 200 μL, and 2.5 μL micropipettes
7. Tweezers

Warning: primary antibodies and secondary antibody-coupled QD should always be carefully kept on ice. Neurobasal medium should be pre-heated and equilibrated in the incubator before use.

2.4 Imaging Setup

There is a wide variety of microscope setups that can be adequate to perform single QD tracking (Fig. 1). The main features needed are:

1. Inverted fluorescence microscope body with appropriate excitation/emission filters adapted to the optical properties of the fluorophores
2. Vibration isolation table supporting the microscope (e.g., TMC Vibration Control, USA) to avoid drifts during acquisitions
3. Magnification objectives in the range of 60x to 100x
4. Mercury lamp
5. EM-CCD camera (e.g., Evolve, Photometrics, USA)
6. Bath heater system to maintain samples at 37 °C (e.g., TC-324B/344B Temperature Controller, Warner Instruments, USA)
7. Acquisition software (e.g., MetaMorph, Molecular Devices, USA)

3 Methods

3.1 Transfections

In order to perform the tracking of an exogenous membrane protein, a transfection needs to be done before the QD experiment is carried on. In many cases, a transfection may also be required to have a marker that may be used to allow co-localization studies (such as a synaptic protein). Whether it is a simple or a double

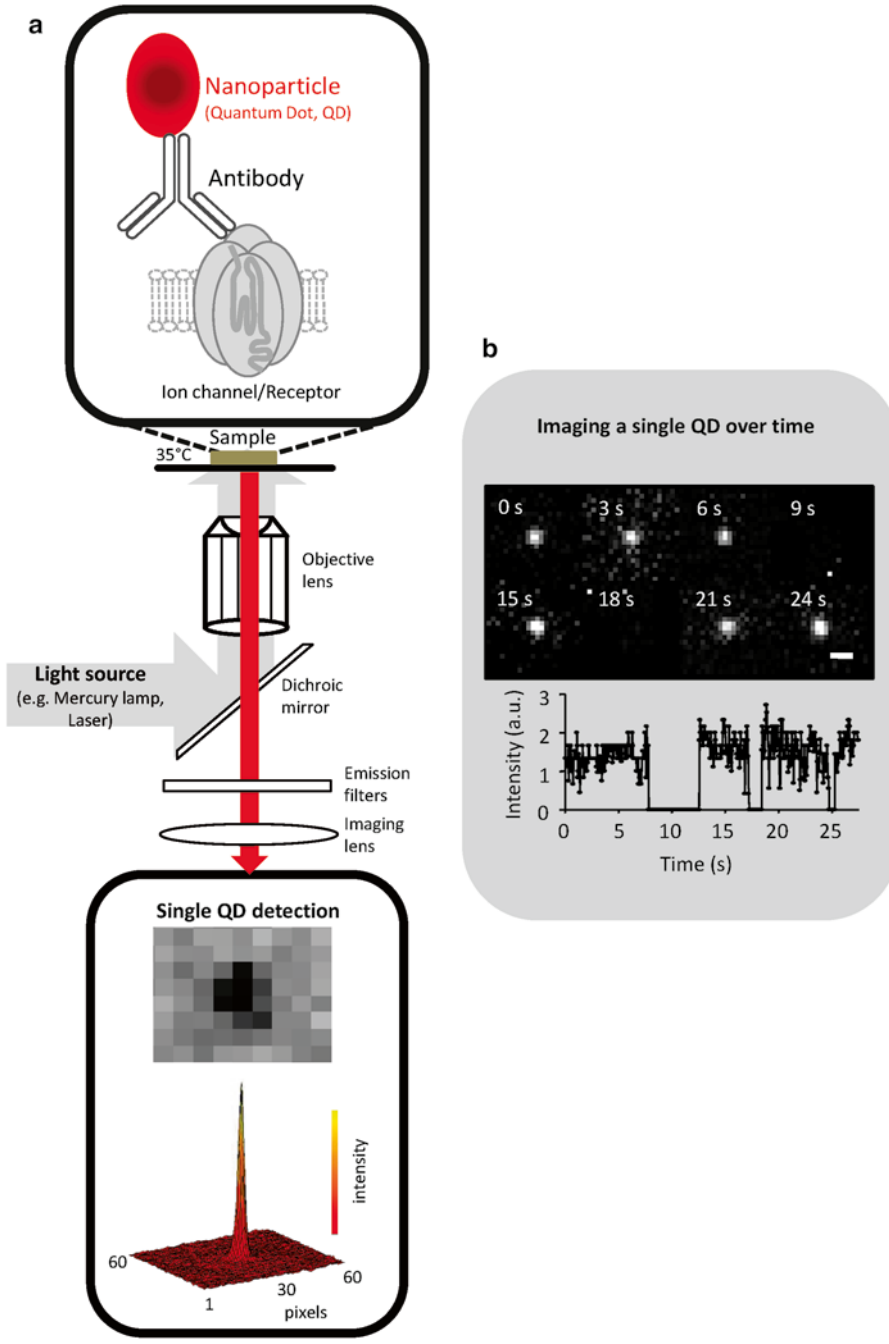

Fig. 1 Schematic microscopy setting to perform single nanoparticle tracking in live brain cells.(**a**) Description of the optic path to achieve single nanoparticle tracking of a quantum dot. The single nanoparticle is part of a complex with an antibody directed against an extracellular epitope of the ion channel/receptor of interest. (**b**) The blinking of a single quantum dot (655 nm emission) is represented. Note the fast change in luminescence over time

transfection, the QD experiment needs to be done once the transfected proteins are expressed (e.g., 24–72 h after transfection).

3.2 QD Labeling of Extracellular Epitopes of Membrane Proteins in Live Neurons

1. Equilibrate a flask of complete medium in the incubator at 37 °C and 5 % CO_2 overnight before experiment. Leave the cap of the flask slightly loose in order to permit gas exchange. In general, 50 mL is more than enough for a typical experiment.
2. One hour before starting the experiment, add bovine serum albumin (BSA) to the medium (final concentration of 1 %). The BSA decreases unspecific binding of QD. Do not agitate the flask, and just dissolve the BSA gently mixing and leaving the flask in the incubator for an hour (*see* **Note 3** for multiple staining).
3. Put in a 6-well plate 3 mL of complete medium with BSA in each well, to wash the coverslip after incubation with antibodies and QD. Leave the plate in the incubator as well.
4. Prepare primary antibody solution mixing 0.5 μL of antibody in 500 μL of medium with BSA (1:1000 dilution, but this concentration should be adjusted according to the particular molecule to be tracked).
5. Vortex the antibody solution gently.
6. Prepare functionalized QD dilution (Fab fragments coupled to QD) by diluting QD stock 1:10000 in medium with BSA. To do this, prepare a pre-dilution 1:10 in PBS, then dilute 1:1000 in the BSA medium.
7. Vortex the functionalized QD solution.
8. Stretch a piece of clean Parafilm over a flat surface to do the incubation with antibodies.
9. Put a 100 μL drop of primary antibody solution over the Parafilm.
10. Carefully grab a coverslip of your cultured neurons with a thin forceps and flip it over the antibody drop, in such a way that the cells are facing the Parafilm (and therefore embedded in antibody solution).
11. Put the Parafilm and coverslip back to the incubator for 10 min.
12. Wash the coverslip by submerging it in three of the wells containing medium with BSA for 10 s each time.
13. Repeat the incubation process but now with a drop of the QD solution, letting it for 10 min inside the incubator.
14. Wash again the coverslip three times in the wells with medium and BSA that haven't been used.

15. Place the coverslip in an imaging chamber and fill the chamber with cell medium (about 200 μL depending on the cell chamber type).
16. Place the chamber in the microscope, controlling the temperature and CO_2 as required for the desired experiment (atmosphere typically fixed at 5 % CO_2 at 37 °C).

3.3 Imaging

Single-molecule tracking can be performed in standard epifluorescence microscopes as long as the camera is sensitive and fast enough to detect individual QD at a fast sampling rate. Make sure you have the right filter sets for your labels. If the instrument has the right equipment, the imaging procedure is straightforward.

1. Choose a cell of interest according to the quality of the labeling and bright field image.
2. Make sure that the number of QD over the cell is high enough to allow a decent statistical analysis but low enough to avoid crossing of trajectories from different QD. If the QD density is too high or too low, then the incubation process needs to be adjusted changing the concentration of QD.
3. Record images of the fluorescent dyes used, as well as a bright field image.
4. Take an image stream of QD (in general a few 100 consecutive frames is enough) at a high sampling rate (at least 20 or 30 images per second).
5. Avoid imaging for long time periods, as the photodamage increases and some of the QD will be internalized. For most cell membrane receptors, imaging can be performed for about 20 min after incubation with QD.

3.4 Image Analysis

Image processing for single-particle tracking is a delicate process, and if possible, it should be performed with the assistance of imaging experts until the needed skills are acquired. Particle tracking methodologies are a research topic on itself, and there are constant improvements and new developments that are better suited for specific applications [2, 3]. There are several available commercial softwares to do automated particle tracking such as Imaris (Bitplane) or Volocity (PerkinElmer), while some laboratories prefer to develop their own codes. Another solution is to use available scripts and plug-ins that run, for example, in Matlab (MathWorks) or ImageJ (NIH).

The first step for particle tracking procedures is the automated detection of the QD in every frame of the stream. To do this, one of the most robust and precise ways is to detect intensity maxima and fit two dimensional Gaussians to obtain the position of the QD. The pointing accuracy of this procedure is mainly given by the quality of the distance traveled by the QD during and each

frame's time exposure. Due to the high signal-to-noise ratio of typical QD tracking experiments, the accuracy could reach about 30 nm [4]. If markers of interest are transfected beforehand (e.g., GFP-tagged synaptic protein), QD can be precisely located within specific membrane compartments – e.g., synaptic, perisynaptic, and extrasynaptic compartments – on each frame of a stream. Identified QD locations can then be projected on a single image to provide a high-resolution distribution of the receptor/QD complexes over the acquisition. After all QD positions are detected, software packages link individual QD positions from one frame to the following one (*see* **Note 4** for blinking reconnection).

Once the detection and tracking algorithms are applied over the QD image streams, the standard way of characterizing the behavior of a diffusing particle is by calculating the mean squared displacement (MSD).

For a trajectory of N positions ($x(t),y(t)$) with times from $t=0$ to $t=N^*\Delta t$, the MSD corresponding to the time interval $\tau = n\Delta t$ can be calculated as follows:

$$\sum_{i=1}^{N-n} \frac{\left[x\left((i+n)*\Delta t\right)-x\left(i*\Delta t\right)\right]^2+\left[y\left((i+n)*\Delta t\right)-y\left(i*\Delta t\right)\right]^2}{N-n}$$

From each MSD, the instantaneous diffusion coefficient may be calculated, measuring how much each QD moves (in μm per second). The linear fit of the first few points (say 4 or 5) of the MSD(τ) plotted against the lag time τ is proportional to the diffusion coefficient:

$$\mathrm{MSD}(\tau) = < r^2 > (\tau) = 4D\tau$$

4 Notes

1. Although still in its infancy, single-particle tracking in cultured organotypic brain slices has also recently been reported. While protocols remain very similar to those developed for dissociated neuronal cultures, we encourage the reader to refer to [1] for more details.
2. Since quantum dots of non-overlapping excitation/emission wavelengths are now available, dual-color tracking experiments can be performed simultaneously using a beam splitter (e.g., DV2 Multichannel Imaging System, Photometrics, USA) to separate acquisition channels.
3. If a particular staining needs to be done (e.g., MitoTracker Green to facilitate detection of synapses), the staining should be done according to the manufacturer's protocol, which could mean doing the staining before or after QD incubation.

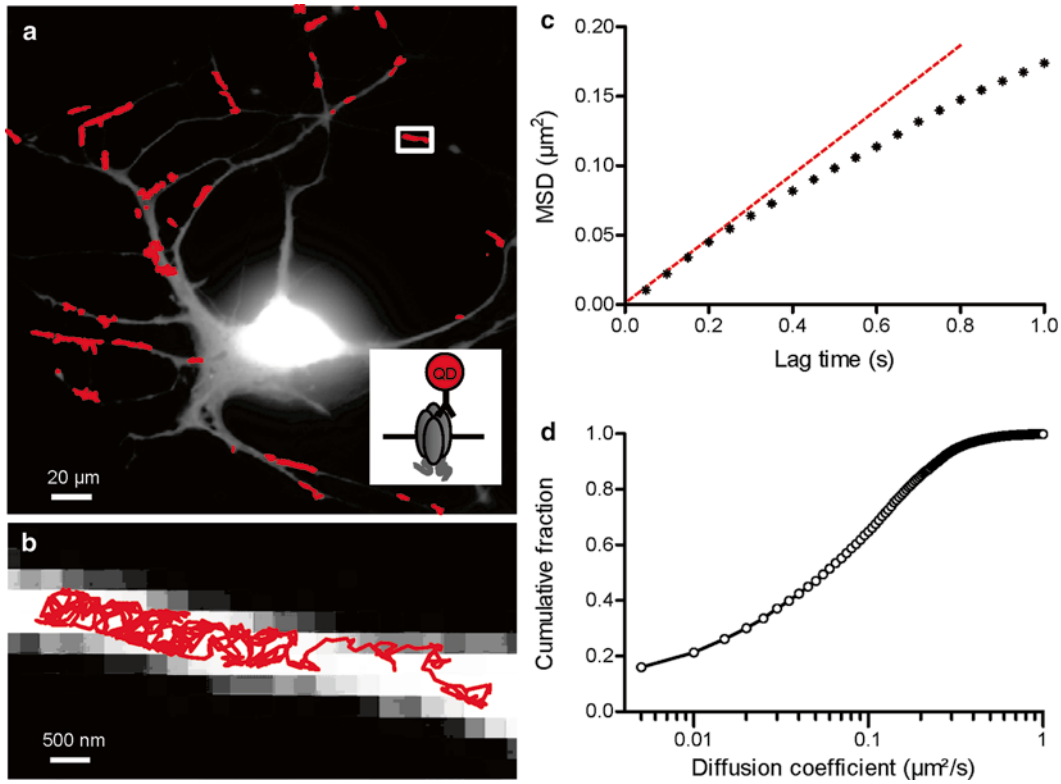

Fig. 2 Single-particle tracking on hippocampal neurons. (**a**) Trajectories of single QD-labeled surface NMDA receptors on the dendrites of a hippocampal neuron (20 Hz acquisition, 30 s duration). *Inset*, schematic representation of a receptor labeled by an antibody coupled to a quantum dot. (**b**) Representative trajectory taken from panel **a** of a single NMDA receptor on a dendrite. (**c**) Plot of the mean square displacement (MSD) versus time of the NMDA receptor surface trajectory presented in panel **b**. The instantaneous diffusion coefficient, *D*, is calculated for each trajectory from a linear fit (*red dotted line*) of the first 4 points of the mean square displacement versus time following the equation $MSD(t) = <r^2>(t) = 4Dt$.(**d**) Cumulative distribution of NMDA receptor instantaneous surface diffusion coefficients. The initial point of the distribution represents the immobile fraction of the population of receptors ($D < 0.005$ µm²/s for typical pointing accuracy)

4. A typical property of QD luminescence is the blinking (Fig. 1b). Up to a certain point, this effect can be corrected in the trajectories analysis imposing conditions to the linkage of trajectories that are adequate to the experimental settings. In particular, automated blinking correction should consider a maximum number of frames to reconnect trajectories and a maximum distance allowed for the displacement during the blink (Fig. 2).

Acknowledgments

This work was supported by the Centre National de la Recherche Scientifique, Agence Nationale de la Recherche, Conseil Régional d'Aquitaine, and Marie Curie Individual Fellowship 326442.

We thank lab members for constructive discussions and critical reading of the manuscript and the Bordeaux Imaging Center for technical support.

References

1. Biermann B, Sokoll S, Klueva J, Missler M, Wiegert JS, Sibarita JB, Heine M (2014) Imaging of molecular surface dynamics in brain slices using single-particle tracking. Nat Commun 5:3024
2. Chenouard N, Smal I, de Chaumont F, Maška M, Sbalzarini IF, Gong Y, Cardinale J, Carthel C, Coraluppi S, Winter M et al (2014) Objective comparison of particle tracking methods. Nat Methods 11:281–289
3. Deschout H, CellaZanacchi F, Mlodzianoski M, Diaspro A, Bewersdorf J, Hess ST, Braeckmans K (2014) Precisely and accurately localizing single emitters in fluorescence microscopy. Nat Methods 11:253–266
4. Groc L, Lafourcade M, Heine M, Renner M, Racine V, Sibarita JB, Lounis B, Choquet D, Cognet L (2007) Surface trafficking of neurotransmitter receptor: comparison between single-molecule/quantum dot strategies. J Neurosci 27:12433–12437
5. Mikasova L, De Rossi P, Bouchet D, Georges F, Rogemond V, Didelot A, Meissirel C, Honnorat J, Groc L (2012) Disrupted surface cross-talk between NMDA and Ephrin-B2 receptors in anti-NMDA encephalitis. Brain 135:1606–1621

Chapter 6

Radioligand Binding Detection of Receptors in Brain Membranes

Fuencisla Pilar-Cuéllar, Alvaro Díaz, Emilio Garro-Martínez, Alicia Martín, Beatriz Romero, and Elsa M. Valdizán

Abstract

Transmitters, hormones, and most of the therapeutic drugs exert their biological functions by generating signals in target cells through interaction with a receptor molecule in the cellular membrane, cytosol, or even at the nucleus of the cell. Because receptors play such a crucial role in cell function, especially within the central nervous system (CNS), we need lab techniques to measure their expression and functionality. There are techniques to determine regulatory changes in receptor number (receptor density), subcellular distribution, anatomical distribution, the physiological function of the receptors, as well as the ligand affinity.

Here we describe a classic way of doing this by exposing cells or tissue membranes to radiolabeled molecules (radioligands) that bind selectively to receptors in the sample (*receptor binding assay*). The functional consequence of the receptor occupancy or level of G-protein activation could be measured by *[^{35}S]GTPγS binding assay*. This assay measures the binding of the non-hydrolyzable analogue [^{35}S]GTPγS ([^{35}S]guanosine-5′-O-(3-thio) triphosphate) to Gα subunits. [^{35}S]GTPγS binding assays, also known as functional binding assays, are carried out in a similar way as radioligand (receptor) binding assays.

The above radiometric assays are useful to differentiate among agonist, antagonist, and inverse agonist activities, in addition to traditional pharmacological parameters of potency and efficacy, as well as receptor constitutive activity and agonist-specific G-protein-coupled signaling. Moreover, radioligand binding assays provide a powerful tool for screening drug candidates for many receptors in drug discovery research.

Key words Radioligand, Membrane homogenates, Saturation binding assays, Competition binding assays, [^{35}S]GTPγS receptor binding, Affinity, Efficacy, Functionality

1 Introduction

The use of radioligands is a well-known method to study the pharmacological characteristics and the regional distribution of receptor proteins. The anatomical localization of the neurotransmitter receptors is studied using autoradiographic methods, which is explained in Chap. 11.

Radioligand assays allow receptor characterization (receptor number or density, subcellular distribution, anatomical distribution, and ligand affinity) by *receptor binding assay* as well as GPCR

Rafael Luján and Francisco Ciruela (eds.), *Receptor and Ion Channel Detection in the Brain: Methods and Protocols*, Neuromethods, vol. 110, DOI 10.1007/978-1-4939-3064-7_6, © Springer Science+Business Media New York 2016

activation by *[^{35}S]GTPγS or functional binding assays*, which enable the differentiation between agonist, antagonist, and inverse agonist activities of the ligands in addition to traditional pharmacological parameters of potency, efficacy, as well as constitutive activity of receptors.

The *receptor binding assays* use specific receptor ligands, either agonists or antagonists, labeled mainly with isotopes as ^{3}H or ^{125}I. The main characteristics of the radioligands are their saturable binding to the receptor, their high affinity binding values, and the reversibility of their binding to the receptor. However, the radioligands also bind nonspecifically to other components in the membrane homogenate. In most cases, even multiple washes cannot remove this nonspecific binding (*see* **Note 1**). To determine the specific binding of the radioligand, it is necessary to include a nonspecific binding condition in the experiment, consisting in the addition of the radioligand together with a very high concentration (100–1000-fold) of another non-labeled molecule also with high affinity for the receptor of interest. By measuring the nonspecific binding and subtracting this from total binding, it is possible to calculate the *specific binding*.

There are different types of *receptor binding assay* experiments which allow the determination of different receptor parameters [1]. The k*inetic assays* are preliminary assays to determine the measure of the time course of ligand dissociation and association, providing a radioligand affinity value for the receptor *(KD)* that should be consistent with that determined with saturation studies.

The *saturation assays* consists in tissue or cell homogenates incubated with a wide range of radioligand increasing concentrations (tenfold below and above the radiolabeled ligand K_D). Data analyses of saturation curves provide measures of radioligand affinity (K_D) and receptor density (Bmax).

In the *competition assays*, a fixed low radioligand concentration (~K_D) and a wide range of competitor (non-labeled) concentrations are used. Data analysis provides information about the competitor's affinity for the receptor (Ki). In both experiments, we can also obtain the Hill parameter (n_H), corresponding to the Scatchard slope (in saturation assays) or the slope of the competition curve (between 20 and 80 % displacement values), which can indicate if there is one ($nH = 1$) or more receptor binding sites ($nH < 0.8$) and if there is positive ($nH > 1$) or negative ($nH < 1$) cooperative binding.

In order to select an adequate radioligand, several aspects should be taken into account, such as its specific activity, selectivity for the receptor of interest, and the level of nonspecific binding, as well as the isotope type (*see* **Note 2**).

[^{35}S]GTPγS or functional binding assays allow determining the activation of the G proteins by GPCRs [2]. Following GPCR activation, GTP replaces GDP on the alpha subunit of the G protein. Functional binding assay is based on radiometric detection of GTP

exchange on the Gα protein subunit by using a non-hydrolyzable radioligand nucleotide GTPγS labeled with ^{35}S. The GTPγS assay works better with Gi-coupled GPCRs. Very low assay windows are usually obtained for Gs- and Gq-coupled receptors, due to [1] the high Gi expression levels relative to Gs or Gq proteins and [2] the exchange rate of these G proteins for GTP. In these experiments, data analyses of agonist-induced stimulation of [^{35}S]GTPγS binding allow to determine agonist effective concentration 50 (EC_{50}) and maximal stimulation (Emax) [3].

There is a huge number of specific radioligands for each receptor subtype to perform receptor binding experiments as well as high number of agonists and antagonist drugs that can be used either in receptor or functional binding experiments. Protocols will be slightly different in terms of buffers, membrane preparation, radioligand, agonists/antagonists, or incubation conditions. Different databases are available to check the wide range of ligands available for a specific receptor (*see* **Note 3**).

Here we are going to describe our lab protocols to label 5-HT_{1A} receptors with [^{3}H]8-OH-DPAT and the [^{35}S]GTPγS functional binding assay using the selective 5-HT_{1A} agonist (±)8-OH-DPAT.

2 Materials

2.1 Buffers

2.1.1 Receptor Binding Assays

1. *Homogenization buffer 1:* 0.05 M Tris–HCl (pH 7.6) and 0.32 M sucrose. To prepare 50 mL of buffer, dissolve 302.9 mg of Tris–HCl and 5.5 g of sucrose in distilled water, and adjust pH to 7.6. Adjust the volume to 50 mL. Store at 4 °C.
2. *Homogenization buffer 2*: 0.05 M Tris–HCl (pH 7.6). To prepare 50 mL of buffer, dissolve 302.9 mg of Tris–HCl in distilled water, and adjust pH to 7.6. Adjust the volume to 50 mL. Store at 4 °C.
3. *Snyder buffer* (SB): 0.05 M Tris–HCl (pH 7.6), 4 mM $CaCl_2$, and 0.1 % ascorbic acid. For serotonin (5-HT) receptor binding, SB should contain 10 μM pargyline (pargyline hydrochloride) [4]. To avoid $CaCl_2$ precipitation, SB should be freshly prepared before the experiment. To prepare 100 mL of SB, dissolve 605.7 mg of Tris–HCl, 44.4 mg of anhydrous $CaCl_2$ (Sigma-Aldrich), and 0.1 g of ascorbic acid (Sigma-Aldrich) in distilled water. Adjust the pH to 7.6 and the volume to 100 mL. Freshly prepare 1 mL of pargyline 10^{-2} M by dissolving 1.9 mg of pargyline in 1 mL of distilled water. Add 100 μL of pargyline 10^{-2} M to 100 mL of SB to obtain SB containing 10 μM pargyline (SBP). Keep on ice until used (*see* **Note 4**).
4. *Washing buffer*: 0.05 M Tris–HCl (pH 7.6). As indicated for homogenization buffer 2, washing buffer should be stored at 4 °C. Prepare in advance 1 L.

2.1.2 Functional ([^{35}S] GTPγS) Binding Buffers

1. *Homogenization buffer 1*: 0.05 M Tris–HCl (pH 7.5). To prepare 100 mL, dissolve 605.7 mg of Tris–HCl in distilled water. Adjust pH to 7.5, and add water to 100 mL. Keep on ice.
2. *Homogenization buffer 2*: 0.05 M Tris–HCl (pH 7.5), 100 mM NaCl, 1 mM EGTA, 3 mM $MgCl_2$, and 1 mM DTT. For 100 mL, dissolve 605.7 mg of Tris–HCl, 584.4 mg NaCl, 38 mg EGTA, 28.6 mg $MgCl_2$, and 15.4 mg DTT in distilled water. Adjust pH to 7.5 and the final volume to 100 mL. Maintain at 4 °C.
3. *Assay buffer* (*see* **Notes 5, 6**, and 7): 0.05 M Tris–HCl (pH 7.5), 100 mM NaCl, 1 mM EGTA, 3 mM $MgCl_2$, 1 mM DTT, 300 μM GDP, and 10 mU/mL adenosine deaminase (ADase) (Sigma-Aldrich; 250 U/150 μL). For 100 mL, add 13.3 mg of GDP and 0.6 μL of ADase to the homogenization buffer 2. Prepare fresh before the experiment. Maintain on ice until used.
4. *Washing buffer*: 0.05 M Tris–HCl (pH 7.5). As indicated for the homogenization buffer 1, prepare 1 L, and maintain at 4 °C.

2.2 Drugs and Reagents (See Note 8)

1. 5-HT (*5-hydroxytryptaminehydrochloride*): to prepare 1 mL stock solution 1 mM, weight 212 μg of 5-HT and dissolve in distilled water. Dilute this initial solution 1:10 (tenfold of the final concentration) to obtain a 100 μM working solution using the assay buffer.
2. WAY-100,635 (*3-[4-(2-Methoxyphenyl)piperazin-1-yl]-2-phenyl-N-tert-butyl-propanamide dihydrochloride*): to prepare 1 mL stock solution 1 mM, weight 468 μg of WAY-100,635 and dissolve in distilled water. Dilute this initial solution 1:10–100 μM using the assay buffer.
3. (±)8-OH-DPAT (*(±)-8-Hydroxy-2-(dipropylamino)tetralin hydrobromide*): to prepare 1 mL stock solution 1 mM, weight 247 μg of (±)8-OH-DPAT and dissolve in distilled water. Dilute this initial solution to 100 μM using the assay buffer.
4. GTPγS (*guanosine 5′-[γ-thio]triphosphate*) tetralithium salt: to prepare 1 mL stock solution 1 mM, weight 563 μg of GTPγS and dissolve in distilled water. Dilute this initial solution 1:10–100 μM using the assay buffer.

2.3 Radioligand (See Note 9)

2.3.1 Receptor Binding Assay

[^{3}H]8-OH-DPAT (8-hydroxy-DPAT and [propyl-2,3-ring-1,2,3-^{3}H]) (NET 929, Perkin Elmer). The specific activity of this radioligand depends on the lot, ranging between 100 and 200 Ci/mmol, with a concentration of 1 mCi/mL.

2.3.2 Functional ([^{35}S] GTPγS) Binding Assay

[^{35}S]GTPγS (guanosine 5'-(gamma-thio)triphosphate, [^{35}S]) (NEG 030H, Perkin Elmer); specific activity, 1250 Ci/mmol; and concentration, 12.5 mCi/mL. As the amount of radioligand

needed in the experiments is usually very small (<1 μL), this radioligand can be diluted 1:10, to obtain a final concentration of 1.25 mCi/mL. If the radioligand is purchased in a 250 μCi format, we should dilute the 20 μL of radioligand (12.5 mCi/mL) by adding 180 μL of 10 mM tricine buffer (pH 7.6) with 10 mM DTT. The radioligand can be aliquoted and stored at −20 °C until used.

2.3.3 Calculations to Prepare Radioligand Concentrations

To calculate the volume of radioligand stock (commercial) solution to be pipetted for the preparation of the initial radioligand concentration used in the assay, we need to know the specific activity (SA) (Ci/mmol) (*see* **Note 10**) and the radioisotope concentration (mCi/mL). Radioactive decay or disintegration should be taken into account especially with short half-life isotopes as ^{35}S (87 days) or ^{125}I (60 days) (*see* **Note 11**). Below, the formula to calculate the volume (μL) of radioligand stock solution in order to prepare 0.5 mL of 20 nM [^{3}H]8-OH-DPAT (SA: 142 Ci/mmol; [1 mCi/mL]) is shown.

$$0.5\,\text{mL} \times \frac{1}{10^3\,\text{mL}} \times \frac{20\,\text{nmol}}{1} \times \frac{142\,\mu\text{Ci}}{\text{nmol}} \times \frac{\mu\text{L}}{1\,\mu\text{Ci}} = 1.42\,\mu\text{L}$$

Check the real concentration of the radioligand by measuring the dpm value in a liquid scintillation counter (*see* **Note 12**). Pipette 50 μL of the prepared solution into a vial containing 2 mL of scintillation liquid and count it. The theoretical dpm value can be calculated using the following formula:

$$50\,\mu\text{L} \times \frac{1}{10^6\,\mu\text{L}} \times \frac{20\,\text{nmol}}{1} \times \frac{142\,\mu\text{Ci}}{\text{nmol}} \times \frac{2.2 \times 10^6\,\text{dpm}}{1\,\mu\text{Ci}} = 312400\,\text{dpm}$$

Add more radioligand or dilute it (using incubation buffer) to obtain the adequate concentration if necessary.

Alternatively, these calculations can be made on the "QuickCalcs" webpage from GraphPad: http://www.graphpad.com/quickcalcs/radcalcform.cfm.

2.4 Tissue Dissection

For receptor studies in CNS, we need to obtain the brain of the experimental animals, dissecting out the areas of interest (*see* **Note 13**). Follow the protocols approved by local Animal Care and Use Committee about sacrificing the animals, avoiding the use of anesthetics (*see* **Note 14**). Place the animal head into an ice for 2 min, and quickly remove the brain from the skull using dissecting tools (i.e., bone rongeurs, tweezers, etc.). Dissect out the different brain structures of interest, put into 1.5 mL tubes, and store at −80 °C until used.

2.5 Membrane Preparation

Membranes for receptor binding assays may be prepared by using a Polytron homogenizer (Polytron Ultra-turrax T-25). In our opinion, a glass/Teflon homogenizer (Potter–Elvehjem homogenizers)

is better for functional binding studies, as it seems to be a milder homogenization procedure. Indeed, we use the Potter–Elvehjem homogenizer for both receptor and functional assays when we have a limited amount of sample.

2.6 Other Materials and Apparatuses

Polypropylene tubes 5 mL (*see* **Note 15**)

- Brandel 24-sample, Semi-automatic cell harvester
- Whatman GF/B or GF/C glass fiber filter
- Liquid scintillation cocktail (Ultima-Flo™ M; Perkin Elmer)
- Plastic scintillation vials (Pico Pro Vial, 4 mL; Perkin Elmer)
- Liquid scintillation counter packard Tri-Carb 2900TR (Packard BioScience Company, USA)

3 Methods

3.1 Receptor Binding Assays

3.1.1 Membrane Fraction Preparation for Receptor Binding

1. Thaw the tissue on ice, and weight the sample.
2. Homogenize the tissue 1:10 (w:v) in homogenization buffer 1, using a Polytron at maximum speed, for 10 s at 4 °C (3 times).
3. Transfer the homogenate to 1.5 mL microtubes and centrifuge at 900 × *g* for 10 min at 4 °C.
4. The supernatant is transferred to another 1.5 mL tube and centrifuged at 48,000 × *g* for 25 min at 4 °C.
5. Discard the supernatant and resuspend the pellet in 10 volumes of homogenization buffer 2. Homogenize with a Polytron.
6. Incubate the homogenate for 15 min, at 37 °C in a thermostatic shaking water bath to eliminate the endogenous neurotransmitter.
7. Cool it down at 4 °C and centrifuge the homogenate at 48,000 × *g* for 25 min at 4 °C.
8. Discard the supernatant and resuspend the pellet in 1:3 volumes of SB.
9. Distribute the homogenate in 0.5 mL aliquots in 1.5 mL tubes, and store at −80 °C until used.

3.1.2 Receptor Binding Saturation Assay

In our laboratory, binding assays are typically performed in a final volume of 250 μL. Until incubation, all the preparation steps should be performed on ice.

1. Thaw membrane homogenate and dilute 1:10 to a final dilution of 1:30 using the homogenization buffer 2 and a Polytron.
2. Measure the protein concentration of a 5 μL aliquot by using a commercial kit (DC™ Protein Assay, BioRad) as described

below (*see* 3.4). With the obtained protein concentration (mg/mL), adjust the membrane preparation to a final concentration of 45–55 μg protein/150 μL of membrane preparation (45–55 μg protein/assay tube).

3. Prepare serial 1:2 dilutions of the radioligand solution using SBP. The range of [^{3}H]8-OH-DPAT concentrations tested in our representative saturation assay to yield an appropriate curve for nonlinear regression analysis methods is 20, 10, 5, 2.5, 1.25, 0.6, 0.3, and 0.15 nM. As we will dilute 25 μL of each radioligand concentration in an assay volume of 250 μL, the "radioligand solution" for the curve should be prepared 10× (200, 100, 50, 25, 12.5, 6.25, 3.13, and 1.56 nM, respectively).
4. Set a rack of 48 polypropylene 5 mL tubes. For each radioligand concentration, label six tubes: three for total binding (T) and three for the nonspecific binding (NS).
5. Pipette the assay components in the respective assay tubes and in the order described in Table 1 (*see* **Note 16**).
6. Vortex the tubes and incubate them at 37 °C for 30 min in a thermostatic shaking water bath (*see* **Note 17**).
7. Prior filtration, presoak GF/B Whatman glass fiber filters using washing buffer for 5 min (*see* **Note 18**).
8. Place the GF/B Whatman glass fiber filter in the Brandel harvester, and filter the tubes contents. Wash the filters three times with 5 mL of cold (4 °C) washing buffer (*see* **Note 19**).
9. Dry the filters at room temperature for 2 h.
10. Place the filter disks for each experimental condition in different vials containing 2 mL of scintillation liquid and vortex.
11. Prepare two additional scintillation vials with 2 mL of scintillation liquid for each radioligand concentration. Add 50 μL of each radioligand concentration.
12. Place the vials in racks and count the vials in a liquid scintillation counter using the appropriate isotope tag.

Table 1
Description of the volumes to pipette into each tube condition in an experiment of receptor binding saturation

[^{3}H]8-OH-DPAT saturation assay	Total (μL)	Nonspecific (μL)
Buffer SBP	75	50
5-HT (10^{-4} M)	–	25
[^{3}H]8-OH-DPAT (200–1.56 nM)	25	25
Membranes	150	150

3.1.3 Receptor Binding Competition Assay

The radioligand concentration used in this experiment is close to its K_D value and can be determined in previous kinetic/saturation assays (as described in Sect. 3.1.2), or obtained in the literature. The concentration of [^{3}H]8-OH-DPAT, WAY-100,635 (competitor), and 5-HT (NS) is prepared tenfold in SBP.

The experiment should be performed as follows:

1. Thaw the membrane homogenates on ice and dilute them to 1:30 in homogenization buffer 2.
2. Measure the protein amount in the sample as described below (*see* 3.4), and adjust to pipette 45–55 μg of protein per tube.
3. Prepare 600 μL of 20 nM [^{3}H]8-OH-DPAT.
4. Prepare 1:10 serial dilutions of WAY-100,635: 10^{-9} to 10^{-4} M using SBP buffer.
5. Prepare 5-HT 100 μM (as indicated in 2.1.3) for the "nonspecific" condition.
6. Set a rack of 24 polypropylene 5 mL tubes for each condition: 3 total, 3 nonspecific binding, and 3 for each competitor concentration. Pipette as indicated in Table 2 (*see* **Note 16**).
7. Incubate at 37 °C for 30 min, in a thermostatic shaking water bath (*see* **Note 17**).
8. Continue as indicated in **steps 7–12** of Sect. 3.1.2.

3.2 Functional Binding Assays ([^{35}S]GTPγS Binding)

3.2.1 Membrane Fraction Preparation for [^{35}S]GTPγS Binding Assay

1. Thaw the tissue on ice and homogenize 1:80 (w:v) in homogenization buffer 1 using a Potter–Elvehjem homogenizer at 800 rpm, 15 strokes on ice.
2. Transfer the homogenate in 1 mL aliquots in 1.5 mL tubes.
3. Centrifuge the homogenate at 240 × *g* for 5 min at 4 °C.
4. Collect the supernatant, place in 1.5 mL tubes, and centrifuge at 21,000 × *g* during 15 min at 4 °C.

Table 2
Description of the volumes to pipette into each tube condition in an experiment of receptor binding competition

[^{3}H]8-OH-DPAT competition assay	Total (μL)	Competitor (μL)	Nonspecific (μL)
Buffer SBP	75	50	50
WAY-100,635 (10^{-9} – 10^{-3} M)	–	25	–
5-HT (10^{-4} M)	–	–	25
[^{3}H]8-OH-DPAT (20 nM)	25	25	25
Membranes	150	150	150

5. Discard the supernatant and resuspend the pellet in homogenization buffer 2.
6. Incubate for 15 min at 37 °C thermostatic shaking water bath to eliminate the endogenous neurotransmitter.
7. Centrifuge at 21,000 × *g* during 15 min at 4 °C.
8. Discard the supernatant and either use immediately or store the pellet at −80 °C until used.

3.2.2 Functional Binding Assay ([^{35}S]GTPγS Binding)

1. Resuspend the pellet of the membrane fraction obtained in 3.2.1 in incubation buffer. Determine the protein concentration in the membrane sample (*see* Sect. 3.4) to know the protein amount used for the assay in order to add 45–55 μg protein/assay tube.
2. The conditions in the experiments are as follows:
   (a) Basal [^{35}S]GTPγS binding
   (b) Agonist-stimulated [^{35}S]GTPγS binding: 10^{-8} to 10^{-4} M (±)8-OH-DPAT
   (c) Antagonism of the agonist-stimulated [^{35}S]GTPγS binding: 10^{-9} to 10^{-4} M (±)8-OH-DPAT + 10 μM WAY-100,635
   (d) Nonspecific [^{35}S]GTPγS binding: 10 μM GTPγS
3. Prepare 700 μL of 1 nM [^{35}S]GTPγS.
4. Prepare 1:10 serial dilutions of (±)8-OH-DPAT: 10^{-8} to 10^{-3} M and 100 μM WAY-100,635 using incubation buffer.
5. Prepare 100 μM GTPγS (as indicated in 2.1.3) for the "nonspecific" condition.
6. Set a rack of 48 polypropylene 5 mL tubes for each condition: six basal, six nonspecific binding, three for each (±)8-OH-DPAT concentration, and three for each (±)8-OH-DPAT concentration + WAY-100,635. Pipette as indicate in Table 6.3 (*see* **Note 16**).
7. Incubate for 30 min at 30 °C in a thermostatic shaking water bath.
8. During the incubation time, pre-soak GF/C Whatman glass fiber filters in washing buffer for 5 min (*see* **Note 18**).
9. Place the GF/C Whatman glass fiber filter in the Brandel harvester, and continue as indicated in **steps 8–12** of Sect. 3.1.2.

3.3 Protein Determination

1. In a 96-well plate, pipette 5 μL of BSA standards of known concentration, with water as blank, and 2.5 and 5 μL of the membrane samples used in the binding experiments. All the samples should be in triplicate.
2. Add 25 μL reagent A of the DC™ protein assay (BioRad).

Table 3
Description of the volumes to pipette into each tube condition in an experiment of functional binding assay

[^{35}S]GTPγS binding assay	Basal (μL)	Agonist (μL)	Agonist + antagonist (μL)	Nonspecific (μL)
Buffer	200	175	150	175
GTPγS (10^{-4} M)	–	–	–	25
(±)8-OH-DPAT (10^{-8} – 10^{-3} M)	–	25	25	–
WAY-100,635 (10^{-4} M)	–	–	25	–
[^{35}S]GTPγS (1 nM)	25	25	25	25
Membranes	25	25	25	25

3. Add 200 μL reagent B of the DC™ protein assay (BioRad).
4. Wait 5 min and quantify at 750 nm wavelength in a plate reader (Mithras LB 940).
5. For the analysis of the optical density values (OD), we should subtract the mean of the blank OD from all the OD values obtained of the rest of the samples.
6. In a GraphPad program sheet, the standard curve OD values are represented in the y-axis and the protein concentration presented in milligrams per mL (mg/mL of protein) in the x-axis. The values are adjusted to a linear regression, setting the blank to 0, and the unknown values for mg/protein are interpolated from the standard curve.

3.4 Data Analysis and Graphical Representation

3.4.1 Analysis of Receptor Binding Assays

The interaction of a ligand with its receptor follows the law of mass action since this interaction is not linear with respect to ligand concentration, protein (receptor) concentration, or time of interaction [5]; therefore, a nonlinear regression analysis is the most accurate mathematical method to analyze data from receptor binding assays.

In saturation assays, binding of a radioligand is measured at equilibrium and analyzed to determine K_D (dissociation constant) and Bmax (receptor expression level). K_D is the concentration where 50 % of the receptors are labeled and reflects the affinity of the receptor for the radioligand. Bmax represents the maximal number of specific binding sites (receptors) labeled by the radioligand. In competition assays, binding is also measured at equilibrium, and two main kinetic parameters are determined, IC_{50} (inhibitory concentration 50) which is the concentration of the unlabelled ligand that displaces the radioligand from half of the specific binding sites, and Ki, the affinity of the competitor for the receptor [6] using the program EBDA/LIGAND or GraphPad Prism [7] (*see* **Note 20**).

Analysis of Saturation Binding Data

Saturation curves are obtained by plotting total, specific, and nonspecific binding dpm values (y-axis) against the real concentration of the radioligand used in the assay (x-axis) (Fig. 1). To obtain the specific binding dpm values, the nonspecific binding data for each radioligand concentration should be subtracted from the total binding data of that radioligand concentration. Real concentrations must be plotted by converting the dpm of each radioligand concentration sample to nanomolar concentration. This can be done using QuickCalcs (GraphPad) http://www.graphpad.com/quickcalcs/radcalcform/.

An example of a saturation isotherm for the binding of [^{3}H]8-OH-DPAT in rat hippocampus is shown in Fig. 1, The dpm mean ± SEM of total, specific, and nonspecific binding for each real

a

Radioligand (nM)	Total binding (dpm) Mean ± S.E.M.	n	Non-specific binding (dpm) Mean ± S.E.M.	n	Specific binding (dpm) Mean ± S.E.M.	n
0.2	190 ± 99	3	20 ± 10	3	170 ± 110	3
0.3	320 ± 120	3	50 ± 12	3	270 ± 100	3
0.6	487 ± 140	3	70 ± 23	3	417 ± 99	3
1.3	820 ± 99	3	90 ± 35	3	730 ± 120	3
2.5	1283 ± 150	3	150 ± 44	3	1133 ± 140	3
5.0	1480 ± 120	3	180 ± 66	3	1300 ± 99	3
10.0	2000 ± 99	3	400 ± 99	3	1600 ± 150	3
20.0	2300 ± 190	3	600 ± 110	3	1700 ± 120	3

c

Nonlin fit	A Specific binding Y
One site -- Specific binding with Hill slope	
Best-fit values	
Bmax	1867
h	0.9981
Kd	1.872
Std. Error	
Bmax	192.2
h	0.1964
Kd	0.5652
95% Confidence Intervals	
Bmax	1468 to 2267
h	0.5896 to 1.407
Kd	0.6967 to 3.048
Goodness of Fit	
Degrees of Freedom	21
R square	0.9143
Absolute Sum of Squares	709582
Sy.x	183.8
Number of points	
Analyzed	24

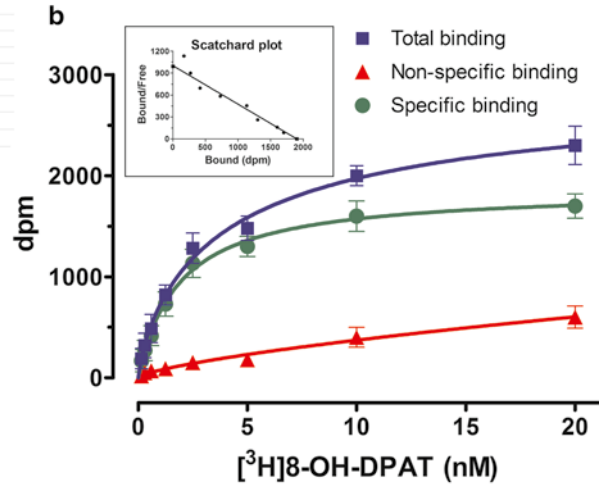

Fig. 1 *Estimation of Bmax and KD for* [^{3}H]8-OH-DPAT in rat hippocampal membranes (*receptor saturation assay)*. In (**a**), a table with the total, nonspecific, and specific binding values for each real radioligand concentration is shown (as mean ± SEM of dpm from triplicates). Note that the specific binding is calculated by subtracting the nonspecific binding data from the total binding data for each radioligand concentration. In (**b**), the dpm from *total* (■), *nonspecific* (▲), and *specific* (●) binding has been plotted against increasing concentrations (*nM*) of the radiolabeled ligand. Note that nonspecific binding is linear and not saturable, whereas specific binding reaches a plateau (an approximation of the Bmax). Insert represents the Scatchard transformation of the data from (**a**), the slope represent $-1/K_D$, and the intercept at the x-axis is an estimate of Bmax. However, K_D and Bmax are usually estimates by nonlinear regression curve fit, as shown in (**c**). In our representative assay, [^{3}H]8-OH-DPAT binds with high affinity (*KD* = 1.87) and in a saturable manner (Bmax = 1867 dpm; 37,340 fmol/mg protein) to one binding site (Hill slope = 0.998)

radioligand concentration is displayed in Fig. 1a. The values of dpm for total, specific, and nonspecific binding are plotted (y-axis) against increasing concentrations of the radiolabeled ligand (real radioligand concentration, x-axis) (Fig. 1b). Note that nonspecific binding is linear and not saturable, whereas specific binding reaches a plateau (an approximation of the Bmax). Fitting of specific dpm to a nonlinear, one site-specific binding with Hill slope in GraphPrism provides estimates of the number of receptors (Bmax) as well as the concentration of [^{3}H]8-OH-DPAT that labels half of the receptors (K_D). In our representative assay, [^{3}H]8-OH-DPAT binds with high affinity ($KD = 1.87$) and in a saturable manner (Bmax = 1867 dpm) to one binding site (Hill slope = 0.998) (Fig. 1c).

Bmax values are usually given as femtomoles per mg of protein (fmol/mg protein) after the determination of the amount of protein present in the tissue sample. Firstly, calculate the dpm/fmol of the radioligand used in the experiment (in our example, [^{3}H]8-OH-DPAT, with an specific activity of 142 Ci/mmol):

$$\frac{142\ \text{Ci}}{\text{mmol}} \times \frac{2.2x10^{12}\ \text{dpm}}{\text{Ci}} \times \frac{\text{mmol}}{10^{12}\ \text{fmol}} = 312.4\ {}^{\text{dpm}}\!/_{\text{fmol}}$$

Then apply this value to the dpm values obtained in the saturation assay to obtain the fmol values for each experimental condition. Finally, divide the fmols obtained by the protein amount present in each test tube (45–55 μg protein) to know the fmol/mg protein. In our example shown in Fig. 1, specific [^{3}H]8-OH-DPAT binding yielded a Bmax = 1867 dpm that corresponds to 37,340 fmol/mg protein (50 μg protein/assay). You can also use "chemical and radiochemical calculators" from GraphPad software website (see http://www.graphpad.com/quickcalcs/radcalcform/).

Analysis of Competition Binding Data

Competition curves are obtained by plotting specific binding as a percentage of total binding versus the log concentration of the competing ligand. Figure 2 shows a representative competition assay in which the specific binding of 2 nM [^{3}H]8-OH-DPAT to 5-HT$_{1A}$ receptors is inhibited by the selective 5-HT$_{1A}$ receptor antagonist WAY-100,635, but not by fluoxetine (a selective serotonin reuptake inhibitor with no affinity for 5-HT$_{1A}$ receptors, Fig. 2a). Data are analyzed with GraphPrism using nonlinear regression (fitting to a One site-Fit Ki, Fig. 2b) in which the concentration and the K_D for the radioligand (hot) are known and constant. The fitting allows us to determine the inhibition constant (Ki) and inhibitory concentration 50 (IC_{50}) of the unlabelled ligand. The analysis assumes that there is only one binding site and that the binding is reversible and at equilibrium. In some cases, the competitor ligand may displace the specific radioligand binding in a biphasic manner, indicating either two binding sites or allosteric modulation. In our example, WAY-100,635, but not fluoxetine,

a

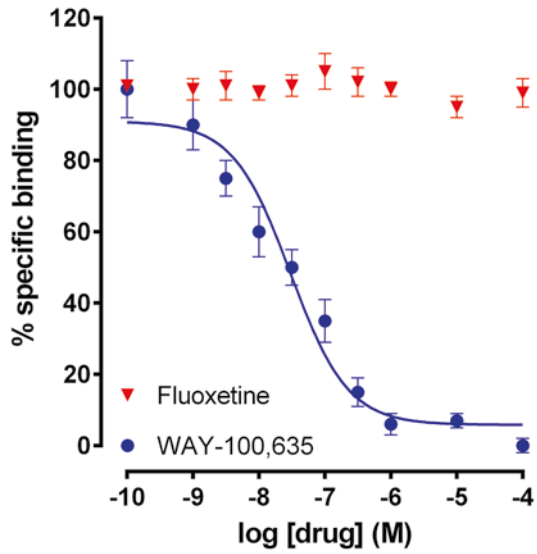

b

Nonlin fit	A	B
	WAY-100,635	Fluoxetine
	Y	Y
1 One site - Fit Ki [2]		Not converged
2 Best-fit values		
3 logKi	-8.038	
4 HotNM	= 2.000	
5 HotKdNM	= 1.900	
6 Bottom	7.894	
7 Top	= 100.0	
8 Ki	9.160e-009	
9 Std. Error		
10 logKi	0.08930	
11 Bottom	3.189	
12 95% Confidence Intervals		
13 logKi	-8.221 to -7.855	
14 Bottom	1.363 to 14.42	
15 Ki	6.012e-009 to 1.396e-008	
16 Goodness of Fit		
17 Degrees of Freedom	28	
18 R square	0.9144	
19 Absolute Sum of Squares	3272	
20 Sy.x	10.81	
21 Constraints		
22 HotNM	HotNM = 2.000	HotNM = 2.000
23 HotKdNM	HotKdNM = 1.900	HotKdNM = 1.900
24 Top	Top = 100.0	Top = 100.0
25		
26 Number of points		24
27 Analyzed	30	30

Fig. 2 Competition curves of 2nM [^{3}H]8-OH-DPAT binding in rat hippocampal membranes. Note how specific [^{3}H]8-OH-DPAT binding was totally inhibited by WAY-100,635 in a concentration-dependent manner (**a**). Nonlinear regression analysis (**b**) shows a high affinity of WAY-100,635 to 5-HT$_{1A}$ receptors (*Ki* = 9.2 nM). By contrast, fluoxetine did not displace specific [^{3}H]8-OH-DPAT binding. Data points are mean ± SEM of triplicate determinations from two representative experiments

completely displaced specific [^{3}H]8-OH-DPAT binding, with a *Ki* = 9.2 nM. These values are consistent with its high affinity to 5-HT$_{1A}$ receptors.

3.4.2 Analysis of [^{35}S] GTPγS Binding Assays

The [^{35}S]GTPγS binding curves are obtained by plotting ligand-induced-specific binding against the log concentration of the ligand used in the assay (agonist or inverse agonist). Nonspecific mean values are subtracted from the other experimental conditions (basal and ligand conditions). Those "specific" values are then referred to basal binding values (100 %). The Emax, maximal response, is usually expressed as % of agonist-induced stimulation of [^{35}S]GTPγS binding over basal binding (100 %). The EC$_{50}$ is the concentration to produce a half-maximal response (Fig. 3b). In the case of antagonists, *K*i values may be determined by two means: an agonist concentration–response curve in the presence of a fixed antagonist concentration (rightward curve shifts) or an antagonist concentration–response curve run at a fixed agonist concentration [8].

In Fig. 3, the analysis (Fig. 3b) and graphical of data (Fig. 3a) obtained from a representative assays using (±)8-OH-DPAT to stimulate [^{35}S]GTPγS binding as described in the methods section are shown (*see* Sect. 3.2.2). Data analysis (nonlinear log[agonist] vs. response–variable slope; GraphPrism,) revealed an Emax = 137.6 %

a

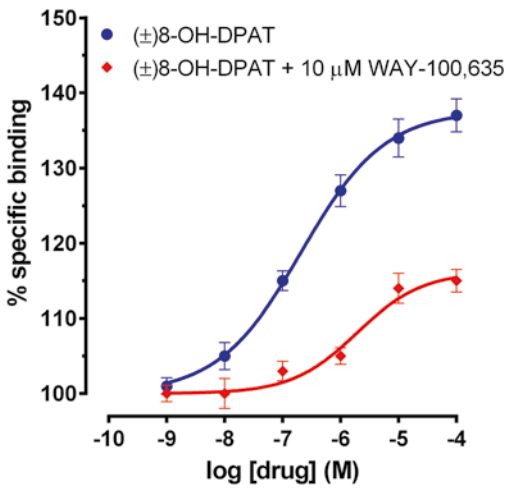

b

	Nonlin fit	A (±)8-OH-DPAT Y	B (±)8-OH-DPAT + 10 μM WAY-100,635 Y
1	log(agonist) vs. response -- Variable slope		
2	Best-fit values		
3	Bottom	= 100.0	= 100.0
4	Top	137.6	116.2
5	LogEC50	-6.680	-5.716
6	HillSlope	0.6059	0.7703
7	EC50	2.089e-007	1.924e-006
8	Span	= 37.64	= 16.19
9	Std. Error		
10	Top	1.826	2.249
11	LogEC50	0.1334	0.2965
12	HillSlope	0.08957	0.3092
13	95% Confidence Intervals		
14	Top	133.7 to 141.6	111.4 to 121.0
15	LogEC50	-6.966 to -6.394	-6.352 to -5.080
16	HillSlope	0.4138 to 0.7980	0.1071 to 1.434
17	EC50	1.081e-007 to 4.038e-007	4.449e-007 to 8.321e-006
18	Goodness of Fit		
19	Degrees of Freedom	14	14
20	R square	0.9680	0.8759
21	Absolute Sum of Squares	106.5	85.11
22	Sy.x	2.758	2.466
23	Constraints		
24	Bottom	Bottom = 100.0	Bottom = 100.0
25			
26	Number of points		
27	Analyzed	17	17
28			

Fig. 3 [^{35}S]GTPγS binding in rat hippocampal membranes. Stimulation of [^{35}S]GTPγS binding by increasing concentrations of (±)8-OH-DPAT and its inhibition by 10 μM WAY-100,635. Data points (mean ± SEM of triplicate determinations from two representative experiments) fit to a nonlinear adjust (**a**), and theoretical Emax (top) and EC_{50} are calculated from the adjust (**b**). In our example, the Emax = 137.6 % with a EC_{50} 0.21 μM of (±)8-OH-DPAT is shifted rightward Emax = 116.2 % with a EC_{50} 1.9 μM

versus basal binding and $pEC_{50} = 6.7$ for (±)8-OH-DPAT-induced stimulation of [^{35}S]GTPγS binding. The specificity of the response was confirmed by the inhibition (±)8-OH-DPAT-induced stimulation of [^{35}S]GTPγS binding in the presence of a fixed concentration of WAY-100,635 (selective 5-HT_{1A} receptor antagonist; 10 μM).

4 Notes

1. Nonspecific binding unlike specific binding does not saturate with increasing radioligand concentrations. For nonspecific binding, it is recommended to choose a ligand that is different than the radioligand.
2. ^{3}H, ^{35}S, and ^{125}I are the most used isotopes in these binding experiments. ^{3}H radioisotopes present low energy but long half-life, while the other two exhibit high energy but shorter half-life. The low energy of ^{3}H confers to the radioligand a great stability, while other high energetic isotopes produce the degradation of the radioligand molecule.
3. There are some useful website databases displaying the radioligands used for different receptors. Among them, the most used are the International Union of Basic and Clinical Pharmacology (IUPHAR) website (http://www.guidetophar-

macology.org/) and the Special Issue "The Concise Guide to PHARMACOLOGY 2013/14," containing articles as "The Concise Guide to PHARMACOLOGY 2013/14: G Protein-Coupled Receptors," "The Concise Guide to PHARMACOLOGY 2013/14: ligand-gated channels," and "The Concise Guide to PHARMACOLOGY 2013/14: transporters" (http://onlinelibrary.wiley.com/doi/10.1111/bph.2013.170.issue-8/issuetoc), edited by the British Journal of Pharmacology [9].

4. Preliminary experiments are necessary to optimize binding buffer composition in order to optimize the binding and avoid the degradation of the radioligand, peptides, or proteins from the sample: Salt and protein concentration should be adjusted, and other reagents as pargyline (monoamine oxidase inhibitor), ascorbic acid (antioxidant), chelating agents (ethylene glycol tetraacetic acid, EGTA, or ethylene diamine tetraacetic acid, EDTA), protease inhibitors (leupeptin or phenylsulfonyl, PMSF), etc., can also be added to the buffer.
5. The [^{35}S]GTPγS incubation buffer should contain Na^+ and Mg^{2+} to minimize the basal [^{35}S]GTPγS binding. The Mg^{2+} ions also keep the receptor in its high affinity state conformation.
6. High GDP concentration is used to reduce basal [^{35}S]GTPγS binding, as the GDP prevents the binding of [^{35}S]GTPγS to the non-heterotrimeric G protein, leading to inactive G proteins.
7. The basal binding results from the activation of different receptors, but the activation of adenosine A_1 receptors by endogenous adenosine are the most relevant. In order to decrease the basal [^{35}S]GTPγS binding values, the enzyme adenosine deaminase or A_1 antagonists in the incubation buffer are included, improving the signal-to-noise ratio.
8. Reagents/drugs are usually prepared at 1 mM in distilled water, and aliquots can be stored at −20 °C (i.e., 1 mM GTPγS aliquots). Other reagents as 5-HT, dopamine, etc. should be freshly prepared. Therefore, check the reagent solubility specifications and stability in the corresponding technical datasheet. Remember that serial dilutions used in the assay must be prepared using the assay buffer.
9. Research use of radioactive materials and disposal of radioactive waste are regulated by government agencies. Be sure that you follow the governmental regulations of your country. Take into account a radioactive waste minimization plan.
10. In general, it is better to choose a radioligand with a high specific activity. The specific activity indicates the amount of radioactivity per molecule of ligand and is usually given in units of

Curies per millimole (Ci/mmol) of ligand. For ^{3}H ligands, the specific activity of the ligand should be over 20 Ci/mmol. The maximal theoretical specific activity per tritium is 29 Ci/mmol. For ^{125}I-labeled ligands, a specific activity of 2200 Ci/mmol means that there is a ^{125}I labeling site per ligand molecule, and 4400 Ci/mmol means two ^{125}I labelings per ligand molecules.

11. The radioactive decay or the disintegration of the isotope is defined as the spontaneous disintegration of a radionuclide with the emission of energetic particles or radiation. The rate of decay is measured in terms of its half-life or $t_{1/2}$ which is the time taken for the activity of a given amount of a radioactive substance to decay to half of its initial value. It may not be very important for ^{3}H-ligands, as it is 12.5 years, but the decay should be taken into account for other isotopes as ^{35}S (87 days) or ^{125}I (60 days). To calculate the fraction of isotope remaining in your radioactive stock solution, you have to use the following formula:

$$\text{Decay factor} = e^{-(0.693/t_{1/2})\times\text{time}}$$

In this formula, the time is the number of days since the radioligand was calibrated. Multiply the decay factor by the concentration on the calibration date (for [^{35}S]GTPγS is 12.5 mCi/mL). The amount of radioligand needed to prepare the radioligand solution should be calculated with the corrected concentration of radioligand.

There are several websites with decay calculators (http://www.radprocalculator.com/Decay.aspx; http://www.hse2.ubc.ca/rad/Calc/calcframe.htm) and iPad, iPhone, and Apple Apps for radiochemical calculations (http://www.perkinelmer.com/Resources/TechnicalResources/ApplicationSupportKnowledgebase/radiometric/calculations.xhtml#Radiochemicalcalculations-app).

12. ^{3}H and ^{35}S release beta energy, which can be measured on an scintillation counter after the addition of liquid scintillation cocktail. The beta energy interacts with the scintillation liquid to produce photons, which are measured by the detector. For ^{125}I that emits both beta-like energy and gamma energy, it can also be used as gamma counter.

13. Binding studies can be also performed on mammalian cell lines, harvesting the cells using a cell scraper (CLS3008 Corning®). The culture cells are centrifuged at 300 × *g* for 5 min at 4 °C, and the pellet is washed using PBS and centrifuged at 300 × *g* for 5 min at 4 °C. The cell pellet can be stored at −80 °C until used.

14. In our laboratory, animals are sacrificed by decapitation since pentobarbital or any other anesthetics may interfere in the results.
15. Glass tubes pretreated with Sigmacote® (Sigma-Aldrich) are used instead of propylene tubes, when working with some high lipophilic radioligands such as [^{3}H]CP 55,940 (to label cannabinoid CB1 receptors) due to its attachment to the labware.
16. Work with radioactive materials in appropriate facilities; monitor yourself and your work area for contamination. The best way to control potentially hazardous radioactive materials is at the source; however, protective clothing provides a good level of secondary protection. Do not wear sandals or open toe shoes, and you should wear gloves and lab coat. A polymethyl methacrylate (PMMA) bench top Beta Shield is used when working with beta-emitting isotopes to avoid any radiation hazards. In the case of ^{125}I-radioligands, an X-ray protective lead glass or radiation shielding must be used. The addition of the different incubation components in the reaction tubes should be as described: buffer, ligand/s, radioligand, and to finish with the membranes. This order would minimize radioactivity contamination, and subsequently, it would produce less radioactive waste disposal. All the contaminated materials should be discarded in the appropriate containers for solid or liquid radioactive waste. Radioactive wastes containing radionuclides with short half-life are commonly stored and allowed to decay prior to its elimination as nonradioactive waste.
17. The preparation of the binding should be performed at 4 °C. For some specific receptors, the incubation temperature should be also 4 °C to prevent the radioligand degradation.
18. The filtration step can be performed with GF/B or GF/C filters depending on the receptor studied. The difference between both filter types is the pore size: 1 μm for GF/B and 1.2 μm for GF/C. The GF/B or GF/C filters can be pretreated with a solution of 0.1–0.5 % (v/v) polyethylenimine (PEI) in washing buffer to reduce the radioligand binding to the filters, as the neutral charge of the PEI can compensate the negative charge of the glass fiber filter. [^{35}S]GTPγS binding experiments should not be treated with PEI. Coating filters with BSA reduces nonspecific binding. Including BSA, salts or detergents in the wash or binding buffer can also help reduce nonspecific binding.
19. In radioactive ligand binding assays (both receptor and [^{35}S]GTPγS binding assays), the separation of the bound ligand from the free ligand can be performed either by centrifugation, dialysis, or gel filtration. However, the most widely used pro-

cedure is filtration, either on a vacuum manifold or by a cell harvester. In recent years, the scintillation proximity assay (SPA technology) has been developed that requires no separation step and allows the design of high-throughput receptor binding assays [10].

20. Different computer programs are available for this purpose: EBDA/LIGAND [7]. Recently, easy-to-use software packages, for both Mac and Windows computers, combine scientific graphing, comprehensive curve fitting (nonlinear regression), understandable statistics, and data organization (GraphPad Prism from GraphPad Software, San Diego, CA, http://www.graphpad.com/scientific-software/prism/, and SigmaPlot from Systat Software, San José, CA, http://www.sigmaplot.com/).

Acknowledgments

This work was supported by Ministerio de Ciencia, SAF07-61862; Ministerio de Economia y Competitividad, SAF2011-25020; and Instituto de Salud Carlos III.

References

1. Yamamura HI, Enna SJ, Kuhar MJ (1990) Methods in neurotransmitter receptor analysis. Raven, Nueva York
2. Selley DE, Stark S, Sim LJ, Childers SR (1996) Cannabinoid receptor stimulation of guanosine-5'-O-(3-[35S]thio)triphosphate binding in rat brain membranes. Life Sci 59:659–668
3. Harrison C, Traynor JR (2003) The 35S GTP-gamma-S binding assay: approaches and applications in pharmacology. Life Sci 74:489–508
4. Snyder SH, Bennett JP Jr (1976) Neurotransmitter receptors in the brain: biochemical identification. Annu Rev Physiol 38:153–175
5. Kenakin TP (1997) The pharmacologic analysis of drug receptor interaction, 3rd edn. Lippincott-Raven, New York
6. Cheng Y, Prusoff WH (1973) Relationship between the inhibition constant (K1) and the concentration of inhibitor which causes 50 per cent inhibition (I50) of an enzymatic reaction. Biochem Pharmacol 22:3099–3108
7. Munson PJ, Rodbard D (1980) Ligand: a versatile computerized approach for the characterization of ligand binding system. Anal Biochem 107:220–239
8. Strange PG (2010) Use of the GTPγS ([35S] GTPγS and Eu-GTPγS) binding assay for analysis of ligand potency and efficacy at G protein-coupled receptors. Br J Pharmacol 161:1238–1249
9. Alexander SPH, Harmar AJ (eds) (2013) Concise guide to pharmacology 2013/14. Br J Pharmacol 170(8):1449–1458.
10. DeLapp NW (2004) The antibody-capture [(35)S]GTPgammaS scintillation proximity assay: a powerful emerging technique for analysis of GPCR pharmacology. Trends Pharmacol Sci 25:400–401

Chapter 7

Recombinant Alphavirus-Mediated Expression of Ion Channels and Receptors in the Brain

Markus U. Ehrengruber and Kenneth Lundstrom

Abstract

Ectopic gene transfer has been a crucial method for neurobiological studies aiming to resolve the function of specific membrane and non-membrane proteins. For this purpose, expression vectors based on Semliki Forest virus, Sindbis virus, and Venezuelan equine encephalitis virus, all members of the alphavirus genus, have been engineered in the form of naked RNA replicons, recombinant viral particles, and layered DNA vectors. By applying these alphaviral vectors to mammalian cell lines, large quantities of integral membrane proteins including ligand- and voltage-gated ion channels as well as G protein-coupled receptors have been expressed, and their functional activity confirmed by both electrophysiological recordings and coupling to G proteins. Furthermore, alphavirus vectors have provided efficient delivery tools for high-level expression of recombinant proteins in cultures of primary neurons and organotypic hippocampal slices as well as upon intracranial injection, in vivo in rodent brain. This chapter describes the generation of infectious but replication-deficient Semliki Forest virus and Sindbis virus particles that are useful for the efficient transduction of neurons in vitro, in situ, and in vivo.

Key words Semliki Forest virus, Sindbis virus, Recombinant protein, Voltage-gated sodium channel, G protein-coupled receptor, Cell line, Primary neuron, Hippocampal slice, Rodent

1 Introduction

Integral membrane proteins including G protein-coupled receptors (GPCRs) and ion channels represent the largest group of drug targets [1, 2]. In contrast to the classic monitoring of ligand binding, much emphasis has recently been given to functional assays such as coupling to G proteins for GPCRs and electrophysiological recordings for ion channels. In this context, efficient gene delivery vectors have become crucial. Among the various vector systems engineered, alphavirus-based vectors have provided efficient gene delivery both in vitro and in vivo and have furthermore generated high transient expression levels of recombinant proteins [3]. Particularly high expression levels of integral membrane proteins have been obtained in mammalian cell lines [4]. Another favorable

Rafael Luján and Francisco Ciruela (eds.), *Receptor and Ion Channel Detection in the Brain: Methods and Protocols*, Neuromethods, vol. 110, DOI 10.1007/978-1-4939-3064-7_7,

feature of alphaviruses is the high preference for transient gene expression in primary neurons [5] and in neurons in hippocampal slice cultures [6].

Alphaviruses are enveloped positive-sense, single-stranded RNA viruses belonging to the Togaviridae family [7]. Among the ~30 members of alphaviruses, Semliki Forest virus (SFV) [8], Sindbis virus (SIN) [9], and Venezuelan equine encephalitis virus (VEE) [10] have been subjected to the engineering of various vectors for recombinant protein expression. In principle, three types of expression systems have been developed. The most commonly used version is based on *replication-deficient recombinant viral particles*, which requires the use of two vectors (Fig. 1a). The expression vector hosts the alphavirus nonstructural genes nsP1-4, the subgenomic 26S promoter, and the gene of interest (Fig. 2). The helper RNA provides the viral structural proteins required for particle production. The generated viral particles are replication-deficient because mainly RNA from the expression vector will be packaged due to the presence of a packaging signal. There is, however, the potential of recombination leading to the formation of full-length infectious virion RNA and to reduce this possibility second-generation helper vectors providing only conditionally infectious particles have been introduced [11]. Prevention of viral recombination can be achieved by using split helper vectors, where the alphavirus capsid and membrane protein genes have been placed on separate helper vectors [12, 13]. Application of replication-deficient alphavirus particles provides high transduction rates in a broad range of host cells and generates high levels of recombinant protein expression of a transient nature under high biosafety conditions.

Replication-proficient recombinant viral particles are generated from a full-length alphavirus genome including an additional subgenomic promoter and the gene of interest, which can be introduced in different regions of the vector (Fig. 1b) [9, 14]. These viral particles provide high-level recombinant protein expression and further production of new infectious viral particles. Utilization of replication-proficient particles extends the duration of recombinant protein expression and improves particularly in vivo gene delivery. However, due to the generation of virus progeny, caution needs to be paid to potential biosafety risks. Alternatively, *layered DNA recombinant vectors* have been engineered, where an upstream DNA polymerase type II promoter initially drives the expression of the alphavirus replicase genes as well as the gene of interest (Fig. 1c) [15]. This type of vector is applied directly as DNA plasmids for transfection of mammalian host cells. The presence of the replicase complex provides the means for high recombinant protein expression, but this technique is compromised by the restricted plasmid DNA transfection efficacy in comparison to viral transduction. However, due to the lack of the alphavirus structural protein

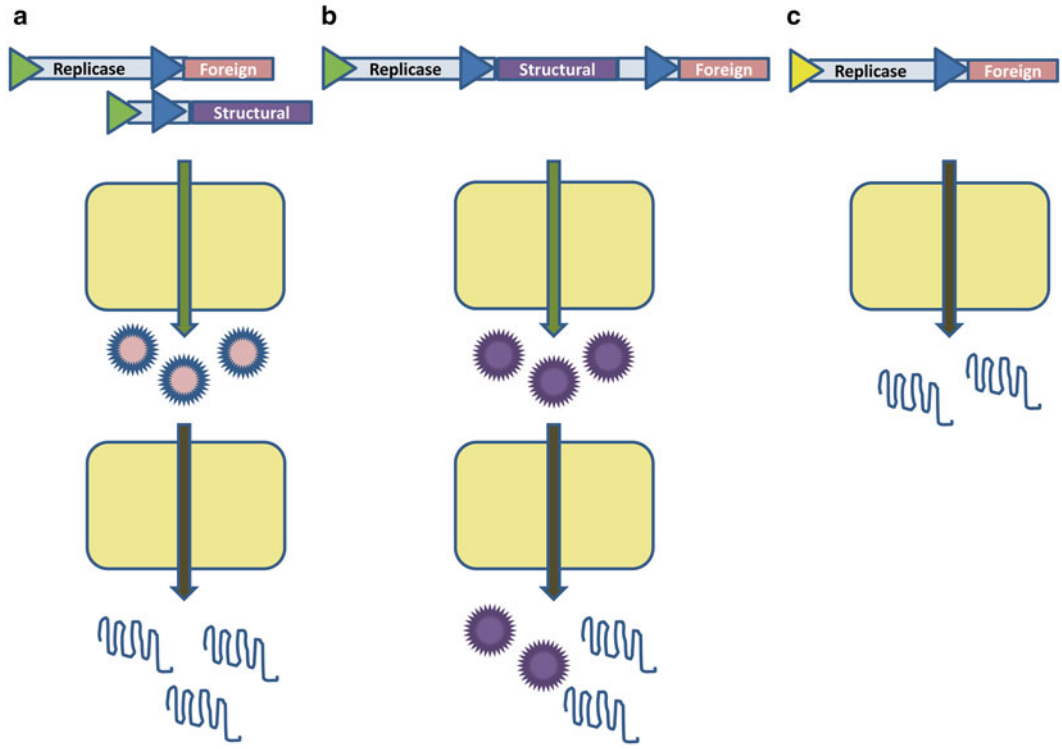

Fig. 1 Different alphavirus vector systems. (**a**) *Replication-deficient vector system:* In vitro transcribed RNA molecules from both the expression vector – carrying the genes for the replicase complex as well as the gene of interest (foreign) – and the helper vector (containing the structural protein genes) are co-transfected into host cells. Mammalian cells are infected with the resulting recombinant particles (that lack the structural protein genes) for high-level recombinant protein expression. (**b**). *Replication-proficient vector:* In vitro transcribed full-genome-length RNA including the gene of interest (foreign) is transfected into host cells, which generate fully replication-competent viral particles. After infection of mammalian cells, recombinant proteins are expressed and new infectious virus progeny will be produced. (**c**). *DNA-layered vectors:* Transfection of mammalian host cells with a DNA expression vector carrying the nonstructural protein genes under the control of a ubiquitous (e.g., cytomegalovirus) or cell type-specific promoter (*yellow arrowhead*) as well as the gene of interest (foreign) results in recombinant protein expression. Green arrowheads indicate the SP6 RNA polymerase promoter, and blue arrowheads illustrate the endogenous alphaviral 26S subgenomic promoter

genes, the use of layered DNA recombinant vectors eliminates any risk of generation of infectious viral particles and therefore ensures the highest possible biosafety level.

The broad host range of alphaviruses has allowed efficient gene delivery not only to mammalian cell lines but also to a number of primary cell cultures. Particularly, neuronal cells have shown a high susceptibility to both SFV and SIN particles, thus rendering alphaviruses useful in neuroscience. For instance, SFV vectors have provided up to 90 % infection rates in cultured primary neurons, resulting in high-level transgene expression [16]. Moreover, injection of SFV and SIN particles into rat organotypic hippocampal

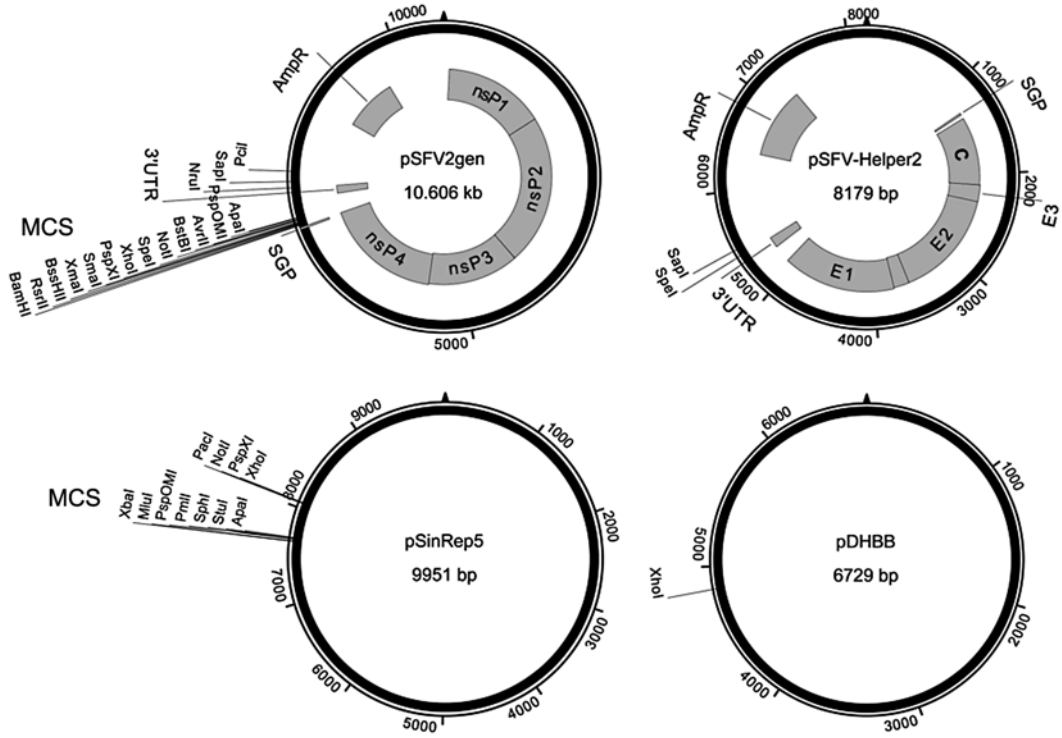

Fig. 2 Alphavirus plasmid maps. SFV expression vector (pSFV2gen) and helper vector (pSFV-Helper2). SIN expression vector (pSinRep5). There are several different SIN helper plasmids, and the choice of which one to use would depend on both the replicon and source of cells [9, 32]. Unique restriction sites for the multiple cloning sites (MCS) and to linearize the plasmids for in vitro transcription are shown; triangles at position zero indicate the location of the SP6 promoter for in vitro transcription. *AmpR* ampicillin resistance gene (β-lactamase), *C* capsid protein gene, *E1, E2, E3 envelope* glycoprotein genes, *nsP* nonstructural protein gene, *SGP* alphaviral subgenomic promoter (driving the expression of the transgene and of the structural protein genes for the vector and helper plasmids, resp.), *3'UTR* alphaviral 3'-nontranslated region including the poly-A tail sequence

slice cultures has provided efficient gene delivery to neurons in situ [6]. When expression was monitored in slices infected with wild-type SFV and SIN encoding the green fluorescent protein (enhanced GFP), more than 90 % of the GFP-positive cells were pyramidal neurons (Fig. 3). Viability of the transduced neurons was confirmed up to 2–5 days post-infection by using propidium iodide exclusion [6] and electrophysiological assays [17]. A less cytotoxic SFV mutant caused a strong temperature-dependent preference for transgene expression in interneurons rather than pyramidal cells [16]. And the SFV(PD) mutant vector not only caused lower cytotoxicity as well as enhanced and prolonged transgene expression but also higher superinfection, which is useful for transduction of neurons with protein multimers [18, 19]. Finally, the SFV(A774nsP) vector, which is based on the A7(74)

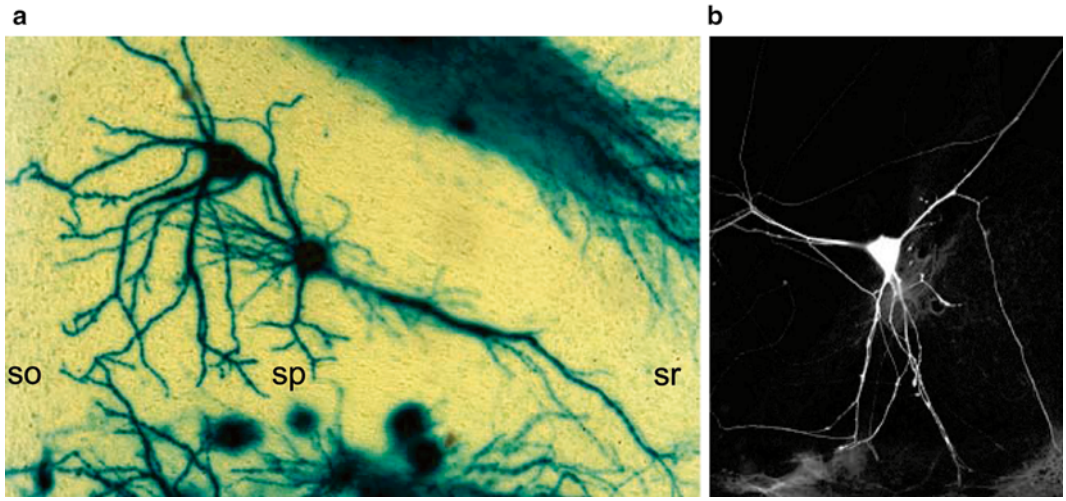

Fig. 3 Alphaviral transduction of neurons in brain slice cultures and of dissociated hippocampal neurons. (**a**). SIN-mediated expression of β-galactosidase (as visualized by X-gal staining, blue) in CA3 pyramidal cells from an organotypic rat hippocampal slice. The hippocampal slice was obtained from a postnatal day 6 rat, cultured for 14 days, and fixed and stained at one day post-infection. so, stratum oriens; sp, stratum pyramidale; sr, stratum radiatum. (**b**) Fluorescence microscopic image showing SFV(PD)-mediated expression of GFP-tagged tau protein in a pyramidal neuron from dissociated hippocampal cells prepared from postnatal day 5 rats, cultured for 19 days, and imaged at one day post-infection

strain, showed temperature-dependent expression in cultured hippocampal neurons and organotypic slices, specifically providing transgene expression in glial cells at 37 °C but neurons at 31 °C [14].

Alphavirus vectors, particularly replication-deficient particles derived from the SFV4 strain [8], have been frequently applied to ectopically express a number of topologically different recombinant proteins [4, 8]. In this context, expression of integral membrane proteins has been of special interest. For instance, a large number of GPCRs have been overexpressed in various mammalian cell lines and subjected to ligand binding studies and functional assays (Table 1) [1, 4, 20]. The rapid virus stock production and the broad host range supported the application of infectious alphaviral particles to study GPCRs with a structural genomics approach [20, 21] that included the large-scale production of GPCRs in mammalian cells cultured in spinner flasks and bioreactors [22]. Ion channels have also been functionally expressed from SFV vectors as demonstrated by ligand binding activity and electrophysiological recordings for the serotonin 5-HT_3 receptor [23, 24] and P2X purinoreceptor [25, 26].

Alphaviral particles have been mostly used for transgenes of up to ~5 kb in size, which reconstitutes the original alphavirus genome length of 11.8 kb and thus permits efficient packaging into the viral capsids. However, SFV vectors can also be used for larger transgenes. In a study focusing on the neuronal voltage-gated sodium channels Nav1.1, Nav1.2, Nav1.3, and Nav1.6 [27], these

Table 1
Ligand binding and functional activity of integral membrane proteins expressed from SFV vectors

Membrane protein	Ligand binding	Functional assay	Reference
GPCRs			
Adrenergic α1B (α1BR) receptor	[^{125}I] HEAT	IP accumulation	[38]
Dopamine D3 receptor	[^{3}H] spiperone		[39]
Histamine H2 receptor	[^{125}I] APT	cAMP stimulation	[40]
Metabotropic glutamate receptor 2/3	[^{3}H]-LY354740		[41]
Metabotropic glutamate receptor 4	[^{3}H]-L-AP4	[γ-^{35}S]GTP binding	[42]
Neurokinin-1 receptor	[^{3}H] substance P	Ca^{2+} release	[43]
Ligand-gated ion channels			
Purinoreceptor P2X4	[^{35}S]ATPγS		[26]
Purinoreceptor P2X1/2		ATP-evoked currents	[25]
Purinoreceptor P2X4	[^{35}S]ATPγS		[26]
Serotonin 5-HT3 receptor	[^{3}H]GR65630	Electrophysiology	[23, 24]
Voltage-gated ion channels			
Sodium channel Nav 1.2		Electrophysiology	[27]
Sodium channel Nav 1.6		Electrophysiology	[27]

APT aminopotentidine, [^{125}I] *HEAT* 125iodo-2-[Beta-(4-hydroxyphenyl)-ethyl-aminomethyl]tetralone, *IP* inositol phosphate

Fig. 4 Application of SFV vectors for the overexpression of voltage-gated sodium channels (Nav). (**a**) Schematic representation of the viral genome lengths, as compared to wild-type SFV4. Bars indicate SFV nonstructural protein genes (*gray*), SFV structural protein genes or transgenes (either the fluorescent reporter gene alone or fused to a specific voltage-gated sodium channel subtype; *black*), and noncoding regions (*white*). (**b**). Viral titers for wild-type SFV particles produced at 37 °C and less cytopathic SFV(PD) particles obtained at 31 °C (means ± SD of 4–9 virus preparations per genome size and viral type). Asterisks indicate significant differences vs. the smaller genome length of 74 % (t-test, $p < 0.05$). (**c**). Transgene expression time course and level in BHK cells for wild-type SFV and less cytopathic SFV(PD) vectors (empty and filled symbols, respectively) encoding fluorescently tagged Nav1.1(E954Q), Nav1.2, Nav1.3(E897Q), and Nav1.6(E937Q) (means ± SD). The point mutations (given in parentheses) confer tetrodotoxin resistance to the Nav subtypes. (**d**). Fluorescence micrographs of BHK cells at 39–51 h after infection with less cytopathic SFV(PD) expressing the different fluorescently tagged sodium channels. (**e**). Western blot analysis for ectopic expression of EGFP-Nav1.2 (*left*) and ECFP-Nav1.6(E937Q) (*right*) in BHK cells at 1 day post-infection. A pan-anti-Nav antibody was used to detect sodium channel protein, whereas an anti-β-actin antibody was used as a control to verify the loading of similar cellular protein amounts in the different lanes. (**f**) Electrophysiological patch-clamp recordings from mouse cortical neurons overexpressing wild-type Nav1.2 (*top row*) and tetrodotoxin-resistant Nav1.2(E942Q) and ECFP-Nav1.6(E937Q) (*bottom row*). Cells were analyzed at 18–24 h after infection with SFV and SFV(PD) encoding the fluorescently tagged channels; recordings in the two bottom panels were done in 0.5 μM tetrodotoxin to isolate the ectopic sodium currents from the endogenous ones. Sample traces of sodium currents obtained upon cellular depolarization to −10 mV are shown; dashed lines represent recordings from non-fluorescent control neurons of the same culture dishes. The top right panel shows the average peak currents (means ± SD) obtained at −10 mV for uninfected control neurons ($n = 9$ cells) as well as neurons overexpressing wild-type Nav1.2 via wild-type SFV ($n = 3$) and less cytopathic SFV(PD) ($n = 3$); *asterisks* indicate significant differences vs. uninfected cells (t-test, $p < 0.05$)

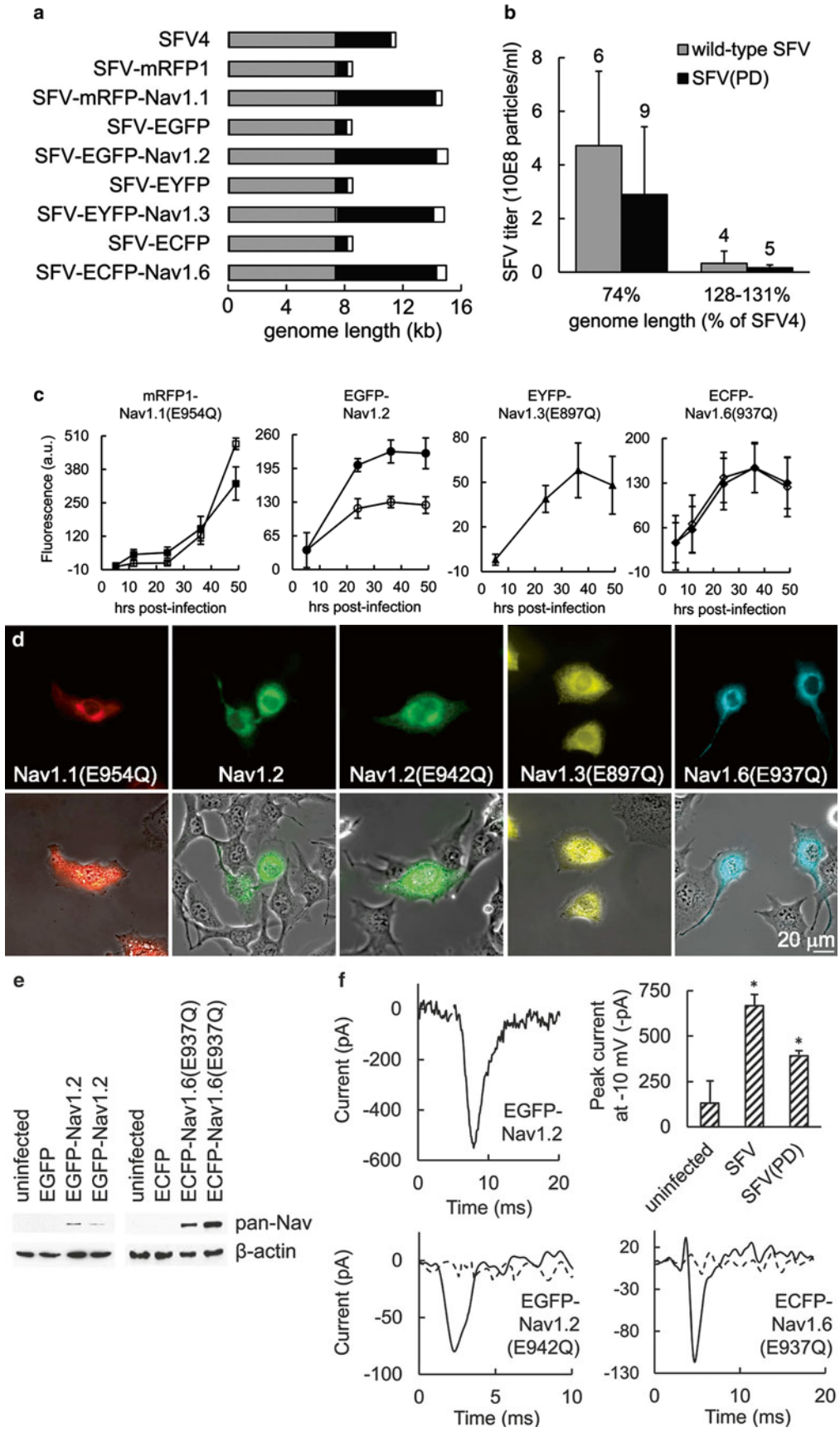
a
SFV4
SFV-mRFP1
SFV-mRFP-Nav1.1
SFV-EGFP
SFV-EGFP-Nav1.2
SFV-EYFP
SFV-EYFP-Nav1.3
SFV-ECFP
SFV-ECFP-Nav1.6
0 4 8 12 16
genome length (kb)
b
wild-type SFV
SFV(PD)
SFV titer (10E8 particles/ml)
6
9
4
5
74%
128-131%
genome length (% of SFV4)
c
mRFP1-Nav1.1(E954Q)
EGFP-Nav1.2
EYFP-Nav1.3(E897Q)
ECFP-Nav1.6(937Q)
Fluorescence (a.u.)
hrs post-infection
d
Nav1.1(E954Q)
Nav1.2
Nav1.2(E942Q)
Nav1.3(E897Q)
Nav1.6(E937Q)
20 µm
e
uninfected
EGFP
EGFP-Nav1.2
EGFP-Nav1.2
uninfected
ECFP
ECFP-Nav1.6(E937Q)
ECFP-Nav1.6(E937Q)
pan-Nav
β-actin
f
Current (pA)
EGFP-Nav1.2
Time (ms)
Peak current at -10 mV (-pA)
uninfected
SFV
SFV(PD)
EGFP-Nav1.2 (E942Q)
ECFP-Nav1.6 (E937Q)

relatively large cDNAs were fused to the differently colored fluorescent reporter genes for monomeric red fluorescent protein (mRFP), enhanced green fluorescent protein (EGFP), enhanced yellow fluorescent protein (EYFP), and enhanced cyan fluorescent protein (ECFP), respectively. The resulting ~7 kb transgenes were inserted into the SFV vector system, creating viral RNA molecules that exceeded the wild-type SFV4 genome by 28–31 % (Fig. 4a) and leading to 20-fold lower titers (Fig. 4b). Despite the reduced viral titers as a consequence of impaired packaging efficiency, the SFV particles were useful to ectopically express the voltage-gated sodium channels in baby hamster kidney (BHK) cells as assayed by fluorescence microscopy (Fig. 4c) and Western blot analysis (Fig. 4d). Most importantly, when applied to primary cultures of mouse hippocampal neurons, functional overexpression of wild-type Nav1.2 currents and tetrodotoxin-insensitive mutant Nav1.2 (E942Q) currents was achieved by both conventional SFV and less cytopathic SFV(PD), as demonstrated by electrophysiological recordings from single fluorescent neurons (Fig. 4e).

With regard to neuroscience, alphavirus vectors have demonstrated efficient delivery and strong but transient expression of reporter genes in rodent brain [28, 29]. Injection of replication-deficient SFV-LacZ particles encoding β-galactosidase into the amygdala and striatum of male Wistar rats resulted in local and transient β-galactosidase expression and no significant difference in control parameters such as body weight, temperature, exploratory behavior, and forced motor performance [28]. Similarly, injection of SIN-LacZ particles into mouse nucleus caudate/putamen and nucleus accumbens septi demonstrated high levels of β-galactosidase expression [29]. Moreover, SIN vectors have been applied for in vivo transfer of calcium/calmodulin-dependent protein kinase IV (CaMKIV) and CREB, which caused enhancement of both NMDA receptor-mediated synaptic responses and "silent synapses" that generate long-term potentiation [30].

2 Materials

The following materials are mandatory for the generation of recombinant alphaviral particles:

- SFV vectors: pSFV2gen and pSFV-Helper2 (available upon request: markus.ehrengruber@kshp.ch, lundstromkenneth@gmail.com)
- SIN vectors: pSINRep5 [31], and DH-BB or other defective helper plasmids (available from Dr. Sondra Schlesinger or Dr. Charles Rice upon request: sondra@wusm.wustl.edu, ricec@mail.rockefeller.edu). For neuronal cells, helper plasmids

containing the glycoproteins derived from TE12 virus should be used [32].

- Restriction endonucleases: *Spe*I, *Nru*I, *Sap*I (for SFV); *Xho*I, *Not*I, *Pac*I (for SIN)
- 0.8 % agarose gel
- 25:24:1 (v/v/v) phenol/chloroform/isoamyl alcohol
- 3 M sodium acetate
- 70 and 95 % ethanol
- 10 × transcription buffer for SFV (below) and commercial 5 × transcription buffer provided with the SP6 polymerase for SIN
  - 10 mM $m^7G(5')ppp(5')G$ sodium salt (Pharmacia or New England Biolabs)
  - 50 mM dithiothreitol (DTT)
  - rNTP mix (10 mM rATP, rCTP, rUTP, 5 mM rGTP (Roche Molecular Biochemicals)
  - 10–50 U/μL RNase inhibitor (Roche Molecular Biochemicals)
  - 10–20 U/μL SP6 RNA polymerase (Roche Molecular Biochemicals, Invitrogen)
- Gel loading buffer
- Molecular weight marker (DNA ladder)
- BHK-21 cells (ATCC #CRL-6281)
- BHK-21 medium: Dulbecco's modified F-12 medium and Iscove's modified Dulbecco's medium + 4 mM glutamine, 10 % fetal calf serum (FCS)
- Phosphate-buffered saline (PBS)
- Trypsin-EDTA (0.5 mg/mL trypsin, 0.2 mg/mL EDTA in PBS)
- 1.5 mL microcentrifuge tubes
- Heating blocks or water baths (37 °C and 80–90 °C)
- Sterile electroporation gap cuvettes (0.2 or 0.4 cm gap, Bio-Rad)
- Electroporator (e.g., Gene Pulser, Bio-Rad)
- Tissue culture flasks (T25 and T75) and dishes (24, 35 or 100 mm) (Nunc)
- Microwell plates (6-, 12-, and 24-well plates) (Costar)
- Falcon tubes (15 and 50 mL) (Becton Dickinson)
- Plastic syringes (10 or 20 mL) with attached 0.22 μm sterile filter (Millipore)

The following material is necessary for the transduction of organotypic brain slice cultures using recombinant alphaviral particles:

- Glass capillaries (e.g., Clark Electromedical Instruments, Pangbourne, UK)
- Electrode puller
- Electrode holder (airtight)
- Autoclavable electrode holder (e.g., metal bin with foam)
- Micromanipulator (e.g., Narishige)
- Metal plate containing a base for a 35 mm Petri dish
- 35 mm Petri dishes (Costar)
- 3-Way valve
- Plastic tubing (inner dimension 1 mm, outer dimension 3 mm)
- Dissection microscope
- Autoclaved microloader pipet tips (Eppendorf)
- Forceps, small scissors
- Cutting medium (roller tube culture medium, 10 mM $MgCl_2$, 0.5 μM tetrodotoxin, e.g., Latoxan)
- Hippocampal slice cultures (e.g., roller tube type)
- Burner

The following material is required for the purification of alphaviral particles, for the β-galactosidase reporter assay, and for Western blots:

- MicroSpin™ S-200 HR Columns (Amersham)
- X-gal stock solutions: 50 mM K ferricyanide (+4 °C); 50 mM K ferrocyanide (+4 °C), 1 M MgCl (room temperature), 2 % X-gal in DMF or DMSO (–20 °C)
- X-gal staining solution: 1 X PBS (1/10 of stock), 5 mM K ferricyanide (1/10 of stock), 5 mM K ferrocyanide (1/10 of stock), 2 mM MgCl (1/500 of stock), 1 mg/mL X-gal (1/20 of stock)
- Mowiol 4–88 containing 2.5 % DABCO (1,4-diazobicyclo-[2.2.2]-octane)
- Lysis buffer (50 mM Tris-HCl. pH 7.6, 150 mM NaCl, 2 mM EDTA, 1 % (v/v) Nonidet P-40 (NP40) (Sigma)
- Hybond ECL nitrocellulose filter (Amersham)
- TBST (TBS with 0.1 % Tween 20)
- ECL Chemiluminescence kit (Amersham)

3 Methods

3.1 Subcloning into SFV and SIN Vectors

Genes of interest are subcloned into the multiple cloning sites (MCS) of the SFV and SIN expression vectors according to general cloning procedures. Verification of correctly cloned inserts is conducted by restriction endonuclease digestions, and nucleotide sequencing can further be applied for insert confirmation. Preparation of Midiprep or Maxiprep DNA is recommended for in vitro transcription reactions. However, initial transcription tests can be carried out from Miniprep DNA.

3.2 DNA Linearization

SFV vectors are linearized by *Spe*I, *Sap*I, or *Nru*I, and SIN plasmids by *Xho*I, *Not*I, or *Pac*I under standard restriction digestion. Agarose gel electrophoresis is applied to confirm complete vector linearization by comparing to uncut plasmid. Linearized plasmids are purified by phenol/chloroform extraction and ethanol precipitation (overnight at –20 °C or 15 min at –80 °C). Ethanol precipitates are centrifuged for 15 min at 18,000 × *g* at +4 °C, washed with 70 % ethanol and re-spun for 5 min. DNA pellets are air dried or lyophilized and resuspended in RNase-free H_2O at a final concentration of 0.5 μg/μL. Instead of phenol-chloroform extraction, linearized DNA can be purified in MicroSpin™ S-200 HR Columns (Amersham) or similar spin columns (e.g., from the Qiagen PCR purification kit) according to the manufacturer's instructions. It is essential that the DNA is RNase-free.

3.3 In Vitro Transcription

Generation of high-titer virus stocks requires in vitro transcription of high-quality RNA. It is recommended that fresh RNA is prepared for each electroporation although RNA storage for weeks is possible at –80 °C. The in vitro transcription reactions should be set up at room temperature to avoid precipitation of spermidine at lower temperatures. The following composition for a 50 μL reaction (sufficient for one electroporation of expression vector RNA and two electroporations for helper RNA) is recommended:

5 μL (2.5 μg) linearized plasmid DNA

5 μL SFV 10X SP6 buffer or 10 μL commercial SIN 5X SP6 buffer

5 μL 10 mM $m^7G(5')ppp(5')G$

5 μL 50 mM DTT

5 μL rNTP mix (10 mM rATP, 10 mM rCTP, 10 mM rUTP, 5 mM rGTP)

x μL RNase-free H_2O to reach a final volume of 50 μL

2 μL (50 U/μL) RNase Inhibitor

5 μL (20 U/μL) SP6 RNA polymerase

The reaction components are added in the listed order, and the mix spun briefly in a microcentrifuge and incubated for 1 h at 37 °C. To verify the quality of in vitro transcribed RNA, 1–4 μL aliquots are loaded on a 0.8 % agarose gel. High-quality RNA is characterized by thick bands without smearing. The size of RNA from the expression vectors is approximately 8 kb (compared to DNA markers) and for helper RNA slightly smaller. It is recommended that the in vitro transcribed RNA is directly used for electroporation. Preferentially, samples stored at −80 °C should be reevaluated before use. Generally the RNA yields from in vitro transcription reactions are in the range of 20–50 μg.

3.4 Electroporation of RNA into BHK Cells

BHK-21 cells have been demonstrated to produce high-titer SFV and SIN stocks. It is essential that the cells used for electroporation possess a low passage number (cultured less than 3 months) and no more than 80 % confluency as old and too dense cell cultures generate significantly lower virus titers. Cells are washed once with PBS, and then 6 mL trypsin-EDTA is added per T175 flask for 5 min at 37 °C. Importantly, cells should be well resuspended to remove clumps, centrifuged for 5 min at $800 \times g$, and resuspended in a small volume (<5 mL) of PBS. To remove any serum that might contain nucleases, the volume is increased to 25 mL with PBS, cells are re-centrifuged for 5 min at $800 \times g$ and resuspended in 2.5 mL PBS per T175 flask, equivalent to $1–2 \times 10^7$ cells per mL. Cells should be used immediately for electroporation although storage for 1 h on ice is acceptable. Next, 0.4 mL BHK cells are transferred to 0.2 cm electroporation cuvettes (or 0.8 mL cells/0.4 cm cuvette), and 20–45 μL recombinant RNA and 20 μL helper RNA are added to each cuvette. Two consecutive electric pulses are applied using the following setting for the Bio-Rad Gene Pulser:

	0.2 cm cuvette	0.4 cm cuvette
Capacitance extender	960 μF	960 μF
Voltage	1500 V	850 V
Capacitor	25 μF	25 μF
Resistance (pulse controller)	∞	Ω disconnected
Expected time constant (tc)	0.8 s	0.4 s

Application of the Bio-Rad Gene Pulser II requires the following modifications:

- The pulse controller should be set to “high range” and “∞.”
- The capacitance rotary switch should be set to “high capacitance.”
- The following settings should be applied: 360 V and 75 μF.

- The obtained resistance for 0.2 cm cuvettes is 10 Ω, and the time constant 0.7–0.8 s.

Upon electroporation, cells are immediately diluted 25-fold in cell culture medium, transferred to T flasks or plates, and incubated at 37 °C overnight in an incubator with 5 % CO_2.

3.5 Lipid-Mediated Transfection of RNA

Lipid-based transfection methods can be used alternatively to electroporation. In this context, DMRIE-C (ThermoFischer Scientific) has been used for successful RNA transfection into BHK-21, COS7, and CHO-K1 cells. BHK-21 cells ($1.5–3 \times 10^5$) are cultured in 35 mm Petri dishes or in 6-well plates to 80 % confluency and then washed with Opti-MEM I reduced-serum medium (Gibco-BRL). Cationic lipid-RNA complexes consisting of 0, 3, 6, 9, 12, and 15 μL plus 10 μL (~5 μg) recombinant RNA and 5 μL (~2.5 μg) helper RNA are mixed with 1 mL Opti-MEM I reduced-serum medium in 1.5 mL microcentrifuge tubes at room temperature and mixed briefly. Lipid-RNA complexes are added immediately to the washed cells and incubated for 4 h at 37 °C. The transfection medium is replaced by complete BHK medium and the cells are incubated at 37 °C overnight.

3.6 Harvest of Recombinant Viral Particles

Efficient recombinant SFV and SIN particle production occurs within the first 24 h post-transfection, yielding titers in the range of $10^8–10^9$ (occasionally 10^{10}) infectious particles per mL. Extension of the culture time to 48 h may increase the titers to some extent, in particular for the less cytopathic variant SFV(PD). The virus-containing medium is carefully removed from the BHK cells and sterilized using 0.22 μm filters (Millipore) to remove cell debris and possible contaminants. Immediately distribute virus stocks in aliquots to avoid repeated cycles of freezing and thawing, which might reduce titers significantly. Virus stocks can be stored for weeks at −20 °C and for years at −80 °C.

3.7 Activation of Recombinant SFV Particles Generated with pSFV-Helper2

Virus stock production from the conventional SFV helper and the SIN helpers renders directly infectious particles, which can be used for infection of host cells. In the case when the second-generation pSFV-Helper2 vector is used for the packaging of recombinant viral particles, only conditionally infectious particles are generated [11]. Activation of these particles is achieved by addition of α-chymotrypsin (20 mg/mL) to the virus stocks at a final concentration of 500 μg/mL and incubation at room temperature for 20 min. The reaction is terminated by adding aprotinin (a trypsin inhibitor, 10 mg/mL) to a final concentration of 250 μg/mL.

3.8 Virus Titer Determination

The replication-deficient nature of the recombinant alphavirus particles described herein prevents direct titer measurement by plaque assays. Indirect titer estimations can be made based on reporter gene expression. In this context, BHK cells plated at a

defined concentration on 6- or 12-well plates or on cover slips are infected with serial dilutions (e.g., fivefold dilutions in the range expected to give 20–50 positive cells per microscope field) of virus stocks expressing GFP or β-galactosidase. Titers are estimated after 48 h incubation at 37 °C. For GFP expression, the number of fluorescent cells is counted and the approximate titers calculated by taking into account the virus dilutions. In the case of β-galactosidase expression, infected cells are washed with PBS and fixed in cold methanol at −20 °C for 5 min. After three washes with PBS, the cells are stained with X-gal staining solution (*see* Materials) at 37 °C or room temperature for at least 2 h, and X-gal (blue)-positive cells counted and the titers estimated similarly as for GFP detection. In the case of available antibodies against the recombinant protein of interest, titers can be determined by immunofluorescence of infected cells on coverslips. After two washes with PBS, the coverslips are fixed for 6 min at −20 °C in methanol, washed three times with PBS, and incubated for 30 min at room temperature in PBS containing 0.5 % gelatin and 0.25 % BSA to prevent unspecific binding. Next, incubate coverslips for 30 min with primary antibody (in the same buffer), wash three times with PBS, and incubate with secondary antibody for 30 min at room temperature. Coverslips are washed three times with PBS, once with H_2O, air dried, and mounted onto glass slides using 10 μL Mowiol 4–88 containing 2.5 % DABCO (1,4-diazobicyclo-[2.2.2]-octane). The immunoreactive cells are counted, and titers estimated as above.

Additionally, a method has been applied for titer determination of SFV particles by using the RNeasy Kit (Qiagen) followed by quantitative RT-PCR amplification [33]. A standard curve for SFV-RNA is obtained by serial dilution of SFV plasmid DNA and then the mean Cts applied to a standard curve equation to determine the cDNA copy number in each sample. The total SFV-RNA copy number present in the original SFV sample is calculated by the multiplication of the cDNA copy number with the conversion factor specific to each sample.

The simplest way to determine the viral titer is by morphology characterization of infected cells using phase contrast light microscopy. Cells infected by alphaviruses show a dramatic decrease in growth and can be distinguished from noninfected cells due to their changed morphology (rounding up) and increased phase contrast, which allows rough titer estimations.

3.9 Gene Expression Evaluation

Rapid evaluation of transgene expression from generated virus stocks to establish the optimal conditions (virus concentration, host cell, time of cell harvest, etc.) can be obtained by Western blotting in case antibodies are available against the protein of interest or against tags incorporated in the vector. Various cell lines (BHK-21, CHO-K1, HEK293) cultured on 6-, 12-, or 24-well plates are infected with serial dilutions of virus stocks, and lysis buffer is added (250, 125, and 62.5 μL lysis buffer per 6-, 12-,

and 24-well plate, respectively) at various times post-infection, followed by a 10 min incubation on ice. The lysed cells are thoroughly resuspended and samples analyzed by 10–12 % SDS-PAGE. After protein material transfer for 30 min, the Hybond ECL nitrocellulose filters are treated with 5 % milk in TBST at +4 °C for 30 min, followed by primary antibody at room temperature for 30 min. The filters are then treated with the secondary antibody at room temperature for 30 min, and specific bands are visualized with the ECL Chemiluminescence kit.

In case no antibodies are available, recombinant protein expression can be monitored by metabolic labeling with ^{35}S-methionine. Cells are infected on multiwell plates as described above. The culture medium is removed, the cells are washed once with PBS, and incubated in starvation medium (Eagle's MEM, 2 mM L-glutamine, 20 mM HEPES) at 37 °C for 30 min. The medium is replaced with 50–100 μCi/mL of ^{35}S-methionine (in starvation medium) and incubated for 20 min at 37 °C. Cells are washed twice with PBS, and then incubated with chase medium (Eagle's MEM, 2 mM L-glutamine, 20 mM HEPES, 150 μg/mL unlabeled methionine) for the appropriate time (15 min to 3 h). Thereafter, the chase medium is removed, the cells are washed once with PBS, and 250 μL lysis buffer per well (6-well plate) is added and incubated for 10 min on ice. The lysed cells are resuspended thoroughly and samples run on 10–12 % SDS-PAGE under standard conditions. The gel is fixed in 10 % acetic acid, 30 % methanol for 30 min at room temperature. The fixation solution is replaced with Amplify® (Amersham) and incubated for 30 min at room temperature. The gel is dried and exposed on Hyperfilm MP for 2–24 h (depending on the signal) at room temperature (or at –80 °C applying radioactivity-intensifying screens), and the radioactive bands are visualized.

3.10 Primary Neurons in Culture

Primary cultures of dispersed hippocampal and cortical neurons can be obtained from embryonic day 18 (E18) rats and are cultured in Neurobasal Medium (Invitrogen) on 24-well plates. Postnatal day 3–5 (P3-5) rat hippocampal neurons are cultured on glass coverslips in 35 mm Petri dishes as described earlier [34]. Briefly, the CA1 and CA3 hippocampal regions are removed from 3-to-5 day old rats, and the neurons recovered by trypsin digestion (10 mg/mL type XI, 0.5 mg/mL DNase I type IV) and mechanical dissociation, followed by culturing in minimal essential medium containing 0.6 % (wt/vol) glucose, 1 mM glutamine, 2.4 g/L NaHCO3, 100 mg/mL bovine transferrin, 25 mg/mL insulin, and 5–10 % FCS at a density of 50,000 cells per 35 mm plastic Petri dish (Falcon) coated with poly-ornithine and Matrigel (Collaborative Research). The cultures are maintained at 37 °C in 95 % air, 5 % CO_2 in a humidified incubator, and the medium is replaced every 3–4 days. After one day in culture, the medium is supplemented with 5 M cytosine-D-arabinofuranoside, and the neurons are used after 10–14 days.

As primary neurons in culture are particularly sensitive to both physical and chemical exposure, the cells should be subjected to as little disturbance as possible. Already minor manipulations such as removal and exchange of medium can be harmful. It is therefore recommended that appropriate amounts of virus are added directly to the primary neurons in culture to avoid removal or addition of medium. We have observed that the medium from BHK-21 cells (in which the virus stocks are generated), under certain conditions, can be toxic to primary neurons in culture. For this reason, methods of virus concentration and medium replacement can be applied to reduce any neurotoxic effect on neurons.

3.11 Virus Stock Purification and Concentration

3.11.1 Ultracentrifugation

A two-phase solution is prepared in ultracentrifuge tubes by the addition of 1 mL of 50 % sucrose solution (bottom) and 3 mL of 20 % sucrose solution (top). Virus stock solution (9 mL for SW 40 Ti and 8 mL for SW 41 Ti) is carefully added onto the 20 % sucrose. The samples are subjected to ultracentrifugation at 160,000*g* (30,000 rpm in SW 40 Ti or SW41 Ti rotor) for 90 min at+4 °C. The alphavirus particles will settle at the interface between the 20 % and 50 % sucrose layers and can be collected by discarding the medium fraction and the bottom 0.8 mL consisting of 50 % sucrose.

3.11.2 Centriprep Concentration

Virus stocks are loaded onto the sample container of the Centriprep concentrator as described by the manufacturer. The assembled concentrator is centrifuged at an appropriate *g*-force (according to the manufacturer's recommendations) until the fluid levels inside and outside the filtrate collector have equilibrated. The device is removed, the airtight seal cap snapped off, and the filtrate decanted. The cap is replaced and the concentrator is centrifuged a second time. The filtrate is decanted, the twist-lock cap loosened, and the filtrate collector removed. The concentrated virus sample is collected with a 1 mL disposable plastic pipette. If desired, further concentration of virus is possible by additional centrifugation after decanting the filtrate.

3.11.3 Affinity Chromatography Concentration

Application of Matrex® Cellufine™ Sulfate (Millipore) allows for virus concentration and efficient removal of endotoxins and other contaminants. The column is packed according to the procedures provided by the manufacturer. The column is equilibrated with adsorption buffer (0.01 M phosphate, 0.1 M NaCl, pH7.5) and samples loaded at pH 7.5. The column is washed with several bed volumes of adsorption buffer to remove nonbinding contaminants. Concentrated virus stocks are eluted with elution buffer (1–2 M NaCl or KCl).

3.12 Cultured Hippocampal Slices

Organotypic slice cultures from rat and mouse hippocampus can be prepared in the roller tube configuration as described earlier [35]. As this technique results in neurons covered by a layer of glial cells, the penetration of viral particles is limited, which has been

addressed by manual injection of alphavirus particles into the extracellular space of the tissue [6]. Microinjections into slices can be achieved with commercially available devices like the Microinjector 5242 (Eppendorf). Alternatively, viral particles can be delivered by using glass micropipettes in an airtight electrode holder on a micromanipulator (e.g., Narishige) commonly used for patch-clamp recordings in electrophysiology. Virus injection can be performed by connecting a 1 mL syringe to the electrode holder via plastic tubing under sterile biosafety level 2 conditions as described [36]. During the injection procedure, the slices should be bathed in a specific medium (cutting medium) to reduce excitotoxic injury.

3.12.1 Micropipette Preparation

Glass capillaries are pulled on an electrode puller to obtain micropipettes with long tips, characteristic of the sharp electrodes used for intracellular recordings. The micropipettes are transferred into an electrode holder and autoclaved.

3.12.2 Assembly of the Virus Injection Setup

The following procedure is required for the setup for virus injections.

- Fix the micromanipulator onto a metal plate with a base for a 35 mm Petri dish.
- Set up the system according to biosafety level 2.
- Mount the electrode holder onto the micromanipulator (ideally with both a coarse and a fine control).
- Connect the electrode holder using plastic tubing with a three-way valve to a 1 mL syringe.
- Insert a 35 mm plastic Petri dish into the base on the metal plate.
- Add 2–3 mL cutting medium (pre-warmed to 37 °C) to the Petri dish.
- Focus the dissection microscope onto the 35 mm Petri dish.

3.12.3 Micropipette Loading

Alphavirus stocks are diluted 10- to 1000-fold in cutting medium. Application of non-diluted virus leads to extremely high infection rates and therefore makes it difficult to identify individual cells expressing the transgene of interest. An autoclaved glass micropipette is filled with 20–30 µL of diluted virus by using a sterile Eppendorf microloader pipette tip. The micropipette is inserted into the assembled, airtight electrode holder (above), and the micropipette tip is cut with sterilized scissors to a final diameter of ~20 µm. Verify that virus solution exits the micropipette tip when positive pressure is applied from the attached 1 mL syringe.

3.12.4 Virus Injection

Cultured hippocampal slices are transferred into 35 mm Petri dishes by using flame-sterilized forceps. The micropipette is lowered into the pyramidal and/or granule cell layer by using the micromanipula-

tor. Virus solution is injected with a short (<2 s) pressure pulse from the 1 mL syringe, and the pressure is released via the three-way valve to terminate the injection. Next, the micropipette is moved into a neighboring site and the injection procedure repeated (10–15 injection sites per slice). Injected slices are bathed in roller tube culture medium for 10–60 s to remove the tetrodotoxin from the cutting medium as well as any non-bound virus particles to lower the biohazardous potential of the slices. The slices are then returned to the culture system and incubated for 1–3 days.

3.13 In Vivo Delivery of Alphavirus Vectors

Both SFV and SIN particles can be used for direct stereotactic injections into rodent brain without any particular purification or concentration procedures [28, 29]. However, any of the above-described purification and concentration procedures can also be applied. SFV vectors have been utilized for injections into male Wistar rats (lbm RoRo, SPF, Biological Research Labs Ltd., Switzerland) [28]. Stereotactic microinjections are performed under general anesthesia with Ketamine/Xylazine (200/10 mg/kg ip) in physiological saline under thermoregulatory control and oxygen supplementation. Craniotomy is conducted with a fine dental drill and injections performed according to coordinates previously described [37]. Stainless-steel injectors are attached to a stereotaxic holder, and the needle lowered into the target area to apply appropriate amounts of virus (10^5 particles into striatum/amygdala/cortex, 10^7 particles into ventricles). A microinfusion pump (Harvard PHD 2000) is used to transfer the virus solution via polyethylene tubing to a 10 μL Hamilton syringe in a volume of 1 μL over 2 min (0.5 μL/min). The injection needle should be left in place for an additional 2 min before slow withdrawal over 1 min. The wound is sutured and animals are kept warm for 3–4 h postsurgery. Alphavirus stocks can be purified and concentrated, but initial studies in rat striatum and amygdala did not reveal any inconvenience of using SFV in the original culture medium for BHK cells [28]. Certain cellular components, such as cerebrospinal fluid (CSF), may be toxic to SFV, resulting in substantially decreased titers when virus stocks are resuspended in CSF (Lundstrom 1999, unpublished results).

4 Notes

1. Generation of high-titer virus stocks relies on high-quality DNA preparations. It is thus highly recommended that commercial Midiprep or Maxiprep DNA kits are used for plasmid DNA preparation.
2. It is advisable to optimize the composition of the in vitro transcription reaction, particularly the concentration of the CAP analogue $m^7G(5')ppp(5')G$. Commercial buffers should be

critically evaluated as the high RNA yields do not necessarily correlate with generation of high virus titers.

3. The transfection/electroporation efficacy can be monitored for constructs with reporter genes by fluorescence (GFP), X-gal staining (β-gal), or immunofluorescence. Likewise, transduction/infection efficacy can be visualized by the same methods for approximate titer evaluations.
4. Filter sterilization of alphavirus stocks with no further purification or concentration is sufficient for many applications. However, neuronal cells are particularly sensitive to certain media (for instance, the medium from BHK-21 cells) and ultracentrifugation or affinity column purification may thus be applied.
5. As primary neurons and hippocampal slices in culture are highly sensitive to physical and chemical interventions, manipulations of the cultures should be kept to a minimum.

Acknowledgments

The authors thank Dr. Sondra Schlesinger for her comments on the manuscript.

References

1. Lundstrom K (2003) Present and future approaches to screening G protein-coupled receptors. Future Med Chem 5:523–538
2. Waszkielewicz AM, Gunia A, Szkaradek N et al (2013) Ion channels as drug targets in central nervous system disorders. Curr Med Chem 20:1241–1285
3. Lundstrom K (2005) Biology and application of alphaviruses in gene therapy. Gene Ther 12: S92–S97
4. Lundstrom K (2001) Semliki Forest virus vectors for rapid and high-level expression of integral membrane proteins. Biochim Biophys Acta 1601:90–96
5. de Hoop MJ, Olkkonen VM, Ikonen E et al (1994) Semliki Forest virus as a tool for protein expression in cultured rat hippocampal neurons. Gene Ther 1 Suppl 1:S28–S31
6. Ehrengruber MU, Lundstrom K, Schweitzer C et al (1999) Recombinant Semliki Forest virus and Sindbis virus efficiently infect neurons in hippocampal slice cultures. Proc Natl Acad Sci U S A 96:7041–7046
7. Strauss JH, Strauss EG (1994) The alphaviruses: gene expression, replication, and evolution. Microbiol Rev 58:491–562
8. Liljeström P, Garoff H (1991) A new generation of animal cell expression vectors based on the Semliki Forest virus replicon. BioTechnology (N Y) 9:1356–1361
9. Bredenbeek PJ, Frolov I, Rice CM et al (1993) Sindbis virus expression vectors: packaging of RNA replicons by using defective helper RNAs. J Virol 67:6439–6446
10. Davis NL, Brown KW, Johnston RE (1989) In vitro synthesis of infectious Venezuelan equine encephalitis virus RNA from a cDNA clone: analysis of a viable deletion mutant. Virology 171:189–204
11. Berglund P, Sjöberg M, Garoff H et al (1993) Semliki Forest virus expression system: production of conditionally infectious recombinant particles. BioTechnology (N Y) 11:916–920
12. Smerdou C, Liljestrom P (1999) Two-helper RNA system for production of recombinant Semliki Forest virus particles. J Virol 73: 1092–1098
13. Schlesinger S (2001) Alphavirus vectors: development and potential therapeutic applications. Expert Opin Biol Ther 1:177–191
14. Ehrengruber MU, Renggli M, Raineteau O et al (2003) Semliki Forest virus A7(74) trans-

duces hippocampal neurons and glial cells in a temperature-dependent dual manner. J Neurovirol 9:16–28

15. DiCiommo DP, Bremner R (1998) Rapid, high level protein production using DNA-based Semliki Forest virus vectors. J Biol Chem 273:18060–18066
16. Lundstrom K, Rotmann D, Hermann D et al (2001) Novel mutant Semliki Forest virus vectors: gene expression and localization studies in neuronal cells. Histochem Cell Biol 115: 83–91
17. Ehrengruber MU, Hennou S, Büeler H et al (2001) Gene transfer into neurons from hippocampal slices: comparison of recombinant Semliki Forest virus, adenovirus, adeno-associated virus, lentivirus, and measles virus. Mol Cell Neurosci 17:855–871
18. Ehrengruber MU, Goldin AL (2007) Semliki Forest virus vectors with mutations in the nonstructural protein 2 gene permit extended superinfection in neuronal and non-neuronal cells. J Neurovirol 13:353–363
19. Lundstrom K, Abenavoli A, Malgaroli A et al (2003) Novel Semliki Forest virus vectors with reduced toxicity and temperature-sensitivity for long-term enhancement of transgene expression. Mol Ther 7:202–209
20. Hassaine G, Wagner R, Kempf J et al (2006) Semliki Forest Virus vectors for overexpression of 101 G Protein-coupled receptors in mammalian host cells. Protein Expr Purif 45: 343–351
21. Lundstrom K, Wagner R, Reinhart C et al (2006) Structural genomics on membrane proteins: comparison of more than 100 GPCRs in 3 expression systems. J Struct Funct Genomics 7:77–91
22. Blasey HD, Lundstrom K, Tate S et al (1997) Development of a process for recombinant protein production at one litre scale with the Semliki Forest virus system. Cytotechnology 24:65–72
23. Werner P, Kawashima E, Reid J et al (1994) Organization of the mouse 5-HT3 receptor gene and functional expression of two splice variants. Mol Brain Res 26:233–241
24. Hovius R, Tairi A-P, Blasey H et al (1998) Characterization of a mouse serotonin 5-HT3 receptor purified from mammalian cells. J Neurochem 70:824–834
25. Evans RJ, Lewis C, Virginio C et al (1996) Ionic permeability of, and divalent cation effects on, two ATP-gated cation channels (P2X receptors) expressed in mammalian cells. J Physiol 497(2):413–422
26. Michel AD, Miller KJ, Lundstrom K et al (1997) Radiolabeling of the rat P2X4 purinoreceptor: Evidence for allosteric interactions of purinoreceptor antagonists and monovalent cations with P2X purinoreceptors. Mol Pharmacol 51:524–532
27. Ehrengruber MU, Lee A, Dutt K et al (2007) High efficiency expression of large voltage-gated ion channels in neurons. Soc. Neurosci; abstract no. 466.5. San Diego, 3–7 Nov 2007
28. Lundstrom K, Richards JG, Pink JR et al (1999) Efficient in vivo expression of a reporter gene in rat brain after injection of recombinant replication-deficient Semliki Forest virus. Gene Ther Mol Biol 3:15–23
29. Altman-Hamandzic S, Groceclose C, Ma J-X et al (1997) Expression of β-galactosidase in mouse brain: utilization of a novel nonreplicative Sindbis virus vector as a neuronal gene delivery system. Gene Ther 4:815–822
30. Marie H, Morishita W, Yu X et al (2005) Generation of silent synapses by acute in vivo expression of CaMKIV and CREB. Neuron 45:741–752
31. Frolov I, Schlesinger S (1996) Translation of Sindbis virus mRNA: analysis of sequences downstream of the initiating AUG codon that enhance translation. J Virol 70:1182–1190
32. Kim J, Dittgen T, Nimmerjahn A et al (2004) Sindbis vector SINrep (nsP2S^{726}): a tool for rapid heterologous expression with attenuated cytotoxicity in neurons. J Neurosci Methods 133:81–90
33. Puglia AL, Rezende AG, Jorge SA et al (2013) Quantitative RT-PCR for titration of replication-defective recombinant Semliki Forest virus. J Virol Methods 193:647–652
34. Malgaroli A, Ting AE, Wendland B et al (1995) Presynaptic component of long-term potentiation visualized at individual hippocampal synapses. Science 268:1624–1628
35. Gähwiler BH (1981) Organotypic monolayer cultures of nervous tissue. J Neurosci Methods 4:329–342
36. Ehrengruber MU, Schlesinger S, Lundstrom K (2011) Alphaviruses: Semliki Forest virus and Sindbis virus vectors for gene transfer into neurons. In: Crawley JN, Gerfen CR, Rogawski MA, Sibley DR, Skolnick P, Wray S (eds) Current protocols in neuroscience. John Wiley & Sons, New York, pp 4.22.1–4.22.27
37. Paxinos G, Watson C (2006) The rat brain in stereotaxic coordinates. Academic Press, San Diego
38. Scheer A, Björklöf K, Cotecchia S et al (1999) Expression of the α1B adrenergic receptor and G protein subunits in mammalian cell lines using the Semliki Forest virus expression system. J Recept Signal Transduct Res 19:369–378

39. Lundstrom K, Turpin MP (1996) Proposed schizophrenia-related gene polymorphism: expression of the Ser9Gly mutant human dopamine D3 receptor with the Semliki Forest virus system. Biochem Biophys Res Commun 225:1068–1072
40. Hoffmann M, Verzijl D, Lundstrom K et al (2001) Recombinant Semliki Forest virus overexpression and pharmacological characterization of the histamine H2 receptor in mammalian cells. Eur J Pharmacol 427:105–114
41. Schweitzer C, Kratzeisen C, Adam G et al (2000) Characterization of [3H]-LY354740 binding to rat mGlu2 and mGlu3 receptors expressed in CHO cells using Semliki Forest virus vectors. Neuropharmacology 39:1700–1706
42. Monastryrskaia K, Lundstrom K, Plahl D et al (1999) Effect of the umami peptides on the ligand binding and function of rat mGlu4a receptor might implicate this receptor in the monosodium glutamate taste transduction. Br J Pharmacol 128: 1027–1034
43. Lundstrom K, Mills A, Buell G et al (1994) High-level expression of the human neurokinin-1 receptor in mammalian cells using the Semliki Forest virus expression system. Eur J Biochem 224:917–921

Chapter 8

Fluorescent Ligands and TR-FRET to Study Receptor–Receptor Interactions in the Brain

Víctor Fernández-Dueñas, Thierry Durroux, and Francisco Ciruela

Abstract

G-protein-coupled receptors (GPCR) mediate a large number of functions within the organism, constituting one of the main drug targets in pharmacological research. In line with this, the phenomenon of GPCR oligomerization has gained interest during the last years, since novel drugs may be developed targeting these kinds of structures. Accordingly, different techniques in order to assess the occurrence of GPCR oligomerization in native tissue have emerged (immunoelectron microscopy, proximity ligation assay, etc.). From them, the most reliable approach consists of engaging a TR-FRET process between fluorescent ligands directed to the putative interacting receptors. Here, we review this methodology used to reveal receptor–receptor interactions in brain tissue.

Key words TR-FRET, Fluorescent ligands, G-protein-coupled receptor, GPCR oligomerization

1 Introduction

G-protein-coupled receptors (GPCRs) constitute a diverse family of proteins that sense a large array of extracellular molecules to prompt cellular responses. The physiology of GPCRs has been intensely studied for many years, from the binding of the extracellular ligand to the coupling and activation of G proteins, which subsequently mediate intracellular signal transduction pathways [1]. Interestingly, the functioning of these kinds of receptors is actually being revised, since it was postulated more than two decades ago that GPCRs may interact forming receptor complexes (i.e., oligomers) at the cell surface of living cells [2, 3]. Accordingly, receptors within an oligomer may establish a close cross-talk that may modify the signal transduction pathways mediating cellular responses. Interestingly, in order to explain these new characteristics, novel pharmacological concepts have been developed, such as functional selectivity or biased agonism [4]. GPCR oligomerization is therefore actually mostly accepted by the scientific community. However, although direct molecular evidences of receptor–receptor

Rafael Luján and Francisco Ciruela (eds.), *Receptor and Ion Channel Detection in the Brain: Methods and Protocols*, Neuromethods, vol. 110, DOI 10.1007/978-1-4939-3064-7_8,

interactions have been largely shown in heterologous expression systems [5], the demonstration of GPCR oligomerization in native tissue has still not been straightforward resolved. Thus, receptor–receptor direct interactions have been usually indirectly assessed by means of genetic (i.e., yeast two-hybrid systems) and biochemical (i.e., co-immunoprecipitation) techniques [6, 7]. However, these approaches do not permit to ensure that receptors are really in close proximity, thus new tools have been recently generated. From them, the most remarkable and precise one consists of engaging a time-resolved fluorescence resonance energy transfer (TR-FRET) process between compatible fluorescent ligands [8, 9]. Accordingly, selective ligands for the receptors forming the putative oligomer are tagged with fluorescent probes, compatible to elicit a TR-FRET process (see below); thus, if they are separated by less than 10 nm, a TR-FRET signal can be readily detected. Of note, this approach takes advantage of the use of lanthanides (i.e., terbium, Tb^{3+}) complexed with cryptate, as donor molecules within the FRET process. Hence, these compounds not only elicit a highly efficient energy transfer, but they also present a high signal-to-noise ratio, since the bleed-through of lanthanide into acceptor emission (i.e. dy647) is negligible. In addition, FRET is time resolved due to the long-lived emission of these rare earth elements [10–12]. Nevertheless, apart from the advantages of the fluorescent probes used, which may allow high temporal selectivity and spectral compatibility, the use of fluorescent ligands presents the major advantage of being applied in native tissue, in which they may bind in unmodified and physiologically expressed receptors. This kind of approach was firstly developed to demonstrate oxytocin receptor dimerization in rat mammary gland [9, 13]. Thus, the oxytocin receptor antagonist phenylpropionyl linear vasopressin was derived with europium chelate as donor and Alexa647 dye as acceptor, and a specific TR-FRET signal was obtained in rat mammary gland membranes. Recently, we designed selective fluorescent ligands in order to undeniably reveal the well-known receptor–receptor interaction between $A_{2A}R$ and D_2R in the striatum [14]. Accordingly, we synthesized the D_2R antagonist *N*-(p-aminophenthyl)spiperone (NAPS) derived with Lumi4-Tb ($NAPS^{Lumi4\text{-}Tb}$) as donor, and the $A_{2A}R$ antagonist SCH442-416 derived with dy647 (SCH^{dy647}). Interestingly, by recording the TR-FRET signal elicited after incubating striatal membranes with the named fluorescent ligands, we definitely resolved the long-standing question concerning D_2R-$A_{2A}R$ assembly in native tissue [14]. Needless to say, contrasting to oxytocin receptors in mammary gland of lactating rat that are highly expressed, GPCRs in brain are usually expressed at low levels and the detection of a specific FRET signal resulting from GPCR-specific interaction is therefore difficult. Thus, although TR-FRET is a sensitive technique that exhibits an excellent signal/noise ratio, the protocol used to reveal D_2R-$A_{2A}R$ oligomerization

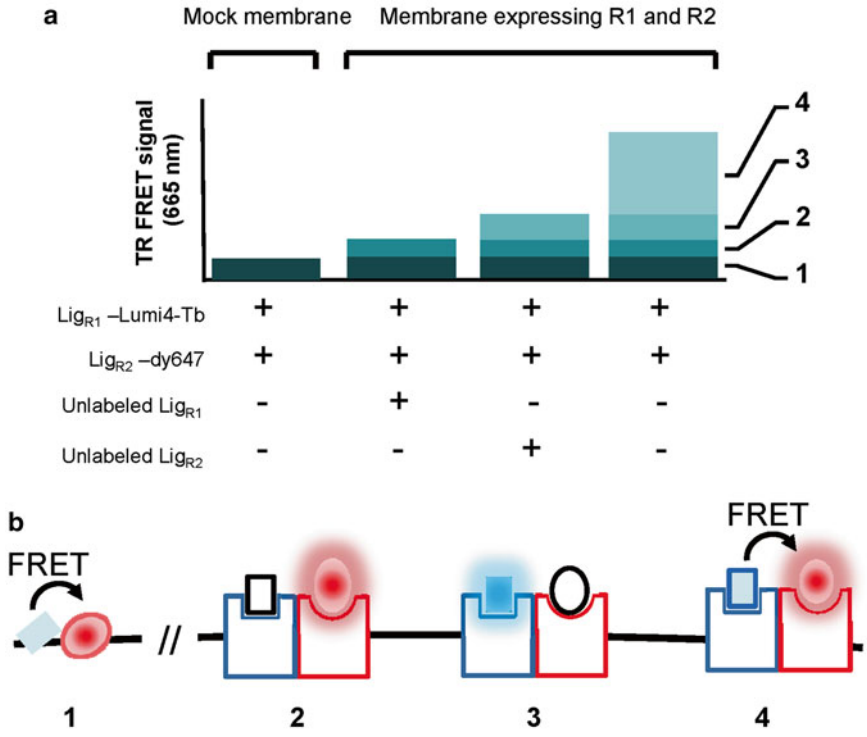

Fig. 1 (**a**) Scheme showing the different conditions that may be assayed to detect the specific TR-FRET signal occurring between two receptors (R1 and R2). (**b**) Diagram illustrating the distinct nonspecific signals that can preclude the observation of the specific TR-FRET signal. *1* Background signal from the device + autofluorescence of the biological samples + nonspecific FRET due to nonspecific binding of ligands; *2* Direct excitation of acceptor; *3* Bleed-through of donor fluorescence in FRET channel; *4* Specific TR-FRET signal

was optimized from the initial protocol [8, 9] to extract specific signal from total FRET signal. Of note, a number of controls should be included, since various nonspecific signals can preclude the observation of the specific FRET signal (Fig. 1): (1) The dynamic FRET resulting from random collision of fluorescent ligands. To overcome this difficulty, experiments should not be performed in homogeneous conditions, but protocol should include washing steps to reduce random collision occurrence. (2) The bleed-through of Lumi4-Tb at the acceptor emission and FRET wavelength (665 nm). It can be estimated when an excess of unlabeled ligand competing with the ligand-Lumi4-Tb for the binding site is added. (3) A FRET due to the nonspecific binding of ligands. Although it is generally weak, it cannot be negligible when ligands are highly hydrophobic, for example. (4) The direct excitation of the acceptor at 337 nm. (5) The autofluorescence of the biological preparation. (6) Background signal of the device. The last three sources of contamination are usually weak and additional optimization of the signal acquisition parameters is not

usually required. In the present chapter, we describe the use of fluorescent ligands and TR-FRET to study receptor–receptor interactions (i.e., $A_{2A}R$ and D_2R) in the striatum. Importantly, this protocol has been optimized based on the particular levels of expression of the former receptors, but it may be applicable for revealing other kind of receptor–receptor interactions in the brain.

2 Materials

2.1 Animals

1. Sprague–Dawley rats (Charles River Laboratories, L'Arbresle, France) weighting 200–250 g.

2.2 Buffers and Reagents

1. Ice-cold lysis buffer: 10 mM Tris–HCl, 1 mM EDTA, 300 mM KCl; pH 7.4.
2. Tris–EDTA buffer: 10 mM Tris–HCl, 1 mM EDTA; pH 7.4.
3. Membrane suspension buffer: 50 mM Tris–HCl (pH 7.4), 10 mM $MgCl_2$; pH 7.4.
4. Tris–Krebs buffer: 20 mM Tris–HCl, 118 mM NaCl, 1.2 Mm KH2PO4, 1.2 mM MgSO4, 4.7 mM KCl, 1.8 mM CaCl2; pH 7.4.
5. Bradford assay: BCA Protein Assay Kit (Pierce Biotechnology, Rockford, IL, USA).
6. BSA (Sigma-Aldrich, St. Louis, MO, USA).
7. Glucose (Sigma-Aldrich)
8. *N*-(p-aminophenthyl)spiperone (NAPS) derived with Lumi4-Tb ($NAPS^{Lumi4\text{-}Tb}$) and SCH442-416 derived with dy647 (SCH^{dy647}) (Cisbio Bioassays, Bagnols-sur-Cèze, France).

2.3 Instrumentation, Equipment, and Software

1. VDI 12 Adaptable Homogenizer (VWR, Radnor, PA, USA).
2. Heraeus Fresco 21 Centrifuge (Thermo Scientific, Waltham, MA, USA).
3. Ultracentrifuge with a swing SW-32-out bucket rotor (Beckman Coulter, Roissy, France).
4. Beckman Ultra-Clear Centrifuge tubes (25 × 89 mm).
5. Black 96-well plate (Greiner Bio-One GmbH, Frickenhausen, Germany).
6. PHERASTAR plate reader (BMG Labtech, Durham, NC, USA).
7. GraphPad Prism software (GraphPad Software, La Jolla, CA, USA).

3 Methods

3.1 Preparation of Purified Striatal Membranes

1. Sacrifice rats weighting 200–250 g by decapitation and dissect the striatum (*see* **Note 1**).
2. Homogenize striatum rapidly in 2 mL of ice-cold lysis buffer with Polytron for three periods of 10 s each (*see* **Notes 2** and **3**).
3. Spun the homogenate for 10 min at 1000 × *g* at 4 °C.
4. Recover the supernatant and centrifuge for 30 min at 12,000 × *g* at 4°C.
5. Discard the supernatant and wash the pellet obtained in 1 mL of ice-cold Tris–EDTA buffer.
6. Centrifuge again for 30 min at 12,000 × *g* at 4°C, and resuspend the pellet in 15 mL of Tris–EDTA buffer containing 10 % sucrose (wt/vol).
7. Layer the sample-containing solution onto 15 mL of Tris–EDTA buffer with 35 % sucrose (wt/vol) (*see* **Note 4**).
8. Centrifuge the preparation for 2 h at 100,000 × *g* at 4°C in a swing SW-32-out bucket rotor.
9. Collect purified striatal membranes at the 10–35 % interface (*see* **Note 5**).
10. Disperse and wash membranes in 30 mL of ice-cold membrane suspension buffer.
11. Centrifuge the sample for 30 min at 40,000 × *g* at 4°C and resuspend in 500 µL of membrane suspension buffer.
12. For each membrane preparation, determine protein concentration by colorimetric assay (e.g., Bradford assay).
13. Fresh membranes are immediately used. Alternately, they can be quickly frozen in liquid nitrogen and stored at –20 °C.

3.2 Labeling of Receptors with the Fluorescent Ligands and TR-FRET Recordings

1. Prepare membranes solutions of 50–100 µg (*see* **Note 6**) in 200 µL of ice-cold Tris–Krebs buffer complete with 0.1 % BSA and 0.1 % glucose, in a 1.5 mL Eppendorf tube.
2. Select fluorescent ligands, with compatible fluorescent moieties to engage a TR-FRET process (*see* **Note 7**) once bound to their respective receptors (Fig. 2a).
3. Prepare the donor and acceptor fluorescent ligands separately in ice-cold labeling Tris–Krebs buffer complete with 0.1 % BSA and 0.1 % glucose, and keep on ice (*see* **Notes 8** and **9**).
4. Prepare non-fluorescent probes also in the labeling buffer and keep on ice (*see* **Note 9**).
5. Mix ligands solutions in a final volume of 200 µL (*see* **Note 10**), add onto membrane suspensions, and incubate overnight at 4 °C with gentle rocking (*see* **Note 11**).

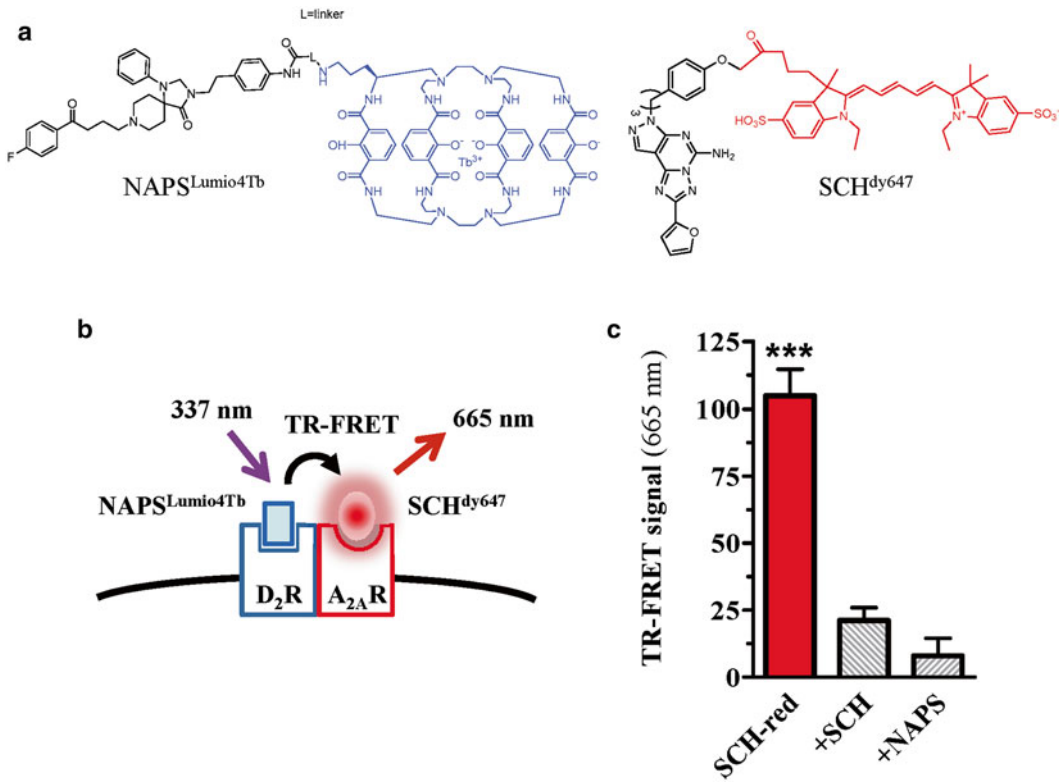

Fig. 2 (**a**) Structure of the D_2R and $A_{2A}R$ fluorescent ligands. (**b**) Diagram illustrating the principle of TR-FRET between the fluorescent ligands bound to D_2R and $A_{2A}R$. (**c**) TR-FRET recordings in rat striatal purified membranes. Membranes were labeled with $NAPS^{Lumi4\text{-}Tb}$ (1 nM) plus (i) SCH^{dy647} (10 nM) (*first column*); (ii) plus SCH^{dy647} (10 nM) and SCH (1 μM) (*second column*); (iii) plus SCH^{dy647} (10 nM) and NAPS (1 μM). The TR-FRET signal obtained when only challenging the fluorescent ligands was significantly higher than the obtained when adding cold ligands (***$P < 0.001$; one-way ANOVA followed by Bonferroni's multiple comparison post hoc test) (Adapted from Fernández-Dueñas et al. [14])

6. Centrifuge the solution for 30 min at 12,000 × *g* at 4 °C to wash unbound ligands, and resuspend the pellet in ice-cold Tris–Krebs buffer.
7. Dispense solutions (100 μL/well) in 96-well black plates and immediately read in a PHERASTAR plate reader (*see* **Note 12** and **13**).
8. Upon excitation of the donor at 340 nm, record signals at 620 nm for the donor (e.g., terbium) and 665 nm for the acceptor (e.g., dy647) (*see* **Note 14**).
9. Subtract from the 665 nm signal the nonspecific FRET signal and especially the bleed-through (*see* **Note 15**) to obtain the specific TR-FRET signal (representative results are shown in Fig. 2).

4 Notes

1. In our protocol, animals are housed and tested in compliance with the guidelines described in the Guide for the Care and Use of Laboratory Animals [15] and following the European Community, law 86/609/CCE, FELASA, and ARRIVE guidelines. Thus, animals are housed in standard cages with ad libitum access to food and water and maintained under controlled standard conditions (12 h dark/light cycle starting at 7:30 AM, 22 °C temperature and 66 % humidity). Our Committee on Animal Use and Care might also approve the protocol.
2. A preliminary manual homogenization can be performed by means of a glass Dounce homogenizer. Both the tissue grinder tube and pestle should be prechilled in a beaker of ice before homogenization.
3. Polytron is usually set at position six. It is recommended to perform homogenization in an ice-bath to preclude sample warming.
4. Creating the gradient layer is a critical step and must be done with extreme care. A pipettor and a 10-mL standard glass or plastic pipette is used, attaching at the end of the tubing a 9–10-cm-long metal tube (Z1 mm inner diameter or 18–20 gauge). Alternately, the metal tube can be attached to a peristaltic pump. Nevertheless, a very slow flow (<1 mL/min) delivery is mandatory.
5. Collection of the purified striatal membranes at the 10–35 % interface is also critical, since contamination of the 35 % phase should be avoided. The procedure is basically the reverse of that used for gradient creation.
6. Optimization of membrane concentration has to be performed for each assay.
7. In the example supplied, D_2R and $A_{2A}R$ ligands were used. Thus, the D_2R antagonist *N*-(p-aminophenthyl)spiperone (NAPS) derived with Lumi4-Tb ($NAPS^{Lumi4\text{-}Tb}$) as donor and the $A_{2A}R$ antagonist SCH442-416 derived with the fluorescent dye dy647 (SCH^{dy647}) (*see* Fig. 2a) were used.
8. Donor and acceptor ligand concentrations are needed to be optimized to obtain an optimal TR-FRET signal. In the example, $NAPS^{Lumi4\text{-}Tb}$ concentration is 1 nM, and SCH^{dy647} concentration is 10 nM.
9. Premixed ligand solutions are prepared 8× concentrated, due to the dilutions performed mixing ligands and the additional dilution by the membranes.

10. To properly analyze TR-FRET results, a series of conditions have to be included. From them, a nonspecific control is obtained with an excess of unlabeled donor or acceptor ligands (i.e., NAPS and SCH442-416), in the presence of donor and acceptor labeled ligands. Similarly, another nonspecific control incubating donor and acceptor ligands in the absence of membranes is performed (note that if available, a knockout condition would be very valuable). Finally, a negative control is obtained by measuring TR-FRET only incubating with the donor.
11. By working at 4 °C, all internalization phenomena are avoided.
12. In order to avoid loss of ligands bound, since a new equilibrium with the new solution may occur, upon resuspending the pellet the solution is readily dispensed and read in the plate reader. Also since the plate readers are generally not thermostated, plates should be kept on ice as much as possible.
13. TR-FRET readings can be performed using other plate readers, for instance, RUBYSTAR (BMG Labtech) or Envision (Perkin Elmer).
14. TR-FRET reading conditions are described elsewhere [14].
15. Bleed-through of Lumi4-Tb at the acceptor emission and FRET wavelength can be determined experimentally when adding an excess of unlabeled ligand competing with ligand-Lumi4-Tb for the same binding site. However, variations from one well to another in membrane concentration can significantly impact the bleed-through. In these conditions, a theoretical bleed-through can also be determined well by well by calculating the 665/620 ratio (r) on a well containing only ligand-Lumi4-Tb. Indeed, the bleed-through at 665 nm is proportional to signal at 620 nm. Therefore, the bleed-through of one sample is equal to the signal measured at 620 multiplied by the ratio r. It is noteworthy that the ratio can vary from one device to another since it depends on the characteristics of the excitation and the emission filters and dichroic mirror. It has therefore to be determined for each device.

Acknowledgments

This work was supported by Ministerio de Economía y Competitividad/Instituto de Salud Carlos III (SAF2014-55700-P, PCIN-2013-019-C03-03 and PIE14/00034), Institució Catalana de Recerca i Estudis Avançats (ICREA Academia-2010), and Agentschap voor Innovatie door Wetenschap en Technologie (SBO-140028) to FC. Also, F.C. and V.F.-D. belong to the "Neuropharmacology and Pain" accredited research group

(Generalitat de Catalunya, 2014 SGR 1251). We thank E. Castaño and B. Torrejón from the Scientific and Technical Services (SCT) group at the Bellvitge Campus of the University of Barcelona for their technical assistance. Also, this work was supported by research grants from the Centre National de la Recherche Scientifique, Institut National de la Santé et de la Recherche Médicale, and by the Plateforme de Pharmacologie-Criblage of Montpellier and the Region Languedoc-Roussillon.

References

1. Lohse MJ, Hein P, Hoffmann C et al (2008) Kinetics of G-protein-coupled receptor signals in intact cells. Br J Pharmacol 153 Suppl:S125–S132. doi:10.1038/sj.bjp.0707656
2. Agnati LF, Fuxe K, Zini I et al (1980) Aspects on receptor regulation and isoreceptor identification. Med Biol 58:182–187
3. Fuxe K, Agnati LF, Benfenati F et al (1983) Evidence for the existence of receptor--receptor interactions in the central nervous system. Studies on the regulation of monoamine receptors by neuropeptides. J Neural Transm 18: 165–179
4. Schulte G, Levy FO (2007) Novel aspects of G-protein-coupled receptor signalling--different ways to achieve specificity. Acta Physiol (Oxf) 190:33–38. doi:10.1111/j.1365-201X.2007.01696.x
5. Ciruela F, Vallano A, Arnau JM et al (2010) G protein-coupled receptor oligomerization for what? J Recept Signal Transduct Res 30:322–330. doi:10.3109/10799893.2010.508166
6. Miller J, Stagljar I (2004) Using the yeast two-hybrid system to identify interacting proteins. Methods Mol Biol 261:247–262. doi:10.1385/1-59259-762-9:247
7. Selbach M, Mann M (2006) Protein interaction screening by quantitative immunoprecipitation combined with knockdown (QUICK). Nat Methods 3:981–983. doi:10.1038/nmeth972
8. Trifilieff P, Rives M-L, Urizar E et al (2011) Detection of antigen interactions ex vivo by proximity ligation assay: endogenous dopamine D2-adenosine A2A receptor complexes in the striatum. Biotechniques 51:111–118. doi:10.2144/000113719
9. Albizu L, Cottet M, Kralikova M et al (2010) Time-resolved FRET between GPCR ligands reveals oligomers in native tissues. Nat Chem Biol 6:587–594. doi:10.1038/nchembio.396
10. Mathis G (1995) Probing molecular interactions with homogeneous techniques based on rare earth cryptates and fluorescence energy transfer. Clin Chem 41:1391–1397
11. Bazin H, Trinquet E, Mathis G (2002) Time resolved amplification of cryptate emission: a versatile technology to trace biomolecular interactions. J Biotechnol 82:233–250
12. Terrillon S, Durroux T, Mouillac B et al (2003) Oxytocin and vasopressin V1a and V2 receptors form constitutive homo- and heterodimers during biosynthesis. Mol Endocrinol 17:677–691. doi:10.1210/me.2002-0222
13. Kern A, Albarran-Zeckler R, Walsh HE, Smith RG (2012) Apo-ghrelin receptor forms heteromers with DRD2 in hypothalamic neurons and is essential for anorexigenic effects of DRD2 agonism. Neuron 73:317–332. doi:10.1016/j.neuron.2011.10.038
14. Fernández-Dueñas V, Taura JJ, Cottet M et al (2015) Untangling dopamine-adenosine receptor-receptor assembly in experimental parkinsonism in rats. Dis Model Mech 8:57–63. doi:10.1242/dmm.018143
15. Clark JD, Gebhart GF, Gonder JC et al (1997) Special report: the 1996 guide for the care and use of laboratory animals. ILAR J 38:41–48

Chapter 9

In Situ Proximity Ligation Assay to Study and Understand the Distribution and Balance of GPCR Homo- and Heteroreceptor Complexes in the Brain

Dasiel O. Borroto-Escuela, Beth Hagman, Miles Woolfenden, Luca Pinton, Antonio Jiménez-Beristain, Julia Oflijan, Manuel Narvaez, Michael Di Palma, Kristin Feltmann, Stfano Sartini, Patrizia Ambrogini, Francisco Ciruela, Riccardo Cuppini, and Kjell Fuxe

Abstract

The existence of homo- and heteroreceptor complexes with allosteric receptor-receptor interactions increases the diversity of receptor function including recognition, trafficking, and signaling. This phenomenon increases our understanding of how brain function is altered through molecular integration of receptor signals. An alteration in specific heteroreceptor complexes or their balance/equilibrium with the corresponding homoreceptors is considered to have a role in the pathogenic mechanisms that lead to mental and neurological diseases, including drug addiction, depression, Parkinson's disease, and schizophrenia. However, despite extensive experimental work supporting the formation of these receptor complexes in cellular models, their detection and visualization in the brain remained largely unknown until recent years, when a well-characterized in situ proximity ligation assay (in situ PLA) was adapted to validate the existence of GPCR homo- and heteroreceptor complexes in their native environment. In this chapter we will describe the in situ PLA procedure as a high selectivity and sensitivity assay to detect and characterize GPCR homo- and heteroreceptor complexes and their balance and distribution ex vivo in the brain by confocal laser microscopy. Herein, we outlined in detail the in situ PLA assay and how to use it in an optimal way on work with formalin-fixed free-floating rat brain sections.

Key words G protein-coupled receptors, Immunohistochemistry, In situ proximity ligation assay, Heteroreceptor complexes, Dimerization, Receptor-receptor interaction, Stoichiometry

1 Introduction

Nervous system-related diseases are highly complex in their etiology. It is not surprising that the underlying pathological processes are poorly understood and treatment possibilities are inadequate. One emerging concept is that direct physical interactions of different receptors named homo-/heteroreceptor complexes may be

Rafael Luján and Francisco Ciruela (eds.), *Receptor and Ion Channel Detection in the Brain: Methods and Protocols*, Neuromethods, vol. 110, DOI 10.1007/978-1-4939-3064-7_9, © Springer Science+Business Media New York 2016

involved with disease onset and progression. Thus, these receptor complexes could potentially serve as a biomarker and/or drug target of the disease [2–4]. Accordingly, the orthosteric targeting of heteroreceptor complexes with pharmacological agents (i.e., bivalent ligands) and the disruption of the receptor-receptor interface by means of interfering peptides may become new therapeutical strategies [5]. Several groups have contributed to the development of the concept of heteroreceptor complexes, in which receptors physically interact to produce either an integrated regulation of receptor tyrosine kinases [2, 5], ion channels [6], and/or an activation of intracellular signaling cascades generating changes in gene expression [7].

Recently, GPCR heteroreceptor complexes were rigorously collected, and their magnitude is represented in a global GPCR heterodimer network (GPCR-HetNet; www.gpcr-hetnet.com) [8]. The results from the GPCR-HetNet indicate a scale-free model in which some of the protomers dominate the connectivity and hold the network together. Using two different hub criteria revealed the following hubs in the network: the dopamine D2 receptor, the beta-2 adrenergic receptor, the growth hormone secretagogue receptor type 1, the mu-type opioid receptor, the secretin receptor, the delta-type opioid receptor, the adenosine A1 receptor, the adenosine A2A receptor, and the cannabinoid receptor 1. Other highly connected protomers were also identified. The emergence of potential allosteric mechanism avenues and higher-order heteroreceptor complexes are also described. Although, in this work, the homoreceptor complex information was excluded, the data highlighted that more than 87 % of the total numbers of protomers identified exist as homoreceptor complexes too [8].

These direct interactions involving GPCRs were demonstrated through diverse biophysical (FRET, BRET, BiFC) and biochemical or microscopy-based procedures (e.g., co-immunolocalization, co-immunoprecipitation, radioligand binding, co-internalization analysis) that assess receptor-receptor interactions in heteroreceptor complexes [1, 9–11]. Each methodology used has provided precise and valuable information which was considered with caution in view of the limitations of the techniques. Some controversy regarding some approaches also emerged [12, 13]. Nevertheless, when these methods are properly assessed, it is possible to safely demonstrate the direct interactions between GPCRs as well as their dynamics [14, 15]. Novel technologies have also been developed, such as real-time FRET experiments in living cells [16] and dual-color fluorescence cross-correlation spectroscopy [17]. However, despite the extensive experimental results obtained with these biophysical/biochemical techniques, supporting the formation of GPCR homo- and heteroreceptor complexes in heterologous systems, the existence of such receptor complexes in their native environment (brain tissue) was not confirmed until recent

years. Thus, a well-characterized in situ proximity ligation assay (in situ PLA) was adapted to validate the existence of GPCR complexes in cellular models first [18] and then in brain sections ex vivo [2, 5, 7, 19–23].

It should be highlighted that until now, most experimental work was focused on the study of receptor-receptor interactions in GPCRs as a phenomenon of binary interactions. In other words, it was only focused on the understanding of face-to-face protomer-protomer interactions and their allosteric receptor-receptor modulation and functional specificities. However, the phenomenon of GPCR oligomerization is a more complex and dynamic process, which involves many more parameters than the classical analysis of the interactions of the two protomers involved [24]. One emerging concept is that direct physical receptor-receptor interactions in heteroreceptor complexes or altered balance with their homoreceptor complex populations can contribute to brain disease progression inter alia of Parkinson's disease [3, 4, 25], depression [5, 26], schizophrenia [21], Alzheimer's, and addiction. When discussing the role of GPCR heteroreceptor complexes, it is of substantial interest to understand the balance/equilibrium between the corresponding homo- and heteroreceptor complexes in the plasma membrane of the cell (Fig. 1). Consider a disruption or shift of this balance as a mechanism of disease development could be important in the discovery of pharmacological targets. We have suggested that the introduction of in situ PLA (Fig. 1) in combination with Western blot, radioligand-binding experiments, and co-immunoprecipitation could open a new window to the understanding of the importance of the balance of the corresponding homo- and heteroreceptor complexes [19].

In this chapter, we will describe the in situ PLA procedure as a high selectivity and sensitivity assay to study and characterize the balance and distribution of GPCR homo- and heteroreceptor complexes ex vivo in the brain using confocal laser microscopy, including a detailed description of how to perform the assay in an optimal way. At the end of the chapter, we will discuss the advantages and disadvantages of this method compared to other available techniques.

2 The In Situ PLA: Principle of the Assay

The in situ PLA is a method that combines the dual recognition of a probe-targeted assay with a split-reporter approach, creating a selective and sensitive method for specific detection of two receptors in close proximity forming a homo- or heteroreceptor complex [27]. In this method a pair of antibodies, in which complementary oligonucleotides have been attached, is used to target the receptor protomers in the receptor complex of interest.

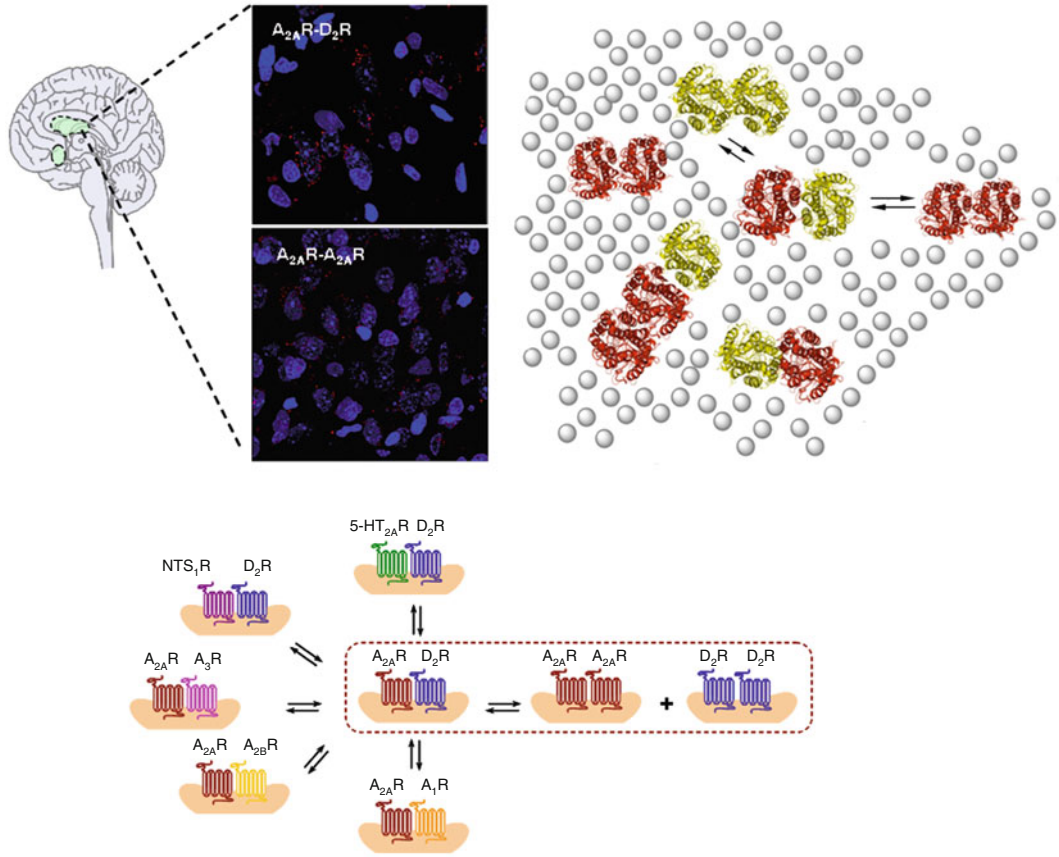

Fig. 1 On the understanding of the balance/equilibrium between GPCR homo- and heteroreceptor complexes in cell populations in the brain. (*Top right*) Schematic representation of the balance between different populations of A2AR-D2R heteroreceptor complexes and their corresponding homoreceptor complexes in a portion of a neural membrane (D2R and A2A homoreceptor complexes are indicated in *red* and *yellow* colour respectively). (*Top left*) The panel represents an example of in situ PLA experiment performed in striatal free-floating sections using primary antibodies of different species directed to adenosine A2A and dopamine D2 receptors. The detected A2A-A2A homoreceptor complexes and A2A-D2R heteroreceptor complexes are seen as *red* clusters (blobs, puncta) in each panel. (*Bottom*) Understanding the complexity of the balance between A2AR-D2R and its homoreceptor complexes, iso A2AR- and iso D2R-heteroreceptor complexes, and other A2A- and D2R-heteroreceptor complexes. Thus, it is clear that the stoichiometry and topology of the complexes is unknown (e.g., A2AR-D2R = A2AR-A2AR + D2R-D2R + A2AR-A2AR-D2R + A2AR-D2R-D2R + A2AR-A2AR-D2R-D2R + A2AR-A2AR-A2AR-D2R-D2R)

Only when the receptor protomers are in close proximity, i.e., interacting in a receptor complex, are the oligonucleotides attached to the antibody able to join together. After hybridization of both proximity probes, enzymatic ligation follows and a circular DNA molecule is formed. This DNA circle strand is a surrogate marker for the detected complexes and serves as a template for amplification (rolling circle amplification (RCA)) using a highly efficient polymerase (e.g., phi29 DNA polymerase). The long single-concatemeric-stranded rolling circle product (RCP), attached to one

of the proximity probes, is a result of the first round amplification, displacing the newly created strand. The RCP is linked to the proximity probe and, thereby, stays attached to one of the two protomer of the receptor complex, allowing to reveal the location of the receptor complex [28]. The RCPs are detected and visualized by hybridization with fluorescent-labeled oligonucleotides complementary to the repeated sequences encoded in the RCPs, which renders them visible for fluorescence microscopy (Fig. 1).

3 Materials

3.1 Buffers

1. Hoffman solution (cryoprotection for free-floating brain sections): 250 mL 0.4 M PBS, ethylene glycol 300 mL, 300 g sucrose, 10 g polyvinylpyrrolidone, and 9 g NaCl. Add high purity water to 1000 mL. Keep the resulting solution in a freezer (cold storage: –20 °C).
2. Phosphate-buffered saline (PBS). PBS is prepared by mixing 0.23 g NaH_2PO_4 (anhydrous; 1.90 mM), 1.15 g Na_2HPO_4 (anhydrous; 8.10 mM), and 9.00 g NaCl (154 mM). Then, add H_2O to 900 mL and, if needed, adjust to desired pH (7.2–7.4) with 1 M NaOH or 1 M HCl. Finally, add H_2O to 1 L, filter, sterilize, and store indefinitely at 4 °C. PBS could also be prepared at a 10× concentration (commercially available at Sigma-Aldrich (Cat. No: P5493-1L)) and stored until dilution into the working solution.
3. Glycine buffer (10 mM): dissolve 0.75 g glycine in 100 mL PBS. Store at 4 °C.
4. Permeabilization buffer: 0.1 % Triton X-100 in PBS (e.g., 0.1 mL Triton X-100 in 100 mL PBS). Store at 4 °C.
5. Blocking solution: Prepare the blocking solution by preparing 0.2 % BSA in PBS (e.g., 0.2 g in 100 mL PBS, stored at 4 °C). Adjust the amount of reagents accordingly so that the total volume is kept at 400 μL × well (12-well plate). Prepare this solution fresh. This blocking solution can be replaced by, e.g., the Duolink blocking solution (Sigma-Aldrich) or the Odyssey blocking buffer (Licor Biosciences). However, choose the blocking agent best suited for the antibodies used. If animal serum is used to replace the BSA, for example, the use of 5 % sterile-filtered goat serum, make sure that it is sterile filtered, as unfiltered serum may increase the amount of background signals.
6. Primary antibodies and proximity probes (oligonucleotide-labeled secondary antibodies), incubation buffer. We strongly recommend to dilute the antibodies in the blocking solution to be used (see above 5).

7. Ligation buffer: 10 mM Tris-acetate, 10 mM magnesium acetate, 50 mM potassium acetate, and pH 7.5 adjusted with HCl. Stored at −20 °C [29].
8. Hybridization-ligation solution: BSA (250 g/mL), T4 DNA ligase (final concentration of 0.05 U/μL), Tween-20 (0.05 %), NaCl 250 mM, ATP 1 mM, and the circularization or connector oligonucleotides (125–250 nM). Circularization or connector oligonucleotides can be designed and synthesized as described previously [29]. Before usage, vortex briefly to mix the ligase with the solution. Alternatively, the ligation buffer and the hybridization-ligation solution can be ordered from Olink Bioscience or Sigma-Aldrich (Cat No. DUO92008).
9. Washing buffer A: 8.8 g NaCl, 1.2 g Tris base, and 0.5 mL Tween-20. Dissolve in 800 mL high purity water and adjust the pH to 7.4 using HCl. Adjust with high purity water to 1000 mL and filter through a 0.22 μm filter. Store at 4 °C.
10. Amplification solution: Instead of preparing the solutions described below [11–13], one amplification solution can be purchased (Olink Bioscience or Sigma-Aldrich (Cat No. DUO92008)) and used.
11. Rolling circle amplification (RCA) buffer: 50 mM Tris-HCl, 10 mM $MgCl_2$, 10 mM $(NH_4)_2SO_4$, and pH 7.5 adjusted with HCl. Stored at −20 °C.
12. RCA solution (final concentration: phi-29 polymerase 0.125–0.200 U/μL, BSA (250 g/mL), 1× RCA buffer, Tween-20 (0.05 %), and dNTP (250 M for each)).
13. Detection solution (final concentration: BSA (250 g/mL), 2 μL sodium citrate 20X (A 20X stock solution consists of 3 M sodium chloride and 300 mM trisodium citrate (adjusted to pH 7.0 with HCl)), 4 μL Tween-20 (0.5 %), and the fluorescence detection by fluorophores (e.g., Texas Red or Alexa 555)-oligonucleotide strand (5 μM) (*see* [29])
14. Washing buffer B: 5.84 g NaCl, 4.24 g Tris base, and 26.0 g Tris-HCl. Dissolve in 500 mL high purity water and adjust the pH to 7.5 using HCl. Then add again high purity water to 1000 mL. Filter through a 0.22 μm filter. Store at 4 °C.
15. Mounting medium (e.g., VectaShield, Vector Labs)

3.2 Brain Tissue Preparation

For the analysis of GPCR homo- and heteroreceptor complexes in the rat brain, we highly recommend the use of formaldehyde-fixed frozen free-floating sections, whose production is described in detail in the following (**Note 1**). First, animals are deeply anesthetized by an intraperitoneal (i.p.) injection of a high dose of pentobarbital (60 mg/mL, [0.1 mL/100 g]) and then perfused intracardially with 30–50 mL ice-cold 4 % paraformaldehyde (PFA)

in 0.1 M phosphate-buffered saline (PBS, pH 7.4) solution. After perfusion, brains are collected and transferred into well-labeled glass vials filled with 4 % PFA fixative solution for 6–12 h. Then, the brains are placed in 10 and 30 % sucrose (0.1 M PBS, pH 7.4) and incubated for 1 day (10 % sucrose) and a number of days (30 % sucrose) at 4 °C with several sucrose buffer changes, until freezing the brain (in a bowl with dry ice: put inside a beaker with isopentane; when the isopentane reaches −45 °C, enter the mold with tissue; once frozen store at −80 °C). Proceed to generate the tissue sections (10–30 μm thick) using a cryostat (stored tissue at −20 °C on the day before cutting). After cutting, store them in Hoffman solution (e.g., in a 24-well plate). Alternatively, to the use of fixed free-floating sections, you can use fixed frozen sections attached to microscopy slides. The mounted sections on slides must be kept at −20 °C until use.

3.3 Proximity Probes: Conjugation of Oligonucleotides to Antibodies

Proximity probes are created through the attachment of oligonucleotides to antibodies. The antibodies are functionalized by either direct covalent coupling of an oligonucleotide [29] or non-covalent coupling by incubating biotinylated antibodies with a streptavidin-modified oligonucleotide [30]. The oligonucleotide component of the proximity probes can be functionalized to either primary antibodies or secondary antibodies. The latter approach avoids the need to conjugate the oligonucleotide components to each primary antibody protomer pair, saving time and costs. Mainly three types of chemical methods can be used for the conjugation of oligonucleotides to antibodies: the maleimide/NHS-esther chemistry (SMCC) [31], the succinimidyl 4-hydrazinonicotinate acetone hydrazone (SANH) [32], or the commercially available Antibody-Oligonucleotide All-in-One Conjugation Kit from Solulink company (http://www.solulink.com/). It is based on two complementary hetero-bifunctional linkers (Sulfo-S-4FB (formylbenzamide) and S-HyNic (hydrazino-nicotinamide)). The act of conjugation can severely affect the ability of some antibodies to bind an antigen. For this reason, different antibodies, conjugation chemistries, and reaction conditions to obtain suitable proximity probes must be tested prior to any experiments. Alternatively, antigen-validated, proximity probes from specialized companies like Duolink (Uppsala, Sweden; http://www.olink.com/) or Sigma-Aldrich can be bought directly.

4 Assay Protocol

1. First, wash the fixed free-floating sections (storage at −20 °C in Hoffman solution) four times with PBS.
2. Quench your brain slices with 10 mM glycine buffer, for 20 min at room temperature (**Note 2**).

3. Wash twice, for 5 min each, with PBS at room temperature.
4. Then incubate with the permeabilization buffer (10 % fetal bovine serum (FBS) and 0.5 % Triton X-100 or Tween-20 in Tris buffer saline (TBS), pH 7.4) for 30 min at room temperature.
5. Wash twice, for 5 min each, with PBS at room temperature.
6. Then incubate with the blocking buffer (0.2 % BSA in PBS) for 30 min at room temperature (**Note 3**). It should be checked regularly that the reaction does not dry out since this will cause a high background signal.
7. Turn on the incubator and preheat the humidity chamber until usage.
8. Incubate the brain sections with the primary antibodies diluted in a suitable concentration in the blocking solution for 1–2 h at 37 °C or at 4 °C overnight (**Note 4**).
9. Wash twice, for 5 min each, with the blocking solution at room temperature under gentle agitation to remove the excess of primary antibodies.
10. In the mean time, if primary antibodies are used in combination with secondary proximity probes, dilute the secondary antibodies proximity probes to a suitable concentration in the blocking solution. It is important to use the same buffer as those for the primary antibody to avoid background staining. Apply the proximity probe mixture to the sample and incubate for 1 h at 37 °C in a humidity chamber. Do not allow the samples to dry as this will also cause artifacts.
11. To remove the unbound proximity probes, wash the slides twice, 5 min each time, with blocking solution at room temperature under gentle agitation.
12. Prepare the hybridization-ligation solution. To ensure optimal conditions for the enzymatic reactions, the sections should be soaked for 1 min in ligation buffer (10 mM Tris-acetate, 10 mM magnesium acetate, 50 mM potassium acetate, pH 7.5 [29]), prior to addition of the hybridization-ligation solution (final concentration: BSA (250 g/mL), T4 DNA ligase buffer, Tween-20 (0.05 %), NaCl 250 mM, ATP 1 mM, and the circularization or connector oligonucleotides 125–250 nM). Circularization or connector oligonucleotides can be designed and synthesized as described previously ([29]). Remove the soaking solution (ligation buffer), and add T4 DNA ligase at a final concentration of 0.05 U/μL to the hybridization-ligation solution. Vortex briefly to mix the ligase with the solution. Apply the mixture immediately to the sections and incubate slides in a humidity chamber at 37 °C for 30 min. Alternatively, the ligation buffer and the hybridization-ligation solution can

be ordered from Olink Bioscience or Sigma-Aldrich (Cat No. DUO92008).

13. To remove the excess of connector oligonucleotides, wash twice, for 5 min each, with the washing buffer A at room temperature under gentle agitation. Tap off all excess washing solution.
14. Prepare the rolling circle amplification mixture. Soak the sections in RCA buffer for 1 min. Remove the soaking solution, and add the RCA solution (final concentration: phi-29 polymerase 0.125–0.200 U/μL, BSA (250 g/mL), RCA buffer, Tween-20 (0.05 %), and dNTP (250 M for each)). Vortex briefly the RCA solution and incubate in a humidity chamber for 100 min at 37 °C. Prepare the detection solution and incubate the sections in a humidity chamber for 30 min at 37 °C. Keep the detection solution in the dark to prevent fluorophore bleaching. From now on, all reactions and washing steps should be performed in the dark. Alternatively to preparing these buffers and solutions by yourself, the amplification mixture and the detection solution can be ordered from Olink Bioscience or Sigma-Aldrich (Cat No. DUO92008).
15. Wash the sections twice in the dark, for 10 min each, with the washing buffer B at room temperature under gentle agitation.
16. Dip the sections in a washing buffer B dilution of 1:10 and let sections dry at room temperature in the dark.
17. The free-floating sections are put on a microscope slide and a drop of appropriate mounting medium (e.g., VectaShield or Dako) is applied. The cover slip is placed on the section and sealed with nail polish. The sections should be protected against light and can be stored for several days at 4 °C or for several months/years at −20 °C (**Note 5**).

5 Quantitative PLA Image Analysis

1. Visualize the sections with fluorescence microscopy equipped with excitation/emission filters compatible with the fluorophores used. The in situ PLA signals have a very characteristic bright sub-micrometer-sized puncta appearance that is easily recognized and distinguishable from potential background fluorescence (*see* Fig. 2). While moving the focus through the sample tissue, appearance and disappearance of PLA signals should be noticeable. Up to a certain density of PLA signals, they appear as discrete dots (puncta, blobs) that can be easily counted/quantified using image analysis software.
2. Analyze the captured images using image techniques to quantify the number of dots. Many commercially image analysis

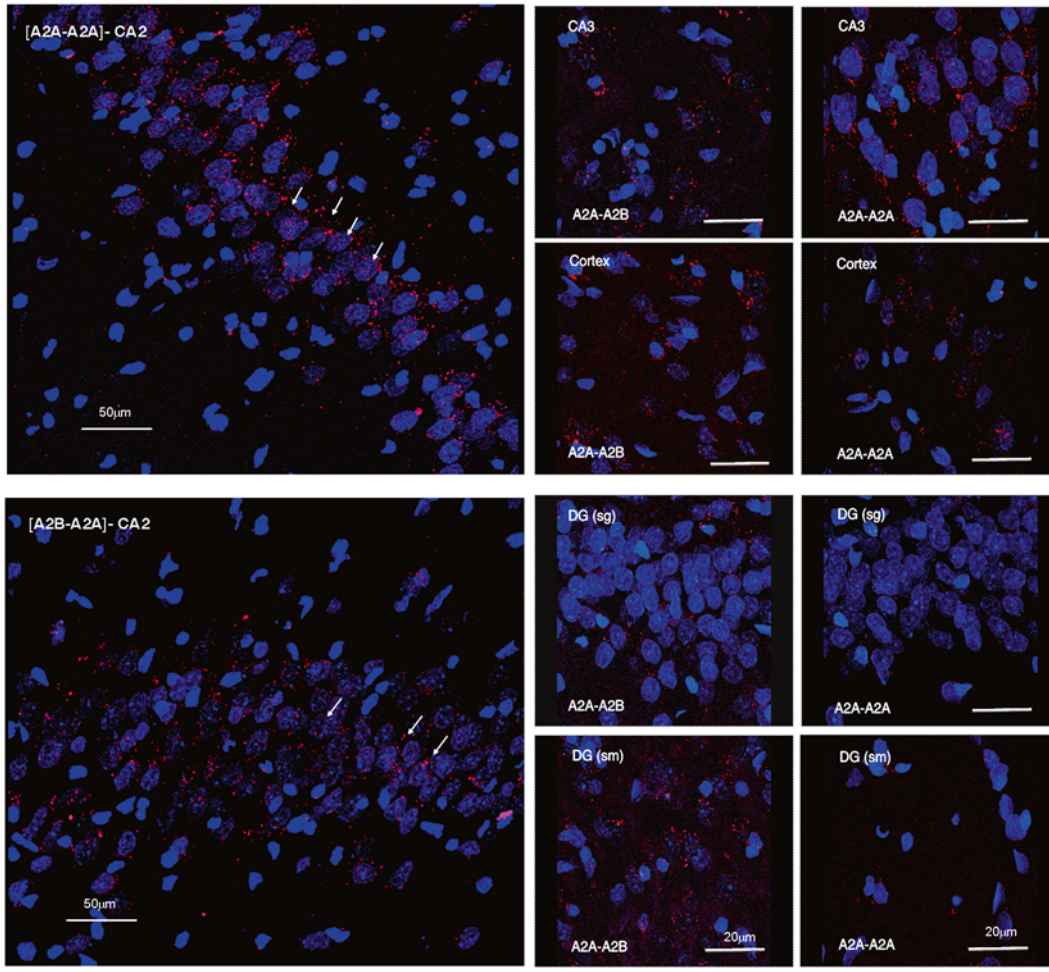

Fig. 2 Examples of in situ PLA assay in the hippocampus formation and cerebral cortex. (*Upper-left panel*) High densities of PLA-positive profiles (*red*) are shown in the pyramidal cell layer CA2 representing the A2A-A2A homoreceptor complexes. (*Lower-left panel*) Medium densities of the PLA-positive blobs are shown in the pyramidal cell layer of the CA2 representing the A2B-A2A isoreceptor complexes. In the two images, *arrows* point to examples of PLA-positive blobs. In the *right panels*, examples of PLA-positive blobs representing A2A-A2B isoreceptor complexes and A2A-A2A homoreceptor complexes are shown from the same regions of the hippocampus formation and the cerebral cortex. There presences in the CA3 regions and in the granular and molecular layers of the dentate gyros are illustrated. The scale bar are shown in the *lower-right panels* (20 µm)

software packages can be used (e.g., Duolink ImageTool (Sigma-Aldrich)), but also free software packages are available (e.g., BlobFinder, CellProfiler).

3. Usually four important parameters should be kept in mind for a proper analysis and result interpretation: (1) the number of DAPI nuclei in the sample field, (2) the number of positive PLA/dots per sample field, (3) the total number of positive

PLA cells/nuclei per sample field, and (4) the diameter sizes of the individual PLA blobs (the diameter may indicate if aggregates (higher order) of receptor complexes exists). Within these four values, it will be possible to get an overall view of the expression/enrichment of GPCR heteroreceptor complexes in the different brain areas analyzed and extract relevant conclusions from the comparisons between brain areas (Fig. 2). We have proposed the molecular phenomenon of receptor-receptor interactions as a fruitful way to understand how brain function can increase through molecular integration of signals. An alteration in specific receptor-receptor interactions or their balance/equilibrium (with the corresponding monomers-homomers) is indeed considered to have a role in the pathogenic mechanisms that lead to various brain diseases. Therefore, targeting protomer-protomer interactions in heteroreceptor complexes or changing the balance with their corresponding homoreceptor complexes in discrete brain regions may become an important field for developing novel drugs, including hetero-bivalent drugs and optimal types of combined treatments. The analysis of animal or human brain material with in situ PLA can reveal if the relative abundance of specific homo- and heteroreceptor complexes in discrete brain regions is altered in brain diseases or under certain drug treatments, for instance, chronic L-dopa treatment in Parkinson's disease [25]. In this analysis, it is important also to determine the ratio between heteroreceptor complex populations versus total number of the two participating protomer populations, using in addition to Western blots, receptor autoradiography, and biochemical binding methods. The two latter methods show the densities and affinities of the two functional receptor populations. The relationship between these parameters will help to normalize the heteroreceptor complexes values for comparison between groups in addition to evaluating the potential changes in the total number of the two protomer populations [19]. Certainly, we cannot compare or determine directly a balance between the homo- and heteroreceptor complexes populations in the same tissue using the in situ PLA approach, because of a technical limitation of the procedure itself. But the method could help us determine each population independently and compare their relative expression levels after an appropriate numerical analysis. Furthermore, increasing importance will be to determine the agonist/antagonist regulation of these homo-/heteroreceptor complexes in order to understand their potential roles as drug targets or as markers of brain disease progression.

6 Advantages and Disadvantages of the PLA Method

In situ PLA can offer advantages by:

1. Giving the opportunity to study the existence of any potential homo- and heteroreceptor complexes, for which a pair of suitable antibodies is available without the need of employing a genetic constructs.
2. The method could be performed in both cells and tissue samples, including human specimens collected from biobanks.
3. The in situ PLA could be useful to monitor the effects of different compounds like agonists and antagonists or their combined treatment on the balance of homo- and heteroreceptor complexes in cells and tissue.
4. The information obtained by the in situ PLA is at the resolution of individual cells or even of subcellular compartments providing profound insights into cellular heterogeneity in tissues.
5. The method also provides an enhanced sensitivity and selectivity compared to many other methods since powerful rolling circle amplification and dual target recognition are used.

As with any method, there are limitations, for instance:

1. The in situ PLA cannot be used in live cells, as fixation it is a prerequisite for the cell/tissue material employed.
2. When studying receptor-receptor interactions, it is important to remember that the method, like many other methods for studying protein-protein interactions, can show that two proteins are in close proximity and, therefore, likely directly interact. Proteins can also interact indirectly through an adapter protein. The maximal distance between two epitopes to give rise to a signal with in situ PLA is 10–30 nm with direct-conjugated proximity probes and slightly longer when secondary proximity probes are used. This distance will be dependent on the size of the receptors/antibodies and the respective length of the attached oligonucleotides. By changing the length of the oligonucleotides, the maximal distance limits can be reduced or increased. However, in general, the functional distance is usually close to the one detected in a FRET assay [27].
3. Another critical parameters for achieving good results is the use of excellent antibodies. Importantly, the antibodies have to be used under optimal conditions taking into consideration parameters such as antibody concentration, epitopes targeted by the antibodies, fixation, antigen retrieval, blocking conditions, etc.

4. A range of controls, both positive and negative ones, should be used to guarantee the specificity of the PLA signal. Positive controls can include cells where the protein is known to be expressed, such as in certain cells or tissues or in cells transfected to express the protein. Negative controls include cells or tissues that do not express the protein or where the protein has been knocked out or downregulated by, e.g., siRNA.

7 Notes

1. As for all antibody-based staining methods, the samples should be sufficiently pretreated to fit the primary antibodies with respect to fixation, permeabilization, and antigen retrieval of the tissue to be investigated. Similar conditions as employed for immunohistochemistry can be used for in situ PLA procedures. For in situ PLA, the common options are fixed paraffin-embedded or cryostat sections. The choice of section is determined by a number of conditions, including the time and skill of the investigator. However, careful consideration of the fixation protocol is especially necessary to ensure the optimal preservation of the morphology of the specimen and target antigen (receptors).
2. Autofluorescence can be brought on by certain endogenous tissue constituents, e.g., fibronectin, lipofuscin, and elastin, and by fixation in aldehydes. Based on this phenomenon, after rehydrating your formalin-fixed frozen sections and before blocking the slices, it is important to incubate them in 10–100 mM glycine PBS, pH 7.4, for 20 min. Glycine solution has the ability to quench autofluorescence caused by reactive groups (free aldehydes) in your cell or tissue-fixed samples. Alternatively to glycine solution, we can employ as well a solution of 50 mM ammonium chloride in PBS for 10 min. or a solution of 1 % sodium borohydride in PBS for 10–20 min. Sodium borohydride is flammable on contact with water and harmful by ingestion or inhalation. Therefore, take adequate precautions. It varies from sample to sample which method works the best, but in formalin-fixed rat brain sections, we had most success with the glycine solution methods. Another measure to avoid or reduce background in your samples is reducing the section thickness, as the intensity of autofluorescence depends on this parameter.
3. To reduce the likelihood of unspecific binding of the antibodies to the tissue, the tissue needs to be blocked by a blocking agent, such as bovine serum albumin (BSA) (by adding 1 μL BSA (10 mg/mL) and 1 μL sonicated salmon sperm DNA (0.1 mg/mL) to 38 μL 0.5 Triton X-100 or Tween-20 in TBS, pH 7.4 [32]). An animal serum like 10 % FBS can be used, but

make sure that it is sterile filtered, as unfiltered serum may increase the amount of background signals. Use the blocking agent best suited for the antibodies used.

4. The conditions for incubation with the primary/secondary antibodies (probes) should be chosen according to the manufacturer's recommendations, or be identified by the users.
5. The intensity of the rolling circle product will go down quickly in some mounting media. It is necessary to use a mounting medium containing anti-fade reagents.

Acknowledgments

This work has been supported by the Karolinska Institutets Forskningsstiftelser 2014/2015 to D.O.B-E and by the Swedish Medical Research Council (62X-00715-50-3) and AFA Försäkring (130328) to KF and D.O.B-E. D.O.B-E belongs to Academia de Biólogos Cubanos.

References

1. Achour L, Kamal M, Jockers R, Marullo S (2011) Using quantitative BRET to assess G protein-coupled receptor homo- and heterodimerization. Methods Mol Biol 756:183–200
2. Borroto-Escuela DO, Narvaez M, Perez-Alea M, Tarakanov AO, Jimenez-Beristain A, Mudo G, Agnati LF, Ciruela F, Belluardo N, Fuxe K (2015) Evidence for the existence of FGFR1-5-HT1A heteroreceptor complexes in the midbrain raphe 5-HT system. Biochem Biophys Res Commun 456(1):489–493
3. Fuxe K, Guidolin D, Agnati LF, Borroto-Escuela DO (2015) Dopamine heteroreceptor complexes as therapeutic targets in Parkinson's disease. Expert Opin Ther Targets 19(3): 377–398
4. Fuxe K, Borroto-Escuela D, Fisone G, Agnati LF, Tanganelli S (2014) Understanding the role of heteroreceptor complexes in the central nervous system. Curr Protein Pept Sci 15(7):647
5. Borroto-Escuela DO, Romero-Fernandez W, Mudo G, Perez-Alea M, Ciruela F, Tarakanov AO, Narvaez M, Di Liberto V, Agnati LF, Belluardo N, Fuxe K (2012) Fibroblast growth factor receptor 1–5-hydroxytryptamine 1A heteroreceptor complexes and their enhancement of hippocampal plasticity. Biol Psychiatry 71(1):84–91
6. Nai Q, Li S, Wang SH, Liu J, Lee FJ, Frankland PW, Liu F (2009) Uncoupling the D1-N-methyl-D-aspartate (NMDA) receptor complex promotes NMDA-dependent long-term potentiation and working memory. Biol Psychiatry 67(3):246–254
7. Narvaez M, Millon C, Borroto-Escuela D, Flores-Burgess A, Santin L, Parrado C, Gago B, Puigcerver A, Fuxe K, Narvaez JA, Diaz-Cabiale Z (2015) Galanin receptor 2-neuropeptide Y Y1 receptor interactions in the amygdala lead to increased anxiolytic actions. Brain Struct Funct 220(4):2289–2301
8. Borroto-Escuela DO, Brito I, Romero-Fernandez W, Di Palma M, Oflijan J, Skieterska K, Duchou J, Van Craenenbroeck K, Suarez-Boomgaard D, Rivera A, Guidolin D, Agnati LF, Fuxe K (2014) The G protein-coupled receptor heterodimer network (GPCR-HetNet) and its hub components. Int J Mol Sci 15(5):8570–8590
9. Borroto-Escuela DO, Flajolet M, Agnati LF, Greengard P, Fuxe K (2013) Bioluminescence resonance energy transfer methods to study G protein-coupled receptor-receptor tyrosine kinase heteroreceptor complexes. Methods Cell Biol 117:141–164
10. Fernandez-Duenas V, Llorente J, Gandia J, Borroto-Escuela DO, Agnati LF, Tasca CI, Fuxe K, Ciruela F (2012) Fluorescence resonance energy transfer-based technologies in the study of protein-protein interactions at the cell surface. Methods 57(4):467–472
11. Skieterska K, Duchou J, Lintermans B, Van Craenenbroeck K (2013) Detection of G protein-coupled receptor (GPCR) dimerization

by coimmunoprecipitation. Methods Cell Biol 117:323–340

12. James JR, Oliveira MI, Carmo AM, Iaboni A, Davis SJ (2006) A rigorous experimental framework for detecting protein oligomerization using bioluminescence resonance energy transfer. Nat Methods 3(12):1001–1006
13. Bouvier M, Heveker N, Jockers R, Marullo S, Milligan G (2007) BRET analysis of GPCR oligomerization: newer does not mean better. Nat Methods 4(1):3–4; author reply 4
14. Marullo S, Bouvier M (2007) Resonance energy transfer approaches in molecular pharmacology and beyond. Trends Pharmacol Sci 28(8):362–365
15. Audet M, Lagace M, Silversides DW, Bouvier M (2010) Protein-protein interactions monitored in cells from transgenic mice using bioluminescence resonance energy transfer. FASEB J Off Publ Fed Am Soc Exp Biol 24(8): 2829–2838
16. Fernandez-Duenas V, Gomez-Soler M, Jacobson KA, Santhosh Kumar T, Fuxe K, Borroto-Escuela DO, Ciruela F (2012) Molecular determinants of a(2a) r-d(2) r allosterism: role of the intracellular loop 3 of the d(2) r. J Neurochem 123(3):373–384
17. Herrick-Davis K, Grinde E, Cowan A, Mazurkiewicz JE (2013) Fluorescence correlation spectroscopy analysis of serotonin, adrenergic, muscarinic, and dopamine receptor dimerization: the oligomer number puzzle. Mol Pharmacol 84(4):630–642
18. Borroto-Escuela DO, Van Craenenbroeck K, Romero-Fernandez W, Guidolin D, Woods AS, Rivera A, Haegeman G, Agnati LF, Tarakanov AO, Fuxe K (2010) Dopamine D2 and D4 receptor heteromerization and its allosteric receptor-receptor interactions. Biochem Biophys Res Commun 404(4):928–934
19. Borroto-Escuela DO, Romero-Fernandez W, Garriga P, Ciruela F, Narvaez M, Tarakanov AO, Palkovits M, Agnati LF, Fuxe K (2013) G protein-coupled receptor heterodimerization in the brain. Methods Enzymol 521: 281–294
20. Trifilieff P, Rives ML, Urizar E, Piskorowski RA, Vishwasrao HD, Castrillon J, Schmauss C, Slattman M, Gullberg M, Javitch JA (2011) Detection of antigen interactions ex vivo by proximity ligation assay: endogenous dopamine D2-adenosine A2A receptor complexes in the striatum. Biotechniques 51(2):111–118
21. Borroto-Escuela DO, Romero-Fernandez W, Narvaez M, Oflijan J, Agnati LF, Fuxe K (2014) Hallucinogenic 5-HT2AR agonists LSD and DOI enhance dopamine D2R protomer recognition and signaling of D2-5-HT2A heteroreceptor complexes. Biochem Biophys Res Commun 443(1):278–284
22. Borroto-Escuela DO, Narvaez M, Di Palma M, Calvo F, Rodriguez D, Millon C, Carlsson J, Agnati LF, Garriga P, Diaz-Cabiale Z, Fuxe K (2014) Preferential activation by galanin 1-15 fragment of the GalR1 protomer of a GalR1-GalR2 heteroreceptor complex. Biochem Biophys Res Commun 452(3): 347–353
23. Romero-Fernandez W, Borroto-Escuela DO, Agnati LF, Fuxe K (2013) Evidence for the existence of dopamine D2-oxytocin receptor heteromers in the ventral and dorsal striatum with facilitatory receptor-receptor interactions. Mol Psychiatry 18(8):849–850
24. Borroto-Escuela DO, Corrales F, Narvaez M, Oflijan J, Agnati LF, Palkovits M, Fuxe K (2013) Dynamic modulation of FGFR1-5-HT1A heteroreceptor complexes. Agonist treatment enhances participation of FGFR1 and 5-HT1A homodimers and recruitment of beta-arrestin2. Biochem Biophys Res Commun 441(2):387–392
25. Antonelli T, Fuxe K, Agnati L, Mazzoni E, Tanganelli S, Tomasini MC, Ferraro L (2006) Experimental studies and theoretical aspects on A2A/D2 receptor interactions in a model of Parkinson's disease. Relevance for L-dopa induced dyskinesias. J Neurol Sci 248(1–2): 16–22
26. Millón C, Flores-Burgess A, Narváez M, Borroto-Escuela DO, Santín L, Parrado C, Narváez JA, Fuxe K, Díaz-Cabiale Z. A role for galanin N-terminal fragment (1-15) in anxiety- and depression-related behaviors in rats. Int J Neuropsychopharmacol. 2014 Oct 31;18(3). pii: pyu064. doi: 10.1093/ijnp/pyu064.
27. Weibrecht I, Leuchowius KJ, Clausson CM, Conze T, Jarvius M, Howell WM, Kamali-Moghaddam M, Soderberg O (2010) Proximity ligation assays: a recent addition to the proteomics toolbox. Expert Rev Proteomics 7(3):401–409
28. Soderberg O, Leuchowius KJ, Kamali-Moghaddam M, Jarvius M, Gustafsdottir S, Schallmeiner E, Gullberg M, Jarvius J, Landegren U (2007) Proximity ligation: a specific and versatile tool for the proteomic era. Genet Eng (N Y) 28:85–93
29. Soderberg O, Leuchowius KJ, Gullberg M, Jarvius M, Weibrecht I, Larsson LG, Landegren U (2008) Characterizing proteins and their interactions in cells and tissues using the in situ proximity ligation assay. Methods 45(3): 227–232

30. Gullberg M, Gustafsdottir SM, Schallmeiner E, Jarvius J, Bjarnegard M, Betsholtz C, Landegren U, Fredriksson S (2004) Cytokine detection by antibody-based proximity ligation. Proc Natl Acad Sci U S A 101(22):8420–8424
31. Soderberg O, Gullberg M, Jarvius M, Ridderstrale K, Leuchowius KJ, Jarvius J, Wester K, Hydbring P, Bahram F, Larsson LG, Landegren U (2006) Direct observation of individual endogenous protein complexes in situ by proximity ligation. Nat Methods 3(12): 995–1000
32. Leuchowius KJ, Weibrecht I, Soderberg O (2011) In situ proximity ligation assay for microscopy and flow cytometry. Curr Protoc Cytom Chapter 9:Unit 9.36

Part II

Neuroanatomical Techniques

Chapter 10

Fluorescent In Situ Hybridization for Sensitive and Specific Labeling

Miwako Yamasaki and Masahiko Watanabe

Abstract

We describe a simplified and efficient protocol for non-isotopic fluorescent in situ hybridization experiments, allowing the implementation of multiple probe analyses at a single-cell resolution. This protocol involves simultaneous and specific hybridization of hapten-labeled riboprobes for mRNAs, followed by probe visualization via immunohistochemical procedures and peroxidase-mediated precipitation of tyramide-linked fluorophores. This procedure can be used to detect virtually any combination of two or three mRNA populations and is therefore a powerful method to characterize neuronal populations expressing a target gene and to determine the expression of genes of interest in the same or distinct cells. A combination of fluorescent in situ hybridization with immunofluorescence and retrograde fluorescent tracer labeling further expands the benefit and utility of histology-based methods. We also provide representative results and troubleshooting for the important steps of this protocol. Once specific probes and tissue sections are obtained, the total length of the entire procedure is 2–3 days.

Key words Fluorescent in situ hybridization, Immunohistochemistry, In situ hybridization, mRNA, Riboprobe, Tyramide signal amplification

1 Introduction

The in situ hybridization (ISH) method allows specific nucleic acid sequences to be detected on histological sections and has been one of the most powerful methods available to examine the spatiotemporal pattern of gene expression. Although the original methods for ISH using radiolabeled probes are highly effective in detecting very low levels of transcripts [1], their major limitations are relatively poor resolution and long exposure time. The more recently developed indirect labeling method, using non-isotopic hapten-conjugated probes that are visualized by antibody staining, has overcome these limitations. Specifically, a fluorescence ISH (FISH) protocol using the tyramide signal amplification (TSA) system has proven the most efficient, because it provides not only specific and reproducible results but also a means of characterizing the

Rafael Luján and Francisco Ciruela (eds.), *Receptor and Ion Channel Detection in the Brain: Methods and Protocols*, Neuromethods, vol. 110, DOI 10.1007/978-1-4939-3064-7_10,

neurochemical identity of given neuronal populations. We have progressively improved and simplified the previously established, single-labeling non-isotopic ISH [2] to obtain a robust and versatile FISH protocol. Here, we provide a detailed description of the techniques and optional approaches to expand the benefits of a histology-based method, including simultaneous detection of two or three mRNAs of interest and concomitant immunofluorescence or retrograde tracer labeling.

1.1 Overview of Procedures

Our FISH protocol entails specific hybridization of hapten-labeled riboprobes to target mRNAs, followed by probe detection using immunohistochemical procedures. The preparation of probes and samples is essentially similar to that of standard isotopic ISH protocols. After choosing the cDNA sequence of interest, a cDNA template for probe production is prepared by polymerase chain reaction (PCR) amplification and subcloned into a Bluescript II plasmid containing the T3 and T7 RNA polymerase promoters. Hapten-conjugated UTP is incorporated into the cRNA probe via in vitro transcription. After hybridization of the probe to the target mRNA, the hapten is recognized by a specific antibody conjugated with horseradish peroxidase (POD). POD then catalyzes and forms a precipitation of tyramide-linked fluorophores around the probe, thus offering a means to localize target mRNAs with spatial precision.

Three different haptens are presently available, digoxigenin (DIG), fluorescein isothiocyanate (FITC), and biotin, and therefore, up to three different mRNAs can be detected simultaneously. For double-labeling FISH (double FISH), a combination of DIG- and FITC-labeled probes is the easiest and most efficient. In double FISH, two probes labeled with different haptens are hybridized at the same time, but then immunostained and visualized sequentially in a two-step procedure. After the first round of deposition of the first hapten, the peroxidase activity of the first antibody-coupled POD is inactivated by hydrogen peroxide incubation. Subsequently, a POD-conjugated antibody against the second hapten is applied and visualized. Routinely, we use fresh-frozen cryostat sections mounted on glass slides; however, when combining with retrograde tracer labeling or immunofluorescence, we use perfusion-fixed free-floating sections instead.

2 Materials

2.1 Preparation and PCR Amplification of the Target cDNA and Plasmid Construction

Alkaline phosphatase (*Escherichia coli* C57) (Takara, Kyoto, Japan, cat. no. 2120A)

Agarose (SeaPlaque GTG) (Lonza, Rockland, ME, USA, cat. no. 50100)

Blunting Kination Ligation (BKL) Kit (Takara, cat. no. 6127)

Chloroform

cDNA library

DNA polymerase (PrimeSTAR HS) (Takara, cat. no. R010A)

Double-distilled water (dDW)

Ethidium bromide

Ethylenediaminetetraacetic acid (EDTA)

ISOGEN (Nippon Gene, Toyama, Japan, cat. no. 317-02501)

QIAquick Gel Extraction Kit (QIAGEN, Hilden, Germany, cat. no. 28704)

Restriction enzymes supplied with 10× buffer (e.g., Takara)

TAE (Tris–acetate–EDTA, 10× stock)

Tris(hydroxymethyl)aminomethane 999

2.2 In Vitro Transcription

Acetic anhydride (WAKO, Tokyo, Japan, cat. no. 146-07271)

Biotin 10× RNA-labeling mix (Roche Applied Science, Mannheim, Germany, cat. no. 11685597910)

DIG 10× RNA-labeling mix (Roche Applied Science, cat. no. 11277073910)

Dimethyl sulfoxide (DMSO)

DNA step ladder (e.g., WAKO, cat. no. 316-00454 and 316-00664)

Ethanol (100 %)

Fluorescein 10× RNA-labeling mix (Roche Applied Science, cat. no. 11685619910)

Formamide

Ribonuclease inhibitor (Toyobo, Tokyo, Japan, cat. no. SIN-201)

RNA polymerase supplied with 10× transcription buffer (e.g., T3 and T7 polymerase; Promega, Madison, WI, USA, cat. no. P208C and P207B, respectively)

RQ1 RNase-free DNase (Promega, cat. no. M610A)

Spermidine

Triethanolamine-HCl (TEA-HCl)

2.3 Preparing Brain Samples, Pre-hybridization, and Hybridization

Dextran sulfate sodium salt (Sigma-Aldrich, St. Louis, MO, USA, cat. no. D8906)

Disodium hydrogen phosphate 12-water

Iodoacetamide

N-Lauroylsarcosine sodium salt

Paraformaldehyde (Merck, Darmstadt, Germany, cat. no. 1.04005.1000)

Parafilm (Bemis, Neenah, WI, USA, cat. no. PM-996)

Silane-coated slide glasses (Muto Pure Chemicals, Tokyo, Japan, cat. no. New Silane II)

Sodium citrate trisodium

Sodium chloride

Sodium dihydrogen phosphate dihydrate

Sodium hydroxide

Tween-20 (polyoxyethylene (20) sorbitan monolaurate)

2.4 Immunohistochemical Detection of Probes

Anti-biotin, POD conjugated (Vector Laboratories, Burlingame, CA, USA, cat. no. SP-3010)

Anti-digoxigenin-POD, Fab fragments (Roche Applied Science, cat. no. 11207733910)

Anti-fluorescein/Oregon Green antibody, HRP conjugate (Invitrogen, Carlsbad, CA, USA, cat. no. A-21253)

DMSO

Hydrogen peroxide

ProLong Gold antifade reagent (Invitrogen, P36930)

Rabbit serum (Millipore, Temecula, CA, USA, cat. no. S20-100ML)

Sheep serum (Millipore, cat. no. S22-100ML)

TSA Plus Fluorescein Systems (PerkinElmer, Waltham, MA, USA, cat. no.NEL744001KT)

TSA Plus Cy3 Systems (PerkinElmer, cat. no. NEL741001KT)

TSA Plus Cy5 Systems (PerkinElmer, cat. no. NEL745001KT)

VECTASHIELD (Vector Laboratories, cat. no. H-1400)

2.5 Equipment (Key Equipment Is Shown in Fig. 1)

Confocal laser scanning microscope (e.g., FV1000, Olympus)

Cryostat (e.g., Leica CM 1900, Leica)

Glass staining jar

Metal slide holder

Moisture chamber

Hybridization incubator (e.g., TAITEC, Tokyo, Japan, cat. no. HB-100)

Polytron homogenizer

Presterilized filter units (e.g., Nalgene, Rochester, NY, USA, cat. no. 291-4545 and 455-0500)

Sealed container (e.g., sealed bento box)

Fig. 1 Key equipment and setup necessary for FISH. (**a**, **b**) After applying diluted riboprobes, sections are coverslipped with a sheet of parafilm (**a**) and placed in a sealed container (**b**). At the bottom of the container, sheets of filter paper soaked in 50 % (vol/vol) formamide solution diluted with DW are spread to maintain humidity. (**c**–**e**) After the overnight hybridization step, parafilm coverslips are removed, and slides are placed in a slide holder (**c**). Sections are then subjected to a series of post-hybridization washes in conventional glass staining jars (**d**) that are immersed and preheated in a water bath (**e**). (**f**) Blocking and probe visualization through immunohistochemical procedures are carried out in a humid chamber. We generally spread a sheet of paper towel soaked in DW to keep humidity

Spectrophotometer (e.g., NanoDrop 2000c, Thermo Fisher Scientific)

UV transilluminator

Water bath (e.g., TAITEC, cat. no. HB-100)

2.6 Reagent Setup

1. *4% paraformaldehyde (wt/vol) in 0.1 M PB (pH7.4, 1 L)*: Dissolve 40 g of paraformaldehyde in 500 mL of dDW, stir at 60 °C, and add 250 μL of 5 N NaOH. Allow the solution to cool, add 500 mL of 0.2 M PB, filter, and store at 4 °C. All steps should be carried out in a fume hood.

2. *Acetylation solution* (*for 200 mL*): Dissolve 3.72 g of TEA-Cl and 1.9 mL of 5 N NaOH in 190 mL of dDW. Make the volume up to 200 mL with dDW, and add 1 mL of acetic anhydride just before use.

   Note Because the acetylation solution remains stable for only a short time period, acetic anhydride should be added just before use.

3. *Hybridization buffer* (*for 500 mL*): Take a glass media bottle with a cap, and mix 250 mL of formamide, 60 mL of 5 M NaCl, 50 g of dextran sulfate, 16.5 mL of 1 M Tris–HCl (pH 8), 10 mL of 50× Denhardt's stock solution, 1 mL of 0.5 M EDTA, 0.5 g of *N*-lauroylsarcosine sodium salt, and 100 mg of tRNA. Add dDW to make the volume up to 500 mL. Put in a shaking incubator at 37 °C for 1–2 days to dissolve, filtrate with presterilized filter units (e.g., Nalgene), dispense into 50-mL plastic tubes, and store at –20 and –80 °C for immediate use and long-term storage (up to 2–3 years), respectively.
4. *20× SSC* (*for 1 L*): Mix 175.3 g of NaCl and 88.2 g of sodium citrate, and add sufficient dDW to make the volume up to 1 L. Autoclave and store at room temperature.
5. *5× SSC* (*for 1 L*): Take 250 mL of 20× SSC and 25 μL of 20 % Tween-20. Make the volume up to 1 L with dDW.
6. *2× SSC* (*for 1 L*): Take 100 mL of 20× SSC and 25 μL of 20 % Tween-20. Make the volume up to 1 L with dDW.
7. *0.1× SSC* (*for 1 L*): Take 5 mL of 20× SSC and 25 μL of 20 % Tween-20. Make the volume up to 1 L with dDW.
8. *Formamide 1* (*for 150 mL*): Mix 75 mL of formamide, 30 mL of 20× SSC, and 7.5 μL of 20 % Tween-20. Make the volume up to 150 mL with dDW.
9. *Formamide 2* (*for 150 mL*): Mix 75 mL of formamide, 15 mL of 20× SSC, and 7.5 μL of 20 % Tween-20. Make the volume up to 150 mL with dDW.
10. *TNT buffer* (*for 2 L*): Mix 200 mL of 1 M Tris–HCl (pH 7.4), 60 mL of 5 M NaCl, and 50 μL of 20 % Tween-20. Make the volume up to 2 L with dDW.
11. *NTE buffer* (*500 mL*): Mix 50 mL of 5 M NaCl, 5 mL of 1 M Tris–HCl (pH 8.0), 5 mL of 0.5 M EDTA, and 12.5 μL of 20 % Tween-20. Make the volume up to 500 mL with dDW.
12. *20 mM iodoacetamide in NTE buffer*: Dissolve 0.37 g of iodoacetamide in 100 mL of NTE buffer.
13. *10% blocking reagent* (Roche Applied Science): Prepare a 10 % stock solution of blocking reagent in 0.1 M maleic acid buffer. Gradually heat to 60 °C to dissolve, autoclave, and store aliquots at –20 °C.

14. *DIG-blocking solution*: Mix 100 % normal sheep serum, 100 % normal rabbit serum, 10 % blocking reagent (Roche Applied Science), and TNT buffer, at a ratio of 1:1:1:7. When combining with immunofluorescence using secondary antibodies against rabbit IgG, omit rabbit serum.
15. *0.5% (wt/vol) TSA-blocking solution*: Dissolve blocking reagent (PerkinElmer) in TNT buffer. Gradually heat to 60 °C, and stir continuously. Store at 4 and –20 °C for immediate use (2–3 months) and long-term storage (1 year), respectively.

3 Methods

3.1 Preparing Riboprobes

This step involves preparation of the cDNA of the gene of interest, PCR amplification of the cDNA, subcloning of the cDNA into plasmids, and in vitro transcription.

3.1.1 Preparation of the Target cDNA

Mouse brain cDNA library preparation: Isolate total RNA from homogenized fresh brains by the acid-phenol method.

1. Homogenize 1 g of fresh mouse brain in a 50-mL plastic tube in 10 mL of ISOGEN (Nippon Gene, Toyama, Japan) using a Polytron homogenizer.
2. Add 2 mL of chloroform and shake vigorously for 3 min.
3. Centrifuge at 3500 rpm for 15 min at 4 °C in a swinging bucket rotor.
4. Transfer the aqueous phase to a new plastic tube and mix with 5 mL of isopropanol.
5. Incubate at room temperature for 10 min.
6. Centrifuge at 3500 rpm for 15 min at 4 °C.
7. Wash the precipitated total RNA with 70 % ethanol.
8. Dissolve in TE buffer (10 mM Tris–HCl, pH 8.0/1 mM EDTA, pH 8.0).
9. Measure the OD260 of the total RNA to calculate the concentration (1.0 OD260 is equivalent to 40 μg/mL of RNA).
10. Construct a cDNA library using the total RNA and the First-Strand cDNA Synthesis Kit according to the manufacturer's instructions (GE Healthcare, Uppsala, Sweden).

3.1.2 PCR Amplification of the Target cDNA

The transcript is initially amplified by PCR using the forward and reverse primers. If the first round of PCR amplification results in low yields, a nested approach is used for the probe production; the product of the first PCR is then used as a template for the second round of PCR using nested forward and reverse primers. Typically, we use a protocol consisting of a series of 35 cycles, each consisting

of 96 °C for 20 s, 56 °C for 2 s, and 72 °C for minutes equivalent to the length (in kb) of PCR products, following a rule of 1 min per 1 kb of length, using PrimeSTAR HS DNA polymerase (Takara). The cDNA fragments are purified by 1 % SeaPlaque GTG agarose gel electrophoresis, followed by extraction from the agarose gel bands using the QIAquick Gel Extraction Kit.

3.1.3 Plasmid Construction

After blunting and kination using the BKL Kit, cDNA fragments are subcloned into an EcoRV site of the pBluescript (SK+), which has been dephosphorylated by bacterial alkaline phosphatase. After mini-preparation of plasmids, the nucleotide sequence of the cDNA fragments is confirmed using the T3 and T7 primers.

3.1.4 Linearization of Plasmid DNA Carrying cDNA of Interest

1. Plasmid digestion with restriction enzyme (37 °C, 2 h).

Plasmid (30 μg)	30 μL
10× buffer	50 μL
100 mM spermidine	5 μL
Restriction enzyme	5 μL
Total	500 μL

2. Run an aliquot (5 μL plus loading dye) on a 1 % agarose gel containing ethidium bromide.
3. Add 2 μL of 20 mg/mL proteinase K and incubate at 37 °C for 30 min.
4. Treat with phenol/chloroform three times.
5. Add 1/20 volumes of 5 M NaCl and 2 volumes of 100 % EtOH, and allow to precipitate at –20 °C for 15 min to 1 h.
6. Spin down, and wash precipitate with 70 % EtOH.
7. Dry, and dissolve in 20 μL of TE.
8. Adjust to 0.5 μg/μL by OD measurement at 260 nm, and store at –20 °C.

3.1.5 In Vitro Transcription

In vitro transcription is performed using 10× DIG/FITC/biotin labeling mixture (Roche Applied Science).

1. For each probe (sense and antisense), add the components listed below to a 1.5-mL tube. Mix and incubate at 37 °C for 2 h.

Linearized plasmid (0.5 μg/μL)	2 μL (1 μg)
5× buffer	4 μL
DTT	2 μL
10× labeling mixture	2 μL

RNase inhibitor	1 μL
DW	8 μL
RNA polymerase	1 μL
Total volume	20 μL

2. Add 3 μL of the following DNase mix and incubate at 37 °C for 30 min.

RNase inhibitor	1 μL
tRNA (20 mg/mL)	1 μL
RQ1 DNase	1 μL
Total volume	3 μL

3. Run an aliquot (1 μL) with loading dye on a 1.5 % agarose gel.
4. Add EtOH precipitation mix and allow to precipitate at −20 °C for more than 1 h.

0.5 M EDTA	0.8 μL
3 M LiCl	1 μL
20 μg/μL glycogen	2 μL
EtOH	65 μL

5. Centrifuge at 12,000 rpm for 20 min.
6. Wash with 70 % EtOH and allow to air-dry.
7. Dissolve in 50 μL DW.
8. Add 50 μL formamide, and store at −20 °C.

3.2 Preparing Brain Samples

In our standard protocol, we use fresh-frozen brain samples sectioned at 20 μm on a cryostat; however, when combining with retrograde tracer labeling and immunofluorescence, we use perfusion-fixed brain sections instead.

3.2.1 Fresh-Frozen Sections

1. Deeply anesthetize mice with diethyl ether, remove the brain from the skull, and place it on powdered dry ice.
2. Set the temperature of the cryostat chamber to −15 °C.
3. Place the frozen brain in the chamber of the cryostat and allow the temperature to equilibrate.
4. Section the freshly frozen brains at 20 μm on a cryostat, mount onto silane-coated glass slides, and allow to air-dry at room temperature. Store slides at −80 °C.

Note 1 Because too many sections on each glass slide may cause falsely uneven and weak hybridization signals, it is advisable to keep the number of sections as few as possible.

Note 2 Because dehydration in the freezer undermines the quality of the hybridization, the sections should be used within a month.

3.2.2 Microslicer Sections of Perfusion-Fixed Brain

These sections are subjected to free-floating ISH carried out using a glass test tube.

1. Under deep pentobarbital anesthesia, perfuse 4 % PFA for 10 min by peristaltic pump (total ~50 mL for a 30-g mouse).
2. Remove the brain and place into the fixative for 3 h at room temperature.
3. Embed brains in 2 % agarose and make 50-μm-thick sections using a microslicer. Store in 0.1 M PB (pH 7.2) containing 0.1 % sodium azide at 4 °C.

Note 1 The cutting and storage buffer should be 0.1 M PB. If sections are cut and stored in PBS, hybridization signals weaken considerably.

Note 2 In some cases, combining longer postfixation (3 days at room temperature) and cryosectioning improves the signal.

3.3 Pre-hybridization

This step entails fixation with paraformaldehyde, acetylation, and pre-hybridization with hybridization buffer. Acetylation is the most critical procedure to reduce nonspecific labeling and increase the signal-to-noise ratio. All procedures are performed at room temperature.

1. Thaw frozen brain sections and allow to air-dry	
2. Incubate sections in 4 % PFA (in PB, pH 7.2)	15 min
3. Wash sections in PBS	~5 min
4. Incubate sections in 70 % EtOH	5 min
5. Incubate sections in 100 % EtOH	5 min
6. Air-dry	~5 min
7. Incubate sections in acetylation solution	10 min
Acetic anhydride should be added just before use	
8. Incubate sections in 2× SSC	5 min
9. Apply hybridization buffer to each slide	
10. Place sections in a humid chamber	30 min to 1 h
11. Incubate sections in 2× SSC	5 min
12. Incubate sections in 0.1× SSC	5 min
13. Incubate sections in 70 % EtOH	5 min
14. Incubate sections in 100 % EtOH	5 min
15. Allow to air-dry	

Note When using prenatal brain sections, dehydration with EtOH helps to avoid the tissue detaching from the glass slide.

3.4 Hybridization

Unlike isotopic ISH using oligo DNA probes, the optimal temperature for this hybridization is high. In our standard protocol, it is 63.5 °C. For some probes, hybridization at a higher temperature would help to improve the signal-to-noise ratio.

1. Add riboprobes to the hybridization buffer at a dilution of 1:1000.
2. Apply hybridization mix to the section, remove visible air drops, and cover with parafilm. Each adult mouse sagittal brain section requires 200–300 μL of hybridization solution.
3. Put glass slides in a sealed plastic container with filter paper soaked in 50 % formamide solution (vol/vol) at the bottom of chamber to maintain humidity.
4. Incubate in a hybridization oven at 63.5 °C overnight (12–16 h).

3.5 Post-hybridization Wash

After gently removing the parafilm coverslip, place slides in a slide holder, and immerse in a glass jar containing washing reagent preheated in a water bath. Procedures in **steps 3–8** and **9** are carried out at 61 °C and room temperature, respectively.

1. Preheat washing solutions to 61 °C in water bath	
2. Immerse slides in jar containing 2× SSC and remove parafilm from slides	
3. Wash sections in 5× SSC (1)	15 min
4. Wash sections in 5× SSC (2)	15 min
5. Wash sections in formamide 1	30 min
6. Wash sections in formamide 2	30 min
7. Wash sections in 0.1× SSC (1)	15 min
8. Wash sections in 0.1× SSC (2)	15 min
9. Wash sections in 0.1× SSC (3)	~5 min

3.6 Blocking

All procedures are carried out at room temperature. For all steps except **steps 5** and **7**, a slide holder is immersed in a glass jar containing each reagent. In **steps 5** and **7**, glass slides are put in a humid chamber with a sheet of paper towel immersed with DW, and one drop (~70 μL) of blocking solution is applied to each section.

1. Incubate sections in NTE buffer	~15 min
2. Incubate sections in 20 mM iodoacetamide in NTE buffer	~15 min
3. Incubate sections in NTE buffer	~10 min
4. Incubate sections in TNT buffer	~5 min

(continued)

5. Incubate sections with DIG-blocking solution	30 min
6. Wash sections in TNT buffer	2–3 min
7. Incubate sections with 0.5 % TSA-blocking buffer	30 min
8. Wash in TNT buffer	

3.7 Immunohistochemical Detection of the First Probe

In double FISH using FITC- and DIG-labeled probes, detection of the FITC probe needs to be carried out first with FITC-conjugated tyramide, because the anti-FITC antibody recognizes FITC precipitate. All procedures are carried out in a humid chamber and at room temperature.

Apply 100–200 μL of POD-conjugated anti-FITC antibody (diluted at 1:1500–1:500 in DIG-blocking solution)	1–2 h
Wash sections in TNT buffer – 3 washes for 5 min each	15 min
Apply 100–200 μL of TSA Plus FITC working solution (TSA Plus FITC stock solution is diluted at 1:200 in 1× Plus Amplification Diluent)	10 min
Wash sections in TNT buffer (1)	~5 min
Wash sections in TNT buffer (2)	~5 min
Incubate sections in 0.6 % hydrogen peroxide solution in TNT buffer	30 min
To inactivate peroxidase activity associated with the detection of the first riboprobe	
Wash sections in TNT buffer – 2 washes for ~5 min each	~10 min

Note For TSA Plus stock solution, we typically add 60 μL of DMSO to TSA Plus Amplification Reagent supplied as a solid.

3.8 Immunohistochemical Detection of the Second Probe

1. Apply 100–200 μL of POD-conjugated anti-fluorescein antibody (diluted at 1:500 in DIG-blocking solution), peroxidase-conjugated anti-DIG antibody	1 h
2. Wash sections in TNT buffer – 3 washes for 5 min each	15 min
3. Apply 100–200 μL of TSA Plus Cy3 working solution (TSA Plus Cy3 stock solution is diluted at 1:200 in 1× Plus Amplification Diluent)	10 min
4. Wash sections in TNT buffer – 2 washes for 5 min each	10 min
5. Incubate sections in 0.6 % hydrogen peroxide solution in TNT buffer	30 min
To inactivate peroxidase activity associated with the detection of the second riboprobe	
6. Wash sections in TNT buffer ×2	~15 min

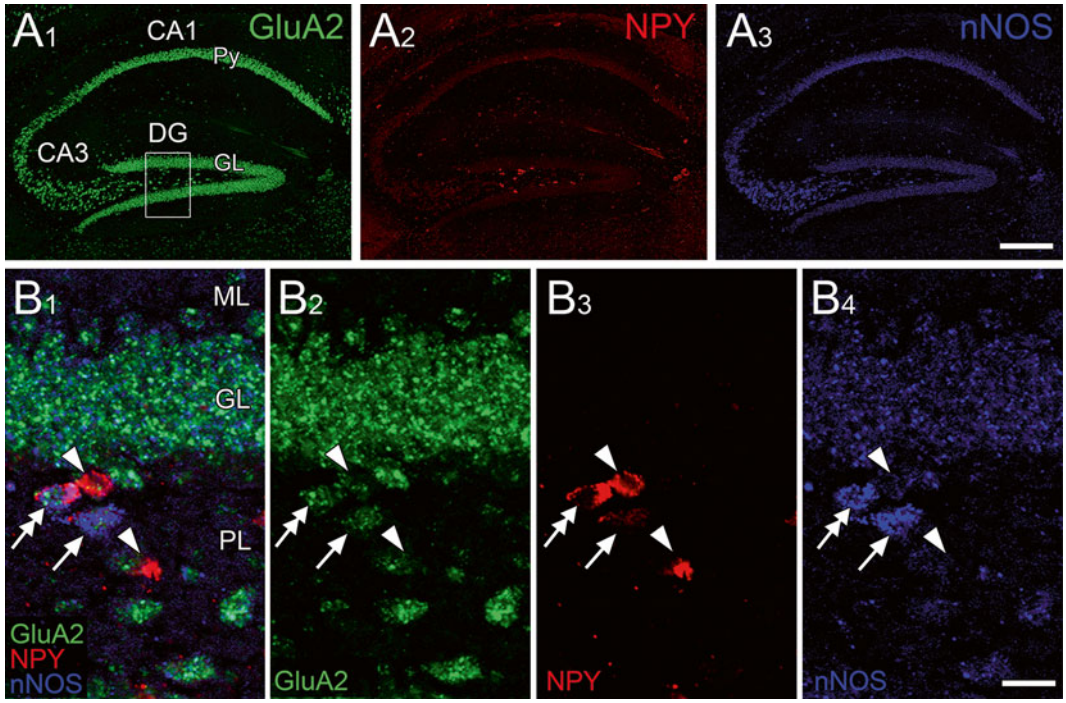

Fig. 2 Simultaneous detection of three different mRNAs by FISH. (**a**) Triple-labeling FISH for GluA2 subunit of AMPA-type glutamate receptor (A_1, *green*), neuropeptide Y (*NPY*; A_2, *red*), and neuronal nitric oxide synthase (*nNOS*; A_3, *blue*) in the hippocampus. Note that while GluA2 expression is intense and widely distributed in the pyramidal cell layer (*Py*) of CA1–3 and the granule cell layer (*GL*) in the dentate gyrus (*DG*), NPY and nNOS expression is limited to a subset of cells dispersed in the hippocampus. (**b**) High-power images of the region indicated in A_1 showing GluA2 expression in the GL and polymorphic cell layer (PL or hilus) in the DG. Color-separated images of B_1 are shown in B_2—B_4. GluA2 expression (B_2, *green*) is much weaker in hilar cells expressing NPY (B_3, *red*) and/or nNOS (B_4, *blue*) than NPY-/nNOS-negative cells. *Double-arrow*, *arrow*, and *arrowheads* indicate NPY+/nNOS+ cells, NPY-/nNOS+ cells, and NPY+/nNOS– cells, respectively. *CA1 and CA3* CA1 and CA3 region of the Ammon's horn, *DG* dentate gyrus, *Py* pyramidal cell layer *GL*, granule cell layer, *ML* molecular layer. Scale bars, **a**, 200 μm; **b**, 10 μm

4 Options

4.1 Triple FISH

We typically use a biotin-labeled probe as the third probe and visualize with Cy5. Representative examples are shown in Fig. 2.

4.1.1 Immunohistochemical Detection of the Third Probe

After visualizing the second probe according to Sect. 3.8,

1. Incubate sections with one drop of blocking solution	20 min
2. Wash briefly with TNT buffer	
3. Incubate with peroxidase-conjugated anti-biotin antibody (2 μg/mL in blocking solution)	1 h
4. Wash sections in TNT buffer – 3 washes for 5 min each	15 min

(continued)

5. Apply 100–200 μL of TSA Plus Cy5 working solution (TSA Plus Cy5 stock solution is diluted at 1:200 in 1× Plus Amplification Diluent)	10 min
6. Wash sections in TNT buffer – 2 washes for 5 min each	10 min
7. Incubate sections in 0.6 % hydrogen peroxide solution in TNT buffer	10 min
8. Wash sections in TNT buffer overnight	

4.2 Counterstaining

We typically use NeuroTrace fluorescent Nissl stains of various colors (Invitrogen) and TOTO3 (Invitrogen). NeuN immunostaining is also useful for quantitative analysis. Sections are incubated with NeuN (Millipore, MAB377; diluted 1:1000 in PBS) for 1 h and visualized with an appropriate secondary antibody.

4.3 Combination with Immunofluorescence

Some antibodies still specifically recognize antigens that have undergone harsh ISH procedures (Fig. 3a, b). When combining with immunofluorescence, microslicer sections are subjected to free-floating ISH using glass test tubes. After probe visualization, sections are subjected to conventional immunofluorescence procedures.

4.4 Combination with Retrograde Tracer Labeling

Combining retrograde tracer labeling with FISH is an effective approach to characterize the neurochemical identity of projection neurons. For this purpose, we typically use Alexa Fluor 488-conjugated cholera toxin subunit b (CTb) (Invitrogen) [3] (Fig. 3c, d). After an appropriate survival period (~2 days), CTb-injected mice were anesthetized and fixed by transcardial perfusion with 4 % PFA. Microslicer sections of 50 μm thick were subjected to free-floating ISH, and after probe visualization, tracer signals were detected by immunofluorescence with a rabbit anti-Alexa Fluor 488 antibody, which were further visualized with an Alexa Fluor 488-conjugated anti-rabbit IgG antibody for 2 h.

5 Notes

1. As the intensity of the fluorescence signal is proportional to the number of hapten-labeled UTP, we recommend using long probes of 600–1000 nt in size. However, in some cases, only

Fig. 3 (continued) cholera toxin subunit b (*CTb; C*, *D_2*, *green*) into the VTA and neuronal nuclear immunostaining by a NeuN antibody (*D_1*, *blue*). Note that the majority of VTA-projecting BST neurons (*arrows*) express GAD67 mRNA. *ac* anterior commissure, *BST* bed nucleus of the stria terminalis, *Cb* cerebellum, *cc* corpus callosum, *Cx* cortex, *Hi* hippocampus, *ic* internal capsule, *LS* lateral septum, *lv* lateral ventricle, *Mb* midbrain, *MO* medulla oblongata, *OB* olfactory bulb, *St* striatum, *Th* thalamus. Scale bars, **a**, 1 mm; **b**, **d**, 10 μm; **c**, 200 μm

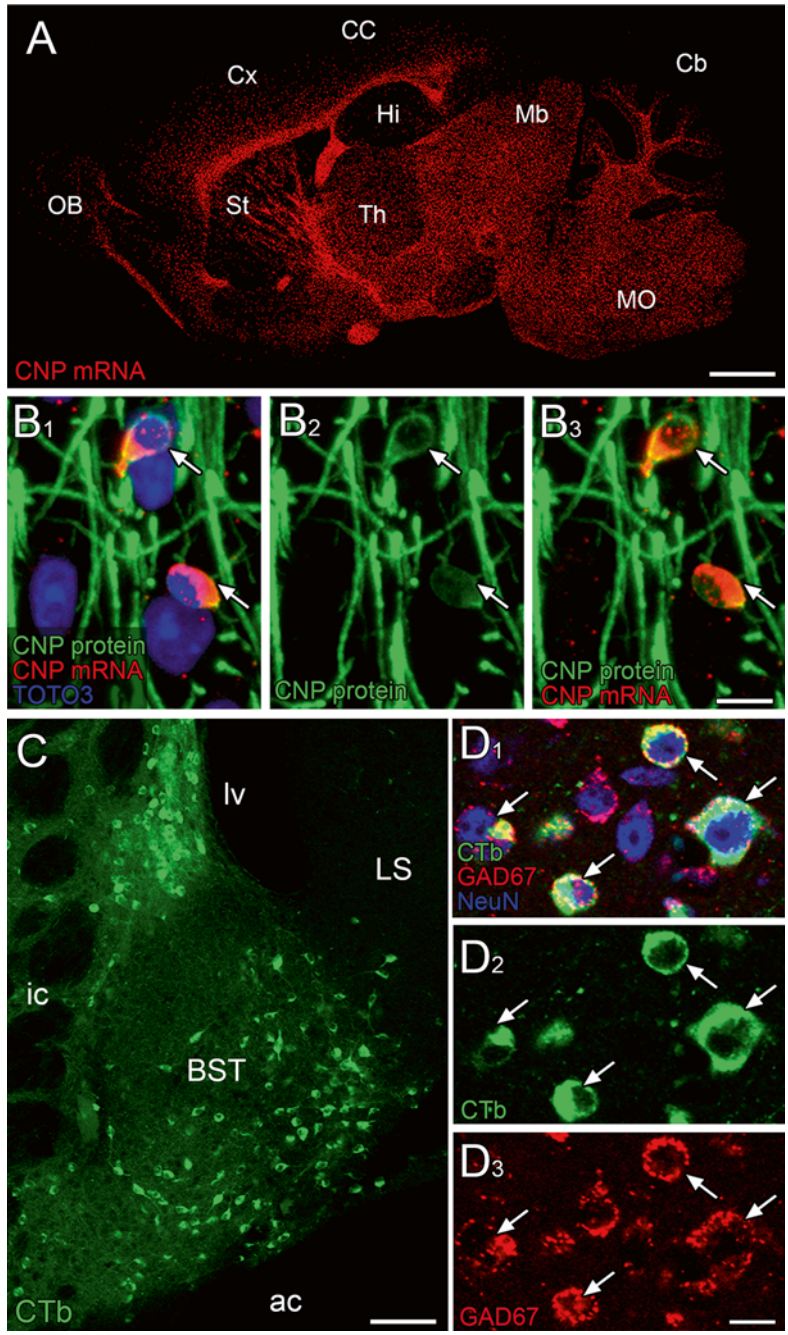

Fig. 3 Combining FISH with immunofluorescence or retrograde tracer labeling. (**a**, **b**) Confirming the co-expression of mRNA and protein of 2′,3′-cyclic nucleotide 3′-phosphodiesterase (CNP), one of the major myelin-associated proteins, in adult mouse brain. (**a**) Overall expression pattern in the whole brain showing that CNP mRNA-expressing cells are distributed densely in the white matter and relatively sparsely in the gray matter. (**b**) Triple fluorescent labeling for CNP mRNA (B_3, *red*), CNP protein (B_2, *green*), and nucleus (B_1, *blue*) in the cerebral cortex. Perikaryal labeling of CNP protein completely overlaps with that of CNP mRNA. Arrows indicate CNP-positive perikarya. Note that putative myelin sheathes are visualized by CNP immunolabeling. (**c**, **d**) Characterizing the bed nucleus of the stria terminalis (BST) neurons projecting to the ventral tegmental area (VTA). FISH for GAD67 (D_3, *red*) is combined with retrograde tracer injection of Alexa Fluor 488-conjugated

the probe covering the full length (e.g., 3000–4000 bp) of the target gene yields both specific and strong signals, whereas in other cases, only a shorter probe generates specific signals. Therefore, the size of the probe should be determined according to the situation (e.g., expression level, sequence homology with other genes, and G/C ratio of the sequence).

2. When performing dFISH, we typically label and visualize the gene of interest with FITC; however, the appropriate combination of FITC/DIG labeling and FITC/Cy3/Cy5 detection differs depending on the situation. When we encounter bleed-through of FITC signals into adjacent detection channels (e.g., Cy3), probes for intensely expressed mRNA are labeled with DIG instead and visualized by Cy3 or Cy5.
3. Because the optimal dilution of a peroxidase-conjugated antibody significantly differs depending on manufacturer and batch number, it needs to be determined empirically.
4. False double-positive cells in dFISH are mainly due to insufficient inactivation of POD associated with the first probe detection or bleed-through from the adjacent channels. To validate the inactivation of the first POD, apply a second tyramide tethered to another fluorophore and confirm that there is no signal from the second one. Possible bleed-through can be also checked in single-label FISH by confocal microscopic observation.
5. When judging the specificity of the probes, the overall expression pattern in the whole brain and each brain region is extremely informative and reliable, so that should be thoroughly examined and compared with results obtained by another method. We generally compare the expression pattern with previous isotopic ISH studies using oligo DNA probes.

Acknowledgments

We thank all lab members for providing informative examples and helpful suggestions.

References

1. John HA, Birnstiel ML, Jones KW (1969) RNA-DNA hybrids at the cytological level. Nature 223(5206):582–587
2. Lein ES, Hawrylycz MJ, Ao N, Ayres M, Bensinger A et al (2006) Genome-wide atlas of gene expression in the adult mouse brain. Nature 445:168–176
3. Kudo T, Uchigashima M, Miyazaki T, Konno K, Yamasaki M, Yanagawa Y, Minami M, Watanabe M (2012) Three types of neurochemical projection from the bed nucleus of the stria terminalis to the ventral tegmental area in adult mice. J Neurosci 32(50):18035–18046

Chapter 11

Autoradiographic Visualization of G Protein-Coupled Receptors in Brain

Rebeca Vidal, Raquel Linge, María Josefa Castillo, Josep Amigó, Elsa M. Valdizán, and Elena Castro

Abstract

In this chapter, two in vitro techniques applied to study the anatomical localization of a receptor are revised: firstly, the receptor binding assay in sections, a technique to assess the location and distribution of a receptor in the tissue (*descriptive and anatomical information*), and, secondly, the [^{35}S]GTPγS-binding assay also in tissue slices, which allows the quantification of the level of G protein activation by a specific GPCR's agonist. The latter technique provides additional information about the coupling efficacy of a receptor to G proteins (*functional autoradiography*), thus enabling the study of the first step in the intracellular signaling pathway after the receptor activation. Both techniques are basically performed for the in vitro autoradiographic visualization of receptors in tissue slices obtained from animal or human postmortem samples.

Key words Receptor autoradiography, [^{35}S]GTPγS receptor binding in sections, G protein-coupled receptor

1 Introduction

Current radiometric techniques allow a detailed study of the differential distribution of a given receptor in different systems, and they can also provide valuable information about their functionality. Many receptors have been discovered and described by using homogenate binding assays, including the pharmacological characterization and the pharmacological profile of different drugs. However, this technique does not allow anatomical resolution. Autoradiography, to overcome this limitation, combines image analysis approaches with the principles of radioligand binding assays. In fact, this technique shares some aspects with the homogenate binding studies, including the receptor-ligand interaction properties such as affinity, specificity, and selectivity.

On the other hand, [^{35}S]GTPγS-binding autoradiography is a technique that, unlike receptor autoradiography, provides

Rafael Luján and Francisco Ciruela (eds.), *Receptor and Ion Channel Detection in the Brain: Methods and Protocols*, Neuromethods, vol. 110, DOI 10.1007/978-1-4939-3064-7_11,

anatomical and functional information at the same time as it unifies the advantages of receptor autoradiography and [^{35}S]GTPγS binding performed on membrane extracts. It is based on the labeling of the first step of the signaling mechanism of GPCRs. Thus, this method allows the visualization of activated receptors, by means of labeling the G proteins with a radioactive non-hydrolyzable analogue of GTP, after their activation by a determined receptor. The agonist binding to the receptor induces some conformational changes in the receptor structure, allowing the interaction with the G protein. The activation of the G protein leads to GDP release from their α-subunit and it is replaced by [^{35}S]GTPγS. Since this analogue is resistant to GTPase-induced hydrolysis, the radioactivity incorporated (what we measure) is proportional to the number of G protein α-subunits activated.

From a methodological point of view, *autoradiographic visualization of the receptor* is carried out by the incubation of the tissue slices with a specific radioligand at suitable conditions of temperature, buffer assay, and time to reach the equilibrium. These conditions are quite similar to those applied to the binding in membranes. Sometimes, it is necessary a previous preincubation in order to eliminate any remaining endogenous ligand or drugs from treatments to avoid their interference in the results of the assay. The radioligand chosen must possess high affinity (K_D in nM order or less) and exhibits low nonspecific binding. In the IUPHAR database (see http://www.iuphar-db.org/), you can also consult the recommended radioligands for a variety of GPCRs. The substance selected to define the nonspecific binding is used in a high concentration (usually between 100 and 1000 times more than the concentration of the radioligand used) and have to exhibit a high affinity for the receptor. After the incubation step with the radioligand, the washing of the slices is performed, generally, at cold temperatures to ensure an optimal specific/nonspecific binding ratio. Then, the slides are quickly dried in a cold air flow to prevent the dissociation phenomenon and the diffusion of the radioligand. The autoradiograms are obtained by the apposition of the slices to a photographic emulsion (a radiosensitive film or a coverslip previously treated with the emulsion) under darkness conditions. The tissues are exposed for a period that depends on the specific activity of the radioligand and the density of receptor measured. The films are then developed and fixed and autoradiograms are generated for further quantification. Image acquisition from autoradiogram can be made using a macroscope coupled to a high-resolution camera or with a high-resolution scanner. The quantification is performed by using different softwares for image analysis (Scion image Scion Corporation, Maryland, USA or Image J). Saturation and competition-binding experiments can be also performed by autoradiography methods (*see* **Note 1**).

Regarding [^{35}S]*GTPγS receptor binding in sections or functional autoradiography*, the first aspect that we should take into consideration is the level of basal [^{35}S]GTPγS binding (in the absence of the agonist) to accurately measure the level of specific agonist-induced stimulation. This basal binding is heterogeneously distributed all throughout the brain and may hinder the measurement of the specific stimulation by an agonist, especially in the case of receptors expressed in a low number or with small coupling efficiency. Another relevant point is the specificity of the response that is confirmed with the inhibition of agonist-induced stimulation of [^{35}S] GTPγS binding by a selective antagonist of the receptor.

In general, the steps are quite similar to those described above for receptor autoradiography. Therefore, only those that differ will be explained. The incubation with [^{35}S]GTPγS is performed under different experimental conditions: in the absence of the agonist (basal binding), in the presence of a selective agonist for the receptor studied (agonist-stimulated binding), agonist plus a selective antagonist (pharmacological specificity), and with an excess of non-labeled GTPγS (nonspecific binding). Then, tissue samples are washed, dried, and exposed to radiosensitive films for 48 h. The quantification process and the analysis of the autoradiograms are as described for conventional autoradiography, using for these purpose commercial standards of ^{14}C.

One of the main limitations of [^{35}S]GTPγS-binding autoradiography is that only pertussis toxin-sensitive G proteins (G_i or G_o) can be labeled with enough sensitivity.

Therefore, agonist-induced stimulation of [^{35}S]GTPγS-binding through G_s or G_q proteins is more difficult to detect probably due to the low spontaneous rate of GDP dissociation and to the relative poor abundance of these proteins in the central nervous system (CNS). Another limitation is that [^{35}S]GTPγS-binding assays do not allow to establish the subtype of G proteins that are activated following receptor stimulation.

Here we set out protocols for 5-HT_{1A} receptor autoradiography by using [^{3}H]8-OH-DPAT as radioligand [1] and the functional autoradiography for G coupling to 5-HT_{1A} receptor by using the selective 5-HT_{1A} agonist 8-OH-DPAT [2].

2 Materials

2.1 Receptor Autoradiography

2.1.1 Reagents

[^{3}H]8-OH-DPAT (8-hydroxy-DPAT, [propyl-2, 3-ring-1, 2, 3-3H]-, specific activity = 100–200 Ci/mmol, concentration of 1 mCi/mL, NET929 Perkin Elmer) (*see* **Note 2**), (±)8-OH-DPAT ((±)-8-hydroxy-2-(dipropylamino)tetralin hydrobromide, ref. H8520, Sigma-Aldrich), 5-HT (serotonin hydrochloride, ref. H9523, Sigma-Aldrich), Tris–HCl (Trizma® hydrochloride, ref. T5941, Sigma-Aldrich), $CaCl_2$ (calcium chloride anhydrous, ref.

499609, Sigma-Aldrich), ascorbic acid (L(+)-ascorbic acid, ref. 0515, Scharlab, S.L.), and pargyline (pargyline hydrochloride, ref. P8013, Sigma-Aldrich)

2.1.2 Buffers

1. *Preincubation buffer*: 170 mM Tris–HCl, 4 mM $CaCl_2$, and 0.01 % ascorbic acid in deionized water at pH = 7.5. This buffer must be made fresh in order to avoid $CaCl_2$ precipitation. The weight of each component will vary depending on the waters of hydration.

   To prepare 180 mL of preincubation buffer (90 mL will be used for the preincubation step and 90 mL for prepare the incubation buffer), a mixture of Tris–HCl (4.82 g), $CaCl_2$ (79.91 mg), and ascorbic acid (18 mg) is dissolved in 180 mL of deionized water. Add few drops of 1 M hydrochloric acid (HCl) to adjust pH.

2. *Incubation buffer*: 170 mM Tris–HCl, 4 mM $CaCl_2$, and 0.01 % ascorbic acid at pH = 7.5 in the presence of 10 μM pargyline and [^{3}H]8-OH-DPAT to achieve a final concentration of 2 nM .

   To prepare 90 mL of incubation buffer, add 90 μL of pargyline (10^{-2} M, 1.96 mg/mL in distilled water) and 25.56 μL commercial stock solution of [^{3}H]8-OH-DPAT to 90 mL of the preincubation buffer. Below it is shown the formula to calculate the volume (μL) of radioactive solution in order to prepare 90 mL of 2 nM [^{3}H]8-OH-DPAT (SA: 142 Ci/mmol; [1 mCi/mL]) (*see* **Note 3**).

$$90\ mL \times \frac{1}{10^3\ mL} \times \frac{20\ nmol}{L} \times \frac{142\ \mu Ci}{nmol} \times \frac{\mu L}{1\ \mu Ci} = 25.56\ \mu L$$

   Stir the buffer gently to ensure that they are well mixed. Check that the concentration is correct (2 nM) by measuring an aliquot of 100 μL of incubation buffer (radioactive solution) in a β-counter to determine the DPM. For the DPM calculation, the equivalence is 1 μCi = 2.2×10^6 DPM. The expected DPM in this sample are calculated according to the formula:

$$100\ \mu L \times \frac{1}{10^6\ \mu L} \times \frac{2\ nmol}{L} \times \frac{142\ \mu Ci}{nmol} \times \frac{2.2x10^6\ dpm}{1\ \mu Ci} = 62480\ dpm$$

   where 142 is the value of specific activity of radioligand in μCi units, 2 nmol/L is the concentration of radioligand necessary for the assay, 100 μL is the volume of the aliquot, and DPM are the units of radioactivity . If the DPM present in this 100 μL aliquot differ from the expected value, we should either add more radioligand or dilute the incubation buffer to obtain the adequate concentration.

3. *Washing buffer*: 170 mM Tris–HCl, pH = 7.5. Prepare about 200 mL.

2.2 [^{35}S]GTPγS Receptor Binding in Sections or Functional Autoradiography

2.2.1 Reagents

[^{35}S]-GTPγS (GTPγS, [^{35}S]-, specific activity = 1250 Ci/mmol, concentration of 12.5 mCi/mL, NEG030H, Perkin Elmer, *see* **Note 2**), GTPγS (guanosine 5′-[γ-thio]triphosphate tetralithium salt, ref. G8634, Sigma-Aldrich), (±)8-OH-DPAT ((±)-8-hydroxy-2-(dipropylamino)tetralin hydrobromide, ref. H8520, Sigma-Aldrich), WAY100,635 (WAY100,635 maleate salt, ref. W108, Sigma-Aldrich), GDP (guanosine 5′-diphosphate sodium salt, ref. G7127, Sigma-Aldrich), EGTA (ethylene glycol-bis(2-aminoethylether)-N,N,N′,N′-tetraacetic acid, ref. E-4378, Sigma-Aldrich), DTT (DL-dithiothreitol, ref. 43819, Sigma-Aldrich), $MgCl_2$ ($MgCl_2.6H_2O$, ref MA0035, Scharlab S.L.), NaCl (ref. SO0225, Scharlab S.L.), Tris–HCl (Trizma® hydrochloride, ref: T5941, Sigma-Aldrich), adenosine deaminase (adenosine deaminase from bovine spleen type X, concentration = 1.08 U/μL, ref. A5043, Sigma-Aldrich)

2.2.2 Buffers

1. *Preincubation buffer*: 50 mM Tris–HCl, 3 mM $MgCl_2$, 0.2 mM EGTA, 100 mM NaCl, 1 mM DTT, 2 mM GDP in water at pH = 7.4. The weight of each component will vary depending on the waters of hydration.

   To prepare 360 mL of preincubation buffer (180 mL will be used to prepare the incubation buffer and 180 mL for the preincubation step of the assay), a mixture of Tris–HCl (2.84 g), $MgCl_2.6H_2O$ (220.3 mg), EGTA (27.9 mg), NaCl (2.10 g), DTT (55.6 mg), and GDP (319.1 mg) is dissolved in 360 m1 of deionized water. Add few drops of 1 M hydrochloric acid (HCl) to adjust pH.

2. *Incubation buffer*: 50 mM Tris–HCl, 3 mM $MgCl_2$, 0.2 mM EGTA, 100 mM NaCl, 1 mM DTT, 2 mM GDP in the presence of 10 mU/mL adenosine deaminase, and [^{35}S]GTPγS to achieve a final concentration of 0.04 nM (*see* **Notes 4** and **5**). Aliquots of 25 μL [^{35}S]GTPγS (stored at –20 °C) are used to prepare the incubation buffer. For that purpose, the content of the commercial bottle of [^{35}S]GTPγS solution is diluted (1:10) by adding 180 μL of 10 mM tricine (pH = 7.6) with 10 mM DTT to 20 μL of the bottle (final concentration of 1.25 mCi/mL).

   To prepare 180 mL of incubation buffer, add 1.8 μL of adenosine deaminase and 7.2 μL of aliquoted [^{35}S]GTPγS (if the decay factor is 1, *see* **Note 6**) to 180 mL of the preincubation buffer. Stir gently to ensure that it is well mixed. Check that the radioligand concentration is correct as indicated above.

3. *Washing buffer*: 50 mM Tris–HCl, pH = 7.4. Prepare about 400 mL.

2.3 Other Materials and Apparatuses

1. Cryostat.
2. β-counter (Liquid Scintillation Counter Packard Tri-Carb 2900TR, Packard BioScience Company, USA).

3. Glass slides (Superfrost® plus, Thermo Scientific) and boxes for storing slides.
4. Coplin jar (ref. S5516).
5. Autoradiography [^{3}H]-standards are commercially available from American Radiolabeled Chemicals (*see* **Note 7**). ^{14}C standards (American Radiolabeled Chemicals) are used to construct the calibration curves for [^{35}S]GTPγS receptor autoradiography.
6. Protection Shields, and bench guard, Dynalon®
7. Autoradiography cassettes (ref 10585785, Fisher Scientific).
8. Radiation-sensitive films (Carestream® Kodak® BioMax® MR film, ref. Z358460, Sigma-Aldrich).
9. Developer (Carestream® Kodak® autoradiography GBX developer/replenisher, ref. P7042, Sigma-Aldrich) and fixer (Carestream® Kodak® autoradiography GBX fixer/replenisher, ref. P7167, Sigma-Aldrich).
10. Scintillation liquid (Ultima-Flo™ M, 2x5L, ref. 6013579, Perkin Elmer).
11. Scintillation vials (Pico Pro Vial 4 mL, ref. 6000252, Perkin Elmer).

3 Methods

3.1 Receptor Autoradiography

3.1.1 Tissue Preparation

In a cryostat (−20 °C), cut three consecutive brain sections of interest (12 μm thick slice) using the glass slides indicated above. Tissue slides are stored (−20 °C) until the day of experiment to prevent protein degradation. Two sections are used to measure the total binding (TB) and the other section for the nonspecific binding (NSB) (*see* **Note 8**).

3.1.2 Assay Protocol (See **Note 9**)

1. Thaw tissue slides at room temperature (20–22 °C, 30 min).
2. Prepare 90 mL of the preincubation buffer (30 mL per coplin jar/condition: TB1, TB2, and NSB). Take 90 mL of the preincubation buffer and fill the three jar coplins which will contain the slides for total (TB1 and TB2) and nonspecific (NSB) binding (30 mL per jar). The volume of the preincubation and incubation buffers depends of the number of tissue slides (and TB and NSB coplin jars) of your experiment. A 30 mL coplin jar can contain up to 11 glass slides.
3. Prepare 90 mL of incubation buffer (as stated in Sect. 2.1.2.2) for TB1, TB2, and NSB conditions and fill the respective coplin jars.
4. Prepare 500 μL of 1 mM (106 μg/500 μL) of serotonin (to define the nonspecific binding) in a glass test tube using deionized water. Pipette 300 μL of 5-HT (1 mM) into the NSB jar coplin.

5. Preincubate the slides into the corresponding jar coplins (TB1, TB2, and NSB) at room temperature for 30 min.
6. Drain the slides and incubate them at room temperature for 30 min. Slides for TB condition are incubated into the 30 mL coplin jars containing the incubation buffer solution, and NSB slides are incubated into the coplin jar containing 30 mL of the incubation buffer solution and 300 μL of 5-HT (1 mM).
7. Wash the slides twice in a 30 mL of ice-cold washing buffer for 5 min.
8. Dip the slides in cold deionized water to remove buffer salts.
9. Then dry rapidly in a cold air stream (at least for 1 h).
10. Put the incubated tissue slides (and also tritium standards) into autoradiography cassettes, and expose them to radiation-sensitive films under red lighting in a dark room.
11. Leave an exposition time of 12 weeks (at 4 °C).
12. At the end of exposition time, thaw the slides at room temperature (1 h) before developing.
13. Develop the film sheets under red lighting in a dark room (*see* **Note 10**).
14. Quantify the autoradiograms as indicated in Sect. 3.3 (*see* also Fig. 1).

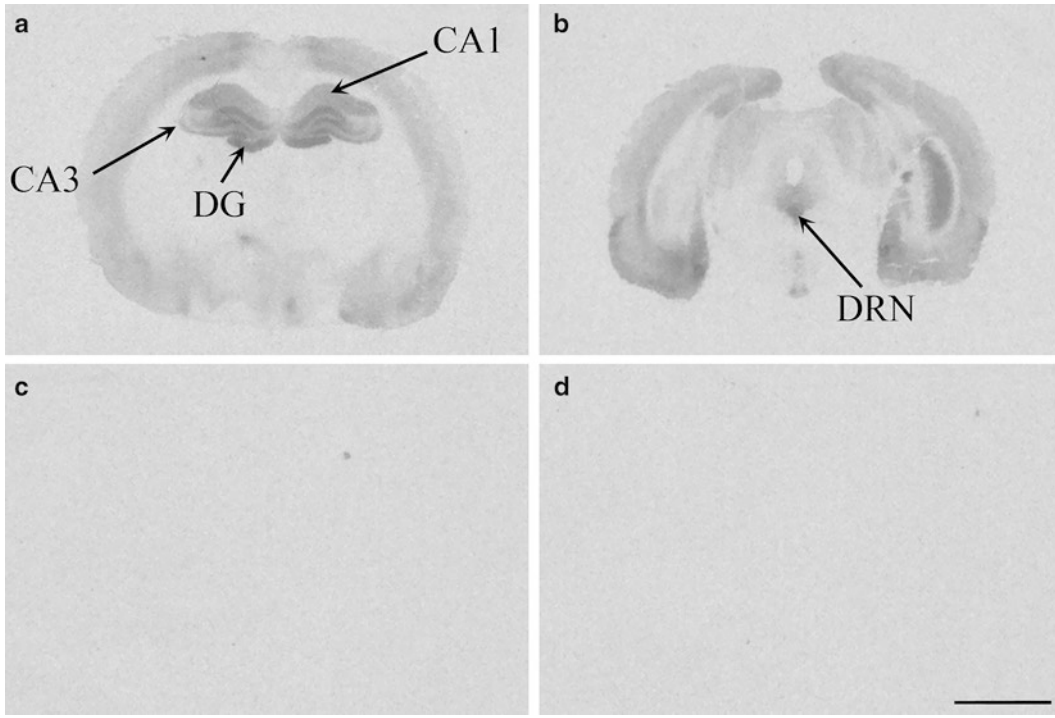

Fig. 1 Autoradiographic illustration of [^{3}H]8-OH-DPAT binding in coronal sections of rat brain. (**a**, **b**) Total binding and (**c**, **d**) nonspecific binding. *CA1* CA1 field of hippocampus, *CA3* CA3 field of hippocampus, *DG* dentate gyrus, *DRN* dorsal raphe nucleus. Bar = 2 mm

3.2 [^{35}S]GTPγS Receptor Binding in Sections or Functional Autoradiography

3.2.1 Tissue Preparation

In a cryostat (−20 °C), cut six consecutive brain sections of interest (12 μm thick) using the glass slides indicated above. Tissue slides are stored (−20 °C) until the day of experiment to prevent protein degradation. Two slides are used to measure the basal binding (B), two slides are used for agonist stimulation (in this example, 8-OH-DPAT-induced stimulation of [^{35}S]GTPγS binding, AB), one slide is used for the nonspecific binding (NSB), and the last slide is used to confirm the pharmacological selectivity (WAY100,635-induced antagonism of 8-OH-DPAT-induced stimulation of [^{35}S]GTPγS binding, AAB). We advise not to store the tissue sections more than one month since longer periods may cause detrimental [^{35}S]GTPγS binding due to protein degradation (*see* **Note 8**).

3.2.2 Assay Protocol (See **Note 9**)

1. Thaw tissue slides at room temperature (20–22 °C, 30 min).
2. Take 180 mL of the preincubation buffer and fill the six jar coplins (30 mL per jar) which will contain the slides for the different conditions: basal (B1 and B2), agonist-stimulated (AB1, AB2), antagonist + agonist (AAB), and nonspecific (NSB) binding.
3. Prepare 180 mL of incubation buffer as stated above (buffers) and fill the respective jar coplins (30 mL/jar coplin).
4. Prepare in a glass test tube 700 μL of 1 mM of 8-OH-DPAT (229 μg/700 μL) in deionized water. Pipette 300 μL to each of the two AB jar coplins.
5. Prepare in a glass test tube 500 μL of 1 mM of GTPγS (281.5 μg/500 μL) in deionized water. Pipette 300 μL into the NSB jar coplin.
6. Prepare in a glass test tube 500 μL of 1 mM of WAY100,635 (269 μg/500 μL) in deionized water. Pipette 300 μL into the AAB jar coplin.
7. Preincubate the slides into the corresponding jar coplins (B1 and B2; AB1 and AB2; AAB and NSB) at room temperature for 30 min.
8. Drain slides and incubate them into the respective jar coplins (2 h at 25 °C).
9. Wash the slides twice in 30 mL of ice-cold washing buffer for 15 min.
10. Dip the slides into cold deionized water to remove buffer salts.
11. Dry them rapidly using cold air stream (at least for 1 h).
12. Put the incubated tissue slides (and also [^{14}C]-labeled standards) into autoradiography cassettes, and expose them to radiation-sensitive films under red lighting in a dark room.
13. Leave an exposition time of 48 h (at 4 °C).
14. At the end of exposition time, thaw the slides at room temperature (1 h) before developing.

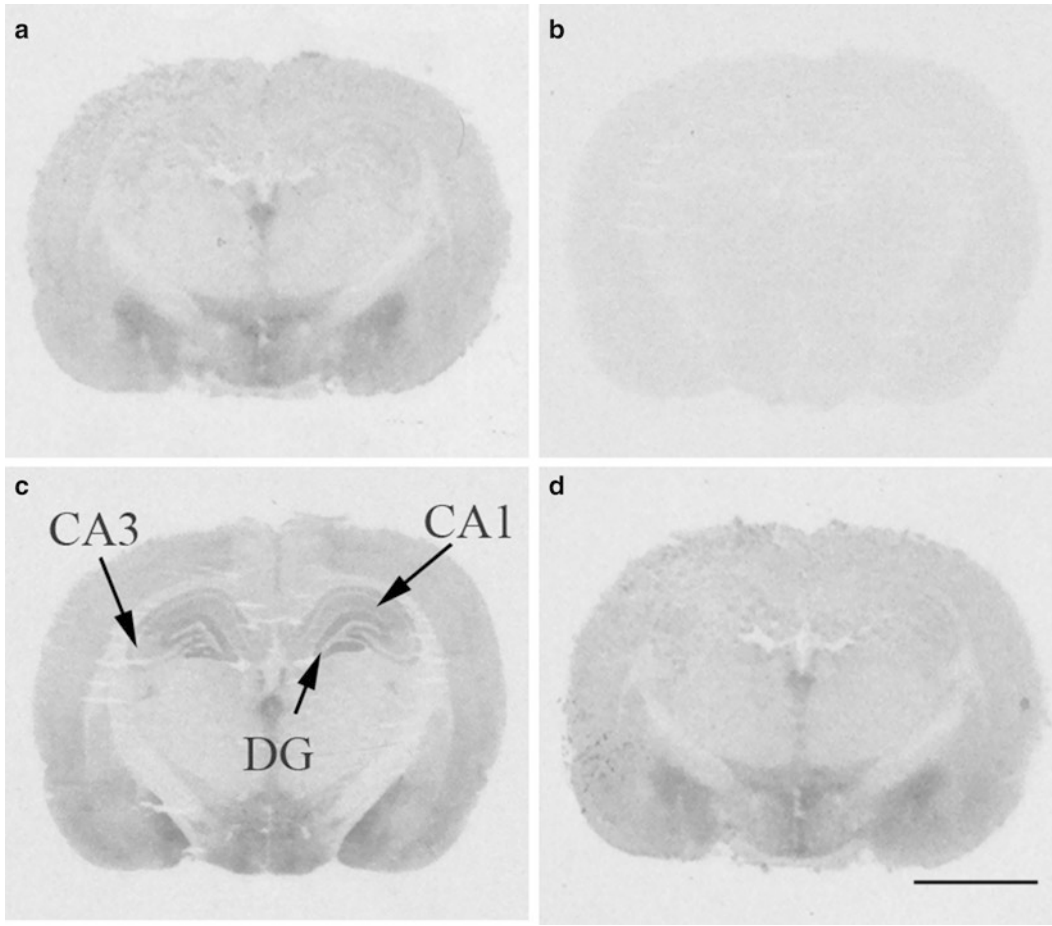

Fig. 2 Autoradiographic illustration of 8-OH-DPAT-stimulated [^{35}S]GTPγS binding in coronal sections of rat brain. (**a**) Basal binding, (**b**) nonspecific binding, (**c**) 8-OH-DPAT (10 μM), and (**d**) 8-OH-DPAT (10 μM) + WAY100,635 (10 μM). *CA1* CA1 field of hippocampus, *CA3* CA3 field of hippocampus, *DG* dentate gyrus. Bar: 2 mm

15. Develop the film sheets under red lighting in a dark room (*see* **Note 10**).
16. Quantify the autoradiogram as indicated in Sect. 3.3 (*see* also Fig. 2).

3.3 Quantification of Autoradiogram

3.3.1 Scanning the Films

A digital image of the autoradiograms is generated using a high-resolution flatbed scanner working in a 256 Gy scale. The film is transilluminated from a light in the scanner lid. The whole firm or selected areas, as convenient, are saved as a *. tif file to be quantified by an image analysis software.

3.3.2 Autoradiograms Quantification

The autoradiograms are quantified using a computer software that allows the measurement of the optical density (OD; gray intensity

as Scion Image; ImageJ). Radioactive standards are used to know the relationship between the radioactivity level and the gray intensity (OD). This relationship fits to a hyperbolic function and that can be transformed in a linear representation (log exposition vs OD). Since it is a lineal regression, the quantification is less accurate for extreme values (overexposed or underexposed areas). Therefore, it is very important to use the appropriate standards to construct the calibration curves. Standards must cover a wide range of radioactivity values (i.e., 0.07–35 nCi/g tissue for ^{3}H and 0.15–110 nCi/g tissue for ^{14}C standard). In our laboratory, we use the Scion Image program to quantify the autoradiograms following these steps:

1. *Creating a calibration curve.* Open the file (*.tif) of a scanned film. For each standard, select an area to measure (with a circle or rectangular tool) and press Ctrl+1 (or select Analyze-Measure). Once you have measured all the standard strips, go to Calibrate (under Analyze menu) and type in the standard values (nCi/g tissue) of each standard strip (under "known" column). Choose the most adequate equation to obtain a good correlation (r^2 close to 1) and save it (i.e., standards as text file) (*see* Fig. 3a–c).
2. *Calibrating the film.* Open the file (*.tif) of the scanned film containing the brain images (it will appear the file name followed by an * symbol). Go to Analyze-Calibrate and open standards text file. This will calibrate the film with the standard calibration curve already obtained. Press OK. Now the file name will appear with an * followed by an ^ symbol (it means the film is calibrated; see red arrows in Fig. 1d, arrows 1 and 2).
3. *Measuring the brain autoradiograms.* Choose the image and select each region of interest within the tissue brain image and with the aid of the tools (usually the freehand selection tool, Fig. 3d, arrow 3). Press Ctrl+1 (or select Analyze-Measure). Results will appear by pressing Ctrl+2 (or selecting Analyze-Show Results). Copy and paste the results (i.e., excel) for further data analysis and statistics. When all the measurements have been made, remember to subtract the NSB to the TB values to obtain the specific binding. Data from receptor autoradiography are expressed as nCi/g tissue and can be converted to fmol/mg tissue, whereas data from functional autoradiography are expressed as % of stimulation versus basal binding (100 %); if basal values are shown, they are usually expressed as nCi/g tissue or fmol/mg tissue.

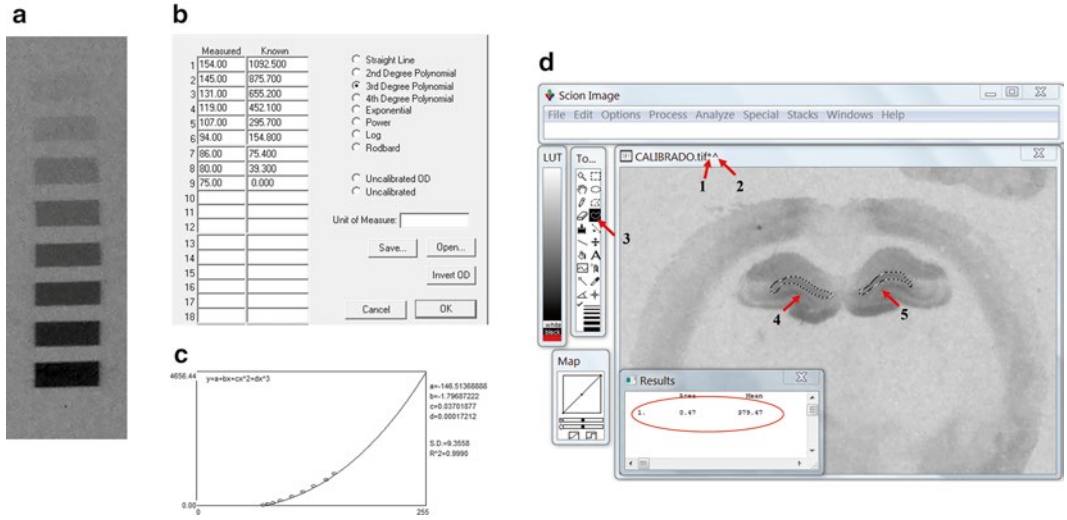

Fig. 3 Illustration of autoradiograms quantification with the Scion program. (**a**) ^{14}C Standard autoradiogram. (**b**): Selected curve calibrations which were "measured" are the optical density (OD) values for each standard strip, and "Known" indicates the values in nCi/g tissue corresponding to each standard strip. (**c**) Calibration curve; the best fit is a polynomial of third degree as can be observed by *r*2 correlation, in this case with a value of 0.9990. (**d**) Measurement of a scanned image using the Scion Image software. The *.tiff file (*arrow 1*) is calibrated (*arrow 2*), and using the freehand selection tool (*arrow 3*), the region/s of interest (*arrows 4 and 5*) are selected. The area and OD values of the selected area are displayed in the "Results" box

4 Notes

1. Saturation autoradiography-binding experiments are carried out in the usual way by increasing the concentration of added radioligand, whereas in competition assays the concentration of radioligand remains constant, and consecutive sections are incubated with increasing concentrations of competitor compound. Thus, the Bmax, $K_{D,}$ and K_i parameters can be also calculated by this method.
2. Research use of radioactive materials are regulated by government agencies. Disposed radioactive waste is regulated by government agencies; be sure you follow government regulations. Take into account a radioactive waste minimization plan.
3. Technical Data Sheets provided by the radioligand manufacture state the parameters to prepare the radioligand working dilutions as well as the calibration date, specific activity, and radioactive concentration. As an example, see http://www.perkinelmer.com/Content/TDLotSheet/NET929_1975348.pdf for [^{3}H]8-OH-DPAT.
4. One of the main issues of [^{35}S]GTPγS binding is the importance of basal binding, which is heterogeneously distributed

throughout the brain. The major challenge is to minimize agonist-independent binding to G proteins without lowering agonist-induced binding. To maximize the agonist-stimulated [^{35}S]GTPγS-binding signal over the background signal, Na^+ and Mg^{2+} are required. Na^+ is important to decrease basal binding as it suppresses agonist-independent [^{35}S]GTPγS binding [3]. On the other hand, Mg^{2+} allows shifting the equilibrium towards the high-affinity state of the receptor. High concentration of GDP is also required in order to suppress basal binding: GDP prevents the binding of [^{35}S]GTPγS to non-heterotrimeric G protein targets and also leads to the formation of inactive forms of G proteins, which can thereafter change bound GDP to [^{35}S]GTPγS when an agonist is added [4, 5].

5. A fraction of the basal binding results from the activation of adenosine A1 receptors by the endogenous adenosine. Thus, the addition of adenosine deaminase (a hydrolytic enzyme) or A1 antagonists in the incubation buffer allows blocking the effect of endogenous adenosine at A1 receptors, reducing basal binding and improving signal-to-noise ratio. The presence of EGTA is also very important to chelate Ca^{2+} and facilitate agonist-stimulated [^{35}S]GTPγS binding.
6. In all the radioactive assays, the decay of the ^{35}S label needs to be taken into account, but it is reasonably stable if stored appropriately. The specific activity is specified as of the calibration date indicated in the manufacturer's datasheet (http://www.perkinelmer.com/Content/TDLotSheet/NEG030H_0215.pdf). This datasheet also contains a table with the corresponding decay factor that should be applied to know the actual specific activity on the day of the assay.
7. ^{3}H (tritium) or ^{125}I standards are the most commonly standards used to generate the calibration curves for receptor autoradiography. The election depends on two factors: anatomical resolution and the exposition period of the emulsion. ^{3}H-radioligands offer the advantage of better resolution, as well as a broad margin of error for small variations in the slice thickness and a long half-life (12.5 years) compared to ^{125}I-radioligands (60 days). Furthermore, one of the main advantages of ^{125}I-radioligands is the high specific activity (between 2000 Ci/mmol and 30–200 Ci/mmol for ^{3}H-ligand) which makes them especially helpful when the receptor density is very low. By contrast, experiments with ^{125}I-radioligands are recommended to be performed as soon as the radioligand is available due to their high decay. Beta-counters are to measure ^{3}H -labeled samples and γ-counters for ^{125}I -labeled samples.
8. Tissue sections from different brain levels and/or replicates for a particular level may be cut for each condition/slide.

Obviously, the total number of tissue sections that a glass slide may contain will depend on the brain size (animal species) and the anatomical level.

9. Work with radioactive materials in radioactive facility, monitor yourself, and your work bench for contamination. The best way to control potentially hazardous radioactive materials is at the source; however, protective clothing provides a good level of secondary protection. Do not wear sandals or open toe shoes; you should wear gloves and lab coat. A polymethyl methacrylate (PMMA) bench top Beta Shield is used when working with beta-emitting isotopes to avoid any radiation hazards. In the case of ^{125}I-radioligands, an X-ray protective lead glass or radiation Shielding must be used. The addition of the different incubation components in the reaction tubes should be as described: buffer, ligand/s, radioligand, and, to finish with, the membranes. This order would minimize radioactivity contamination, and subsequently it would produce less radioactive waste disposal. All the contaminated material should be discarded in the appropriate containers for solid or liquid radioactive waste. Radioactive wastes containing radionuclides with short half-life are commonly placed into storage and allowed to decay prior to their elimination as nonradioactive waste.
10. In order to produce a radiographic image, the processing procedure for the film is sequenced as follows: developing, rinsing, fixing, washing, and drying. The procedure is performed under safe-light conditions (red light in a dark room). These steps can be carried out using trays or tanks with the aid of metal film hangers. Alternatively, the films may be developing by using an automated process.

    Step I: Developing – immerse the film in the developing solution for 5 min at 20 °C (do not agitate).
    Step II: Rinsing – rinse the film in clear tap water (2–3 s) and drain it.
    Step III: Fixing – immerse film into the fixer solution for 5 min and then drain.
    Step IV: Washing – wash the film twice for 5 min clear tap water.
    Step V: Drying – dry at room temperature (i.e., hanging it by using a clip attached to one corner of film or using a film hanger).

Acknowledgments

This work was supported by Ministerio de Ciencia, SAF07-61862, Ministerio de Economía y Competitividad SAF2011-25020, and Instituto de Salud Carlos III.

References

1. Pazos A, Palacios JM (1985) Quantitative autoradiographic mapping of serotonin receptors in the rat brain. I. Serotonin-1 receptors. Brain Res 346:205–230
2. Castro ME, Diaz A, Del Olmo E, Pazos A (2003) Chronic fluoxetine induces opposite changes in G protein coupling at pre and postsynaptic 5-HT_{1A} receptors in rat brain. Neuropharmacology 44:93–101
3. Happe HK, Bylund DB, Murrin LC (2001) Agonist-stimulated [^{35}S]GTPgammaS autoradiography: optimization for high sensitivity. Eur J Pharmacol 422(1–3):1–13
4. Sim LJ, Selley DE, Childers SR (1995) In vitro autoradiography of receptor-activated G proteins in rat brain by agonist-stimulated guanylyl 5′-[γ-[^{35}S]thio]-triphosphate binding. Proc Natl Acad Sci U S A 92:7242–7246
5. Sóvágó J, Dupuis DS, Gulyás B, Hall H (2001) An overview on functional receptor autoradiography using [^{35}S]GTPγS. Brain Res Rev 38:149–164

Chapter 12

Analysis of the Expression Profile and Regional Distribution of Neurotransmitter Receptors and Ion Channels in the Central Nervous System Using Histoblots

Elek Molnár

Abstract

The histoblot method is a reliable and convenient way to compare the regional distribution and expression level of different proteins in brain samples without compromising the integrity of antibody-binding sites by tissue fixation, which is required for conventional immunocytochemistry. Fixation introduces covalent modifications, cross-linking and/or denaturation of proteins. These chemical modifications often alter the antibody-binding sites, and cross-linked molecules may hinder the access of antibody to epitopes. The direct transfer of native proteins from unfixed frozen tissue sections to an immobilising matrix offers much improved accessibility of the transferred proteins for immunochemical analysis. The histoblot method has been successfully applied to analyse the regional distribution of several neurotransmitter receptors, ion channels and other proteins in the adult and developing brains. While this technique lacks cellular resolution, it provides high sensitivity and much improved consistency compared to conventional immunohistochemical techniques, which is essential for reliable quantitative comparisons of overall expression levels of proteins in different brain regions. Compared to conventional immunoblot analysis of protein extracts from dissected brain regions, histoblots provide more accurate and direct information about the anatomical localisation of proteins. In this chapter we describe the histoblot protocol we have used for the identification of quantitative changes in a wide range of neurotransmitter receptors and ion channels in various brain regions.

Key words Alkaline phosphatase, Antibodies, Cryostat section, Expression level, Histoblot, Immunoblot, Immunostaining, Localisation, Nitrocellulose membrane

1 Introduction

Mapping of the regional expression profiles of various receptors, ion channels and other proteins is frequently applied for a wide range of studies of the central nervous system (CNS). While conventional immunohistochemical techniques are often able to reveal the anatomical distribution of endogenous proteins in the brain tissue at relatively high resolution, they also have several limitations that could undermine protein target recognition by antibodies [1].

Rafael Luján and Francisco Ciruela (eds.), *Receptor and Ion Channel Detection in the Brain: Methods and Protocols*, Neuromethods, vol. 110, DOI 10.1007/978-1-4939-3064-7_12,

Immunohistochemical analysis requires the fixation of the brain tissue to preserve morphology and to protect samples from the rigours of processing and staining techniques. Fixatives stabilise cells and tissues via either introducing covalent cross-linkages (e.g. aldehydes such as glutaraldehyde or formalin) or by denaturing proteins (e.g. acetone and methanol) or a combination of both. These changes in target proteins often reduce the ability of antibodies to access and/or recognise their epitopes in fixative-treated tissue samples. Variations in the application of fixatives (e.g. during trans-cardial perfusion of animals) or the potential loss of proteins from tissue sections during the various treatment steps can have a major impact on the consistency of immunolabelling [1]. This inherent variability of immunohistochemical approaches often hinders quantitative comparisons of protein expression levels in different brain samples.

Immunoblot analysis of tissue extracts obtained from dissected brain samples is widely used to study quantitative changes in protein levels. Electrophoretic separation of proteins and their subsequent transfer to blotting membranes allows the reliable and specific identification of immunoreactive bands with the correct molecular weights. While this approach is often used to validate the selectivity of antibody labelling, immunoblotting also has significant limitations. For example, (i) inaccuracies in the dissection of various brain regions, (ii) variability associated with lengthy and complex sample preparation procedures (e.g. tissue homogenisation, subcellular fractionation and protein extraction techniques), and (iii) proteolytic degradation of samples (e.g. due to post-mortem delays in human) can undermine spatial resolution, reproducibility and quantification.

To combine the fine anatomical resolution offered by conventional immunohistochemistry with optimal accessibility of immobilising matrix-bound proteins for immunochemical detection, various in situ blotting (histoblot) techniques were developed for the regional mapping of various protein targets [2–4]. These techniques are based on the direct transfer of native proteins from unfixed frozen tissue sections to an immobilising matrix (e.g. nitrocellulose transfer membrane). The blotted membranes can be subjected to similar immunochemical detection and quantification procedures that are widely used for conventional immunoblotting of electrophoretically separated proteins. These histoblots proved to be a convenient and highly reliable method for the mapping of neurotransmitter receptors (Fig. 1) [5–10], ion channels [11, 12] and other CNS proteins [13–15]. While the spatial resolution of histoblot technique is similar to radioligand autoradiography and in situ hybridisation histochemistry, it is not suitable for the investigation of protein distribution at the cellular and subcellular levels.

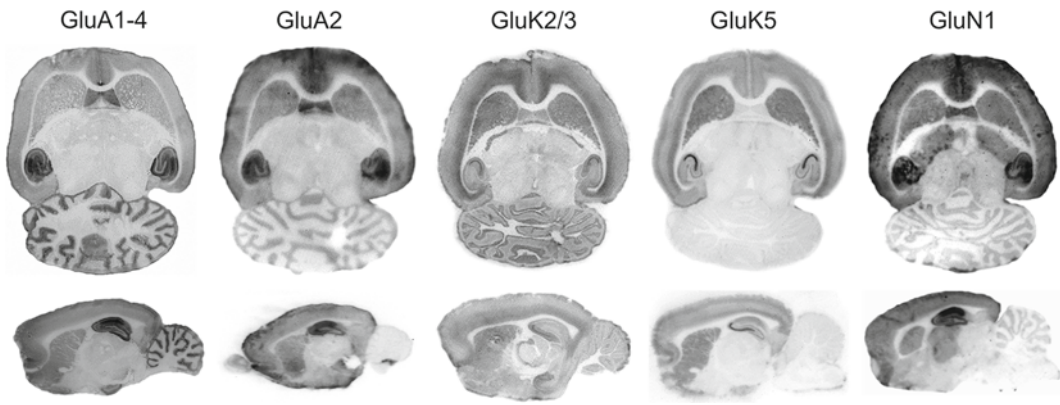

Fig. 1 Regional distribution of ionotropic glutamate receptor subunit proteins. Histoblots of horizontal (*top panels*) and sagittal (*bottom panels*) sections of adult rat brains were immunolabelled with affinity-purified GluA1-4 [16], GluA2, GluK2/3 (Abcam, Cambridge, UK), GluK5 [18] and GluN1 [16] subunit selective antibodies (Images were provided by Dr. Simon M. Ball)

This chapter describes the histoblot protocol that we have successfully applied for the mapping and quantitative comparisons of neurotransmitter receptor (Fig. 1) [9, 16–21] and ion channel [11] expression levels in different brain regions. The experimental procedures described below were initially used for studies of glutamate receptors in rodent brain samples at different developmental stages [22] or following the induction of seizures [23–26]. However, the same methodology and theoretical principles are also applicable to other protein targets in the CNS. Furthermore, the same methodology can also be used for the investigation of human brain samples (Fig. 2), which are often very challenging targets for conventional immunohistochemical or immunoblotting approaches.

2 Materials

2.1 Buffers

1. Transfer buffer: 48 mM Tris-base, 39 mM glycin, 2 % (w/v) sodium dodecyl sulphate (SDS), 20 % (v/v) methanol and pH ≈ 10.5 (not adjusted). To prepare 100 mL of transfer buffer, dissolve 0.58 g Tris-base, 0.29 g glycin and 2 g SDS in deionised water and add 20 mL of methanol before volume is adjusted to 100 mL.
2. Tris buffer with saline and Tween 20 detergent (TBST buffer): 10 mM Tris–HCl (pH 8.0), 150 mM NaCl and 0.05 % (v/v) Tween 20. To prepare 1000 mL of TBST buffer, dissolve 1.21 g Tris-base, 8.77 g NaCl and 0.5 mL (or 0.552 g) Tween 20 and adjust pH to 8.0 using HCl before volume is adjusted to 1000 mL.

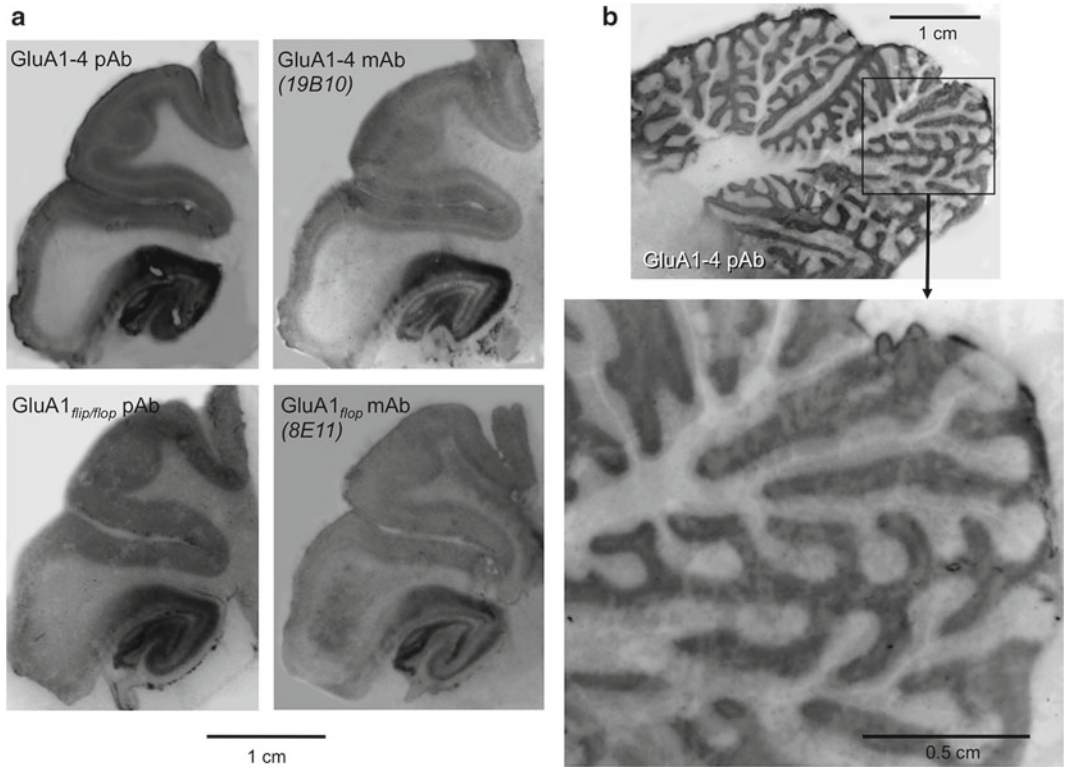

Fig. 2 Regional distribution of AMPA receptor subunits in human brain samples. Histoblots of human hippocampal (**a**) and cerebellar (**b**) sections were labelled with anti-GluA1-4 [16], anti-GluA1*flip/flop* [27] polyclonal rabbit antibodies (*pAb*) or anti-GluA1-4 (*19B10*) and anti-GluA1flop (*8E11*) monoclonal mouse antibodies (*mAb*) [9] to visualise the distribution of the corresponding subunit proteins

3. Blocking solution: 5 % (w/v) skimmed milk powder in TBST. Dissolve 5 g milk powder in 100 mL TBST.
4. Radioimmunoprecipitation assay buffer supplemented with ethylenediaminetetraacetic acid (EDTA) (RIPEA buffer): 20 mM Tris–HCl (pH7.5), 60 mM NaCl, 0.4 % (v/v) Triton X-100, 0.1 % (w/v) SDS, 0.4 % (w/v) deoxycholic acid, sodium salt and 2 mM EDTA disodium dihydrate. To prepare 1000 mL of RIPEA buffer, dissolve 2.423 g Tris-base, 3.5 g NaCl, 4 mL (or 4.28 g) Triton X-100, 1 g SDS, 4 g deoxycholic acid, sodium salt and 0.7443 g EDTA disodium dihydrate in deionised water and adjust pH to 7.5 using HCl before volume is adjusted to 1000 mL.
5. Deoxyribonuclease I [EC 3.1.21.1] (DNase I) buffer: 100 mM Na-acetate (pH5.0) and 5 mM $MgSO_4$. For 500 mL DNase I buffer, dissolve 6.8 g Na-acetate $3xH_2O$ (or 4.1 g anhydrous Na-acetate) and 0.616 g $MgSO_4$ $7xH_2O$ (or 0.301 g anhydrous $MgSO_4$) and adjust pH to 5.0 using acetic acid.

6. Strip buffer: 0.1 M Tris–HCl (pH 7.0), 2 % (w/v) SDS and 0.1 M β-mercaptoethanol. To prepare 200 mL of strip buffer, dissolve 2.423 g Tris-base and 4 g SDS in deionised water and adjust pH to 7.0 using HCl before volume is adjusted to 200 mL. Just before use, transfer solution into a fume hood and add 0.7 mL (or 0.78 g) β-mercaptoethanol (0.1 M final concentration).
7. Alkaline phosphatase (AP) buffer: 0.1 M Tris–HCl (pH 9.5), 0.1 M NaCl and 5 mM $MgCl_2$. For 1000 mL AP buffer, dissolve 12.14 g Tris-base, 5.84 g NaCl and 1.01 g $MgCl_2$ $6xH_2O$ in deionised water and adjust pH to 9.5 using HCl or NaOH before volume is adjusted to 1000 mL.
8. AP developer: 0.33 % (w/v) nitro blue tetrazolium (NBT), 0.66 % (w/v) 5-bromo-4-chlor-3-indolyl phosphate (BCIP), 0.1 M Tris–HCl (pH 9.5), 0.1 M NaCl and 5 mM $MgCl_2$.
   8.1. Prepare 5 % (w/v) NBT solution in 70 % (v/v) dimethylformamide (DMF) and 30 % (v/v) deionised water. For 200 µL NBT solution, use 0.01 g NTB, 140 µL DMF and 60 µL deionised water.
   8.2. Prepare 5 % (w/v) 5-bromo-4-chlor-3-indolyl phosphate (BCIP) solution in 100 % DMF. For 200 µL BCIP solution, dissolve 0.01 g BCIP in 200 µL DMF.
   8.3. AP developer should be prepared just before use: Add 16 µL of 5 % NBT and 33 µL BCIP solutions to 5 mL AP buffer and mix.
9. AP stopper (phosphate-buffered saline, PBS): 1.5 mM KH_2PO_4, 8.5 mM Na_2HPO_4 (pH 7.5), 137 mM NaCl and 3 mM KCl. To prepare 1000 mL, dissolve 0.204 g anhydrous KH_2PO_4, 1.207 g anhydrous Na_2HPO_4 (or 1.513 g Na_2HPO_4 $2xH_2O$), 8.01 g NaCl and 0.224 KCl. Confirm that pH is 7.5 and adjust volume to 1000 mL.

3 Methods

3.1 Preparation of Brain Sections for Histoblots

Prepare 10 µm thick cryostat sections of frozen unfixed brains for histoblots. Trans-cardial perfusion of animals and cryoprotection of brain tissue are not necessary. The transfer of proteins from unfixed section onto nitrocellulose membranes will preserve anatomical organisation of brain samples without compromising antigenicity by fixation.

1. Anaesthesia: Follow national and international guidelines for the care and handling of animals. Use approved protocols for anaesthesia and killing of animals appropriate for the species used for experiments.

2. Freshly removed brains should be cleared of dura and surface blood vessels. Regions of interest need to be dissected from larger brains (e.g. human brain samples).
3. For freezing the brain tissue, use isopentane (at least 500 mL in a long beaker) prechilled to –35–40 °C on dry ice or in –80 °C freezer. Place the brain tissue onto aluminium foil and remove liquid using filter paper. Gently immerse the brain (without the aluminium foil) into the prechilled isopentane. The brain tissue can be damaged or deformed if there is not enough isopentane in the beaker, and the brain hits the bottom too soon. It takes about 5 min to completely freeze an adult whole rat brain in isopentane. For the removal of brains from the isopentane, use a chilled forceps to prevent its sticking to the brain tissue.
4. Frozen brains should be secured individually with prechilled soft paper towels in prechilled Falcon tubes (50 mL capacity), which can be used for storage and transportation. The brains should be stored at –80 °C or on dry ice during transportation.
5. Transfer samples to –20 °C freezer overnight before cryostat sectioning.
6. Use Tissue-Tek® O.C.T™ to attach brain samples to specimen chocks in the desired orientation and position. Keep samples at –20 °C.
7. Set cryostat chamber and block temperature to –20 °C, knife to –17–18 °C or use your own optimised temperature settings. Trim down brain samples to the region of interest and then collect 10 μm thick sections and thaw and mount them onto cleaned, uncoated glass microscope slides. Mount some of the sections onto poly-l-lysine or gelatin-coated glass slides for Nissl staining. Keep brain sections at –20 °C until they are processed for histoblotting or at –80 °C for longer-term storage.

3.2 Transfer of Proteins from Brain Sections onto Nitrocellulose Membranes

Use a pair of powder-free gloves to avoid contamination of the membranes by fingerprints.

1. Cut Whatman filter paper (Nr. 1001917 or Nr. 3030917) to the appropriate size (about 3 × 3 cm for rat brains).
2. One by one dip both ends of the filter papers into transfer buffer (48 mM Tris-base, 39 mM glycin, 2 % (w/v) SDS, 20 % (v/v) methanol, pH ≈ 10.5) and lay them onto a clear glass surface without trapped air bubbles. Build up three layers of moist filter papers and put dry filter papers immediately next to them (both sides) to remove any excess liquid. Papers should not release buffer even under pressure.
3. Use the appropriate size (e.g. 2.4 × 2.4 cm for rat brain) of nitrocellulose membrane paper (e.g. Schleicher & Schuell, BA

85, 0.45 μm, Nr 401196). Proteins should be transferred onto the outer (convex) surface in the roll. This surface needs to be marked with an identification number of the section using a pencil at one of its corners. Do not use pen.

4. Fully dip the nitrocellulose membrane into transfer buffer and layer the membrane on the top of the stack of wet filter papers without trapped air bubbles.
5. Without horizontal movement, carefully place the glass slide with the brain section facing down onto the nitrocellulose membrane in a way that no air bubbles remain.
6. Apply a weight (e.g. inverted full 1000 mL laboratory glass bottle with plastic top on) gently from one side to remove trapped air and leave it for 30 s without any movement.
7. Immerse glass side with the attached nitrocellulose membrane facing down into blocking buffer (5 % (w/v) skimmed milk powder in TBST) and leave it for one hour without agitation. Nitrocellulose membrane will normally detach from glass slide. If not, peel it off gently using a forceps. Discard used filter papers; you need to prepare new ones for each transfer to avoid contamination of the nitrocellulose membranes.
8. Transfer nitrocellulose membranes into appropriate size petri dishes (or 6 well plates) filled with blocking buffer.
9. Prepare DNase I solution (you will need 2 mL/well): add 10 Units of DNase I stock (RNase-free) to 2 mL DNase I buffer.
10. Rinse membranes in TBST once for 1 min. From this point samples should be placed on a shaker for subsequent steps to make sure that the whole membrane is evenly exposed to buffers and reagents.
11. Incubate nitrocellulose membranes in DNase I solution at 37 °C for 20 min. The enzymatic degradation of DNA will improve access to membrane-bound protein epitopes.
12. Wash nitrocellulose membranes in RIPEA for 20 min.
13. Wash nitrocellulose membranes in TBST for 2×10 min.
14. Add β-mercaptoethanol to strip buffer under fume hood (you will need 1 mL/well).
15. Remove TBST and add strip buffer (1 mL/well) to nitrocellulose membranes under fume hood. Seal petri dishes (or plates with lids) tightly using parafilm and incubate at 45 °C for 1 h. This step will remove adhering tissue residues from the nitrocellulose membrane.
16. Remove strip buffer and wash nitrocellulose membranes in RIPEA buffer for 10 min.
17. Wash in TBST for 2×5 min.
18. Incubate in blocking solution for 1 h.

3.3 Immunolabelling

19. Dilute primary antibody in blocking solution (200 μL/blot). While optimum concentration needs to be determined for each primary antibody, 1 μg/mL is usually a good starting point for affinity-purified antibodies.
20. Seal nitrocellulose membranes with primary antibodies into small plastic pockets (prepare these just slightly bigger than the nitrocellulose membrane) using an impulse sealer and incubate samples at 4 °C overnight on shaker or rotating wheel in cold room.
21. Remove membranes from plastic pockets and place them in RIPEA-containing petri dishes for washing for 20 min. Use TBST instead of RIPEA if the expected immunolabelling is weak.
22. Wash in blocking solution for 2 × 10 min.
23. Dilute alkaline phosphatase-labelled secondary antibody in blocking solution (e.g. 1:5000 dilution of donkey anti-rabbit IgG-AP, Promega; 1 mL/well). Add 1 mL of diluted secondary antibody to membranes and incubate on shaker for 90 min at room temperature (~20 °C).
24. Wash membranes in RIPEA for 20 min. Use TBST instead of RIPEA for this step if the expected immunolabelling is weak.
25. Wash membranes in TBST for 2 × 10 min and rinse it one more time in TBST briefly.
26. Prepare AP developer as described above and add 1 mL/well.
27. Develop alkaline phosphatase reaction at room temperature (~20 °C) as long as required. Usually it takes about 5–30 min to get clear labelling. Leave it at 4 °C overnight if there is no detectable labelling after 30 min.
28. Stop AP reaction using PBS and rinse membranes three times in fresh PBS.
29. Store membranes in PBS at 4 °C until scanning or photography. Do not dry membranes before images are captured because labelling will fade.

4 Notes

1. Using temperatures below –40 °C for the freezing of brain samples may result in the fragmentation of the frozen brain tissue or difficulties with cutting of sections using cryostat. Following appropriate freezing, even relatively large brain areas (e.g. cryostat sections of whole human cerebellum, hippocampus, striatum, etc.) can be processed for histoblotting (Fig. 2).

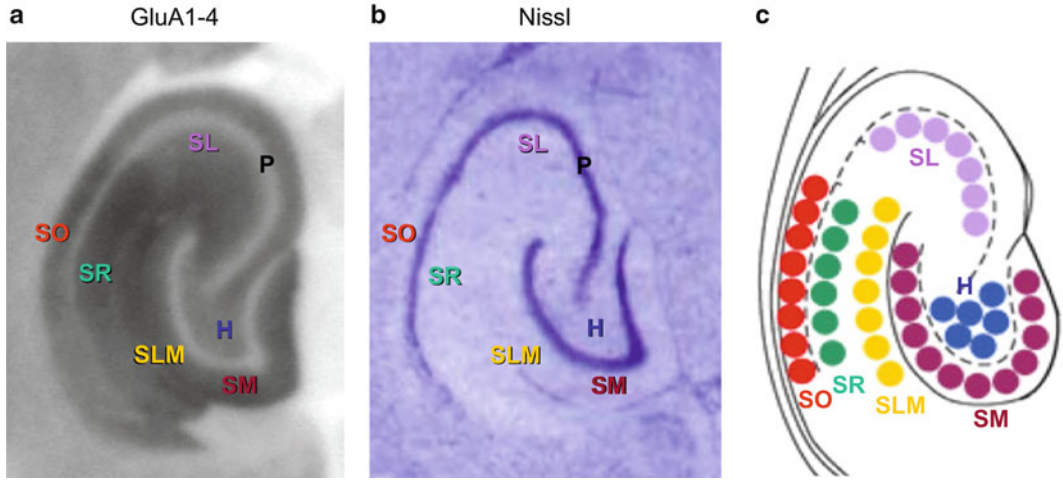

Fig. 3 Illustration of the sampling method used to compare immunoreactivities in different hippocampal regions. (**a**) Hippocampal region of a rat brain histoblot immunolabelled with a rabbit polyclonal anti-GluA1-4 antibody [16]. (**b**) Nissl-stained sections facilitate the identification of different brain regions after immunostaining for sampling of immunoreactivity. (**c**) The colours on the schematic diagram represent layers of the hippocampal formation: *red* stratum oriens (*SO*), *green* stratum radiatum (*SR*), *yellow* stratum lacunosum-moleculare (*SLM*), *plum* stratum moleculare of dentate gyrus (*SM*), *blue* hilum of dentate gyrus (*H*), *lilac* stratum lucidum of CA3 (*SL*). Density readings can be taken by placing open circular cursors with a diameter of 0.1 mm at the indicated adjacent positions along SO (*8 circles*), SR (*6 circles*), SLM (*7 circles*), SM (*12 circles*), H (*6 circles*), SL (*7 circles*). See text and Refs. [11, 19, 20, 22–26] for details and examples

2. Accurate setting of the thickness of the cryostat sections is essential for quantitative comparisons. Based on our experience, 10 μm thick sections (that likely to represent a single cell layer) are ideal for histoblots. This is consistent with previous studies [3]. Because the unfixed frozen brain sections are also suitable for the study of radioligand binding sites using autoradiography and for in situ hybridisation histochemistry analysis of mRNA distribution, these can be performed in parallel to complement the histoblot mapping of the corresponding proteins.
3. Nissl staining of adjacent sections can help with the accurate identification of immunopositive brain structures (Fig. 3). For Nissl staining use poly-l-lysine or gelatin-coated glass slides. After overnight drying at room temperature (~20 °C), wash slides in 70 % (v/v) ethanol for 2 min. Use 1 % (w/v) aqueous cresyl violet for 5 min. Remove excess stain by washing in tap water. Wash slides in 10 % (v/v) methylated spirits containing a few drops of acetic acid. Wash slides in methanol three times and once in xylene before mounting in DPX mountant (BDH Laboratory Supplies, Poole, UK) for microscopy or scanning.

4. Nitrocellulose membranes with transferred brain proteins (after **step 18** under 3.2) can be stored at –20 °C for several weeks without deterioration of antigenicity and subjected to immunostaining later. For storage, place blotted nitrocellulose membranes between two layers of filter papers (e.g. Whatman filter paper Nr. 1001917 or Nr. 3030917) pre-soaked in blocking buffer. Seal nitrocellulose membranes with filter papers into small plastic pockets using an impulse sealer and store them at –20 °C.
5. Optimum dilution and incubation conditions need to be established for each primary and secondary antibody. Most affinity-purified primary antibodies produce good immunolabelling at 1 μg/mL concentration following overnight incubation at 4 °C. Alkaline phosphatase-conjugated secondary antibodies at 1:5000 dilution, applied for 90 min at room temperature (or overnight at 4 °C), are generally suitable for the visualisation of primary antibodies. While the use of horseradish peroxidase-conjugated secondary antibodies in combination with enhanced chemiluminescence is frequently used to amplify signal for conventional immunoblots, this detection system reduces the resolution of histoblots therefore less suitable than the above-described alkaline phosphatase-based visualisation of immunoreactivity.
6. Primary antibodies that produce specific labelling on immunoblots often fail to recognise the same protein targets in fixed tissue samples using conventional immunohistochemistry. Because the presentation of proteins in histoblots is very similar to conventional immunoblots, antibodies are more likely to work in both techniques. However, the use of appropriate positive and negative controls is required to confirm the specificity of immunolabelling obtained with histoblots [1]. Omitting the primary antibody and using sera obtained from immunised animals before the first injection of the antigen ('pre-immune serum') instead of the primary antibody are frequently used negative controls. In addition, primary antibodies should be preabsorbed with excess of the corresponding antigenic peptide or protein. Under these conditions, the labelling of endogenous proteins presented on histoblots is blocked by the saturation of antibodies with the antigens. While this control will show that the antibody binds to the antigen, it does not exclude the possibility of cross-reactions with other proteins. It is often very helpful to use two different antibodies raised against different epitopes of the same target protein. If patterns of staining are the same with both antibodies, this is strong circumstantial evidence in favour of specificity [1, 17]. The ideal control sample is tissue obtained from a transgenic animal, which lacks the target antigen. Comparison of the

distribution of immunoreactivity with images obtained by using other localisation techniques (e.g. autoradiography using radioligands or in situ hybridisation histochemistry) could provide additional supporting evidence. For example, areas where the presence or absence of the target antigen is expected based on these complementary imaging approaches can be used as positive and negative controls, respectively, [1].

7. While in most histoblot experiments 5 % (w/v) skimmed milk powder containing blocking solution is able to minimise non-specific labelling, normal serum or fish skin gelatin (3–5 % w/v) can be used as an alternative if the background labelling is high. Unlike normal serum, bovine serum albumin (BSA) or milk, fish gelatin does not contain IgG or serum proteins that could cross-react with mammalian antibodies. Also, fish gelatin effectively blocks non-specific binding sites on nitrocellulose membranes and suitable for the dilution of antibodies during immunostaining procedures [9].
8. Digital greyscale images of histoblots can be produced by standard desktop scanners, which provide even and consistent illumination of nitrocellulose membranes even if several are scanned at the same time for quantitative comparisons. Membranes should remain wet during scanning to prevent the fading of immunopositive areas. Therefore, wet nitrocellulose membranes should be covered with a transparent plastic sheet after they are laid on the glass surface of the scanner. In addition to keeping the membranes wet, the plastic sheet also helps with the removal of trapped air bubbles from under the nitrocellulose membranes.
9. Image analysis and processing can be performed using Adobe® Photoshop® (Adobe Systems, San Jose, CA, USA) or Image J (NIH Image, Bethesda, MD, USA; http://imagej.nih.gov/ij) software. Greyscale images need to be captured and treated identically to allow comparison of pixel densities (arbitrary units) of immunoreactivity in different brain regions. The pixel density can be measured using open circular cursors with a set diameter (e.g. 0.1 mm), which is appropriate for the region of interest (Fig. 3). The cursors should be placed in different brain regions identified based on adjacent cresyl violet-stained sections [11, 19, 20, 23]. For example, different regions of the hippocampus can be analysed by placing circular cursors with a diameter of 0.1 mm at adjacent positions along the *stratum oriens*, *stratum radiatum*, *stratum lacunosum-moleculare*, *stratum moleculare* of dentate gyrus, *hilum* of dentate gyrus and *stratum lucidum* of CA3 (Fig. 3). The same approach can be applied to other brain regions. About ten different background determinations need to be performed near the brain protein containing areas of the immunostained nitrocellulose membranes. The average of these

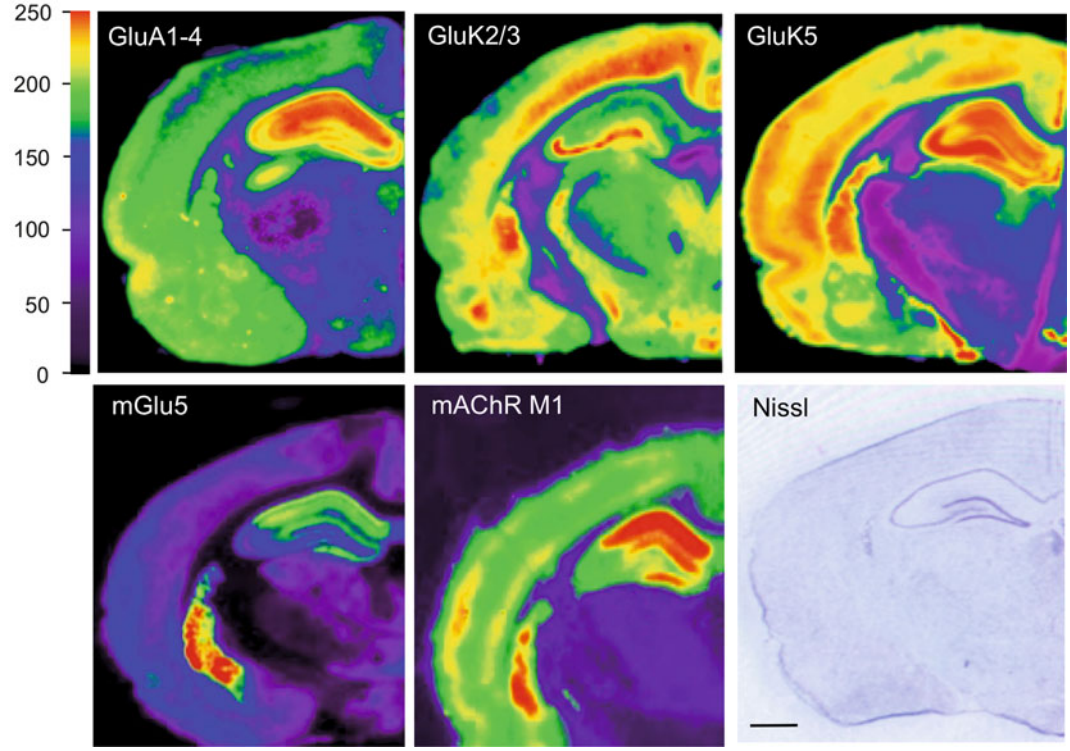

Fig. 4 Colour gradients illustrate the regional expression profiles of different neurotransmitter receptor proteins. Histoblots of coronal rat brain sections were immunostained for either ionotropic glutamate receptor subunits GluA1-4 [16], GluK2/3, GluK5 (Abcam, Cambridge, UK), metabotropic glutamate receptor isoform 5 (*mGlu5*) or muscarinic acetylcholine receptor M1 (*mAChR M1*) [20]. Greyscale histoblot images were converted to colour gradients using gradient mapping [19–21]. *Scale bar*, 1 mm (Images were provided by Dr. Simon M. Ball)

background values needs to be subtracted from the average pixel densities measured within various brain regions. Following background corrections, the average pixel density for the whole region from one animal should be counted as one 'n'. Differences between corresponding brain regions of different animals should be assessed using a two-way analysis of variance (ANOVA) and further compared with the Bonferroni post hoc test, at a minimum confidence level of $p < 0.05$.

10. For illustration purposes greyscale histoblot images can be converted to colour gradients using the gradient mapping function of Adobe® Photoshop® (Adobe Systems, San Jose, CA, USA) [19–21] (Fig. 4).

Acknowledgements

I am grateful to Professor Peter Streit (1945–2008, Brain Research Institute, University of Zurich), for introducing me to the histoblot technique. I would like to thank Drs Simon M Ball, Ik-Hyun

Cho and Endre Dobó for their contributions to the refinement of the histoblot method. This research was supported by Grant from the Biotechnology and Biological Sciences Research Council, UK (Grant BB/J015938/1).

References

1. Molnár E (2013) Immunocytochemistry and immunohistochemistry. In: Langton PD (ed) Essential guide to reading biomedical papers: recognising and interpreting best practice. Wiley-Blackwell, Chichester, West Sussex, UK, pp 117–128
2. Taraboulos A, Jendroska K, Serban D, Yang S-L, DeArmond SJ, Prusiner SB (1992) Regional mapping of prion proteins in brain. Proc Natl Acad Sci USA 89:7620–7624
3. Okabe M, Nyakas C, Buwalda B, Luiten PGM (1993) In situ blotting: a novel method for direct transfer of native proteins from sectioned tissue to blotting membrane: procedure and some applications. J Histochem Cytochem 41: 927–934
4. Jendroska K, Hoffmann O, Schelosky L, Lees A, Poewe W, Daniel SE (1994) Absence of disease related prion protein in neurodegenerative disorders presenting with Parkinson's syndrome. J Neurol Neurosurg Psychiatry 57: 1249–1251
5. Benke D, Wenzel A, Scheuer L, Fritschy JM, Mohler H (1995) Immunobiochemical characterization of the NMDA-receptor subunit NR1 in the developing and adult rat brain. J Recept Signal Transduct Res 15:393–411
6. Wenzel A, Scheurer L, Künzi R, Fritschy JM, Mohler H, Benke D (1995) Distribution of NMDA receptor subunit proteins NR2A, 2B, 2C and 2D in rat brain. Neuroreport 7:45–48
7. Wenzel A, Villa M, Mohler H, Benke D (1996) Developmental and regional expression of NMDA receptor subtypes containing the NR2D subunit in rat brain. J Neurochem 66:1240–1248
8. Rogers SW, Gahring LC, White HS (1998) Glutamate receptor GluR1 expression is altered selectively by chronic audiogenic seizures in the Frings mouse brain. J Neurobiol 35: 209–216
9. Tönnes J, Stirli B, Cerletti C, Behrmann JT, Molnár E, Streit P (1999) Regional distribution and developmental changes of GluR1-flop protein revealed by monoclonal antibody in rat brain. J Neurochem 73:2195–2205
10. Court JA, Martin-Ruiz C, Graham A, Perry E (2000) Nicotinic receptors in human brain: topography and pathology. J Chem Neuroanat 20:281–298
11. Fernández-Alacid L, Watanabe M, Molnár E, Wickman K, Luján R (2011) Developmental regulation of G protein-gated inwardly-rectifying K^+ (GIRK/Kir3) channel subunits in the brain. Eur J Neurosci 34:1724–1736
12. Ferrándiz-Huertas C, Gil-Mínguez M, Luján R (2012) Regional expression and subcellular localization of the voltage-gated calcium channel β subunits in the developing mouse brain. J Neurochem 122:1095–1107
13. Schulz-Schaeffer WJ, Tshöke S, Kranefuss N, Dröse W, Hause-Reitner D, Giese A, Groschup MH, Kretzschmar HA (2000) The paraffin-embedded tissue blot detects PrPSc early in the incubation time in prion diseases. Am J Pathol 156:51–56
14. Kimura KM, Yokoyama T, Haritani M, Narita M, Belledy P, Smith J, Spencer YI (2002) *In situ* detection of cellular and abnormal isoforms of prion protein in brains of cattle with bovine spongiform encephalopathy and sheep with scrapie by use of a histoblot technique. J Vet Diagn Invest 14:255–257
15. Beliczai Z, Varszegi S, Gulyas B, Halldin C, Kasa P, Gulya K (2008) Immunohistoblot analysis on whole human hemispheres from normal and Alzheimer diseased brains. Neurochem Int 53:181–183
16. Pickard L, Noël J, Henley JM, Collingridge GL, Molnar E (2000) Developmental changes in synaptic AMPA and NMDA receptor distribution and AMPA receptor subunit composition in living hippocampal neurons. J Neurosci 20:7922–7931
17. Pickard L, Noël J, Duckworth JK, Fitzjohn SM, Henley JM, Collingridge GL, Molnar E (2001) Transient synaptic activations of NMDA receptors lead to the insertion of native AMPA receptors at hippocampal neuronal plasma membranes. Neuropharmacology 41:700–713
18. Gallyas F, Ball SM, Molnar E (2003) Assembly and cell surface expression of KA-2 subunit-containing kainate receptors. J Neurochem 86:1414–1427
19. Callaerts-Vegh Z, Beckers T, Ball SM, Baeyens F, Callaerts PF, Cryan JF, Molnar E, D'Hooge

R (2006) Concomitant deficits in working memory and fear extinction are functionally dissociated from reduced anxiety in metabotropic glutamate receptor 7-deficient mice. J Neurosci 26:6573–6582

20. Jo J, Ball SM, Seok H, Oh SB, Massey PV, Molnar E, Bashir ZI, Cho K (2006) Experience-dependent modification of mechanisms of long-term depression. Nat Neurosci 9:170–172
21. Ball SM, Atlason PT, Shittu-Balogun OO, Molnár E (2010) Assembly and intracellular distribution of kainate receptors is determined by RNA editing and subunit composition. J Neurochem 114:1805–1818
22. Jouhanneau J-S, Ball SM, Molnár E, Isaac JTR (2011) Mechanisms of bi-directional modulation of thalamocortical transmission in barrel cortex by presynaptic kainate receptors. Neuropharmacology 60:832–841
23. Kopniczky Z, Dobó E, Borbély S, Világi I, Détári L, Krisztin-Péva B, Bagosi A, Molnár E, Mihály A (2005) Lateral entorhinal cortex lesions rearrange afferents, glutamate receptors, increase seizure latency and suppress seizure-induced c-fos expression in the hippocampus of adult rat. J Neurochem 95:111–124
24. Világi I, Dobó E, Borbély S, Czégé D, Molnár E, Mihály A (2009) Repeated 4-aminopyridine induced seizures diminish the efficacy of glutamatergic transmission in the neocortex. Exp Neurol 219:136–145
25. Borbély S, Dobó E, Czégé D, Molnár E, Bakos M, Szűcs B, Vincze A, Világi I, Mihály A (2009) Modification of ionotropic glutamate receptor-mediated processes in the rat hippocampus following repeated, brief seizures. Neuroscience 159:358–368
26. Borbély S, Czégé D, Molnár E, Dobó E, Mihály A, Világi I (2015) Repeated application of 4-aminopyridine provoke an increase in entorhinal cortex excitability and rearrange AMPA and kainate receptors. Neurotox Res 27:441–452
27. Molnár E, Baude A, Richmond SA, Patel PB, Somogyi P, McIlhinney RAJ (1993) Biochemical and immunocytochemical characterization of antipeptide antibodies to a cloned GluR1 glutamate receptor subunit: cellular and subcellular distribution in the rat forebrain. Neuroscience 53:307–326

Chapter 13

Immunohistochemistry for Ion Channels and Their Interacting Molecules: Tips for Improving Antibody Accessibility

Kohtarou Konno and Masahiko Watanabe

Abstract

Elucidating the molecular organization at synapses is essential for understanding brain function and plasticity. Immunohistochemistry is widely used as a sensitive and specific method in morphological studies. There are specific antibodies directed against receptors, ion channels, and their interacting molecules; however, it is sometimes difficult and ineffective to visualize synaptic proteins by conventional immunocytochemistry. This is mainly owing to the fact that the cross-linking of proteins by chemical fixation hampers the accessibility of antibodies to antigen molecules. This is particularly true for receptors and ion channels condensed in the synaptic cleft, postsynaptic density, or trigger zone of action potentials. To overcome this problem, researchers have devised methods to improve immunohistochemical detection of proteins that are hidden or prone to be hidden in condensed molecular matrices. Of these methods, mild chemical fixation by low paraformaldehyde concentrations or fresh frozen sections is often effective in detecting such *hidden* proteins. Moreover, pretreatment of sections with proteases such as pepsin is a prerequisite to detect proteins embedded in the core of the postsynaptic density, for example, NMDA-type glutamate receptors and their interacting PSD-95 protein family. In this chapter, we introduce these improving techniques for light microscopic immunohistochemistry.

Key words Immunofluorescence, Immunohistochemistry, Antigen retrieval, Antigen exposure, Low-concentration paraformaldehyde, Pepsin pretreatment, Fresh frozen section

1 Introduction

For immunohistochemical studies, tissues and cells are fixed by appropriate aldehyde fixatives to preserve structure and antigenicity. Four percent paraformaldehyde (PFA) in phosphate buffer is the most commonly used fixative. Glutaraldehyde is further added for ultrastructural preservation for immunoelectron microscopy, but the antigenicity of most proteins is greatly reduced by the addition of this aldehyde. Aldehyde fixatives form protein-protein and protein-nucleic acid cross-links. Chemical fixation by aldehyde fixatives hampers the antigen-antibody reaction and worsens the

Rafael Luján and Francisco Ciruela (eds.), *Receptor and Ion Channel Detection in the Brain: Methods and Protocols*, Neuromethods, vol. 110, DOI 10.1007/978-1-4939-3064-7_13,

accessibility of antibodies in two ways, by the breakdown or conformational changes of antigen epitopes and by the cross-linking and shrinkage of tissues. These events often lower the sensitivity and specificity of immunohistochemical detection notably for receptors, ion channels, and related molecules that are condensed in the synaptic cleft, postsynaptic density, or trigger zone of action potentials.

To overcome this problem, several laboratories have tried to uncover such hidden proteins by immunohistochemistry. Fritschy et al. [1] have reported that microwave irradiation of fixed brain tissues lowers nonspecific staining and improves immunohistochemical staining for $GABA_A$ receptors, but not for NMDA-type glutamate receptors. They further found that microwave irradiation of unfixed or fresh frozen sections enhances immunohistochemical staining for both receptor types. Lorincz and Nusser [2] used a low-pH-based 1–2 % PFA fixation, which increases the intensity of immunohistochemical staining for $GABA_A$ receptors, ionotropic glutamate receptors, and voltage-gated K^+ and Na^+ channels. Therefore, the choice and condition of chemical fixation are important factors to improve immunohistochemical detection.

Even if chemical fixation is milder using low PFA concentrations or by immersive fixation of fresh frozen sections, proteins in the *core* of the postsynaptic density, such as NMDA-type glutamate receptors and their interacting PSD-95 protein family, are still resistant to conventional immunohistochemical detection and require rigorous antigen-exposure processing. To this end, we have developed section pretreatment by proteases, such as pepsin, which is designed to break the cross-linking of protein-protein and protein-nucleic acid interactions and facilitate accessibility of antibodies to antigen epitopes [3–5].

To find optimal immunohistochemical conditions for proteins of interest, we routinely pretest the effects of lowering of PFA concentrations, section pretreatment by pepsin, and use of fresh frozen sections. In this chapter, we describe these procedures to improve immunohistochemical detection of synaptic proteins at the microscopic level.

2 Materials

2.1 Immunohistochemistry with Paraffin Sections

2.1.1 Fixation

1. PFA. To prepare 1 L of 1 or 4 % PFA in 0.1 M sodium phosphate buffer (PB, pH7.4), 10 g or 40 g of PFA powder is dissolved in 500 mL of distilled water. After filtration of PFA solution by filter paper, 500 mL of 0.2 M PB is added. For safety reasons, all these steps should be carried out wearing protective clothing and gloves and in a fume hood.

2. 0.2 M sodium PB (pH 7.4). One hundred and sixteen grams of $Na_2HPO_4 \cdot 12H_2O$ and 11.8 g $NaH_2PO_4 \cdot 2H_2O$ is dissolved in distilled water to make 2 L of 0.1 M PB.
3. Nembutal (Abbott Laboratories, North Chicago, IL, USA; 50 mg/mL sodium pentobarbital) or somnopentyl (Schering-Plough, Germany; 64.8 mg/mL sodium pentobarbital). Intraperitoneal injection at 1 mL/kg body weight. For anesthesia of small laboratory animals, such as mice, anesthetic diluted with sterile saline is convenient.
4. Peristaltic pump.
5. Scissors and tweezers.
6. Phosphate-buffered saline (PBS, pH 7.4). 435 g of NaCl, 116 g of $Na_2HPO_4 \cdot 12H_2O$, and 11.8 g of $NaH_2PO_4 \cdot 2H_2O$ are dissolved in distilled water to make 5 L of 10 × PBS stock solution. PBS (150 mM NaCl in 10 mM PB, pH 7.4) is prepared by 1:9 dilution of 10 × PBS stock solution with distilled water.

2.1.2 Preparation of Paraffin Sections

1. Dehydration series. Glass containers containing an ascending series of ethanol (50, 70, 80, 90, 95, and 100 %) and xylene are placed in a thermostatic chamber (37 °C). Glass containers with xylene-paraffin (1:1), paraffin-1, paraffin-2, and paraffin-3, are placed in a thermostatic oven (65 °C).
2. Paraffin wax. TissuePrep Embedding Media (Fisher Scientific, USA).
3. Tissue-Tek Mega-Cassette (Sakura Finetek Japan, Japan).
4. SM 200R sliding microtome (Leica, Germany) with S35 microtome blade (Feather, Japan).
5. Slide glass coated with silane (Muto Pure Chemicals, Japan).
6. Water bath for floating paraffin section (Takashima, Japan).
7. Paraffin stretcher (Sakura Finetek Japan, Japan).

2.1.3 Antigen-Retrieval and Antigen-Exposing Treatments

1. Rehydration series. Paraffin sections are dewaxed and rehydrated by dipping in glass containers containing xylene and a descending series of ethanol (100, 95, 90, 80, 70, and 50 %), with 1 min for each step. After rehydration, glass slides are rinsed in distilled water and then PBS.
2. Immunosaver and Retriever oven (Electron Microscopy Sciences, Hatfield, PA, USA)
3. Pepsin stock solution. 100 mg/mL of pepsin stock solution is prepared by dissolving 2 g of pepsin powder (Dako Japan, Japan) in 20 mL of distilled water. After completely dissolving in solution, pepsin stock solution is aliquoted into 1.5 mL plastic tubes and immediately frozen for stock in the freezer at −80 °C.
4. Water bath.

2.1.4 Immunohistochemical Staining

1. PBS.
2. Humidified chambers.
3. 10 % Normal blocking serum: 10 % of normal serum from the same host species as secondary antibodies. Never use normal blocking serum from host species of the primary antibody.
4. Primary antibodies. Usually, primary antibodies are used at 1 μg/mL for affinity-purified antibodies or diluted to 1:2000 for antisera.
5. Species-specific fluorophore-linked secondary antibodies. Secondary antibodies are diluted to 1:200 for use.
6. Vectashield mounting medium (Vector Laboratories, USA).
7. Cover glass slips (Matsunami, Japan).

2.2 Immunohistochemistry with Fresh Frozen Sections

Materials for immunohistochemistry with fresh frozen sections are essentially the same as those with paraffin sections, except for the following:

1. Powdered dry ice.
2. Tissue-Tek O.C.T. compound (Sakura Finetek Japan, Japan).
3. CM 1900 Cryostat (Leica, Germany) with high-profile disposable microtome blades (Leica, Germany).

3 Methods

3.1 Immunohistochemistry with Paraffin Sections

This section explains procedures for immunofluorescence with paraffin sections, which are less sensitive in immunohistochemical detection compared with microslicer and cryostat sections. Nevertheless, paraffin sections are useful and reproducible, especially when antigen-exposing techniques such as pepsin pretreatment are required. Improved detection by use of low PFA concentrations and pepsin pretreatment is also true for microslicer and cryostat sections and immunoperoxidase.

3.1.1 Fixation

Four percentage PFA in 0.1 M PB is the standard fixative for light microscopic immunohistochemistry. Nevertheless, it should be kept in mind that the concentration of PFA is a critical factor that affects the accessibility of antibodies to antigen molecules, particularly those condensed in the synaptic cleft, postsynaptic density, and action potential trigger zone. Tissue shrinkage by dehydration and embedding in paraffin wax further hinders antibody accessibility compared with immunohistochemistry using microslicer and cryostat sections. If one encounters unexpectedly low immunohistochemical signals, the use of 1 % PFA is worth a try. *See* Chap. 17 for transcardial perfusion.

After perfusion with two volumes of 4 or 1 % PFA fixative for 10 min using a peristaltic pump, brain tissues are excised from the

skull and immersed in the same fixative for 2 h at room temperature and then rinsed with PBS. Fixed brains are stored in PBS at 4 °C until sectioning.

3.1.2 Preparation of Paraffin Sections

Fixed brain samples packed in a Tissue-Tek Mega-Cassette are dehydrated by ethanol and xylene in a thermostatic chamber at 37 °C and immersed in paraffin wax in a thermostatic oven at 65 °C. The time required for each dehydration and immersion step depends on the size of tissue specimens. For mouse brains, 3–6 h is sufficient for each step. Finally, brain samples are dipped in melted pure paraffin wax in a metal mold for several hours and then cooled to be solidified in the refrigerator. After complete cooling, paraffin blocks are taken out from the mold and attached to wooden blocks.

Paraffin sections (4–5 μm in thickness) are prepared on a SM 200R sliding microtome. Sections are floated on water at room temperature and then transferred to a water bath at approximately 40 °C. After a complete stretch, paraffin sections are mounted on glass slides coated with silane and dried on a paraffin stretcher plate at 40 °C overnight. Paraffin sections are housed in glass slide boxes and stored at room temperature for several years or more.

3.1.3 Antigen-Retrieval and Antigen-Exposing Treatments

After dewaxing and rehydration, paraffin sections should be subjected to either antigen-retrieval or antigen-exposing treatment. Antigen-retrieval treatment is performed by heating paraffin sections in a citrate- or EDTA-based buffer and is quite effective in the detection of unhidden molecules, i.e., conventional molecules that antibodies can freely access when using microslicer and cryostat sections. Antigen-exposing treatment by protease digestion is essential for any sections to detect hidden molecules that are embedded in the core of the postsynaptic density, such as NMDA-type glutamate receptors and their interacting PSD-95 protein family.

We use Immunosaver for antigen-retrieval treatment. Immunosaver diluted to 1:200 with water is poured into a glass container and placed in a retriever oven. When heated up to 95 °C, a metal rack with rehydrated glass slides is dipped in Immunosaver solution and heated at 95 °C for 30 min.

For antigen-exposing treatment, we prefer pepsin because its activation and inactivation are readily controlled by lowering pH and neutralization, respectively. Glass containers containing 0.2 N HCl to 37 °C are pre-warmed at 37 °C in a water bath. After adding 1/100 volume of thawed pepsin stock solution (final pepsin concentration is 1 mg/mL), rehydrated paraffin sections are dipped and digested at 37 °C. Incubation for 10 min is optimal for paraffin sections of adult brains, while that for 2–3 min is optimal for paraffin sections of neonatal brains and for microslicer and cryostat sections of adult brains. When using paraffin sections of 4 % PFA-fixed brains, a combination of Immunosaver and pepsin treatments is often effective compared with pepsin treatment alone.

3.1.4 Immunohistochemical Staining

All immunohistochemical incubation is performed in a humidified chamber at room temperature, and PBS is used as a washing and diluent buffer. Nonspecific binding of primary antibodies is prevented by 20 min incubation with 10 % normal serum. Sections are then incubated overnight with primary antibodies at appropriate dilution that yields specific signals with minimal nonspecific labeling. After three rinses in PBS for 5 min each, sections are incubated with a secondary antibody for 2 h. After rinsing in PBS, glass slides are covered by coverslip with anti-fade mounting medium. Fluorescent images are taken using confocal or fluorescence microscopy.

Figure 1 shows examples of immunofluorescence using 1 % PFA-fixed paraffin sections of adult mouse brains, which are subjected to antigen-exposing treatment by pepsin digestion and immunoreacted with primary antibodies against AMPA receptor GluA1, GluA2, GluA3, and GluA4 and NMDA receptor GluN1, GluN2B, GluN2C, and GluN2D.

3.2 Immunofluorescence with Fresh Frozen Sections

As originally reported by Fritschy et al. [1], we have also experienced great improvement in immunohistochemistry with the use of fresh frozen sections. This method is particularly effective when immunohistochemical detection targets hidden proteins or proteins prone to be hidden in the postsynaptic density, including ionotropic glutamate receptor GluA, GluN, and GluD subunits, and their interacting PSD-95 and transmembrane AMPA receptor regulatory proteins [6]. However, the effectiveness with the use of fresh frozen sections varies greatly depending on the primary antibodies used, even if they are raised against the same proteins.

3.2.1 Preparation of Fresh Frozen Sections

Under deep anesthesia, the carotid artery is transected for bleeding, and brain tissues are excised from the skull and immediately frozen in powdered dry ice. Brain tissues are stored in the freezer at –80 °C until use. The temperature of the cryostat chamber is set at –15 °C, and brain tissues are placed in the chamber at least for 30 min. Brain tissues are then embedded in Tissue-Tek O.C.T. compound, and frozen sections (20 μm in thickness) are prepared on a CM 1900 Cryostat. Sections are mounted on silane-coated slide glass and dried by sending room temperature wind through the dryer. Fresh frozen sections can be stored for a few weeks at –80 °C until the experiments.

3.2.2 Fixation of Sections and Immunohistochemical Staining

Sections on glass slides are air dried and warmed up to room temperature. They are fixed by dipping in 4 % PFA in 0.1 M PB for 15 min and rinsed with PBS. If necessary, fresh frozen sections are subjected to pepsin treatment before immunohistochemical staining (*see* Sect. 3.1.3). All immunohistochemical incubation is performed in a humid chamber at room temperature, similar to immunohistochemistry with paraffin sections.

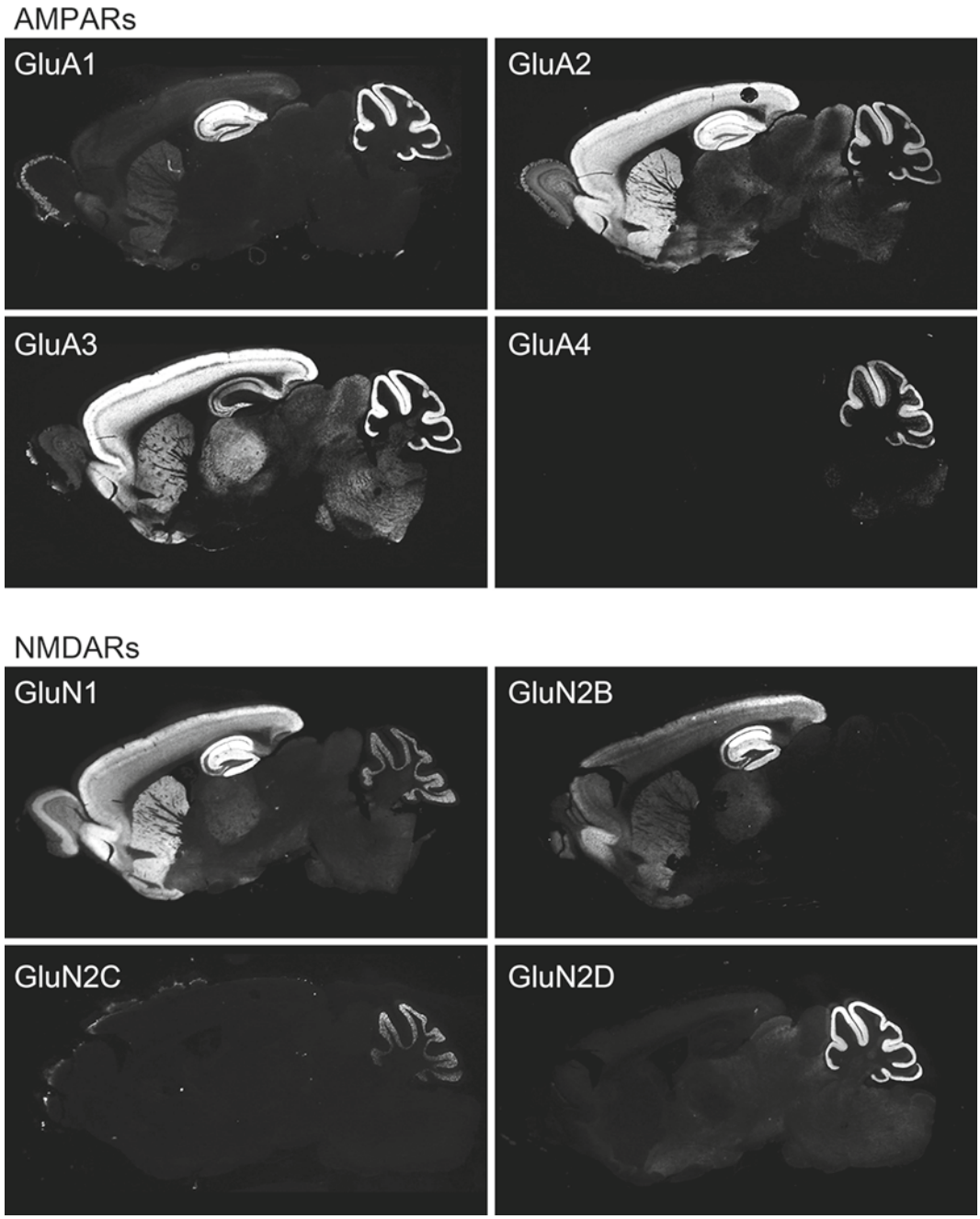

Fig. 1 Immunofluorescence using 1 % PFA-fixed paraffin sections for AMPA receptor subunits GluA1, GluA2, GluA3, and GluA4 and NMDA receptor subunits GluN1, GluN2B, GluN2C, and GluN2D

Figure 2 shows examples of immunofluorescence using fresh frozen sections of adult mouse brains. Sections are immunoreacted for AMPA receptor subunits GluA1 and GluA2 and for PSD-95.

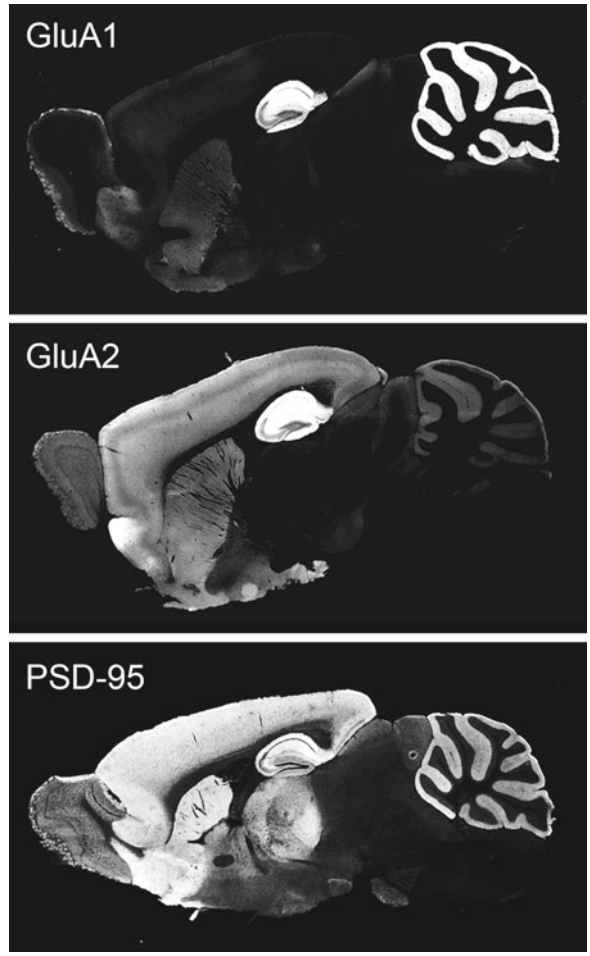

Fig. 2 Immunofluorescence using fresh frozen sections for AMPA receptor subunits GluA1 and GluA2 and PSD-95

References

1. Fritschy JM, Weinmann O, Wenzel A, Benke D (1998) Synapse-specific localization of NMDA and GABA(A) receptor subunits revealed by antigen-retrieval immunohistochemistry. J Comp Neurol 12:194–210
2. Lorincz A, Nusser Z (2010) Molecular identity of dendritic voltage-gated sodium channels. Science 328:906–909
3. Fukaya M, Kato A, Lovett C, Tonegawa S, Watanabe M (2003) Retention of NMDA receptor NR2 subunits in the lumen of endoplasmic reticulum in targeted NR1 knockout mice. Proc Natl Acad Sci U S A 100:4855–4860
4. Fukaya M, Watanabe M (2000) Improved immunohistochemical detection of postsynaptically-located PSD-95/SAP90 protein family by protease section pretreatment. A study in the adult mouse brain. J Comp Neurol 426: 572–586
5. Watanabe M, Fukaya M, Sakimura K, Manabe T, Mishina M, Inoue Y (1998) Selective scarcity of NMDA receptor channel subunits in the stratum lucidum (mossy fiber-recipient layer) of the hippocampal CA3 subfield. Eur J Neurosci 10: 478–487
6. Konno K, Matsuda K, Nakamoto C, Uchigashima M, Miyazaki T, Yamasaki M, Sakimura K, Yuzaki M, Watanabe M (2014) Enriched expression of GluD1 in higher brain regions and its involvement in parallel fiber-interneuron synapse formation in the cerebellum. J Neurosci 28: 7412–7424

Chapter 14

Localization of GFP-Tagged Proteins at the Electron Microscope

Sara Gil-Perotin, A. Cebrián-Silla, V. Herranz-Pérez, P. García-Belda, S. Gil-García, M. Fil, J.S. Lee, M.V. Nachury, and José Manuel García-Verdugo

Abstract

The cloning of green fluorescent protein (GFP) has opened a new arena of protein labeling and has become a new alternative to existing markers or dyes. Main advantages are its stability and its fluorescent activity independent on the binding of other ligands or proteins. The use of GFP-tagged proteins has found multiple applications in molecular biology such as lineage tracing assays, cell fusion assessment, and/or immunodetection, among others. High-resolution imaging combined with immunogold labeling for GFP provides the best correlation with subcellular localization, and it allows detection of membrane-bound GFP-tagged receptors and cytosolic and/or nuclear proteins. In this chapter, we attempt to summarize the state-of-the-art in GFP detection, current protocols, advantages, and pitfalls, and we describe a method, used in our laboratory, which combines confocal fluorescence microscopy with transmission electron microscopy (TEM) for the study of cell cultures at the ultrastructural level.

Key words Pre-embedding immunogold labelling, Fluorescent-tagged protein, Cre-recombinase, Correlative light and electron microscopy, High-resolution techniques

1 Introduction

In recent years, the green fluorescent protein (GFP), isolated from the jellyfish *Aequorea victoria* [1], has become an essential tool for molecular biology purposes. Its use as a reporter gene includes monitoring gene expression or cell transformation, lineage tracing, and protein localization, among others. These functions achieve their maximum goal when combined with high-resolution imaging. To this regard, immunogold labeling for GFP provides the best correlation with GFP expression and subcellular localization, and it allows detection of membrane-bound GFP-tagged receptors and cytosolic and/or nuclear proteins.

Rafael Luján and Francisco Ciruela (eds.), *Receptor and Ion Channel Detection in the Brain: Methods and Protocols*, Neuromethods, vol. 110, DOI 10.1007/978-1-4939-3064-7_14,

In this chapter, we attempt to summarize the state-of-the-art in GFP detection, current protocols, advantages, and pitfalls, and we describe a method, used in our laboratory, which combines confocal fluorescence microscopy with transmission electron microscopy (TEM) for the study of cell cultures at the ultrastructural level. Ultrastructural analysis under the electron microscope of GFP-tagged proteins, adds a value regarding the relationship between GFP signal and other cellular components. This strategy is potentially useful in a myriad of applications such as cell transport, vesicle trafficking, autophagy, cell division, etc.

1.1 Examples of the Application of GFP in Biology

In the case of GFP-related tools, molecular technology has assisted relevantly to the field of biology. Developing of GFP-tagged proteins by gene engineering allows the visualization of GFP fusion proteins and their cell dynamics upon expression in cell cultures or in transgenic organisms [2]. It has also become an alternative tool to other existing markers. To design GFP-tagged proteins is not an easy task, because GFP is a bulky protein (29 KDa) that can alter folding or function of the protein of interest (Fig. 1a). At the end of the chapter, we add some considerations to take into account when designing a GFP-tagged protein (*see* **Note 1**).

Combination with *cre-recombinase* technology has been a major step forward to carry out modifications at specific sites in the DNA of cells (Fig. 1b). In our laboratory, it has been relevant for cell fusion studies [3, 4]. We used transgenic mice in which all cells had inhibited the expression of *LacZ* gene (flanked by loxP sites) under the control of a promoter corresponding to a constitutive gene. When cells expressing cre-recombinase-GFP fusion protein, fused or transferred genetic information (or the protein itself) to tissues in transgenic mice, cre-recombinase eliminated loxP sites by recombination allowing for *LacZ* expression, and therefore, making possible the visualization of transplanted cells by immunofluorescence (GFP+ cells) and target cells by beta-gal staining.

In the field of embryonic development and adult stem cells, increasing resources are being dedicated to develop novel strategies for lineage tracing. Cre recombination has been *adorned* with the addition of a ligand-binding domain to estrogens (ER^{T2}) that allows to successfully induce specific temporal Cre activity. *Cre* gene is fused to a mutated estrogen receptor in which the ligand-binding site is specific for tamoxifen (an estrogen receptor antagonist) due to a greater affinity for the receptor. The addition of tamoxifen (pulse) allows the Cre-ER^{T2} complex to enter the

Fig. 1 (continued) GFP-positive cells can be observed in different organs or tissues. (**c**) $CreER^{T2}$ lineage tracing. Crossing $CreER^{T2}$ transgenic mice with Rosa26 mice, the latter with *GFP expression* halted by loxP sites does not induce recombination. However, when tamoxifen is injected, cre-recombinase is expressed, and recombination takes place and, therefore, GFP expression. When GFP expression depends on specific stem cell promoters, it is possible to follow stem cell progeny by studying animals at certain time points from tamoxifen addition

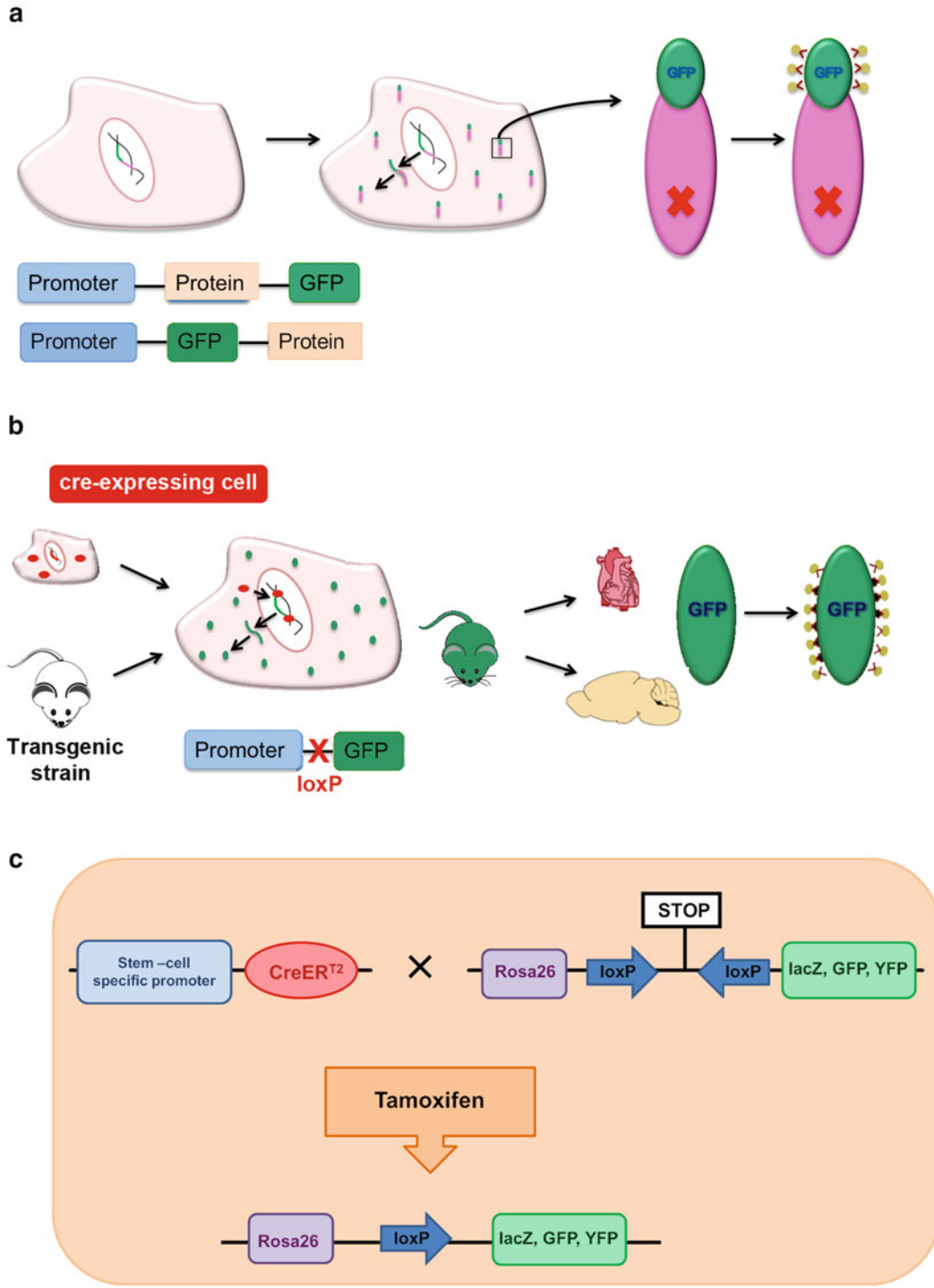

Fig. 1 GFP applications in cell biology. (**a**) GFP-tagged proteins. GFP protein can be fused to the C-terminal or the N-terminal domain of the protein of interest. In the case of successful expression, splicing, and translation, GFP can be visualized with a fluorescent microscope or under the TEM by performing gold pre-embedding immunohistochemistry against GFP. (**b**) An example of cre-recombinase and GFP-based fusion/communication studies. Upon cell transplantation of cre-expressing cells (constitutively or under specific promoters) into a transgenic strain of mice with *GFP gene* preceded by loxP sites (non-expressed), cre-recombinase, if transferred, recombines DNA and eliminates loxP sites, and therefore *GFP gene* is transcribed.

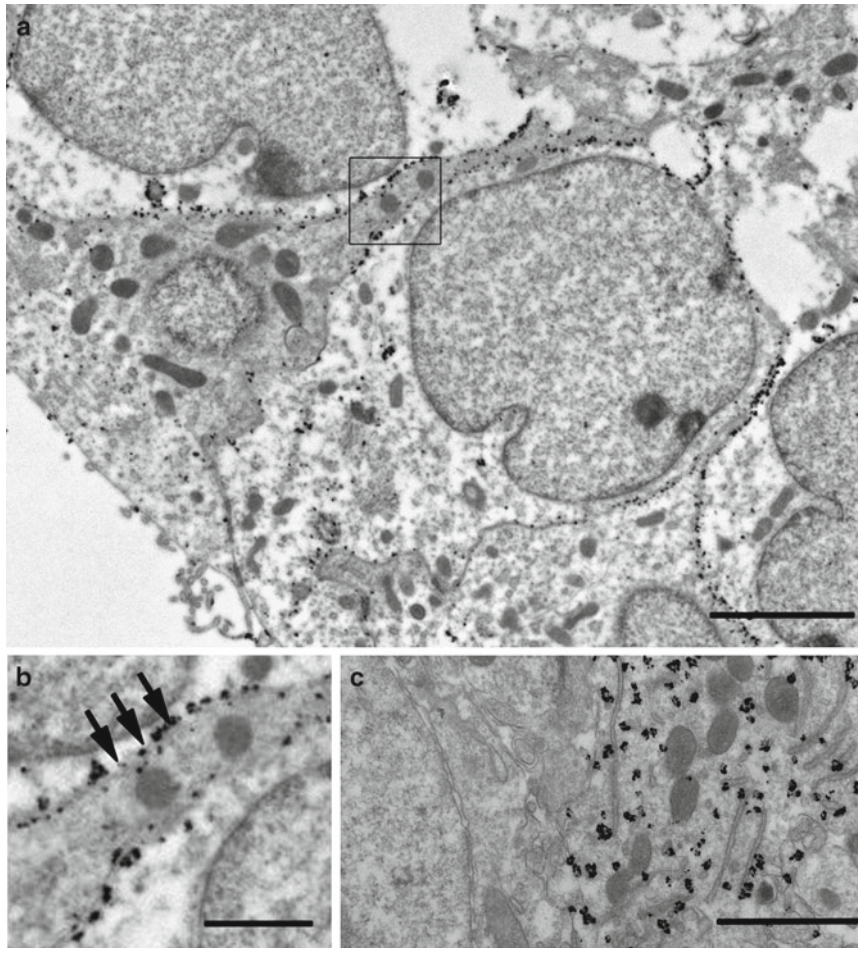

Fig. 2 Micrographs of GFP immunogold in different applications. (**a**) Lineage tracing of vimentin progeny in vimentin-mGFP-creRT2 transgenic mice upon tamoxifen induction. Tamoxifen induces expression of membrane-bound GFP under vimentin promoter (scale, 5 μm); (**b**) detail of membrane-bound gold particles (scale, 1 μm); (**c**) Iba1 microglial marker expression by immunogold labeling. Microglia cell (*right*) labeled with gold particles apposed to a Purkinje cell in postnatal mouse cerebellum (scale, 1 μm)

nucleus and exert the recombination activity to induce a targeted mutation (Fig. 1c). Therefore, it allows to perform "pulse and chase" experiments. If the targeted mutation includes the expression of GFP under a certain promoter, cells pertaining to a specific lineage (determined by the promoter) express GFP and can be visualized (short chase time), as it can be their progeny at longer chase periods.

In all mentioned cases, specific protocols for GFP immunogold labeling have allowed us to visualize GFP expression in certain types of cells and to determine the subcellular localization of the proteins of interest (Fig. 2). We further describe these methods in the following sections. However, a scientific hindrance related to GFP detection has led us to many brainstorming sessions, and we

would like to share with the readers the steps followed to bypass the obstacle. We overexpressed a GFP-fused form of a protein involved in centriole elongation, by transfection of U2OS osteosarcoma cells in culture dishes. We could detect GFP-positive structures at the fluorescence microscope, but upon processing samples for electron microscopy, we were unable to correlate ultrastructure with fluorescence signal in the same cell [5]. To overcome this limitation, we used correlative light and electron microscopy (CLEM) successfully. CLEM combines the advantages of both light (LM) and TEM, providing an essential tool for the study of the cell structure and function. CLEM gathers a group of visual techniques trying to overcome their individual limitations, becoming an increasingly used approach in cell biology nowadays.

2 Materials

2.1 Buffers and Solutions

1. Phosphate buffer (PB): 0.1 M PB at pH 7.4. PB is made of monobasic sodium phosphate (NaH_2PO_4) and dibasic sodium phosphate (Na_2HPO_4), both at a final concentration of 0.1 M.
2. Saline solution: 0.9 % NaCl and 0.1 % heparin (from a 5 % aqueous stock solution) in double-distilled H_2O.
3. Fixative solution I: 4 % paraformaldehyde (PFA) (Sigma, St Louis, MO, USA) and 0.5 % glutaraldehyde (GA) (from a 25 % aqueous stock solution; Electron Microscopy Sciences, EMS, Hatfield, PA, USA) in 0.1 M PB. Since it is a highly cross-linking agent and toxic, use it in a fume hood.
4. Agar solution: 4 % agar in 0.1 M PB.
5. Sodium borohydride solution: 1 % borohydride ($NaBH_4$) (Sigma) in double-distilled H_2O.
6. Cryoprotectant solution: 25 % sucrose in 0.1 M PB.
7. 2-Methylbuthane, 99 % (Sigma).
8. Blocking solution I: 0.3 % BSAc (Aurion, The Netherlands) in 0.1 M PB.
9. Primary antibody: chicken anti-GFP antibody (1:200; Aves Labs, Tigard, OR, USA) in blocking solution I.
10. Blocking solution II: 0.5 % BSAc (Aurion) and 0.1 % fish skin gelatin (Aurion) in 0.1 M PB.
11. Secondary antibody: goat anti-chicken antibody conjugated to colloidal gold (1:50; Ultra Small; Aurion) in blocking solution II. This solution is light sensitive; keep in the dark.
12. Sodium acetate solution: 2 % sodium acetate ($C_2H_3O_2Na \cdot 3H_2O$) in double-distilled H_2O.

13. Silver enhancement solution: mix equal parts of developer and enhancer reagents in a dark chamber immediately before use (Silver enhancement kit, Silver Enhancement R-Gent SE-LM, Aurion).
14. Gold toning solution: 0.05 % gold chloride (AuCl) (Sigma) in double-distilled H_2O. This solution is light sensitive; keep in the dark.
15. Sodium thiosulfate solution: sodium thiosulfate 0.3 % ($Na_2S_2O_3 \cdot 5H_2O$) in double-distilled H_2O. This solution is light sensitive; keep in the dark.
16. Fixative solution II: 2 % GA (from an aqueous 25 % stock solution) in 0.1 M PB. Since it is a highly cross-linking agent and toxic, use it in a fume hood.
17. DAPI solution: prepare a 300 nM solution of 4′,6-diamino-2-fenilindol (DAPI; Sigma) in double-distilled H_2O.
18. Fixative solution III: 3.5 % GA in 0.1 M PB. Store in the dark at 4 °C for up to a month. Since it is a highly cross-linking agent and toxic, use it in a fume hood.
19. Fixative solution IV: 4 % PFA. Store in the dark at 4 °C for up to a week. Since it is a highly cross-linking agent and toxic, use it in a fume hood.

2.2 Labware and Other Equipment

1. Dry ice.
2. Culture multi-well dish or plates.
3. Photoetched glass gridded coverslips (Bellco, Vineland, NJ, USA).
4. Vibratome (VT1000S; Leica Microsystems Inc, Germany).
5. Ultramicrotome (UC6; Leica).
6. Confocal inverted microscope (FV1000; Olympus, Japan).
7. Transmission electron microscope (Tecnai G^2 Spirit; FEI, The Netherlands).

3 Methods

3.1 GFP Pre-embedding Immunogold Labeling (Fig. 3)

1. Perfuse (4 mL/min) with freshly prepared saline solution (5 min) and fixative solution I (15 min) or alternatively fix small tissue pieces in this fixative solution (*see* **Note 2.1**). Postfix in 4 % PFA overnight at 4 °C.
2. Wash three times for 10 min each with 0.1 M PB to remove fixative.
3. Embed tissue in 4 % agar and cut 50-μm-thick vibratome slices.
4. For aldehyde inactivation, incubate 50-μm-thick sections in 1 % sodium borohydride in 0.1 M PB for 30 min at room

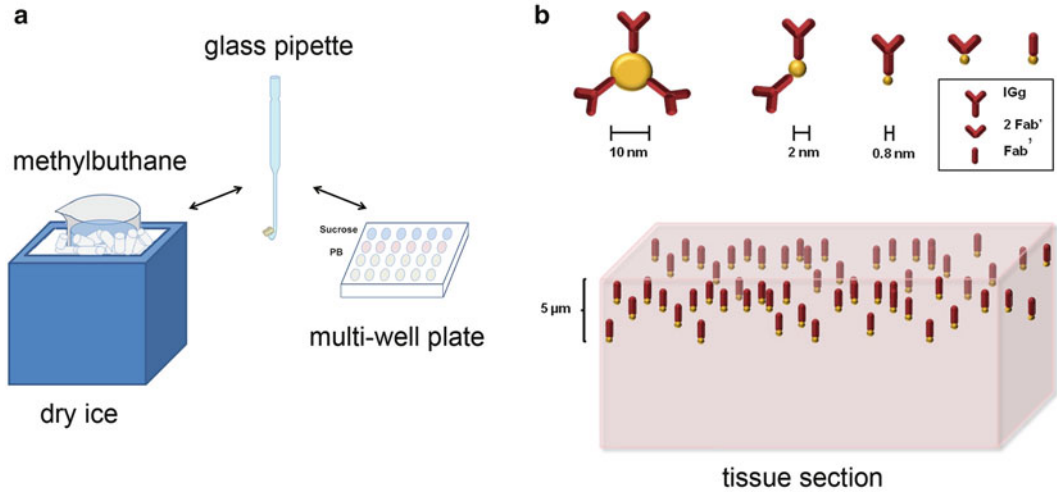

Fig. 3 GFP immunogold pre-embedding. (**a**) Freeze-thaw cycles. Following pretreatment with sucrose, tissue sections, held gently with a glass pipette, are introduced in a Pyrex® beaker filled with 2-methylbuthane on dry ice. After a few seconds, the sections are put into the sucrose solution. The procedure is repeated 3–5 times. Finally, the slices are introduced in 0.1 M PB. (**b**) Size of gold particles for immunogold labeling determines their penetration. Colloidal gold particles' sizes from 10 nm to ultrasmall 0.8 nm, bound from multiple IgGs to single Fab'. Penetration is improved when using 0.8 nm gold particles in comparison with the 10 nm

temperature (RT). Wash with 0.1 M PB every 10 min for 1 h. Bubbles should disappear.

5. Immerse in cryoprotectant solution for 30 min under mild agitation at RT.
6. Freeze sections in 2-methylbuthane on dry ice (−60 °C) for a few seconds, and thaw them in the cryoprotectant solution. Repeat 4–5 times and transfer them into ice-cold 0.1 M PB (*see* ***Note 2.2***).
7. Block with blocking solution I for 1 h at RT.
8. Incubate in chicken anti-GFP primary antibody solution for 36–60 h under mild agitation at 4 °C.
9. Wash three times for 10 min each with 0.1 M PB to remove primary antibody. From this step, all incubations should be performed in the dark.
10. Block with blocking solution II for 1 h at RT.
11. Incubate in gold-conjugated goat anti-chicken antibody overnight under mild agitation at RT.
12. Rinse 3 times with 0.1 M PB for 10 min each.
13. Wash in sodium acetate solution 3 times for 15 min each.
14. Proceed with silver enhancement using silver enhancement solution. The signal should increase slowly within 10–20 min. Check under a light microscope (GFP signal should be observed as a dark labeling).

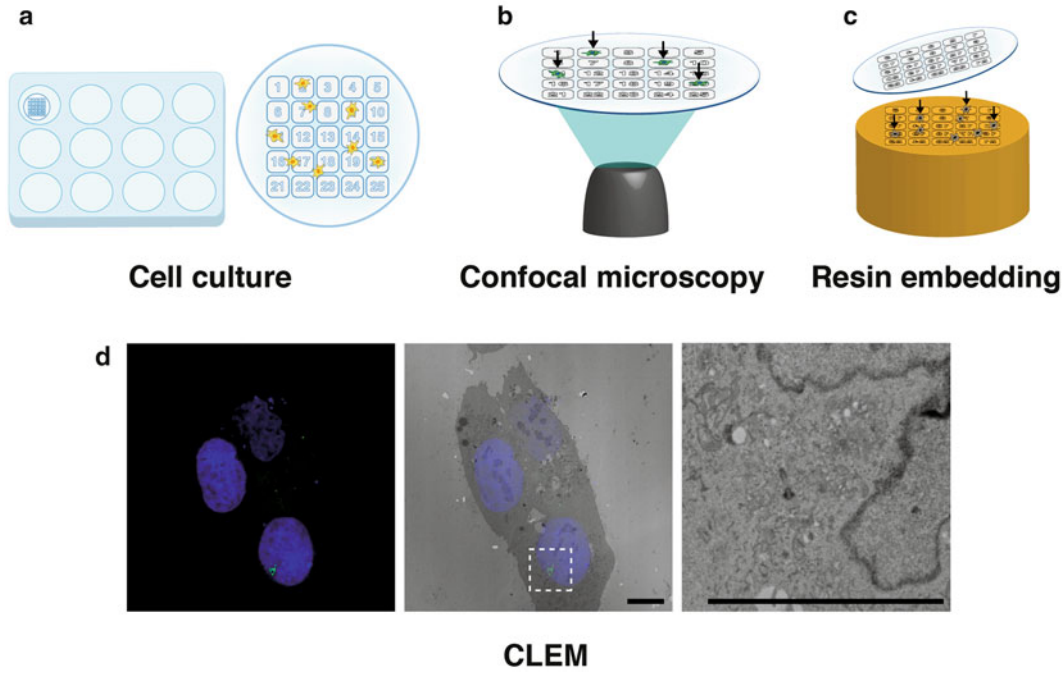

Fig. 4 CLEM procedure for cell cultures. (**a**) Cell culture. Fluorescence-labeled cells are grown on gridded coverslips in multi-well plates to facilitate their identification. Cell number should be adjusted to a final confluency of ~50 %. (**b**) Confocal microscopy. Identify cells of interest (*arrows*) in the gridded coverslip and note their position in the grid. Acquire bright-field images and fluorescence confocal Z-stacks at different magnifications. (**c**) Resin embedding. Process coverslips for TEM by embedding in epoxy resin. Cells and the gridded pattern will be transferred to the surface of the resin block upon removal of the coverslip. Obtain serial ultrathin sections from these blocks. (**d**) CLEM. Use fluorescence images to identify cells of interest in TEM (*left panel*). Align fluorescence and TEM photomicrographs in order to obtain overlaid CLEM images (*middle panel*). High-resolution details are obtained using TEM (*right panel*; corresponds to inset in previous image). *Scale bars*, 10 μm

15. Wash in sodium acetate solution 3 times for 5 min each.
16. Incubate in gold toning solution for 30 min at RT.
17. Wash in sodium thiosulfate solution twice for 10 min at 4 °C (sections will become gray).
18. Rinse 3 times with 0.1 M PB for 10 min each at RT.
19. Postfix in fixative solution II for 30 min at RT.
20. Rinse 5 times with 0.1 PB for 5 min each at RT.
21. Prepare samples for Durcupan™ embedding following standard methods.

3.2 Correlative Light-Electron Microscopy for Cell Culture Study

1. Seed mammalian adherent cell lines on photoetched glass gridded coverslips in adequate culture dishes (Fig. 4a). Adjust cell number for a final confluence of ~50 % (*see* **Note 3.1**). Culture at 37 °C, 5 % CO_2 under standard sterility conditions.

2. Label cultured cells using a fluorescent dye by an appropriate method depending on experimental needs (e.g., expression of GFP-tagged proteins or microinjection of fluorescent molecules).
3. Fixate cells as follows: discard culture medium, wash three times for several seconds with 0.1 M PB, and incubate in 4 % paraformaldehyde in 0.1 M PB for 10 min (should you require live-cell imaging, *see* **Note 3.2**). All steps should be performed using pre-warmed solutions and at 37 °C.
4. Discard fixative solution and replace by 0.1 M PB at room temperature.
5. Counterstain cell nuclei by incubation in DAPI solution for 5 min. Rinse the samples three times briefly in 0.1 M PB. This is an optional step, but it greatly aids in further steps and in final image alignment.
6. Use a confocal microscope to identify cells of interest on the coverslip and note their position within the grid (Fig. 4b).
7. Obtain bright-field and fluorescence images at different magnifications to register the arrangement of cells within the grid. Take also a high magnification Z-stack of selected cells in order to be able to correlate similar planes in fluorescence and EM images later on.
8. Further fixate cells by incubation in 3.5 % glutaraldehyde in 0.1 M PB for 1 h at 4 °C. This two-step fixation is required in order to maintain fluorescence (which is affected by glutaraldehyde) while ensuring ultrastructural preservation.
9. Transfer the coverslips from culture dishes to plates suitable for subsequent Durcupan™ resin embedding for electron microscopy.
10. Wash three times for 5 min each with 0.1 M PB to remove any excess of fixative.
11. Postfix samples by incubation in 2 % osmium tetroxide (OsO_4; EMS) in 0.1 M PB for 90 min with gentle agitation.
12. Embed samples in epoxy resin (e.g., Durcupan™) following standard methods [6].
13. Prepare containers slightly smaller in size than the coverslips (e.g., Eppendorf tube caps), and fill them completely with epoxy resin.
14. Place photoetched gridded coverslips, cell side facing down, on top of resin-filled containers and in contact with epoxy resin.
15. Let the resin infiltrate the cells overnight at room temperature on a flat surface.
16. The following day, fill new containers with fresh resin and transfer the coverslips to the new containers.

17. Let the resin polymerize in an oven at 65 °C for 48 h.
18. Remove resin blocks from their molds. Use a heated knife if needed.
19. Remove coverslips by repeated immersion in liquid nitrogen and warm water (*see* **Note 4.2**). Cells and the grid pattern will be transferred as a mirror image to the surface of the resin block. Individual grid cells can be identified and marked for the next step using a microscope (Fig. 4c).
20. Use an ultramicrotome to trim just selected grid cells in the resin blocks. Then cut serial ultrathin sections (70–80 nm) using a diamond knife, and contrast with Reynolds lead citrate solution for 10 min. Gently wash with ultrapure water.
21. Use fluorescence images to identify cells of interest under the electron microscope trying to find remarkable features as a guide. Try to match Z-stack images with similar planes in serial ultrathin sections to produce a harmonious final composition.
22. Use imaging software to overlay fluorescence and electron microscopy images. Adjust images' opacity, scale, and position to align correctly both images. Merge composite images and export as a single file (Fig. 4d).

4 Notes

4.1 Considerations When Designing a GFP-Tagged Protein

4.1.1 Subcellular Localization of the Protein within the Cell

Proteins containing signal peptides within their sequence determining their final location in the cell (membrane, inclusion bodies, endoplasmic reticulum, etc.) can be strikingly interfered by GFP fusion. This is due to several reasons: it can structurally impede protein synthesis and/or binding to the endoplasmic reticulum membrane, or it can interrupt the function of the signal peptide (e.g., GPI-anchored proteins). In this case, we recommend to double-check subcellular location predictor software (www.expasy.org) and with extensive fluorescence analyses of tissues or cells upon GFP expression.

4.1.2 Formation of Secondary Structures

It is recommended to avoid GFP tagging when GFP sequence is complementary to regions of the gene of interest. This may cause the mRNA to fold into secondary structures by base complementarity. This is a rare event, and it is more likely to occur between the GFP gene and specific sequences contained in the introns of our gene. In this case, mRNA precursors fold into secondary structures, and mRNA might fail to be spliced or processed. This could be avoided by applying local DNA aligning tools to both sequences (http://blast.ncbi.nlm.nih.gov/Blast.cgi).

4.1.3 Protein Function

GFP can interfere with the function of the protein by misfolding of secondary and tertiary structures or by disruption of the active site of the protein. It can also prevent binding to DNA (e.g., transcription factors). We recommend to test functionality of the protein with more than one functional assay and to use, at least, two different forms of the protein tagged to GFP (fusion with the C-terminal and N-terminal domains). The addition of a short sequence of neutral amino acids (e.g., alanine) between the GFP protein and our protein of interest could give more flexibility to the complex, and we also recommend it.

4.2 Pre-embedding Immunogold Labeling

4.2.1 Tissue and Fixation

Karnovsky's fixative (2 % PFA and 2.5 % GA) is one of the preferred fixative solutions for EM studies. PFA rapidly penetrates into the tissue and GA establishes strong protein bounds; their combination achieves a proper ultrastructural quality [7]. Nonetheless, the concentration of GA in the solution prevents immunodetection of GFP. For this reason, tissues and cells set for immunodetection under the electron microscope must be fixed with a solution that establishes a middle ground between antigen detection and ultrastructure preservation.

4.2.2 Permeabilization and Secondary Antibodies

The main limitation of the protocol for pre-embedding immunogold histochemistry is the low penetration of the antibodies. In conventional immunoprotocols, antibody penetration can be improved by adding detergents. However, their use greatly affects membrane integrity, what could generate a relevant decrease in the quality of the sample under the EM. In consequence, a new strategy has been developed in which the tissue pieces are cryoprotected and afterward are subjected to several freeze-thaw cycles, which quickly create and dissolve small crystals, facilitating the permeation of the membranes while avoiding major damages on the ultrastructure. In specific occasions when exposure to GFP antibodies is limited, for instance, when GFP-tagged proteins are located in the nucleus, it can be appended an extra step before cryoprotection by adding 0.1 % Triton-X for 30 min.

A second approach to increase the penetration of the antibodies is to use secondary antibodies combined to gold particles, small enough to penetrate the tissue. These ultrasmall gold particles also yield enhanced labeling efficiency due to their better labeling of antibodies, because each antibody has at least one individual gold particle bound to it. With this structure, both the overall size of the conjugates and the steric hindrance decreased, allowing a large number of gold particles per antigen [8].

4.3 CLEM

4.3.1 Cell Confluence

Adjust cell confluence depending on the duration of the experiment so that the plate is not fully confluent at the end of the procedure. A confluent plate will make identification very difficult under the EM. The shape and arrangement of cells will be used as landmarks for their later identification.

4.3.2 Live-Cell Imaging

Alternatively, live-cell image acquisition can be performed directly using an inverted fluorescence microscope, and after which, cells should be fixated by removing culture medium, gently washing three times for several seconds each in 0.1 M PB, and incubating in 3.5 % GA in 0.1 M PB for 10 min (in this case, continue with **step 9**).

4.4 Safety

1. Use a fume hood.
2. Use gloves and protective glasses for this process, since small pieces of glass can break away causing injuries.

Acknowledgments

We thank M. Salomé Sirerol-Piquer, Clara Alfaro-Cervelló, Ulises Gómez-Pinedo, and Mario Soriano-Navarro for their useful contribution. We thank Dr. Engelhardt for kindly provide mGFP transgenic mice, and Maria Duran-Moreno for sharing her GFP picture. This work was supported by Spanish MINECO grants (Instituto Salud Carlos III-RETIC TerCel and SAF2012-33683, to JMGV) and pre- and postdoctoral fellowships (AP2010-4264 and CM12/00014 to ACS and SGP, respectively), the University of Valencia predoctoral fellowship (to PGB), and Generalitat Valenciana predoctoral fellowship Santiago Grisolia (to MF).

References

1. Shimomura O, Johnson FH, Saiga Y et al (1962) Extraction, purification and properties of aequorin, a bioluminescent protein from the luminous hydromedusan, Aequorea. J Cell Comp Physiol 59(3):223–239
2. Chalfie M, Tu Y, Euskirchen G et al (1994) Green fluorescent protein as a marker for gene expression. Science 263(5148):802–805
3. Alvarez-Dolado M, Pardal R, Garcia-Verdugo JM, Fike JR, Lee HO, Pfeffer K, Lois C, Morrison SJ, Alvarez-Buylla A (2003) Fusion of bone-marrow-derived cells with Purkinje neurons, cardiomyocytes and hepatocytes. Nature 425(6961):968–973, Epub 2003 Oct 12
4. Mazo M, Gavira JJ, Abizanda G et al (2010) Transplantation of mesenchymal stem cells exerts a greater long-term effect than bone marrow mononuclear cells in a chronic myocardial infarction model in rat. Cell Transplant 19(3):313–328. doi:10.3727/096368909X480323
5. Thauvin-Robinet C, Lee JS, Lopez E et al (2014) The oral-facial-digital syndrome gene C2CD3 encodes a positive regulator of centriole elongation. Nat Genet 46:905–911. doi:10.1038/ng.3031
6. Sirerol-Piquer MS, Cebrián-Silla A, Alfaro-Cervelló C et al (2012) GFP immunogold staining, from light to electron microscopy, in mammalian cells. Micron (Oxford, England: 1993) 43(5):589–599. doi:10.1016/j.micron.2011.10.008
7. Hayat MA (1972) Principles and techniques of electron microscopy, vol 1 and 2. Van Nostrand Reinhold Company, New York
8. Hainfeld JF, Robinson JM (2000) New frontiers in gold labeling: symposium overview. J Histochem Cytochem 48(4):459–460

Chapter 15

Pre-embedding Methods for the Localization of Receptors and Ion Channels

Rafael Luján

Abstract

Pre-embedding techniques are some of the most widely used approaches in immunoelectron microscopy applied to the neurosciences, providing unexpected insights into the structure-function of neurotransmitter receptors and ion channels in the brain. These techniques involve immunoreactions with antibodies before embedding and ultrathin sectioning. As a result, they are very sensitive and show excellent resolution and good ultrastructural and antigenicity preservation. Among other advantages, pre-embedding techniques are useful for simultaneous observation of labelled tissue at the light and electron microscopic levels, as well as for quantitative analysis and 3D reconstructions. There are two main pre-embedding techniques based on the label attached to the secondary antibody: the pre-embedding immunoperoxidase method, which uses an active enzyme such as horseradish peroxidase (HRP), and the pre-embedding immunogold method, which uses a small-sized gold particle. The pre-embedding immunoperoxidase technique provides valuable information on regional distribution of receptors, while the pre-embedding immunogold technique is reliable for the localization of receptors along the neuronal surface of any specific compartment or organelle. In this chapter, we introduce pre-embedding immunoperoxidase and immunogold procedures used primarily on brain sections in both single and double labelling and also discuss the limitations inherent to these approaches.

Key words Pre-embedding immunoperoxidase, Pre-embedding immunogold, Immunohistochemistry, High-resolution techniques, Electron microscopy, Silver enhancement, Permeabilization, Extrasynaptic receptor, Double labelling, Quantification

1 Introduction

Determining the precise subcellular localization of neurotransmitter receptors and/or ion channels is crucial for understanding their function in specific neuron populations of the brain, and pre-embedding approaches have been widely used for this purpose. Pre-embedding methods involve immunolabelling steps before samples are embedded in resin, such that primary and secondary antibodies can penetrate throughout the whole depth of the tissue sample. As a result, pre-embedding techniques are highly sensitive and render good ultrastructural and antigenicity preservation.

Rafael Luján and Francisco Ciruela (eds.), *Receptor and Ion Channel Detection in the Brain: Methods and Protocols*, Neuromethods, vol. 110, DOI 10.1007/978-1-4939-3064-7_15,

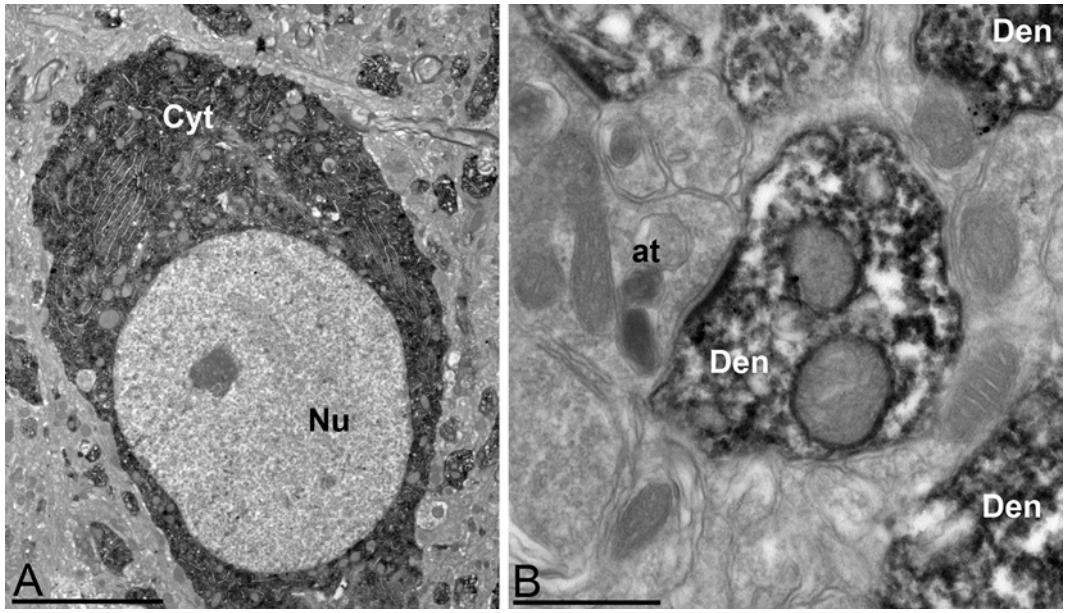

Fig. 1 Electron micrographs showing immunoreactivity for the GIRK2 subunit of the G protein-gated inwardly rectifying K^+ channel, as demonstrated by a pre-embedding immunoperoxidase method in the ventral tegmental area (VTA) of the mouse brain. (**a**) In the soma of VTA dopaminergic neurons, the peroxidase reaction end product for GIRK2 diffuses and fills the whole cytoplasm (*Cyt*) of the neuron, but the nucleus (*Nu*) of the cell lacks immunoreactivity. (**b**) In the neuropil, the peroxidase reaction end product for GIRK2 fills the dendritic shafts (*Den*) of dopaminergic neurons, which establish synaptic contacts from axon terminals (*at*). *Scale bars*: **a** 5 μm; **b** 0.5 μm

In addition, they allow the observer to visualize and correlate the same immunolabelled tissue or cell, both at the light and electron microscopic levels. Furthermore, these techniques have been successfully used in quantitative analyses and in 3D reconstructions that employ serial ultrathin sections.

Pre-embedding techniques involve antibody molecules that can be visualized using two different types of labels. One label is an active enzyme (the horseradish peroxidase or HRP) that has the ability to induce formation of a coloured reaction product from a suitable substrate system, resulting in the designated pre-embedding immunoperoxidase technique. The other label is a gold particle, giving rise to what is called the pre-embedding immunogold technique. Each of these approaches has its advantages and disadvantages; the pre-embedding immunoperoxidase method (Fig. 1) is the most sensitive and provides valuable information on the regional distribution of neurotransmitter receptors and/or ion channels. The HRP technique has been used to fill specific neurons and trace their dendrites to determine types of synaptic contacts. However, given the diffusible nature of the peroxidase reaction end-product, we cannot exclude the possibility

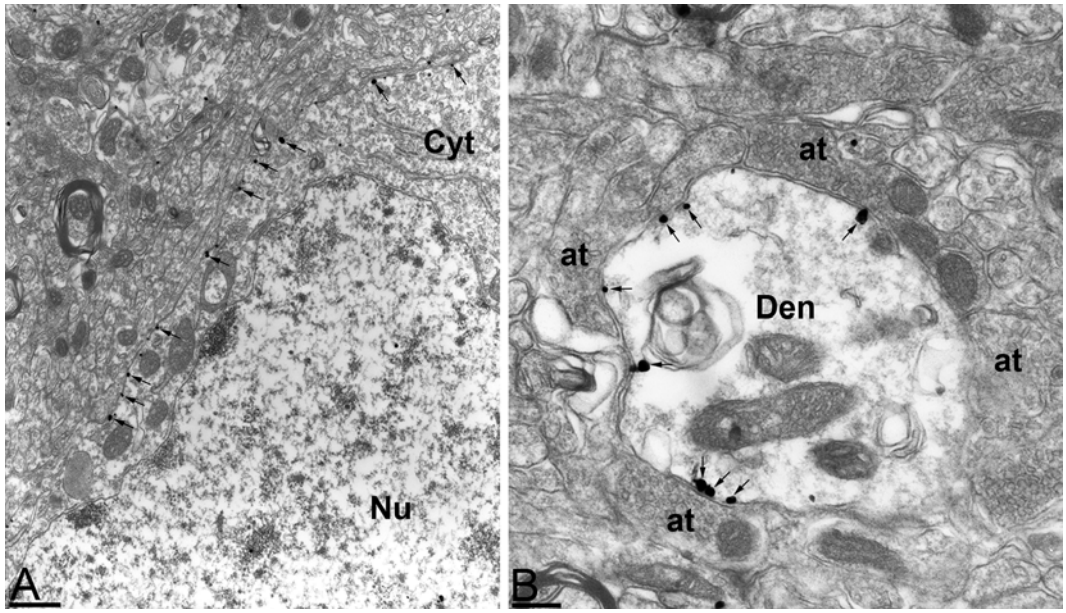

Fig. 2 Electron micrographs showing immunoreactivity for the GIRK2 subunit of the G protein-gated inwardly rectifying K^+ channel, as demonstrated by a pre-embedding immunogold method in the ventral tegmental area (VTA) of the mouse brain. (**a**) Immunoparticles for GIRK2 are localized along the somatic plasma membrane (*arrows*) of VTA dopaminergic neurons. (**b**) In the neuropil, immunoparticles for GIRK2 are localized along the extrasynaptic plasma membrane (*arrows*) of dendritic shafts (*Den*) of dopaminergic neurons. *At* axon terminal, *Cyt* cytoplasma, *Nu* nucleus. *Scale bars*: **a** 0.5 μm; **b** 0.2 μm

that the labelling observed in specific cellular organelles or compartments did not originate from neighbouring places [1]. The pre-embedding immunogold method (Fig. 2), on the other hand, produces a nondiffusible label; therefore, the precise site of the reaction can be determined. Furthermore, this method is reliable for the localization of receptors at extrasynaptic and perisynaptic sites in single and serial sections and has been successfully used to quantify neurotransmitter receptors and ion channels along the plasma membrane [2–4]. However, this technique also has limitations; the strength of labelling decreases with depth, and antibodies may penetrate unevenly into brain tissue. For example, synaptic receptors or any other proteins located at putative glutamatergic synapses are generally not detected using this method (the post-embedding immunogold technique should be used in such cases; *see* Chap. 16). Only inhibitory synapses seem to be labelled for signalling proteins using the pre-embedding immunogold method. In conclusion, the two methods provide complementary information about cellular and subcellular locations of neurotransmitter receptors or ion channels and are best used in combination.

The successful application of pre-embedding immunohistochemical techniques depends directly on the adequate preservation of antigenicity, the capacity of primary and secondary antibodies to infiltrate throughout the tissue and the specificity in the recognition of antigens by primary antibodies. Therefore, proper handling of brain samples is required. This process involves an appropriate fixative solution, the permeabilization of membranes, the correct visualization of the molecules whose ultrastructural location needs to be unambiguously determined and an appropriate embedding resin. Taking all these issues into consideration, this chapter describes the main scope and protocols of pre-embedding immunohistochemical techniques. These methods have been successfully utilized in our laboratory for the examination and analysis of subcellular localization of neurotransmitter receptors and ion channels at the electron microscopic level in the brain using both single and double labelling. The experimental procedures provided are derived from studies on mGlu and $GABA_B$ receptors and potassium channels [1–4]. However, the general principles and methods can be applied to other plasma membrane or intracellular proteins. Furthermore, the same methodology can also be successfully applied to elucidate the distribution of neurotransmitter receptors and ion channels during development [3, 5, 6] and adulthood [1–4], as well as for nearly any protein in practically every organism and tissue.

2 Materials

2.1 Buffers

The two most commonly used buffers are phosphate (PB) and Tris (TB) and their saline version, PBS and TBS, respectively. PB and PBS are used at a final working dilution of 0.1 M, while TB and TBS at a dilution of 0.05 M.

1. *Phosphate buffer* (*0.1 M*, *pH 7.4*). Phosphate buffer consists of two components: monobasic sodium phosphate (NaH_2PO_4) and dibasic sodium phosphate (Na_2HPO_4). The weight of each component will vary depending on the waters of hydration. The pH is adjusted by mixing the two components in the appropriate amounts.

   To prepare 1 L of 0.2 M sodium phosphate buffer (PB), pH7.4, combine $Na_2HPO_4 \cdot 2H_2O$ (35.6 g) and $NaH_2PO_4 \cdot 2H_2O$ (31.2 g), each at 0.2 M, in the ratio 4:1. If necessary, add a few drops of 1 M sodium hydroxide (NaOH) in distilled water to adjust pH. The stock solution of 0.2 M PB can be stored at 4 °C for several weeks. To prepare 0.1 M PB (pH 7.4), dilute equal volumes of the 0.2 M PB stock solution with distilled water.

2. *Phosphate-buffered saline* (*0.1 M*, *pH 7.4*). PBS is prepared by mixing 0.9 % NaCl with 0.1 M PB.
3. *Tris buffer* (*0.05 M*, *pH 7.4*). Tris buffer (TB) can be prepared in several ways. For reliable accuracy and reproducibility, we recommend preparing a stock solution of 0.05 M TB (pH 7.4 at 25 °C) by dissolving 6.61 g Trizma HCl (Sigma-Aldrich, St. Louis, USA) and 0.97 g Trizma Base (Sigma-Aldrich) in 1000 mL of distilled water. Desiccate the reagents before weighing.
4. *Tris-buffered saline* (*0.05 M*, *pH 7.4*). Once stock solution of 0.05 M TB is ready, TBS is prepared by mixing 0.9 % NaCl with TB. This buffer can be stored at 4 °C for several weeks.

2.2 Tissue and Fixation

Brain tissue must be fixed before pre-embedding immunohistochemistry. An appropriate fixation is very important for preserving antigenicity and ultrastructure. However, optimal conditions for good ultrastructural preservation contrast the optimal conditions required for good preservation of antigenicity. Therefore, degree of fixation involves a compromise between achieving the best possible immunolabelling and minimal disruption of ultrastructure. Several types of fixative solutions and fixation conditions have been used to localize different antigens in the brain and other tissues. A mixture of paraformaldehyde and a low concentration of glutaraldehyde (0.05–0.5 %) is a popular fixative for pre-embedding immunoelectron microscopy.

1. Anaesthesia (Nembutal or ketamine-xylazine 1:1, 0.1 mL/kg bw). Follow the protocols approved by the local Animal Care and Use Committee. The care and handling of animals prior to and during the experimental procedures should be in accordance with National and International Regulations.
2. Buffers: 0.2 M PB, pH 7.4.
3. Paraformaldehyde (supplied as powder; EMS, Hatfield, USA). Keep at room temperature in a dry place. PFA is very toxic in contact with skin, by inhalation and if swallowed. Therefore, always wear protective clothing and gloves, and handle in a fume hood.
4. Glutaraldehyde (EM grade, supplied as a 25 % aqueous solution; EMS). This reagent can be stored at 4 °C. Glutaraldehyde is also very toxic, so follow safety notes described above for paraformaldehyde.
5. Fixative solution: It must be freshly prepared using 4 % paraformaldehyde and 0.05 % glutaraldehyde in 0.1 M PB, pH 7.4.

   To prepare 1000 mL of 4 % paraformaldehyde/0.05 % glutaraldehyde in 0.1 M PB, pH 7.4: dissolve 40 g of paraformaldehyde in 300 mL of distilled water, make up to 500 mL

with distilled water, filter and add 500 mL 0.2 M PB and 2 mL of 25 % glutaraldehyde. For safety reasons, all these steps should be carried out in a fume hood.

6. Peristaltic pump (Fisher Scientific, Pittsburg, USA).
7. Needle (20 gauge).
8. Small scissors, fine scissors, clamps and tweezers (EMS).

2.3 Sectioning of the Brain

Although there are different ways to cut the brain, those procedures requiring cryoprotection and freezing of specimens to be sectioned are not recommended for immunoelectron microscopy. The vibrating microtome, which allows brains to be cut at room temperature or 4 °C immediately after perfusion-fixation, is the most appropriate apparatus, and the immunohistochemical techniques are performed using free-floating sections (around 50–70 μm thickness).

1. Vibrating microtome (Vibratome, Leica)
2. Double-edged stainless steel razor blades (EMS)
3. Instant glue
4. Buffer: 0.1 M PB, pH7.4
5. Twenty four-well culture plate
6. Paintbrush (size 0–1) to transfer sections

2.4 Membrane Permeabilization

Following perfusion-fixation, in order to enhance the penetration of immunoreagents and favour accessibility to several antigens, it may be necessary to disrupt the plasma membranes to some extent. This can be achieved either by freeze-thawing, which mechanically disrupts the membranes by producing small ice crystals or by incubating the sections with the detergent Triton X-100, which dissolves part of the lipid bilayer of membranes.

2.4.1 Triton X-100

1. Triton X-100
2. Buffer: 0.05 M TBS, pH7.4

2.4.2 Freeze-Thaw

1. Sucrose, to prepare cryoprotectant solutions of 10 and 30 % in 0.1 M PB
2. Buffer: 0.1 M PB, pH7.4
3. Liquid nitrogen, stored in Dewar flask

2.5 Pre-embedding Immunohistochemistry

1. Buffers: (a) 0.1 M PB, pH7.4; (b) 0.1 M PBS, pH 7.4; (c) 0.05 M TB, pH 7.4; (d) 0.05 M TBS, pH 7.4.
2. Shaker (JP Selecta, Barcelona, Spain).
3. Refrigerator.
4. Primary antibodies (*see* **Note 1**).

5. Normal serum (*see* **Note 2**). This reagent can be aliquoted in small tubes and stored at –20 °C.
6. Biotinylated secondary antibodies (Vector Laboratories): working dilution of 1:200 in TBS.
7. Secondary antibodies conjugated to 1.4 nm gold particles (Nanoprobes Inc.): working dilution of 1:100 in TBS.
8. ABC (avidin-biotin-peroxidase complex) Vectastain kit (Vector Laboratories).
9. 3.3′-Diaminobenzidine tetrahydrochloride (DAB, Sigma-Aldrich): 0.05 % in TB. The solution is light sensitive. It can be stored at –20 °C.
10. Hydrogen peroxide: working solution of 1 % in distilled water to give a final concentration of 0.01 % (i.e. 20 μL H_2O_2/2 mL DAB solution).
11. Glutaraldehyde: 1 % in PB. Follow safety notes described in Sect. 2.2.
12. HQ Silver intensification kit (Nanoprobes Inc.). Store the HQ Silver kit in the freezer at –20 °C. A couple of hours before use, maintain kit at room temperature, in a dark place, to allow melting of the three solutions in the kit.

2.6 Processing Sections for Electron Microscopy

1. Buffers: 0.1 M PB, pH 7.4.
2. Osmium tetroxide (OsO_4, Sigma-Aldrich): 1 % in 0.1 M PB, pH 7.4 (*see* **Note 3**). Very toxic and volatile, so always wear protective clothing and gloves, and handle in a fume hood. It may be stored at 4 °C for several weeks.
   Osmium tetroxide can be supplied in the form of crystals in sealed ampoules, which should be scrupulously cleaned using soap and water, as should all glass items coming into contact with osmium. In this case, a stock solution of 2 % osmium tetroxide in double-distilled water is made first. To prepare the stock solution, open a 1 g ampoule of osmium tetroxide and dissolve in 50 mL of double-distilled water. Osmium tetroxide is slow to dissolve, and the solution should be prepared at least 24 h in advance. Place the vial containing the osmium solution inside a second container, and store in a fume hood, in the dark. Finally, a working fixative solution (1 % in 0.1 M PB) is prepared just before use by mixing equal parts of 2 % aqueous stock solution with an equal part of 0.2 M PB.
3. Uranyl acetate: 1 % in Milli-Q water. Incubation of sections with uranyl acetate before dehydration, also known as *en bloc staining*, improves their contrast when examined at the electron microscope. Protect from light to prevent the precipitation of uranyl acetate during incubation. Very toxic, so always wear protective clothing and gloves, and handle in a fume hood.

4. Graded series of ethanol in water (50, 70, 90, 95 and 100 %) for dehydration.
5. Dry absolute ethanol: absolute ethanol with anhydrous cupric sulphate.
6. Propylene oxide (EMS). It is extremely toxic in contact with skin, by inhalation and if swallowed and also volatile and flammable. Do not wear protective gloves, as this substance will dissolve them, and handle in a fume hood.
7. Epoxy resin: Durcupan ACM (Sigma-Aldrich).
   One of the most commonly used epoxy resins is Durcupan ACM, which facilitates flat embedding (see below) of the samples on slides. This resin consists of four components: epoxy resin (designated component A), hardener (component B), an accelerator (component C) and component D. Each component has a long shelf life if bottles are properly closed and stored in a dry place. Certain components of the epoxy resin are toxic, so always wear protective clothing and gloves, and handle in a fume hood.
   Prepare the epoxy resin by weighing 10 g of component A, 10 g of component B, 0.3 g of component D and 0.3 g of component C in a disposable plastic beaker, always following this sequence: A, B, D and C. Mix thoroughly with a disposable plastic pipette in order to obtain satisfactory results. The bubbles that form during this mixing process will rise to the surface in 5–10 min. If a different amount of epoxy resin is needed, follow the ratio 10:10:0.3:0.3 g. This ratio results in a Durcupan epoxy resin of medium hardness. Unused epoxy resin can be stored for several months at –20 °C, but we recommend using a freshly prepared mixture. Resin waste should be collected in a disposable beaker and allowed to polymerize at 60 °C for 24 h, before disposal.
8. Oven (temperature range up to 200 °C) to polymerize the epoxy resin.
9. Adhesive labels.
10. Paintbrush or toothpick.
11. Glass slides and coverslips.
12. Polyethylene moulds for embedding samples for electron microscopy (EMS).

2.7 Ultrathin Sectioning

1. Ultramicrotomo (Leica, Vienna, Austria)
2. Diamond knife (Diatome, Biel, Switzerland)
3. Glass knifemaker (Leica EM KMR3)
4. Glass knives (EMS)

5. Pioloform-coated single slot copper grids (EMS)
6. Forceps to handle grids (EMS)
7. Grid storage box (EMS)

2.8 Staining of Ultrathin Sections

Although tissue sections can be examined in the electron microscope after immunohistochemical reactions, it is usually necessary to counterstain using heavy metal solutions to improve contrast. The most commonly used stain is Reynold's lead citrate.

1. Lead citrate solution. Store at 4 °C. Wear protective gloves.
   Prepare lead citrate solution by weighing 0.133 g lead nitrate ($Pb(NO_3)_2$) and 0.176 g tri-sodium citrate ($Na_3C_6H_5O_7$). Add 4.8 mL of double-distilled water to the lead nitrate and shake vigorously to dissolve. Add the tri-sodium citrate to the lead nitrate solution and shake gently until a milky suspension is formed. Immediately, add 0.2 mL 4 M NaOH and mix well until the solution becomes totally clear. Note that sodium carbonate is formed when the lead citrate solution is exposed to air. Transfer the solution to a 10 mL glass bottle with a screw cap for storage, and wrap it with aluminium foil.
2. Sodium hydroxide pellets (Sigma-Aldrich).
3. Laboratory film (e.g. Parafilm).
4. Methods

3 Methods

3.1 Tissue and Fixation

1. Fix the brain by perfusion-fixation (*see* **Note 4**).
2. Set up peristaltic pump. Place open end of tubing into the beaker of saline and fixative solution (in ice). Fill both tubes, but fill the common tube with saline only. Avoid air bubbles in any of the tubes. The volume of fixative solution should be scaled to size of animal.
3. Perform deep anaesthesia of the animal by intraperitoneal injection of ketamine-xylazine 1:1 (0.1 mL/kg b.w.). Allow a few minutes for anaesthesia to occur, indicated by the loss of reflex responses. For instance, pinch the toes to judge the level of response to painful stimuli.
4. Place the animal on its back on a Styrofoam board, and pin out all four limbs at the feet using small needles.
5. Cut the skin just below the diaphragm with small scissors to expose the liver. Cut the ribs laterally, bend the chest backward and fix it with a clamp to allow easy access to the heart. Once the chest is opened, the animal can no longer breathe; therefore, the following steps should be carried out as quickly as possible. Lack of oxygen (anoxia) causes poor preservation of the ultrastructure and may compromise antigenicity.

6. Remove any excess adipose or connective tissue from the heart. Separate the thymus with a small spatula and make sure the ascending aorta is visible.
7. Make a small cut in the left ventricle using fine scissors.
8. Insert a blunt needle connected to the end of the tubing into the left ventricle. Secure needle by clamping in place near the point of entry into the heart, and turn on the peristaltic pump. Then immediately cut the right atrium using fine scissors.
9. Perfuse the animal with saline for 1 min or until the liver becomes paler and the blood has been cleared from the body. At this point, switch to the fixative solution and continue perfusion for 15 min (*see* **Note 5**). Check tail and neck flexibility as good indicators of how well the animal is being fixed; a well-fixed animal should have a stiff tail and neck.
10. Turn off the peristaltic pump. The animal should be stiff at this point. Cut the head, remove brain from the skull and wash in 0.1 M PB, pH7.4.
11. After perfusion is completed, the animal carcass should be wrapped and placed in a plastic bag in a freezer, until properly disposed of in the animal housing facility.
12. Wash brain thoroughly in PB, for 2 h, before sectioning.

3.2 Sectioning of the Brain

1. Cut brain areas of interest into blocks. If sagittal sections are required, separate hemispheres with a razor blade along the midsagittal plane. If coronal sections are required, cut brains into two to three different tissue blocks (for instance, one containing the olfactory bulbs and the main part of the striatum, one containing the whole hippocampus and thalamus and one containing the cerebellum). Wash blocks four times with 0.1 M PB, pH7.4, for 15 min each.
2. Mount and stick one brain hemisphere or a tissue block on the vibratome's specimen holder, using fast glue.
3. Fill the vibratome reservoir with 0.1 M PB and cut 50- to 70-μm thick sections (*see* **Note 6**).
4. Collect the sections with a brush, and place each section in a well of the 24-well plate containing PB.
5. Store sections in 0.1 M PB, at 4 °C (*see* **Note 7**).

3.3 Membrane Permeabilization

3.3.1 Freeze-Thaw

1. Prepare cryoprotectant solutions: (1) 10 % sucrose in 0.1 M PB; (2) 30 % sucrose in 0.1 M PB.
2. Once tissue blocks containing brain areas of interest have been obtained after perfusion-fixation, place them in 10 % sucrose in 0.1 M PB and shake gently until tissue blocks sink.
3. Place tissue blocks in 30 % sucrose in 0.1 M PB and shake gently until they sink.

4. Drain off the excess sucrose and place the tissue blocks in an empty plastic beaker.
5. Drop the beaker quickly into liquid nitrogen without full submersion, so the tissue blocks are in contact with the liquid nitrogen through the wall of the beaker. Allow the tissue blocks to freeze completely, and immediately let the blocks thaw in 0.1 M PB, at room temperature.
6. Wash the tissue blocks twice with 0.1 M PB, for 15 min each.
7. Section tissue blocks in a vibrating microtome (*see* Sect. 3.2).

3.3.2 Triton X-100

1. Prepare a blocking solution of 10 % normal goat serum in TBS containing 0.05 % Triton X-100.
2. Incubate sections and shake gently for 1 h, at room temperature.
3. Wash the sections four times with TBS, for 15 min each.

3.4 Pre-embedding Immunoperoxidase

1. Wash sections three times with 0.1 M PB, for 15 min each, to remove any remaining fixative. Then rinse sections with TBS, for 30 min.
2. Block non-specific binding by incubating sections in TBS blocking solution containing 10 % normal serum, for 1 h. If permeabilization with detergent is needed, go to **step 1** of Sect. 3.3 before incubating in blocking solution.
3. Incubate sections in primary antibody diluted in TBS containing 1 % normal serum, at 4 °C, for 12–24 h (*see* **Note 8**).
4. Wash the sections four times with TBS, for 15 min each.
5. Incubate sections in biotinylated secondary antibody in TBS containing 1 % normal serum, at room temperature, for 2–4 h.
6. Wash the sections three times with TBS, for 15 min each.
7. Incubate sections in ABC in TBS, at room temperature, for 2 h (*see* **Note 9**).
8. Wash the sections twice with TBS, for 15 min each.
9. Wash the sections twice with TB, for 15 min each.
10. Incubate sections for 15 min in a solution of 0.05 % DAB in TB, at room temperature.
11. Add hydrogen peroxide to the DAB solution to reach a final concentration of 0.01 %, and incubate for a further 2–3 min (*see* **Note 10**).
12. Stop reaction in TB and then wash the sections 4 times with TB, for 10 min each.

3.5 Pre-embedding Immunogold

1. Wash sections three times with 0.1 M PB, for 15 min each, to remove any excess of fixative and once with TBS, for 30 min.
2. Block non-specific binding by incubating sections with 0.5 mL of blocking solution consisting of TBS containing 10 % normal serum, for 1 h.
3. Remove the blocking solution and replace it with 0.5 mL of primary antibody diluted in TBS containing 1 % normal serum, at 4 °C, for 12–24 h (*see* **Note 8**).
4. Wash the sections four times with TBS, for 15 min each.
5. Incubate the sections with 0.5 mL of 1.4 nm gold compound-conjugated secondary antibody (use at 1:100 dilution) in TBS containing 1 % normal serum, at room temperature, for 2 h (*see* **Note 11**).
6. Wash the sections four times with TBS, for 15 min each, and once with PB, for 15 min.
7. Postfix the sections with 1 mL of 1 % (w/v) glutaraldehyde in PB, at room temperature, for 10 min (*see* **Note 12**).
8. Remove the glutaraldehyde solution and wash the sections three times with PB, for 10 min each, followed by two washes in 1 mL of Milli-Q water, for 10 min each.
9. Prepare the silver intensification solution immediately before use by mixing equal volumes of the three reagents (components A, B and C) from the HQ Silver enhancement kit, in a dark room, at room temperature.
10. Place the sections in 0.5 mL of silver intensification solution at room temperature, for 6–8 min, in the dark (*see* **Note 13**).
11. Remove the silver intensification solution and stop reaction with Milli-Q water.
12. Wash the sections four times in 1 mL of Milli-Q water, for 5 min each, in the dark. Although reaction stops with washing, the silver-enhanced slices may continue to darken during washing and storage. Therefore, do not store, and process sections for electron microscopy as soon as possible.

3.6 Double Labelling Pre-embedding HRP-Immunogold

1. Wash the sections three times with 0.1 M PB, for 15 min each, to remove any remaining fixative. Then wash sections with TBS, for 30 min.
2. Block non-specific binding by incubating sections in TBS blocking solution containing 10 % normal animal serum, for 1 h.
3. Incubate the sections in a cocktail of two primary antibodies raised in different species and diluted in TBS containing 1 % normal animal serum, at 4 °C, for 12–24 h (*see* **Note 8**).
4. Wash the sections four times with TBS, for 15 min each.

5. Incubate the sections in a cocktail of two secondary antibodies, biotinylated and 1.4 nm gold compound-conjugated in TBS containing 1 % normal serum, at room temperature, for 2–4 h (*see* **Note 11**).
6. Wash the sections three times with TBS, for 15 min each.
7. Wash the sections once with PB, for 15 min.
8. Postfix the sections with 1 mL of 1 % (w/v) glutaraldehyde in PB, at room temperature, for 10 min (*see* **Note 12**).
9. Remove the glutaraldehyde and wash the sections twice with PB, for 10 min each.
10. Wash the sections once with Milli-Q water, for 10 min.
11. Silver intensification: prepare the solution immediately before use by mixing equal volumes of the three reagents (components A, B and C) from the HQ Silver enhancement kit, at room temperature, in a dark room. Incubate sections in 0.5 mL of silver intensification solution at room temperature, for 6–8 min, in the dark (*see* **Note 13**).
12. Remove the silver intensification solution and stop reaction with Milli-Q water.
13. Wash the sections four times in 1 mL of Milli-Q water, in the dark, for 5 min each.
14. Wash the sections twice with TBS, for 15 min each.
15. Incubate sections in ABC in TBS, at room temperature, for 2 h (*see* **Note 9**).
16. Wash the sections twice with TBS, for 15 min each.
17. Wash the sections twice with TB, for 15 min each.
18. Incubate sections for 15 min in a solution of 0.05 % DAB in TB, at room temperature.
19. Add hydrogen peroxide to the DAB solution to reach a final concentration of 0.01 %, and incubate for a further 2–3 min (*see* **Note 10**).
20. Stop reaction in TB and then rinse the sections four times with TB, for 10 min each.

3.7 Processing Sections for Electron Microscopy

1. Wash the sections three times with 0.1 M PB, for 15 min each.
2. Postfix the sections with 1 % osmium tetroxide in 0.1 M PB, for 30 min (*see* **Note 14**).
3. Wash the sections five times with 0.1 M PB, for 8–10 min each, to remove all traces of osmium and then wash once with distilled water, for 8–10 min.
4. Stain with 1 % uranyl acetate solution in distilled water, for 30 min.

5. Dehydrate the sections with 50, 70, 90, 95 and 100 % ethanol, for 10–15 min each, and then 100 % dry ethanol, for 10–15 min (*see* **Note 15**).
6. Incubate with propylene oxide twice, for 10–15 min each. Use glass pipettes, as propylene oxide dissolves plastic pipettes.
7. Infiltrate in epoxy resin (e.g. Durcupan) for 4 h and then proceed with flat embedding (*see* **Note 16**).
8. Polymerize the resin by heating in an oven, at 60 °C, for 48 h.
9. With the unused epoxy resin, fill the polyethylene moulds (capsules) up to the top and place in an oven for polymerization, at 60 °C, for 24 h.

3.8 Ultrathin Sectioning

1. Remove the coverslip. Observe the sections with a stereomicroscope and choose the brain region of interest.
2. Trim the area of interest by making four small cuts in the section using a scalpel. The small sample will detach from the slide.
3. Take one block of resin polymerized in the polyethylene capsules. Stick the small sample on the tip of the resin block with fast glue, and let dry for 10–15 min.
4. In an ultramicrotome, trim the sample on the resin block with a single-edged razor blade.
5. Fit the block into the ultramicrotome and align the block face with a glass knife.
6. Remove the empty resin from the top of the sample using a glass knife. Then change to a diamond knife.
7. Cut ultrathin sections (60–80 nm thickness) with the ultramicrotome.
8. Collect short ribbons of sections on pioloform-coated slot grids and let dry. Store the grids in a grid box.

3.9 Staining of Ultrathin Sections

1. Prepare the lead citrate solution (*see* Sect. 2.8).
2. Take a plastic or glass Petri dish with a piece of laboratory film and place a few sodium hydroxide pellets in one of the sides.
3. Draw up the lead citrate solution into a Pasteur pipette, placing individual drops on the laboratory film.
4. Place grids with ultrathin sections onto the drops of the lead citrate solution. Leave for 1.5–3 min.
5. Wash the grids three times in double-distilled water, for several seconds each.
6. Blot the bottom of the grid with filter paper and then allow grids to dry at room temperature. Place grids in a grid box.

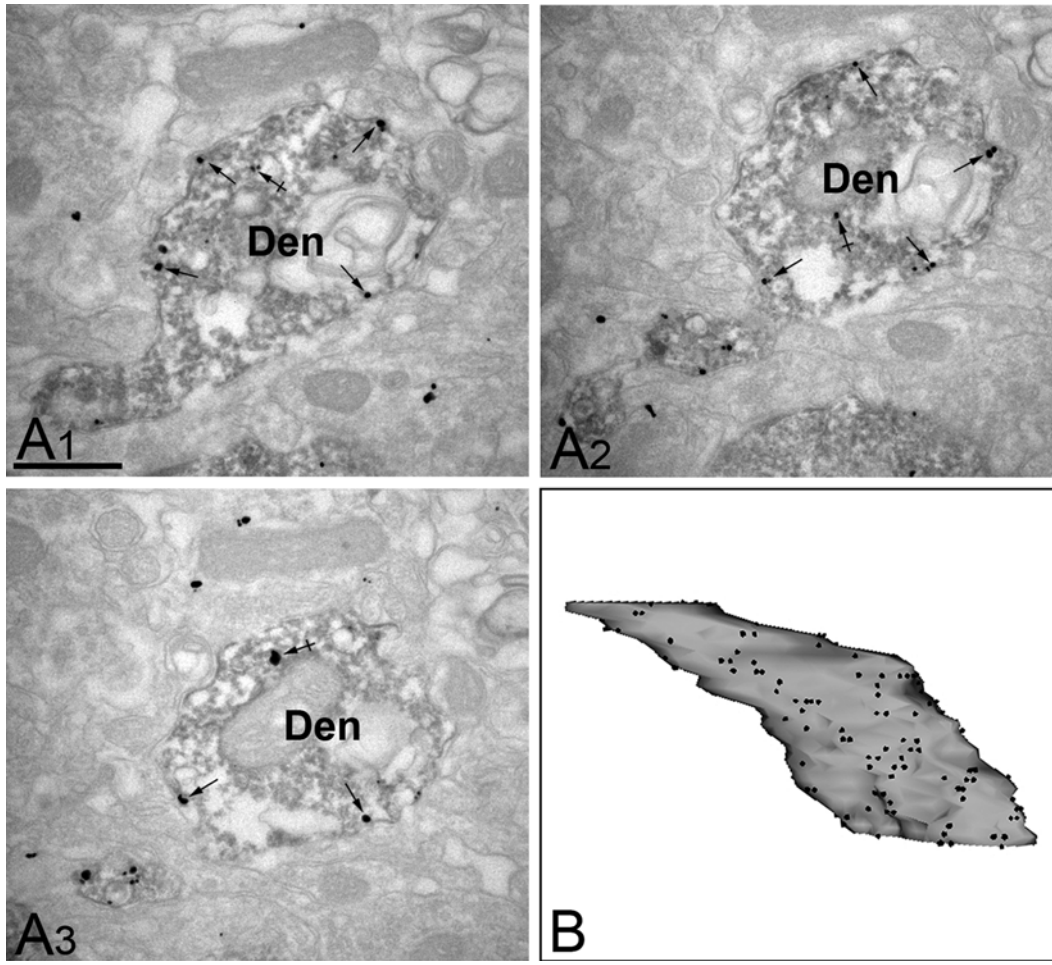

Fig. 3 Electron micrographs showing immunoreactivity for tyrosine hydroxylase (TH), a marker of dopaminergic neurons, and the GIRK2 subunit of the G protein-gated inwardly rectifying K^+ channel, as demonstrated by a double-labelling pre-embedding method in the ventral tegmental area (VTA) of the mouse brain. (**a1**–**a3**) Three serial sections of the same dendritic shaft in the VTA. The peroxidase reaction end product (TH immunoreactivity) diffuses and fills the dendritic shafts (*Den*) of dopaminergic neurons, whereas immunoparticles (GIRK2 immunoreactivity) were located along the extrasynaptic plasma membrane (*arrows*) and at intracellular sites (*crossed arrows*). (**b**) Three-dimensional reconstruction from 25 serial sections of a VTA dopaminergic dendrite. *Black dots* represent immunogold particles on the front surface of the dendrite. *Scale bar*: **a** 0.5 μm

7. Examine sections with a transmission electron microscope. Figs. 1, 2 and 3 show examples of immunolabelling for GIRK2, a G protein-gated inwardly rectifying K^+ channel subunit in the ventral tegmental area of the mouse brain, using pre-embedding immunoperoxidase, pre-embedding immunogold and double-labelling pre-embedding HRP-immunogold methods.

4 Notes

1. Primary antibodies that work well by western blotting, immunocytochemistry or immunohistochemistry at the light microscopic level do not necessarily work on tissue prepared for electron microscopy. When testing out antibodies for the first time for immunoelectron microscopy, suitable positive and negative control tests should be performed. Negative controls involve brain regions that are known to contain the antigen of interest, while positive controls use brain regions or cell types that do not to contain a given antigen. An additional negative control includes the substitution of the primary antibody with nonimmune immunoglobulin from the same species and at the same dilution. A very popular and widely used control, the so-called adsorption control, consists of adsorbing the primary antibody with the peptide antigen employed to generate the antibody. Although this eliminates the binding of the antibody to the protein in the section, we now know that it may not bind to the same protein used to generate the primary antibody.
2. Normal serum helps to prevent the secondary antibody from cross-reacting with endogenous immunoglobulins in the tissue. Normal serum should be from the species in which the secondary antibody was raised. For instance, if the primary antibody is raised in rabbit and the secondary antibody is raised in goat (i.e. goat anti-rabbit antibody), then normal goat serum should be used.
3. Osmium tetroxide is used as a secondary fixative following aldehyde fixation, since its rate of penetration is too slow to prevent artefacts if used initially. This chemical is extremely toxic, and volatile fumes are very corrosive, especially to mucous membranes. Therefore, osmium solutions should be prepared and handled in a fume hood, always wearing protective clothing, disposable gloves and eyewear. The used osmium solutions should be disposed of properly. For convenience and safety in the laboratory, aqueous solutions of osmium tetroxide in sealed 2-mL glass ampoules can be purchased.
4. Fixation of the tissue can be carried out by immersion or by vascular perfusion. Although immersion-fixation is generally employed for post-mortem or biopsy specimens and cultured cells, perfusion-fixation is recommended for most purposes, including for use with small animals. For instance, it yields very good morphology preservation in highly vascular tissues like the brain or the liver. The perfusion-fixation method allows the removal of blood from the animal, giving rise to a very rapid and uniform fixation. It consists of administering the fixative

into the aorta of deeply anaesthetized animals, either using a peristaltic pump or a gravity-powered mechanism, for 15–20 min. For postnatal animals, post-fixation in the same fixative for several hours (from 2 h to overnight) is recommended.

5. When perfusing the animal, the flow rate of the solution entering the cardiovascular system affects fixation and the preservation of structure. If the flow rate is too high, blood vessels may break the endothelial wall, causing leakage of the fixation from the cardiovascular system. This will decrease the flow rate, producing a slow fixation and a compromised structural preservation. Similarly, if the flow rate of the fixative solution is too low, fixation is slow and will also produce a compromised structural preservation. To adjust the flow rate, change the speed of the peristaltic pump so that with a 20-gauge needle, a solution beam of about 4–5 cm is created.
6. The section thickness is not a critical factor for the immunolabelling process. However, sections thinner than 40 μm are difficult to handle with a paintbrush and there is an increased risk that the tissue will break. Sections thicker than 100 μm are easy to handle but turn very dark after osmification, making it impossible to observe gross structure of the section in the light microscope. In our experience, a section of 50–70 μm is a good thickness, affording both easy handling and identification at the light microscopic level of the different brain regions present in the section after epoxy resin embedding.
7. Tissue blocks left uncut for several days display degradation of antigens. Therefore, for better results with pre-embedding techniques, tissue blocks should be cut immediately following fixation-perfusion and fresh sections used. Tissue sections that are left on the bench at room temperature rapidly dampen antigenicity and ultrastructure preservation, and factors like heat, dryness or exposure to ultraviolet light contribute to this deterioration. For optimal antigen preservation, the most common practice is to keep sections in 0.1 M PB, add 0.05 % sodium azide, wrap the vial in aluminium foil and store at 4 °C. Do not use sections for immunoelectron microscopy after 1 week of storage, as the ultrastructure and antigenicity preservation deteriorate quickly with time.
8. The optimal dilution of any antibody should be determined in a trial test using a wide range of concentrations. In general, the final concentration of antibodies should be approximately 0.5–4 μg/mL for pre-embedding conditions. The binding of any antibody to an antigen is affected by the concentration of the antibody, the number of sections incubating per volume of antibody solution and the duration and temperature of the incubation. Therefore, all these parameters should be optimized in each case, taking into account that short incubations ought to be carried out at room temperature and long incubations at 4 °C.

9. In the case of kits from Vector Laboratories, the avidin-biotin-peroxidase complex (ABC) is made by mixing solution A (avidin), diluted 1:100, with solution B (biotinylated peroxidase), diluted 1:100, in TBS. This complex should be made 30 min before use. There are several kits available from Vector Laboratories; the Elite kit possesses greater sensitivity, but it is more expensive and produces more background reaction if the antibody binds non-specifically to the tissue.
10. Monitor the speed of the peroxidase reaction, which depends on the antigen and concentration of immunoreagents, by watching the development of colour within the sections. Immunolabelled areas should appear dark brown, whereas areas lacking the specific antigen, as well as control sections (lacking primary or secondary antibodies), should appear white. The intensity of reaction can be checked with the light microscope, but because the DAB reaction is light sensitive, exposure to intense light should be very short. Stop the reaction quickly with TB.
11. Two different types of gold reagents are commercially available for pre-embedding techniques. One uses colloidal gold particles (ranging in size from 5 to 50 nm in diameter) that are based on hydrophobic interactions with immunoglobulins. However, this association is very weak, and dissociated immunoglobulins lacking gold particles can be formed. The second type consists of 1.4 nm gold particles bound covalently to the immunoglobulin (nanogold, Nanoprobes Inc.), thus avoiding the formation of IgG that lack gold particles. Since the main constraint of the pre-embedding immunogold method is the limited penetration of immunoreagents through tissue, use of the second reagent described, nanogold, is highly recommended. Fab' nanogold conjugate is also available (use at 1:100 dilution). The smaller size of this molecule allows deeper penetration into the tissue, therefore producing better immunogold labelling for some antibodies. Since 1.4-nm gold particles are too small to be visualized directly at the electron microscope, immunoparticles must be intensified with silver deposits in order to increase their diameter.
12. Use of 0.1 M PB is recommended for this procedure. Although PBS has also been extensively used as a fixative dilution buffer or as a washing solution, Cl^- ions from NaCl have been shown to inhibit the silver intensification reaction.
13. There are several protocols for silver intensification. The HQ Silver intensification kit (Nanoprobes, Inc.) is one of the most widely used. It produces small silver particles that are approximately 20–40 nm in diameter. It is easy to use and prepared by thoroughly mixing equal volumes of three components (initiator, moderator and activator). However, this kit is light sensitive

and all steps should be carried out in the dark. In addition, the silver intensification reaction does not work efficiently at temperatures below 20 °C. At room temperature, the intensification process is quite fast and it normally takes 6–8 mins to achieve silver particles of good size. Longer periods of incubation yield very large silver particles, increasing the possibility of two or more independent silver particles fusing into a single larger particle. A series of different intensification times should be tested to determine the optimum size of the immunoparticles. Alternatively, the silver intensification kit from AURION (www.aurion.nl/) can be used, which is light insensitive, has low viscosity and allows easy control of size of silver particles under the light microscope. It also consists of three components (enhancer, initiator and activator) that are straightforward to use following the manufacturer's instructions.

14. When osmium tetroxide is added to the vials, sections rapidly turn black and become rigid and fragile, so vigorous agitation should be avoided. One major problem associated with the osmium tetroxide step is that strong osmication and high OsO_4 concentrations dissolve the silver deposited on the immunogold particles. There are three possible solutions: (1) after osmication, do not leave the sections washing in 0.1 M PB overnight, and continue processing for electron microscopy; (2) reduce osmication to 0.5 % for 10–15 min; and (3) prepare a new stock solution of 4 % osmium tetroxide in distilled water.

15. Before dehydration and eventual immersion in propylene oxide, a substance that dissolves the plastic of the 24-well culture plate, transfer sections from the plate to individual glass vials. Perform dehydration in the glass vials with 50 and 70 % ethanol. Then, using a paintbrush, transfer sections to a slide as quickly as possible to avoid evaporation of the ethanol. Cover the slide with a coverslip and add 90, 95 and 100 % ethanol, for 10–15 min each (ethanol will reach the section by capillarity). The use of slides during this step of dehydration ensures that sections are completely flat before resin infiltration and polymerization. Finally, the sections are transferred back to glass vials to carry out the second 100 % ethanol dehydration and final steps.

16. To perform infiltration with epoxy resin, transfer the sections to aluminium boats using a paintbrush. Add 1–2 mL of freshly prepared resin to each aluminium boat and ensure that the sections remain fully immersed and do not float on the resin. To perform the flat-embedding step, use a toothpick to very carefully remove the sections from the aluminium boats and place them on a slide. Add a few drops of resin to the sections and ensure that they remain completely covered. Place a coverslip over the sections and remove any excess resin with filter paper.

Acknowledgments

The author would like to thank Alexandra Salewski, MSc., for the English revision of the manuscript. This work was supported by the grants BFU-2012-38348 and CONSOLIDER CSD2008-00005 from the Spanish Ministry of Education and Science, the European Union (HBP – Project Ref. 604102) and the Junta de Comunidades de Castilla-La Mancha (PPII-2014-005-P).

References

1. Luján R, Nusser Z, Roberts JDB, Shigemoto R, Somogyi P (1996) Perisynaptic location of metabotropic glutamate receptors mGluR1 and mGluR5 on dendrites and dendritic spines in the rat hippocampus. Eur J Neurosci 8: 1488–1500
2. Luján R, Roberts JDB, Shigemoto R, Somogyi P (1997) Differential plasma membrane distribution of metabotropic glutamate receptors mGluR1α, mGluR2 and mGluR5, relative to neurotransmitter release sites. J Chem Neurochem 13:219–241
3. Ballesteros-Merino C, Lin M, Wu WW, Ferrandiz-Huertas C, Cabañero MJ, Watanabe M, Fukazawa Y, Shigemoto R, Maylie J, Adelman JP, Luján R (2012) Developmental profile of SK2 channel expression and function in CA1 neurons. Hippocampus 22:1467–1480
4. Padgett CL, Lalive AL, Tan KR, Terunuma M, Muñoz MB, Pangalos MN, Martínez-Hernández J, Watanabe M, Moss SJ, Luján R, Lüscher C, Slesinger PA (2012) Methamphetamine-evoked depression of GABA(B) receptor signaling in GABA neurons of the VTA. Neuron 73: 978–989
5. López-Bendito G, Shigemoto R, Fairén A, Luján R (2002) Differential distribution of group I metabotropic glutamate receptors during rat cortical development. Cereb Cortex 12:625–638
6. López-Bendito G, Shigemoto R, Kulik A, Paulsen O, Fairén A, Luján R (2002) Expression and distribution of metabotropic GABA receptor subtypes $GABA_BR1$ and $GABA_BR2$ during rat cortical development. Eur J Neurosci 15: 1766–1778

Chapter 16

Post-embedding Immunohistochemistry in the Localisation of Receptors and Ion Channels

Rafael Luján and Masahiko Watanabe

Abstract

Post-embedding techniques are powerful approaches for the analysis of the chemical architecture of the brain and have proved useful to investigate disease processes at the molecular level. These techniques involve immunohistochemical reactions on tissue that is previously fixed, dehydrated, embedded in resin and sectioned. As a result, immunoreactions only occur on the surface of the sections, and this make post-embedding techniques to have lower sensitivity than other immunoelectron microscopy approaches. However, among other advantages, post-embedding techniques are the only reliable methods to localise any receptor/ion channel at excitatory synapses and also enable the simultaneous localisation of different molecules in the cell or subcellular compartments using secondary antibodies conjugated with gold particles of different size. In this chapter, we introduce the post-embedding immunoperoxidase for light microscopy and post-embedding immunogold for electron microscopy and also discuss the limitations inherent to these approaches. We describe the main scope and protocols which have been successfully utilised at our research centres for the examination and analysis of neuronal surface and intracellular and receptor/ion channel in the brain.

Key words Post-embedding immunogold, Post-embedding HRP, Immunohistochemistry, High-resolution techniques, Electron microscopy, Freeze-substitution, Cryofixation, Synaptic receptor, Double labelling, Quantification

1 Introduction

The hallmark of post-embedding techniques involves performing immunohistochemical reactions on tissue that is previously fixed, dehydrated, embedded in resin and sectioned prior to subsequent light or electron microscopy examination and analysis. Generally speaking, post-embedding techniques can be used for the same reasons as pre-embedding techniques, that is, to determine the precise subcellular localisation, exact number and position of a given target molecule in a biological tissue. The choice of whether to apply a pre- or post-embedding method to the detection of an antigen in any particular tissue depends on the properties of primary antibody and accessibility of the antigen.

Rafael Luján and Francisco Ciruela (eds.), *Receptor and Ion Channel Detection in the Brain: Methods and Protocols*, Neuromethods, vol. 110, DOI 10.1007/978-1-4939-3064-7_16,

Two main methods have been devised for post-embedding immunohistochemical techniques based on the use of different makers: (1) Post-embedding immunohistochemistry combined with biotinylated secondary antibodies enables the visualisation of antigenic sites on semithin sections at the light microscopic level, and (2) post-embedding immunohistochemistry combined with colloidal gold conjugates enables the visualisation of molecules on ultrathin sections at the electron microscopic level. The latter technique exceeds by far the resolution offered by enzyme-based techniques, which rely on the analysis of a dense reaction product that has a diffusible nature, and therefore, it is difficult to quantify. The theoretical distance between antigenic sites and the centre of the gold particle determines the spatial resolution of the post-embedding immunogold procedure, defined by the length of the antibody bridge and the size of the colloidal gold particle. Thus, for instance, using 10 nm gold particles, and a primary and a secondary antibody (both IgGs with a diameter of ~8 nm), the spatial resolution of the technique should be ~21 nm. The resolution will be better if gold particles are directly coupled to the primary antibody or using the Fab fragment of an IgG secondary antibody and will be worse when using gold particles above 10 nm.

The post-embedding immunohistochemical techniques have several advantages over those that use pre-embedding:

1. A major advantage offered by post-embedding techniques is that each antigen molecule present at the surface of the section has the same probability of being immunodetected, regardless of its subcellular distribution. Thus, this is the only reliable method to localise any receptor/ion channel at excitatory synapses, because the entire cut length of the plasma membrane is uniformly exposed to the antibodies as the sections are directly floated on to the solutions [1–3].
2. Tissue penetration problem characteristics of the pre-embedding immunohistochemistry, where diffusion barriers may constrain immunolabelling or some structures that contain the receptor/ion channel may remain unlabelled due to the limited antibody penetration though the tissue, are minimised because of small thickness of sections.
3. The previous two advantages provide a better condition for quantitative analysis of the receptor/ion channel density compared to pre-embedding conditions.
4. Serial sections of the same tissue, cell or subcellular compartment can be incubated and examined with different antibodies or control solutions.
5. The use of secondary antibodies conjugated with gold particles of different size (for instance, 5 nm, 10 nm, 15 nm, 20 nm, etc.) enables the simultaneous localisation of different receptors/

ion channels in the same neuron population or subcellular compartments.

6. Once resin-embedded tissue blocks are available, they can be used for a very long time, also allowing optimisation of the immunolabelling conditions and repetition of experiments in the same tissue without having to use more animals.
7. The post-embedding immunolabelling procedure takes only a few hours distributed in two consecutive days to complete compared to the several days needed to complete pre-embedding immunolabelling methods.

There are, however, some disadvantages to the post-embedding techniques:

1. The absence of osmium tetroxide treatment in the processing of the tissue embedded in acrylic resins results in poor preservation of membranes and low contrast for all the neuronal organelles.
2. Antigenicity is frequently lost during the dehydration and embedding procedures. This is the reason why the post-embedding method appears to be less sensitive than the pre-embedding methods. Indeed, many antibodies that provide labelling under pre-embedding conditions fail to provide a signal under post-embedding conditions. For instance, a much lower density of extrasynaptic receptors/ion channels is revealed with the post-embedding method than under pre-embedding [4, 5].
3. Since in the post-embedding method immunoreactions occur on the surface of the ultrathin sections, the proportion of antigen molecules that is available for primary and secondary antibodies binding is significantly reduced when compared with the pre-embedding mode, resulting in the lower sensitivity of the former technique.

The sequence steps in the processing of tissue for post-embedding immunohistochemistry involve (1) fixation, (2) dehydration, (3) embedding, (4) sectioning, (5) immunoreaction and (6) analysis of sections. Each of those steps can be performed in many different ways. Therefore, it is difficult to provide a standard protocol because many laboratories have their own procedure. The reasons for such large amount of protocols are that each researcher has unique set of requirements and that each new target antigen needs individual evaluations to set up optimal experimental conditions. In fact, this is why post-embedding immunohistochemical techniques are always challenging and sometimes frustrating, although certainly very rewarding when immunoreactions works properly. This chapter describes the scope and protocols of post-embedding immunohistochemical techniques at the light and electron microscopic level that have been successfully utilised at our

laboratories for the examination and analysis of the subcellular localisation of neurotransmitters, neurotransmitter receptors and ion channels in the brain using single and/or double labelling. The experimental procedures provided are derived from studies on AMPA and NMDA receptors, as well as GIRK and SK potassium channels [1, 5–8]. However, the general principles and methodologies can be applied to other receptors and ion channels. In addition, the same procedures have also been successfully applied to (1) elucidate the distribution of receptors and ion channels during development [5, 7], (2) demonstrate the presence of receptors and amino acid transmitter in the same synapses [3, 8], (3) combine with anterograde tracing to identify transmitters and receptors in specific fibre projections [9] and (4) investigate disease mechanisms involved in disease states, for instance, the analysis of SK2 channels redistribution in experimental ischemia and hypoxia following cardiac arrest [10].

2 Materials

2.1 Buffers

Use phosphate (PB) and Tris (TB) buffers and their saline version, PBS and TBS, respectively. PB and PBS are used at a working dilution of 0.1 M. TB and TBS are used at a working dilution of 0.05 M.

1. *Phosphate buffer* (*0.1 M*, *pH7.4*). Phosphate buffer contains monobasic sodium phosphate (NaH_2PO_4) and dibasic sodium phosphate (Na_2HPO_4). The weight of each component will vary depending on the waters of hydration. The pH is adjusted by mixing the two components in the appropriate amounts.

   To prepare 1 L of 0.2 M sodium phosphate buffer (PB), pH7.4: a mixture of $Na_2HPO_4{\cdot}2H_2O$ (35.6 g) and $NaH_2PO_4{\cdot}2H_2O$ (31.2 g), each at 0.2 M, in the ratio 4:1, has a pH of about 7.4. If necessary, add a few drops of 1 M sodium hydroxide (NaOH) in distilled water to adjust pH. The stock solution of 0.2 M PB can be stored at 4 °C for several weeks. To prepare 0.1 M PB (pH 7.4), dilute equal volumes of the 0.2 M PB stock solution with distilled water.

2. *Phosphate-buffered saline* (*0.1 M*, *pH7.4*). PBS is prepared by mixing 0.9 % NaCl with 0.1 M PB.

3. *Tris buffer* (*0.05 M*, *pH7.4*). Tris buffer (TB) can be prepared in several ways. For precise accuracy and reproducibility, it is recommended to obtain a stock solution of 0.05 M TB (pH 7.4 at 25 °C), by dissolving 6.61 g Trizma HCl (Sigma-Aldrich, St. Louis, USA) and 0.97 g Trizma Base (Sigma-Aldrich) in 1000 mL of distilled water.

4. *Tris-buffered saline* (*0.05 M*, *pH7.4*). Once stock solution of 0.05 M TB is ready, TBS is prepared by mixing 0.9 % NaCl with TB. This buffer can be stored at 4 °C for several weeks.

2.2 Chemical Fixation

As for pre-embedding immunoelectron microscopy, the choice of appropriate fixative conditions is a critical step to perform successful post-embedding immunohistochemistry and aims to find the right balance between preservation of tissue ultrastructure and preservation of antigens in a state that can be recognised by the primary antibodies. In a given fixative solution, the concentration of glutaraldehyde is more critical than the concentration of paraformaldehyde, because glutaraldehyde has two reactive aldehyde groups, making this fixative a very efficient cross-linker. Fixatives with a high concentration of glutaraldehyde provide good ultrastructure preservation, whereas fixatives with low concentration or no glutaraldehyde provide the optimal preservation of antigenicity. However, the amount of glutaraldehyde that an antigen can tolerate to still produce a strong immunolabelling in the tissue is very difficult, if not impossible, to predict. Although for some membrane proteins the presence of 1 % glutaraldehyde in the fixative solution has proved to be compatible with a strong immunogold signal, this is not the case for most membrane proteins. Thus, our standard fixative solution is based on the use of 0.1 % glutaraldehyde combined with 4 % paraformaldehyde, which can be used when the first screening a novel receptor/ion channel target. In cases where the antigenicity of target molecules is highly sensitive to glutaraldehyde and even to paraformaldehyde, the use of 1–4 % paraformaldehyde may give good results.

1. Anaesthesia (Nembutal 50 mg/mL or Somnopentyl 64.8 mg/mL at 1 mL/kg b.w.). Follow the protocols approved by local Animal Care and Use Committee. The care and handling of animals prior to and during the experimental procedures should be in accordance with National and International regulations.
2. Buffers: 0.2 M PB, pH 7.4.
3. Paraformaldehyde (supplied as powder; EMS, Hatfield, USA). Keep at room temperature in a dry place. PFA is very toxic by contact with the skin, inhalation and ingestion. Therefore, always wear protective clothing and gloves and handle in a fume hood.
4. Glutaraldehyde (EM grade, supplied as a 25 % aqueous solution; EMS). This reagent can be stored at 4 °C. Glutaraldehyde is very toxic, so follow safety notes described above for paraformaldehyde.
5. Fixative solution: freshly prepare 4 % paraformaldehyde and 0.1 % glutaraldehyde in 0.1 M PB, pH 7.4.

   To prepare 1000 mL of 4 % paraformaldehyde + 0.1 % glutaraldehyde in 0.1 M PB, pH 7.4: dissolve 40 g paraformaldehyde in 300 mL of distilled water, make up to 500 mL with distilled water, filter, add 500 mL 0.2 M PB and add 4 mL of

25 % glutaraldehyde. For safety reasons, all these steps should be carried out in a fume hood.

6. Peristaltic pump (Fisher Scientific, Pittsburgh, USA).
7. Needle (20 gauge).
8. Small scissors, fine scissors, clamps and tweezers (EMS).

2.3 Brain Sectioning

1. Vibrating microtome (Vibratome, Leica).
2. Double-edge stainless steel razor blades (EMS).
3. Instant glue.
4. Buffer: 0.1 M PB, pH7.4.
5. Twenty-four-well culture plate.
6. Paintbrush (size 0–1) to transfer sections.

2.4 Cryofixation

Cryofixation can be used as an alternative to or in combination with chemical fixation, and its major goal is to immobilise molecules and stop metabolic activities in the cell. Several cryofixation techniques can be used for brain tissue: slam-freezing (also known as cold metal block freezing), plunge freezing, propane jet freezing and high-pressure freezing. In all procedures, the freezing must achieve very rapid cooling rates so as to minimise damage to the sample caused by ice crystal formation. To ensure high-quality preservation of brain tissue, we used cryofixation with slam-freezing in combination with freeze-substitution and Lowicryl resin embedding. Currently, high-pressure freezing is considered as the most reliable method of cryofixation and can also be combined with freeze-substitution. The description on how to perform high-pressure freezing is described in Chap. 17.

1. Freezing apparatus (Leica EM CPC; Leica, Vienna, Austria).
2. Buffer: 0.1 M PB, pH7.4.
3. Cryoprotectant solutions: sucrose 1 M and 2 M in 0.1 M PB.
4. Liquid nitrogen.
5. Paintbrush (size 0–1) to transfer sections.

2.5 Freeze-Substitution

Once frozen, the brain tissue is transferred from the cryofixation unit to the freeze-substitution unit. During freeze-substitution, water within the frozen samples is gradually substituted with pure methanol at −80 °C, and then brain sections are gradually warmed and embedded in acrylic resin (*see* **Note 1**). Even though the tissue may have been previously chemically fixed by perfusion, the freeze-substitution step reduces the harmful effects that the dehydration and embedding reagents have on antigenicity preservation.

1. Automatic freeze-substitution machine (AFS; Leica, Vienna, Austria).
2. Dry absolute methanol.

3. Liquid nitrogen.
4. 0.5 % Uranyl acetate in dry absolute methanol. This solution is slow to dissolve, and it should be prepared at least 30 min before use. Light sensitive, so during preparation of the solution, enwrap the bottle of flask with aluminium foil. Protect from light to prevent the precipitation of uranyl acetate during incubation and filter before use. Very toxic, so always wear protective clothing and gloves and handle in a fume hood.
5. Lowicryl HM20 resin (EMS) (*see* **Note 2**). Lowicryl HM20 resin has three components: Crosslinker D, Monomer E and Initiator C. The resin is prepared by weighing 2.98 g of Crosslinker D and 17.02 g of Monomer E and mixing gently by bubbling a continuous stream of dry nitrogen gas into the mixture with a disposable glass pipette. Add 0.1 g of Initiator C to the final solution and mix again gently in the same way. Humidity will interfere with the polymerisation of the resin. Avoid inhaling the vapours from the Lowicryl resin, as they are toxic. Wear protective clothing and gloves, and use a well-ventilated fume hood for mixing the components of the resin.

2.6 Processing Sections for Electron Microscopy

Post-embedding immunohistochemistry of brain tissue at the light microscopic level involves postfixation with osmium tetroxide and embedding in epoxy resin.

1. Buffers: 0.1 M PB, pH 7.4.
2. Osmium tetroxide (OsO_4, Sigma-Aldrich): 1 % in 0.1 M PB, pH 7.4 (*see* **Note 3**).
3. 1 % Uranyl acetate in Milli-Q water. The incubation of sections with uranyl acetate before dehydration, also known as en bloc staining, improves their contrast when examined at the electron microscope. Protect from light to prevent the precipitation of uranyl acetate during incubation. Very toxic, so always wear protective clothing and gloves and handle in a fume hood.
4. Graded series of ethanol in water (50, 70, 90, 95 and 100 %) for dehydration.
5. Dry absolute ethanol: absolute ethanol with anhydrous cupric sulphate.
6. Propylene oxide (EMS). It is extremely toxic by contact with the skin, inhalation and ingestion and also volatile and flammable. Do not wear protective gloves, as it will dissolve them, and handle in a fume hood.
7. Epoxy resin: Durcupan ACM (Sigma-Aldrich). Prepare the epoxy resin by weighing 10 g of component A, 10 g of component B, 0.3 g of component D and 0.3 g of component C, in a disposable plastic beaker always following this order A:B:D:C. Mix thoroughly with a disposable plastic pipette in

order to obtain satisfactory results. The bubbles that form during this mixing process will rise to the surface in 5–10 min. If other amount of epoxy resin is needed, follow the ratio 10:10:0.3:0.3 g. This ratio allows obtaining a Durcupan epoxy resin of medium hardness. Unused epoxy resin can be stored for several months at –20 °C, but it is recommended to use freshly prepared mixture. Resin waste should be collected in a disposable beaker and allowed to polymerise at 60 °C for 24 h before disposal.

8. Oven, to polymerise the epoxy resin.
9. Adhesive labels.
10. Paintbrush or toothstick.
11. Glass slides and coverslips.
12. Polyethylene moulds for embedding samples for electron microscopy (EMS).

2.7 Coating Slides with Gelatine and Semithin Sectioning

1. Gelatine-coating solution: to prepare 1 L of gelatine-coating solution, pour 1 L of deionised water in a beaker. Place the beaker a hot plate with a stir bar at medium speed and add 5 g of gelatine; temperature of the heating should not exceed 45 °C. After the gelatine has dissolved, add 0.5 g of chromium potassium sulphate [$CrK(SO_4)_2$]. Then, filter the solution and allow cooling down at room temperature before use.
2. Filters.
3. Glass slides.
4. Hot plate and magnetic stirrer.
5. Slide racks.
6. Staining dishes.
7. Thermometer.
8. Diamond knife (Diatome, Biel, Switzerland).
9. Glass knifemaker (Leica EM KMR3).
10. Glass knifes (EMS).
11. Slide storage box (EMS).
12. Toluidine blue solution: 0.5 % toluidine blue and 1 % sodium borate in distilled water. Filter before use and store at room temperature.

2.8 Ultrathin Sectioning of Lowicryl-Embedded Tissue

When sectioning Lowicryl resins, well polymerised tissue blocks of HM20 behave much like tissue blocks of epoxy resins and, therefore, will section easily. However, if the Lowicryl resin is not properly polymerised, sectioning becomes difficult and, in addition, the resulting sections can break up during the immunolabelling step.

1. Ultramicrotome (Leica, Vienna, Germany).
2. Diamond knife (Diatome, Biel, Switzerland).

3. Glass knifemaker (Leica EM KMR3).
4. Glass knifes (EMS).
5. Pioloform-coated single-slot nickel grids (EMS) (*see* **Note 4**).
6. Forceps to handle grids (EMS).
7. Grid storage box (EMS).

2.9 Immunolabelling Semithin Sections: Post-embedding HRP

This procedure involves cutting semithin sections (0.5–2 μm-thick) from epoxy resin-embedded tissue blocks and collecting them on glass slides, followed by etching of the resin and removal of osmium tetroxide, before performing immunohistochemical reactions, dehydration and covering slides with coverslips.

1. Buffers: (a) 0.05 M TBS, pH7.4; (b) TBS containing 0.1 % Triton X-100 (TBST).
2. Sodium ethanolate (*see* **Note 5**). Filter before use. Perform this step in darkness, as the solution is light sensitive.
3. Sodium meta-periodate ($NaIO_4$). Prepare a 1 % solution of sodium meta-periodate in distilled water (*see* **Note 6**).
4. Human serum albumin (HSA; supplied as powder, Sigma) (*see* **Note 7**). Can be stored at 4 °C.
5. Monoclonal or polyclonal primary antibodies.
6. Biotinylated secondary antibodies (Vector Laboratories): working dilution of 1:200 in TBS.

2.10 Immunolabelling Ultrathin Sections: Post-embedding Immunogold

This procedure involves cutting ultrathin sections (70–100 nm-thick) from Lowicryl resin-embedded tissue blocks and collecting them on pioloform-coated single-slot nickel grids, before performing immunohistochemical reactions.

1. Buffers: (a) 0.05 M TBS, pH7.4; (b) TBS containing 0.1 % Triton X-100 (TBST).
2. Human serum albumin (supplied as powder, Sigma). Can be stored at 4 °C.
3. Monoclonal or polyclonal primary antibodies.
4. Secondary antibodies conjugated with colloidal gold. In case of single-labelling experiments, use secondary antibodies conjugated to 10 nm colloidal gold particles. If double is required, also use secondary antibodies conjugated to 5 nm or 15 nm colloidal gold particles. As secondary antibodies conjugated to smaller gold particles yield higher immunogold labelling, this bias should be considered for the combination of molecules and gold particle diameters in double labelling.

2.11 Staining of Ultrathin Sections

Non-osmicated tissue processed by cryofixation and freeze-substitution and embedded in Lowicryl HM20 exhibits low contrast in the electron microscopic level. Therefore, it is always

necessary to counterstain using heavy metal solutions to improve contrast. The most commonly used methodology for the post-embedding immunogold technique involves the use of uranyl acetate followed by Reynold's lead citrate.

1. Uranyl acetate: 5 % solution in 40 % ethanol. Filter before use. Follow safety notes described in Sect. 2.3. The use of this solution before staining with Reynold's lead citrate is very effective to get images with high contrast.
2. Reynolds's lead citrate solution. Store at 4 °C. Wear protective gloves.

   Prepare lead citrate solution by weighing 0.133 g lead nitrate ($Pb(NO_3)_2$) and 0.176 g tri-sodium citrate ($Na_3C_6H_5O_7$). Add 4.8 mL of double-distilled water to the lead nitrate and shake vigorously to dissolve. Add the tri-sodium citrate to the lead nitrate solution and shake gently until a milky suspension is formed. Immediately, add 0.2 mL 4 M NaOH and mix well until the solution becomes totally clear. Note that sodium carbonate is formed when the lead citrate solution is exposed to air. Transfer the solution to a 10 mL glass bottle with a screw cap bottle for storage and wrap it with aluminium foil.
3. Sodium hydroxide pellets (Sigma-Aldrich).
4. Laboratory film (e.g. Parafilm).

3 Methods

3.1 Tissue and Fixation

1. Fix the brain by perfusion fixation.
2. Set up peristaltic pump. Place open end of tubing into the beaker of saline and fixative solution (in ice). Fill both tubes, but fill the common tube entirely with only saline. Avoid air bubbles in any of the tubes. The volume of fixative solution should be scaled to size of animal.
3. Deep anaesthesia of the animal by intraperitoneal injection of ketamine-xylazine 1:1 (0.1 mL/kg b.w.). Allow a few minutes for anaesthesia to occur, indicated by the loss of reflex responses. For instance, pinch the toes to judge the level of response to painful stimulus.
4. Place the animal on its back on a styrofoam or cork board and pin out all four limbs at the feet using small needles.
5. Cut the skin just below the diaphragm with a small scissors to expose the liver. Cut the rips laterally and bend the chest backward and fix it with a clamp to allow an easy access to the heart. Once the chest is opened, the animal can no longer breathe, and therefore, all following steps should be carried on

as quickly as possible. The lack of oxygen (anoxia) causes bad preservation of the ultrastructure and may compromise antigenicity.

6. Remove any excess of adipose or connective tissue on the heart. Separate the thymus with a small spatula and make sure that ascending aorta is visible.
7. Make a small cut in the left ventricle using a fine scissors.
8. Place a blunt needle connected to the end of the tubing into the left ventricle or the ascending aorta. Secure needle by clamping in place near the point of entry in the heart and turn on peristaltic pump. Then immediately cut the right atrium using a fine scissors. In small rodents like mice and neonatal pups, 25G sharp needle is inserted to the left ventricle.
9. Perfuse the animal with saline for 1 min or until the liver has got a lightened coloration and blood has been cleared from the animal body. At this point, switch to the fixative solution and perfuse 2–3 volumes of the body weight for 10 min. Check tail and neck flexibility as good indicators to know how well the animal is being fixed; a well-fixed animal should have stiff tail and neck. Note that excessive saline perfusion or prolonged time from chest opening to the onset of perfusion will cause hypoxic changes in subcellular structures, such as the stacking of the smooth endoplasmic reticulum in neuronal dendrites and somata.
10. Turn off the peristaltic pump. The animal should be stiff at this point. Cut the head, remove brain from the skull and wash in 0.1 M PB, pH7.4.
11. After completion of perfusion, the animal carcass should be wrapped and placed in a plastic bag in a freezer until properly disposed of in the animal house facility.
12. The brain is washed thoroughly in PB during 2 h before sectioning

3.2 Sectioning of the Brain

1. Cut brain areas of interest into blocks. Wash blocks four times for 15 min each with 0.1 M PB, pH7.4.
2. Mount and stick one brain hemisphere or a tissue block on the vibratome's specimen holder using the fast glue.
3. Fill the vibratome reservoir with 0.1 M PB and cut: (1) 50–70-μm thick sections for epoxy resin embedding and (2) 400-μm thick sections for Lowicryl resin embedding.
4. Collect the sections with a brush, and place each section into a well of the 24-well plate containing 0.1 M PB.
5. Store sections in 0.1 M PB at 4 °C (*see* **Note 8**).

3.3 Cryofixation

1. Wash freshly fixed tissue 4 times for 15 min each in 0.1 M PB, pH7.4.
2. Place sections (400 μm thickness, cut with a vibratome) in cryoprotectant solutions of 1 M sucrose, until they sink, and then in 2 M sucrose, overnight at 4 °C (*see* **Note 9**).
3. Switch on Leica EM CPC and fill dewars with liquid N_2. Carry out the slam-freezing of the sections, following manufacturer's instructions.

3.4 Freeze-Substitution

1. Fill the freeze-substitution machine (Leica AFS) with liquid nitrogen.
2. Choose the appropriate settings (time and temperature) for the different steps. In order to program and to operate the machine, follow the manufacturer's instructions.
3. Place all the holders and substitution media into the machine to reach the working temperature and wait until the machine has equilibrated –80 °C.
4. Place frozen sections in the chamber of the freeze-substitution machine. All following steps are carried out in this machine.
5. Place sections in 0.5 % uranyl acetate in dry absolute methanol at –80 °C overnight.
6. Wash four times for 2 h each with dry absolute methanol at –80 °C.
7. Warm from –80 to –50 °C at 10 °C/h in the AFS machine in the evening.
8. Resin infiltration: infiltrate with a mixture of dry methanol: Lowicryl HM20 (1:1) for 2 h.
9. Change to a mixture of dry methanol:Lowicryl HM20 (1:2) for 2 h.
10. Infiltrate in pure Lowicryl HM20 for 2 h. Leave in pure Lowicryl HM20 overnight at –50 °C.
11. Embedding process: transfer the sections into freshly prepared Lowicryl HM20 resin in embedding moulds at –50 °C.
12. Start UV light polymerisation for 48 h at –50 °C.
13. Warm from –50 to 18 °C at 10 °C/h under continuous UV irradiation, and continue UV polymerisation at 18 °C for 24 h.
14. Remove the tissue blocks from moulds, label blocks and store them at room temperature.

3.5 Processing Sections for Electron Microscopy

1. Wash the sections 3 times for 15 min each with 0.1 M PB.
2. Postfix the sections with 1 % osmium tetroxide in 0.1 M PB for 30 min.

3. Wash the sections 5 times for 8–10 min each with 0.1 M PB to remove all traces of osmium and then wash once for 8–10 min with distilled water.
4. Stain with 1 % uranyl acetate solution in distilled water for 30 min.
5. Dehydrate the sections with 50, 70, 90, 95 and 100 % ethanol for 10–15 min each and then 100 % dry ethanol for 10–15 min.
6. Propylene oxide twice for 10–15 min each. Use glass pipettes, as propylene oxide dissolve plastic pipettes.
7. Infiltration in epoxy resin (e.g. Durcupan) for 4 h and flat-embedding.
8. Polymerise the resin by heating in an oven at 60 °C for 48 h.
9. With the unused epoxy resin, fill the polyethylene moulds (capsules) up to the top and place in an oven at 60 °C for 24 h for polymerisation.

3.6 Coating Slides with Gelatine and Semithin Sectioning

1. Pour the gelatine-coating solution into a large staining dish, which will be used for dipping the slides.
2. Place the glass slides into the staining racks. Use clean, dry slides. To achieve that, wash slides in hot soapy water and rinse them thoroughly in tap water, followed by deionised water.
3. Dip the racks of slides into the gelatine-coating solution for about 2 min. To shake off any air bubbles on the slides, agitate the slide rack gently. Then, remove the racks slowly from the gelatine-coating solution, protect them from dust and allow slides to dry in the racks overnight in a 40–50 °C oven.
4. Remove the slides from the racks and place them in slide boxes and store at room temperature until use.
5. Mark several circles with a diamond pencil on the reserve side of the gelatine-coated slides. These marks will help identify later positioning of semithin sections.
6. To obtain semithin sections from the epoxy resin-embedded tissue blocks, place the block in an ultramicrotome and trim the area of interest with a single-edge razor blade.
7. Fit the block into the ultramicrotome, align the block face with a glass knife and remove the empty resin from the top of the sample using a glass knife. Then change to a diamond knife.
8. Cut semithin sections (0.5–2 μm thickness) with the ultramicrotome.
9. Transfer sections to droplets of distilled water overlaying the scored circles on the gelatine-coated slides. Place one semithin section in each scored circle.
10. Place slides on a hot plate to dry up.

3.7 Ultrathin Sectioning

1. Observe the Lowicryl HM20 blocks with a stereomicroscope and carefully trim them with a single-edge razor blade.
2. Fit the block into the ultramicrotome and align the block face with a glass knife.
3. Remove the empty resin from the top of the sample using a glass knife. Then change to a diamond knife.
4. Prepare semithin sections (0.5–2 μm thickness) with a glass knife. Follow the same steps as described in Sect. 3.6.
5. Stain the semithin sections with a toluidine blue solution and then examine with the light microscope (*see* **Note 10**).
6. Cut ultrathin sections (60–80 nm thickness) with the ultramicrotome.
7. Collect one to a few sections on pioloform-coated slot nickel grids and let dry. Store the grids in a grid box.

3.8 Post-embedding on Semithin Sections

1. Place glass slides containing the semithin sections in a coplin jar.
2. Immerse slides in sodium ethanolate at room temperature for 40 min.
3. Drain well and wash slides 3 times for 5 min each with absolute ethanol.
4. Wash slides 3 times for 5 min each with distilled water.
5. Pre-treat epoxy semithin with 1 % sodium meta-periodate in distilled water for 7 min.
6. Wash slides 3 times for 5 min each with distilled water.
7. Wash slides twice times for 5 min each with TBS 0.05 M, pH7.4.
8. Dry slides around the semithin sections with filter paper and place slides flat in a humid chamber (*see* **Note 11**).
9. Block nonspecific binding by applying drops of 10 % normal serum of appropriate species in TBS containing to the semithin sections for 1 h.
10. Apply drops of primary antibody diluted in TBS containing 1 % normal serum to the semithin sections and incubate overnight at 4 °C.
11. Wash slides 3 times for 10 min each with TBS.
12. Apply drops of in biotinylated secondary antibody in TBS containing 1 % normal serum to the semithin sections and incubate for 2 h at room temperature.
13. Wash slides 3 times for 10 min each with TBS. Make up avidin-biotin-peroxidase (ABC) during this step, as the solution needs to be prepare 30 min before use.
14. Incubate semithin sections in ABC in TBS for 2 h at room temperature.

15. Wash slides twice for 10 min each with TBS. Then, rinse slides once with TB for 10 min.
16. Incubate slides for 15 min in coplin jars in a solution of 0.05 % 3,3′-diaminobenzidine tetrahydrochloride (DAB, Sigma-Aldrich) in TB at room temperature. The solution is light sensitive. Very toxic, so always wear protective clothing and gloves, and handle in a fume hood.
17. Add 0.01 % hydrogen peroxide (H_2O_2) to the DAB solution. For instance, add 500 μL 1 % H_2O_2 to 50 mL of 0.05 % DAB. Incubate for around 6 min.
18. Wash slides 3 times for 10 min each with distilled water.
19. Add 4 drops of 4 % OsO_4 in distilled water and then wash slides 4 times for 10 min each with distilled water.
20. Dehydration: place slides in 50 % ethanol, 70 % ethanol, 90 % ethanol, 95 % ethanol, 100 % ethanol and dry absolute ethanol for 10 min each step.
21. Clearing: two changes in xylene for 10 min each.
22. Mount with standard light microscopy mounting medium (for instance, DPX).
23. Examine sections in a light microscope. Figure 1 shows examples of immunolabelling for the neurotransmitter GABA in the mouse cerebellum by post-embedding immunoperoxidase at the light microscopic level.

3.9 Post-embedding on Ultrathin Sections

1. Place grids, sections down, on drops of filtered blocking solution consisting of 2 % HSA in TBST for 30 min at room temperature.
2. Place grids in drops of primary antibody in filtered TBST with 2 % HSA at 27 °C overnight. If double labelling is required, prepare a cocktail of the two primary antibodies raised in different species in filtered TBST with 2 % HAS and place grids in drops of antibodies' solution at 27 °C overnight.
3. Wash grids 3 times for 15 min each with TBST. To do the first wash, pick up each grid with forceps and dip it in three small vials of filtered TBST. Excess buffer is dried off the forceps and grids with filter paper. The second and third washes are performed on drops of filtered TBST.
4. Place grids in drops of 2 % HSA in TBST for 10 min at room temperature.
5. Place grids in drops of 10 nm gold-conjugated secondary antibody (*see* **Note 12**) diluted 1:10 in TBST with 2 % HSA for 2 h at room temperature. If double labelling is required, prepare a cocktail of the two secondary antibodies conjugated with 10 nm and 15 nm colloidal gold, both diluted 1:10 in TBST with 2 % HSA for 2 h at room temperature.

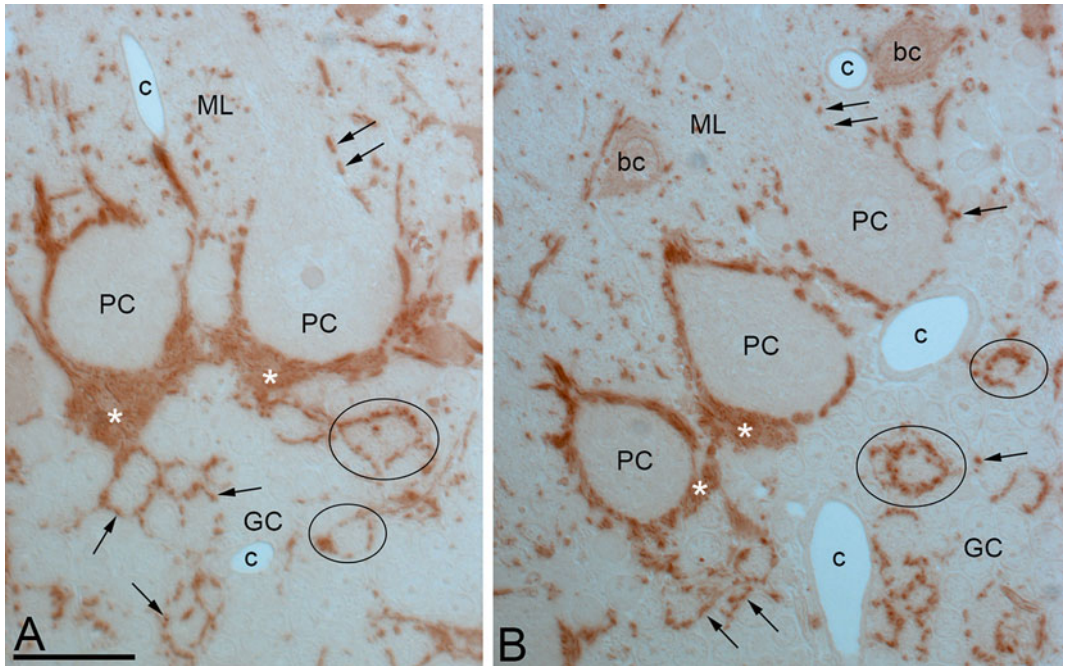

Fig. 1 Immunoreactivity for GABA on coronal semithin sections (0.5 μm) from the adult cerebellar cortex using a post-embedding immunoperoxidase method at the light microscopic level. (**a**, **b**) GABA-positive cell bodies, corresponding to basket cells (*bc*), appear in the molecular layer (*ML*) above Purkinje cells (*PC*). Numerous GABA-positive varicosities are observed in the surrounding neuropil (*arrows*). Numerous puncta immunolabelled for GABA were also seen, particularly in pinceau-like structures (*white asterisk*) around the somata of Purkinje cells. In the granule cell layer, immunolabelling for GABA was intense in cerebellar glomerulli (e.g. *black circles*), corresponding to the expression of the neurotransmitter in the axon terminals of Golgi cells. Abbreviations: *c* capillary, *GC* granule cell layer, *ML* molecular layer, *PC* Purkinje cell layer. Scale bar, 20 μm

6. Wash grids 4 times for 10 min each in TBS. For the first wash, pick up each grid and dip it in three small vials of filtered TBS. The second, third and fourth washes are performed on drops of filtered TBS.
7. Let grids dry at room temperature.

3.10 Staining of Ultrathin Sections

1. Prepare 5 % uranyl acetate in 40 % ethanol.
2. Prepare the lead citrate solution (*see* Sect. 2.9).
3. Take a glass Petri dish with a piece of laboratory film and place tissue paper soaked in water around the edge of the dish to form a humidity chamber.
4. Place grids in a uranyl acetate solution for 90 s at room temperature and in darkness.
5. Rinse grids 3 times for several seconds each in double-distilled water. To do the first wash, pick up each grid with forceps and dip it in three small vials of double-distilled water. Excess buffer is dried off the forceps and grids with filter paper. The second

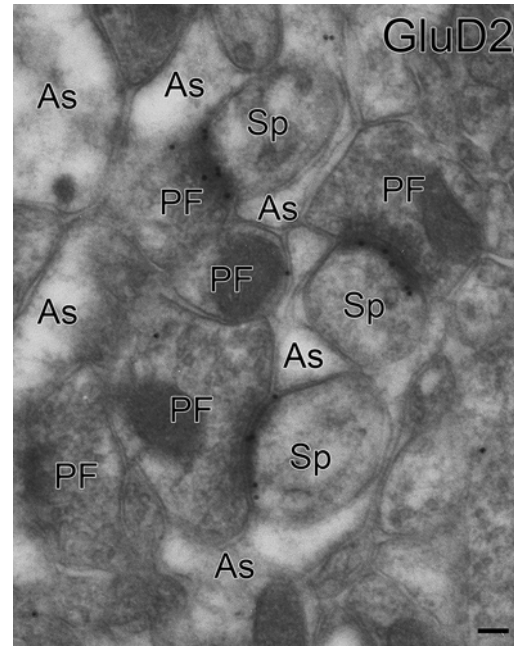

Fig. 2 Electron micrographs showing glutamate receptor GluD2 in the cerebellar cortex. Note that immunogold particles are selectively deposited in the postsynaptic density of Purkinje cell spines (*Sp*) in contact with parallel fibre terminals (*PF*) (This picture was provided from Dr. K. Konno in Hokkaido University Graduate School of Medicine, Japan). *As* astrocytic processes. Scale bar, 100 nm

and third washes are performed on drops of double-distilled water. Let grids dry at room temperature.

6. Take a plastic or glass Petri dish with a piece of laboratory film and place a few sodium hydroxide pellets in one of the sides. Sodium hydroxide reduces the formation of sodium carbonate (an insoluble electrondense precipitate) when the lead citrate solution is exposed to air during the next steps.
7. Take up the lead citrate solution with a Pasteur pipette, placing individual drops on the laboratory film.
8. Place grids with ultrathin section down on the drops of the lead citrate solution. Leave for 1.5–3 min.
9. Wash the grids 3 times for several seconds each in double-distilled water. Follow the same procedure as described in step number 4.
10. Blot the bottom of the grid with filter paper and place and then allow grids to dry at room temperature. Place grids in a grid box.
11. Examine sections in a transmission electron microscope. Figures 2 and 3 show examples of immunolabelling for glutamate receptor GluD2 at parallel fibre-Purkinje cell synapses

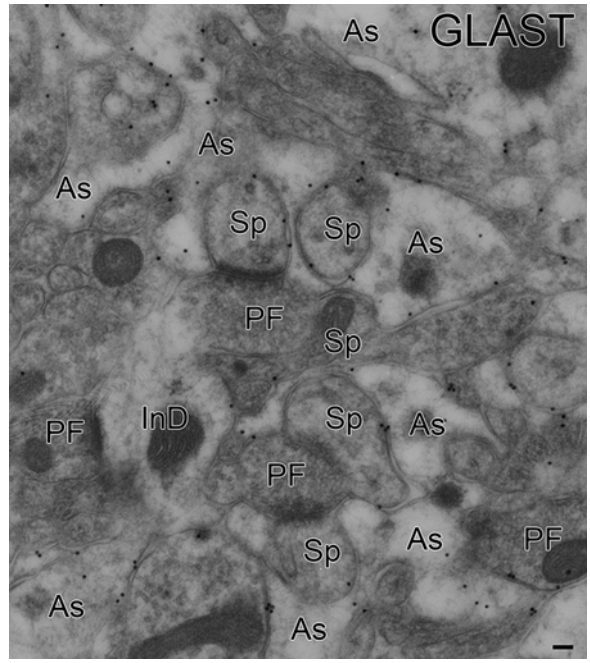

Fig. 3 Electron micrographs showing glutamate transporter GLAST in the cerebellar cortex. Note that immunogold particles are selectively deposited on the cell membrane of astrocytic processes (*As*) enwrapping various neuronal elements. *InD* interneuron dendrite, *PF* parallel fibre terminal, *Sp* Purkinje cell spine (This picture was provided from Dr. K. Konno in Hokkaido University Graduate School of Medicine, Japan). Scale bar, 100 nm

and for glutamate transporter GLAST on Bergmann glia, respectively, in the mouse cerebellum by single-labelling post-embedding immunogold techniques.

3.11 Controls

The controls of experiment that confirm the sensitivity (positive controls) and specificity (negative controls) are of practical importance. For those who are not familiar with post-embedding immunohistochemistry, positive controls are essential to test whether and confirm that materials and methods adopted are working. To this end, post-embedding immunohistochemistry is applied to model molecules which have been demonstrated to be well suited for this technique, such as postsynaptic molecules PSD-95 and GluD2 and astroglia-specific molecule GLAST (Figs. 2 and 3), using primary antibodies that have been validated in previous studies. Once selective signals are obtained in specific cellular and subcellular elements, the factors that influence the sensitivity, such as the choice of fixatives and antibodies and the condition of incubations, can be optimised first using model molecules and then for molecules of interest.

Negative controls are essential to validate the authenticity of yielded signals. The best negative control is achieved by negative labelling in mutant animal models defective in the genes of interest. However, such knockout animals and tissues are not always available or obtainable. In such instances, one should test by second-best negative controls, as described in Chap. 1 (3.5. Specificity tests).

4 Notes

1. Great care must be taken when selecting the most appropriate embedding resin for post-embedding immunohistochemistry. There are many resins available and only a few of them have proved useful for post-embedding immunogold techniques. Resins can be broadly categorised as water immiscible (for instance, epoxy resins like Durcupan, Epon, Araldite and Spurr) and water miscible (for instance, acrylic resins like the Lowicryls, LR White and LR Gold), each having advantages and disadvantages. Epoxy resins are not often used for immunoelectron microscopy because heating is required for resin polymerisation and this step can compromise the detection of the epitopes. However, some epitopes survive heating (for instance, amino acids such as GABA, glutamate or glycine), and thus, some antibodies do remain active in these resins. The most widely used resins to detect most antigens using post-embedding immunogold techniques are acrylic resins, particularly Lowicryls. For instance, Lowicryl resin, such as HM20, is a hydrophilic acryl resin having a low viscosity that is an advantage to infiltrate into the tissue. It is a low-temperature cured resin that can be polymerised at −50 °C under UV irradiation, thus minimising the lost of antigenicity during embedding.
2. Lowicryl resins consist of four variants (K4M, HM20, K11M and HM23), which differ in their hydrophobic and hydrophilic properties and the temperature at which they freeze. These acrylic resins provide improved antigenicity preservation over epoxy resins for the high-resolution localisation of neurotransmitter receptors using post-embedding immunohistochemistry. The most commonly used acrylic resin for receptor/ion channel localisation is Lowicryl HM20. Another acrylic resin giving good results for post-embedding immunohistochemistry is Unicryl (BioCell International).
3. Osmium tetroxide is very toxic and volatile, so always wear protective clothing and gloves, and handle in a fume hood. The solution can be stored at 4 °C for several weeks. The used osmium solutions should be disposed of properly. For convenience and safety in the laboratory, aqueous solutions of

osmium tetroxide in sealed glass 2 mL ampoules can be purchased. In addition, osmium tetroxide can be supplied in the form of crystals in sealed ampoules. In such case, ampoules and all glass items contacting osmium should be scrupulously clean using soap and water. Prepare a stock solution of 4 % osmium tetroxide in double-distilled water by opening a 1 g ampoule of osmium tetroxide and dissolving it in 25 mL of double-distilled water. The osmium tetroxide is slow to dissolve, so make sure to prepare the stock solution at least 24 h in advance. Place the vial containing the osmium stock solution inside a second container, seal it and store in a fume hood in darkness. Finally, a working fixative solution (1 % in 0.1 M PB) is prepared just before use.

4. For post-embedding immunogold, nickel grids are recommended to copper grids, since nickel is inert and have high resistance to chemical damage when immuno or enzyme solutions are used during incubations. However, the magnetic properties of nickel grids can be very annoying when handling and produces astigmatism in the transmission electron microscope. In such cases, non-magnetic forceps are needed to handle grids, and a demagnetising coil is required to demagnetise the nickel grids. On the other hand, grids coated with a plastic support film such as Pioloform are essential due to the fragility of Lowicryl resin sections and because they are subjected to many washings in the process of immunolabelling and contrasting.
5. Sodium ethanolate (also known as ethanolic NaOH) is used to remove epoxy resin from the semithin sections, allowing full accessibility of all immunoreagents to the antigen. We use a saturated solution of sodium ethanolate, which is prepared by mixing 50 g of NaOH with 300 mL of absolute ethanol in a bottle. Wrap the bottle with a black bag or simply leave the solution in the dark for several days until it turns brown before use. The degree of epoxy resin removed by sodium ethanolate depends on the incubation time, and therefore, we recommend performing some trials. To avoid poor structure preservation and ultimately destruction of the tissue, do not do incubate semithin sections long periods. Note that this etching treatment substantially lowers the antigenicity in some cases.
6. Sodium meta-periodate is an oxidising agent, always used prior to incubation with the primary antibodies, that removes osmium tetroxide (OsO_4) from the semithin and/or ultrathin sections, thus allowing some antibodies to recognise their antigens on osmicated, epoxy resin tissue.
7. Human serum albumin can be replaced with fish gelatin, ovalbumin or non-fat dried milk to prevent nonspecific immunolabelling.

8. To avoid degradation of antigens, we recommend cutting tissue blocks immediately after fixation-perfusion and use fresh sections for better result in the post-embedding techniques. Tissue sections that are left on the bench at room temperature rapidly dampen antigenicity and ultrastructure preservation, and factors like heat, drying or exposure to ultraviolet light contribute to this deterioration.
9. The cryoprotection step for freeze-substitution can also be carried out by placing sections in 10, 20, or 30 % glycerol in 0.1 *M* Tris-maleate buffer, pH 7.4, overnight [1]. The choice of whether to use glycerol instead of sucrose in the cryoprotection solution depends on the nature of the antigen. It is recommended to do trials, first using cryoprotection with 2 *M* sucrose. If the preservation of antigenicity is not appropriate, then cryoprotection with glycerol can be used instead.
10. Examination of semithin sections is important to assess the quality of fixation, to orient the tissue and to select the constituents to be investigated with the electron microscope. Cells fixed well are darkly stained with the toluidine blue solution compared to those fixed incompletely.
11. To maintain humidity in the humid chamber, place filter paper soaked in water around the edge of the chamber and keep it closed and sealed whenever possible.
12. Gold particles of 10 nm size are easy to visualise on the ultrathin sections at the electron microscope level. Gold particles of a bigger size (e.g. 15 or 20 nm, up to 40 nm) are also available that are easier to visualise at electron microscope level but appear to provide less sensitivity to the post-embedding method. For double-labelling experiments, it is recommended to use a combination of 5 nm and 10 nm (or 10 nm and 15 nm) size gold particles. Owing to the low sensitivity of the post-embedding immunogold method, we may add polyethyleneglycol (5 mg/mL), which dissolves lipids, to the final solution to facilitate the penetration of the 10 nm colloidal gold secondary antibodies and therefore to improve immunolabelling in our ultrathin sections.

Acknowledgements

This work was supported by the grant BFU-2012-38348 and the grant CONSOLIDER CSD2008-00005 from the Spanish Ministry of Education and Science, by grant PPII-2014-005-P from the Junta de Comunidades de Castilla-La Mancha and by grant HBP-604102 from the European Union. We thank Dr. Kohtarou Konno for his help to this chapter.

References

1. Nusser Z, Luján R, Laube G, Roberts JDB, Molnar E, Somogyi P (1998) Cell type and pathway dependence of synaptic AMPA receptor number and variability in the hippocampus. Neuron 21:545–559
2. Landsent AS, Amiri-Moghaddam M, Matsubara A et al (1997) Differential localization of δ glutamate receptors in the rat cerebellum: coexpression with AMPA receptors in parallel fiber-spine synapses and absence from climbing fiber-spine synapses. J Neurosci 17:834–842
3. Matsubara A, Laake JH, Davanger S, Usami S, Ottersen OP (1996) Organization of AMPA receptor subunits at a glutamate synapse: a quantitative immunogold analysis of hair cell synapses in the rat organ of Corti. J Neurosci 16:4457–4467
4. Luján R, Nusser Z, Roberts JDB, Shigemoto R, Somogyi P (1996) Perisynaptic location of metabotropic glutamate receptors mGluR1 and mGluR5 on dendrites and dendritic spines in the rat hippocampus. Eur J Neurosci 8: 1488–1500
5. Ballesteros-Merino C, Lin M, Wu WW, Ferrandiz-Huertas C, Cabañero MJ, Watanabe M, Fukazawa Y, Shigemoto R, Maylie J, Adelman JP, Luján R (2012) Developmental profile of SK2 channel expression and function in CA1 neurons. Hippocampus 22:1467–1480
6. Pérez-Otaño I, Luján R, Tavalin SJ, Plomann M, Modregger J, Liu X-B, Jones EG, Heinemann SF, Lo DC, Ehlers MD (2006) Endocytosis and synaptic removal of NR3A-containing NMDA receptors by PACSIN1/syndapin1. Nat Neurosci 9:611–621
7. Fernández-Alacid L, Watanabe M, Molnar E, Wickman K, Luján R (2011) Developmental regulation of G protein-gated inwardly-rectifying (GIRK/Kir3) channel subunits in the brain. Eur J Neurosci 34:1724–1736
8. Takumi Y, Ramirez-Leon V, Laake P, Rinvik E, Ottersen OP (1999) Different modes of expression of AMPA and NMDA receptors in hippocampal synapses. Nat Neurosci 2: 618–624
9. Ragnarson B, Ornung G, Ottersen OP, Grant G, Ulfhake B (1998) Ultrastructural detection of neuronally transported choleragenoid by post-embedding immunocytochemistry in freeze-substituted Lowicryl HM20 embedded tissue. J Neurosci Methods 80:129–136
10. Allen D, Nakayama S, Kuroiwa M, Nakano T, Palmateer J, Kosaka Y, Ballesteros C, Watanabe M, Bond CT, Luján R, Maylie J, Adelman JP, Herson PS (2011) SK2 channels are neuroprotective for ischemia-induced neuronal cell death. J Cereb Blood Flow Metab 31: 2302–2312

Chapter 17

High-Resolution Localization of Membrane Proteins by SDS-Digested Freeze-Fracture Replica Labeling (SDS-FRL)

Harumi Harada and Ryuichi Shigemoto

Abstract

Visualizing molecular localization at high resolution contributes to understanding of their functions and roles in physiological and pathological conditions. Sodium dodecyl sulfate-digested freeze-fracture replica labeling (SDS-FRL) is a powerful electron microscopy method to study high-resolution two-dimensional distribution of transmembrane proteins and their tightly associated proteins on platinum-carbon replica. During treatment with SDS, unfixed proteins and intracellular organelle are dissolved and integral membrane proteins captured and stabilized by carbon and platinum deposition are denatured, retaining most of their antigenicity, and exposed on exoplasmic and protoplasmic surfaces of lipid monolayers. The exposure of these antigens on the surface of replica facilitates the accessibility of antibodies and therefore provides higher labeling efficiency than those obtained with other immunoelectron microscopy techniques. In this chapter, we describe the protocols of SDS-FRL adapted for mammalian brain samples and an additional procedure for fluorescence-guided electron microscopy for replica immunolabeling.

Key words Freeze-fracture replica, SDS, Immunogold labeling, Integral membrane proteins, Electron microscopy

1 Introduction

The SDS-FRL, sodium dodecyl sulfate-digested freeze-fracture replica labeling technique was invented by Fujimoto in 1995 to study two-dimensional distribution of integral membrane proteins and lipids in cellular membranes [1]. The original technical concept of low-temperature replica method for electron microscopy (EM) was reported in the 1950s and developed into freeze-fracture replica method in the 1960s to obtain the faithful structure of living cells [2, 3]. However, the identification of each cellular profile solely on the basis of morphological features of fractured face of the replica was often difficult in complex tissues such as the brain because fracture occurs randomly. The SDS-FRL enables us to identify various cellular profiles under the electron microscope by

Rafael Luján and Francisco Ciruela (eds.), *Receptor and Ion Channel Detection in the Brain: Methods and Protocols*, Neuromethods, vol. 110, DOI 10.1007/978-1-4939-3064-7_17,

immunogold labeling for marker proteins. We have modified this technique for brain samples and successfully visualized molecules in identified cellular components at high resolution [4–8]. We also found that SDS-FRL empowers us to quantify the number of receptors and ion channels with high labeling efficiencies that are close to 100 % [4, 8]. This chapter describes the protocol of SDS-FRL adapted for mammalian brain samples, which we routinely use in our laboratory. We also describe an additional fluorescence-guided method for immunogold labeling, which reduces time and effort for finding labeled profiles under the electron microscope.

Freeze-fracture replicas of brain tissues can be prepared in three steps: fixation of tissue specimen with paraformaldehyde, freezing under high pressure, and replication by deposition of carbon and platinum following fracturing. Fixing tissue specimen with low concentration (0.5–2 %) paraformaldehyde provides not only equable fracturing and replication but also stable labeling efficiency. Fixed brain samples are cut into 70–150 μm thick slices using a vibratory slicer followed by freezing with a high-pressure freezer, which allows stable and even freezing. The frozen samples are fractured by a physical force, and carbon and platinum are deposited on the fractured face to make replicas. The lipid bilayers of cell membrane tend to split into two parts at their hydrophobic center under frozen condition, which results in the exposure of two kinds of inner face of the membrane: exoplasmic fracture face (E-face) and the protoplasmic fracture face (P-face) [9]. The first carbon deposition captures the exposed phospholipids and integral membrane proteins serving as physical fixation and stabilization. The second platinum-carbon deposition gives shadows that increase the contrast for EM images. The final carbon deposition supports the carbon-platinum layers and increases the mechanical strength [10].

The unfixed proteins or intracellular organelle are dissolved in the following SDS treatment. Transmembrane proteins and their tightly bounded associated proteins are exposed on the surface of replica [11], allowing antibodies to reach their antigens easily in the following immunogold labeling. At the same time, fixed proteins are denatured by SDS, making antigen-antibody binding similar to that in the immunoblotting method [1]. Therefore many antibodies suitable for immunoblot are usable for SDS-FRL as well. Along with these advantages mentioned above, SDS-FRL has also potential disadvantages in comparison with other EM-labeling methods. First, it must be noted that the integral membrane proteins are partitioned into either of the E-face or P-face when the membranes are fractured. The ratio of the partition can be affected by binding of these molecules to associated proteins located in the intracellular and extracellular surfaces of the membrane and is not readily predictable. Antibodies raised against extracellular domains should be used to visualize the target proteins partitioned into the

E-face, whereas antibodies raised against intracellular domains should be used for those partitioned into the P-face. Second, the retainment of the membrane proteins on the replica may be affected by the balance between strength of chemical fixation and stringency of SDS treatment. For example, weak fixation or excessive SDS treatment can cause false-negative results by intensively removing associated proteins or even integral membrane proteins [11]. Third, the fracturing process may not be always random. Specific cellular profiles with smooth contour, for example, may be more frequently fractured than other profiles with more complicated shapes. Such sampling bias could affect quantitative analyses in some cases.

Although we should carefully take these limitations into consideration, SDS-FRL is a unique method that facilitates two-dimensional protein localization analyses at high resolution and with high sensitivity.

2 Materials

2.1 Buffers

1. 0.2 M phosphate buffer (PB), pH 7.4. To prepare 1 L of solution: dissolve 38.4 g of sodium phosphate monobasic dihydrate (NaH_2PO_4-$2H_2O$) and 7.8 g of sodium hydroxide (NaOH) in 900 mL of MilliQ water and adjust the pH to 7.4. Add MilliQ water to make the volume to 1 L. NaOH makes skin corrosion and causes serious eye damage. Handle with protective wears.
2. 0.1 M PB, pH 7.4: dilute above 0.2 M PB by 50 % with MilliQ water.
3. 25 mM phosphate-buffered saline (PBS): PBS is made by adding 0.9 % sodium chloride (NaCl) into 25 mM PB.
4. 50 mM tris-buffered saline (TBS). To prepare 1 L of solution: mix 50 mL of 1 M Tris-HCl (pH 7.4) and 9 g of NaCl in MilliQ water. Adjust the volume to 1 L with MilliQ water.

2.2 Tissue Fixation

1. Anesthesia (sodium pentobarbital: 300 mg/mL. Dilute by 20 % with filter-sterilized 25 mM PBS before use).
2. 25 mM PBS.
3. 0.1 M PB.
4. 2 % Paraformaldehyde (PFA) solution (2 % PFA in 0.1 M PB with 15 % v/v picric acid solution, adjust pH to 7.3–7.4 with 1 N HCl). Paraformaldehyde is hazardous by contact skin, inhalation, and ingestion. Handle under a fume hood with protective, e.g., safety goggles, gloves, and safety clothes. Picric acid is explosive when dry. Prepare PFA solution every time before use and keep no longer than 1 week since paraformaldehyde polymerizes

when it is in aqueous condition and reduces its efficiency of fixation. For preparation of 1 L solution: dissolve 20 g paraformaldehyde in 280 mL of MilliQ water at 60 °C with stirring. Add 1.0 g of NaOH to increase the alkalinity and dissolve paraformaldehyde completely. Add 150 mL of saturated picric acid solution and 500 mL of 0.2 M PB. Cool down the solution to room temperature and adjust the pH to 7.3–7.4 with 1 N HCl. Adjust the volume to 1 L with MilliQ water. Filtrate the solution using filter paper and keep at 4 °C until use.

5. Peristaltic pump with silicon tubes.
6. Forceps.
7. Surgical scissors.
8. Syringes (1 mL size).
9. Needles (26–27 gauge).

2.3 Slice Preparation and Cryoprotection

1. Vibratory Slicer (LinearSlicer Pro 7, DOSAKA EM, Japan or VT1200 Leica)
2. Fine paint brushes (size 1–2)
3. Razor blades (wipe with acetone before use to remove oil used in manufacture)
4. 0.1M PB, ice-cold
5. 10–30 % glycerol in 0.1 M PB (prepare 30 % glycerol in 0.1 M PB and dilute with 0.1 M PB to make 10 and 20 % solution)

2.4 Freezing

1. High-pressure freezing machine (HPM010 or HPM100, Leica).
2. Metal polisher (GLANOL, Faserit GmbH, Germany).
3. Chamois leather: use for polishing copper specimen carriers with metal polisher.
4. Copper specimen carriers: 3 mm disk on 4.6 mm disk in diameter with 0.3 mm height each (in total 0.6 mm height). Polish the surface with metal polisher using chamois leather and keep in acetone until use to avoid formation of rust.
5. Punch, to make 1.5 mm hole in diameter.
6. Ophthalmic scissors.
7. Double-faced tapes: 80 or 140 μm of thickness and choose depending on the thickness of tissue slices. Make a 1.5 mm hole using a punch and put on a copper specimen carrier. Trim off extra tapes with ophthalmic scissors along the edge of 3 mm disk.
8. Fine paint brushes (size 0–1).
9. Forceps.
10. Liquid nitrogen for freezing and storage of frozen samples.

2.5 Fracturing and Replication

1. Freeze-fracture machine (JFD V, JEOL, Japan or BAF060, Leica).
2. Liquid nitrogen for cooling down the machine and handling frozen samples.
3. 50 mM TBS.
4. Porcelain spot plate.
5. Platinum loops: prepare from platinum wires of 0.8–1.0 mm in diameter. Make a 2–3 mm-sized loop and place at the tip of a Pasteur pipette. Heat the tip of a Pasteur pipette to close the tip and fix the platinum loop.
6. Forceps.

2.6 SDS-Digestion

1. 2.5 % SDS solution (2.5 % SDS, 20 % sucrose in 15 mM Tris-HCl, pH 8.3): store at room temperature. SDS has acute toxicities with skin/eye irritation. Handle with protective wears.
2. Glass vials with caps (14.75 mm in diameter, 45 mm in height).
3. Hybridization incubator (HB-100, TAITEC, Japan).

2.7 Immunogold/ Fluorescence Labeling

1. 2.5 % SDS solution, pH 8.3.
2. Washing buffer (0.1 % Tween-20 + 0.05 % bovine serum albumin (BSA) + 0.05 % NaN_3 in TBS): replicas are fragile and occasionally stick to platinum loops or a porcelain spot plate. Low concentration of BSA prevents replicas from adhering to platinum loops or porcelain plates. Store at 4 °C.
3. Blocking buffer (5 % BSA in washing buffer). Store at 4 °C.
4. Antibody dilution buffer (1 % BSA in washing buffer). Store at 4 °C.
5. 50 mM TBS.
6. MilliQ water.
7. Porcelain spot plate.
8. Platinum loops.
9. Humid box: prepare with 1-well plates (Nunc OmniTray with lid, non-treated, Thermo Fisher Scientific). Put laboratory film (e.g., Parafilm) in the bottom of a 1-well plate and place wet papers at the corner to keep the humidity. Seal the lid with laboratory film.
10. Shaker (KS 130 basic, IKA, Germany).
11. Refrigerating shaker (Multitron standard, INFORS HT, Switzerland).
12. Primary antibodies.
13. Gold particle-conjugated secondary antibodies.
14. Fluorescence-labeled secondary antibodies.

15. Pioloform-coated copper mesh grids (Electron Microscopy Sciences, USA).
16. Filter papers.
17. Fine forceps.
18. Grid storage box (Electron Microscopy Sciences, USA).

3 Methods

3.1 Fixation and Tissue Preparation

1. Set tubes to the peristaltic pump. Fill the tubes with 25 mM PBS. Confirm absence of air bubbles in the tube. Set a 26–27 gauge needle to the tip of the tube.
2. Adjust the flow rate of the peristaltic pump to 6–7 mL/min (*see* **Note 1**).
3. Anesthetize an animal with the 60 mg/mL sodium pentobarbital. Inject 1 mL · volume/kg · bodyweight of sodium pentobarbital intraperitoneally using a 26–27 gauge syringe needle. Let the animal free for several minutes until it falls into a sleep. Proceed with the following steps under deep anesthesia.
4. Check the depth of anesthesia by performing a toe-pinch test. Pinch one of the toes of anesthetized animal to elicit a reflex reaction. If there is a reflex, the anesthesia is not sufficient. Wait some more minutes or inject additionalamount of anesthesia if needed. Repeat the toe-pinch test until the reflex disappears.
5. Pinch the abdominal outer skin of the animal with forceps. Cut it with surgical scissors to expose the inner skin/muscles.
6. Pinch the abdominal inner skin/muscles by forceps. Cut it with surgical scissors. Internal organs will be exposed.
7. Cut the diaphragm and expose the heart. Do not injure the heart, liver, or any other organs.
8. Cut the ribs to open the thoracic cavity of the animal.
9. Start the peristaltic pump. Insert the 27 gauge needle connected to the tip of peristaltic pump tube into the left ventricle of the heart.
10. Cut the right atrium of heart with scissors to perfuse the solution transcardially. Avoid leakage from the nose or mouth of the animal. Adjust the flow rate of the peristaltic pump accordingly.
11. Perfuse 50 mM PBS for several minutes to wash out blood. The color of the liver becomes pale yellowish-brown.
12. Change the perfusion solution to 2 % PFA. Avoid trapping air bubbles in the tube.

13. Perfuse the fixative solution transcardially for 12 min.
14. Stop the peristaltic pump. Remove the needle from the heart.
15. Decapitate the fixed animal. Remove the scalp with scissors to expose the skull.
16. Remove muscles attached to the skull with scissors. Cut caudal edge of the skull with scissors along the midline. Remove the skull with forceps to expose the fixed brain. Avoid damaging the surface of the brain with forceps, scissors, or the skull.
17. Hold up the exposed brain with forceps. Cut the optic nerves by scissors to isolate the brain.
18. Immerse the isolated fixed brain in 0.1 M PB. Store at 4 °C. Normally good structures will be preserved for 1 week with this condition.

3.2 Brain Slice Preparation

1. Set a razor blade to the vibratory slicer. Make sure that the angle of blade is properly set ralative to the stage.
2. Remove the excess solution from the fixed brain using filter papers. Trim off the extra parts of the brain with a razor blade.
3. Glue the fixed brain on the stage. Fill ice-cold 0.1 M PB in the buffer bath.
4. Slice the fixed brain into 70–150 μm thick slices.
5. Collect slices containing the region of interest with a fine brush. Keep slices in ice-cold 0.1 M PB. Store at 4 °C until use.

3.3 Cryoprotection

1. Prepare 10 %, 20 %, and 30 % glycerol in 0.1 M PB solutions.
2. Transfer the slices into 10 % glycerol in 0.1 M PB. Incubate slices for 20 min at room temperature with shaking at 80 rpm (*see* **Note 2**).
3. Transfer the slices into 20 % glycerol in 0.1 M PB. Incubate slices for 20 min at room temperature with shaking at 80 rpm (*see* **Note 2**).
4. Transfer the slices into 30 % glycerol in 0.1 M PB. Incubate slices for several hours ~ up to 1 overnight at 4 °C with shaking (*see* **Note 3**).

3.4 High-Pressure Freezing

1. Prepare the high-pressure freezing machine. Air-heat for 1 h to dry up. Fill alcohol and adjust the alcohol pressure to 3–4 bar.
2. Prepare specimen slices. Trim off the extra parts from the region of interest with a trimming blade. Make the trimmed slices smaller than 1.4 mm in diameter.
3. Put a specimen slice in the hole of double-faced tape attached on a specimen carrier with a fine painting brush. Fill the blank space around the specimen slice with 30 % glycerol in 0.1 M PB. Sandwich the specimen with a non-taped carrier (*see* **Note 4**).

4. Freeze the sandwiched specimen slices with carriers using a high-pressure freezing machine. Frozen carriers must be transferred into liquid nitrogen immediately after the freezing.
5. Transfer frozen carriers into each cryovial. Store them in liquid nitrogen until use.

3.5 Freeze-Fracture

1. Prepare the freeze-fracture machine. Fill liquid nitrogen; wait until the vacuum becomes lower than 10^{-5} Pa. The temperature of specimen stage and knife is colder than –175 °C. Set the temperature of specimen stage at –140 °C.
2. Cool down the specimen holder with liquid nitrogen just before use (*see* **Note 5**).
3. Load frozen carriers into the specimen holder in liquid nitrogen.
4. Insert the specimen holder into specimen chamber of the freeze-fracture machine. Start heating of the stage up to –140 °C. Wait until the vacuum becomes lower than 10^{-5} Pa.
5. Adjust the height of carbon and platinum/carbon rods to 1.5 mm.
6. Insert the knife into specimen chamber. Open the specimen holder by moving the knife toward one direction. Specimens will be fractured when the holder has opened.
7. Retract the knife. Start evaporation of carbon with the stage angle of 90° and rotation of the stage. Make 5 nm thick of carbon layer by monitoring the value of quartz crystal.
8. Change the angle of stage to 60°. Start evaporation of platinum/carbon. Make 2 nm thickness of platinum/carbon layer by monitoring the value of quartz crystal (*see* **Note 6**).
9. Change the angle of stage back to 90°. Start evaporation of carbon with stage rotation. Make 15–20 nm of carbon layer by monitoring the value of quartz crystal.
10. Take out the specimen holder from the specimen chamber.
11. Thaw specimens in 50 mM TBS at room temperature. Check the carbon/platinum deposition under a stereomicroscope.

3.6 SDS-Digestion

1. Pick up each specimen with carbon/platinum deposition using a looped platinum wire. Put them into 750 μL of 2.5 % SDS solution in each glass vial.
2. Digest the attached tissue with SDS. Set the temperature of incubator at 80 °C. Incubate the specimens for 18 h with rocking at 50 rpm (*see* **Note 7**).
3. SDS-digested replicas can be stored in SDS solution until use at room temperature.

3.7 Immunolabeling

1. Wash replicas with 1 mL of fresh 2.5 % SDS solution for 10 min with shaking (80 rpm) at room temperature.
2. Wash replicas for 3 times with 1 mL of washing buffer at room temperature with shaking, 10 min each.
3. Block nonspecific binding sites with 30 μL of blocking buffer for 1 h at room temperature with shaking.
4. Prepare primary antibody solution. Dilute antibody with antibody dilution buffer into the appropriate concentration. Use 30 μL of diluted antibody for each replica sample (*see* **Note 8**).
5. Transfer the replicas into 30 μL of diluted primary antibody solution. Incubate in a humid box for longer than 1 overnight (>18 h) at 15 °C with shaking (40 rpm).
6. Wash replicas with washing buffer for 3 times at room temperature with shaking (80 rpm), 10 min each.
7. Block nonspecific binding sites with 30 μL of blocking buffer in a humid box for 30 min at room temperature with shaking (80 rpm).
8. Prepare secondary antibody solution. Dilute gold nanoparticle-conjugated secondary antibody against the primary antibodies (e.g., 5 nm gold-conjugated goat anti-rabbit IgG) to 1/30 with blocking buffer. Use 30 μL of diluted antibody for each replica sample (*see* **Note 8**).
9. Transfer replicas into 30 μL drop of diluted secondary antibody. Incubate in a humid box for 1 overnight (>18 h) at 15 °C with shaking (40 rpm).
10. Wash replicas with 1 mL of washing buffer for 10 min at room temperature with shaking (80 rpm). If fluorescence labeling is required, proceed with the steps decribed in 3.8.
11. Wash replicas twice with 1 mL of 50 mM TBS at room temperature with shaking (80 rpm) for 10 min each.
12. Transfer replicas into 1 mL of MilliQ water.
13. Pick up replicas on grids in MilliQ water. Dry grids in the air and store them at room temperature until examining with electron microscope (Fig. 1).

3.8 Fluorescence Labeling for LM Detection

1. Wash replicas with 1 mL of washing buffer twice at room temperature with shaking (80 rpm) for 10 min, each.
2. Block nonspecific binding sites with 30 μL of blocking buffer in a humid box for 30 min at room temperature with shaking.
3. Prepare fluorescent antibody solution. Dilute fluorescence dye-conjugated antibody against the secondary antibody (e.g., Alexa Fluor 488 donkey anti-goat IgG) to 1/200 with blocking buffer. Use 30 μL of diluted antibody for each replica sample.

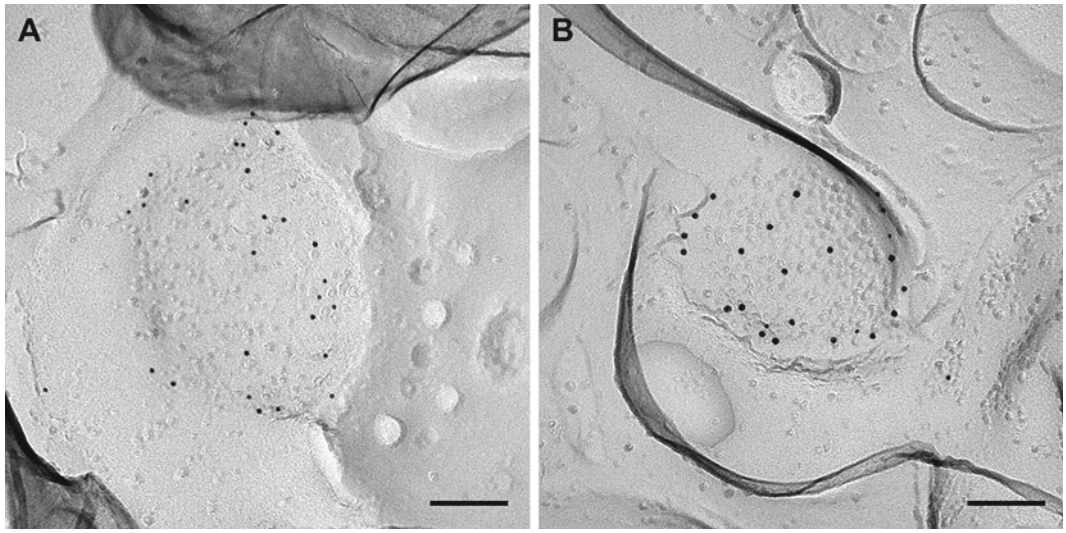

Fig. 1 Electron micrographs showing immunoreactivity for Cav2.1 subunit of P/Q-type voltage-dependent calcium channels (**A**) and GluD2 subunit of glutamate receptors (**B**) at the parallel fiber – Purkinje cell synapse in the rat cerebellum. Gold particles of 5 and 10 nm sizes were used to label Cav2.1 and GluD2, respectively. Gold particles for Cav2.1 are localized on the P-face of parallel fiber varicosities, which have synaptic vesicles in cross-fractured terminals. They are preferentially distributed in concave structures indicating presynaptic active zone (**A**). GluD2 labeling was mostly found in intramembrane particle clusters on the E-face, which mark glutamatergic postsynaptic membrane specialization (**B**). *Scale bars*; 100 nm

4. Transfer replicas into 30 μL drop of diluted fluorescent antibody. Incubate for 2 h at 37 °C or 1 overnight (>18 h) at 15 °C in a humid box with shaking (40 rpm).
5. Wash replicas with 1 mL of washing buffer for 10 min at room temperature with shaking (80 rpm).
6. Wash replicas twice with 1 mL of 50 mM TBS for 10 min each at room temperature with shaking.
7. Transfer replicas into 1 mL of MilliQ water.
8. Pick up replicas on grids in MilliQ water. Dry grids in the air completely.
9. Place grids on a siliconized glass slide to examine under an epifluorescent microscope.
10. Mount MilliQ water on a grid and cover with a siliconized coverslip.
11. Check the location of fluorescence.
12. Remove the coverslip and take out the grids. Let them dry in the air to proceed with electron microscope observation (Fig. 2).

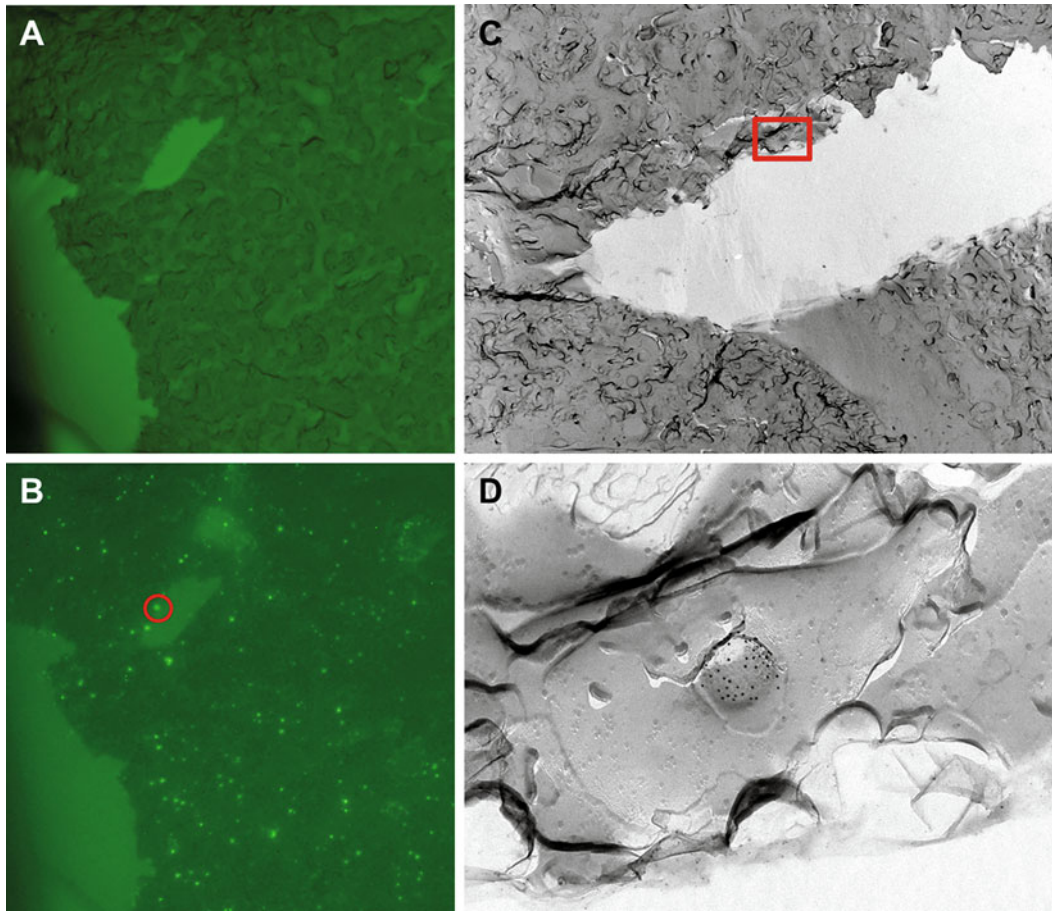

Fig. 2 Correlative fluorescence LM-EM analysis. GluD2 was visualized with 10 nm gold particles and Alexa 488 fluorescent labeling. Replica was first examined by an epifluorescence microscope (**A**, bright field; **B**, fluorescence) to map positive signals on a low-magnification replica images. The fluorescence-positive spots (*red circle* in **B**) were then examined under EM (**C**, **D**) with the map obtained by LM. (**D**) Magnified image shown in *red rectangle* in **C**

4 Notes

1. Choose slower flow rate for juvenile animals and faster rate for adults.
2. Slices must be kept in the solution so that they will not be dried. Dried slices will have salt precipitates on the surface and it may influence on some structures. Normally slices will sink into the bottom of the solution after 20 min incubation. Longer incubation will be needed in case slices are still floating in the solution.
3. Too long incubation in glycerol may cause artificial aggregations of intramembrane particles.

4. Remove air bubbles and adjust the height of filler solution and double-faced tape. Both of insufficient or excess amounts of filler can cause a failure in freezing. Insufficient filler will introduce air bubbles in between specimen carriers. Air bubbles or excess amount of filler may disassemble the sandwich of specimen carriers under high pressure.
5. Large air bubbles will appear when liquid nitrogen was poured onto the specimen holder. These bubbles will disappear when it has cooled down and become same temperature as liquid nitrogen.
6. Platinum/carbon evaporation may be omitted if fluorescent labeling is weak. Platinum can cause reflection of laser which decreases the signal/noise ratio of fluorescence images.
7. The standard condition for SDS treatment is 18 h incubation at 80 °C. Adjust the stringency of SDS treatment by modifying the incubation time and temperature appropriate to each antibody.
8. Multiple labeling is also possible by using antibodies generated in different host animals in combination with different sizes of gold particles to label each antibody. Make sure to use antibodies raised against extracellular domains to visualize proteins located on the E-face and antibodies raised against intracellular domains for those on the P-face. If the target proteins are closely localized to each other, it is recommended to perform sequential labeling to avoid steric hindrance of antibodies for the firstly applied primary antibody. In this case, labeling with the other primary antibodies will be compromised.

Acknowledgments

We thank Mitsuru Ikeda for preparing replica images used in Fig. 2.

References

1. Fujimoto K (1995) Freeze-fracture replica electron microscopy combined with SDS digestion cytochemical labeling of integral membrane proteins. Application to the immunogold labeling of intercellular junctional complexes. J Cell Sci 108:3443–3449
2. Hall CE (1950) A low temperature replica method for electron microscopy. J Appl Phys 21:61–67
3. Bullivant S, Ames A 3rd (1966) A simple freeze-fracture replication method for electron microscopy. J Cell Biol 29:435–447
4. Tanaka J, Matsuzaki M, Tarusawa E, Momiyama A, Molnár E, Kasai H, Shigemoto R (2005) Number and density of AMPA receptors in single synapses in immature cerebellum. J Neurosci 25:799–807
5. Hagiwara A, Fukazawa Y, Deguchi-Tawarada M, Ohtsuka T, Shigemoto R (2005) Differential distribution of release-related proteins in the hippocampal CA3 area as revealed by freeze-fracture replica labeling. J Comp Neurol 489:195–216
6. Masugi-Tokita M, Tarusawa E, Watanabe M, Molnár E, Fujimoto K, Shigemoto R (2007) Number and density of AMPA receptors in individual synapses in the rat cerebellum as revealed by SDS-digested

freeze-fracture replica labeling. J Neurosci 27: 2135–2144

7. Antal M, Fukazawa Y, Eördögh M, Muszil D, Molnár E, Itakura M, Takahashi M, Shigemoto R (2008) Numbers, densities, and colocalization of AMPA- and NMDA- type glutamate receptors at individual synapses in the superficial spinal dorsal horn of rats. J Neurosci 28:9692–9701
8. Indriati DW, Kamasawa N, Matsui K, Meredith AL, Watanabe M, Shigemoto R (2013) Quantitative localization of Cav2.1 (P/Q-type) voltage-dependent calcium channels in Purkinje cells: somatodendritic gradient and distinct somatic coclustering with calcium-activated potassium channels. J Neurosci 33:3668–3678
9. Fujimoto K (1997) SDS-digested freeze-fracture replica labeling electron microscopy to study the two-dimensional distribution of integral membrane proteins and phospholipids in biomembranes: practical procedure, interpretation and application. Histochem Cell Biol 107:87–96
10. Fujita A, Fujimoto T (2007) Quantitative retention of membrane lipids in the freeze-fracture replica. Histochem Cell Biol 128: 385–389
11. Rash JE, Davidson KGV, Kamasawa N, Yasumura T (2005) Freeze-fracture replica immunogold labeling (FRIL) in biological electron microscopy. Microsc Microanal 11: 138–139

Chapter 18

Application of Virus Vectors for Anterograde Tract-Tracing and Single-Neuron Labeling Studies

Hiroyuki Hioki, Hisashi Nakamura, and Takahiro Furuta

Abstract

Elucidating neuronal circuits is fundamental issue for understanding how the brain works and implements higher-order functions. Various viral vectors have been developed and become valuable tools for the analysis of neuronal circuits in the central nervous system. Sindbis virus vector is very useful for anterograde labeling of neurons, since the vector expresses reporter protein rapidly and strongly. Furthermore, the vector makes it possible to visualize whole structures of a single neuron by injecting adequately diluted virus solution. After immunoperoxidase staining with a tyramine-based signal amplification technique, two-dimensional reconstruction of a single neuron is performed with a virtual slide system and graphic software. In this chapter, we describe a set of single-neuron tracing method in exact detail. On the other hand, Sindbis virus vector shows very high cytotoxicity by shutting off host cellular transcription and translation and is not suitable for the experiments requiring long-term expression of transgene. In the previous study, we developed novel lentivirus vector and succeeded in neuron-specific and high-level sustained gene expression. This novel vector is expected to be applied as a sensitive anterograde tracer in addition to Sindbis virus vector.

Key words Sindbis virus, Membrane-targeting signal, Anterograde tracing, Single-neuron tracing, Reconstruction, Lentivirus, Tet-Off system

1 Introduction

Visualization of neurons is the first key step in understanding the brain structure. Recombinant viral vectors are now considered to be powerful tools for labeling of neurons, since they can be directly delivered to any specific region of the animal brain at any time. Among available vectors, Sindbis virus vector is of great advantage to rapid and high-level expression of reporter protein, since the infected neurons express a large amount of the protein under the strong viral subgenomic promoter. In the previous studies, we developed Sindbis virus vector, which express palmitoylation (pal) site-attached green fluorescent protein (palGFP) [2] or monomeric red fluorescent protein (pal-mRFP1) [15]. The palmitoylated fluorescent protein, palGFP or pal-mRFP1, is targeted to the

Rafael Luján and Francisco Ciruela (eds.), *Receptor and Ion Channel Detection in the Brain: Methods and Protocols*, Neuromethods, vol. 110, DOI 10.1007/978-1-4939-3064-7_18,

plasma membrane and can clearly visualize the edges of neuronal cells. Taken together, Sindbis virus vector expressing palGFP or pal-mRFP1 works as a highly sensitive anterograde tracer [3, 6, 9, 13–15, 19].

The vector also enables us to visualize whole structure of a single neuron by injecting adequately diluted virus solution due to the powerful viral subgenomic promoter. Indeed, we succeeded in efficient visualization of single neurons and demonstrated the axonal arborizations of single mesencephalic dopamine neurons [12], motor and sensory thalamic neurons [10, 11, 17], and layer V cortical projection neurons in the rat presubiculum [8]. In this chapter, we describe the detailed procedures: (1) preparation of Sindbis virus particles, (2) visualization of a single neuron in the dorsal lateral geniculate nucleus (LGd) by way of example, and (3) complete reconstruction of a single LGd neuron (Figs. 1 and 2). In addition, the vector is also compatible with electron microscopic observation (*see* Chap. 19).

Although Sindbis virus vector is useful for anterograde labeling and single-neuron tracing experiments, the vector possesses a serious drawback. After the infection, the vector shuts off the host cellular transcription and translation and exhibits high cytotoxicity [1, 21]. Thus, other types of virus vectors such as lentivirus vectors are desirable for the experiments requiring long-term gene expression. Lentivirus vectors offer unique advantages of stably integrating transgenes into the genome of the infected cells and of providing the basis for sustained gene expression. However, lentivirus vectors with ubiquitous promoters including cytomegalovirus promoter weakly express transgenes in both neuronal and glial cells in the central nervous system. In the previous study, we addressed those long-standing issues and succeeded in achieving high-level and neuron-specific gene transduction in vivo by constructing novel system, "Double Lentiviral Vector Tet-Off Platform" [5]. Since the vectors should be one of the valuable tools in the field of basic and clinical neurosciences, we also introduce the production of lentivirus particles under serum-free condition and show the example of anterograde labeling (Fig. 3).

Fig. 1 (continued) found, the section containing the labeled neuron was counterstained with propidium iodide or NeuroTrace green, respectively, to identify the location of the infected neuron. (**c**) The cell body and dendrites of the labeled neuron were observed under a fluorescent microscope. (**d**) After the immunoperoxidase staining for GFP or mRFP1 with the BT-GO amplification method, the axon fibers of a single-labeled LGd neuron were observed in the V1. (**e**) Cortical axons formed many varicosities in the V1. (**f**) The single-labeled LGd neurons also sent axon collaterals to the Rt. *Amp* ampicillin resistance gene, *APt* anterior pretectal nucleus, *ColE1* ColE1 origin, *DAB* diaminobenzidine, *LGd* dorsal lateral geniculate nucleus, *LP* lateral posterior thalamic nucleus, *nsP1 ~ 4* nonstructural genes 1 ~ 4, *Rt* reticular thalamic nucleus, *SP6* SP6 promoter

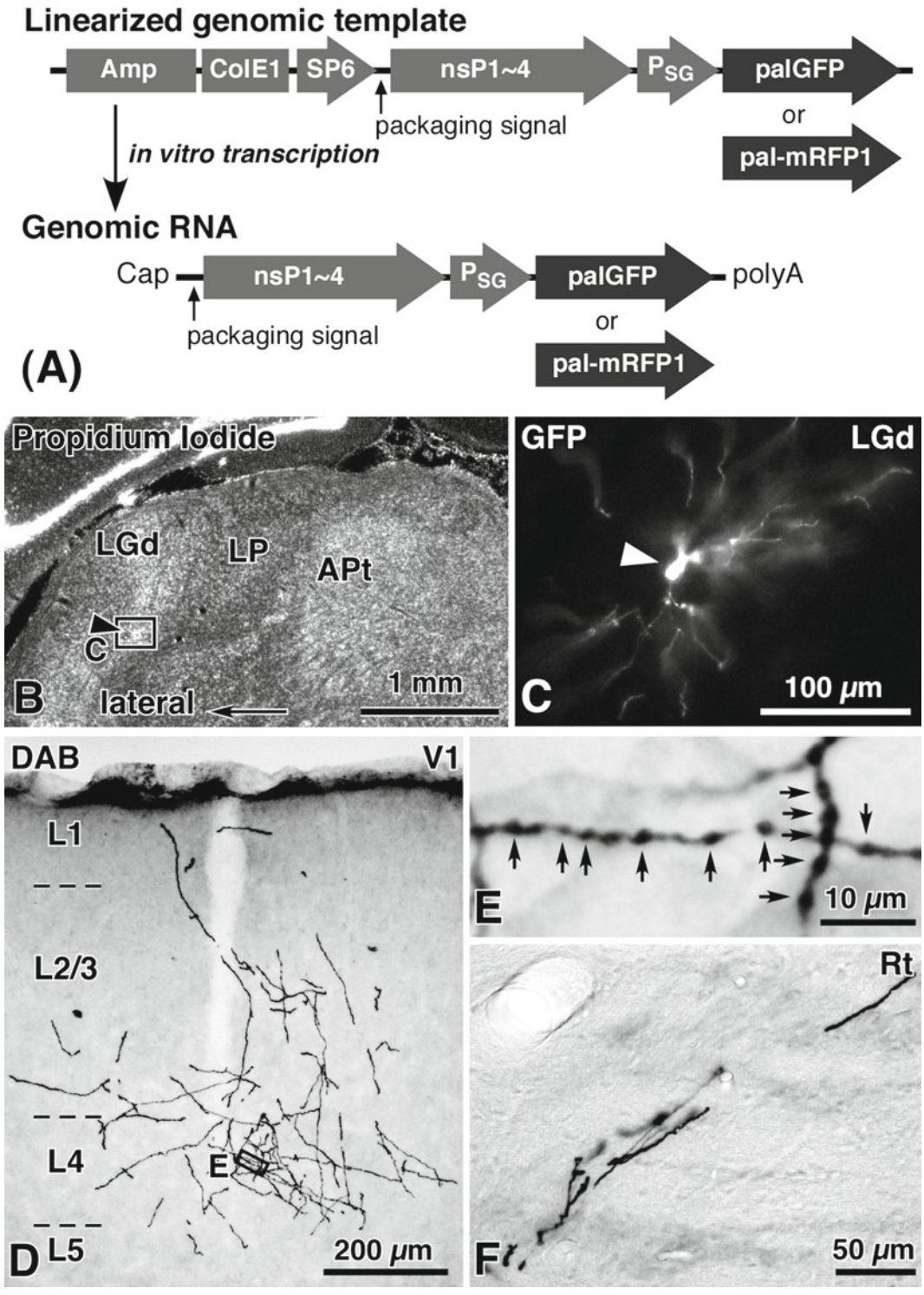

Fig. 1 Visualization of a single neuron in the dorsal lateral geniculate nucleus with Sindbis virus vector. (**a**) After inserting membrane-targeted green or red fluorescent protein (palGFP or pal-mRFP1) into pSinRep5, the plasmid was linearized with restriction enzyme. Subsequently, genomic RNA was produced by SP6 in vitro transcription. (**b**) When a neuron infected with palGFP (*arrowheads* in **b**, **c**) or pal-mRFP1 Sindbis virus was

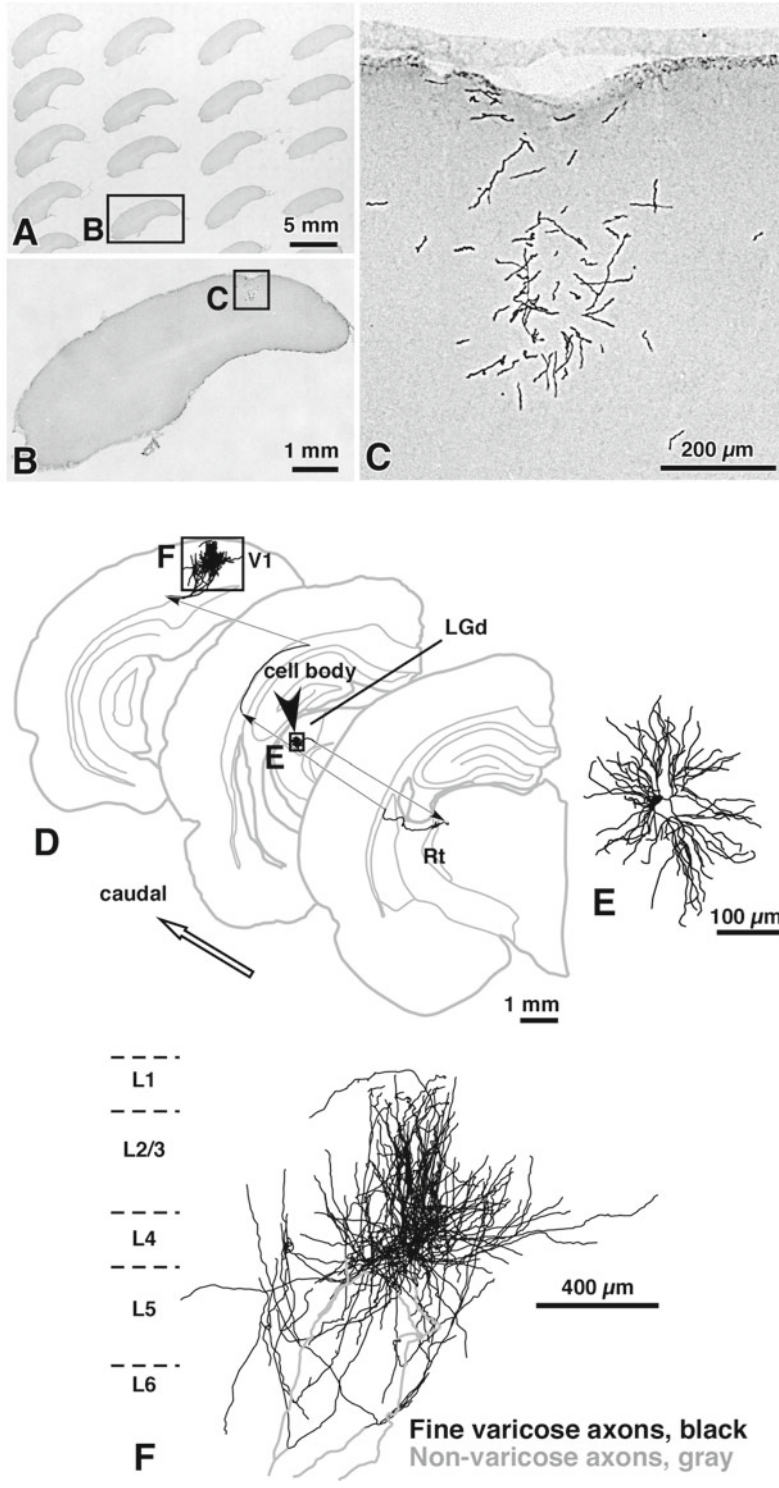

Fig. 2 Reconstruction of a single LGd neuron. (**a**) The coverslipped sections on the glass slides were automatically captured by digital slide scanner TOCO. (**b**) The images of each section were trimmed away from the glass slides images and saved as 8-bit TIFF files with graphic software Canvas 12. (**c**) The axons on the screen were traced and digitized with a digital pen tablet and graphic software Canvas 12. (**d**) All dendritic and axon fibers of a single LGd neuron were reconstructed completely. (**e**) The LGd neuron had multipolar dendrites. (**f**) The axon fibers of the single LGd neuron were mainly observed in L2–4 of the V1. The fine varicose and non-varicose axons are indicated in *black* and *gray*

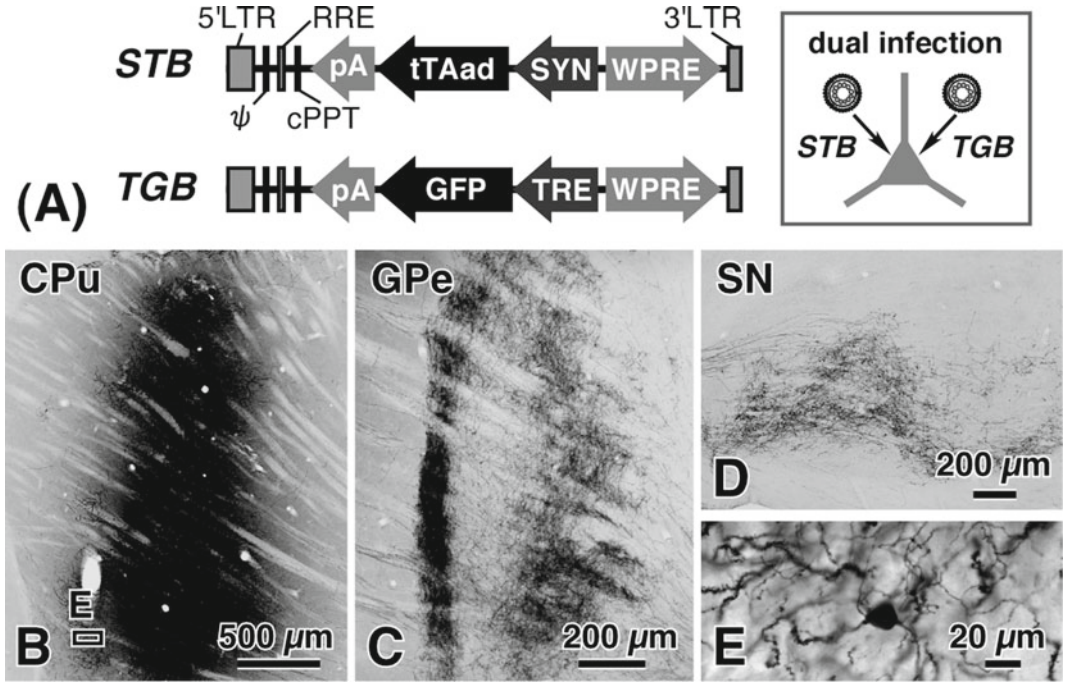

Fig. 3 High-level expression of reporter protein in neostriatal neurons by Tet-Off lentivirus vectors. (**a**) "Double Lentiviral Vector Tet-Off Platform" is composed of two elements—regulator and response lentivirus vectors. The regulator vector, *STB*, expresses an improved version of the tetracycline-controlled transactivator (tTAad) under the control of human synapsin I (SYN) promoter [4]. The tTAad binds to TRE-tight promoter and strongly activates the transcription of GFP in the response vector, *TGB*. (**b**–**e**) One week after the injection of a mixture of *STB* and *TGB* into CPu, GFP was visualized by immunoperoxidase staining without BT-GO amplification method. The immunoreactivity for GFP was very strong not only in the injection site (CPu) but also in the projection targets (GPe and SN). *cPPT* central polypurine tract, *CPu* caudate putamen, *GPe* globus pallidus external segment, *LTR* long terminal repeat, *ψ* HIV-1 packaging signal, *pA* polyadenylation signal derived from the bovine growth hormone (BGH) gene, *RRE* HIV-1 Rev response element, *SN* substantia nigra, *WPRE* woodchuck hepatitis virus posttranscriptional regulatory element

2 Materials

2.1 Preparation of Sindbis Virus Particles

We obtained "Sindbis Expression System" from Life Technologies (#K750-01) and inserted palGFP or pal-mRFP1 sequence into the MCS of genomic template, pSinRep5. The sequence information and materials are available upon request. The production and concentration of virus vectors are based on the manufacturer's instructions with some modifications. In addition to basic equipment for molecular biology, the following materials are necessary for virus production and concentration. The experiments should be approved by the Committee for Recombinant DNA Study.

2.1.1 In Vitro Transcription

1. Genomic plasmid, pSinRep5-palGFP [2] or pSinRep5-pal-mRFP1 [15].
2. Helper plasmid, DH(26S) (Life Technologies).
3. Proteinase K solution (#19131, QIAGEN).
4. Restriction enzymes (NotI and XhoI).
5. mMESSAGE mMACHINE™ SP6 (#AM1340, Life Technologies).

2.1.2 Preparation of Cells

1. Baby hamster kidney cells (BHK cells, Life Technologies).
2. αMEM(−) (#12561-056, Life Technologies).
3. αMEM(+): Add fetal bovine serum (FBS) to a final concentration of 5 %.
4. PBS(−) (#14249-95, Nacalai Tesque).
5. Trypsin solution: TrypLE Express Enzyme (#12605-010, Life Technologies).
6. 175-cm^2 flask (#661160, Greiner Bio-One).

2.1.3 Electroporation of Cells

1. Gene Pulser® II Electroporation System (Bio-Rad).
2. 0.4-cm electroporation cuvette (#165-2088, Bio-Rad).
3. αMEM(+).
4. 100-mm tissue culture plastic dish (Advanced TC, #664960, Greiner Bio-One).

2.1.4 Concentration of Sindbis Virus Particles

1. 50 mM Tris–HCl solution: 50 mM Tris–HCl, pH7.4, 100 mM NaCl, 0.5 mM EDTA.
2. 55 % sucrose solution: 55 % sucrose (w/v) in 50 mM Tris–HCl, pH7.4, 100 mM NaCl, 0.5 mM EDTA.
3. 20 % sucrose solution: 20 % sucrose (w/v) in 50 mM Tris–HCl, pH7.4, 100 mM NaCl, 0.5 mM EDTA.
4. Ultracentrifuge: Optima L-90K (Beckman Coulter).
5. SW 41 Ti rotor (Beckman Coulter).
6. SW 41 centrifuge tube: 50 Ultra-Clear™ tubes 14×89 mm (#344059, Beckman Coulter).

2.2 Injection

Stereotaxic coordinates for the LGd are determined according to the rat brain atlas [18].

1. Anesthesia: 7 % (w/v) chloral hydrate in water. All animal care and use should be in accordance with the National Institutes of Health Guide for the Care and Use of Laboratory Animals, and the experiments also should be approved by the Committee for Animal Care and Use and that for Recombinant DNA Study.
2. Sindbis virus expressing palGFP [2] or pal-mRFP1 [15].

3. PBS: 5 mM sodium phosphate-buffered 0.9 % (w/v) saline, pH7.4.
4. BSA: bovine serum albumin (#01863-77, Nacalai Tesque).
5. Stereotaxic Instrument (David Kopf).
6. Fine tweezers.
7. Picospritzer II (General Valve Corporation).
8. N_2 gas.
9. Hand drill (Minimo®, MINITOR).
10. Steel hole cutter (#BS1214, MINITOR).

2.3 Fixation

1. Anesthesia: 7 % (w/v) chloral hydrate in water.
2. PBS.
3. Fixative solution: 3 % (v/v) formaldehyde, 75 % (v/v) saturated picric acid (equal to 0.95 % (w/v) picric acid), and 0.1 M Na_2HPO_4 (adjusted with NaOH to pH7.2) (*see* **Note 1**).
4. Needle (18 gauge).
5. Tweezers.
6. Surgical scissors.

2.4 Sectioning

1. 0.1 M PB: 0.1 M sodium phosphate buffer (pH7.4) (*see* **Note 2**).
2. 30 % (w/v) sucrose in 0.1 M PB.
3. O.C.T. Compound (#4583, Sakura Finetek Japan).
4. Dry ice powder.
5. Freezing microtome (Leica).
6. 24-well cell culture plate (#662160, Greiner Bio-One).

2.5 Fluorescent Nissl-Like Staining

1. PBS.
2. PBS-X: PBS containing 0.3 % (v/v) Triton X-100.
3. Propidium iodide (#29037-76, Nacalai Tesque).
4. NeuroTrace 500/525 green fluorescent Nissl stain (#N21480, Life Technologies).
5. Non-coated glass slides.
6. Axioplan 2 epifluorescence microscope (Carl Zeiss).
7. 10× objective lens (Plan-NEOFLUAR, NA = 0.3, Carl Zeiss).
8. 1.25× objective lens (EC Plan-NEOFLUAR, NA = 0.03, Carl Zeiss).
9. QICAM FAST digital monochrome camera (QImaging).

2.6 Immunoperoxidase Staining

1. H_2O_2.
2. PBS.
3. PBS-X.

4. Affinity-purified rabbit antibody to GFP [20] or mRFP1 [6].
5. PBS-XCG: PBS-X containing 1 % (v/v) normal goat serum and 0.12 % (w/v) λ-carrageenan (*see* **Note 3**).
6. Biotinylated goat antibody to rabbit IgG (#BA-1000, Vector Laboratories).
7. ABC: VECTASTAIN Elite ABC Standard Kit (#PK-6100, Vector Laboratories).
8. Dimethyl sulfoxide.
9. Tyramine hydrochloride (#T2879-1G, Sigma-Aldrich).
10. Biotin–NHS: Biotin N-hydroxysuccinimide Ester (#203112, Merck).
11. Monoethanolamine.
12. Biotinylated tyramine (BT) solution: Mix equal volumes of 281 mM biotin–NHS and 288 mM tyramine hydrochloride in dimethyl sulfoxide. Incubate the mixture overnight at RT protected from light. Add 1/10 volume of monoethanolamine to inactivate the remaining free biotin–NHS. Incubate the mixture for 4 h at RT protected from light. BT solution is stable for up to 2 months at 4 °C. For longer storage, freeze the solution at −20 °C or below and avoid repeated freezing and thawing.
13. GO: Glucose oxidase (257 U/mg, #16831-14, Nacalai Tesque).
14. β-D-glucose (#16804-32, Nacalai Tesque).
15. 0.1 M PB.
16. DAB: Diaminobenzidine-4HCl.
17. 0.5 M Tris–HCl solution: 0.5 M Tris in water (adjusted with HCl to pH 7.6).
18. Gelatinized glass slides.
19. Graded series of ethanol in water (30, 50, 70, and 95 %).
20. Xylene.
21. NEW MX: Mounting medium (Matsunami Glass).

2.7 Reconstruction of Dendrites and Axons

1. TOCO: Digital slide scanner (CLARO).
2. 10× objective lens (EC Plan-Neofluar, NA = 0.30, Carl Zeiss).
3. Digital pen tablet (Bamboo Tablet).
4. Canvas 12: Graphic software (ACD Systems International Inc.).

2.8 Counterstaining with Cresyl Violet

1. Graded series of ethanol in water (30, 50, 70, and 95 %).
2. Xylene.
3. Cresyl violet.
4. 20 mM acetate buffer (pH 4.8).

5. Acetic acid.
6. Chloroform.
7. NEW MX: Mounting medium (Matsunami Glass).

2.9 Preparation of Lentivirus Particles

We obtained "ViraPower™ Lentiviral Expression System" from Life Technologies (#K4937-00) and constructed genomic plasmids, pLenti6PW-STB and pLenti6PW-TGB [5]. In the previous study, we also established the method for production of VSV-G pseudotyped lentivirus under serum-free condition and introduce the procedure with attention to detail.

2.9.1 Production of Lentivirus Vector under Serum-Free Condition

1. pLenti expression plasmid: pLenti6PW-STB or pLenti6PW-TGB [5] (*see* **Note 4**).
2. Helper plasmids: ViraPower™ Packaging Mix (#K4975-00, Life Technologies). The mixture contains pLP1, pLP2, and pLP/VSVG plasmids.
3. 293FT cells (#R700-07, Life Technologies).
4. PBS(−) (#14249-95, Nacalai Tesque).
5. OptiMEM(−) (#31985-070, Life Technologies).
6. OptiMEM(+): Add FBS to a final concentration of 2%.
7. Trypsin solution: TrypLE Express Enzyme (#12605-010, Life Technologies).
8. Lipofectamine® 2000 (#11668027, Life Technologies).
9. Virus Production Medium: UltraCULTURE™ (#12-725F, LONZA) containing 0.1 M MEM Non-essential Amino Acids (NEAA, #11140050, GIBCO), 4 mM L-glutamine (#25030-081, GIBCO), 2 mM GlutaMAX (#35050-061, GIBCO), and 1 mM Sodium Pyruvate (#11360-070, GIBCO). This medium can be stored at 4°C for 1 month.
10. 100-mm tissue culture plastic dish (#664160, Greiner Bio-One).
11. BioCoat™ poly-D-lysine 100-mm dish (#354469, Corning).
12. Round-bottom polystyrene 5-mL tube (#352058, BD Bioscience).

2.9.2 Concentration of Lentivirus Particles

1. 0.45-μm filter (#UFC2BHK08, Millipore).
2. 55 % sucrose solution: 55 % sucrose (w/v) in 50 mM Tris–HCl, pH 7.4, 100 mM NaCl, 0.5 mM EDTA.
3. PBS(−) (#14249-95, Nacalai Tesque).
4. Ultracentrifuge: Optima L-90K (Beckman Coulter).
5. SW 41 Ti rotor (Beckman Coulter).
6. SW 41 centrifuge tube: 50 Ultra-Clear™ tubes 14×89 mm (#344059, Beckman Coulter).
7. Amicon Ultra-15 Ultracel-100K (#UFC910008, Millipore).

3 Methods

3.1 Production and Concentration of Sindbis Virus Vector

3.1.1 In Vitro Transcription

1. Linearize 2–3 μg of the genomic plasmid (pSinRep5-palGFP or pSinRep5-pal-mRFP1) and helper plasmid (DH26S) with restriction enzymes, NotI and XhoI, respectively.
2. Check whether or not the plasmids are completely linearized by agarose gel electrophoresis with around 500 ng of the digested plasmids.
3. Add 1/10 volume of proteinase K solution into the remaining digest and incubate at 37 °C for 30 min.
4. Purify the plasmids by phenol–chloroform extraction and ethanol precipitation.
5. Resuspend the pellet DNA to a concentration of 0.5 μg/μL in RNase-free water.
6. Mix the following reagents at RT and incubate for 2 h at 37 °C.

RNase-free water	2 μL
Linearized DNA	2 μL (1 μg)
2 × Ribonucleotides mix	10 μL
20 mM GTP	2 μL
10 × Transcription buffer	2 μL
10 × SP6 Enzyme mix	2 μL/20 μL

7. Measure the concentration of the transcribed RNA. Generally, you can obtain 10–20 μg of RNA from 1 μg of DNA template.
8. Check the quality of RNA by agarose gel electrophoresis with around 500 ng of the transcription reaction. If you wish to accurately size the RNA, denaturing gel electrophoresis should be performed (*see* **Note 5**).

3.1.2 Preparation of Cells

1. Grow BHK cells, 80–90 % confluent, in a 175-cm^2 flask containing 30 mL of αMEM(+).
2. Aspirate the medium and wash the cells with PBS(−).
3. Add 5 mL of trypsin solution into the flask and incubate for 2 min in CO_2 incubator.
4. Briefly pipette the solution to obtain a single-cell suspension.
5. Transfer the cells to a sterile 50-mL conical tube.
6. Add 5 mL of αMEM(+) to the flask and transfer the cells to the 50-mL conical tube.
7. Centrifuge the cells at 200 × *g* for 5 min at 4 °C.

8. Resuspend the cells in 10 mL of αMEM(−).
9. Centrifuge the cells at 200 × *g* for 5 min at 4 °C.
10. Resuspend the cells in 10 mL of PBS(−).
11. Centrifuge the cells at 200 × *g* for 5 min at 4 °C.
12. Resuspend the cells in 500 μL of PBS(−).

3.1.3 Electroporation of Cells

1. Turn on Gene Pulser® II Electroporation System, and set "low cap" and "voltage" to 50 μF and 0.85 kV, respectively.
2. Transfer 0.5 mL of the cell suspension into a 0.4-cm electroporation cuvette and place the cuvette on ice.
3. Add 5–10 μg of the genomic and helper RNA and mix gently but thoroughly.
4. Place the cuvette in the electroporation device and check the sample resistance. It should be between 0.10 ~ 0.20 Ω.
5. Pulse the cell suspension twice. Actual time constant and voltage will be 0.90 ms and 0.90 kV, respectively.
6. Place cells on ice for 5 min.
7. Transfer the electroporated cells to 9.5 mL of αMEM(+) in a 100-mm plate. Rinse the cuvette with the cell suspension to collect all the cells.
8. Grow the cells for 24–36 h.
9. Place the medium into a 50-mL conical tube.
10. Centrifuge the medium at 2,000 × *g* for 10 min at 4 °C.
11. Replace the supernatant into a 50-mL conical tube and store at –80 °C.

3.1.4 Concentration of Sindbis Virus Particles

1. Wash SW 41 centrifuge tube with 70 % EtOH, and then let it air-dry.
2. Add 1 mL of 55 % sucrose solution into the tube.
3. Layer 3 mL of 20 % sucrose solution onto the 55 % sucrose cushion.
4. Place sample solution on top of the 20 % sucrose solution. Fill tube about 2 mm from top with 50 mM Tris–HCl solution.
5. Centrifuge at 160,000 × *g* for 90 min at 4 °C to sediment the virus particles onto the 55 % sucrose cushion.
6. Discard the top fraction containing the medium (about 8 mL), and remove 1.5 mL of the 20 % sucrose.
7. Collect virus particles from the 20 %/55 % interface in a total volume of 1.5 mL.
8. Divide the solution into 100 μL aliquots and store at –80 °C.
9. Determine actual virus titer by adding serial dilutions of virus solution to BHK cells.

3.2 Injection

1. Dilute palGFP and pal-mRFP1 Sindbis virus vectors to $3–6 \times 10^5$ infectious units (IU) with PBS containing 2 % (w/v) BSA, and mix the two diluted solution (*see* **Note 6**).
2. Anesthetize rats by intraperitoneal injection of 7 % (w/v) chloral hydrate solution (3.5 mL/kg b.w.). Allow a few minutes for anesthesia to occur.
3. Place the anesthetized rats in a stereotaxic instrument, and adjust the incisor bar until the heights of bregma and lambda were equal in order to achieve the flat skull position.
4. Make an incision on the scalp along the midline and expose the skull.
5. Thin the skull above the LGd of rats bilaterally (4.0–5.2 mm posterior to the bregma and 3.7–3.9 mm lateral to the midline) using a hand drill (Minimo®) with a steel hole cutter, and carefully remove the remaining bones using fine tweezers to expose the brain surface.
6. Load 0.2 μL of the Sindbis virus vectors mixture into a glass micropipette, and attach the micropipette to a Picospritzer II.
7. Move the tip of the micropipette to the LGd of rats (4.0–5.2 mm posterior to the bregma, 3.7–3.9 mm lateral to the midline, and 4.3–4.7 mm deep from the brain surface) (*see* **Note 7**).
8. Inject 0.2 μL of the virus mixture into the LGd by pressure for 5 min.
9. Repeat the **steps 6–9** to inject the virus vectors mixture into the contralateral LGd.
10. The rats are allowed to survive for 36–48 h (*see* **Note 8**).

3.3 Fixation

1. Anesthetize rats deeply by intraperitoneal injection of 7 % (w/v) chloral hydrate solution (7.0 mL/kg b.w.). Allow a few minutes for anesthesia to occur.
2. Open the abdominal cavity with surgical scissors, insert the 18-gauge needle from the left ventricle of the heart into the aorta, and cut the right atrial appendage (*see* **Note 9**).
3. Perfuse with 300 mL of PBS to remove the blood from the circulatory system.
4. Perfuse with 300 mL of fixative solution.
5. Remove the scalp, skull, and dura mater with bone forceps and tweezers.
6. Remove the brain and place it in fixative solution for 4 h at RT.

3.4 Sectioning

1. Replace the fixative with 30 % (w/v) sucrose in 0.1 M PB to cryoprotect brain tissue.
2. Place the brain on the stage of a freezing microtome with a 2:1 mixture of 30 % (w/v) sucrose: O.C.T. Compound, and briefly freeze them with dry ice powder (*see* **Note 10**).
3. Adjust the stage angle to keep the coronal plane of the brain horizontal.
4. Layer 30 % (w/v) sucrose in 0.1 M PB on the surface of the brain, and freeze the sucrose solution and brain completely by embedding in dry ice powder on the stage for at least 5 min (*see* **Note 11**).
5. Cut the brain into 50-μm-thick coronal sections on a freezing microtome, and collect the sections serially in 24-well cell culture plate with 0.1 M PB.

3.5 Fluorescent Nissl-Like Staining

1. Observe the sections including the injection site under an Axioplan 2 epifluorescence microscope with a filter set for GFP (excitation filter, 450–490 nm; emission, 515–565 nm) or mRFP1 (excitation, 530–585 nm; emission, ≥615 nm).
2. Check whether or not a single neuron is labeled with palGFP or pal-mRFP1 Sindbis virus (*see* **Note 12**).
3. Wash the sections containing palGFP- or pal-mRFP1-expressing neuron with PBS-X at RT for 10 min twice.
4. Incubate the sections for 30 min at RT with 40 μg/mL propidium iodide or 1/200-diluted NeuroTrace 500/525 green-fluorescent Nissl stain in PBS-X.
5. Wash the sections with PBS-X at RT for 10 min twice.
6. Mount the sections onto non-coated glass slides and coverslip the sections with PBS.
7. Capture the digital fluorescence images with a QICAM FAST digital monochrome camera using 1.25× and 10× objective lens, and determine the location of palGFP- or pal-mRFP1-labeled neuron.

3.6 Immunoperoxidase Staining

3.6.1 ABC Method for the Sections Containing the Cell Body and Dendrites

1. Pick up the sections containing the cell body and dendrites of the infected neuron from the serial sections (*see* **Note 13**).
2. Wash the sections with PBS at RT for 10 min twice.
3. Incubate the sections for 30 min at RT with 1 % (v/v) H_2O_2 in PBS.
4. Wash the sections with PBS-X at RT for 10 min twice.
5. Incubate the sections overnight at RT with 0.4 or 0.2 μg/mL affinity-purified rabbit antibody to GFP or mRFP1 in PBS-XCG.

6. Wash the sections with PBS-X at RT for 10 min twice.
7. Incubate the sections for 1 h at RT with 10 μg/mL biotinylated goat antibody to rabbit IgG in PBS-XCG.
8. Wash the sections with PBS-X at RT for 10 min twice.
9. Incubate the sections for 1 h at RT with 1/100-diluted ABC in PBS-X (*see* **Note 14**).
10. Wash the sections with PBS at RT for 10 min twice.
11. Incubate the sections for 30–60 min at RT with 0.02 % (w/v) DAB and 0.0001 % (v/v) H_2O_2 in 50 mM Tris–HCl (pH 7.6).
12. Wash the sections with PBS at RT for 10 min twice.

3.6.2 ABC Method with BT-GO Amplification for the Remaining Serial Sections

1. Perform same steps above (2–9 in Sect. 3.6.1).
2. Wash the sections with 0.1 M PB at RT for 10 min twice.
3. Incubate the sections for 5 min at RT with the mixture containing 2.55 μM BT, 3 μg/mL of GO, and 2 % (w/v) BSA in 0.1 M PB (*see* **Note 15**).
4. Add β-D-glucose to 2 mg/mL and mix the solution and sections well.
5. Incubate the sections for 30 min at RT (*see* **Note 16**).
6. Perform same steps above (8–12 in Sect. 3.6.1).
7. Mount all the stained sections serially onto gelatinized glass slides.
8. Dry up the sections.
9. Soak the glass slides in ethanol–water mixtures of 30, 50, and 70 % (v/v) at RT for 30 min each, and dip the slides into 95 % (v/v) ethanol in water.
10. Soak the glass slides in ethanol overnight at RT.
11. Dip the glass slides into xylene–ethanol mixture of 50 % (v/v), and soak the slides in xylene overnight at RT.
12. Coverslip the sections with mounting medium NEW MX.

3.7 Reconstruction of Dendrites and Axons

1. Capture a whole coronal section into a large color image with a spatial resolution of 1.038 μm/pixel using digital slide scanner TOCO with a 10× objective lens (*see* **Note 17**).
2. Trace and digitize the axons and dendrites of stained LGd neurons on the images with a digital pen tablet and graphic software Canvas 12 (*see* **Note 18**).
3. Superimpose the digitized fibers from all the sections with graphic software Canvas 12.

3.8 Counterstaining with Cresyl Violet

1. Soak the coverslipped glass slides in xylene at RT until mounting agent has dissolved.
2. Remove cover glasses from the glass slides.

3. Dip the glass slides in xylene–ethanol mixture of 50 % (v/v), ethanol and ethanol–water mixtures of 95, 70, 50, and 30 % (v/v) at RT.
4. Soak the glass slides for 15–60 min at RT into 0.2 % (w/v) cresyl violet and 30 % (v/v) ethanol in 20 mM acetate buffer (pH4.8).
5. Wash the glass slides with 70 % (v/v) ethanol in water.
6. Wash the glass slides with 95 % (v/v) ethanol and 2 % (v/v) acetic acid in water.
7. Wash the glass slides with 42.5 % (v/v) ethanol, 50 % (v/v) chloroform, and 2 % (v/v) acetic acid in water.
8. Dip the glass slides into ethanol–water mixture of 95 % (v/v), ethanol, xylene–ethanol mixture of 50 % (v/v), and xylene.
9. Coverslip the sections again with mounting medium NEW MX.
10. Determine the cortical layers and areas where the reconstructed LGd neurons project.

3.9 Preparation of Lentivirus Vector

3.9.1 Production of Lentivirus Vector under Serum-Free Conditions

1. The day before transfection, plate 293FT cells in a 100-mm tissue culture plate such that they will be 90–95 % confluent on the day of transfection.
2. Pre-warm 7 mL of OptiMEM(+) on the poly-D-Lysine-coated 100-mm dish.
3. For each transfection sample, prepare DNA–Lipofectamine™ 2000 complexes as follows:
   (a) In a round-bottom polystyrene 5-mL tube, mix 9 μg of ViraPower™ Packaging Mix and 3 μg of pLenti expression plasmid, pLenti6PW-STB or pLenti6PW-TGB, with 1.5 mL of OptiMEM(−). Mix gently and incubate at RT for 5 min.
   (b) In a round-bottom polystyrene 5-mL tube, dilute 36 μL of Lipofectamine™ 2000 with 1.5 mL of OptiMEM(−). Mix gently and incubate at RT for 5 min.
   (c) After the 5 min incubation, combine the diluted DNA with the diluted Lipofectamine™ 2000, and mix gently.
   (d) Incubate at RT for 20 min with gentle shaking to allow the DNA–Lipofectamine complexes to form.
4. While DNA–Lipofectamine complexes are forming, prepare 293FT cells for virus production as follows:
   (a) Remove the medium and wash the cells once with 5 mL of PBS(−).
   (b) Add 2 mL of trypsin solution to the monolayer and incubate for 3 min in CO_2 incubator.
   (c) Briefly pipette the solution to obtain a single-cell suspension.

(d) Transfer the cells to a 50-mL conical tube and add 2 mL of OptiMEM(+).

(e) Centrifuge the cells at 200 × *g* for 3 min at 4 °C.

(f) Aspirate off the medium and resuspend the cells with 150 μL of OptiMEM(+).

5. Add the resuspended cells into 3 mL of DNA–Lipofectamine complexes.
6. Incubate them at RT for 5 min.
7. Add mixture of the cells and DNA–Lipofectamine complexes to the poly-D-Lysine-coated 100-mm dish containing pre-warmed OptiMEM(+).
8. Mix gently by rocking the dish back and forth.
9. Incubate the cells in CO_2 incubator.
10. After 8–12 h, remove the medium containing the DNA–Lipofectamine complexes and replace with 12 mL of "Virus Production Medium."

3.9.2 Concentration of Lentivirus Particles

1. Harvest virus-containing supernatant 48–72 h (60 h recommended) post-transfection by removing medium to a 50-mL conical tube.
2. Centrifuge at 2,000 × *g* for 15 min at 4 °C to pellet cell debris.
3. Collect the supernatant, and then filter the virus supernatant through a sterile, 0.45-μm low-protein-binding filter (*see* **Note 19**).
4. Wash SW 41 centrifuge tube with 70 % EtOH, and then let it air-dry.
5. Add 1 mL of 55 % sucrose solution into the tube.
6. Place 11 mL of sample solution on top of the 55 % sucrose solution. If the sample volume is less than 11 mL, mess up with PBS(−).
7. Centrifuge at 160,000 × *g* for 3 h at 4 °C in a SW 41 rotor to sediment the virus particles onto the 55 % sucrose cushion.
8. Discard the top fraction containing the medium (about 10.5 mL).
9. Collect virus particles from the medium/55 % interface in a total volume of 1 mL.
10. Concentrate the virus solution with Amicon® Ultra-15 Centifugal Filter Concentrator as follows:

(a) Add virus solution to the Amicon Ultra filter device.

(b) Centrifuge at 3,000 × *g* for 0.5–1 h at 10 °C in a fixed-angle rotor.

(c) Discard the through and add 12 mL of PBS(−).

(d) Repeat the centrifugation for a total of three times to exchange buffer.

(e) Insert a pipette into the bottom of the filter device and withdraw the sample using a side-to-side sweeping motion to ensure total recovery of the concentrated virus solution. Final volume will be around 200 μL.

11. Divide the solution into 10 μL aliquots and store at –80 °C.
12. Determine actual virus titer by adding serial dilutions of virus solution to 293FT cells.

4 Notes

1. After preparing the fixation solution, leave it at least overnight at RT to hydrate formaldehyde completely.
2. To prevent the blade from getting rust, PB but not PBS should be used for sectioning. In addition, after the sectioning, the blade should be washed thoroughly with deionized water and then ethanol.
3. Lambda carrageenan makes the incubation medium highly viscous and contributes to avoiding uneven binding of antibodies to sections [7].
4. The plasmid DNA for transfection should be clean and contains low endotoxin levels. We usually purify plasmid DNA with PureLink™ HiPure Plasmid Kits (#K2100-04, Life Technologies). Instead, you purify the plasmid by cesium chloride equilibrium centrifugation.
5. There are originally three enzyme sites (XhoI, NotI, and PacI) for linearization of the genomic DNA template (pSinRep5). However, since pSinRep5-palGFP and pSinRep5-pal-mRFP1 contain additional XhoI site between the subgenomic promoter and start codon, XhoI digestion is not suitable for linearization purpose.
6. BSA blocks the nonspecific binding of the virus particles to the surface of pipette tips, tubes, and glass micropipettes and, thus, contributes to a linear decrease in virus titer with dilution. The optimal IU of Sindbis virus vector for single-neuron labeling depends on the target neurons. For example, in the case of the lateral posterior thalamic nucleus (LP), $3–6 \times 10^4$ IU (ten times lower IU than in the case of LGd) of the virus is optimum concentration. The mix injection of palGFP and pal-mRFP1 Sindbis virus allows us to improve the success rate of single infections [16].
7. Nakamura H, Hioki H, Furuta T, Kaneko T (2015) Different cortical projections from three subdivisions of the rat lateral

posterior thalamic nucleus: a single-neuron tracing study with viral vectors. Eur J Neurosci. 41:1294–1310.

8. When the tip of the glass micropipette reaches to the target point, move the micropipette 0.5 mm upward to make space for the injection of virus solution.
9. Although glial cells are also infected with Sindbis virus, they die more quickly than neurons. To label neurons selectively, rats should be allowed to survive at least 36 h after the virus injection. The optimal survival time depends on neuron subtypes. In the case of LGd neurons, 36–48 h are enough to label completely, and longer survival time may result in the abnormal morphology of dendrites and/or cell body.
10. Before perfusion, cut and smooth the tip of the 18-gauge needle to avoid stabbing the wall of the blood vessel.
11. The mixture of sucrose solution and O.C.T. Compound enables us to slice the brain tissue smoothly, as compared with the case of using O.C.T. Compound alone.
12. Layering sucrose solution on the surface of the brain protects from melting during sectioning.
13. In the single-neuron tracing study, we generally use the hemispheres containing only one infected neurons expressing pal-GFP or pal-mRFP1, since it is difficult to isolate the entangled axons of two or more LGd neurons in the tracing and reconstruction steps.
14. The expression level of reporter protein is substantially higher in the soma and dendrites than that in the distal axons. Although ABC method is enough to visualize the cell body and dendrites of the infected neuron, BT-GO amplification should be performed to visualize the cortical axons completely.
15. Before incubation with the sections, mix solutions A and B of the ABC kit at 1/100 dilution each in PBS-X and incubate the mixture for at least 30 min.
16. The concentration of BT for BT-GO amplification should be determined by end user (a range of from 0.128 to 1280 μM).
17. During BT-GO reaction, H_2O_2 is produced by glucose oxidation, and the signal amplification saturates within 30 min.
18. TOCO takes 11 images with different focuses at a site of the section (1412×1063 μm), selects automatically the best focused image at each site, and fuses those partially overlapping 20–63 XY images into a large image, in the normal mode of the scanner.
19. The axons and dendrites are reconstructed two-dimensionally section by section onto the coronal plane. Axons or dendrites are sometimes out of focus at the place where the multiple

nerve fibers cross one another. To trace the axons and dendrites precisely, light microscopic observation is required.

20. When we inject lentivirus vector into the rodent brain and just label neuronal cells, the purity of virus solution is not so much a problem. Although virus solution become very viscous, ultracentrifugation step can be skipped and directly moved to ultrafiltration with Amicon® Ultra-15 Centifugal Filter Concentrator.

Acknowledgments

This work was supported by Grants-in-Aid from The Ministry of Education, Culture, Sports, Science, and Technology (MEXT) and Japan Society for the Promotion of Science (JSPS); Grant numbers: for Scientific Research (24500408 and 15K14333 to H.H.; 24500408 and 15H04266 to T.F.); for Exploratory Research (15K14333 to H.H.); and for Scientific Research on Innovative Areas, "Neuronal Diversity and Neocortical Organization" (25123709 to H.H.), "Foundation of Synapse and Neurocircuit Pathology" (22110007 to H.H.), and "Adaptive Circuit Shift" (15H01430 to H.H.).

References

1. Dryga SA, Dryga OA, Schlesinger S (1997) Identification of mutations in a Sindbis virus variant able to establish persistent infection in BHK cells: the importance of a mutation in the nsP2 gene. Virology 228:74–83
2. Furuta T, Tomioka R, Taki K, Nakamura K, Tamamaki N, Kaneko T (2001) In vivo transduction of central neurons using recombinant Sindbis virus: Golgi-like labeling of dendrites and axons with membrane-targeted fluorescent proteins. J Histochem Cytochem 49: 1497–1508
3. Furuta T, Timofeeva E, Nakamura K, Okamoto-Furuta K, Togo M, Kaneko T, Deschênes M (2008) Inhibitory gating of vibrissal inputs in the brainstem. J Neurosci 28:1789–1797
4. Hioki H, Kameda H, Nakamura H, Okunomiya T, Ohira K, Nakamura K, Kuroda M, Furuta T, Kaneko T (2007) Efficient gene transduction of neurons by lentivirus with enhanced neuron-specific promoters. Gene Ther 14:872–882
5. Hioki H, Kuramoto E, Konno M, Kameda H, Takahashi Y, Nakano T, Nakamura KC, Kaneko T (2009) High-level transgene expression in neurons by lentivirus with Tet-Off system. Neurosci Res 63:149–154
6. Hioki H, Nakamura H, Ma YF, Konno M, Hayakawa T, Nakamura KC, Fujiyama F, Kaneko T (2010) Vesicular glutamate transporter 3-expressing nonserotonergic projection neurons constitute a subregion in the rat midbrain raphe nuclei. J Comp Neurol 518: 668–686
7. Hioki H, Okamoto S, Konno M, Kameda H, Sohn J, Kuramoto E, Fujiyama F, Kaneko T (2013) Cell type-specific inhibitory inputs to dendritic and somatic compartments of parvalbumin-expressing neocortical interneuron. J Neurosci 33:544–555
8. Honda Y, Furuta T, Kaneko T, Shibata H, Sasaki H (2011) Patterns of axonal collateralization of single layer V cortical projection neurons in the rat presubiculum. J Comp Neurol 519:1395–1412
9. Ito T, Hioki H, Nakamura K, Tanaka Y, Nakade H, Kaneko T, Iino S, Nojyo Y (2007) Gamma-aminobutyric acid-containing sympathetic preganglionic neurons in rat thoracic spinal cord send their axons to the superior cervical ganglion. J Comp Neurol 502:113–125
10. Kuramoto E, Furuta T, Nakamura KC, Unzai T, Hioki H, Kaneko T (2009) Two types of

thalamocortical projections from the motor thalamic nuclei of the rat: a single neuron-tracing study using viral vectors. Cereb Cortex 19:2065–2077

11. Kuramoto E, Ohno S, Furuta T, Unzai T, Tanaka YR, Hioki H, Kaneko T (2015) Ventral medial nucleus neurons send thalamocortical afferents more widely and more preferentially to layer 1 than neurons of the ventral anterior-ventral lateral nuclear complex in the rat. Cereb Cortex 25:221–235
12. Matsuda W, Furuta T, Nakamura KC, Hioki H, Fujiyama F, Arai R, Kaneko T (2009) Single nigrostriatal dopaminergic neurons form widely spread and highly dense axonal arborizations in the neostriatum. J Neurosci 29:444–453
13. Nakamura K, Matsumura K, Kaneko T, Kobayashi S, Katoh H, Negishi M (2002) The rostral raphe pallidus nucleus mediates pyrogenic transmission from the preoptic area. J Neurosci 22:4600–4610
14. Nakamura K, Matsumura K, Hübschle T, Nakamura Y, Hioki H, Fujiyama F, Boldogköi Z, König M, Thiel HJ, Gerstberger R, Kobayashi S, Kaneko T (2004) Identification of sympathetic premotor neurons in medullary raphe regions mediating fever and other thermoregulatory functions. J Neurosci 24: 5370–5380
15. Nishino E, Yamada R, Kuba H, Hioki H, Furuta T, Kaneko T, Ohmori H (2008) Sound-intensity-dependent compensation for the small interaural time difference cue for sound source localization. J Neurosci 28: 7153–7164
16. Ohno S, Kuramoto E, Furuta T, Hioki H, Tanaka YR, Fujiyama F, Sonomura T, Uemura M, Sugiyama K, Kaneko T (2012) A morphological analysis of thalamocortical axon fibers of rat posterior thalamic nuclei: a single neuron tracing study with viral vectors. Cereb Cortex 22:2840–2857
17. Paxinos G, Watson C (2007) The rat brain in stereotaxic coordinates. Academic, San Diego
18. Suzuki Y, Kiyokage E, Sohn J, Hioki H, Toida K (2015) Structural basis for serotonergic regulation of neural circuits in the mouse olfactory bulb. J Comp Neurol 523:262–280
19. Tamamaki N, Nakamura K, Furuta T, Asamoto K, Kaneko T (2000) Neurons in Golgi-stain-like images revealed by GFP-adenovirus infection in vivo. Neurosci Res 38:231–236
20. Toribio R, Ventoso I (2010) Inhibition of host translation by virus infection in vivo. Proc Natl Acad Sci U S A 107:9837–9842
21. Nakamura H, Hioki H, Furuta T, Kaneko T (2015) Different cortical projections from three subdivisions of the rat lateral posterior thalamic nucleus: a single-neuron tracing study with viral vectors. Eur J Neurosci. 41: 1294–1310.

Chapter 19

Analysis of Synaptic Connections at the Electron Microscopic Level Using Viral Vectors

Takahiro Furuta, Keiko Okamoto-Furuta, and Hiroyuki Hioki

Abstract

Anterograde tracing using Sindbis virus vector resolves several problems of conventional tracers. Usage of the Sindbis virus as a neural tracer prevents the axons passing through the injection site from being labeled because the virus does not infect from axons. Combining the methodological merit of the virus tracer with electron microscopic technique, we analyze morphological characteristics of ultrastructure of axon terminals which are provided specifically from the region of interest, and thus we can systematically extract information of synaptic organization from complicated neural networks. Here, we introduce a method where Sindbis virus labeling is combined with an immunoelectron microscopic technique. Using this technique, we observe synaptic contacts and GABA immunoreactivity in ultrastructure of axon terminals which are revealed to be projected from the virus injection site.

Key words Sindbis virus, Anterograde tracing, Electron microscopy, GFP, Post-embedding immunostaining

1 Introduction

Tract tracing techniques contribute to visualization of axonal arborizations and to morphological analysis of architecture of the neural network [1]. Several kinds of anterograde tracers (e.g., biocytin, BDA, PHAL, and so on) have been used for tract tracing in the previous studies. We use these anterograde tracers in the hope that the tracers are taken up by neural cell bodies at the injection site and are transported toward the axon terminals. We expect that the labeled axons and boutons in a target area were provided from the neurons which were located in the injection site. However, the conventional anterograde tracers are often taken up from passing axons or axon terminals [2], and, thus, it is possible that, in the target area, the tracers label the "undesirable" axons and terminals, which come from other areas than the injection site.

In our previous study, we wanted to visualize axon terminals which originate from the interpolar subnucleus of the spinal

Rafael Luján and Francisco Ciruela (eds.), *Receptor and Ion Channel Detection in the Brain: Methods and Protocols*, Neuromethods, vol. 110, DOI 10.1007/978-1-4939-3064-7_19,

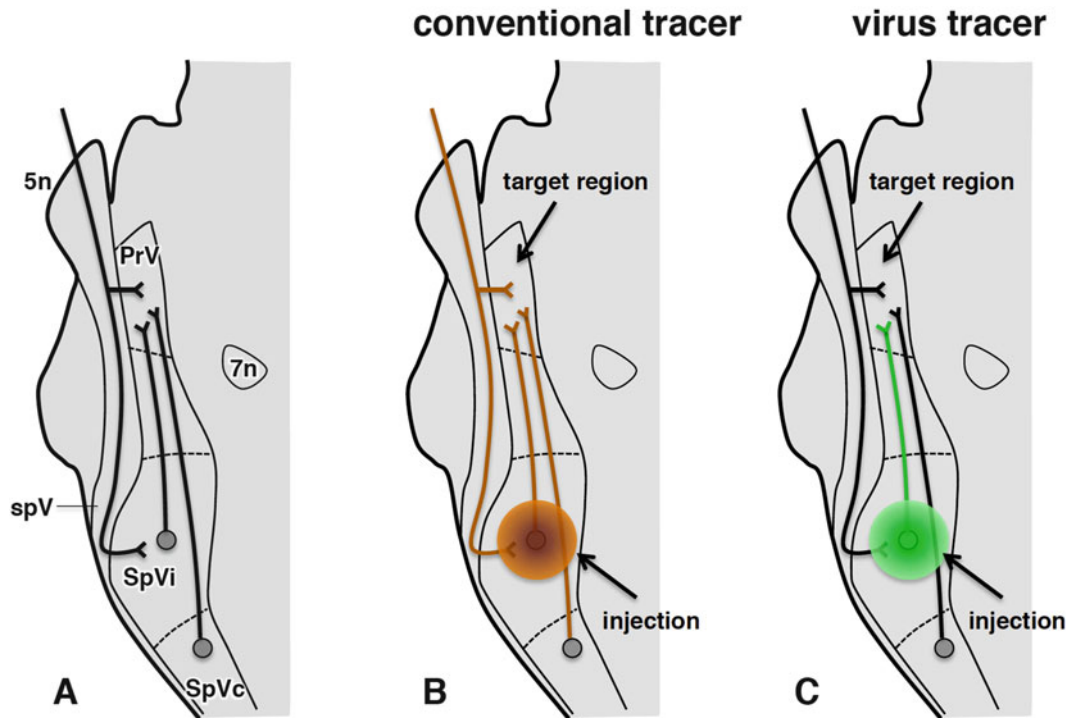

Fig. 1 Schematic drawing showing a merit of anterograde labeling by the virus tracer. (**a**) A part of neural circuit connections is described in a horizontal plane of the brainstem. In the trigeminal complex, the principal trigeminal nucleus (PrV) receives inputs from the trigeminal nerve (primary afferents, 5n), the interpolar subnucleus of the spinal trigeminal nucleus (SpVi), and the caudal subnucleus of the spinal trigeminal nucleus (SpVc). (**b**) Conventional tracers label not only neural elements which are derived from the injection site but also axons which pass through the injection site. (**c**) Sindbis virus tracer infects only from cell bodies and dendrites and thus labels only neurons in the injection site

trigeminal nucleus (SpVi) and terminate in the principal trigeminal nucleus (PrV) to know the inter-subcortical connections of the trigeminal nuclei complex in the brainstem [3]. The PrV receives axonal inputs not only from the SpVi but also from the trigeminal nerve (primary afferents) and caudal subnucleus of the spinal trigeminal nucleus (SpVc) (Fig. 1a). If we use a conventional anterograde tracer, three kinds of axonal inputs (from the SpVi, trigeminal nerve, and SpVc) might be labeled, and we cannot discriminate SpVi input from other inputs (Fig. 1b). In this case, a virus tracer, membrane-targeted GFP-expressing recombinant Sindbis virus (palGFP Sindbis virus, [4]), is very useful because the virus is infected at the cell body and rarely at passing axons or axon terminals (Fig. 1c). We developed palGFP Sindbis virus as an efficient anterograde tracer. Details of palGFP Sindbis virus are described in Chap. 18. Actually, we reported that the palGFP Sindbis virus was occasionally infected from axons and retrogradely labeled neurons [4]. This retrograde labeling was observed only when we used

injection pipettes of large tip diameter and injected a lot of amount of virus solution. If we use a thin-tip pipette to inject the virus, neurons are labeled only anterogradely.

In the functional structure of neural circuits, synaptic connection is one of the most essential features. Synaptic structures are so small that we have to use electron microscopy to observe and analyze them. By combining the electron microscopic technique with tracer labeling or immunohistochemistry, we can obtain more detailed information of the synaptic organization of neural circuits: synaptic connectivity of long-projecting axons, chemical characteristics of pre-/postsynaptic structures and so on. Here, we introduce a method to apply the virus labeling to electron microscopic analysis accompanied with a post-embedding immunostaining [5]. Using this technique, we observed GABA immunoreactivity in axon terminals which were projected from the SpVi to the PrV at ultrastructure level.

2 Materials

2.1 Surgery for Virus Injection

1. Anesthetics. ketamine and xylazine.
2. Sindbis virus solution. Culture medium of virus production is centrifuged to concentrate the virus particles in sucrose gradient. The titer is adjusted to 2×10^10 infective U/mL.
3. Animal. Male Sprague-Dawley rats, 250–300 g B.W.
4. Injection pipette. Glass micropipettes are pulled from borosilicate glass capillaries (2.0 mm OD).
5. Stereotaxic apparatus. Narishige SR-6R.
6. Microinjection system. Picospritzer II (General Valve Corporation, East Hanover, NJ).

2.2 Fixation

1. Prefixative perfusion solution. 5 mM phosphate-buffered saline (PBS, pH7.4)
2. Fixative. Phosphate buffer (0.1 M, pH7.4) containing 4 % formaldehyde and 0.5 % glutaraldehyde
3. Irrigator. Two bottles equipped with a two-way tube
4. Scissors and knife
5. Cannula. Small-sized cannula for rat aorta

2.3 Sectioning on a Vibrating Microtome

1. Vibrating microtome. Microslicer DTK-1000, Dosaka, Kyoto, Japan
2. Razor blade
3. Glue
4. Cutting buffer. 5 mM PBS (pH7.4)
5. Paintbrush

2.4 Immunohistochemical Staining for GFP

1. Wash buffer. 5 mM PBS (pH 7.4) and 0.1 M phosphate buffer (PB, pH 7.4)
2. Primary antibody. Affinity-purified anti-GFP guinea pig antibody [6]
3. Secondary antibody. Gold-conjugated anti-guinea pig IgG goat antibody (Nanoprobes, Yaphank, NY)
4. Incubation buffer. PBS containing 2 % normal donkey serum and 0.2 % Photo-Flo
5. Plastic well plate
6. Shaker
7. Silver enhancement. HQ Silver kit (Nanoprobes, Stony Brook, NY)

2.5 Preparation for Ultrathin Sectioning

1. Osmification. 1 % osmium tetroxide in 0.1 M PB
   a. 0.5 % osmium tetroxide in 0.1 M PB
2. Ethanol. 50, 70, 90, 99, and 100 % ethanol in DDW
3. Uranyl solution. 1 % uranyl acetate in 70 % ethanol
4. Propylene oxide
5. Resin. Durcupan ACM kit (Fluka, Buchs, Switzerland). A:B:C:D = 10:10:0.3:0.3
6. Silicone-coated slide glass and cover glass
7. Oven

2.6 Ultrathin Sectioning

1. Light microscope
2. Stereoscopic microscope
3. Razor blade
4. Rocket made of the resin
5. Glue
6. Ultramicrotome. EM UC6 (Leica, Heidelberg, Germany)
7. Knife of synthetic diamond. Sumi knife 45°
8. Diamond knife. Diatome Ultra 45°
9. Membrane-coated grid. Pioloform-coated mesh nickel grids (VECO, Netherlands)
10. Forceps

2.7 Post-embedding Immunohistochemistry for GABA

1. Etching solution. 0.1 % periodic acid in DDW
2. Tris-buffered saline (TBS). 50 mM TBS (pH 7.4)
3. Blocking solution. TBS containing 2 % normal donkey serum and 0.05 % Photo-Flo
4. Primary antibody. Anti-GABA rabbit antibody (SIGMA)

5. Secondary antibody. Colloidal gold (diameter: 15 nm) conjugated anti-rabbit IgG goat antibody (Amersham)
6. Uranyl acetate solution. 50 % ethanol with 2 % uranyl acetate in DDW
7. Reynolds lead citrate solution

3 Methods

3.1 Virus Injection Surgery

1. Anesthetize a rat deeply by a mixture of ketamine (75 mg/kg b.w.) and xylazine (5 mg/kg b.w.). Cut hair on the heads. Place the rat in a stereotaxic apparatus. Throughout the surgery, a deep level of anesthesia is maintained by additional doses of anesthetics.
2. Cut the skin of the vertex and expose the skull. Make a burr hole on the occipital bone. Make a small cut on the dura by a sharp-tip knife.
3. Lower a glass pipette which contains the virus solution (*see* **Note 1**) through the cut on the dura to place the tip of the pipette at the planned injection site. The virus solution (0.2–0.5 μL) is slowly (*see* **Note 2**) injected by air pressure through the glass micropipette attached to Picospritzer II.
4. Remove the pipette 5 min after the injection. Stitch the skin. The rat is then returned to the animal house.

3.2 Fixation

1. After survival periods of 36–48 h, the rat is fixed.
2. Anesthetize a rat deeply by a mixture of ketamine (75 mg/kg b.w.) and xylazine (5 mg/kg b.w.). Perfuse transcardially with 50–200 mL of PBS followed by 300 mL of fixative solution.
3. After the perfusion was completed, remove the brain from the skull, and put it into a bottle containing the same solution with the fixative. After immersion fixation of 1 h, the fixative is replaced with PBS.

3.3 Sectioning of the Brain

1. Using a razor blade, cut the fixed brain into a small block of the brainstem, which contained the trigeminal complex.
2. Mount and stick the block on a vibration microtome by glue.
3. Fill the specimen holder with 5 mM PBS. Cut the block horizontally into 50 μm thick sections.
4. The sections are collected with a brush and stored in 0.5 mM PBS at 4 °C.

3.4 Immunohistochemistry for GFP

1. Incubate the sections in blocking solution, 5 mM PBS containing 20 % normal donkey serum and 0.2 % Photo-Flo, for 1 h. After the blocking procedure, the sections are incubated

overnight with primary antibody solution, 5 mM PBS containing anti-GFP guinea pig antibody (0.05 μg/mL), normal donkey serum (2 %), and Photo-Flo (0.2 %), at 4 °C. We use a shaker for the incubation.

2. Wash the sections three times in PBS (3 × 10 min).
3. Incubate the sections overnight in the second antibody solution, 5 mM PBS containing gold-conjugated anti-guinea pig IgG goat antibody (1:100 diluted) and normal donkey serum (2 %), at 4 °C.
4. Wash the sections three times in PBS (3 × 10 min).
5. The sections are subjected for additional fixation in 2 % glutaraldehyde in 5 mM PBS for 10 min. After the additional fixation, wash the sections twice in PBS (2 × 5 min).
6. Wash the sections twice in DDW (2 × min). Then, silver intensification is performed with reaction time of 10–15 min (*see* **Note 3**). After the completion of the silver enhancement, wash the sections twice in DDW (2 × 5 min).
7. Wash the sections twice in 0.1 M PB (2 × 5 min).

3.5 Preparation for Ultrathin Sectioning

1. Treat the sections in the osmification solution (1 % osmium tetroxide in 0.1 M PB for 1 min and then with 0.5 % osmium tetroxide in 0.1 M PB) at 4 °C for 20 min.
2. Dehydrate the sections in 50 % ethanol for 10 min.
3. Make the sections react with 1 % uranyl acetate in 70 % ethanol for 40 min.
4. Dehydrate the sections in 90 % ethanol (10 min), in 99 % ethanol (10 min), and then in 100 % ethanol twice (2 × 10 min).
5. Soak the sections in propylene oxide twice for 10 min each.
6. Soak the sections in a mixture of propylene oxide and the resin (1:1) for 1 h.
7. Overnight infiltration in the resin at room temperature.
8. To make flattened plastic samples, embed the sections in the resin by putting the sections between a silicone-coated cover glass and silicone-coated slide glass. Some weights should be put on the cover glass.
9. Polymerize the sections and resin by heating them in an oven at 60 °C for 2 days.
10. Carefully remove the cover glass from the slide glass with a new razor blade. The embedded sections stick to the cover glass or slide glass. Carefully remove the samples.

3.6 Ultrathin Sectioning

1. Identify the region of interest under a light microscope.
2. Cut a sample to make a small piece which contains the region of interest under a stereoscopic microscope.

3. Mount the small piece of the sample on a flat-tipped rocket of the resin by glue. Trim the sample on the rocket by a razor blade.
4. Place the rocket in a ultramicrotome, and then expose surface of the tissue in the resin sample by a Sumi knife.
5. Make ultrathin sections (about 70 nm thickness) with a diamond knife. Ribbons of the ultrathin sections are collected and mounted on Pioloform-coated grids.

3.7 Post-embedding Immunohistochemistry for GABA

1. Etching of the mounted ultrathin sections with 0.1 % periodic acid in DDW for 5 min.
2. Wash the grids in DDW three times (3 × 3 min) and then in TBS three times (3 × 1 min).
3. Block nonspecific binding by incubating sections in blocking solution, TBS containing 2 % normal donkey serum, and 0.05 % Photo-Flo (10 min).
4. Reaction with the primary antibody. Incubate grids overnight at 4 °C with TBS containing anti-GABA rabbit antibody (1:1000 diluted), 2 % normal donkey serum, and 0.05 % Photo-Flo.
5. Wash the grids in TBS three times (3 × 5 min).
6. The grids are further subjected for blocking in TBS containing 2 % normal donkey serum and 0.05 % Photo-Flo for 10 min.
7. Make the samples react with the second antibody at room temperature in TBS containing colloidal gold-conjugated anti-rabbit IgG goat antibody (1:100 diluted), 2 % normal donkey serum, and 0.05 % Photo-Flo for 2–4 h.
8. Wash the grids in TBS (3 × 5 min) and DDW (2 × 5 min).
9. Perform electron staining in uranyl acetate solution for 20 min and in lead citrate solution for 2 min. Before EM examination, the grids are washed in DDW and dried at room temperature.
10. The sample is observed with a transmission electron microscope. Figure 2d shows that a terminal positive for GFP (arrows, silver precipitations) exhibits GABA immunoreactivity (arrowheads, gold particles) and establishes synaptic connections with a dendrite. The GFP immunoreactivity indicates that the labeled terminal is derived from the injection site (SpVi).

4 Notes

1. If we want to prevent virus infection from passing axons, glass pipettes of thin tip (diameter: 5–10 μm) should be used for injections of virus solution in the surgery. The virus which was injected with a thin-tip pipette is seldom infected from axons,

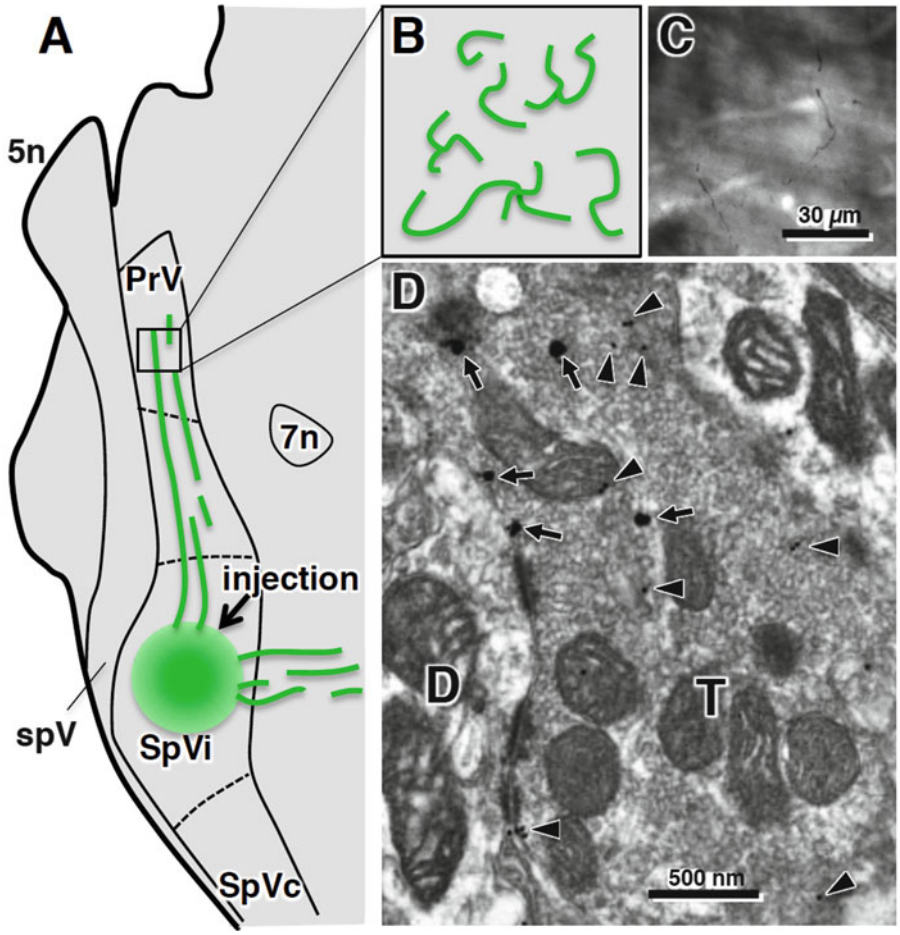

Fig. 2 An example of electron microscopic analysis combined with the virus tracer labeling. (**a**) The Sindbis virus was injected into the SpVi. Neural elements of neurons in the injection site are labeled by GFP (*green*). (**b**) In the target area (PrV), axons and axon terminals which are derived from the injection site (SpVi) are visualized by GFP. (**c**) After immunogold staining for GFP and silver enhancement process, GFP-positive axons and axon terminals can be observed under a light microscope. (**d**) High-power electron micrograph of a GFP-positive terminal. Large black silver precipitates (*arrows*) indicate the presence of GFP, and *small black dots* (*arrowheads*) show post-embedding immunogold reactivity for GABA. The GFP-positive terminal (*T*) establishes symmetrical synaptic contacts on a dendrite (*D*)

although we occasionally observed retrograde labeling when we used thick-tip pipettes. Thus, we suspect that the retrograde labeling is caused by virus infection from "stumps" of broken axons. The thin-tip pipettes also have a merit of preventing spilling over of the injection solution.

2. When we inject solution into brain tissue by pressure, we should go slowly. If we inject it quickly, the solution escapes along the outer wall of the injection pipette and spills over. We take at least 5 min to inject solution of 0.1–0.5 μL and wait for another 5 min before we remove the pipette from the brain.

3. The length of the silver enhancement reaction should be optimized by pilot experiments and further adjusted in each trial by checking staining in the sections. In our procedure, the low concentration (0.05 μg/mL) of the primary antibody for GFP causes low background staining and thus leads sections light in color even after the silver enhancement process. Please notice that if the color of the sections turns darker during the silver enhancement, the reaction should be too much. It is recommended that the silver labeling in GFP-positive axons is checked under a light microscope in each trial.
4. Etching is a very important process in the post-embedding immunostaining because antibodies cannot access the antigens under the resin. The etching process also works to reduce hydrophobicity of ultrathin sections and grids. The hydrophobicity of the specimens and grids would be a problem in the handling of samples during reaction with solutions.

Acknowledgments

This work was supported by the Ministry of Education, Science, Sports, and Culture of Japan Grants (15H04266, 15H01430 and 15K14333). We thank Dr. H. Bokor for the helpful advice on post-embedding immunostaining methods.

References

1. Deller T, Naumann T, Frotscher M (2000) Retrograde and anterograde tracing combined with transmitter identification and electron microscopy. J Neurosci Methods 103:117–126
2. McDonald AJ (1992) Neuroanatomical labeling with biocytin: a review. Neuroreport 3: 821–827
3. Furuta T, Timofeeva E, Nakamura K, Okamoto-Furuta K, Togo M, Kaneko T, Deschenes M (2008) Inhibitory gating of vibrissal inputs in the brainstem. J Neurosci 28:1789–1797
4. Furuta T, Tomioka R, Taki K, Nakamura K, Tamamaki N, Kaneko T (2001) In vivo transduction of central neurons using recombinant Sindbis virus: Golgi-like labeling of dendrites and axons with membrane-targeted fluorescent proteins. J Histochem Cytochem 49:1497–1508
5. Somogyi P, Hodgson AJ, Chubb IW, Penke B, Erdei A (1985) Antisera to gamma-aminobutyric acid. II. Immunocytochemical application to the central nervous system. J Histochem Cytochem 33:240–248
6. Tamamaki N, Nakamura K, Furuta T, Asamoto K, Kaneko T (2000) Neurons in Golgi-stain-like images revealed by GFP-adenovirus infection in vivo. Neurosci Res 38:231–236

Chapter 20

Morphological and Neurochemical Characterization of Electrophysiologically Identified Cells

Yoshiyuki Kubota

Abstract

It is now well known that there are many neuron subtypes in brain. For instance, a few subtypes of pyramidal cell in each layer and 10 or more non-pyramidal cell subtypes are found in neocortex. Their activity and functional role in the microcircuit are different among each cell subtype. Therefore, neuron subtype identification is very important to understand the functional role of the recorded neurons whose physiological firing properties are studied. Neuronal subtypes are morphologically and neurochemically distinct, so histological and immunohistochemical staining of the recorded cells promotes the cell identification. In this chapter, histological tissue preparation methods, for chemical marker identification, dendritic and axonal arborization tracing analysis, and observation by electron microscopy including block face scanning microscopy, of biocytin-injected recorded cells are described.

Key words Slice physiology, Immunohistochemistry, Biocytin, DAB, Dendrite, Axon, Neurolucida, Microwave, Resin

1 Introduction

The cortex is composed of 6 layers. Different connections among outputs, inputs [1], and the many different neuronal subtypes [2–9] occur in the microcircuits of each layer to result in our higher brain function. For instance, two major pyramidal cell subtypes are known in cortical layer V: corticopontine (CPn) cells projecting to the ipsilateral pons and crossed-corticostriatal (CCS) cells projecting to both sides of the striatum [6], and each has a distinct functional role in cortical microcircuits [10]. They are so called thick-tufted and slender-tufted cells, respectively [11]. The firing [12] and connection properties [13], transcription factor Ctip2 expression [9], and dendritic complexity [6] are different between CPn and CCS cells (Fig. 1). Pyramidal cells in layer II/III are also composed of a few subtypes with different projections [2, 14]. Non-pyramidal cells are the other major neuron type and are the inhibitory neurons of cortex (Fig. 1). They can be classified into

Rafael Luján and Francisco Ciruela (eds.), *Receptor and Ion Channel Detection in the Brain: Methods and Protocols*, Neuromethods, vol. 110, DOI 10.1007/978-1-4939-3064-7_20,

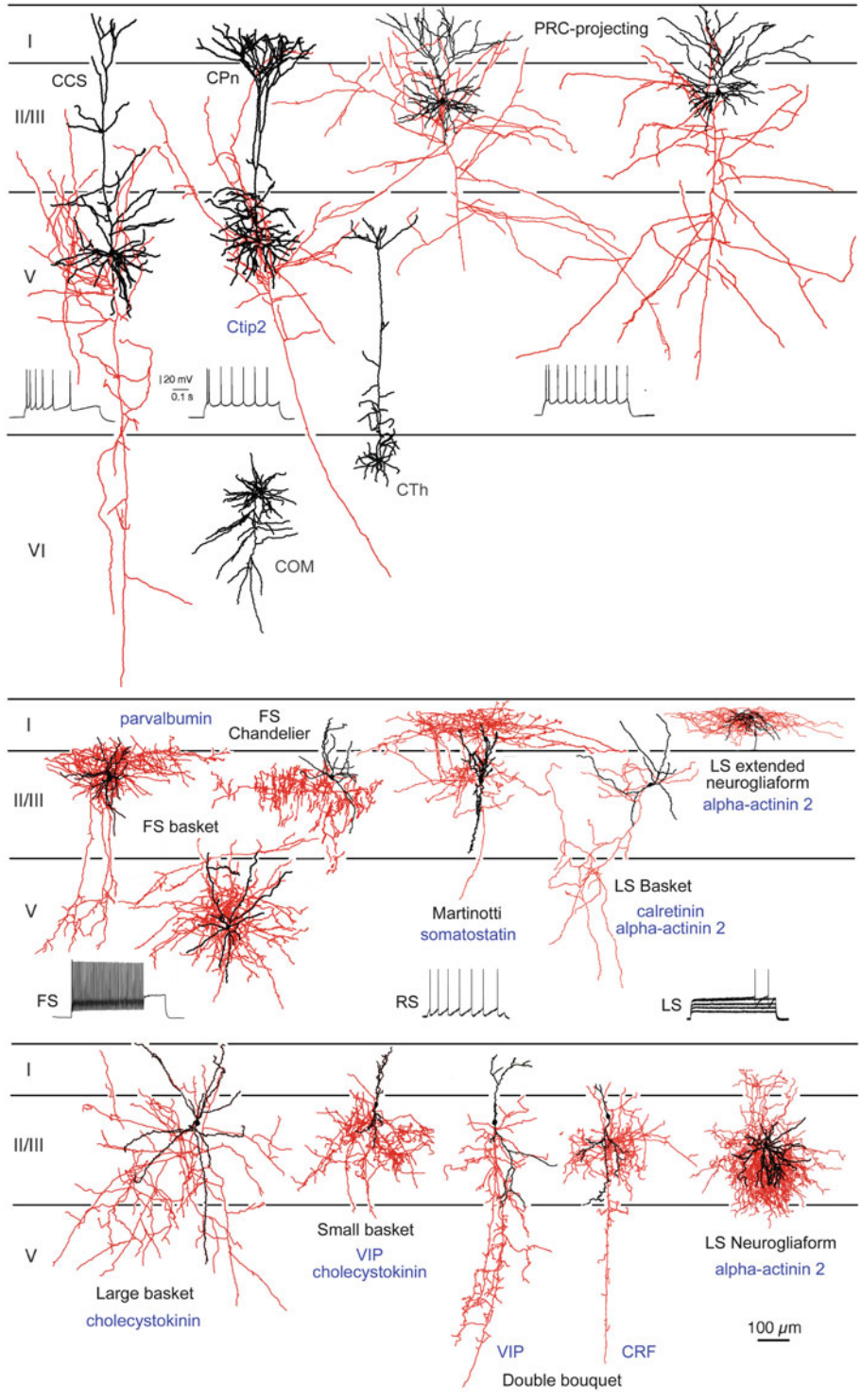

Fig. 1 Subtypes of cortical pyramidal and non-pyramidal cells. *Upper panel* show drawings of different subtypes of cortical pyramidal cells in layer II/III, V, and VI, and *lower panels* non-pyramidal cells in different layers. Cell soma and dendrites are shown in black, and axonal fibers are shown in *red*. The examples of firing patterns after step-current injection are shown. *CCS* crossed-corticostriatal, *CPn* corticopontine, *PRC* perirhinal cortex, *COM* commissural, *CTh* corticothalamic, *FS* fast spiking, *LS* late spiking, *RS* regular spiking, *CRF* corticotropin-releasing factor, *VIP* vasoactive intestinal polypeptide

more than ten subtypes [3, 4], and even more subtypes are found in hippocampus [15]. The morphology, firing properties, neurochemical marker expression, and functional connectivity are different among the various subtypes [3, 4, 15–19]. Altogether, we can identify at least more than 20 neuron subtypes in the cortex, and their activity is different during the different states of brain activity. Therefore, neuron activity analysis with subtype identification is very important to understand the functional architecture of the neuronal microcircuit. In most cases, the different cell subtypes are morphologically and neurochemically distinct, so morphological study of the physiologically analyzed cells should be a key issue for cell subtype identification. Therefore, determining different three distinct properties of a recorded neuron is key for the identification of the neuronal subtype: first, electrophysiological membrane property (fast spiking or regular spiking, etc); second, morphology of the neuron (dendritic and axonal arborization patterns, somatic shape, etc); and third, neurochemical marker expression (neurotransmitter, calcium binding protein, neuropeptide, transcription factor, and so on).

In this chapter, the histological staining protocols with fundamental principles and/or practical tips to investigate morphological and neurochemical characterization of the recorded cell are described step by step. The fixation is fundamentally important. Rapid microwave-enhanced fixation provides a good tissue preservation [20, 21]. Resection of the fixed slice to thinner sections raises the possibility to get a good immunoreactivity of neurochemical markers of the recorded cell soma as well as good and complete staining of the dendrites and axons [8]. Preparation of the slice tissue for electron microscopy (EM) observation provides information about connectivity with synapses of the recorded cell [22]. These anatomical investigations promote our understanding of the functional role of the recorded cells and contribute to brain microcircuit architecture analysis.

2 Material

2.1 Fixation

2.1.1 Paraformaldehyde

The fixative including paraformaldehyde must be fresh, because paraformaldehyde is known to degrade to formic acid easily. To prevent the chemical reaction, the fixative can be stored in a plastic tube (Fig. 2c) and kept in a freezer (−20 or −30 °C) right after making it. The paraformaldehyde is toxic for oral, skin, and respiratory contact and is a suspected carcinogen, so proper protection with a lab coat and lab gloves is essential. It is also important to work in a fume hood to prevent inhalation.

2.1.2 Glutaraldehyde

Glutaraldehyde is a strong fixative and is used to fix brain tissue for electron microscopic observation. Glutaraldehyde is also toxic for oral, skin, and respiratory system, so preventative measures as with

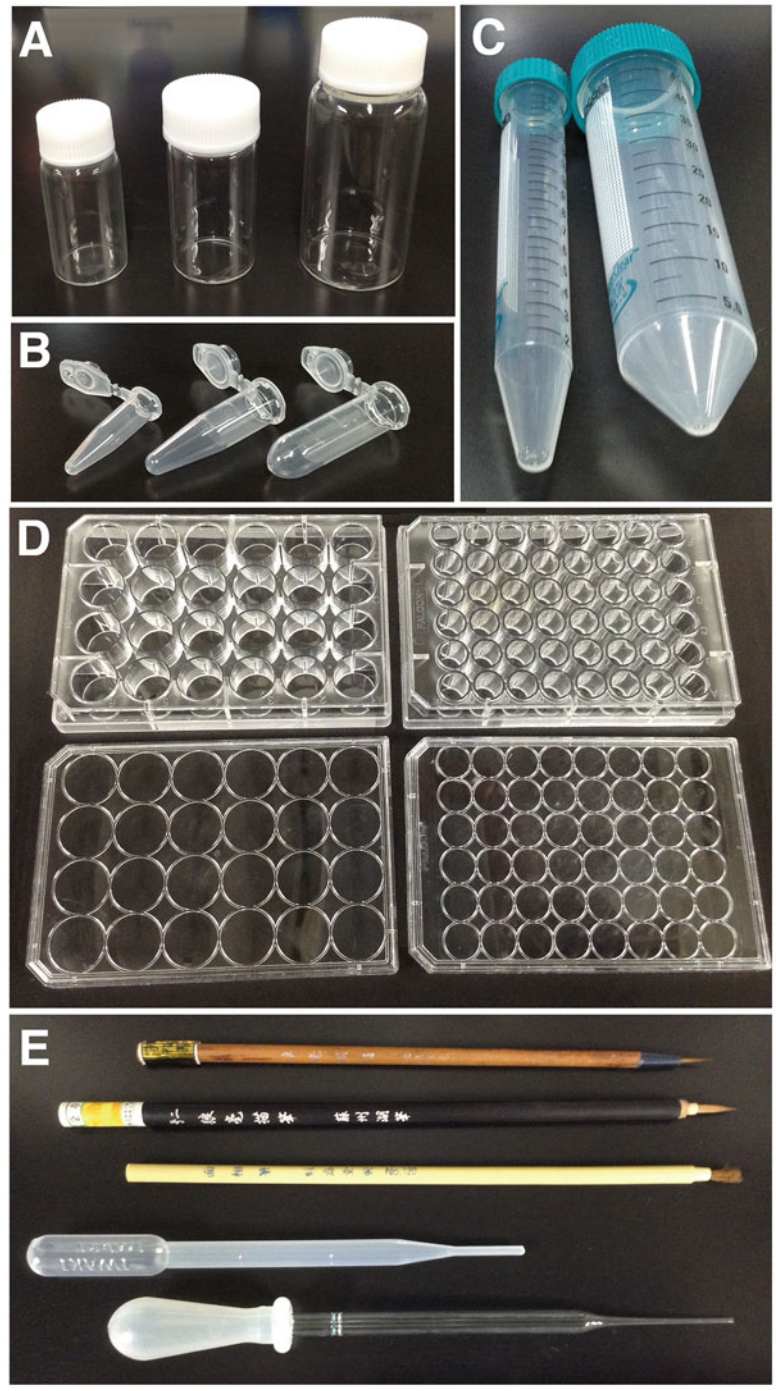

Fig. 2 Tools for histological experiments. (**a**) Glass screw vials. From left, 9, 13.5 and 30 mL volume. (**b**) Plastic microtubes. From left, 0.5, 1, and 2 mL volume. (**c**) Plastic centrifuge tubes. Left, 15 mL; right, 50 mL. (**d**) Multiwell culture plates. Upper left, size 24 wells; upper right, size 48 wells; lower, lids. (**e**) Brushes, plastic a disposable Pasteur pipette, a glass disposable Pasteur pipette. The tip of the glass pipette is polished by heat to prevent mechanical damage to the slice

paraformaldehyde are mandatory. Although tissue fixed with high glutaraldehyde (0.5 % ~) is known to show less immunoreactivity for a small number of primary antisera, most primary antisera are unaffected. This is probably because of the incubation buffer containing proteins and TX, which are believed to stabilize the IgG protein in the primary antiserum and expose the epitope in the tissue.

2.1.3 Picric Acid

Picric acid is a yellow powder and toxic for oral or skin contact, so protection with lab coat and lab gloves is required. Picric acid was used as an explosive to power cannonballs. In solid form it may explode following strong physical shock, friction, or vibration. To prevent explosion, usually water of 20 % is added to the picric acid by weight ratio, or picric acid saturated aqueous (1.2 or 1.3 %) solution is used. The fixative containing this reagent is known to be good for the ultrastructure preservation [23].

2.1.4 How to Make Fixative

100 mL fixative of 4 % paraformaldehyde, 0.2 % picric acid, 0.1 % glutaraldehyde in 0.1 M phosphate buffer (PB).

1. Put 50 mL of 0.2 M PB in Erlenmeyer flask. Stir and heat up to 60 °C on a hot plate magnetic stirrer.
2. Add 4 g of paraformaldehyde. Cover the mouth of the flask with plastic wrapping film to prevent evaporation. No need to add NaOH to change the pH to neutral, because the buffer keeps neutrality even after the paraformaldehyde dissolves.
3. It takes about 10 min to dissolve the paraformaldehyde powder in the hot buffer.
4. Cool it down in ice bath.
5. Filter it with filter paper.
6. Add 0.2 g of picric acid and stir on a magnetic stirrer.
7. Add 0.4 mL of 25 % glutaraldehyde.
8. Add Milli-Q water or distilled water up to 100 mL.
9. Aliquot 2 mL of the fixative into small screw vials of 5 mL volume size and put them in freezer (−20 or −30 °C) for storage (Fig. 2a).
10. Just before using it, take out from the freezer and thaw.
11. Used fixative should be stored in a plastic fixative waste tank, not poured into drain. It should then be dealt with by a chemical-disposal facility.

For high-quality electron microscopic ultrastructure, use fixative with high glutaraldehyde concentration: 4 % paraformaldehyde, 0.2 % picric acid, and 0.5–2 % glutaraldehyde in 0.1 M PB.

2.1.5 Preparation of Microwave for Rapid Microwave-Enhanced Fixation

1. Use a typical small kitchen microwave oven (Fig. 3a).
2. Take out the turn table.
3. Choose a few spots for trial microwave irradiation to identify the spots receiving the most microwave power (Fig. 3b) because the microwave intensity is variable dependent on the point.
4. Place a glass vial with cold 2 mL buffer at one of the spots (Fig. 3b) and measure temperature (Fig. 2c). The vial must be the same type used for the slice tissue fixation.
5. Switch on the microwave for 10 or 20 s, and measure the temperature of the buffer. Compare the increased temperature among the various spots. The spot that the temperature increased most is the suitable location for the microwave-enhanced fixation since it gets the most intense microwave. Note the location for the microwave-enhanced fixation.
6. Put three beakers with 500 mL of water at other locations in the microwave oven, which prevents extra heating of the tissue by absorbing excess microwave radiation (Fig. 3d).
7. Determine the irradiation time for which the temperature of the cold 2 mL buffer in the screw vial remains lower than 40 °C after the microwave irradiation to prevent the tissue denaturalization. Usually 10–20 s should be enough.

2.2 Resection of the Fixed Slice

In some experiments, the dendrites, soma, and axon of a biocytin-injected neuron fail to stain entirely, and/or the immunoreaction in the soma is faintly positive or false negative. This probably results from the incomplete penetration of the avidin/biotin complex: ABC complex (VECTASTAIN Elite ABC, Vector laboratories) and/or primary antiserum into the slice of 300 μm thickness. To get the better staining, resection of the 300 μm thick slices into 50 μm thick sections is one option.

2.2.1 Resection Method

1. Preparation of tools (Fig. 4a):

① Glass plate a: 2.5 cm × 5 cm × 6 mm, ultramicrotome glass strips (Fig. 4a①).

② Plastic plate for agar embedding: 1.5 cm square with about 3 mm in thickness (Fig. 4a②).

③ Large glass slide for holding the plastic plate (Fig. 4a③).

④ Blade tool: assembled three glass slides and a stainless blade with glue. It is for cutting the upper surface perfectly parallel to the bottom surface of the agar block that embeds the slice (Fig. 4a④).

⑤ Glass plate b: This should be larger than the blade tool (Fig. 4a⑤).

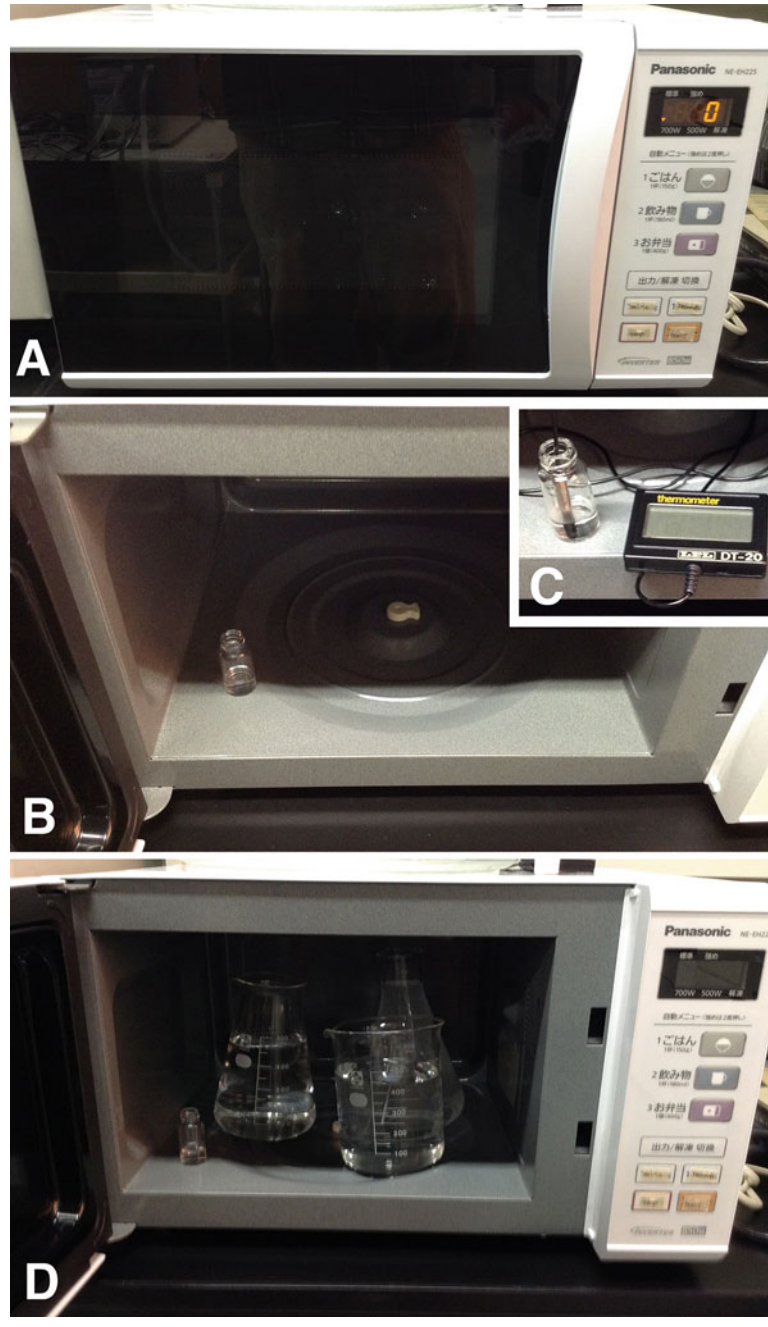

Fig. 3 Microwave for rapid microwave-enhanced fixation. (**a**) Kitchen microwave oven. (**b**) Fixed position of a glass vial for the rapid microwave-enhanced fixation. (**c**) Measuring changes in liquid temperature in the vial. (**d**) Microwave with excess amount of water to exclude overheating of the sample in the glass vial

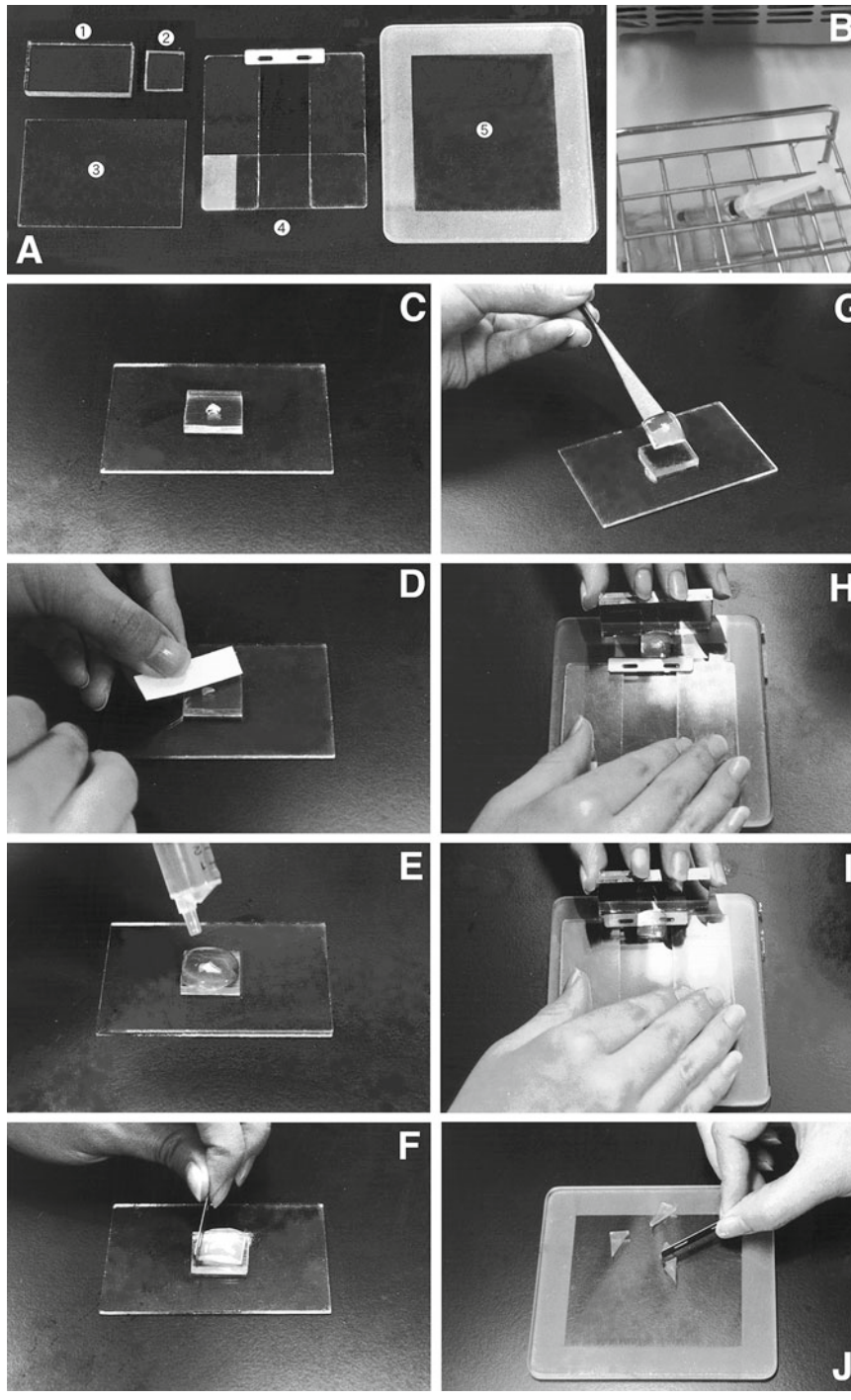

Fig. 4 Resection of fixed slice, step 1: Sequence of resection process for agar embedding. (**a**) Tools for resection of fixed slice. ① Glass plate a. ② A plastic plate for agar embedding. ③ A large glass slide. ④ A blade tool. ⑤ Glass plate b. (**b**) Agar mix solution in syringe is incubated in 43 °C water chamber. (**c**) Fixed slice on top of the plastic plate. (**d**) Removing excess water with filter paper. (**e**) Placing the melted agar mix solution onto the slice. (**f**) Trimming the agar block. (**g**) Get the trimmed agar block onto flat portion of drug spoon. (**h**) Placing the agar block on the glass place b. To hold one edge of the agar block with the glass board a. (**i**) Cutting the surface of the agar block by sliding the blade tool. (**j**) Trimming extra part of the agar block (This figure is reproduced and modified from Yasuo Kawaguchi (2009) [24] with permission from Yoshioka-shoten, Kyoto, Japan)

2. Preparation of solution:

   Agar mix solution (2.5 % agar, 0.25 % agarose): 1.125 g agar + 0.125 g agarose + 55 mL Milli-Q water

   1. Add 1.125 g agar and 0.125 g agarose in 55 mL Milli-Q water. Heat them in microwave to dissolve completely taking care not to overheat that may cause boiling over.
   2. Take the one part of the melted agar mix solution in syringe and float it in hot water bath (about 42–47 °C) to keep its liquid state (Fig. 4b).
   3. Put the rest of the melted agar mix solution in a laboratory dish in about 4–5 mm depth and place it in refrigerator to be solidified. This is used for the base for the resection.

3. How to resection the slice:

   Step 1 (Fig. 4)

   1. Prepare all tools for resection and agar solution (Fig. 4a, b).
   2. Stack the plastic board (3 mm thick and 1.5 cm square) on a flat glass board. Put the fixed slice, as flat as possible, on the plastic board (Fig. 4c). The slice can be covered with agar for stability. The plastic board may be omitted and the slice placed directly on the glass board. A plastic cylinder of about 1 cm length cut from a 5 or 10 mL plastic syringe is then placed on the glass board surrounding the slice.
   3. Remove excess water with filter paper (Fig. 4d).
   4. Drop the agar solution (42–47 °C) over the slice gently to cover it about 3–4 mm high (Fig. 4e).
   5. The agar becomes solid after about a minute. Then trim the agar block embedding the slice roughly to keep agar part at least 4 or 5 mm from the slice edge (Fig. 4f).
   6. Get the trimmed agar block onto the flat portion of drug spoon (Fig. 4g).
   7. Put the trimmed agar block on the flat glass plate b and hold one side of the agar block against the wall of the glass plate a (Fig. 4h).
   8. Cut the surface of the agar block by sliding the blade tool on the glass plate b (Fig. 4i). Then the upper and lower surface of the agar block must be nicely parallel.
   9. Trim the extra portion of the agar at about 2 mm from the slice edge of the agar block (Fig. 4j).

   Step 2 (Fig. 5)

1. Glue the solid agar mix base on cutting board of a slicer (Leica VT1000S, Vienna, Austria). Cut the agar mix base surface with a blade equipped with the slicer to make the surface of the agar mix base parallel to the cutting plane (Fig. 5a).

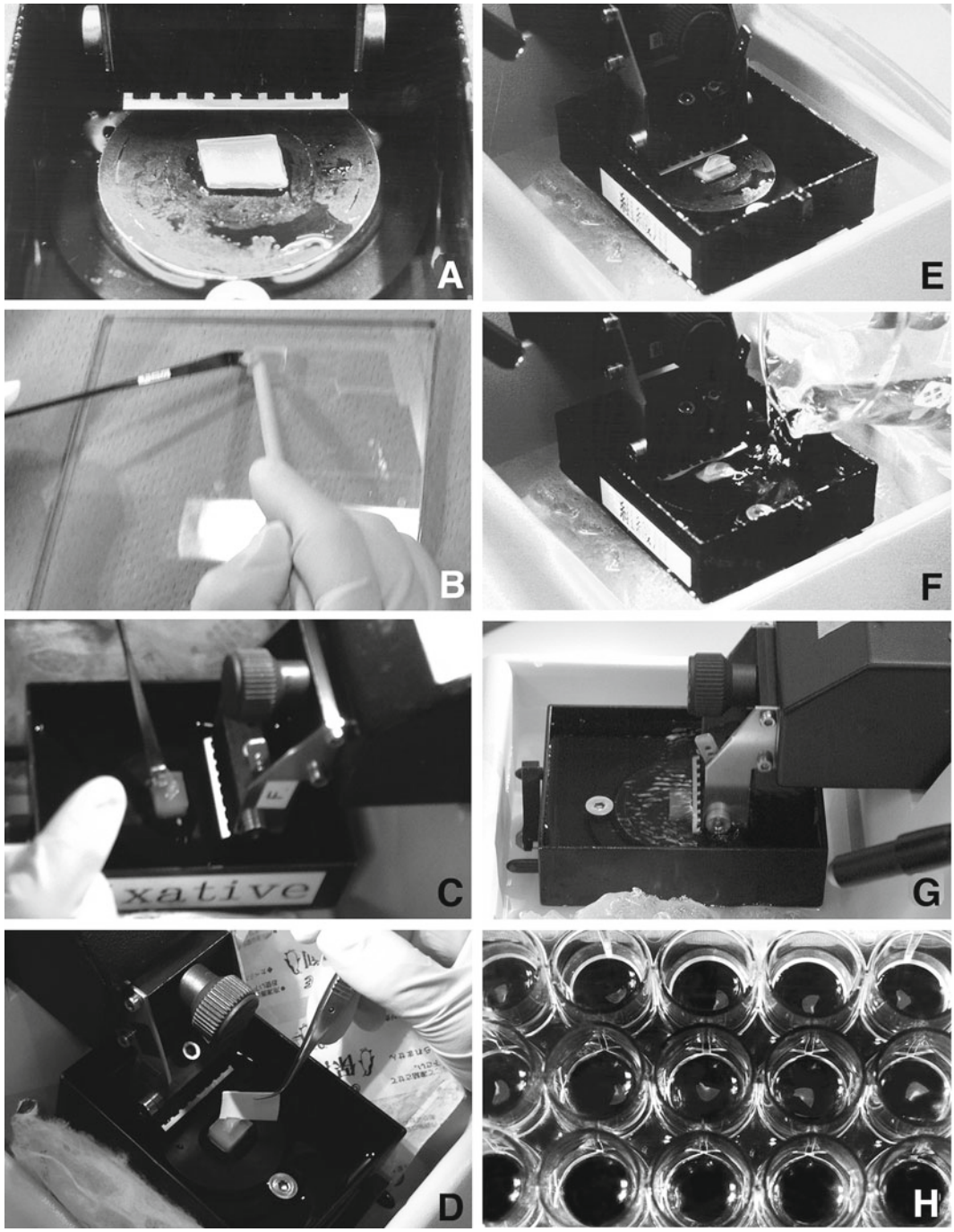

Fig. 5 Resection of fixed slice, step 2: sequence of resection process with slicer. (**a**) Section the agar base to make the surface parallel to the cutting plane. (**b**) Getting the trimmed agar block on drug spoon with brush. (**c**) Placing the agar block on spread glue on surface of the agar base with the slice side up. (**d**) Removing excess glue with filter paper. (**e**) Preparing for re-section. (**f**) Pouring cold buffer. (**g**) Re-sectioning in 50 μm thickness. (**h**) Collecting the sections in multiwell (This figure is reproduced and modified from Yasuo Kawaguchi (2009) [24] with permission from Yoshioka-shoten, Kyoto, Japan)

2. Put a drop of glue on the surface of the agar mix base and spread it evenly using the flat portion of the drug spoon. Gently and carefully place the trimmed agar block embedding the fixed slice on the agar mix base using a small drug spoon (Fig. 5b, c). The slice should be upper side of the agar block.
3. Remove excess amount of glue carefully with filter paper (Fig. 5d).
4. The slice surface should be parallel to the cutting plane (Fig. 5e).
5. Pour cold 0.1 M PB in the cutting tray (Fig. 5f).
6. Resection the slice at 50 μm thickness (Fig. 5g).
7. Collect the sections into a plastic multiwell using a small soft brush (Fig. 5h).

2.3 Freeze and Stock

2.3.1 Recipe of a Cryoprotectant Solution (30 % Glycerol, 30 % Ethylene Glycol, 0.04 M PBS) [25]

1. Mix: glycerol 60 mL, ethylene glycol 60 mL, 0.4 M PB 20 mL and 5 M NaCl 2.3 mL.
2. Add Milli-Q water or distilled water up to 200 mL.

2.3.2 Store Sections in the Cryoprotectant Solution

1. Put about 2 mL of the cryoprotectant solution in a small glass screw vial (Fig. 2a).
2. Place sections in the vial with a small brush gently and cap tightly (Fig. 2e).
3. Put them in a plastic container and store in −30 °C freezer. The sections can be good for the histochemical staining more than a year.

2.4 Immunohistochemical Staining

2.4.1 Immersion Buffer for LM Tissue: 10 % Normal Goat Serum (NGS), 2 % Bovine Serum Albumin (BSA), and 0.5 % Triton X-100 (TX) in 0.05 M Tris Buffer Saline (TBS)

10 mL NGS (S-1000, Vector Laboratories, Burlingame, U.S.A.), 2 g BSA, 2.5 mL 20 % TX are dissolved in 50 mL 0.1 M TBS and add Milli-Q water up to 100 mL.

2.4.2 Immersion Buffer for EM Tissue: 10 % NGS, 2 % BSA, 0 % or 0.04 % TX in 0.05 M TBS

10 mL NGS, 2 g BSA, and none or 0.2 mL 20 % TX are dissolved in 50 mL 0.1 M TBS and add Milli-Q water up to 100 mL.

2.4.3 Storage of the immersion buffer

Aliquot the Immersion Buffer into 1 or 2 mL in Plastic Microtubes (Fig. 2b) and Store Them in −20 or −30 °C Freezer Until Use.

2.5 Histological Staining

2.5.1 ABC Complex

ABC complex (VECTASTAIN Elite ABC, Vector laboratories) is avidin/biotinylated peroxidase complex and a highly sensitive reagent due to the large number of enzyme molecules.

How to make ABC solution with 0.04 % TX in 0.05 M TBS:

Add 10 μL each of A and B solutions of ABC complex into 1 mL 0.05 M TBS.

Incubate the mixed solution on a shaker for about 30 min.

Add 20 μL of 20 % Triton X solution to the mixed ABC solution.

2.5.2 Features of Nickel-Diaminobenzidine Tetrahydrochloride (DAB) Molecule

DAB is a carcinogen/mutagen for bladder cancer and so on, so protect yourself with a lab coat and lab gloves. DAB can aggregate easily around dirt or dust; therefore, a dish or vial for this reagent must be very clean. DAB is susceptible to contamination from oxidizing agents, such as kitchen bleach. However, the by-product altered by the hypochlorite also is mutagenic. Therefore, used DAB solution and the by-product of DAB molecule should be stored in a DAB waste plastic bottle, not poured into drain. It should then be dealt with by a chemical-disposal facility. Collect DAB-contaminated wastes (disposable plastic pipettes, pipette tips, papers, etc.) and keep them in a plastic bag for incineration. The DAB is light sensitive, especially direct sunlight.

2.5.3 How to Make the Nickel-DAB Solution

1. Add 2 mg of DAB and 30 mg of nickel (II) ammonium sulfate hexahydrate in 10 mL of 50 mM Tris-HCl, pH 7.6 and stir to dissolve well. It must be done in a dark place or dark box, because DAB is light sensitive, especially direct sunlight.
2. Use the solution on the day; otherwise aliquot the nickel-DAB solution into 1 or 2 mL in a plastic microtube (Fig. 2b) and store them in −20 or −30 °C freezer until use.
3. At a time of use, warm up a little bit to melt the DAB solution completely.

2.6 Osmium Fixation, Dehydration, and Embedding

2.6.1 Osmium Tetroxide: OsO4

Osmium tetroxide is a very harmful reagent, so protect yourself with a lab coat and lab gloves and work in a fume hood to prevent inhalation. We usually keep 4 % aqueous osmium tetroxide solution in special a glass bottle with a plug and cap that is specialized for the osmium tetroxide solution (Fig. 6a, b) and keep the bottle in a can or additional bottle to shut in the harmful gas (Fig. 6d). Otherwise, the inside of the refrigerator, where the osmium tetroxide bottle is stored, will become blackish by the osmium tetroxide gas. This reagent comes usually as 1 g of solid in a glass ampule (Fig. 6c). Wear plastic gloves. Wash the surface of the ampule carefully and scratch the center pit for entire circumference with an

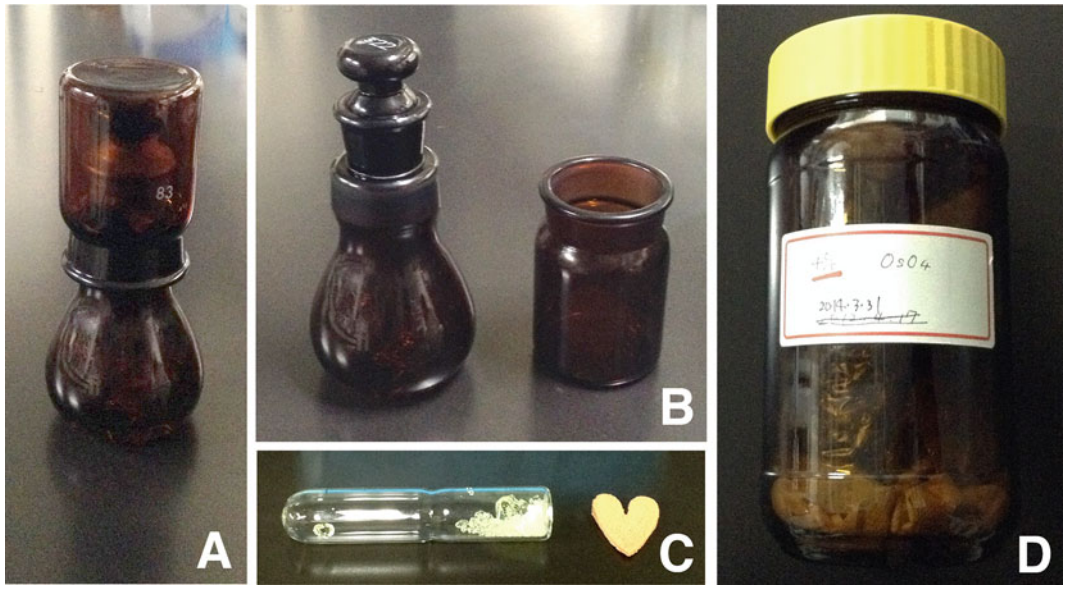

Fig. 6 Osmium tetroxide. (**a**) An osmium tetroxide stock solution glass container. (**b**) The container has an inner stopper and outer cap, double protected. (**c**) *Left*: A glass ampule contains 1 g of osmium tetroxide. *Right*: an ampule cutter to scratch the center pit. (**d**) The container is placed in this bottle for double protection

ampule cutter (Fig. 6c). Wash it carefully with Milli-Q water and put it in the special glass bottle (Fig. 6a, b) and plug it. Shake the bottle gently to break the ampule. It should be quite easily broken inside the bottle. Add 25 mL Milli-Q water and cap completely. Leave on shaker for hours until dissolved completely. Keep the 4 % aqueous osmium tetroxide solution bottle in the other can or bottle with some light impact absorber (Fig. 6d) and put it in a refrigerator. Used osmium tetroxide should be stored in a plastic osmium tetroxide waste bottle, not poured into the drain. Entrust it to a waste-disposal vendor.

2.6.2 Uranyl Acetate

Uranyl acetate is slightly radioactive and emits alpha rays, so protect yourself with a lab coat and lab gloves, and do not inhale. Even a thin sheet of paper can block the alpha rays. A half-life of uranium 238 is 4.468 billion years, so it is important not to drink nor inhale it. The uranyl acetate is light sensitive, especially direct sunlight. Uranyl acetate can be dissolved in water or 70 % ethanol, but it takes sometimes more than an hour. While dissolving on a magnet rotator, cover it with aluminum foil or in a paper box. Used uranyl acetate solution should be stored in a plastic uranyl waste bottle, not poured into a drain, and then properly disposed of.

2.6.3 Resin for Electron Microscopy (EM) Tissue Embedding

Resin (epon) is a skin carcinogen, so protect yourself with a lab coat and lab gloves. In case of touching resin directly, remove it with ethanol from skin. After resin polymerization, it becomes just a plastic and is not a carcinogen anymore. Resin that has absorbed water cannot be polymerized completely and will not be hard enough for ultrathin sectioning, so be sure the moisture of the room should be lower than about 50 %. The section embedded in the resin must be dehydrated completely. Used resin is collected in a disposable plastic or aluminum foil cup and place in 60 °C oven for 24–48 h for polymerization and then put in a trash box.

2.6.4 How to Make Resin

Epon 812 (TAAB, Aldermaston, UK)

Measure epon raw materials in a disposable plastic cup as follows, 28.5 g epon 812, 15.0 g DDSA, and 14.5 g MNA. Mix them thoroughly with a disposable plastic stick or a disposable plastic Pasteur pipette for about 10 min then add 0.7 g DMP-30. Mix well for 10 min. Aliquot it in the glass vials with a screw cap, and keep them in −30 °C freezer until use (Fig. 7a). At the time of use, take it from the freezer and leave for about an hour to warm up to room temperature, and then open the cap. If you open the cap of the vial that is still frozen, the glass wall inside the vial gets condensation. Consequently the epon gets water, and it cannot be polymerized enough for ultrathin section cutting.

Durcupan ACM (Sigma-Aldrich, St. Louis, USA)

Measure Durcupan ACM raw materials in a disposable plastic cup as follows: 11.4 mL (13.2 g) part A, 10 mL (10.9 g) part B, and 0.3 mL (0.31g) part C. Mix them thoroughly with a disposable plastic stick or a disposable plastic Pasteur pipette for about 10 min and add 0.05–0.1 mL (0.06 - 0.12 g) part D. Mix them well for 10 min, yielding a hard resin when polymerized. Aliquot it in the glass vials with a screw cap, and keep them in −30 °C freezer until use (Fig. 7a). At the time of use, take it from the freezer and leave it for about an hour to warm up to room temperature, and then open the cap. If you open the cap of the vial that is still frozen, the glass wall inside the vial gets condensation. Consequently, the epon gets water and it cannot be polymerized enough for ultrathin section cutting.

2.6.5 How to Wash Glass Vials Contaminated with Epon

Epon has high viscosity and is not water soluble. The glass vials and plastic caps contaminated with epon are kept in ethanol for a while to remove epon on the wall surface. Then wash them with a regular way using water and soap. The contaminated ethanol should be entrusted to a waste-disposal vendor.

2.6.6 Propylene Oxide

Propylene oxide is highly volatile and a probable carcinogen, so protect yourself with a lab coat and lab gloves and work in a fume hood to prevent inhalation. United States Environmental Protection Agency (EPA) has classified propylene oxide as a Group B2, probable human carcinogen. Used propylene oxide should be

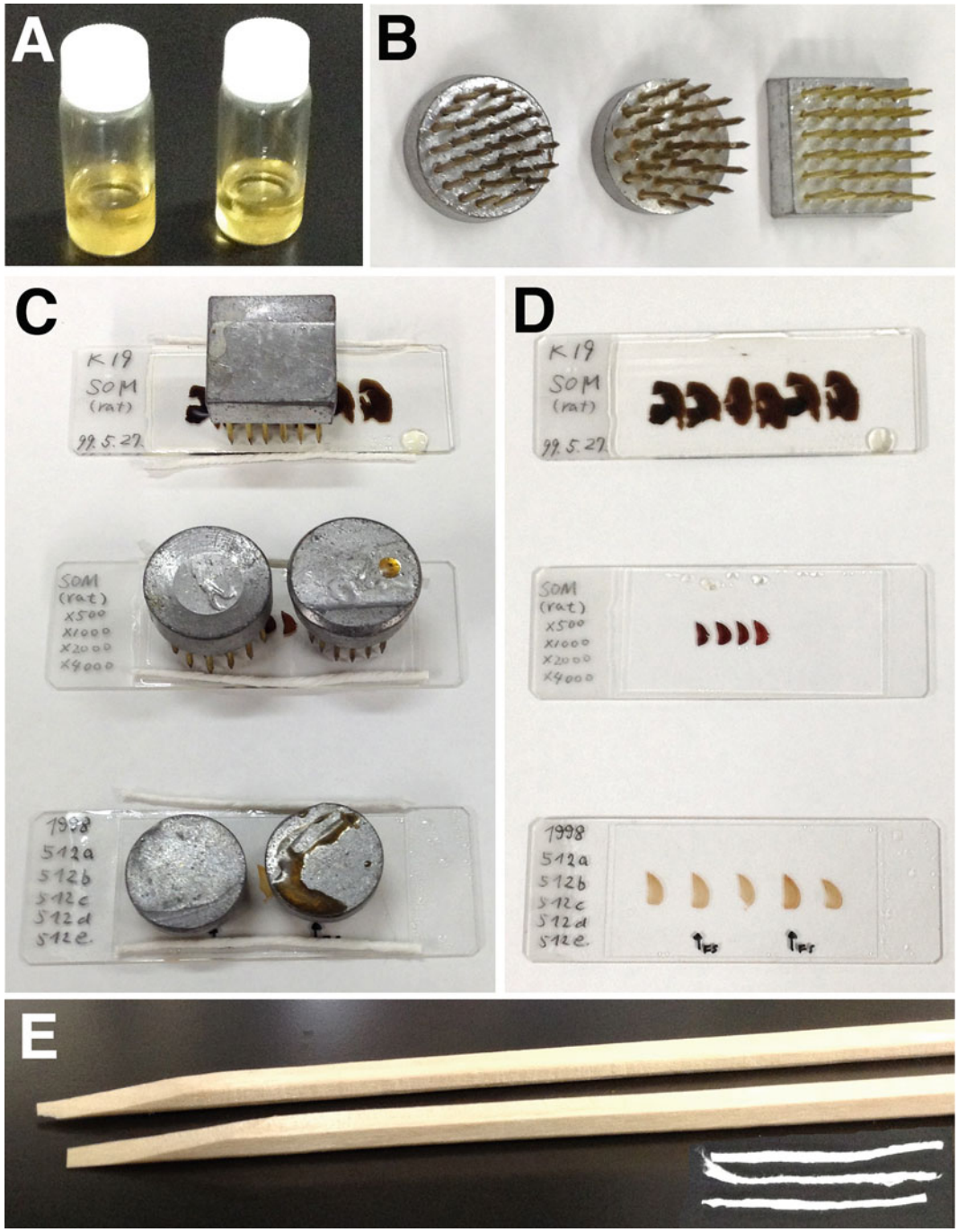

Fig. 7 Tissue embedding with resin. (**a**) Frozen resin in glass screw vials. (**b**) Small kenzans or frogs: needle-point holders. (**c**) The kenzans are used as weight to push the coverslip to ooze out excess amount of resin before polymerization. The paper strips absorb the oozing out resin from the side. (**d**) The specimen embedded in polymerized resin. *Upper*: perfused brain sections for EM preparation. *Middle*: re-sectioned slice for EM preparation. *Bottom*: re-sectioned slice for LM preparation with 0.1 % osmium tetroxide. (**e**) Disposable chop-sticks with the sharp flat tip for taking the section out from viscid pure resin. The tip end is cut sharp with cutter knife. Paper strips of lab paper are shown in *bottom right*

stored in a corrosion resistance plastic waste bottle, not poured into drain, because it dissolves drainage pipe made of vinyl chloride. Entrust it to a waste-disposal vendor.

2.6.7 Lead Aspartate

Lead aspartate is toxic and classified a probable carcinogenic (Category 2A) by the International Agency for Research on Cancer. The reagent brings about lead poisoning. Protect yourself with a lab coat and lab gloves. Used lead aspartate should be stored in a plastic waste bottle, not poured into a drain. Entrust it to a waste-disposal vendor.

2.6.8 How to Make Walton's Lead Aspartate [26]

Add 0.998 g of L-aspartic acid in 250 mL of Milli-Q water. The aspartic acid may be easier to dissolve in water with the pH adjusted to 3.8 with KOH. This stock solution is stable for a few months in refrigerator. Dissolve 0.066 g of lead nitrate in 10 mL of aspartic acid stock solution and adjust the pH to 5.5 with fresh 1 N KOH. The lead aspartate solution is placed in a 60 °C oven for 30 min and must be dissolved completely. Just before use, the solution is filtered with a 0.22-μm Millipore syringe filter.

2.6.9 Microwave with Temperature Control (Fig. 8)

Microwave with temperature control (PELCO BioWave Pro, Ted Pella, inc. Redding, USA) is designed for efficient processing of dehydration and resin penetration process (Fig. 8). Microwave irradiation is controlled with a set temperature to ensure no overheating of the sample tissue. It has an exhaust pipe to place in a fume hood or connect to an exhaust pipe line directly, to avoid contamination of the laboratory air.

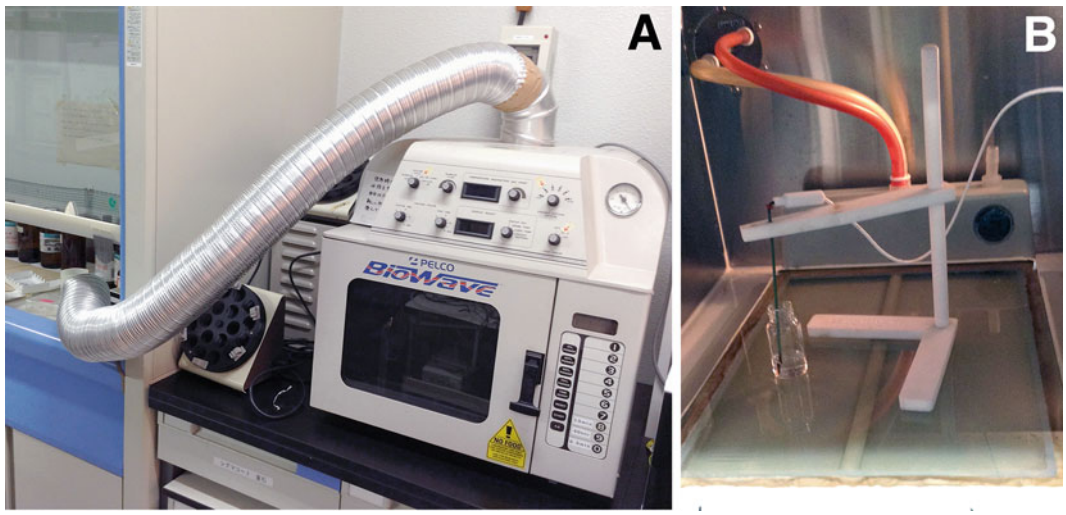

Fig. 8 Temperature-controlled microwave. (**a**) Overview of the temperature-controlled microwave. Exhaust duct leads to the fume hood in the *left*. (**b**) Thermometer for temperature control is inserted in the liquid in the glass vial. The base is a water circulator to exclude overheating the tissue

2.7 Perfusion for In Vivo Recording

Mix 0.5 mL 1 M $MgCl_2$ $6H_2O$, 8.5 g sucrose and 20 mL 0.1 M PB. Add Milli-Q water up to 100 mL.

2.7.1 Preparation of Solution

Prefixative (100 mL)

Fixative (100 mL)

Same as in Sect. 20.2.1.4 Aliquot the fixative and prefixative in plastic tubes and store them in a –20 or –30 °C freezer (Fig. 2c).

3 Methods

3.1 Slice Fixation

1. After a whole cell recording using patch pippete electrode with internal solution containing 0.5% - 1% biocytin, put the slice in fixative, 4 % paraformaldehyde, 0.2 % picric acid, 0.1 % glutaraldehyde in 0.1 M PB in the screw vial, and microwave for 10–20 s (Fig. 3) [5, 6, 19, 27, 28]. Then, put the vial on ice to cool the fixative down as soon as possible. The slice in the fixative should be kept on a shaker in a refrigerator overnight at 4 °C.
2. Wash the slice with 0.1 M PB the next day.

3.2 Slice Resection [24]

1. Wash in 0.1 M PB
2. Resection the 300 μm thickness slice into 50 μm thick sections with the agar mix using slicer (Leica VT1000S, Vienna, Austria) (Figs. 4 and 5).
3. Collect them in 0.1 M PB in a 24 plastic multiwell plate on ice (Fig. 5h).

3.3 Freeze and Stock

The sections or slices can be conveniently kept in the cryoprotectant solution [25] and stored in a freezer at –20 °C or –30 °C for more than a year. The storage method can keep the sections in good condition for histological staining for more than a year.

1. Put the sections in the cryoprotectant solution: 30 % glycerol, 30 % ethylene glycol, and 0.04 M PBS in a glass small screw vial (5–10 mL volume size).
2. Put them in a freezer.

3.4 Neurochemical Characterization with Immunohistochemical Staining [5, 8, 27, 28]

All the steps are processed at 4 °C.

1. Place the sections in 0.05 M TBS (or 0.05 M PBS) in a plastic multiwell plate (Fig. 2d) with a brush gently (Fig. 2e).
2. Suppress intrinsic peroxidase reactions by incubating sections with 1 % H_2O_2 in TBS for 30 min.
3. Wash sections with 0.05 M TBS for 10 min 3 times

4. Incubate sections with two primary antisera in immersion buffer overnight.

   For example:

   Anti-calretinin developed in rabbit diluted 1:1000, Swant #7696

   Anti-parvalbumin developed in mouse diluted 1:4000, Sigma-Aldrich #P-3171

   Immersion buffer for LM: 10 % NGS, 2 % bovine serum albumin, and 0.5 % TX in TBS

   Immersion buffer for EM: 10 % NGS, 2 % bovine serum albumin, and 0 % or 0.04 % TX in TBS

   The primary antisera for the double labeling should be developed in different species. Dilution rate of the primary antiserum should be determined by your own laboratory carefully.

5. Wash sections with TBS for 10 min 3 times.
6. Incubate sections in fluorescence conjugated secondary antiserums in the immersion buffer in a dark box overnight.

   Alexa 488 anti rabbit IgG diluted 1:200 (Life Technologies, Carlsbad, U.S.A.)

   Alexa 594 anti rat IgG diluted 1:200 (Life Technologies)

   Cross-reactivity of the secondary antiserum against IgG developed in different species must be carefully checked in preliminary experiments. It is better to use secondary antisera cross-absorbed against the other species IgG.

7. Wash sections in TBS for 10 min 3 times.
8. Incubate sections in AMCA (Alexa 350) streptavidin in TBS for 3 h in a dark box at RT.

   AMCA streptavidin diluted 1:2000 (Life Technologies)

   Alternatively, Texas red streptavidin can be used. In that case, use Alexa 350 or Alexa 633 anti rat IgG instead of the Alexa 594 anti rat IgG as a secondary antiserum.

9. Wash sections in TBS for 10 min 3 times each.
10. Mount on the glass slide and embed with FluoroGuard Antifade Reagent (Bio-Rad Laboratories, Hercules, USA). Spacer of the same thickness as the section (50 μm) should be embedded side by side to retain the section thickness (Fig. 9c). Double-sided tape of 30 μm thickness helps both retaining thickness and holding a coverslip conveniently (Fig. 9c).
11. After LM observation (Fig. 9), take the sections out from the glass slide gently with a brush and put them in TBS.

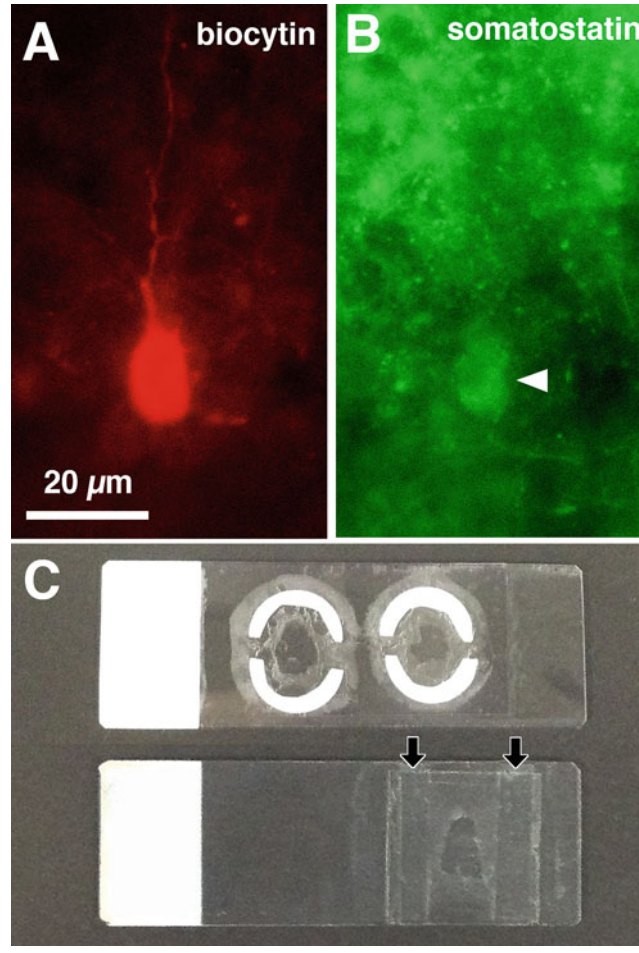

Fig. 9 Immunohistochemical staining. (**a**) Alexa 594 labeled biocytin-injected cortical non-pyramidal cell. (**b**) The recorded cell expresses somatostatin immunoreaction (*arrowhead*). (**c**) Slides prepared for a fluorescent microscopy. *Upper slide* embeds two sections with 50 μm thick spacers (*white*). *Bottom slide* embeds a section between strips of double-sided lucent tape of 30 μm thickness (*arrows*)

3.5 Histological Staining [2, 7, 9, 13, 27, 29–32]

All the steps are processed at 4 °C.

1. Wash sections with 0.05 M TBS (or 0.05 M PBS).
2. Suppress intrinsic peroxidase reactions by incubating sections with 1 % H_2O_2 in TBS for 30 min.
3. Wash sections with 0.05 M TBS for 10 min 3 times.
4. Incubate sections in ABC complex (1:100, Elite ABC, Vector) in 0.04 % TX in TBS for 3 h at RT or overnight at 4 °C.
5. Wash the sections in TBS for 10 min, 2 times.
6. Wash the sections in 0.05 M Tris-HCl buffer (TB) for 5 min.

Nickel-DAB staining or DAB staining method

A. Nickel-DAB staining

Visualize the recorded neuron by dark blue-black color.

1. Incubate the sections in nickel-DAB solution for 30 min in dark.
2. Add H_2O_2 for final concentration 0.01 % for 0.5–2 min.

   Add 10 μL of 1 % H_2O_2 solution in 1 mL nickel-DAB solution while agitating the well slowly. The reaction time is usually 0.5–1 min.
3. Wash the sections in TB to stop the nickel-DAB reaction.
4. Observe the cell under a light microscopy.
5. If the cell is stained appropriately, then wash the sections in TBS for 5 min 3 times. If the cell is still very weakly stained, then repeat the nickel-DAB reaction process (2).
6. Wash the sections in 0.1 M PB.

B. DAB staining

Visualize the recorded neuron by brown color.

1. Incubate the sections in DAB solution (50 mg/100 mL in TB) for 30 min in dark.
2. Add H_2O_2 for final concentration 0.01 % for 2–20 min.

   Add 10 μL of 1 % H_2O_2 solution in 1 mL DAB solution while agitating the well slowly. The reaction time is usually 2–5 min.
3. Wash the sections in TB to stop the DAB reaction.
4. Observe the cell under a light microscopy.
5. If the cell is stained appropriately, then wash the sections in TBS for 5 min 3 times. If the cell is still very weakly stained, then repeat the DAB reaction process (2).
6. Wash the sections in 0.1 M PB

3.6 Osmium Post-fixation, Dehydration, and Embedding

3.6.1 Conventional Tissue Process for LM (Fig. 7)

Section thickness becomes less than a half, maybe only 10 % or less.

1. Wash sections in 0.05 M PB.
2. Place the sections on a silane-coated glass slide (Sigmacote; Sigma-Aldrich) and dry them out.
3. 0.1 % osmium tetroxide in 0.1 M PB for 10 min.

This process should be done in a moist box in a fume hood.

4. Wash sections in Milli-Q water for 3 times.
5. 50 % ethanol for 5 min.
6. 70 % ethanol for 5 min.

7. 80 % ethanol for 5 min.
8. 90 % ethanol for 5 min.
9. 95 % ethanol for 5 min.
10. 99.5 % ethanol for 5 min.
11. 100 % ethanol twice for 5 min.
12. Embed with resin (epon or Durcupan ACM) at 60 °C for 48 h. Use only a few small drops of 100 % resin for embedding. Put metal weight on the top of the coverslip to remove excess amount of the resin. The resin oozing from the side should be absorbed with lab paper (Fig. 7).

    or

12. Xylene for 5 min (two times) and embed with Entellan New (E. Merck, Darmstadt, Germany)
13. LM observation.

3.6.2 Tissue Process for LM with Preserved Section Thickness (Fig. 7)

This method preserves the original section thickness up to about 90 % [33]; therefore, this is appropriate for tracing dendrites and axons.

1. Place the sections in 0.1 M PB in a glass screw vial with a brush (Fig. 2).
2. 0.1 % osmium tetroxide in 0.1 M PB for 60 min.
3. Wash the sections in 0.1 M PB for 10 min 3 times.
4. Wash the sections in Milli-Q water for 5 min.
5. 50 % ethanol for 5 min at 4 °C on shaker.
6. 70 % ethanol for 5 min at 4 °C on shaker.
7. Place the section between a glass slide and coverslip for 15 min in 70 % ethanol to make the section perfectly flat.
8. Place the sections back to the glass screw vial with 80 % ethanol for 5 min at 4 °C on shaker.
9. 90 % ethanol for 5 min at 4 °C on shaker.
10. 95 % ethanol for 5 min at RT on shaker.
11. 99.5 % ethanol for 5 min at RT on shaker.
12. 100 % ethanol twice for 5 min at RT on shaker for 2 times.
13. 50 % resin (epon or Durcupan ACM) in ethanol for 1 h on shaker.
14. Tissue sections are then mounted on glass slide with thin flat tip of disposable chopsticks (Fig. 7e) and embedded in pure resin and covered with a coverslip. The osmium tetroxide-fixed tissue is very fragile, so handle with care.
15. Put a metal weight on the top of the coverslip to remove excess amount of the resin. The resin oozing from the side should be absorbed with lab paper (Fig. 7).

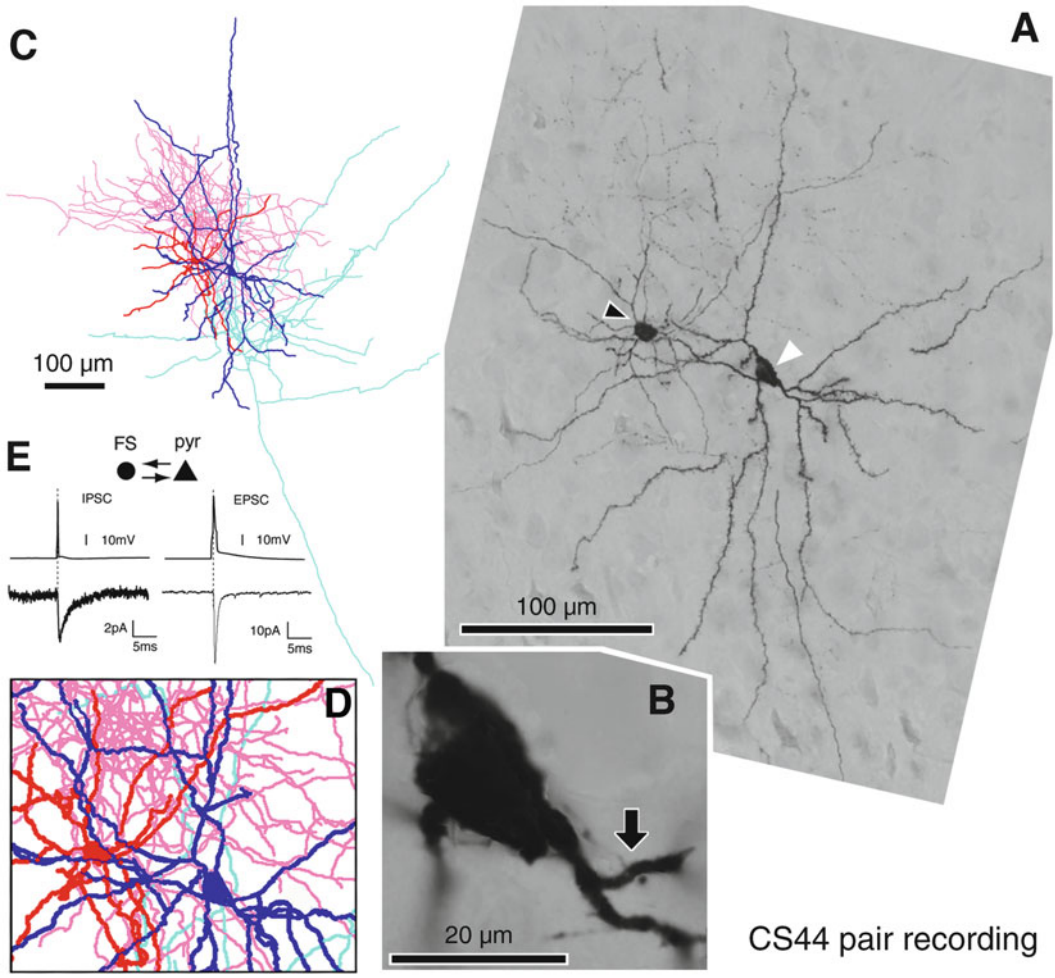

Fig. 10 Recorded cell staining and tracing [19]. (**a**) Focus stack light micrograph of biocytin injected an FS basket non-pyramidal cell (*arrowhead*) and a pyramidal cell (*white arrowhead*) in layer V of rat cortex. (**b**) Enlarged pyramidal cell soma with the FS basket cell axon contact (*arrow*). (**c**) Reconstruction of the pyramidal cell soma-dendrites (*blue*) and axon (*sky blue*), The FS basket cell soma-dendrites (*red*) and axon (*pink*). (**d**) Close-up of the proximal area of the pair cells in the same magnification as in (**a**). (**e**) Average IPSC response in the pyramidal cell (*bottom left*) to a single AP elicited in the FS basket cell (*upper left*). Average EPSC response in the FS basket cell (*bottom right*) to a single AP elicited in the pyramidal cell (*upper right*)

16. Place the specimen in a 60 °C oven for 48 h for polymerization. Place the resin-contaminated paper in the oven for the polymerization. The resin is wiped off with paper from the resin-contaminated chopstick, which is also placed in the oven for the polymerization and reuse.
17. LM observation (Fig. 10). The tissue sections embedded in polymerized resin should be in good condition for many years as were the specimens prepared by Santiago Ramon y Cajal.

3.6.3 Tissue Process for EM [34, 35] (Fig. 7)

This method preserves the original section thickness at about 90 % [33]; therefore, this is the appropriate method to trace dendrites and axons.

1. Place the sections in 0.1 M PB in a glass vial with a screw cap for 10 min
2. 1 % Osmium tetroxide, 1.5 % potassium ferrocyanide in 0.1 M PB for 60 min
3. Wash the sections in 0.1 M PB for 10 min 3 times.
4. 1 % osmium tetroxide in 0.1 M PB for 60 min.
5. Wash the sections in 0.1 M PB for 10 min 3 times.
6. Wash the sections in Milli-Q water for 5 min 3 times.
7. Incubate the sections in 1 % uranyl acetate in Milli-Q water in dark for 40 min.
8. Wash the sections in Milli-Q water for 10 min 3 times.
9. 50 % ethanol for 5 min at 4 °C on shaker.
10. 70 % ethanol for 5 min at 4 °C on shaker.
11. Place the section between a glass slide and coverslip for 15 min in 70 % ethanol to make the section perfectly flat.
12. Place the sections back to the glass screw vial with 80 % ethanol for 5 min at 4 °C on shaker.
13. 90 % ethanol for 10 min at 4 °C on shaker.
14. 95 % ethanol for 15 min at RT on shaker.
15. 99.5 % ethanol for 15 min at RT on shaker.
16. 100 % ethanol twice for 10 min at RT on shaker for 2 times.
17. 50 % resin (epon or Durcupan ACM) ethanol for 2–3 h or overnight at RT on shaker.
18. Put 100 % resin for a few hours or overnight. Tissue sections are then mounted on a Sigmacote (Sigma-Aldrich) coated or siliconized glass slide with the thin flat tip of disposable chopsticks (Fig. 7e). They are embedded in 100 % resin and covered with the coated coverslip.
19. Put metal weight on top of the coverslip to remove excess amount of the resin. The resin oozing from the side should be absorbed with lab paper (Fig. 7).
20. Place the specimen in a 60 °C oven for 48 h for polymerization. The resin-contaminated paper is also placed in the oven for polymerization. The resin is wiped off with paper from the resin-contaminated chopstick, which is also placed in the oven for the polymerization and reuse.
21. LM observation (Fig. 10).

3.6.4 Dehydration Using Temperature Controlled Microwave (Fig. 8) [13]

1. Wash the sections in Milli-Q water for 5 min.
2. 50 % ethanol for 5 min at 4 °C on shaker.
3. 70 % ethanol for 5 min at 4 °C on shaker.
4. Place the section between a glass slide and coverslip for 15 min in 70 % ethanol to make the section perfectly flat.
5. Place the sections back to the glass screw vial with 80 % ethanol. Place it in microwave and put the thermometer sensor in the ethanol. Adjust the temperature control under 37 °C and microwave for 40 s. Larger amount of ethanol for the microwave dehydration result in smaller temperature increase. Then place it on ice (4 °C) on shaker for 5 min. Dehydration in microwave should be without a cap and on shaker should be with a cap.
6. 90 % ethanol for 40 s in microwave with temperature <37 °C and then 5 min on shaker at 4 °C
7. 95 % ethanol for 40 s in microwave with temperature <37 °C and then 5 min on shaker at 4 °C.
8. 99.5 % ethanol for 40 s in microwave with temperature <37 °C and then 5 min on shaker at RT.
9. 100 % ethanol for 40 s in microwave with temperature <37 °C and then 5 min on shaker at RT for 2 times.
10. Propylene oxide or anhydrous acetone for 40 s in microwave with temperature <45 °C without a cap and then 5 min on shaker at RT. The cap of the vial must be tightly closed to prevent evaporation. Put enough amount of propylene oxide or anydrous acetone, because it is very evaporable during heating by microwave. Repeat this step twice.
11. 50 % resin (epon or Durcupan ACM (Sigma-Aldrich)) acetone/propylene oxide for 15 min in microwave <45 °C. Use the other glass vial with similar amount of water to measure temperature with thermometer sensor.
12. Put 100 % resin (epon or Durcupan) overnight. Tissue sections are then mounted on a Sigmacote (Sigma-Aldrich) coated or siliconized glass slide with thin flat tip of disposable chopsticks (Fig. 7e). They are embedded in pure epon or Durcupan ACM and cover with the coated coverslip.
13. Put metal weight on the top of the coverslip to remove excess amount of the resin. The resin oozing from the side should be absorbed with lab paper (Fig. 7).
14. Place the specimen in a 60 °C oven for 48 h for polymerization. The resin-contaminated paper is also placed in the oven for the polymerization. The resin is wiped off with paper from the resin-contaminated chopstick, which is also placed in the oven for the polymerization and reuse.
15. LM observation (Fig. 10).

3.6.5 Tissue Processed for Serial Block Face Scanning Electron Microscopy (SBEM)

Coal-black color of ferrocyanide (reduced)-osmium tetroxide-thiocarbohydrazide-osmium tetroxide (rOTO) following by en block uranyl acetate-staining and lead aspartate-staining protocol [26, 36–38] (Fig. 11b). Cacodylate buffer used in the fixative and buffer instead of 0.1 M PB can enhance electron density of the tissue [26, 36]. However, it should be handled with care since it contains arsenic.

1. Take light micrographs of the stained cell.
2. Place the sections in 0.1 M PB in a glass screw vial and wash them for 10 min.
3. 1 % osmium tetroxide, 1.5 % potassium ferrocyanide in 0.1 M PB for 60 min. Sections turn to black color.
4. Wash the sections in Milli-Q water for 5 min 3 times.
5. Fresh 1 % thiocarbohydrazide (TCH) solution for 20 min at room temperature.

   Add 0.1 g TCH to 10 mL Milli-Q water and place in a 60 °C oven for 1 h. Agitate or shake the bottle gently every 10 min for resolving. Cool down and filter this solution with a 0.22 μm Millipore syringe filter (Millipore, Billerica, USA) right before use.
6. Wash the sections in Milli-Q water for 5 min 3 times.
7. 2 % Osmium tetroxide in Milli-Q water for 30 min.
8. Wash the sections in Milli-Q water for 5 min 3 times.

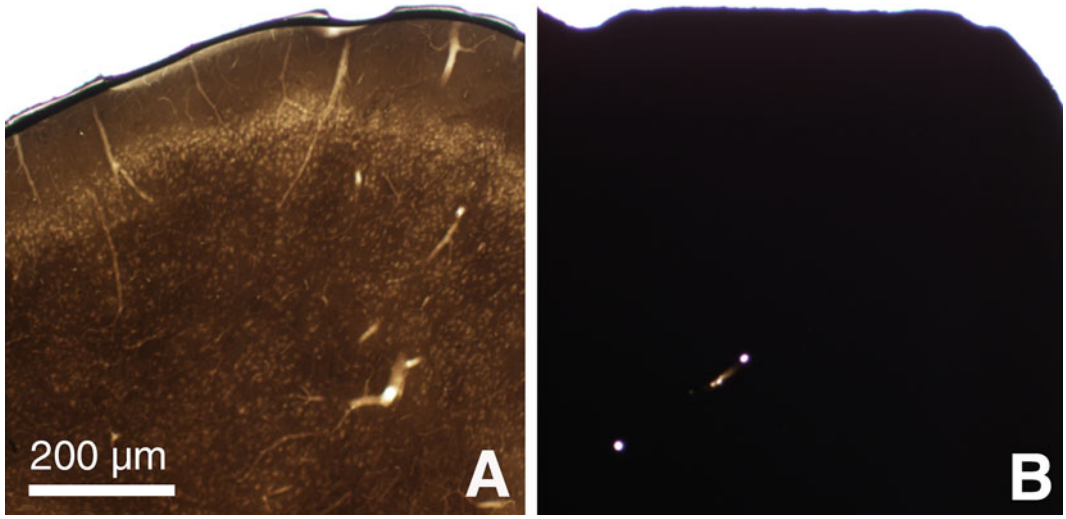

Fig. 11 Conventional osmium tetroxide staining versus heavy metal staining using rOTO *and en block* lead staining. (**a**) 50 μm thick section of cortex processed with conventional osmium tetroxide staining. (**b**) 50 μm thick cortical section processed with rOTO and en block lead staining. The section is completely dark, and light penetrates through only perpendicularly oriented blood vessels

9. Place the sections in 1 % uranyl acetate in Milli-Q water in dark at 4 °C for overnight.
10. Wash the sections in Milli-Q water for 10 min 3 times.
11. Placed sections in the Walton's lead aspartate solution, and put it in a 60 °C oven for 30 min.
12. Wash the sections in Milli-Q water for 10 min 3 times.
13. Dehydrate and embed sections with Durcupan ACM using the same processes in the Sects. 3.6.2 or 3.6.3.
14. Place the specimen in a 70 °C oven to polymerize for 72 h for harder polymerization as SBEM requires a tissue block with hard resin.

3.6.6 Perfusion for In Vivo Recording

1. After in vivo recording using juxtacellular electrode [18, 32], by which biocytin is injected into the recorded cell, the rat is perfused through heart with 5–10 mL prefixative solution of body or room temperature, following 200 mL fixative (4 % paraformaldehyde, 0.2 % picric acid, 0.1 % glutaraldehyde in 0.1 M PB) of body or room temperature for 150–250 g weight rat.
2. Leave brain in the animal body for a few hours at room temperature.
3. Take it out and put it in cold 0.1 M PB.

4 Notes

4.1 Rapid Microwave-Enhanced Fixation and Dehydration

Penetration of the fixative in the brain slice of 300 μm thickness is rather slow. It may not penetrate the entire tissue depth for an hour or so [39]. During the penetrating period, the neurons in the middle of the slice would get no oxygen, or glucose, which is bad for the neurons and the tissue, may degenerate. This affects ultrastructure of the tissue. Fixation with microwave promotes the fixative penetration into the tissue and provides better preservation of tissue structure [20, 21]. The reagent for the dehydration and resin penetration is also accelerated using microwave. It must be done under good temperature control to exclude the heat damage.

4.2 Tips for Good Immunohistochemistry

1. Triton X-100 (TX)
   It is necessary to dilute high viscosity liquid TX for the accurate measurement of its quantity. TX is a detergent that causes micro damage to cytoplasmic membranes and thus allows the IgG of primary antisera to penetrate into tissue. As a result, the tissue preservation may also get damaged to some extent. It is not a problem for LM observation, but the ultrastructure may not be good for EM observation. Therefore, it is highly recommended to use the immersion buffer without TX for

EM tissue preparation; however, the one containing low TX, for instance, 0.04 % TX, is OK.

2. Immersion buffer for primary and secondary antiserum
   The immersion buffer contains high concentration of protein: 10 % NGS and 2 % BSA. Concentrations of the primary and secondary antisera are extremely low: 1:100 ~ 1:10,000. The IgG protein may be more stable in solution rich in protein than water/buffer. Therefore, the NGS and BSA probably help the IgG proteins to be stabilized in the immersion buffer solution and consequently the tissue gets a good immunoreaction. In addition the NGS and BSA may have a background blocking effect on the immunoreaction of the tissue.
3. Whole cell recording
   Whole cell patch pipette records dialyze intracellular contents as biocytin enters a neuron. Short recording times therefore facilitate subsequent immunohistochemical detection, especially of soluble cytoplasmic molecules such as parvalbumin, calbindin D28K, and calretinin which may be lost during a long dialysis. Five to ten minutes or even shorter recording times are recommended to detect soluble cytoplasmic molecules by immunohistochemistry. Biocytin can penetrate throughout neuronal structures including dendrites and axons during records of this duration. In contrast, immunodetection of neuropeptides is not compromised by long recordings since these molecules tend to be fixed to the Golgi apparatus or other organelles.

4.3 Comparison of Nickel-DAB and DAB Staining Methods

DAB method stains the intracellular structure of the recorded cell very dark. The electron dense DAB-osmium product covers all of the intracellular space. This makes it easy to identify the recorded cell with electron microscopy; however, this obscures the intracellular structure, such as small vesicles in a presynaptic bouton, postsynaptic density of postsynaptic structures, microtubules in a dendrite and axon, etc. Nickel-DAB staining method reduces this problem. The nickel is involved in the DAB aggregation and prevents the light transmission to make the color dark at light microscopy (LM) with a shorter reaction time than the conventional DAB method. During the followed osmium tetroxide staining process, probably the nickel is detached from the DAB aggregation somehow, but osmium tetroxide takes the place to keep the similar darkness at the LM (Fig. 12a, d). However, DAB aggregation itself is a lot lighter because of the shorter reaction time. Consequently, the tissue may contain a lot weaker electron density of DAB-osmium tetroxide aggregation than the conventional DAB method. The small vesicles in presynaptic terminals and postsynaptic density (PSD) of the nickel-DAB-stained recorded neurons are visible more clearly than the DAB-stained recorded cells (Fig. 12b, c, e, f). This feature of the nickel-DAB protocol is a useful advantage to detect synaptic contacts.

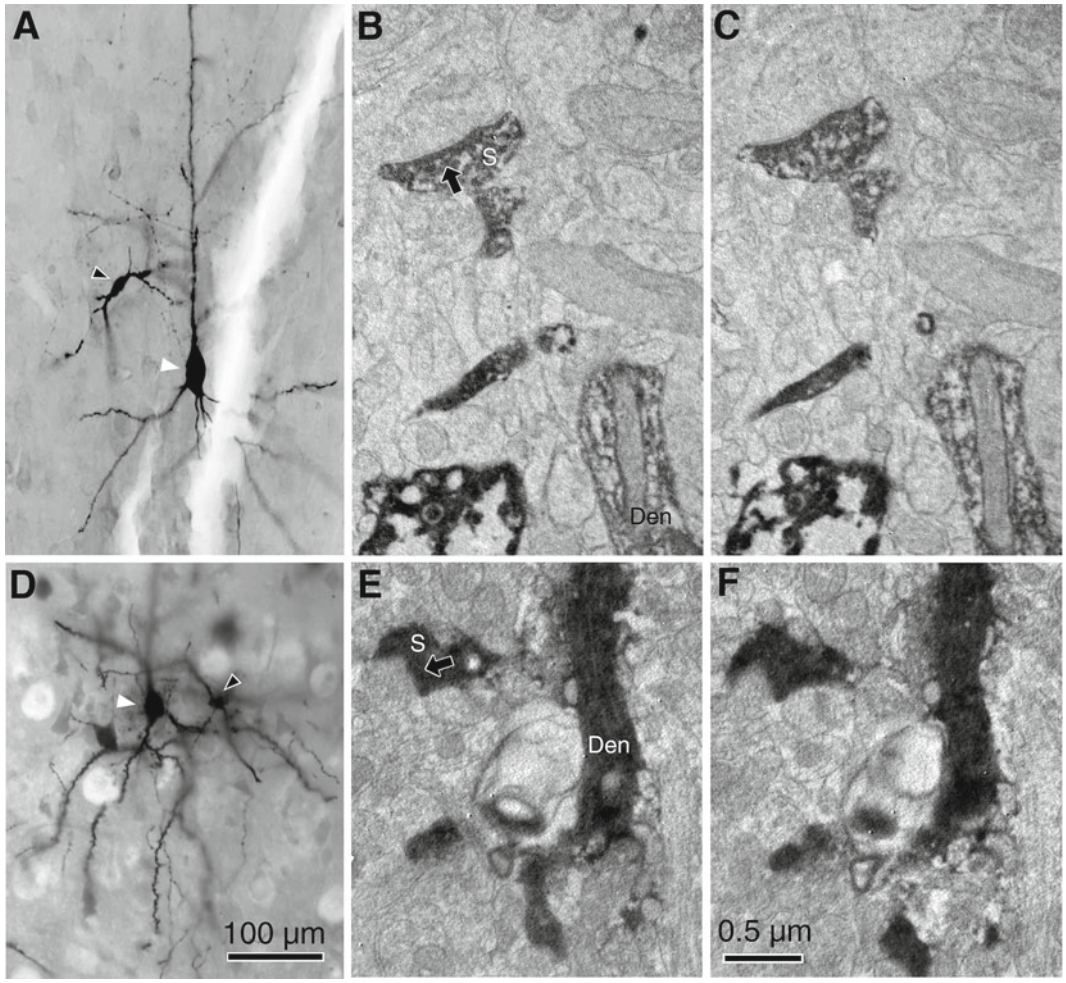

Fig. 12 Comparison of light micrographs and electron micrographs between nickel-DAB and DAB staining method. (**a**) A Recorded pyramidal (*white arrowhead*) and an FS basket cell (*arrowhead*) in cortical layer V stained by nickel-DAB protocol. (**b**, **c**) Successive serial electron micrographs in 50 μm thickness. The intracellular structure of the nickel-DAB-stained dendrite (*Den*) and spine (*S*) is visible. PSD (*arrow*) is visible. (**d**) **A** Recorded pyramidal (*white arrowhead*) and an FS basket cell (*arrowhead*) in cortical layer V stained by conventional DAB protocol. (**e**, **f**) Successive serial electron micrographs in 50 μm thickness. The intracellular structure of the DAB-stained dendrite (*Den*) and spine (*S*) is obscured by the dark dense reaction products. PSD (*arrow*) is not visible

4.4 Embedding Sections with the Resin

The resin is viscous liquid. The osmium tetroxide-treated tissue sections are very hard and fragile. The section quite easily breaks into small pieces in the viscous 100 % pure resin; therefore, handling of the sections should be done very carefully with the chopstick tool (Fig. 7e). Get the fragile sections on the flat tip of the tool gently and transfer to the Sigmacote-coated glass slide. In case of very fragile sections, you may skip the 100 % resin incubation.

Place a few drops/a grain of rice size of 100 % resin on the Sigmacote-coated glass slide, and place the sections in 50 % resin propylene oxide on the 100 % resin. Leave it for about 30 min for the propylene oxide to evaporate and then cover with a Sigmacote-coated coverslip.

The excess amount of resin must be removed with the method using the metal weight to ooze the resin from the side of the coverslip; otherwise the thickness of the preparation slide becomes thick, and the stained neurons may not be able to be focused well with a high magnification objective lens of short working distance. Air bubbles should not be embedded right above or below the stained cell, as this will interfere with LM observation.

4.5 Heavy Metal Staining Procedure for SBEM

SEM requires heavy metal staining which can be accomplished with the coal-black color of ferrocyanide (reduced)-osmium tetroxide-thiocarbohydrazide-osmium tetroxide (rOTO) following by en block uranyl acetate-staining and lead aspartate-staining protocol [26, 36, 37]. The heavy metal staining makes the section black, and the stained cell cannot be observed because of the dense black color of the section after the staining (Fig. 11) [40]. To identify the DAB stained cell, it is important to know the location of the cell in comparison with blood vessels that are clearly visible (Fig. 11b). The heavy metal staining procedure is also good for the other SEM-based observation systems, such as focus ion beam (FIB/SEM), automated tape-collection ultramicrotome (ATUMtome)/SEM system, because the tissue processed with this method requires less dwell time to capture scanning electron micrograph than that with the conventional EM staining method using less metal. The image quality improvement and shorter imaging time are advantages of this method [40].

4.6 Tips for Good Perfusion

1. For a good perfusion, the critical issue is successful and reliable supply of the fixative solution into the cardio vascular system. To increase the success rate, penetrate the injection needle (19G, Fig. 13a) through the apex into the left ventricle and furthermore into the ascending aorta. Clip it in the aorta to stabilize it for an adult rat with a bulldog clamp (Fig. 13c). Cut the right atrium to release blood and allow the flow of the fixative after circulation through the body. File the sharp needle tip of the perfusion needle until blunted (Fig. 13); otherwise the sharp tip penetrates the wall of the aorta. For a small rat or mouse, penetrate the injection needle (24G or 21G, Fig. 13a) through apex into the left ventricle and clip the needle in the heart to stabilize with the bulldog clamp (Fig. 13b).
2. Prefixative solution contains Mg that is a blocker of NMDA receptor and may be effective for decreasing neuron activity. We use only a small amount of the prefixative, 5–10 mL, before

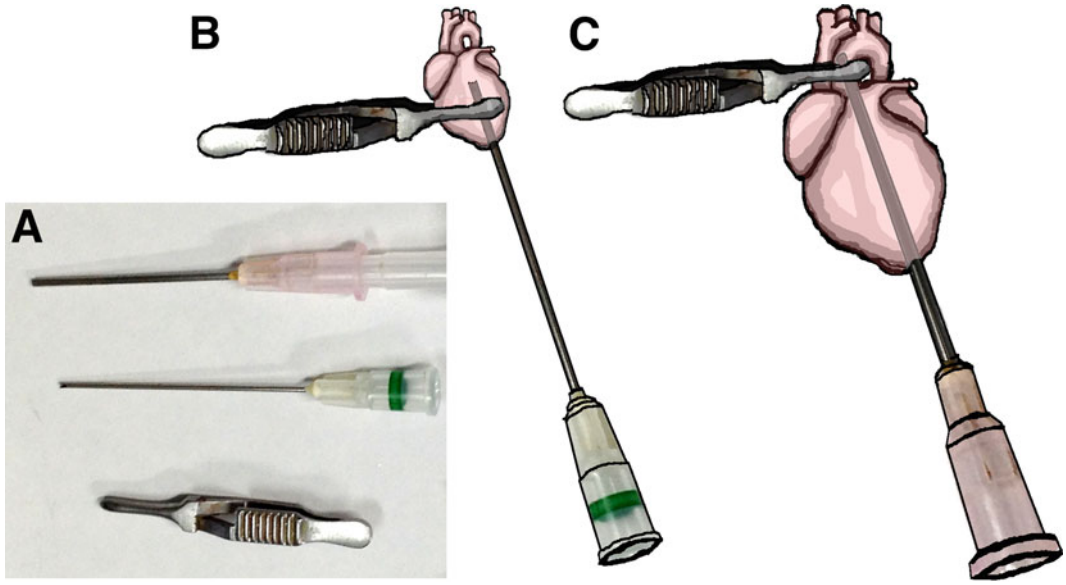

Fig. 13 Appropriate needle locations for perfusion. (**a**) From *upper*, a disposable 19 G injection needle with a blunted tip, a disposable 24 G injection needle with a blunted tip, a bulldog clamp. (**b**) For a small rat or mouse, penetrate the injection needle (24G or 21G) through apex into the left ventricle and clip the needle in the heart to stabilize with the bulldog clamp. (**c**) For an adult rat, penetrate the injection needle (19G) through the apex into the left ventricle and furthermore into the ascending aorta. Clip it in the aorta to stabilize it for an adult rat with a bulldog clamp

the perfusion using the fixative. This may reduce time without oxygen before killing neurons. Sucrose in the prefixative adjusts osmolarity to keep good tissue structure during perfusion of the prefixative. Picric acid and glutaraldehyde are added in the fixative to fix tissue well and increase the rigidity. Those reagents almost likely do not prevent immunoreactivity. The picric acid is yellow, which helps to see the border between the transparent prefixative and yellowish fixative in the transparent plastic tube of perfusion set.

3. The warm prefixative/fixative has a good effect on ultrastructure, because iced prefixative/fixative may shrink the muscle and blood vessels. The temperature also influences microtubule structure, which is neuronal cytoskeleton to maintain dendrites, axons as well as spine shape. It is known to depolymerize into stable αβ-tubuline dimers after the cooling down to 4 °C [41]. The spines are known to disappear in chilled ACSF [42]

4.7 Special features of Slice Tissue

The neuronal death is initiated upon slices cutting. Densely packed neuroglial profiles are found over several microns near their cut surfaces, presumably acting to remove neuronal debris. In contrast,

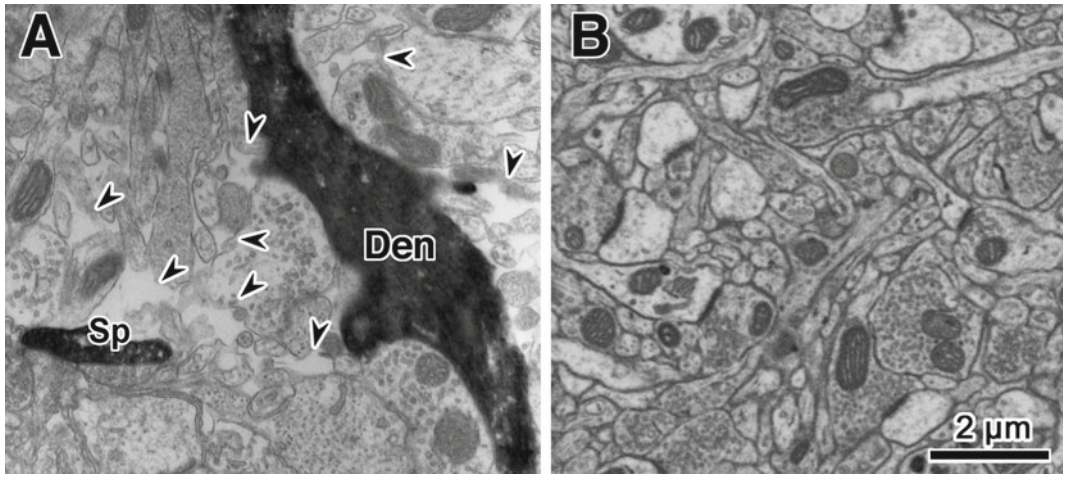

Fig. 14 Comparison of the ultrastructure of rat cortex from slice and perfused brain. (**a**) Many empty spaces are found in slice tissue (*arrowhead*). The dendrite (*Den*) and spine (*Sp*) of a recorded Martinotti cell are stained strongly with DAB after biocytin filling [35]. (**b**) In perfused brain tissue, neuronal and glial structures are densely packed without distinct intercellular space

neuronal profiles are sparsely distributed with many empty spaces at deeper sites in slices (Fig. 14a) [22]. Possibly neuroglia occupy these spaces in healthy brain tissue (Fig. 14b) [43]. A dense neuroglial layer at the slice surface may obstruct antiserum or ABC complex penetration, while penetration within the slice may be facilitated. Resectioning slices into thin sections is therefore needed to optimize staining.

Acknowledgments

We thank Drs. Yasuo Kawaguchi, Satoru Kondo, Mieko Morishima, Fuyuki Karube, and Yasuharu Hirai for neuron drawings, photos, and micrographs in the figures and Drs. Steven R. Vincent, Richard Miles and Fuyuki Karube for valuable comments. This work was supported by Grant-in-Aid for Scientific Research (B) (25290012), Grant-in-Aid for Scientific Research on Innovative Areas "Neural creativity for communication (No. 4103)" (24120718) and "Adaptive circuit shift (No. 3603)" 26112006 from the MEXT of Japan; The Imaging Science Program of National Institutes of Natural Sciences (NINS); Toyoaki Scholarship Foundation; and The Uehara Memorial Foundation.

References

1. Jones EG (1984) Laminar distribution of cortical efferent cells. In: Cerebral Cortex, vol 1. Cellular Components of the Cerebral Cortex, Plenum, New York, pp 521–553
2. Hirai Y, Morishima M, Karube F, Kawaguchi Y (2012) Specialized cortical subnetworks differentially connect frontal cortex to parahippocampal areas. J Neurosci 32:1898–1913
3. Kawaguchi Y, Kubota Y (1997) GABAergic cell subtypes and their synaptic connections in rat frontal cortex. Cereb Cortex 7:476–486
4. Kubota Y (2014) Untangling GABAergic wiring in the cortical microcircuit. Curr Opin Neurobiol 26:7–14
5. Kubota Y, Shigematsu N, Karube F, Sekigawa A, Kato S, Yamaguchi N, Hirai Y, Morishima M, Kawaguchi Y (2011) Selective coexpression of multiple chemical markers defines discrete populations of neocortical GABAergic neurons. Cereb Cortex 21:1803–1817
6. Morishima M, Kawaguchi Y (2006) Recurrent connection patterns of corticostriatal pyramidal cells in frontal cortex. J Neurosci 26:4394–4405
7. Otsuka T, Kawaguchi Y (2011) Cell diversity and connection specificity between callosal projection neurons in the frontal cortex. J Neurosci 31:3862–3870
8. Uematsu M, Hirai Y, Karube F, Ebihara S, Kato M, Abe K, Obata K, Yoshida S, Hirabayashi M, Yanagawa Y et al (2008) Quantitative chemical composition of cortical GABAergic neurons revealed in transgenic venus-expressing rats. Cereb Cortex 18:315–330
9. Ueta Y, Otsuka T, Morishima M, Ushimaru M, Kawaguchi Y (2014) Multiple layer 5 pyramidal cell subtypes relay cortical feedback from secondary to primary motor areas in rats. Cereb Cortex 24:2362–2376
10. Morita K, Morishima M, Sakai K, Kawaguchi Y (2012) Reinforcement learning: computing the temporal difference of values via distinct corticostriatal pathways. Trends Neurosci 35:457–467
11. Groh A, Meyer HS, Schmidt EF, Heintz N, Sakmann B, Krieger P (2010) Cell-type specific properties of pyramidal neurons in neocortex underlying a layout that is modifiable depending on the cortical area. Cereb Cortex 20:826–836
12. Otsuka T, Kawaguchi Y (2008) Firing-pattern-dependent specificity of cortical excitatory feed-forward subnetworks. J Neurosci 28: 11186–11195
13. Morishima M, Morita K, Kubota Y, Kawaguchi Y (2011) Highly differentiated projection-specific cortical subnetworks. J Neurosci 31:10380–10391
14. Ueta Y, Hirai Y, Otsuka T, Kawaguchi Y (2013) Direction- and distance-dependent interareal connectivity of pyramidal cell subpopulations in the rat frontal cortex. Front Neural Circuits 7:164
15. Klausberger T, Somogyi P (2008) Neuronal diversity and temporal dynamics: the unity of hippocampal circuit operations. Science 321:53–57
16. Jiang X, Wang G, Lee AJ, Stornetta RL, Zhu JJ (2013) The organization of two new cortical interneuronal circuits. Nat Neurosci 16:210–218
17. Lee S, Kruglikov I, Huang ZJ, Fishell G, Rudy B (2013) A disinhibitory circuit mediates motor integration in the somatosensory cortex. Nat Neurosci 16:1662–1670
18. Puig MV, Ushimaru M, Kawaguchi Y (2008) Two distinct activity patterns of fast-spiking interneurons during neocortical UP states. Proc Natl Acad Sci U S A 105:8428–8433
19. Yoshiyuki Kubota, Satoru Kondo, Masaki Nomura, Sayuri Hatada, Noboru Yamaguchi, Alsayed A. Mohamed, Fuyuki Karube, Joachim Lubke, Yasuo Kawaguchi (2015) Functional effects of distinct innervation styles of pyramidal cells by fast spiking cortical interneurons eLife (2015) eLife.07919
20. Jensen FE, Harris KM (1989) Preservation of neuronal ultrastructure in hippocampal slices using rapid microwave-enhanced fixation. J Neurosci Methods 29:217–230
21. Login GR, Dvorak AM (1988) Microwave fixation provides excellent preservation of tissue, cells and antigens for light and electron microscopy. Histochem J 20:373–387
22. Kubota Y, Kawaguchi Y (2000) Dependence of GABAergic synaptic areas on the interneuron type and target size. J Neurosci 20: 375–386
23. Somogyi P, Takagi H (1982) A note on the use of picric acid-paraformaldehyde-glutaraldehyde fixative for correlated light and electron microscopic immunocytochemistry. Neuroscience 7:1779–1783
24. Kawaguchi Y (2009) Anatomical and histological analysis of neurons recorded with electrophysiological method using whole cell electrode. In: Shin patch clamp jikkenn gijutsuho,

2009/10/26 edn, pp 118–131. Yoshioka Shoten in Japanese

25. Alcantara S, Ruiz M, D'Arcangelo G, Ezan F, de Lecea L, Curran T, Sotelo C, Soriano E (1998) Regional and cellular patterns of reelin mRNA expression in the forebrain of the developing and adult mouse. J Neurosci 18:7779–7799
26. Deerinck T, Bushong EA, Lev-Ram V, Shu X, Tsien RY, Ellisman MH (2010) Enhancing serial block-face scanning electron microscopy to enable high resolution 3-D nanohistology of cells and tissues. Microsc Microanal 16:1138–1139
27. Kawaguchi Y, Kubota Y (1993) Correlation of physiological subgroupings of nonpyramidal cells with parvalbumin- and calbindinD28k-immunoreactive neurons in layer V of rat frontal cortex. J Neurophysiol 70:387–396
28. Kawaguchi Y, Kubota Y (1998) Neurochemical features and synaptic connections of large physiologically-identified GABAergic cells in the rat frontal cortex. Neuroscience 85: 677–701
29. Kawaguchi Y (1993) Groupings of nonpyramidal and pyramidal cells with specific physiological and morphological characteristics in rat frontal cortex. J Neurophysiol 69: 416–431
30. Kawaguchi Y (1995) Physiological subgroups of nonpyramidal cells with specific morphological characteristics in layer II/III of rat frontal cortex. J Neurosci 15:2638–2655
31. Puig MV, Watakabe A, Ushimaru M, Yamamori T, Kawaguchi Y (2010) Serotonin modulates fast-spiking interneuron and synchronous activity in the rat prefrontal cortex through 5-HT1A and 5-HT2A receptors. J Neurosci 30:2211–2222
32. Ushimaru M, Ueta Y, Kawaguchi Y (2012) Differentiated participation of thalamocortical subnetworks in slow/spindle waves and desynchronization. J Neurosci 32: 1730–1746
33. Karube F, Kubota Y, Kawaguchi Y (2004) Axon branching and synaptic bouton phenotypes in GABAergic nonpyramidal cell subtypes. J Neurosci 24:2853–2865
34. Kubota Y, Hatada SN, Kawaguchi Y (2009) Important factors for the three-dimensional reconstruction of neuronal structures from serial ultrathin sections. Front Neural Circuits 3:4
35. Kubota Y, Karube F, Nomura M, Gulledge AT, Mochizuki A, Schertel A, Kawaguchi Y (2011) Conserved properties of dendritic trees in four cortical interneuron subtypes. Sci Rep 1:89
36. Mikula S, Binding J, Denk W (2012) Staining and embedding the whole mouse brain for electron microscopy. Nat Methods 9:1198–1201
37. Willingham MC, Rutherford AV (1984) The use of osmium-thiocarbohydrazide-osmium (OTO) and ferrocyanide-reduced osmium methods to enhance membrane contrast and preservation in cultured cells. J Histochem Cytochem 32:455–460
38. Naoki Shigematsu, Yoshifumi Ueta, Alsayed A. Mohamed, Sayuri Hatada, Takaichi Fukuda, Yoshiyuki Kubota, Yasuo Kawaguchi (2015) Selective thalamic innervation of rat frontal cortical neuronsCerebral Cortex, (Advanced online publication) doi: 10.1093/cercor/bhv124http://cercor.oxfordjournals.org/content/early/2015/06/03/cercor.bhv124.abstract?sid=c935d413-2c23-4747-b336-aa30cc60c216
39. Hayat MA (2000) Electron microscopy biological applications, 4th edn. Cambridge University Press, Cambridge
40. Kubota Y (2015) New developments in electron microscopy for serial image acquisition of neuronal profiles. Microscopy (Oxf) 64:27–36
41. Fiala JC, Kirov SA, Feinberg MD, Petrak LJ, George P, Goddard CA, Harris KM (2003) Timing of neuronal and glial ultrastructure disruption during brain slice preparation and recovery in vitro. J Comp Neurol 465: 90–103
42. Kirov SA, Petrak LJ, Fiala JC, Harris KM (2004) Dendritic spines disappear with chilling but proliferate excessively upon rewarming of mature hippocampus. Neuroscience 127:69–80
43. Kubota Y, Hatada S, Kondo S, Karube F, Kawaguchi Y (2007)Neocortical Inhibitory Terminals Innervate Dendritic Spines Targeted by Thalamocortical AfferentsJ. Neurosci 27: 1139-1150.

Part III

Functional Techniques

Chapter 21

Using Electrophysiology to Study Synaptic and Extrasynaptic Ionotropic Receptors in Hippocampal Neurons

Ian D. Coombs and David Soto

Abstract

Electrophysiology is an exceptionally useful tool for neuroscience research due to the intrinsic electrical excitability of neurons and the significant array of ion channels present in both neurons and glia. Diverse electrophysiological techniques may be applied to neurobiology ranging from measurements of cell populations in broad brain regions to measurements of single channels in patches of plasma membrane. One of the strengths of electrophysiology as a tool is the ability to measure the properties of known ion channels in heterologous systems, then dissect the diverse pharmacology and biophysics of neuronal responses to finally better understand which component channels and their features determine the biologically critical outputs of neurons and circuits.

Patch-clamp electrophysiology allows recording of neuronal receptors at both the synaptic and extrasynaptic level. The specific techniques described here permit the study of both populations independently by measuring miniature excitatory synaptic currents and currents derived from somatic receptors. The resolution and accuracy of the techniques described in the chapter are high (in the sub-picoampere and sub-millisecond ranges). Further, these methodologies provide valuable information about the behavior of the receptors in their native environment where they coexist with auxiliary, modulatory, and anchoring proteins.

In this chapter, we firstly describe the methodology for preparing hippocampal neuronal cultures. Secondly, we describe the process of recording and analyzing miniature postsynaptic currents. Finally, we describe in detail the technique of fast agonist application onto outside-out patches obtained from the soma of neurons. We discuss common problems found with these approaches and present tips to assist researchers new to the field so they may rapidly master the techniques.

Key words Hippocampal neurons, Cells in culture, Synaptic receptors, Extrasynaptic receptors, Whole-cell, mEPSCs, Fast application of agonist, Outside-out patches, Non-stationary fluctuation analysis, Channel conductance

Rafael Luján and Francisco Ciruela (eds.), *Receptor and Ion Channel Detection in the Brain: Methods and Protocols*, Neuromethods, vol. 110, DOI 10.1007/978-1-4939-3064-7_21,

1 Introduction

Electrophysiology is essential for the study of the central nervous system since the primary function of neurons is to receive, process, and then transmit electrical signals. The signals are created by voltage- and ligand-gated ion channels, and identifying the properties of these constituents is fundamental for understanding their physiological roles in neurons and glial cells. Broadly speaking, electrophysiological techniques can be divided into indirect methods that employ extracellular electrodes – noninvasive methods such as EEG – and direct methods that use micropipettes to make contact with the cell of interest. The latter include intracellular recording techniques, where an electrode is inserted into a cell, and patch clamp, where the pipette makes contact with the cell membrane in the cell-attached, whole-cell, inside-out or outside-out configurations. In this chapter, we will focus on two different configurations allowing the recording of synaptic activity (whole cell) and extrasynaptic activity (outside out) in the context of ionotropic receptor physiology. Results obtained with these techniques can be combined with molecular biology, imaging, or behavioral studies to correlate changes at the molecular or cellular level with a physiological effect.

This chapter first describes an easy, efficient, and relatively fast protocol to isolate and culture hippocampal neurons for electrophysiological recording. The successful recording of synaptic activity is critically dependent on the density and connectivity of the culture. Too few neurons due to low cell viability or plating density will be translated into poor-quality cultures with low connectivity. Too many cells however may lead to difficulty in visualization or too much activity, which can be counterproductive while attempting analysis. Optimal density gives healthy neurons with healthy membranes, which in turn leads to stable seals between the neuronal membrane and recording electrodes. Damaged membranes or unhealthy cells will present unstable and leaky seals, greatly increasing recorded noise and therefore decreasing current resolution. The protocol described here is proven to create healthy hippocampal cultures with a good degree of connectivity and healthy membranes allowing the recording of both spontaneous postsynaptic currents and agonist-evoked currents from membrane patches.

Miniature excitatory postsynaptic currents (mEPSCs) are randomly occurring events caused by activation of ligand-gated ion channels following the spontaneous release of a single presynaptic vesicle. They can be detected in the postsynaptic cell body as fast changes in current with a risetime of less than 1 ms and a decay of several milliseconds. The study of mEPSCs provides important information about both the pre- and postsynaptic cell. Thus, changes in event amplitude are normally ascribed to postsynaptic changes while an alteration in mEPSC frequency is indicative of

changes in release probability at the presynaptic level; therefore, mEPSCs can be used to study different forms of synaptic plasticity. Additionally, analysis of voltage dependence and peak-scaled non-stationary fluctuation analysis (NSFA) can help identification of the synaptic receptors. EPSCs are recorded in the whole-cell configuration. The experimenter can therefore dictate the intracellular media and finely control the composition of key components important for the function and behavior of the studied channels such as polyamines, ATP, GTP, and Ca^{2+}.

"Outside-out" patches are pieces of membrane excised from a cell (e.g., the soma of neurons) with the extracellular surface facing the bath solution and the intracellular surface in contact with the pipette solution. This configuration allows the study of receptor gating because it is possible to apply rapid pulses of agonist to receptors on a pseudo-synaptic timescale. The rapid application of agonist can be used to analyze channel kinetics and pharmacology and extract the single-channel conductance by directly resolving openings or through NSFA. NSFA in patches has a distinct advantage over peak-scaled NSFA from whole neurons in revealing accurate information not only of the channel's weighted mean conductance but also the peak open probability. Both techniques will be covered here and two NSFA macros for the data analysis software "Igor Pro" are attached.

This chapter details protocols and tips to effectively record synaptic and extrasynaptic receptors from hippocampal neurons in culture. The methods and principles herein are perfectly applicable to other types of neurons, such as cortical or cerebellar granule cells in culture.

2 Material

2.1 Hippocampal Pyramidal Neuron Culture Preparation

2.1.1 Buffers and Solutions

1. HBSS (Hank's balanced salt solution). Used primarily as a washing solution during the cell dissociation process to maintain pH and osmotic balance and to provide cells with essential inorganic ions and glucose.

   HBSS has the following composition (in g/L): KCl 0.4; KH_2PO_4 0.06; $NaHCO_3$ 0.35; NaCl 8; Na_2HPO_4 0.048; $CaCl_2$ 0.14; $MgCl_2{\cdot}6H_2O$ 0.1; $MgSO_4{\cdot}7H_2O$ 0.1; D-Glucose 1; Phenol Red 0.01; pH 7.4 with NaOH; osmolarity 280–300 mOsm/Kg adjusted with sucrose if needed.
   The pH indicator (phenol red) is optional but can be useful for confirming the adequacy of the HBSS pH buffer.

2. Trypsin stock solution. Add 250 mg of trypsin from bovine pancreas (Type XI; Sigma T-1005) into 20 mL of HBSS and 476.62 mg of HEPES (titration form; FW 238.31) to reach a final HEPES concentration of 100 mM and a final trypsin concentration of 500 μM. Store in 0.5 mL aliquots at −20 °C.

3. Ovomucoid solution. Ovomucoid is a glycoprotein found in egg whites that is used to inhibit trypsin. A highly concentrated bovine serum albumin (BSA) solution could also be used. The ovomucoid solution here uses both proteins.

   To make ovomucoid (plus BSA) solution, add 10 mg/mL each of ovomucoid and BSA to HBSS. Since the ovomucoid solution can become quite acidic, it is necessary to add HEPES at a final concentration of 10 mM. The solution must be prepared fresh on the day of the culture and should be filtered with a 0.22 ∅ sterile filter.

4. Plating media. This will be used during the first hours of the culture following seeding.

   To prepare 10 mL of plating medium, mix 8.8 mL of minimal essential medium (MEM; Sigma-Aldrich; Ref#51412C), 0.5 mL of heat-inactivated fetal bovine serum (FBS; Invitrogen/Life Technologies, Ref#10500-056), 0.5 mL of heat-inactivated horse serum (HS; Sigma-Aldrich, Ref# H1270), 20 µL penicillin/streptomycin solution (from 5000 IU/mL to 5000 mg/mL stock, respectively; Sigma-Aldrich, Ref#P0781), 100 µL L-glutamine (from 200 mM stock; Sigma-Aldrich, Ref#G7513), and 80 µL glucose at 2.5 M.

5. Maintenance medium. This will be used to maintain the culture following the removal of the plating media.

   To prepare 100 mL of maintenance medium, mix 96.1-mL Neurobasal-A (Invitrogen/Life Technologies, Ref#10888-022), 2 mL of B-27 serum-free supplement (50×; Invitrogen/Life Technologies, Ref#17504-044), 1-mL penicillin/streptomycin solution (same stock and source as previously described), 0.5-mL glutaMAX (100×; Invitrogen/Life Technologies, Ref#A12860-01) and 1.33 mL of 2.5 M glucose.

2.1.2 Poly-D-Lysine Preparation

Poly-D-lysine (PDL) and poly-L-lysine (PLL) are synthetic molecules with molecular weights ranging from 500 to 550 kDa primarily used to promote cell adhesion in culture. They are positively charged polymers that help bind negative charges to glass/plastic surface. PDL is usually preferred over PLL because it is not degraded by proteases released by cells in culture.

1. Dilute PDL (1 mg/mL Sigma-Aldrich, Ref #0899) in PBS, water, or 0.1-M borate buffer (prepared by adding 1.24-g boric acid and 1.9-g sodium tetraborate in 400-mL water; pH 8.5) to a final working concentration of 0.1–0.5 mg/mL (*see* **Note 1**).
2. Apply 200 µL of PDL to the top of 12 mm ∅ coverslips (VWR International, Ref#631-1557) in a 24-well plate.
3. Leave overnight at 37 °C.
4. Copiously rinse 2–3 times with distilled sterile water.
5. Use the PDL-coated coverslips between 1 and 3 days after preparation (*see* **Note 2**).

2.1.3 Dissection Material

1. Large scissors.
2. Small scissors.
3. Fine straight forceps.
4. Fine curved forceps.
5. Very fine forceps (two) to dissect the hippocampi.
6. Small spatula.
7. Scalpel.
8. Plastic Pasteur pipettes (five).
9. Glass Pasteur pipettes with three decreasing tip diameters made by snapping the original tapered end then fire polishing. These are then sigmacoated (Sigmacote®; Sigma-Aldrich, Ref#SL-2) and autoclaved.

Sigmacote® is a special silicone solution in heptane that forms a covalent, microscopically thin film on glass and acts as a water repellant. It is used to minimize cell adhesion to the glass when doing a mechanical dissociation of the tissue.

2.2 Electrophysiological Recordings

2.2.1 Electrophysiological Solutions and Blockers

There are two basic solutions for electrophysiological experiments: extracellular (or physiological) and intracellular solution. These solutions are intended to closely resemble the extracellular and intracellular milieu in terms of salt concentrations and pH. The composition of the solutions varies depending on the recordings to be carried out. Documented here are those commonly used in our laboratory to record glutamatergic mESPCs and outside-out somatic patches from hippocampal neurons:

1. The extracellular (external) solution contains (in mM): NaCl 140; KCl 3.5; HEPES 10; Glucose 20; $CaCl_2$ 1.8; $MgCl_2$ 0.8; pH 7.4 with NaOH; osmolarity 280–300 mOsm/Kg adjusted with sucrose if needed. Magnesium should be removed from the extracellular solution if NMDARs activity is recorded since they are blocked by this cation at the negative voltages normally used to record their activity.
2. The intracellular (pipette) solution contains (in mM): K-Gluconate 116; KCl 6; NaCl 8; HEPES 10; EGTA 0.2; MgATP 2.0; Na_3GTP 0.3; pH7.2 with KOH; osmolarity 270 mOsm/Kg adjusted with sucrose if needed (*see* **Notes 3** and 4).
3. Blockers are necessary to eliminate basal neuronal activity (allowing exclusive recording of mEPSCs) and the unwanted activation of other receptor types. These blockers should be added to the extracellular recording solution.
   - Action potential blockers: Tetrodotoxin (TTX; Tocris Bioscience; Ref#1069) selectively blocks voltage-gated sodium channels inhibiting the propagation of action potentials and thus evoked synaptic transmission.

- NMDAR blockers: D-AP5 (Tocris Bioscience; Ref#0106) is a competitive antagonist for GluN2 subunits and the most frequently used NMDAR blocker. We use it at 50–100 μM since the EC_{50} of AP5 ranges from 0.3 to 4 μM depending on subtype [4]. 25 μM 5,7-dichlorokynurenic acid (Tocris Bioscience; Ref#0286), a competitive antagonist acting on the glycine site of the GluN1 subunit, can be used in combination with AP5 to ensure complete NMDAR blockade.
- AMPA and Kainate receptor blockers: several quinoxalinedione compounds (CNQX, DNQX, NBQX) are a suitable option to block both AMPA and kainate receptors. However, we normally use NBQX at 50 μM since it has been reported that CNQX and DNQX act as a partial agonist rather than antagonist in native AMPARs containing auxiliary subunits [4] although the activation is less than 5 % than for a full agonist.
- $GABA_A$ blockers. There are several compounds that might be used to block ionotropic $GABA_A$ receptors. We normally use SR95531 (gabazine; Tocris Bioscience; Ref#1262) at 20 μM, bicuculline (Tocris Bioscience; Ref#0130) at 50 μM, or picrotoxin (Tocris Bioscience; Ref#1128) at 100 μM. The choice can depend on the experiment: SR95531 is a good selective blocker, but is expensive. Bicuculline has been reported to block calcium-activated potassium channels while picrotoxin is cheap but can also inhibit glycine receptors.

2.2.2 Building a Fast Application Tool for Rapid Solution Exchange

Fast application onto outside-out patches is a vital tool for studying ligand-gated ion channel properties. Rapid application of solutions can be achieved using a theta tube (theta shaped) where two solutions constantly flow on either side of a narrow septum. The theta tube is attached to a piezoelectric device to quickly and reproducibly control movement between the solutions. To create a FAT, we pull the borosilicate theta capillaries with a vertical puller.

1. Place the borosilicate theta capillary (OD 1.5 mm; Sutter Instruments; Ref#BT-150-10) in a Vertical puller suited for multi-barrel electrodes (PE-22 model; Narishige, Japan). Other pullers can be used (PA-10 from ESF or L/M-3P-A from List Medical).
2. Run the puller. The heat from the coil will melt the borosilicate glass, and it will stretch in its middle without breaking.
3. Once pulled, remove the stretched capillary from the pipette puller taking care not to snap it. An accidental break will undoubtedly create a jagged end that can affect the septum and ultimately the quality of the exchange.

4. Constrain one end of the glass and under a dissecting microscope, score or nick the glass at its narrowest point with help of a diamond tip. There is no need to cut the whole perimeter of the glass; in fact, simply by touching the thinnest part of the stretched glass with the tip of the diamond, a scratch can be made. This scratch should be made at the point where the septum meets the glass perimeter.
5. Next, gently flex the free end of the glass away from the point of the scratch and the glass will snap in two equal halves. Check that the glass has a clean fracture point with no jagged edges.
6. Insert tubing in the back of the glass. Tubing with different increasing diameters will be needed to allow full connection to the test solution reservoirs. For the glass used here, polyethylene tubes of 0.61 mm OD × 0.28 mm ID and 0.97 mm OD × 0.58 mm ID (Warner Instruments; Ref#64-0750 and 64-0752) are suitable. Cutting the narrowest tubing at an oblique angle, flattening it, or stretching it slightly may be necessary to insert it in the narrow space available.
7. Seal the connection between the glass and the tubes to prevent leakage of solutions and accidental detachment. An epoxy resin such as Araldite is ideally suited for the purpose, but must be allowed to fully cure for 4+ hours before solutions are pushed through. High-pressure solutions will otherwise force gaps between the softer resin and the glass.

2.2.3 Electrophysiology Equipment

1. Air table (Newport Corporation, CA)
2. Faraday cage
3. Pipette puller (PC-10; Narishige, Japan or P-97; Sutter Instrument, CA)
4. FAT Puller (PE-22; Narishige, Japan)
5. Forge (MF-830; Narishige, Japan)
6. Microscope with DIC (IX50; Olympus, Japan)
7. Macro-/micromanipulator for the recording electrode (PatchStar Micromanipulator; Scientifica, UK)
8. Macropositioner for the "fast-application" tool (Scientifica, UK)
9. DCC camera connected to monitor or computer (C4742-98; Hamamatsu Photonics, Japan)
10. Patch-clamp amplifier (Axopatch 200B; Molecular Devices, CA)
11. Digital/analog converter (Digidata 1440A; Molecular Devices, CA)
12. Filtering unit (900CT/900L8L; Frequency Devices, IL)
13. Piezoelectric device (PiezoMove Z-Actuator; P-601.30 L; Physik Instrumente, Germany)

14. Piezoelectric Amplifier Module (E-505.00; Physik Instrumente, Germany)
15. Diamond tip
16. Diverse material for electrophysiology (BNC cables, silver wire, AgCl ground electrodes, glass capillaries)

3 Methods

3.1 Hippocampal Pyramidal Neuron Culture (Modified from Patten et al. [3])

1. Prepare the coverslips with PDL as described in Materials (Sect. 2.1.2). This is best done the day before.
2. Pre-warm to 37 °C two 15-mL centrifuge tubes with 5-mL HBSS (Sect. 2.1.1; point 1), another tube with 6 mL of ovomucoid solution (Sect. 2.1.1; point 3), and a fourth tube containing 2 mL of plating medium (*see* Sect. 2.1.1; point 4).
3. Prepare several petri dishes (animals used +1) for storing hippocampi during preparation by filling with precooled sterile HBSS in a laminar flow hood.
4. In the same laminar flow hood, prepare the trypsin solution for digestion of brain tissue: add 0.5 mL of trypsin stock (previously prepared; Sect. 2.1.1; point 2) to 5.5 mL of HBSS. Pass the solution through a 0.22 ∅ sterile filter and place in a petri dish at 37 °C in a sterile incubator.
5. In a tissue culture hood, set up three beakers with Sylgard (or another "soft" material) in the bottom to avoid damage of the dissection material. One beaker should contain 70 % EtOH, another, doubled distilled sterile water, and a third, HBSS. Place the dissection tools (scissors and forceps) in the beaker containing EtOH 70 % before use.
6. Use two or three P1-3 rat pups (four or six hippocampi). When extracting and dissociating the hippocampi, it is advisable to work on one brain at a time until the whole hippocampus for each hemisphere is isolated. Store the two dissected hippocampi in a petri dish with cold HBSS (point 3), and repeat points 7 and 8 (below) with the next animal before eventually processing all the extracted hippocampi together (points 9 onward).
7. Firstly, behead the animal with the large scissors according to the approved animal guidelines/protocol. Place the head in a precooled HBSS containing petri dish on top of a cold surface to perform subsequent steps (we work on top of petri dishes filled with frozen water to keep temperature of the tissue low and minimize cell death).
8. Remove the skin of the skull. Make a sagittal cut of the skull carefully with small scissors from back to front. Carefully detach the braincase so as not to damage the brain tissue. Extract the whole brain with a small spatula and discard the cerebellum.

Make a sagittal incision with the scalpel to separate both hemispheres. Remove surrounding tissue and extract the hippocampus from each hemisphere. The dissection material should be passed through the EtOH, water, and HBSS in the beakers to minimize the risk of contamination of the culture with the bacteria present in the skin of the animals. After the dissection, place hippocampi in a precooled HBSS petri dish (point 3).

9. Once all hippocampi are removed, chop each hippocampus into four to five pieces (1–2 mm length) with a scalpel. From here onward, all steps should be performed in the vertical flow hood (culture hood).
10. Transfer the tissue using a plastic Pasteur pipette into the pre-warmed trypsin enzyme solution and incubate it at 37 °C (in 5 % CO_2, 95 % O_2 atmosphere to stabilize pH at 7.4) for 10 min. Try to minimize the volume of HBSS transferred to the trypsin solution when doing the transfer.
11. Wash the tissue twice with 5 mL of pre-warmed HBSS (point 2). For this step, transfer the tissue with plastic Pasteur pipettes to the HBSS and resuspend by gentle flicking.
12. Transfer the tissue into plating medium (2 mL) and triturate into a single cell suspension with the sigmacoated glass Pasteur pipettes (prepared as explained in Sect. 2.1.3 point 9): pass the tissue 15–20 times through the large bore pipette, then 20 times through the medium, then 20 times through the smallest.
13. Layer the dissociated cells carefully on top of the pre-warmed 6 mL of ovomucoid solution (Sect. 2.1.1; point 3). First remove any bubbles from the top of the ovomucoid solution, then draw the cells into one of the glass Pasteur pipettes and very gently place the tip at the solution interface, bleeding the cell suspension slowly onto the ovomucoid solution so that cells remain in the very top layer.
14. Centrifuge at 1000× g (roughly 2000–2400 r.p.m. depending on the rotor radius of the centrifuge used) for 10 min.
15. Discard the supernatant by aspiration, avoiding drying the pellet.
16. Transfer the pelleted cells to a 50-mL tube and fully resuspend in 12 mL of plating medium (Sect. 2.1.1; point 4). Resuspension should be vigorous (creating froth) using a plastic Pasteur pipette.
17. Count cells in a Neubauer chamber and seed at the desired density. For electrophysiological experiments, the recommended density is 50,000–100,000 cells/well to ensure a well-connected culture. Thus, to yield a 24-well plate, it will be necessary to dissociate $1.2–2.4 \times 10^6$ cells. We normally obtain $1–2 \times 10^6$ cells/brain, so 2–3 brains are normally sufficient. Plate the appropriate volume-adding plating media if needed to reach a 0.5 mL final volume per coverslip to ensure a homogeneous cell distribution.

18. Incubate for 1 h in the cell culture incubator at 37 °C before adding 1 mL of pre-warmed plating media.
19. After 3 h, remove the plating media and replace with 1.5–2 mL of maintenance media (Sect. 2.1.1, point 5).
20. After 2–3 days in vitro (d.i.v), add the antimitotic cytosine-β-D-arabinofuranoside (AraC; Sigma-Aldrich, Ref#C6645) at a final concentration of 5 μM from a 10 mM stock (1 μL in a 2-mL well), which avoids excessive glial proliferation. If AraC is added too early (1 d.i.v.), neurons will not grow well.
21. Change half of the media every 7 days (*see* **Note 5**). Neurons will be ready for electrophysiology experiments at 14–21 d.i.v.

3.2 Patch-Clamp Electrophysiology

The specific electrophysiological experiments described in the following sections are for researchers with a rudimentary knowledge of electrophysiology who have previously been "in contact" with patch-clamp experiments. It is not possible to describe the principles, requirements, and practice of electrophysiology in just one chapter. However, for those readers completely unfamiliar with electrophysiology, there are many excellent guides available (e.g., Molleman [2]). From this starting point, we will now explain in detail the steps between preparing the neurons for recording and analyzing the data.

3.2.1 Setting Up the Experimental Rig: The Perfusion System

It is important that cultured neurons have their external solution constantly perfused which removes debris and cytotoxic agents released by any dying cells in the vicinity. In order to exchange the bath solution and to apply drugs or blockers, a perfusion system is needed.

1. Prepare reservoir/s for the extracellular solution – the most commonly used reservoirs are 50- or 20-mL syringes. It is recommended to use syringes with the "Luer cap" system to avoid accidental detachment of the tubing. A three-way stopcock (Polymedicure LTD; Ref#1006) connected to the reservoir syringe is needed to prime, control, drain, and clean the system. All the reservoirs should be attached either to the inside of the Faraday cage or to a tripod stand not in direct contact with the vibration table. The inflow system described here uses only gravity to which a useful addition is to use flow regulators (Palex Medical; Ref#406867) which if needed can reduce the inflow to the desired rate of 1–2 mL/min.
2. Connect the tubes from the reservoirs to the inlet system. We use a commercial mini-manifold (Warner Instruments; Ref#64-0211) that allows up to six incoming lines to be attached to a final inlet. In the case of the fast-application tool, two extracellular solutions will be coupled to the back of the application device (this will be explained in more detail in the following sections).

3. Position an outlet system into the chamber. Although many people use a vacuum system, we recommend a gravity system to avoid noise artifacts and sudden drops in the bath level due to the suction (however, *see* **Note 6** for common ways to overcome this). A gravity outflow system needs to be primed to work. This can be achieved with a syringe at the end of the outflow tubing connected by a Luer stopcock (Warner Instruments; Ref#64-0165). This inflow-outflow system relies on both having a similar rate. If the inflow is too high, the recording chamber will eventually flood. A low inflow rate and the bath will eventually be drained below the level of the outlet nozzle, allowing air bubbles into the system. The use of flow regulators on the inlet while measuring the volume of solution drained through the outlet can assist in striking the right balance.
4. Transfer the coverslip from the culture dish to the bath. The HEPES-based buffer negates the necessity for the carbogen bubbling required for carbonate-buffered solutions, though perfusion should still be maintained at all times. Once the target cell is found, the first step toward recording currents is to form a tight electrical seal between your recording electrode and the cell membrane, which is vital for high-quality electrophysiological experiments. We will describe in Sects. 3.2.2 and 3.2.3 the techniques to facilitate this first step.

3.2.2 *Pipette Preparation*

1. Recording pipettes are made from borosilicate capillaries (hollow glass rods) by pulling them in a horizontal or vertical puller. This can create very fine recording electrodes with tip resistances varying from 3 to 12 MΩ depending on the type of recording and chosen cell type (*see* **Note 7**).
2. Setting the correct capillary pulling parameters can be a slow process. For vertical pullers (PC-10; Narishige), there are two necessary steps: the first is a very high temperature step to stretch and thin the glass. This step is terminated once the glass has melted and has fallen around 1 cm onto a switch, which both catches the electrode and turns off the heat. The heating element is automatically repositioned to the center of the stretched section, the switch/stop is removed, and a lower temperature is applied to the glass which once melted is allowed to fall totally away, breaking the glass. To optimize electrode resistance, the most influential step is to adjust the temperature of the second pull. Higher temperatures result in the glass being more fluid and it will stretch further before breaking yielding a smaller opening and a higher resistance, lower temperatures result in the glass being more brittle thus breaking at a higher diameter and lower resistance. Horizontal pullers have more parameters to set up than vertical ones (in which the experimenter sets up just the temperature and the weight to

stretch the capillary) as, for example, heating values for the coil, pulling velocity, or cooling time and delay.

3. Place the glass capillary (in our case, GC120F-10 from Harvard Apparatus for whole-cell experiments or GC150F-7.5 for pulled patches) into the puller (horizontal puller P-97 by Sutter Instruments or vertical puller PC-10 by Narishige), clamp it according to the manufacturer instructions, and run the program (*see* **Notes 8 and 9**). The tips of the produced electrodes are then polished (*see* **Note 10**).
4. Backfill the recording electrode with intracellular solution (Sect. 2.2.1 point 2). Due to the small inner diameter of the electrode (0.69 and 0.86 mm), a special applicator will be needed, e.g., a Hamilton syringe. We use commercially available loading tips (World Precision Instruments, FL; Ref#MF28G-5) coupled to a small 0.2 μm diameter filter (Minisart RC4 from Sartorius Stedim Biotech; Ref#17821) and a 1-mL syringe. It is important to filter the intracellular solution, as dust and other particles could interfere with the sealing process.
5. Fix the recording pipette into the holder of the preamplifier/headstage. We use a custom-made holder rather than that supplied with the amplifier (*see* **Note 11**).
6. Electrode holders have an auxiliary channel for the connection of tubing that allows for the application of positive pressure when the electrode is introduced into the bath. This prevents obstruction of the tip with any cellular debris or dust that could be encountered before reaching the cells and greatly improves the chances of success when creating a seal on a neuron.

3.2.3 Sealing onto the Neurons

1. Once the pipette is in the bath, measure the electrode resistance by means of a 5-mV step (the "seal test") applied by the amplifier. The Axon pClamp software has an internal oscilloscope that directly gives a readout of the tip resistance. Note that the applied positive pressure normally decreases the apparent resistance of the electrode, so this is best assessed by briefly releasing the pressure.
2. Place the pipette close to the target neuron by using the micrometric manipulator. Adjust the pipette offset until the amplifier reads zero current. To maximize the chances of establishing a good seal, try not to make contact close to the edges of the neuron where cytoplasm is scarce or in the center of the soma where the nucleus is present.
3. To make the seal, advance the pipette toward the cell until the resistance increases, i.e., the current caused by the 5 mV step at the oscilloscope slightly decreases. This means that the glass has contacted the phospholipid bilayer. At this point, release the positive pressure and gently apply negative pressure (suc-

tion) to make the seal. The sealing process can be difficult in neurons compared with cell lines (*see* **Note 12**). Every experimenter has his/her tips to maximize the chances of sealing, and regularly trying subtle variations can improve the technique of even the most experienced of electrophysiologists.

4. Before the gigaseal (a seal with a resistance of at least 1 GΩ) is formed, it is recommended to gradually apply negative voltage to the pipette (from 0 to −60 or −80 mV). This will help with the gigaseal formation. When the seal is formed, it is common to observe the firing of the neuron as inward-outward rapid spikes.
5. Once the resistance between the glass and the membrane of the neuron has reached the gigaseal, release the negative pressure and wait 1 min to allow further stabilization of the seal, which can ultimately go beyond 50 GΩ (e.g., a −1 pA holding current at −50 mV). The higher the initial resistance, the greater the chances of having a low noise, high resistance breakthrough of the cell membrane.

3.2.4 Whole-Cell Configuration

1. Once in cell-attached mode (having formed a gigaseal), apply a pulse of negative pressure either by gentle suction (by mouth) or by using a syringe coupled to the holder (*see* **Note 13**).
2. When the whole-cell configuration is reached, a rapid whole-cell transient will appear (*see* **Note 14**). This is normally accompanied by elevated noise due to the activity of the neuron and the postsynaptic currents.
3. Apply extracellular solution containing blockers. The addition of TTX will suppress action potentials and the cell will become "quiet." Next, use the amplifier to measure the membrane capacitance (Cm) and the series resistance (Rs) by canceling the capacitive transients caused by the 5 mV seal test.

3.3 Miniature EPSC Recordings

This section will focus on the recording and data analysis of iGluR-mediated mEPSCs. Miniature events derived from the activation of other ionotropic receptors (e.g., nicotinic acetylcholine receptors) may need other recording conditions in terms of the ionic composition of the recording solutions and/or voltage-clamping conditions of the membrane. Nonetheless, those events can be analyzed in roughly the same way.

3.3.1 mEPSC Recordings

The required configuration for mEPSC recordings is whole cell as explained in Sects. 3.2.3 and 3.2.4. Other types of recordings can be made in the whole-cell configuration, which include applying agonist to the bath and measuring the agonist-evoked currents at a given potential. It is also possible to study voltage-gated currents by applying a protocol of voltage pulses. Here, we will outline the optimal conditions for recording mEPSCs from hippocampal neurons.

1. Acquisition mode. Once the whole-cell mode is achieved satisfactorily, run a "free-mode/gap-free" continuous protocol. This will record the whole-cell current nonstop until terminated by the experimenter at the end of the experiment (*see* **Note 15**).
2. Filtering frequency. The raw analog signal contains both the output of the cell along with high levels of thermal and electrical noise. If all of this noise is retained, it will greatly detract from the appearance and information available from the data. The Axon amplifier has a low-pass filter that removes high-frequency noise. While additional filtering can be performed on digitized data after the experiment, information cannot be recovered from over-filtered data so we recommend not acquiring data filtered at greater than 5 kHz (10 kHz if noise analysis is to be performed).
3. For measuring the amplitude of mEPSCs, the ideal sampling frequency should be set no lower than 10 KHz (one datapoint acquired every 100 μs; *see* **Note 16**). When acquiring data, analog signals are converted to digital (automatically by the AD/DA converter, Digidata 1440 Series Axon Instruments), i.e., the analog output of the cell is transformed into discrete current-time datapoints in order to store the data. Thus, a high sampling frequency (or sampling rate) will represent the analog signal well, while low sampling rates can result in an irretrievable loss of information (especially in rapid events). In our hands, by recording mEPSCs at different sampling rates, no significant changes in the recorded amplitude or kinetics of mEPSCs are detected when the sampling frequency is 5, 10, or 50 KHz. Below 5 KHz (1–2 KHz), there is too few points to well represent the mEPSC, and estimates for amplitude are decreased (*see* **Note 17**).
4. Avoid recordings with too much leak (*see* **Note 18**). In general, more than −100 pA of leak will decisively reduce the quality of the recording. If the leak cannot be brought below this level, e.g., by applying negative pressure, move onto the next cell. Analyzing leaky, poor-quality data is far more time consuming and much more difficult than analyzing data from cells with a low leak.

3.3.2 mEPSC Analysis

The software with which we perform mEPSC analysis is Igor Pro (http://www.wavemetrics.com). While the analysis is not difficult, it is certainly helpful to be familiar with Igor Pro and the free-software plug-in NeuroMatic (designed by Dr. Jason Rothman, UCL; http://www.neuromatic.thinkrandom.com). NeuroMatic contains an assortment of Igor Pro functions for analyzing electrophysiological data relatively easy. Here, we describe the basic procedure to detect mEPSCs and extract the parameters that define them.

1. Import the data file (termed "waves") into Igor Pro. In our case, it is an axon binary file (.abf) recorded with pClamp10 software: Igor/Neuromatic/Import Waves.
2. Detection of the miniature events: NeuroMatic Panel/Event tab. Set the following criteria: threshold < baseline (for inward currents like glutamate-activated responses at a negative potential); threshold: 3–5 (*see* **Note 19**). Click the "auto" button to run detection of the events.
3. Transform the detected events to waves. This will create a new "wave" for each detected event. To do so, select NeuroMatic Panel/Event tab/Events 2 waves. Once clicked, set a minimum "time before event" of 5 ms, so each event has its own stretch of baseline, and a minimum "time after event" of 20–40 ms, allowing the current to decay back to the baseline.

   When transforming events to waves, in the dialog box "limit data to time before next spike," choose NO. This avoids the detected events being prematurely truncated in the instance of a second event appearing in the tail. This is common when there is a high frequency of mEPSCs and several events are present in the defined time window. They must be excluded, as the truncated records interfere with the proper averaging of the full events.
4. Set the baseline for all detected events. In the NeuroMatic Panel, in the second box from top, select "EV_Event0_" to visualize/work with the event waves rather than the whole record. Then use the NeuroMatic Panel/Main tab/Baseline box to subtract the baseline current (from e.g. 0–4 ms).
5. Once the baseline for each event is set to zero, it is possible to reject those events incorrectly detected as mESPCs, with multiple events or not clear enough for the analysis (*see* **Note 20**).

   It is useful to create a plot of all events (NeuroMatic/Main tab/Plot Box) to easily identify bad events (e.g., those with two or more overlapping mEPSCs in the chosen time window). Double clicking on the outlier trace will open a Dialog Box showing the name of the event (e.g., EV_Event0_A325). Bad events can be then excluded by selecting the trace in question in the main window then clicking the "SetX" checkbox on the top right part of the NeuroMatic panel. However, given the very large number of mEPSCs normally detected, this broad visual approach will in general only identify the clearest few events not suitable for the analysis.

   It is therefore recommended to check all individual events. To visualize all single events one by one, use the [<] and [>] boxes in the NeuroMatic panel to move sequentially through the events. Those events included in the SetX will remain excluded for all subsequent analysis (*see* **Note 20**).

6. Once all necessary events have been excluded, the analysis of desired parameters can be performed (normally amplitude and risetime). This can be measured as individual values from each event or from the average of the events (see next point). In the NeuroMatic panel/Stats tab/Stats1 panel, change the default "Max" to "Min" to measure the minimum current amplitude. In the same box, ---Neg Peak---, "Risetime" will calculate the 10–90 % risetime (from the baseline to the peak) in a time window chosen by the experimenter ("t_bgn" and "t_end"). Clicking the "All waves" option will then calculate the minimum current and risetime for every individual event, storing the values in a new wave "ST_MinY0_Rall_A0" and "ST_RiseT0_Rall_A0" (*see* **Note 21**).
7. The risetime and amplitude of mEPSCs can alternatively be taken from an average of all retained mEPSCs events. First create the average "wave" for those events: NeuroMatic panel/Main tab/Average. This will create a new "wave" with the prefix "Avg_". To measure the parameters of this new wave, select "Avg_" in the NeuroMatic selection box (second from top). A single wave will appear on the main plot window. Follow the same analysis protocol as above (point 6) to calculate amplitude and risetime (*see* **Note 22**).
8. As the conductance of synaptic channels will depend on receptor subtype and association with auxiliary subunits, calculating this conductance can help to identify their composition. This conductance can be measured using peak-scaled non-stationary fluctuation analysis (psNSFA). psNSFA relies on the stochastic or random nature of channel openings which leads changes in current variance that are a function of channel conductance and open probability. By analyzing the variance of a receptor population over time or, in our case, analyzing groups of mEPSCs, certain features of the constituent channels can be evaluated. The fundamental tenet is that for, e.g., a 100 pA response, the variance yielded from fifty 2 pA channels will be clearly different from that yielded from one hundred 1 pA channels, despite the macroscopic mean current being identical. If sufficient mEPSCs are recorded, their variance around the peak-scaled mean current will yield a parabolic relationship, the initial slope of which will depend on the conductance of the receptors recorded. We attach an Igor Pro macro (Appendix 1, *see* **Note 23**) that will perform peak-scaled NSFA to mEPSCs detected, aligned, and averaged as detailed above and fits them using a parabola-fitting protocol (Appendix 2, *see* **Note 24**). For a more detailed explanation of variance analysis, *see* Hartveit and Veruki [1].
9. Before running the macro, position two cursors on the averaged record (dragging the circle and square icons in the bot-

tom left corner of the graph window), one at the peak and the other at the steady-state point. The averaged mEPSCs must be the top window when the macro is initialized. The set averaged must also be selected in the NeuroMatic window.

10. Run the macro. A prompt for the name of the set of data to be analyzed, the time window of the baseline, the number of bins, and the recording voltage appear. After the prompt is answered, two plots are produced; the first is the average current with the axes removed. If wanted, calibrator bars can be attached (Graph/Packages/Append Calibrator). The second presents the binned current variance and fitted parabola along with calculated values for conductance (*see* **Note 25** if the fit fails).

3.4 Outside-Out Recordings

This section will focus on the excision of membrane patches from the soma of neurons, the rapid application of agonist (glutamate) onto these patches, and analytical techniques to study the gating properties of the receptors activated.

3.4.1 Fast Agonist Application Preparation

Fast application of agonist into outside-out patches can be achieved by means of a theta tube attached to a piezoelectric device to finely control the application. The making of this fast-application tool (FAT) is detailed in Sect. 2.2.2.

1. Attach the FAT to the piezoelectric stack. Generally, piezoelectric stacks have a clamping system incorporated to attach other components.
2. Prepare solutions (control and agonist) that will flow through the FAT. Add sucrose (2.5 mg/mL) to one of the solutions; we normally add it to the agonist. The sucrose will change its density, and when both solutions flow out the FAT, a visible interface between both non-mixing solutions will be created that will allow for appropriate fine positioning of the pipette.
3. Dilute the other solution with water. We normally dilute the control (agonist-free) solution. This creates an electrical offset between solutions that will be evident when the tip of the recording pipette crosses the solutions. Alternatively, a separate line can be set up with a much more pronounced dilution, e.g., 50 %. This creates a much larger potential difference requiring less averaging when checking the exchange (see point 5 below).
4. Specific blockers should be added to both control and agonist solutions to prevent the activation of unwanted native channels. For example, when glutamate is used to activate AMPA receptors present on neuronal patches, the GluN2 antagonist D-AP5 should be added to both solutions to avoid any NMDA receptor activity. Alternatively, although not ideal, AMPA can be used as agonist.

5. Check the speed of exchange. For fast-gating receptors such as AMPARs, it is vital to have a very fast exchange of solutions. The risetime of AMPAR responses can be as fast as 200 μs so the solution exchange should preferably better than this. To measure the rate of solution exchange, an open recording pipette is placed close to the boundary between the solutions and positive pressure applied to the pipette. Jumping between the diluted control and undiluted agonist solutions changes the baseline current. By averaging multiple pulses and measuring the 10–90 % risetime, the speed of exchange can be assessed. The exact positioning might vary from one day to another and needs to be checked during experimental setup and after each patch. Common artifacts relating to incorrect positioning of the tip are shown in Fig. 1 (also *see* **Note 26**).
6. Software, such as pClamp from Axon, controls the piezoelectric device by applying a precisely timed voltage step. The duration and magnitude of the voltage can both be varied to create the perfect exchange. For measurements of deactivation, the protocol should be varied to create a 1-ms duration step; for desensitization, we normally use a 100-ms duration (also *see* **Note 27**).
7. Filtering the signal. An external filter is normally needed to smooth the input to the piezoelectric controller. An unfiltered signal leads to extremely rapid movement of the FAT and physical artifacts, i.e., reverberations become apparent. We use an external filter (900CT/900L8L, Frequency Devices), which has the effect of smoothing the voltage signal to the piezoelectric device and can eliminate reverberations without adversely affecting exchange rate, 100 Hz is a good starting point. Overfiltering, e.g., <70 Hz should be avoided as this can slow the signal too much and, while eliminating artifacts, will nonetheless lead to bad exchange quality (*see* Fig. 1).
8. The frequency of the pulses is also important, too low, and the total recording will last longer than needed, increasing the chances of the patch degrading. Too fast and channel desensitization can build up leading to response rundown. AMPARs fully recover from desensitization within 1 s, though some isoforms, e.g., GluA4flip, almost totally recover after just 50 ms.
9. Other useful protocols can be established to help fully characterize the properties of the channel. These include recovery from desensitization where from a steady-state current, agonist is removed then reapplied at increasing intervals, so, for example, intervals of 2–20 (Δ2 ms), 25–70 (Δ5 ms), 80–300 (Δ20 ms), and 400–1000 (Δ100 ms) will give a sensible distribution of datapoints to map out AMPAR recovery.
10. As well as varying the timing of application, the voltage during the application can also be varied. This is a vital tool for identi-

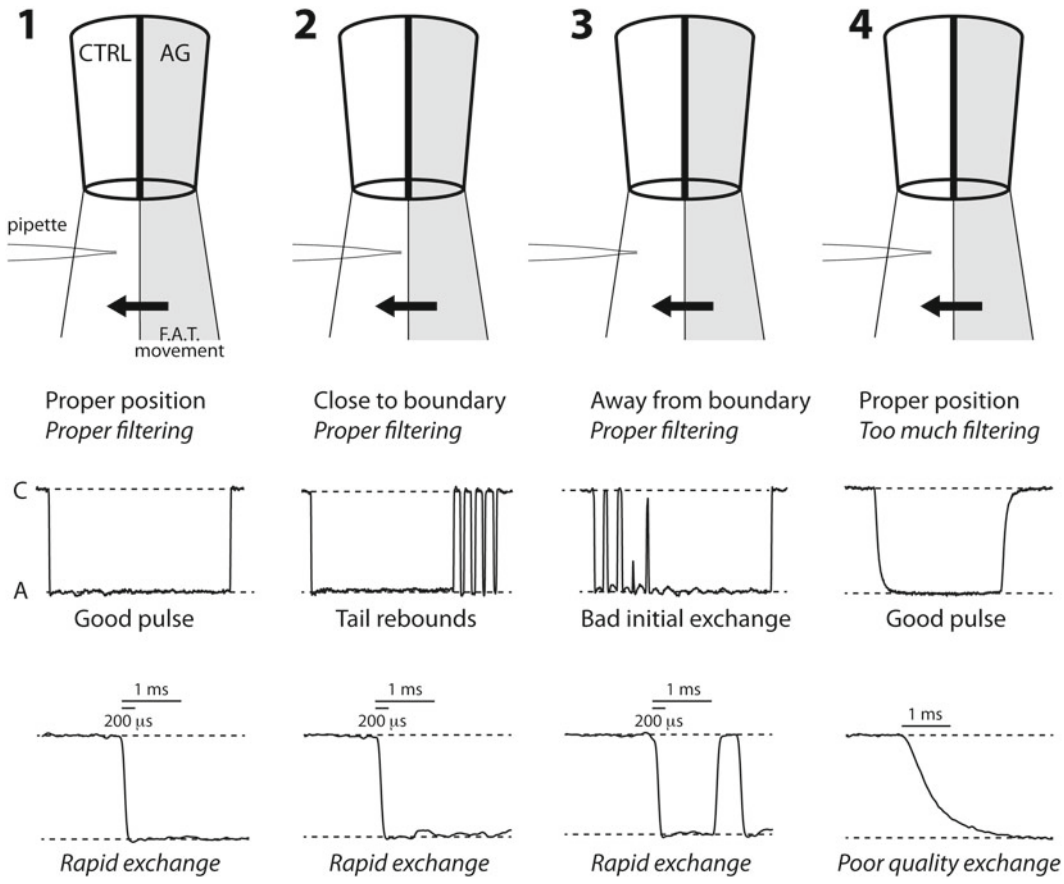

Fig. 1 Pipette positioning and signal filtering are crucial for optimizing exchange times. *Pipette positioning.* The correct positioning of the recording pipette (relative to the boundary) determines the quality of a 20-ms agonist pulse (*CTRL* and *C* control solution, *AG* and *A* agonist solution). In *1* and *4* the position is optimal – in terms of eliminating reverberation errors – and hence there is a clean exchange. *2* and *3* demonstrate the typical reverberation errors seen if the tip of the pipette is either too close (*2*) or too far away (*3*) from the boundary. *Signal filtering.* For fast agonist-application experiments (~200 μs exchange), correct filtering of the rectangular pulse sent to the piezoelectric device is crucial. In *1–3*, the voltage signal received by the piezoelectric actuator is optimally filtered and the initial exchange is ultrafast (<200 μs). In *4*, excessive filtering of the voltage signal results in a poor initial exchange (>1 ms). NB If the signal is under-filtered or unfiltered, reverberation errors such as those shown in *2* and *3* cannot be avoided, even with optimal pipette positioning. Equally, if solution flow rates are too slow, or the FAT is damaged in some way, poor exchanges like in *4* will always result

fying, among other things, the calcium permeability of AMPARs, which are blocked by polyamines in a voltage-dependent manner.

11. Once the proper position, protocol, and filtering are found, a camera coupled to a display (through the computer or separate monitor) allows reproducibility of positioning (*see* **Note 28**). Once the settings have been optimized, a line should be drawn

on the monitor (with nonpermanent marker!) corresponding to the visible solution interface. A circle can then be drawn around the position of the tip. Next time a patch is pulled, both the FAT (if moved) and recording electrode can therefore be returned to the same spots leading to perfect exchange during the experiment. By destroying the patch at the end of the experiment, the quality of the exchange can be confirmed, though it should be noted that the measured exchange across a destroyed patch is often not as fast as across an open electrode, but is still sufficient to prove no large artifacts were present in the exact position used.

3.4.2 Patch Excision

1. Once the whole-cell configuration has been achieved (*see* **Note 29**), it is possible to excise a small piece of membrane containing somatic receptors. This will be attached to the tip of the recording electrode and will be under very good electrical control with high resistance, low leak, and therefore high sensitivity to small currents.
2. To extract the piece of membrane, pull the electrode away slowly by means of the micrometric manipulator (*see* **Note 30**). In doing so, a small patch of membrane will be stretched and will eventually break. Once it breaks, the lipid bilayer will seal itself automatically. This configuration is called an "outside-out" patch. The extracellular parts of the receptors are left facing the bath while the intracellular part of the receptors is in contact with the pipette solution.
3. Once the patch is excised, the tip of the pipette must be located in the proper position to apply the agonist (*see* Sect. 3.4.1) and the recording protocols can commence.

3.4.3 Study of Channel Properties by Means of NSFA

1. The recording protocols required for (non-peak scaled) NSFA are identical to those used for studying receptor desensitization and deactivation (*see* Sect. 3.4.1.6). The only proviso is that because noise analysis looks at variance during changing open probability, it is essential for a large number of applications to be recorded to get sufficient data at all open probabilities. This is particularly true for AMPARs, which have very fast kinetics and therefore have precious few datapoints gathered near the peak, high open probability region of the response. While we have had success with as few as 18 applications for large responses, recording over 50 is preferable and there is no upper limit – the more traces the better.
2. Import the .abf file into Igor with NeuroMatic as in Sect. 3.3.2. Igor/NeuroMatic/Import Waves. Plot the waves (NeuroMatic/Main/Plot) to gauge the overall quality of the record and to identify any unsatisfactory sweeps, e.g., due to momentary perfusion noise, mobile phone signal, etc. or if the

leak changes drastically during the record in which case the leaky sections should be discarded (added to SetX).

3. Subtract the baseline from all satisfactory individual traces (waves). NeuroMatic/Main/Baseline. The acquisition protocol should be set up to include at least 20 ms of baseline before the agonist application to allow an accurate subtraction.
4. Measure the minimum current, i.e., the peak negative current. NeuroMatic/Stats. Select Min and make sure the selected time window includes the peak ("t_begin" and "t_ end" as previously described). Click the "All waves" button and a wave called "ST_MinY0_RAll_A0" is created containing the minimum values for each trace.
5. Perform stability analysis on the peak currents by selecting "ST_MinY0_RAll_A0" in NeuroMatic/Analysis/Stability-Stationary. NSFA relies on the same number of channels being available at each agonist application, so any rundown of the response is unacceptable and can be identified using this test. Once a satisfactory selection of sweeps is identified, they should be included in a new set, e.g., Set1, for further analysis. (NeuroMatic/Sets/Define). A second pass refinement of the stability analysis is available; this can be useful if the signal fluctuates slowly up and down over time and is incorrectly identified as stable by the algorithm. This gives further cause to record "excessive" numbers of applications >200, in case large sections have to be discarded.
6. Align all stable traces. "Jitter" or poor time alignment of applications can lead to additional current variations independent of channel noise. Records are best aligned at the start of the rise; we use the 10 % point. Calculate the risetime from the chosen set of traces, i.e., NeuroMatic/Waves/Set1. To calculate the risetime: NeuroMatic/Stats1/---Neg Peak---/Risetime and choose 10–90 %. Click "All waves." Three waves are created "ST_RiseT0_RS1_A0" containing the risetime, as well as _ RiseBX0_ (the 10 % time point) and _RiseEX0_ (the 90 % time point). Use NeuroMatic/Main/Align to align all waves to ST_RiseBX0_RS1_A0. Plot the waves and expand the rising phase to confirm the alignment has been successful.
7. Average the aligned, stable traces. This average can be used for kinetic analysis to extract time constants of decay, peak currents, and steady-state currents.
8. Position two cursors on the averaged record (dragging the circle and square icons in the bottom left corner of the graph window), one at the peak and the other at the steady-state point to perform NSFA. While a cursor on the peak datapoint is not essential to extract a conductance value from the records, the macro will use it to derive the peak open probability.

9. Run the macro (Coombs_Soto_NSFA; Appendix 3 and *see* **Note 23** to utilize the macro in Igor). The average sweep to be analyzed must be the top window when the macro is initialized. The waves analyzed must also be selected in the NeuroMatic window (e.g., Set1 should be chosen). A prompt appears requiring the set of data to be analyzed, the time window of the baseline, the number of bins, and the recording voltage – if compensating for junction potential errors, these should be accounted for here (*see* **Note 31**). A smoothing function can also be applied if the record has lots of high-frequency noise, though in general this leads to a slight underestimation of the channel conductance.
10. The macro compares the data sweeps in a pairwise fashion, i.e., Sweep 1 is compared to Sweep 2, Sweep 2 to Sweep 3, etc. The total variance present at each time point across all pairs of records is calculated. Each time point is then binned by amplitude, and the total variance from all points in each bin is averaged. Finally, a parabolic function (SigworthNSNA; Appendix 2) is fitted to the current-variance relationship (but *see* **Note 25** if the fit fails).
11. The macro produces two plots. The first is the average current with the axes removed. If wanted, calibrator bars can be attached (Graph/Packages/Append Calibrator). The second presents the binned current variance and fitted parabola along with calculated values for conductance and peak open probability.

4 Notes

1. Poly-D-Lysine is toxic to cells, so do not exceed the stated concentration and ensure complete washing of the coverslips before plating the cells. Keep the diluted PDL solution frozen, preferably at –80 °C when not in use (and do not refreeze once an aliquot has been defrosted).
2. If PDL-coated coverslips are stored for longer than 1 month, the PDL becomes degraded (even when stored at 4 °C). This might interfere with the proper attachment of the cells. One hallmark of degraded PDL is nonhomogeneous cultures where "islands" of neurons grow together leaving large empty spaces between cells.
3. K-$MeSO_3$ can be used instead of K-Gluconate since it minimizes rundown of calcium-activated currents over time. GTP is included to conserve GTP-mediated activity in neurons since the activity of some channels and channel-modulating proteins depends on GTP. ATP is included as an energy source. Including EGTA at 0.2 mM and adding no calcium maintains

a nearly free calcium concentration inside the cell. Free EGTA is quite insoluble so either use an EGTA salt or make a pH7.4 potassium EGTA stock solution using KOH to neutralize the pH. QX-314 (Tocris Bioscience; Ref#1014) is an intracellular blocker of voltage-gated sodium currents that can be added to the recording intracellular solution at 2.5 mM.

4. It can be useful to include a dye in the intracellular solution to be able to identify the neuronal morphology both during the experiment and afterward when cells can be fixed and imaged, e.g., with Lucifer Yellow at 0.05–0.5 mg/mL (Sigma-Aldrich; Ref#L0259). Alexa dyes are best avoided as recent evidence suggests they can modulate levels of free polyamines, affecting the properties of Kir channels and Ca^{2+}-permeable AMPA/KA receptors.
5. Replacing the medium only once a week avoids the removal of neurotrophic factors produced by glial cells. If medium is exchanged too often (2–3 days), the growth factor levels might decrease to levels compromising culture development.
6. Suction-based outflow systems suffer from high variability primarily due to issues of surface tension. Solution can build up in the recording chamber when out of contact with the suction tube, but once contact is made and the surface tension is broken, the majority of the solution can be drawn out before contact is lost. The process then repeats leading to variations in the baseline and excessive noise. In order to reduce this risk, an oblique opening of the outflow pipe nozzle, such as a small plastic tube cut at a 45° angle assists in breaking surface tension. Alternatively, placing the outlet onto a small piece of Whatman® cellulose filter paper which is in contact with the solution will similarly ensure an unbroken flow. Glass capillaries or the tip of a syringe needle can also be used as the outlet nozzle; however, they are tricky to accurately manufacture or can lead to electrical noise, respectively.
7. For whole cell, we recommend 3–5 MΩ; lower resistances than this in general make sealing onto the cell less successful. Higher resistance tips (6–7 MΩ) can be used for whole-cell purposes if the sealing process is proving difficult, or if the cell is small; however, it can compromise the quality of the recordings by raising the series resistance. For outside-out patches, tip resistances between 8 and 12 MΩ are recommended. Below 8 MΩ, the larger amount of pulled membrane might become unstable in the flow of applied solutions. Above 12 MΩ, it becomes tough to break through the membrane of the cell to reach the whole-cell configuration.
8. Using two different types of capillaries is necessary to reproducibly produce electrodes of these different resistances. We use

glass from Harvard Apparatus with different inner and outer diameters. Specifically, it is GC120F-10 for whole cell (1.2 mm OD × 0.69 mm ID; Ref#30-0044) and GC150F-7.5 (1.5 mm OD × 0.86 mm ID; Ref#30-0060) for outside-out patches. Each type of glass should only be used in the appropriate holder (*see* **Note 11**). However, small-tip diameter electrodes can be obtained from 1.2 mm OD capillaries if only the smaller holder is available, e.g., ISO-S-1.2G. It is difficult to reproducibly pull electrodes of <6 MΩ with the thicker-walled glass however.

9. The pair of pipettes resulting from the pulling of the capillary may slightly differ in both shape and tip resistance. Horizontal pullers from Sutter more reliably create two identical pipettes. While the use of a more economical vertical puller by Narishige might result in subtle differences between pipettes from the same pulling, this is normally within acceptable limits and the extent of fire polishing can be adjusted accordingly (*see* **Note 10**).
10. To maximize the chances of sealing, polishing the tip of the electrode is recommended. Polishing the tip smoothens the rough edges created as the pipette is fabricated, which would have made forming a seal more difficult and could even cause membrane damage. This polishing can be done by means of a Forge (Narishige MF-830). When polishing the tip, its diameter will slightly decrease, hence increasing the electrode resistance. This has to be taken into account when setting the puller parameters and making the electrodes.
11. Stability of the pipette's position is crucial for long experiments. The unwanted movement or drift of electrodes during patch-clamp recordings is common, especially during changes in pipette pressure. Furthermore, pipette drift can result in the loss of the seal or a great increase in Rs (series resistance), compromising the quality of the record. We use a holder specifically developed for Axon 200B amplifiers (ISO-S-1.5G or ISO-S-1.2G depending on the glass outer diameter; G23 Instruments, UK). This holder is designed to clamp the pipette at two points rather than the standard one. This greatly reduces the chance of undesired movements and thus increases the mechanical stability of the recording.
12. If it is proving difficult to establish a seal between the recording pipette and the cell membrane, it is common practice to dilute the intracellular solution with distilled water by 4–5 %. This often improves both the sealing and the stability of the patch throughout the recording process.
13. Breaking through the membrane without affecting the seal quality can be difficult in neurons. We recommend increasing negative pressure gently and gradually rather than with a single

stronger pulse. This can be achieved with a 1-mL syringe coupled to the tubing system that is connected to the holder.

14. A slow or small transient may mean a poor breakthrough with high series resistance. The problem can often be fixed using further negative pressure, which may also be required if series resistance increases during the recording.
15. It is recommended to check the series resistance (or access resistance) often (every 2–3 min) and correct the capacitance offsets accordingly. Rs is the total resistance that the current must flow through and is a combination of the pipette resistance and any membrane resistance. A high series resistance leads to poor-quality data with less time resolution and errors in voltage clamping the cell. Changes in series resistance during the experiment in general mean the electrode is becoming blocked by residual membrane from the cell, which can commonly be removed by application of additional negative pressure. An oscilloscope will allow continuous monitoring with no need to stop the recording.
16. The sampling frequency should be always at least double the low-pass filtering frequency. For example, if we set the filtering frequency at 2 KHz, we should use a sampling frequency of at least 4 KHz; otherwise further information will be lost.
17. For easy visualization of data during a recording, it is possible to record in two channels simultaneously, one channel capturing the unfiltered data and the other being passed through a filter at 1 or 2 kHz. This filtered channel can either be acquired or merely displayed on your oscilloscope and, especially with very small responses, can inform a decision of whether the record will prove analyzable.
18. A low leak current is important to ensure correct voltage-clamp of the neuron. The leakier the seal, the less reliable the recording is. This is because the signal-noise ratio greatly decreases and it becomes harder to distinguish mEPSCs due to fluctuations in the baseline current. Further, the larger the total current injected, the greater any voltage error created by series resistance becomes. As well as seal quality, the baseline current also depends on the size and endogenous properties of the cell.
19. For the detection of the miniature events, the baseline threshold is normally set at 3–5 (pA). Background noise is normally between 2 and 4 pA in good quality recordings. So, setting a background noise threshold of 3–4 pA should be enough to detect most miniature events. If background noise is too high (or the recording trace is unstable), setting a threshold of 3–4 pA before the miniature event detection will include many "events" that are not real mEPSCs. On the other hand, the use of a high threshold to detect events (10–12 pA) may overlook

some real events that could prove analyzable. Thus, it is recommended to run a macro to assist with correct detection: Noise_Histogram (original source S.G. Cull-Candy's laboratory, UCL, London – available on request from the authors). This macro scans periods of baseline between events and returns the most appropriate threshold for the event detection in each record. Although not critical, this macro can help to avoid subjectivity and thus ensure consistency of analysis.

20. Spontaneous mEPSCs in general display very varied risetimes. Thus, fast (risetime 0.2–0.3 ms) and slow (>2 ms) events are commonly present in the same recording. This has to be taken into account when grouping events for averaging. Risetime variation might result from receptor subpopulations with distinct properties, for example, receptors composed of different subunits. However, a slow risetime might be indicative of distal events occurring far from the cell body that are subject to the cable filtering that occurs in dendrites. It is therefore useful to have a cutoff risetime, e.g., 1–1.5 ms above which events are discarded since very slow events will have lost much information compared to fast-rising events and are poorly comparable.
21. For small responses, baseline noise and/or peak noise can become a large factor when measuring the 10–90 % risetime introducing inaccuracies. These errors can be decreased by clicking on "y = 10–90 %" and typing in the new values, e.g., 20–80 %. These more neutral measures are less likely to be influenced by noise and can allow a more successful alignment.
22. The number of events needed for a reliable average is high (over 400–500 events) since the amplitude of mEPSCs in cultured hippocampal neurons varies considerably. A small sample size could induce errors especially in the calculation of the miniature event size. For example, for a parameter measured from 400 mEPSCs, the analysis of 300–400 events chosen at random normally generates a 0.5–2 % error compared with the average value from 400. Analysis of 200–300 random events can create a 3–5 % error compared with the average value from 400. When the analysis involves less than 100 mEPSCs (randomly chosen), errors can be as high as 20–30 % compared with the measurement of 400 events.
23. To import the "Coombs_Soto_NSFA" and the "peak-scaled_NSFA" macros into Igor: Igor/Windows/New/Procedure, name as desired and leave in "plain text format." Type or paste the text of the macros (Appendixes 1 and 3). Once finished, compile (Igor/Macro/Compile) and the macros are ready to

go. To run it on the desired average: Igor/Macro/and select your chosen name.

24. The macros fit a parabola using the function "SigworthNSNA." To add this equation to your curve-fitting options, create a new procedure in Igor: Igor/Windows/New/Procedure, name as desired and leave in "plain text format." Type or paste the text of the function (Appendix 2). Save this new procedure in Igor/Igor Procedures. From now on, when Igor is opened, the function will appear in the curve-fitting list.
25. If the binned variance data deviates significantly from a parabolic shape, the autofit section of the macro may well fail. If by eye it seems that a parabola should be fitted, or if only one or two datapoints seem to be problematic, it is possible to fit the data "by hand." Simply apply cursors to the binned datapoints between which you wish to fit and use analysis/curve fitting to use the Sigworth NSNA equation. Constrain the background variance to the calculated value and estimate an appropriate unitary current and number of channels. The data should now be fitted.
26. When measuring the exchange between the control and agonist solution from the FAT, the flow rate of the solutions will determine the speed of the exchange. As a general rule, the higher the flow, the better the exchange is; however, a fast flow commonly leads to patch instability and destruction (*see* Fig. 2.3). One approach is to initially check the exchange at high flow rates before gradually decreasing the flow until just before the exchange time becomes compromised.

    Coating recording pipettes with Sylgard® polymer reduces their fast capacitance thus decreasing background noise and increasing the quality of whole-cell recordings. However, we find that if Sylgard is applied for fast-application experiments, the incidence of slow artifact noise or "wobble" is greatly increased. This suggests that the added weight or volume of the Sylgard makes the electrode and the recording more sensitive to mechanical noise resulting from the movement of the FAT.
27. It is important that both desensitization and deactivation protocols have satisfactory exchange from the same position, since if the electrode is moved during a recording, open-electrode test pulses at the end of the experiment will only reflect the final position. Establishing a position that has a little leeway is also advisable; when checking the exchange, always try moving the electrode a little in all three axes; if the exchange is instantly lost in any direction, it may be better to adapt the conditions slightly.

28. The position and orientation of the pipette tip in relation to the solution interface are another key factor in determining both a fast exchange and the stability of patches. In principle, any angle of the recording pipette relative to the solution interface could create a suitably fast exchange, but there are certain limitations (Fig. 2). The more directly the recording electrode faces the solution flow, the less stable the patches, in general, are. However, if the angle of the pipette is facing away from the flow (Fig. 2.2), or if the electrode is introduced from the "wrong" side (Fig. 2.4), the exchange may be suboptimal. In general, the best compromise is to have the recording electrode perpen-

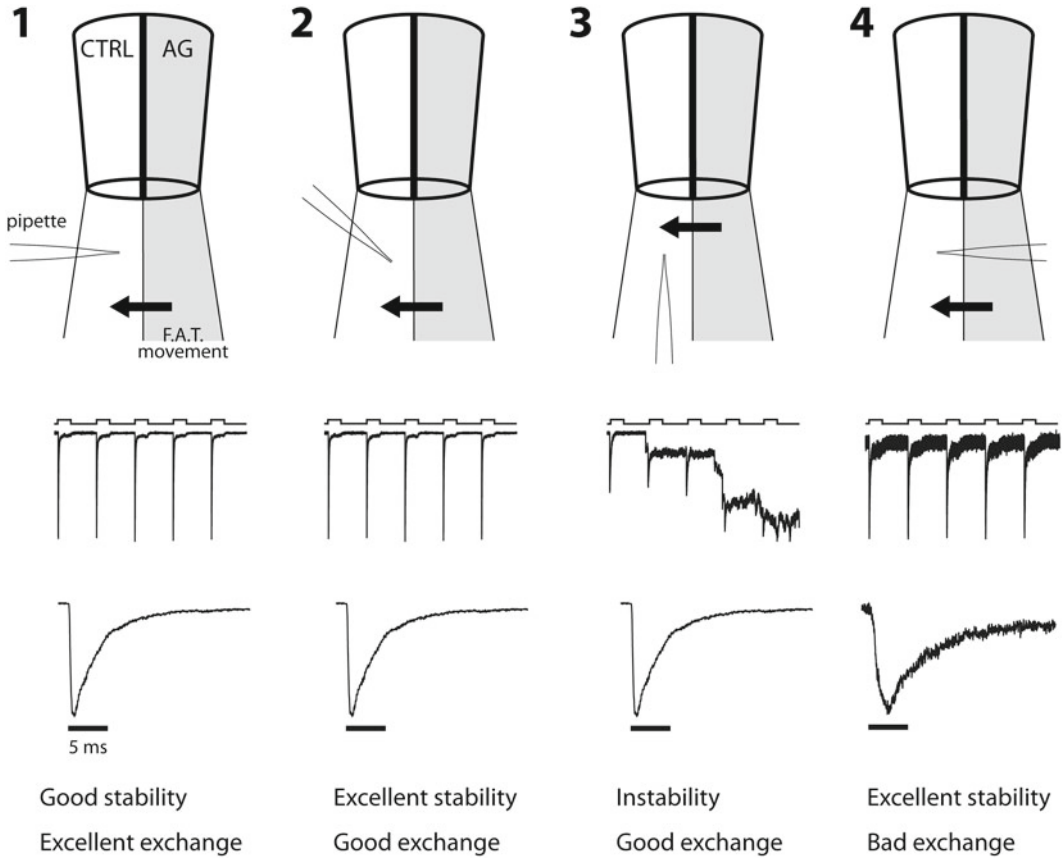

Fig. 2 Fast solution exchange and patch stability depend on the recording pipette orientation. *1* and *2* show configurations where the patch pipette is placed perpendicular (*1*) or almost perpendicular – up to 45° (*2*) to the boundary of the solutions. Patches from *1* to *2* (not directly facing the flow) tend to have good stability and a fast rise of the peak current due to good exchange of solutions. When the pipette is located in parallel to the boundary and directly facing the solution flow (*3*), patches are normally unstable and do not last for long periods of time. A configuration where the agonist solution is reaching the tip of the pipette from "behind" (*4*) is not optimal as the body of the electrode can slightly disperse or distort the agonist solution, thus interfering with the quality of the solution interface. Since the exchange of solutions is slowed, this will affect the risetime of the current and peak amplitude and kinetic measurements

dicular to the solution exchange offering both good stability and exchange. These guidelines are empirical, based on personal experience and are intended as a starting point for finding the best conformation for each individual setup.

29. Do not apply too much negative pressure when forming the seal. This draws the plasma membrane into the pipette, and when pulled, the patch will have a tendency to form deep in the pipette. This results in the receptors being partially shielded from the solutions, meaning the agonist application will not be fast, i.e., the risetime of the activated current might be slow.
30. In our hands, the best way to excise patches is by using a 45° angle for pulling back. However, this is quite variable and angles from vertical to horizontal might work best at any given moment. In general, if on a given day patches are hard to come by, try making subtle modifications to your technique. The angle of patch pulling is one such variable.
31. Junction potential errors result from the difference in ionic composition of the intracellular and extracellular solutions and are present at the junction between them, in our situation the tip of the open electrode. The presence of predominantly high mobility cations in the extracellular solution (Na^+) and low mobility cations in the intracellular solution (K^+ or Cs^+) leads to a net influx of positive charge into an open electrode. An equilibrium stage is only reached when there is a buildup of positive charge in the pipette, typically around 5 mV for $NaCl_{ext}/CsCl_{int}$. As a result, the electrode offset set before sealing onto a cell includes this potential, i.e., when the pipette offset is set to 0 pA, this is not 0 mV, but is actually +5 mV. Once the electrode has sealed onto the membrane, however, this junction is lost, so all subsequent measurements include this error. A recording potential set at −60 mV is actually therefore −55 mV. pClamp contains standard values for the mobility of ions and can calculate the expected junction potential for two solutions. This can be accounted for before the experiment by altering the command voltage, though we recommend a post hoc approach.

Acknowledgments

We wish to thank Saad Hannan for initial assistance with hippocampal cultures and David DiGregorio whose noise analysis macro we have modified. This work is supported by the Spanish Ministry of Science and Technology co-funded with European Union funds FEDER (Grant BFU-2011-24725) and the European Commission (FP7-PEOPLE-2011-CIG; Grant 293498). David Soto is supported by the "Ramón y Cajal" Programme (RyC-2010-05970). Ian Coombs is supported by Wellcome Trust (086185/Z/08/Z)

and MRC (MR/J002976/1) Programme Grants (awarded to Stuart Cull-Candy and Mark Farrant).

Appendix 1: Igor Macro for Peak-Scaled Non-stationary Fluctuation Analysis

```
#pragma rtGlobals=1       // Use modern global
access method.
   Macro PeakscaledNSNA()
       execute "PSNSNA()"
   end
   Function PSNSNA()
//start by initializing strings (the names of
important bits) and waves (the contents)
      string  NSNAAvg,Identifier,BackgroundVarName
       string /g Variance,Average,BinnedVarianc
e,BinnedAverage,STDEV, Binnedgraph, CurrentAvg,
FittedParabola
       string /g layoutName="DisplayFormat"
        variable bslnstart=0  // begin time to
calculate back ground variance
       variable bslnend=4
       variable smoothing_in=0
       variable numbins_in=30
       variable bin=1 //0 if no, 1 if yes
       variable /g smoothing=0
        variable /g BackgroundVar //calculated
background variance
       variable /g xLim
       variable /g yLim
       variable /g ScalePt
       variable /g ScaleMag
       variable /g ScaleFact
       variable /g numbins=0
       variable /g binstart=0 //pA
       variable /g binend=0
       variable DrivingForce=-55
       variable /g Conduct=0
       variable /g Popen
//Make a prompt window for user input of impor-
tant values
      Prompt bslnstart, "Baseline start point (ms)"
       Prompt bslnend, "Baseline end point (ms)"
        Prompt NSNAAvg,"Average Wave",popup,Wave
List("avg_*",";","")
          Prompt smoothing_in, "smooth factor
(binomial)"
```

```
        Prompt Identifier,"enter file suffix for
identification"
       Prompt numbins_in, "number of bins"
      Prompt DrivingForce, "enter voltage (mV)"
       DoPrompt "enter wave",NSNAAvg,bslnstart,
bslnend,smoothing_in,Identifier,numbins_
in,DrivingForce
        if(V_flag==1)          //If there is no
selected wave then it cancels
           return 0 //cancel do prompt
       endif
        smoothing=smoothing_in                //
rename input values for use
       numbins=numbins_in
       Duplicate /o $NSNAAvg NonStatAvg
       Duplicate /o NonStatAvg NonStatVar
       Duplicate /o NonStatAvg ScaleAvg
      Average="Avg"+Identifier                //
This is why you need to enter suffix, to give
fresh names to these values
       Variance="Var"+Identifier
       BinnedAverage="Avg_Bin_"+Identifier
       BinnedVariance="Var_Bin_"+Identifier
       CurrentAvg="Current_"+Identifier
       BackgroundVarName="BackVar"+Identifier
       FittedParabola="FittedNoise"+Identifier
       STDEV="Var_SD"+Identifier
              variable   chncnt,wvcnt,numSweeps
///initialize more variables to name each sweep
      string wvlist,wvName,wvName2,NonStatAvgName
       wave NonStatVar
       string tempwave
       wave chanselect
       wave waveselect
       nvar smoothing
       NonStatVar=0
       numSweeps=0
              wavestats /q/R=(xcsr(A),xcsr(B))
NonStatAvg  ////Gets stats of the average cur-
rent wave in analysis window
                        xLim=V_min+(0.05*V_min)
////sets a limit of 5% under the minimum
           ScalePt=xcsr(A)
           ScaleMag=V_min
    for (chncnt = 0; chncnt < numpnts(ChanSelect);
chncnt += 1) // loops through each time point in
the input waves, normally in ChanA (ChanSelect)
```

```
                    if (ChanSelect[chncnt] != 1)
///If only one sweep, end the macro as noise
analysis cannot be performed.
                continue
            endif
           wvlist = GetChanWaveList(chncnt)   ///
this is a neuromatic function that returns the
list of selected waves for a particular channel
       for (wvcnt = 0; wvcnt < ItemsInList(wvList);
wvcnt += 1)               ///Loops through each
sweep (for the timepoint in question from chncnt)
             wvName = StringFromList(wvcnt, wvList)
///gets the current wave
               wvName2 = StringFromList(wvcnt+1,
wvList)    ///gets the next wave for pairwise
comparison
                     if (exists(wvName) == 0)
///keep going until wvName is 0 i.e. it has gone
through every wave
                  continue
                endif
                   duplicate /o  $wvName, Sweep
///Get values for each pair of waves
                    ScaleFact = Sweep(ScalePt)/
ScaleMag   ///These two lines scale the average
peak to the correspnding datapoint in the sweep
                ScaleAvg = NonStatAvg*ScaleFact
                                if  (smoothing>1)
///Smooth out the records
                    smooth smoothing, Sweep
                endif
                  NonStatVar+=(ScaleAvg-Sweep)^2
///Square the difference to get the variance,
add variances
                numSweeps+=1
            endfor
          NonStatVar/=(numSweeps-1)    ///final cal-
culation of variance by dividing by total number,-1
       endfor
            ////calculate and print background
variance
           wavestats /q /R=(bslnstart,bslnend)
NonStatVar      ////NonStatVar is the wave with
the variance at each timepoint, this is just in
the baseline window
          BackgroundVar=V_avg       //This gives
the average variance in the background range
```

```
            print "background variance (pA^2)
is:", BackgroundVar
             wavestats /q/R=(xcsr(A),xcsr(B))
NonStatAvg  ////Gets stats of the average cur-
rent wave in analysis window
                        xLim=V_min+(0.05*V_min)
////sets a limit of 5% under the minimum
       wavestats /q/R=(xcsr(A),xcsr(B)) NonStatVar
////Gets stats of average Variance wave
                        yLim=V_max+(0.05*V_max)
////sets a limit of 5% over the maximum
            duplicate /o /R=(xcsr(A),xcsr(B))
NonStatVar $Variance                        ////
Duplicates section  of variance between cursors
            duplicate /o /R=(xcsr(A),xcsr(B))
$NSNAAvg  $Average             ////Renames sec-
tion  of current between cursors
            duplicate /o /R=(xcsr(A),xcsr(B))
$NSNAAvg  BckVr                ////Renames sec-
tion as other type of string/wave, never got
that distinction
          if (bin==1)
               duplicate /o $Average AvgForBin
////more renaming to put things in the right form
              duplicate /o $Variance VarForBin
               make /o/N=(numbins) NonStatAvg_Bin
////Gets new waves to contain data from binned records
                           make  /o/N=(numbins)
NonStatVar_Bin
              make /o/N=(numbins) NonStatVarSD
                           wave      VarForBin,
AvgForBin,NonStatAvg_Bin,NonStatVar_
Bin,NonStatVarSD
       variable incwave
       variable incAvg //increment through binning
       nvar numbins,binstart,binend
       variable /g binwidth=0
       variable count_if=0
       variable count_if_sd=0
       variable /g waveEndForSD=0
      NonStatAvg_Bin=0  /////initializing loops
       NonStatVar_Bin=0
       NonStatVarSD=0
       incavg=0
       wavestats /Q AvgForBin
       waveEndForSD=V_npnts-2     /////The num-
ber of comparisons is less because the end points
have only one neighbour
```

```
        Binwidth=(V_min-V_max)/numbins     /////
Binwidth is in current and is the full range
sliced up
       print "binwidth is", binwidth
       variable countbins=0
       for (incAvg=1;incAvg<=numbins;incAvg+=1)
/////Binning routine, loops for each bin
                binstart=V_min-(incAvg*Binwidth)
/////calculates upper and lower limits of the bin
           binend=binstart+binwidth
         count_if=0                          /////
reinnitializes counts
           count_if_sd=0
               for  (incwave=0;incwave<(V_npnts-
1);incwave+=1)                               /////
Runs through each datapoint in cursor range
                    if((AvgForBin[incwave]<binst
art) && (AvgForBin[incwave]>=binend))     /////
If in bin range then include in bin
                             NonStatAvg_Bin[incavg-
1]+=AvgForBin[incwave]      /////Add current and
variance to binpoint
                             NonStatVar_Bin[incavg-
1]+=VarForBin[incwave]
                  if(incwave<waveEndForSD) /////
This calculates errors for error bars on each
variance point
                               NonStatVarSD[incavg-
1 ] + = ( V a r F o r B i n [ i n c w a v e + 1 ] -
VarForBin[incwave])^2
                          count_if_sd+=1
                     endif
                     count_if+=1
                endif
           endfor
                NonStatAvg_Bin[incavg-1]/=count_if
/////Total value divided by number of contributors
           NonStatVar_Bin[incavg-1]/=count_if
           NonStatVarSD[incavg-1]/=2*(count_if_
sd-1)          /////Divide error bars by number
of contributors*2
                               NonStatVarSD[incavg-
1]=sqrt(NonStatVarSD[incavg-1])           /////
Take sqrt of it. to give SD
       endfor
      print "number of executed bins",countbins
```

```
                    duplicate /o NonStatAvg_Bin
$BinnedAverage                ////// Back again,
duplicate binned stuff
                    duplicate /o NonStatVar_Bin
$BinnedVariance
                    duplicate /o NonStatVar_Bin
$BinnedVariance
                    duplicate /o NonStatAvg_Bin
$FittedParabola
                duplicate /o NonStatVarSD $STDEV
//for standard error bars
             endif
          BckVr=BackgroundVar              //////
Duplicting background var
           duplicate /o BckVr $BackgroundVarName
//////More renaming
            Binnedgraph="MeanVarBin"+Identifier
           if(wintype(Binnedgraph)==0)
                display /k=1 $BinnedVariance vs
$BinnedAverage    //make graphs for binned data
               DoWindow /C $Binnedgraph
           ModifyGraph mode=4,marker=19,msize=4
               ModifyGraph rgb=(0,0,0)
               AppendToGraph $BackgroundVarName
vs $Average                //////Add background
variance
               ModifyGraph mode=0
               ShowInfo
                    ErrorBars   $BinnedVariance
Y,wave=($STDEV,$STDEV) //////Stick error bars on
               SetAxis/A
               SetAxis bottom 2, xLim
            ModifyGraph mode( $BinnedVariance)=4
               endif
         Make/D/N=3/O W_coef              //////
Do a fit
           W_coef[0] = {BackgroundVar,-0.5,100}
//////Make first guesses for variance fit
            FuncFit/H="100" SigworthNSNA W_coef
$BinnedVariance       /X=$BinnedAverage       /
D=$FittedParabola  /W=$STDEV /I=1     /////Hold
backvar,;fit N,i
          Conduct = w_coef[1]/DrivingForce*1000
           Popen = V_min/(w_coef[1]*w_coef[2])
          TextBox /w=$Binnedgraph/N=test/C/F=0/
E=1/A=MT           "G(pS)="+num2str(Conduct)+"\
r"+"N="+num2str(w_coef[2])+        "\r"+"PoPeak
="+num2str(Popen) //////Display it
```

```
                AppendToGraph $FittedParabola vs
$BinnedAverage
           ModifyGraph lstyle($FittedParabola)=
3,rgb($FittedParabola)=(0,0,0),mode($BinnedVar
i a n c e ) = 3 , r g b ( $ B a c k g r o u n d V a r N
ame)=(34816,34816,34816)
                  Label left "Variance (pA\\
S2\\M)";DelayUpdate
           Label bottom "Current (pA)"
               display NonStatAvg
               DoWindow /C $CurrentAvg
               ModifyGraph rgb=(0,0,0)
         ModifyGraph tick=3,noLabel=2,axThick=0
           NewLayout /N=Layoutname
          AppendLayoutObject graph $Binnedgraph
           AppendLayoutObject graph $CurrentAvg
       ModifyLayout frame=0,trans=1;DelayUpdate
           ModifyLayout left($Binnedgraph)=100,
top($Binnedgraph)=370,width($Binnedgraph)=300,
height($Binnedgraph)=350;DelayUpdate
           ModifyLayout left($CurrentAvg)=60,to
p($CurrentAvg)=100,width($CurrentAvg)=400,heig
ht($CurrentAvg)=300
   print "Conductance = ",Conduct
   print "PoPeak        = ",Popen
   end
   ////////////////////////////////////////////
////////////////////////////////
```

Appendix 2: Sigworth NSNA Function

```
#pragma rtGlobals=1        // Use modern global
access method.
   Function SigworthNSNA(w,x) : FitFunc  //sig-
worth non-stationary noise analysis fit with
background variance
       Wave w
       Variable x
         //CurveFitDialog/ These comments were
created by the Curve Fitting dialog. Altering
them will
       //CurveFitDialog/ make the function less
convenient to work with in the Curve Fitting
dialog.
       //CurveFitDialog/ Equation:
       //CurveFitDialog/ f(x) = var_back + i*I -
((I*I)/N)
```

```
        //CurveFitDialog/ End of Equation
         //CurveFitDialog/ Independent Variables
1
        //CurveFitDialog/ x
        //CurveFitDialog/ Coefficients 3
        //CurveFitDialog/ w[0] = var_back
        //CurveFitDialog/ w[1] = i
        //CurveFitDialog/ w[2] = N
        return w[0] + w[1]*x-((x*x)/w[2])
   End
```

Appendix 3: Igor Macro for Non-stationary Fluctuation Analysis

```
#pragma rtGlobals=1        // Use modern global
access method.
   Macro PairwiseNSNA()
       execute "NSNA()"
   end
   Function NSNA()
   //start by initializing strings (the names of
important bits) and waves (the contents)
       string  NSNAAvg,Identifier,BackgroundVarN
ame
       string /g Variance,Average,BinnedVarianc
e,BinnedAverage,STDEV,             Binnedgraph,
CurrentAvg,FittedParabola
       string /g layoutName="DisplayFormat"
        variable bslnstart=0  // begin time to
calculate back ground variance
       variable bslnend=20
       variable smoothing_in=0
       variable numbins_in=10
       variable bin=1 //0 if no, 1 if yes
       variable /g smoothing=0
        variable /g BackgroundVar //calculated
background variance
       variable /g xLim
       variable /g yLim
       variable /g numbins=0
       variable /g binstart=0 //pA
       variable /g binend=0
       variable DrivingForce=-55
       variable /g Conduct=0
       variable /g Popen
   //Make a prompt window for user input of
important values
```

```
        Prompt bslnstart, "Baseline start point
(ms)"
       Prompt bslnend, "Baseline end point (ms)"
        Prompt NSNAAvg,"Average Wave",popup,Wave
List("avg_*",";","")
          Prompt smoothing_in, "smooth factor
(binomial)"
         Prompt Identifier,"enter file suffix for
identification"
        Prompt numbins_in, "number of bins"
       Prompt DrivingForce, "enter voltage (mV)"
                              DoPrompt      "enter
wave",NSNAAvg,bslnstart,bslnend,smoothing_
in,Identifier,numbins_in,DrivingForce
         if(V_flag==1)          //If there is no
selected wave then it cancels
           return 0 //cancel do prompt
        endif
       smoothing=smoothing_in            //rename
input values for use
        numbins=numbins_in
        Duplicate /o $NSNAAvg NonStatAvg
        Duplicate /o NonStatAvg NonStatVar
      Average="Avg"+Identifier                  //
This is why you need to enter suffix, to give
fresh names to these values
        Variance="Var"+Identifier
        BinnedAverage="Avg_Bin_"+Identifier
        BinnedVariance="Var_Bin_"+Identifier
        CurrentAvg="Current_"+Identifier
        BackgroundVarName="BackVar"+Identifier
        FittedParabola="FittedNoise"+Identifier
        STDEV="Var_SD"+Identifier
               variable   chncnt,wvcnt,numSweeps
///initialize more variables to name each sweep
        string wvlist,wvName,wvName2,NonStatAvgN
ame
        wave NonStatVar
        string tempwave
        wave chanselect
        wave waveselect
        nvar smoothing
        NonStatVar=0
        numSweeps=0
     for (chncnt = 0; chncnt < numpnts(ChanSelect);
chncnt += 1) // loops through each time point in
the input waves, normally in ChanA (ChanSelect)
```

```
                    if (ChanSelect[chncnt] != 1)
///If only one sweep, end the macro as noise
analysis cannot be performed.
                continue
            endif
           wvlist = GetChanWaveList(chncnt)   ///
this is a neuromatic function that returns the
list of selected waves for a particular
channel
                    for (wvcnt = 0; wvcnt <
ItemsInList(wvList)-1; wvcnt += 1)          ///
Loops through each sweep (for the timepoint in
question from chncnt)
                  wvName = StringFromList(wvcnt,
wvList)          ///gets the current wave
                wvName2 = StringFromList(wvcnt+1,
wvList)    ///gets the next wave for pairwise
comparison
                      if (exists(wvName) == 0)
///keep going until wvName is 0 i.e. it has gone
through every wave
                    continue
                endif
                   duplicate /o  $wvName, Sweep
///Get values for each pair of waves
                duplicate /o  $wvName2, Sweep2
                                if  (smoothing>1)
///Smooth out the records
                    smooth smoothing, Sweep
                    smooth smoothing, Sweep2
                endif
                    NonStatVar+=(Sweep2-Sweep)^2
///Square the difference to get the variance,
add variances
                numSweeps+=1
            endfor
           NonStatVar/=2*(numSweeps)     ///final
calculation of variance by dividing by total
number, and 2 since each wave was used twice
        endfor
             ////calculate and print background
variance
            wavestats /q /R=(bslnstart,bslnend)
NonStatVar      ////NonStatVar is the wave with
the variance at each timepoint, this is just in
the baseline window
```

```
            BackgroundVar=V_avg          //This
gives the average variance in the background
range
             print "background variance (pA^2)
is:", BackgroundVar
              wavestats /q/R=(xcsr(A),xcsr(B))
NonStatAvg  ////Gets stats of the average cur-
rent wave in analysis window
                         xLim=V_min+(0.05*V_min)
////sets a limit of 5% under the minimum
              wavestats /q/R=(xcsr(A),xcsr(B))
NonStatVar   ////Gets stats of average Variance
wave
                         yLim=V_max+(0.05*V_max)
////sets a limit of 5% over the maximum
             duplicate /o /R=(xcsr(A),xcsr(B))
NonStatVar $Variance                      ////
Duplicates  section    of  variance  between
cursors
             duplicate /o /R=(xcsr(A),xcsr(B))
$NSNAAvg  $Average            ////Renames sec-
tion  of current between cursors
             duplicate /o /R=(xcsr(A),xcsr(B))
$NSNAAvg  BckVr               ////Renames sec-
tion as other type of string/wave, never got
that distinction
           if (bin==1)
                duplicate /o $Average AvgForBin
////more renaming to put things in the right
form
              duplicate /o $Variance VarForBin
             make /o/N=(numbins) NonStatAvg_Bin
////Gets new waves to contain data from binned
records
                           make  /o/N=(numbins)
NonStatVar_Bin
              make /o/N=(numbins) NonStatVarSD
                           wave     VarForBin,
AvgForBin,NonStatAvg_Bin,NonStatVar_
Bin,NonStatVarSD
      variable /g binsize //calculated bin cut-
off   /////seems to not be used at all
       variable incwave
          variable  incAvg  //increment  through
binning
       nvar numbins,binstart,binend
       variable binsize_prev
       variable /g binwidth=0
       variable count_if=0
```

```
        variable count_if_sd=0
        variable /g waveEndForSD=0
          NonStatAvg_Bin=0     /////initializing
loops
        NonStatVar_Bin=0
        NonStatVarSD=0
        incavg=0
        wavestats /Q AvgForBin
        waveEndForSD=V_npnts-2     /////The num-
ber of comparisons is less because the end points
have only one neighbour
         Binwidth=(V_min-V_max)/numbins     /////
Binwidth is in current and is the full range
sliced up
        print "binwidth is", binwidth
        variable countbins=0
        for (incAvg=1;incAvg<=numbins;incAvg+=1)
/////Binning routine, loops for each bin
                binstart=V_min-(incAvg*Binwidth)
/////calculates upper and lower limits of the
bin
            binend=binstart+binwidth
          count_if=0                          /////
reinnitializes counts
            count_if_sd=0
                for  (incwave=0;incwave<(V_npnts-
1);incwave+=1)                                /////
Runs through each datapoint in cursor range
                    if((AvgForBin[incwave]<binst
art) && (AvgForBin[incwave]>=binend))     /////
If in bin range then include in bin
                            NonStatAvg_Bin[incavg-
1]+=AvgForBin[incwave]      /////Add current and
variance to binpoint
                            NonStatVar_Bin[incavg-
1]+=VarForBin[incwave]
                  if(incwave<waveEndForSD) /////
This calculates errors for error bars on each
variance point
                              NonStatVarSD[incavg-
1 ] + = ( V a r F o r B i n [ i n c w a v e + 1 ] -
VarForBin[incwave])^2
                         count_if_sd+=1
                    endif
                    count_if+=1
                endif
            endfor
              NonStatAvg_Bin[incavg-1]/=count_if
/////Total   value   divided   by   number   of
contributors
```

```
            NonStatVar_Bin[incavg-1]/=count_if
            NonStatVarSD[incavg-1]/=2*(count_if_
sd-1)          /////Divide error bars by number
of contributors*2
                                NonStatVarSD[incavg-
1]=sqrt(NonStatVarSD[incavg-1])           /////
Take sqrt of it. to give SD
        endfor
       print "number of executed bins",countbins
                    duplicate /o NonStatAvg_Bin
$BinnedAverage                 //////Back again,
duplicate binned stuff
                    duplicate /o NonStatVar_Bin
$BinnedVariance
                    duplicate /o NonStatVar_Bin
$BinnedVariance
                    duplicate /o NonStatAvg_Bin
$FittedParabola
                duplicate /o NonStatVarSD $STDEV
//for standard error bars
             endif
          BckVr=BackgroundVar              //////
Duplicting background var
           duplicate /o BckVr $BackgroundVarName
//////More renaming
            Binnedgraph="MeanVarBin"+Identifier
            if(wintype(Binnedgraph)==0)
                 display /k=1 $BinnedVariance vs
$BinnedAverage    //make graphs for binned data
                DoWindow /C $Binnedgraph
            ModifyGraph mode=4,marker=19,msize=4
                ModifyGraph rgb=(0,0,0)
                AppendToGraph $BackgroundVarName
vs $Average                //////Add background
variance
                ModifyGraph mode=0
                ShowInfo
                     ErrorBars   $BinnedVariance
Y,wave=($STDEV,$STDEV)  //////Stick error bars
on
                SetAxis/A
                SetAxis bottom 2, xLim
             ModifyGraph mode( $BinnedVariance)=4
                endif
          Make/D/N=3/O W_coef              //////
Do a fit
           W_coef[0] = {BackgroundVar,-0.5,100}
//////Make first guesses for variance fit
```

```
            FuncFit/H="100" SigworthNSNA W_coef
$BinnedVariance       /X=$BinnedAverage       /
D=$FittedParabola  /W=$STDEV /I=1     /////Hold
backvar,;fit N,i
          Conduct = w_coef[1]/DrivingForce*1000
           Popen = V_min/(w_coef[1]*w_coef[2])
          TextBox /w=$Binnedgraph/N=test/C/F=0/
E=1/A=MT           "G(pS)="+num2str(Conduct)+"\
r"+"N="+num2str(w_coef[2])+        "\r"+"PoPeak
="+num2str(Popen) //////Display it
              AppendToGraph $FittedParabola vs
$BinnedAverage
           ModifyGraph lstyle($FittedParabola)=
3,rgb($FittedParabola)=(0,0,0),mode($BinnedVar
i a n c e ) = 3 , r g b ( $ B a c k g r o u n d V a r N
ame)=(34816,34816,34816)
                  Label  left  "Variance  (pA\\
S2\\M)";DelayUpdate
           Label bottom "Current (pA)"
               display NonStatAvg
               DoWindow /C $CurrentAvg
               ModifyGraph rgb=(0,0,0)
         ModifyGraph tick=3,noLabel=2,axThick=0
           NewLayout /N=Layoutname
          AppendLayoutObject graph $Binnedgraph
           AppendLayoutObject graph $CurrentAvg
       ModifyLayout frame=0,trans=1;DelayUpdate
           ModifyLayout left($Binnedgraph)=100,
top($Binnedgraph)=370,width($Binnedgraph)=300,
height($Binnedgraph)=350;DelayUpdate
           ModifyLayout left($CurrentAvg)=60,to
p($CurrentAvg)=100,width($CurrentAvg)=400,heig
ht($CurrentAvg)=300
   print "Conductance = ",Conduct
   print "PoPeak        = ",Popen
   end
   ////////////////////////////////////////
////////////////////////////////
```

References

1. Hartveit E, Veruki ML (2007) Studying properties of neurotransmitter receptors by non-stationary noise analysis of spontaneous postsynaptic currents and agonist-evoked responses in outside-out patches. Nat Protoc 2:434–448. Hoboken, NJ
2. Molleman A (2003) Patch clamping – an introductory guide to patch clamp electrophysiology. Wiley, New York
3. Patten D, Foxon GR, Martin KF, Halliwell RF (2001) An electrophysiological study of the effects of propofol on native neuronal ligand-gated ion channels. Clin Exp Pharmacol Physiol 28:451–458
4. Traynelis SF, Wollmuth LP, McBain CJ, Menniti FS, Vance KM, Ogden KK, Hansen KB, Yuan H, Myers SJ, Dingledine R (2010) Glutamate receptor ion channels: structure, regulation, and function. Pharmacol Rev 62:405–496

Chapter 22

Biophysical Methods to Analyze Direct G-Protein Regulation of Neuronal Voltage-Gated Calcium Channels

Norbert Weiss and Michel De Waard

Abstract

Neuronal voltage-gated calcium channels play an essential role for calcium entry into presynaptic endings responsible for the release of neurotransmitters. In turn, and in order to fine tune synaptic activity, numerous neurotransmitters exert a potent negative feedback over the calcium signal provided by G-protein-coupled receptors that can be recognized by characteristic biophysical modifications of the calcium current. There are two main biophysical approaches to analyze direct G-protein regulation of voltage-gated calcium channels: the so-called double-pulse method, which is indirectly assessed by the gain of current produced by a depolarizing prepulse potential, and the "subtraction" method that allows the analysis of G-protein regulation from the ionic currents induced by regular depolarizing pulses. The later method separates the ionic currents due to nonregulated channels from the ion currents that result from a progressive departure of G-proteins from regulated channels, thereby providing valuable information on the OFF kinetics of G-protein regulation. In this chapter, we introduce these "double pulses" and "subtraction" procedures for use primarily with single cells and also discuss the limitations inherent to these two approaches.

Key words Calciumchannel, Ca_v2 channel, G-protein-coupled receptor, G-proteins, Gβγ-dimer, Prepulse facilitation, Biophysical method

1 Introduction

Presynaptic voltage-gated calcium channels (VGCCs), primarily $Ca_v2.1$ and $Ca_v2.2$ channels, represent two of the most important players in the initiation of the Ca^{2+} signal by converting electrical impulses into intracellular Ca^{2+} elevations responsible for the release of neurotransmitters [6]. In turn, these channels are strongly regulated by a negative feedback mechanism provided by the activation of G-protein-coupled receptors (GPCRs) (for review, see [8, 36]). To date, up to 20 GPCRs have been described to modulate VGCCs (Table 1).

Direct inhibition of the Ca^{2+} channels occurs through the direct binding of G-protein βγ-dimer onto various structural molecular determinants of the Ca_v2-subunit [36]. At the whole

Rafael Luján and Francisco Ciruela (eds.), *Receptor and Ion Channel Detection in the Brain: Methods and Protocols*, Neuromethods, vol. 110, DOI 10.1007/978-1-4939-3064-7_22, © Springer Science+Business Media New York 2016

Table 1
Neurotransmitter- and receptor-mediated G-protein modulation of Ca_v2 channels

Neurotransmitter	Receptor	Ca_v channel	Tissue/species	Reference
Ach	M4	$Ca_v2.2$	SCG/rat	Bernheim et al. [2]
	M2	$Ca_v2.1$ & $Ca_v2.2$	SCG/mouse	Shapiro et al. [39]
Adenosine	A1	$Ca_v2.2$	Ciliary ganglion/chicken	Yawo and Chuhma [50]
		$Ca_v2.2$	DRG/chicken	Kasai and Aosaki [29]
		$Ca_v2.1$ & $Ca_v2.2$	Cerebellum/rat	Dittman and Regehr [10]
		$Ca_v2.2$ & $Ca_v2.3$	Hippocampus (CA3 → CA1)/rat	Wu and Saggau [47]
ATP/ADP	P2Y	$Ca_v2.2$	SCG/rat	Brown et al. [5], Filippov et al. [16]
Dopamine	D2	HVA	DRG/chicken	Marchetti et al. [32]
Endocannabinoids	CB1	$Ca_v2.1$	SCG/rat	Garcia et al. [18]
		$Ca_v2.1$, $Ca_v2.2$ & $Ca_v2.3$	Cerebellum	Brown and Russell [4]
GABA	GABA B	$Ca_v2.1$ & $Ca_v2.2$	DRG/rat	Dolphin and Scott [12]
			DRG/chicken	Deisz and Lux [9], Grassi and Lux [22]
			Cerebellum/rat	Dittman and Regehr [10]
		$Ca_v2.2$ & $Ca_v2.3$	Hippocampus (CA3 → CA1)/ guinea pig	Wu and Saggau [48]
		$Ca_v2.2$	SCG/rat	Filippov et al. [17]
Galanin	GalR1	$Ca_v2.2$	Hypothalamus/rat	Simen et al. [40]
Glutamate	mGluR1	$Ca_v2.2$	SCG/rat	Kammermeier and Ikeda [27]
LHRH	LHRH-R	$Ca_v2.2$	SCG/bullfrog	Elmslie et al. [15] Boland and Bean [3], Kuo and Bean [30]
Noradrenaline	α2-adrénergique	$Ca_v2.2$	SCG/bullfrog	Bean [1]
		$Ca_v2.2$	SCG/rat	Garcia et al. [19]
		Non-L	NG108-15	Docherty and McFadzean [11], McFadzean and Docherty [33]

NPY	Y2	Non-L $Ca_v2.2$	SCG/rat SCG/rat	Plummer et al. [35] Toth et al. [43]
Opioids – enkephalins	μ	$Ca_v2.2$	NG108-15	Kasai [28]
Opioids – dynorphins	κ	Non-L	DRG/rat	Bean [1]
Serotonin	5HT-1A	Non-L	Spinal neuron/lamprey	Hill et al. [23]
Somatostatin	SS-R	$Ca_v2.2$	DRG/rat	Ikeda and Schofield [26]
			SCG/rat	Ikeda and Schofield [25]
Substance P	NK1	$Ca_v2.2$	SCG/rat	Shapiro and Hille [38]
VIP	VIP-R	$Ca_v2.2$	SCG/rat	Zhu and Ikeda [52]

SCG superior cervical ganglion, *DRG* dorsal root ganglion

cell level, this regulation is recognized by various phenotypical modifications of the Ca^{2+} current, including a decrease of the inward current amplitude [3, 49], and in some cases a depolarizing shift of the voltage-dependence curve of current activation [1], and a slowing of activation [32] and inactivation kinetics [51]. In addition, short highly depolarizing voltage step, usually applied around +100 mV before the current eliciting pulse ("double-pulse" protocol), is sufficient to reverse, at least partially, most of the landmarks of G-protein inhibition. This protocol produces a so-called prepulse facilitation [13, 24, 37]. While the inhibition of the Ca^{2+} current has been attributed to the direct binding of G-protein βγ-dimer to the Ca_v2-subunit (referred as "ON" landmark for the onset of the inhibition), all the other landmarks including the slowing of current kinetics and prepulse facilitation can be described as variable time-dependent dissociation of Gβγ-dimer from the channel (referred as "OFF" landmarks for the arrest of the inhibition) and consequent recovery from G-protein inhibition [14, 41, 44]. Hence, proper attribution and precise quantitative evaluation of "ON" and "OFF" landmark parameters are necessary to assess the sensitiveness of a given calcium channel/GPCR complex and most importantly provide essential insight into the dynamic regulation of presynaptic calcium channels by G-proteins and GPCRs.

In this chapter, we provide a step-by-step illustration of the two main analytical methods that can be used to extract and describe the main parameters of "ON" and "OFF" G-protein landmarks. It is assumed that the reader already masters specific cell culture preparations and basic single cell patch-clamp recordings.

2 Methods

2.1 Biophysical Analysis of G-Protein Regulation by the "Double-Pulse" Method

The electrophysiological protocol classically used in the "double-pulse" method is shown in Fig. 1a. Initially introduced by Scott and Dolphin [37] and then widely adopted [13, 24], the method consists of comparing the peak current amplitude elicited by a given test pulse before (P1) and after (P2) application of a depolarizing prepulse of variable voltages and durations, both in control and G-protein-activated conditions. An example of current recordings is shown in Fig. 1b for $Ca_v2.2/\beta_3$ channels expressed in *Xenopus oocytes* in response to a 500 ms long test pulse elicited at 10 mV and a prepulse at 70 mV of variable durations. Notably, in control condition, a significant extent of current inactivation is produced by application of depolarizing prepulses as evidenced by a net decline of the peak current amplitude. In contrast, under G-protein activation, prepulse applications induce a current facilitation as evidenced by net-increased peak current amplitudes that

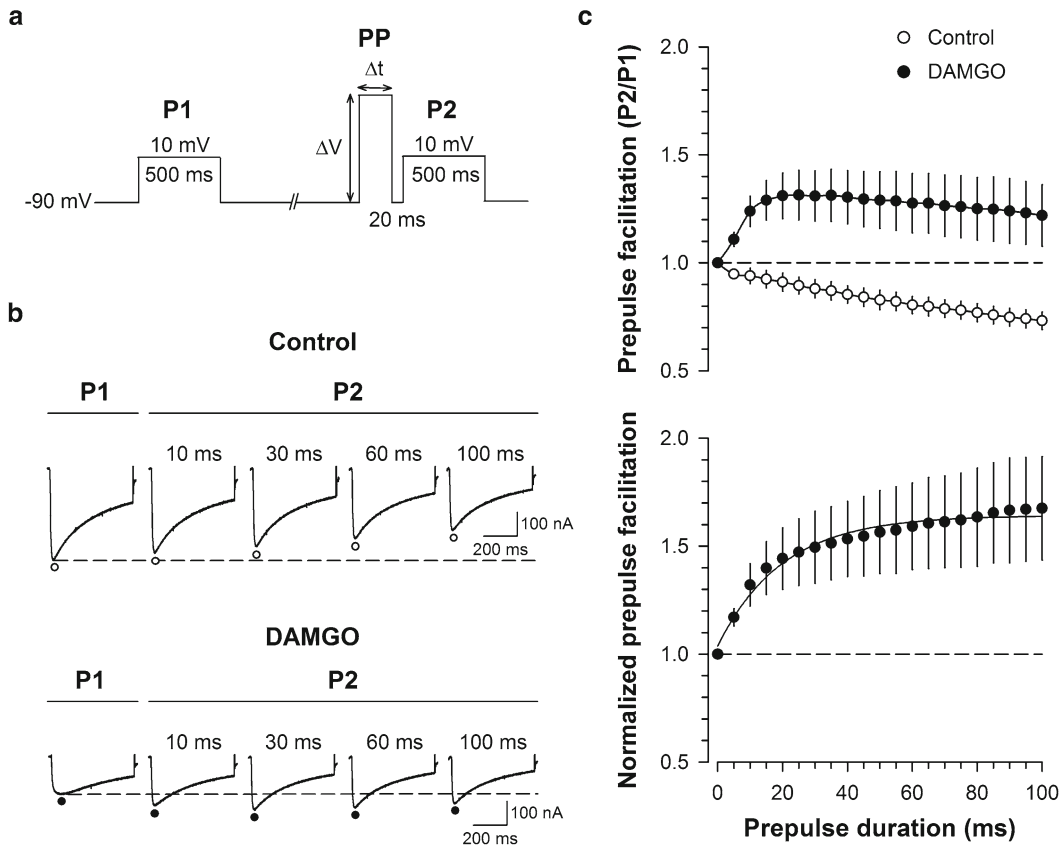

Fig. 1 Analysis of G-protein regulation by the "double-pulse" method. (**a**) Experimental protocol to measure prepulse-induced facilitation using the "double-pulse" method. P1 and P2, eliciting current pulses; *PP* prepulse. (**b**) Representative current traces recorded before and after G-protein activation by DAMGO, elicited by 500 ms P1 at 10 mV and 500 ms P2 at 10 mV following PP at 70 mV of variable durations. (**c**) Peak current amplitude ratio (P2/P1) for control (*open circles*) and DAMGO (*filled circles*) conditions (*top panel*). Normalized prepulse facilitation ($P2/P1_{DAMGO}$)/($P2/P1_{Control}$) to eliminate the prepulse-induced inactivation component resulting to the net prepulse facilitation kinetic. Fitting the result by a single exponential provides the time constant τ and maximal extent of prepulse facilitation (current recovery) (*bottom panel*) (Reproduced from Weiss and De Waard [45])

usually progressively decline with longer depolarizing prepulses. Under those conditions, elicited P2 currents are affected by a gain of current resulting from the dissociation of G-proteins from the channel (recovery from inhibition) and a loss of current due to channel inactivation induced by depolarizing prepulses. For short duration prepulses, the gain of current is predominant, whereas the tendency is inverted by increasing prepulse duration, at time points where G-protein dissociation saturates but channel inactivation increases. The control condition contains only the prepulse-induced inactivation component, whereas both the facilitation component and the inactivation component are present under

G-protein activation. Figure 1c illustrates the average behavior of normalized peak currents (P2/P1) plotted as a function of prepulse duration for both control and G-protein-activated conditions for a prepulse potential of 70 mV. In order to eliminate the inactivation component and isolate the net facilitation component under G-protein activation condition, the evolution of P2/P1 ratio observed under G-protein activation is normalized with regard to the evolution of P2/P1 ratio measured in control condition. The resulting result can then be best fitted by a single exponential function, providing the time constant of G-protein dissociation from the channel (t) and the maximal extent of current facilitation (current recovery). While τ provides important information about the kinetics of G-protein regulation, the extent of current facilitation assed by the "double-pulse" method indirectly gives access to the maximal amplitude of current inhibition that the activation of G-protein produced.

Note 1 Extracting parameters of G-protein regulation using the "double-pulse" method implies that control and G-protein-inhibited channels inactivate at the same rate and with a same extent. It also implies that the voltage dependence of this inactivation is not altered by G-protein inhibition. If this condition is not fulfilled, then the normalization procedure is flawed by approximation. So far, little information is available about the inactivation properties of the inhibited channel, but evidence points to the fact that G-protein-inhibited channels inactivate slower than control channels [15].

2.2 Biophysical Analysis of G-Protein Regulation by the "Subtraction" Method

In contrast to the "double-pulse" method, the "subtraction" method avoids the use of depolarizing prepulses and is not affected by possible alteration in channel inactivation kinetics induced by G-protein binding. This method extracts parameters of G-protein regulation from ionic currents elicited by regular depolarizing pulses by separating the ionic currents due to nonregulated channels from the ionic currents that result from the progressive unbinding of G-proteins from the regulated channel (current recovery). A step-by-step illustration of this method is illustrated in Fig. 2 using a representative example of a $Ca_v2.2/\beta_3$ channel expressed in *Xenopus oocytes* inhibited by application of the μ-opioid receptor agonist DAMGO.

1. Control ($I_{Control}$) and DAMGO-inhibited (I_{DAMGO}) currents, recorded before and after μ-opioid receptor activation, respectively, were triggered by a test pulse at 10 mV (Fig. 2a).
2. Subtracting I_{DAMGO} from $I_{Control}$ provides $I_{Inhibited}$, the amount of inhibited current upon G-protein activation (Fig. 2b, blue trace). The time course of the inhibited current is affected by both the recovery from G-protein inhibition that occurs

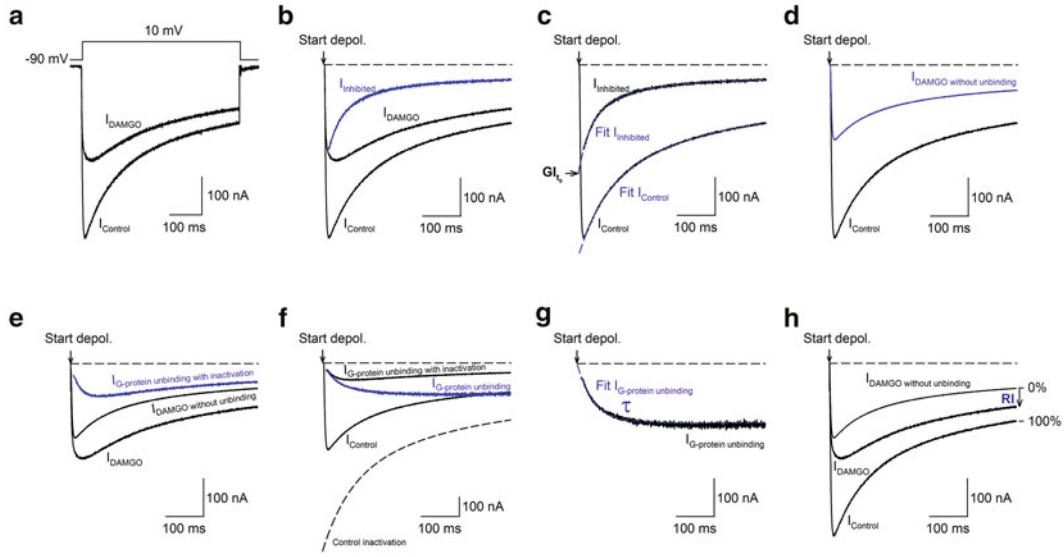

Fig. 2 Step-by-step illustration of the analysis of G-protein regulation by the "subtraction" method. (**a**) Representative current traces elicited at 10 mV for control ($I_{Control}$) and DAMGO (I_{DAMGO}) conditions. (**b**) Inhibited current ($I_{Inhibited}$, *blue trace*) under G-protein activation obtained by subtracting I_{DAMGO} from $I_{Control}$. The *dashed line* represents the zero current level and the *arrow* the start of the depolarization. (**c**) $I_{Control}$ and $I_{Inhibited}$ were extrapolated to $t = 0$ ms (start of the depolarization) by fitting traces (*blue dashed lines*) with a single and double exponential, respectively, in order to determine the maximal extent of G-protein inhibition (GIt_0). (**d**) Estimate of the fraction of control currents that is present in I_{DAMGO} ($I_{DAMGO\ without\ unbinding}$, *blue trace*) and that is due to a population of control channels. It is obtained by the following equation: $I_{Control} \times (1 - GIt_0)$. (**e**) The fraction of I_{DAMGO} current that recovers from G-protein inhibition (G-protein-inhibited channel population) is shown in *blue* ($I_{G\text{-}protein\ unbinding\ with\ inactivation}$) obtained by subtracting $I_{DAMGO\ without\ unbinding}$ from I_{DAMGO}. (**f**) The kinetics of G-protein dissociation ($I_{G\text{-}protein\ unbinding}$, *blue trace*) from G-protein-inhibited channels is obtained by dividing $I_{G\text{-}protein\ unbinding\ with\ inactivation}$ by the normalized control inactivation component (*dashed line* obtain by fitting $I_{Control}$ with a single exponential). (**g**) Fit of $I_{G\text{-}protein\ unbinding}$ (*dashed blue line*) by a single exponential decrease provides the time constant τ of G-protein dissociation from the channel. (**h**) Measure of the percentage of recovery from G-protein inhibition (RI) at the end of 500 ms pulse at 10 mV by $RI = (I_{DAMGO} - I_{DAMGO\ without\ unbinding})/(I_{Control} - I_{DAMGO\ without\ unbinding}) \times 100$ (Reproduced from Weiss and De Waard [45])

during the current eliciting pulse (conversion of G-protein-inhibited channels toward non-inhibited channels) and by the voltage-dependent inactivation of the channel that occurs during the eliciting pulse.

Note 2 One assumption is made that G-protein-bound channels do not undergo openings. It is worth to mention that ion-conducting openings of presumably G-protein-bound channels were initially proposed [7, 31], which could potentially affect the kinetics of $I_{Inihibited}$. However, openings of G-protein-bound channels remain difficult to assess directly and would require further investigation.

3. At the start of the eliciting pulse ($t = 0$ ms), there has been no recovery from G-protein inhibition, no opening from G-protein-bound channels, and inactivation has not taken place yet. Hence, in order to estimate the maximal extent of current inhibition produced by G-protein activation, I_{Control} and $I_{\text{Inhibited}}$ traces are extrapolated to $t = 0$ ms with a single and double exponential function, respectively (Fig. 2c, fits in blue). Fitting $I_{\text{Inhibited}}$ to $t = 0$ ms provides the first parameter of G-protein regulation termed GIt_0 for G-protein-induced current inhibition at the start of the depolarization and represents the maximal extent of current inhibition before any recovery process takes place ($GIt_0 = I_{\text{Inhibited}}\ t_0 / I_{\text{Control}}\ t_0 \times 100$ when expressed as percentage).
4. Applying this percentage of G-protein inhibition to I_{Control} results in $I_{\text{DAMGO without unbinding}}$, the theoretical current that would result from G-protein inhibition if the dissociation of G-proteins from the channel during the eliciting pulse did not occur at all (Fig. 2d, blue trace).
5. Subtracting $I_{\text{DAMGO without unbinding}}$ from I_{DAMGO} provides $I_{\text{G-protein unbinding with inactivation}}$ (Fig. 2e, blue trace). This current contains both the gain of current due to G-protein dissociation from the inhibited channels (recovery from inhibition) and inactivation of the gained current.

Note 3 The kinetics of the $I_{\text{G-protein unbinding with inactivation}}$ current are apparent since the gain of current is affected by inactivation, whereas inactivation is itself altered by the gain of current. Since the gained current results from the conversion of G-protein-inhibited channels toward non-inhibited channels, the real inactivation kinetics should be similar to the one of the non-inhibited channels. The amplitude of $I_{\text{G-protein unbinding with inactivation}}$ current will also depend on what extent inactivation of the channel may undergo during the depolarization when still in the G-protein-inhibited state. However, this inactivation will be significantly less than with a high depolarizing prepulse as the one that is applied in the "double-pulse" method.

6. In order to extract the net G-protein dissociation component, $I_{\text{G-protein unbinding with inactivation}}$ is divided by a normalized curve that depicts the inactivation of non-inhibited channels obtained by fitting I_{Control} by a single exponential function (Fig. 2f, dashed line). The resulting current $I_{\text{G-protein unbinding}}$ (Fig. 2f, blue trace) reflects the net kinetics of G-protein dissociation from the channel and reaches a stable plateau where no G-protein dissociation occurs anymore.
7. The kinetic τ of G-protein dissociation from the channel is obtained by fitting $I_{\text{G-protein unbinding}}$ by a decreasing single exponential function (Fig. 2g, blue dashed line). This time constant

represents the second essential parameter of G-protein regulation of voltage-gated calcium channels.

8. Finally, in order to get an estimate of the maximal fraction of G-protein-inhibited channels that recover from inhibition during the eliciting pulse, the percentage of current that had recovered from inhibition (RI) is measured such that: $RI = 100 \times (I_{DAMGO} - I_{DAMGO\ without\ unbinding}) / (I_{Control} - I_{DAMGO\ without\ unbinding})$ at a time point where $I_{G\text{-}protein\ unbinding}$ reaches a plateau. RI represents the third critical parameter that describes the calcium channel regulation by G-proteins.

3 Concluding Remarks

The biophysical analysis of direct G-protein regulation of voltage-gated calcium channels has been largely performed using the "double-pulse" method. This technique is easy to apply in both primary neurons in culture and heterologous expression systems including various mammalian cell lines and *Xenopus oocytes* and has been widely recognized and accepted. However, this approach makes the postulate that nonregulated and G-protein-inhibited channels inactivate with the same kinetics. Currently, because of technical difficulties to experimentally investigate this feature, there are no clear data in the literature supporting this assumption. In contrast, it is likely that G-protein bound channels inactivate at a slower rate than nonregulated channels, potentially introducing a significant bias to this procedure. This likelihood stems from the fact that Gβγ-dimers bind predominantly on one channel determinant that has been involved in the control of inactivation [42]. In contrast, the "subtraction" method does not require that G-protein-bound channels inactivate with the same kinetics than nonregulated channels. Moreover, this method does not require the application of a depolarizing prepulse that is usually applied along with an interpulse that provides an incentive for G-protein reassociation with the channel, therefore underestimating the real extent of G-protein dissociation. The "subtraction" analysis is exclusively based on current traces elicited at regular membrane voltages, before and after G-protein activation. Most importantly, this method allows the analysis of G-protein regulation at physiological membrane potential, providing a better understanding of the physiological dynamics of the regulation. It uncovers the importance of the offset of G-protein regulation in physiological processes rather than exclusively putting the emphasis on the onset of G-protein inhibition. This is a particularly important aspect of G-protein regulation knowing that neuronal networks undergo a significant extent of tonic G-protein activation. On the other hand, an inherent limitation of this approach is that it is limited to a range

of membrane potentials where ionic currents can be effectively measured. Although this method has been developed and validated on heterologous expressed channels, it is likely that it can also be suitable for analyzing G-protein regulation of voltage-gated calcium channels in native neuronal environment.

In summary, both of the described methods are not model independent and are both affected by their intrinsic assumptions and/or limitations. However, they provide similar qualitative information about the kinetics of the G-protein regulation and are therefore extremely informative in terms of how G-protein-coupled receptors dynamically regulate voltage-gated calcium channel in health and diseased state. Indeed, mutations in the genes encoding VGCCs linked to neurological disorders including hemiplegic migraine type 1 have been shown to alter direct G-protein regulation of mutated channels [20, 21, 34, 46]. Hence, perfect analysis of G-protein regulation of mutated channels not only contributes to our understanding of the associated channelopathies but also represent important signaling information for potential new therapeutic strategies.

Acknowledgments

Research in NW's laboratory is supported by the Czech Science Foundation (grant 15-13556S), the Ministry of Education Youth and Sports (grant 7AMB15FR015), and the Institute of Organic Chemistry and Biochemistry.

References

1. Bean BP (1989) Neurotransmitter inhibition of neuronal calcium currents by changes in channel voltage dependence. Nature 340:153–156
2. Bernheim L, Beech DJ, Hille B (1991) A diffusible second messenger mediates one of the pathways coupling receptors to calcium channels in rat sympathetic neurons. Neuron 6: 859–867
3. Boland LM, Bean BP (1993) Modulation of N-type calcium channels in bullfrog sympathetic neurons by luteinizing hormone-releasing hormone: kinetics and voltage dependence. J Neurosci 13:516–533
4. Brown CH, Russell JA (2004) Cellular mechanisms underlying neuronal excitability during morphine withdrawal in physical dependence: lessons from the magnocellular oxytocin system. Stress 7:97–107
5. Brown DA, Filippov AK, Barnard EA (2000) Inhibition of potassium and calcium currents in neurones by molecularly-defined P2Y receptors. J Auton Nerv Syst 81:31–36
6. Catterall WA (2011) Voltage-gated calcium channels. Cold Spring Harb Perspect Biol 3:a003947
7. Colecraft HM, Patil PG, Yue DT (2000) Differential occurrence of reluctant openings in G-protein-inhibited N- and P/Q-type calcium channels. J Gen Physiol 115: 175–192
8. De Waard M, Hering J, Weiss N, Feltz A (2005) How do G proteins directly control neuronal Ca2+ channel function? Trends Pharmacol Sci 26:427–436
9. Deisz RA, Lux HD (1985) gamma-Aminobutyric acid-induced depression of calcium currents of chick sensory neurons. Neurosci Lett 56:205–210
10. Dittman JS, Regehr WG (1996) Contributions of calcium-dependent and calcium-independent mechanisms to presynaptic inhibition at a cerebellar synapse. J Neurosci 16:1623–1633
11. Docherty RJ, McFadzean I (1989) Noradrenaline-induced inhibition of voltage-sensitive

calcium currents in NG108-15 hybrid cells. Eur J Neurosci 1:132–140

12. Dolphin AC, Scott RH (1987) Calcium channel currents and their inhibition by (-)-baclofen in rat sensory neurones: modulation by guanine nucleotides. J Physiol 386:1–17
13. Doupnik CA, Pun RY (1994) G-protein activation mediates prepulse facilitation of Ca2+ channel currents in bovine chromaffin cells. J Membr Biol 140:47–56
14. Elmslie KS, Jones SW (1994) Concentration dependence of neurotransmitter effects on calcium current kinetics in frog sympathetic neurones. J Physiol 481:35–46
15. Elmslie KS, Zhou W, Jones SW (1990) LHRH and GTP-gamma-S modify calcium current activation in bullfrog sympathetic neurons. Neuron 5:75–80
16. Filippov AK, Brown DA, Barnard EA (2000) The P2Y(1) receptor closes the N-type Ca(2+) channel in neurones, with both adenosine triphosphates and diphosphates as potent agonists. Br J Pharmacol 129:1063–1066
17. Filippov AK, Couve A, Pangalos MN, Walsh FS, Brown DA, Moss SJ (2000) Heteromeric assembly of GABA(B)R1 and GABA(B)R2 receptor subunits inhibits Ca(2+) current in sympathetic neurons. J Neurosci 20:2867–2874
18. Garcia DE, Brown S, Hille B, Mackie K (1998) Protein kinase C disrupts cannabinoid actions by phosphorylation of the CB1 cannabinoid receptor. J Neurosci 18:2834–2841
19. Garcia DE, Li B, Garcia-Ferreiro RE, Hernandez-Ochoa EO, Yan K, Gautam N, Catterall WA, Mackie K, Hille B (1998) G-protein beta-subunit specificity in the fast membrane-delimited inhibition of Ca2+ channels. J Neurosci 18:9163–9170
20. Garza-Lopez E, Gonzalez-Ramirez R, Gandini MA, Sandoval A, Felix R (2013) The familial hemiplegic migraine type 1 mutation K1336E affects direct G protein-mediated regulation of neuronal P/Q-type Ca2+ channels. Cephalalgia 33:398–407
21. Garza-Lopez E, Sandoval A, Gonzalez-Ramirez R, Gandini MA, Van den Maagdenberg A, De Waard M, Felix R (2012) Familial hemiplegic migraine type 1 mutations W1684R and V1696I alter G protein-mediated regulation of Ca(V)2.1 voltage-gated calcium channels. Biochim Biophys Acta 1822:1238–1246
22. Grassi F, Lux HD (1989) Voltage-dependent GABA-induced modulation of calcium currents in chick sensory neurons. Neurosci Lett 105:113–119
23. Hill RH, Svensson E, Dewael Y, Grillner S (2003) 5-HT inhibits N-type but not L-type Ca(2+) channels via 5-HT1A receptors in lamprey spinal neurons. Eur J Neurosci 18:2919–2924
24. Ikeda SR (1991) Double-pulse calcium channel current facilitation in adult rat sympathetic neurones. J Physiol 439:181–214
25. Ikeda SR, Schofield GG (1989) Somatostatin blocks a calcium current in rat sympathetic ganglion neurones. J Physiol 409:221–240
26. Ikeda SR, Schofield GG (1989) Somatostatin cyclic octapeptide analogs which preferentially bind to SOMa receptors block a calcium current in rat superior cervical ganglion neurons. Neurosci Lett 96:283–288
27. Kammermeier PJ, Ikeda SR (1999) Expression of RGS2 alters the coupling of metabotropic glutamate receptor 1a to M-type K+ and N-type Ca2+ channels. Neuron 22:819–829
28. Kasai H (1992) Voltage- and time-dependent inhibition of neuronal calcium channels by a GTP-binding protein in a mammalian cell line. J Physiol 448:189–209
29. Kasai H, Aosaki T (1989) Modulation of Ca-channel current by an adenosine analog mediated by a GTP-binding protein in chick sensory neurons. Pflugers Arch 414:145–149
30. Kuo CC, Bean BP (1993) G-protein modulation of ion permeation through N-type calcium channels. Nature 365:258–262
31. Lee HK, Elmslie KS (2000) Reluctant gating of single N-type calcium channels during neurotransmitter-induced inhibition in bullfrog sympathetic neurons. J Neurosci 20:3115–3128
32. Marchetti C, Carbone E, Lux HD (1986) Effects of dopamine and noradrenaline on Ca channels of cultured sensory and sympathetic neurons of chick. Pflugers Arch 406:104–111
33. McFadzean I, Docherty RJ (1989) Noradrenaline- and enkephalin-induced inhibition of voltage-sensitive calcium currents in NG108-15 hybrid cells. Eur J Neurosci 1:141–147
34. Melliti K, Grabner M, Seabrook GR (2003) The familial hemiplegic migraine mutation R192Q reduces G-protein-mediated inhibition of P/Q-type (Ca(V)2.1) calcium channels expressed in human embryonic kidney cells. J Physiol 546:337–347
35. Plummer MR, Rittenhouse A, Kanevsky M, Hess P (1991) Neurotransmitter modulation of calcium channels in rat sympathetic neurons. J Neurosci 11:2339–2348
36. Proft J, Weiss N (2015) G-protein regulation of neuronal calcium channels: back to the future. Mol Pharmacol 87:890–906
37. Scott RH, Dolphin AC (1990) Voltage-dependent modulation of rat sensory neurone calcium channel currents by G protein activation: effect of a dihydropyridine antagonist. Br J Pharmacol 99:629–630

38. Shapiro MS, Hille B (1993) Substance P and somatostatin inhibit calcium channels in rat sympathetic neurons via different G protein pathways. Neuron 10:11–20
39. Shapiro MS, Loose MD, Hamilton SE, Nathanson NM, Gomeza J, Wess J, Hille B (1999) Assignment of muscarinic receptor subtypes mediating G-protein modulation of Ca(2+) channels by using knockout mice. Proc Natl Acad Sci U S A 96:10899–10904
40. Simen AA, Lee CC, Simen BB, Bindokas VP, Miller RJ (2001) The C terminus of the Ca channel alpha1B subunit mediates selective inhibition by G-protein-coupled receptors. J Neurosci 21:7587–7597
41. Stephens GJ, Brice NL, Berrow NS, Dolphin AC (1998) Facilitation of rabbit alpha1B calcium channels: involvement of endogenous Gbetagamma subunits. J Physiol 509:15–27
42. Stotz SC, Hamid J, Spaetgens RL, Jarvis SE, Zamponi GW (2000) Fast inactivation of voltage-dependent calcium channels. A hinged-lid mechanism? J Biol Chem 275:24575–24582
43. Toth PT, Bindokas VP, Bleakman D, Colmers WF, Miller RJ (1993) Mechanism of presynaptic inhibition by neuropeptide Y at sympathetic nerve terminals. Nature 364:635–639
44. Weiss N, Arnoult C, Feltz A, De Waard M (2006) Contribution of the kinetics of G protein dissociation to the characteristic modifications of N-type calcium channel activity. Neurosci Res 56:332–343
45. Weiss N, De Waard M (2007) Introducing an alternative biophysical method to analyze direct G protein regulation of voltage-dependent calcium channels. J Neurosci Methods 160:26–36
46. Weiss N, Sandoval A, Felix R, Van den Maagdenberg A, De Waard M (2008) The S218L familial hemiplegic migraine mutation promotes deinhibition of Ca(v)2.1 calcium channels during direct G-protein regulation. Pflugers Arch 457:315–326
47. Wu LG, Saggau P (1994) Adenosine inhibits evoked synaptic transmission primarily by reducing presynaptic calcium influx in area CA1 of hippocampus. Neuron 12:1139–1148
48. Wu LG, Saggau P (1995) GABAB receptor-mediated presynaptic inhibition in guinea-pig hippocampus is caused by reduction of presynaptic Ca2+ influx. J Physiol 485:649–657
49. Wu LG, Saggau P (1997) Presynaptic inhibition of elicited neurotransmitter release. Trends Neurosci 20:204–212
50. Yawo H, Chuhma N (1993) Preferential inhibition of omega-conotoxin-sensitive presynaptic Ca2+ channels by adenosine autoreceptors. Nature 365:256–258
51. Zamponi GW (2001) Determinants of G protein inhibition of presynaptic calcium channels. Cell Biochem Biophys 34:79–94
52. Zhu Y, Ikeda SR (1994) VIP inhibits N-type Ca2+ channels of sympathetic neurons via a pertussis toxin-insensitive but cholera toxin-sensitive pathway. Neuron 13:657–669

Chapter 23

Electrophysiological Recordings in Behaving Animals

Agnès Gruart and José M. Delgado-García

Abstract

The electrophysiological measurement of changes in synaptic strength taking place during the acquisition of new motor and cognitive abilities, and during other physiological conditions, is an excellent tool for studying the role of different receptors and/or ion channels in the nervous system of alert behaving experimental animals. Many different molecular and subcellular components, including their complex mechanisms, have specific roles and underlie the physiological basis of learning and memory phenomena. In the past few years, various sophisticated methods (genetically manipulated animals, light stimulation systems, pharmacokinetic protocols, etc.) have emerged as valuable tools to be considered together with the more classic in vivo electrophysiological techniques. Recent methodological and technical (use of multiple recording microelectrodes, telemetric recordings, etc.) improvements will help to refine the level of collected results. In addition, new mathematical routines and modeling procedures are also exponentially increasing the level of data analysis and representation. The aim of all these classic and contemporary procedures is, as far as possible, to study motor and cognitive processes in vivo. The present chapter will deal with different stimulating and recording procedures that can be used in alert behaving mammals during the acquisition, retrieval, or extinction of new abilities.

Key words In vivo electrophysiology, Electrode, Field postsynaptic potentials, Action potential, Neuronal identification, Synaptic activity, Synaptic strength

Abbreviations

EMG	Electromyography
fEPSP	Field excitatory postsynaptic potential
HFS	High-frequency stimulation
LTP	Long-term potentiation
PSTH	Peristimulus time histogram

In the past few years, there has been a notable advance in the knowledge of the structure and localization of many different neurotransmitter receptors and/or ion channels that are essential for the proper understanding of the specific roles of different neuronal structures. Moreover, these functions are currently studied in

Rafael Luján and Francisco Ciruela (eds.), *Receptor and Ion Channel Detection in the Brain: Methods and Protocols*, Neuromethods, vol. 110, DOI 10.1007/978-1-4939-3064-7_23,

increasingly complex preparations, from basic neuron electrophysiological properties to the involvement of neural circuits in the acquisition of new motor and cognitive abilities. The use of different learning paradigms is a good experimental strategy because it can place the experimental animal (and its nervous system) in different situations that need the specific activation of different neural circuits. The in vivo approach to the study of electrophysiological phenomena taking place at selected cortical and subcortical neuronal and synaptic sites during the precise moment of learning acquisition can be very useful for the proper integration of the important information already collected from in vitro and molecular studies [1, 2].

Recent efforts have been aimed at taking advantage of genetically manipulated mice, some of them with changes in the expression of neuronal receptors, neurotransmitters, and/or ionic channels. The electrophysiological results of these in vivo manipulations during different learning tasks allow proposing interesting hypotheses about the role of such molecular elements in the behaving animal. For example, it is known that hippocampal N-methyl-D-aspartate (NMDA) receptors are involved in the acquisition of conditioned eyeblink responses and the induction of long-term potentiation (LTP), both studied in behaving mice at the CA3-CA1 synapse [1, 3]. LTP seems to depend on both local dendritic protein synthesis and nuclear transcription processes, but many different signaling pathways have also been proposed as key responsible sources of the postsynaptic changes that produce LTP and classical conditioning. Moreover, different types of presynaptic receptor (adenosine A_1 and A_{2A}, cannabinoid CB1, muscarinic and nicotinic cholinergic, $GABA_A$ and $GABA_B$ metabotropic glutamate, TrkB, etc.) are also able to exert specific excitatory or inhibitory effects on transmitter release and/or in different phases (habituation, conditioning, extinction, recall, etc.) of learning and memory tasks (*see* Refs. [4–6] for some examples of such studies). These results open new perspectives for studying different receptors and molecular signals, mainly through genetically manipulated mice together with the use of selective pharmacological tools.

Procedures to carry out electrophysiological recordings in behaving animals follow three main steps: (i) electrode preparation, (ii) surgical procedures to implant the electrodes and to prepare the animals for recording sessions, and (iii) recording the selected neuronal activity, followed by data analysis and representation. Although many distinctive features can be taken into account (depending on the species, brain structure to be studied, task to be tested, etc.) in these in vivo electrophysiological recordings, some standard procedures have been already described [7–10]. Finally, it is important to point out that all the procedures included in this chapter should be carried out in laboratories located inside an animal house facility. For most countries, animals cannot go back into an animal house once they have left it. Moreover, any manipulation

in live animals must adhere strictly to international, national, and local regulations for the use of experimental animals. The number of subjects used for any protocol also has to follow the recommendations laid out in the law.

1 Materials

1.1 Electrode Preparation

1.1.1 Stimulating Electrodes

1. Enameled silver wire of 200–500 μm in diameter (A-M Systems, Carlsborg, WA, USA) (*see* **Note 1**).
2. Teflon-coated tungsten wire of 25–50 μm in diameter (Advent Research, Eynsham, UK).
3. Teflon-coated, annealed stainless steel wire of 50 μm in diameter (A-M Systems) for stimulating peripheral nerves in small animals (mice and rats).
4. Seven-stranded, Teflon-coated, stainless steel wire of 250 μm in diameter (A-M Systems) for stimulating peripheral nerves in large animals (rabbits and cats).
5. Hypodermic syringe needles of 21 gauge (0.873 mm in diameter and 40 mm long) or 25 gauge (0.556 mm in diameter and 16 mm long).
6. Fast-acting glue (Loctite® Super Glue with easy brush; Henkel Corp., Germany).

1.1.2 Recording Electrodes

1. Glass capillary tubing of different (1–3 mm) diameters.
2. Pipette puller (Narishige PE-22, Tokyo, Japan).
3. 2M sodium chloride (NaCl) solution.
4. Syringes of 20 mL with hypodermic needles.
5. Acrodisc® syringe filters with HT Tuffryn® membrane (Cardinal Health, Vaugan, ON, Canada).
6. Teflon-coated tungsten wire of 25–50 μm in diameter (Advent Research).
7. Seven-stranded, Teflon-coated, stainless steel wire of 250 μm in diameter for electromyographic (EMG) recordings (A-M Systems).
8. Stainless steel self-tapping screws. A diameter of 1.17 mm is indicated for small animals (mice and rats) and a diameter of around 2–5 mm for large animals (rabbits and cats).
9. Uncoated silver wires of 200 μm in diameter (A-M Systems) for grounds. For large animals, the ends of an external ring electrode made of silver (1 mm in diameter, A-M systems) are introduced into a hole drilled in the skull. During recordings, external ground cables can be attached easily to this external ring.

1.1.3 General Material

1. Soldering material (solder station, tin, magnifying glasses, clamp for magnifying glasses, insolating substances, etc.).
2. Fine scissors, Dumont #5 forceps, scalpels, spatulas, etc.
3. Primer (Loctite® 406; Henkel Corp.).
4. Cyanoacrylate primer (Loctite® 770; Henkel Corp.).
5. Sockets for microelectronics of 4 and 6 pins (RS Components; Allied Electronics, Inc., USA).
6. Bone wax (Ethicon®, Johnson & Johnson Intl., Beerse, Belgium).
7. Self-tapping screws of 1.9 mm (cat no. 19010–20) for attaching the grounds to the cranium of the animal (Fine Science Tools Inc., Foster City, CA, USA).

1.2 Electrode Implantation during Surgery

1. Stereotaxic atlas for the animal species (mouse, rat, rabbit, etc.).
2. Stereotaxic frame and accessories (manipulator X, Y, Z adjustments, electrode holder, head holders, ear bars, etc.) (David Kopf Instruments, Tujunga, CA, USA).
3. Pulse oximeter (Canl-425SV, MED Associates Inc., St. Albans City, VT, USA, for rabbits, and MouseOx Plus® Starr Life Sciences, Oakmont, PA, USA, for mice and rats).
4. Body temperature control system (TR-200, Fine Science Tools Inc., for rabbits, and Kent Scientific, Boston, MA, USA, for mice and rats) and electrical blankets.
5. For anesthesia, we recommend the hypnotic drug ketamine (Ketamidor®, 25 mg/kg) and the sedative drug xylazine (Rompun®, 3 mg/kg), the two delivered by intramuscular injection.
6. Fluotec 5 (Ohmeda-Fluotec, Tewksbury, MA, USA) with mouse or rat anesthesia mask (David Kopf Instruments).
7. Intravenous catheter of 24 gauge (Abbocath®) connected to an adjustable flow probe.
8. Micro drill and carbon steel burrs (NE 120, NSK Dental-Spain, Madrid, Spain).
9. Surgical material (fine scissors, forceps, microspatulas, scalpels, needle holder, suture and needles, bulldog serrefine clamps, etc.).
10. Poupinel (dry heat; cat. no 2000787) sterilizer (Selecta, Barcelona, Spain).
11. Pharmaceuticals (antibiotics, gotu kola extract, Ringer's solution, etc.).
12. Transparent gel to protect the cornea (Methocel® 2 %, CIBA vision, UK).

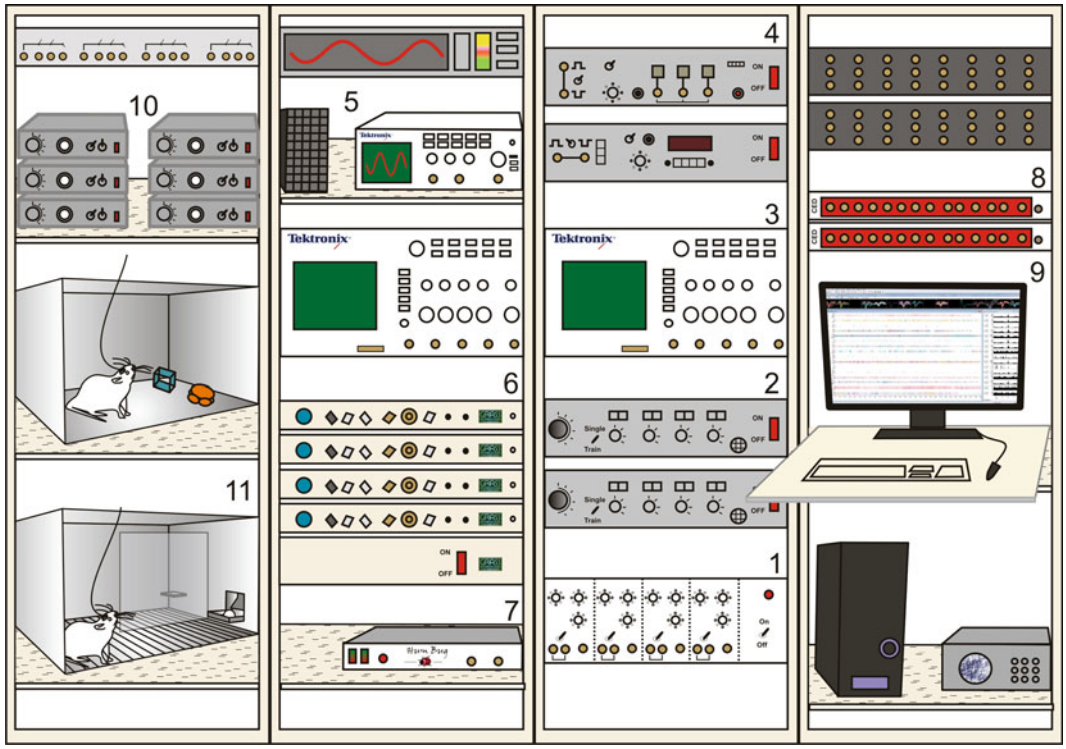

Fig. 1 A diagrammatic representation of a setup for instrumental conditioning of behaving rats. (*1*) Triggering panel, (*2*) stimulators, (*3*) oscilloscope, (*4*) analyzers of spike profiles, (*5*) programmable function generators, (*6*) amplifiers for signal recordings, (*7*) 50–60 Hz noise removal without filtering, (*8*, *9*) data acquisition and storage systems, (*10*) isolation units, and (*11*) adapted boxes for object recognition (*top*) or for operant conditioning (*bottom*)

13. Cotton swabs, gauzes, and absorption triangles.
14. Syringes of 1, 2, 5 and 10 mL, together with hypodermic syringe needles of 21 and 25 gauge.
15. Inlay pattern resin (dental cement) that includes powder, liquid, and lubricant (DuraLay®, Reliance Dental Mfg. Co., Worth, IL, USA).
16. Surgical microscope (CLS 150MR, Leica, Madrid, Spain).
17. Surgery lamp (Derungs, SX50, H. Waldmann GmbH & Co., Villingen-Schwenningen, Germany).
18. Adaptable surgical table (Cibertec).

1.3 Electrophysiological Recordings

1. Grounded metallic racks to support all the equipment and to prevent any electrical noise in recordings (Fig. 1).
2. When recordings are carried out with glass micropipettes implanted daily, a micromanipulator (Canberra, from Narishige) is needed, together with a commercial amplifier (model 1700,

A-M systems) with a headstage probe for high-impedance electrodes.

3. Differential amplifiers for recording extracellular electrophysiological activity using glass pipettes or metallic electrodes around 1–10 MΩ of impedance within a bandwidth of 0.1 Hz–10 KHz (Grass P511, Grass-Telefactor, West Warwick, RI, USA).
4. 50–60 Hz noise removal without additional filtering (Hum Bug®, Digitimer, Hertfordshire, UK).
5. Stimulus isolation units (ISU-220) attached to a programmable stimulator (model CS-220, Cibertec, Madrid, Spain).
6. Window discriminator (model PDV125, Cibertec).
7. Programmable function generators (model PG5110, Tektronix, Beaverton, OR, USA).
8. Digital storage oscilloscopes (model TDS2000C, Tektronix). The use of two or three oscilloscopes simultaneously allows seeing the same signal on different time scales.
9. High-performance data acquisition interface (Power1401-3, CED, Cambridge, UK).
10. Computer with a multichannel data acquisition and analysis package (Spike2, CED).
11. Surgical microscope (M400E, Leica, Madrid, Spain).
12. A homemade Faraday box large enough to contain the equipment (Skinner box, restrainer box, resting box, open field, etc.) where the animal is tested.

2 Methods

2.1 Electrode Preparation

From the first action potential recorded intracellularly many years ago with an electrode inserted into a giant squid axon to the multiple unitary recordings carried out simultaneously in multiple brain sites combined (sometimes) with optical tools, many different types of electrode for stimulation and recording have been designed and used in animal research. With the growth of this technology, some basic electrophysiological recording principles must be kept in mind in order to record neuronal action potentials properly. The increasing sophistication of the types of electrode also requires a deeper awareness in the interpretation and limits of collected recordings. The impairment in animal movements and the damage (because of electrode size and equipment restrictions) that these ambitious techniques can produce also have to be considered when we want to use them in behaving animals (e.g., during performance of selective learning tasks). In this section we will address the basic procedures and the necessary steps for stimulation and recording in small and large behaving mammals.

2.1.1 Stimulating Electrodes

1. Bipolar stimulating electrodes are made with 200–500 μm silver wire glued with some drops of cyanoacrylate (Loctite® Super Glue with easy brush) and separated between 0.1 and 1 mm at their active ends. The enamel is removed from the electrode tip for around 0.1–1 mm, to have a reduced area of stimulation. The electrode's length depends on the neural structure to be reached.
2. Bipolar stimulating electrodes designed to evoke field synaptic potentials are made from four units of 50 μm, Teflon-coated, tungsten wire (Advent Research). The wires are woven together and linked by applying a layer of primer (Loctite® 406) and, 30 min afterward, a layer of glue (Loctite® 770). Four hours later, these four joined wires are cut at different lengths, and each tip is bared of Teflon for 100–200 μm. The final assembly is a step-down electrode in which each wire can reach slightly different areas in the selected brain site. To stimulate a bigger area, the same procedure can be used adding together three or more electrodes.
3. Bipolar electrodes for nerve stimulation (e.g., trigeminal nerve) are made with seven-stranded, Teflon-coated, stainless steel wire introduced inside a 21-gauge hypodermic syringe needle. For small animals, Teflon-coated, annealed stainless steel wire of 50 μs (A-M Systems) introduced inside a 25-gauge hypodermic syringe needle is used. Electrode tips are bared of their isolating cover for 0.5 mm and bent as a hook to allow a stable insertion in the tissue close to the nerve.

2.1.2 Recording Electrodes

1. The diameter and material of the glass micropipette depend on the depth of the selected brain structure. For large animals (rabbits and cats), glass electrodes can be made of borosilicate glass of 3 mm external diameter, with a thick wall to withstand the pulling. For small animals (mice and rats), it is better to use borosilicate glass of 1.5 mm external diameter, with an inside filament to facilitate its filling.
2. The first step is to pull the glass, using a micropipette puller, to a useful length of 25–30 mm. Keep in mind that although the tip of the glass electrode may be very fine (around 1–2 μm), the posterior portion could be around 1–2 mm and able to stretch and even damage the brain tissue.
3. Recording electrodes for field postsynaptic potentials, or local field potentials, are made from two to four units of 50 μm, Teflon-coated, tungsten wire (Advent Research). The wires are woven together and linked by applying a layer of primer (Loctite® 406) and, 30 min afterward, a layer of glue (Loctite® 770). Four hours later, these joined wires are cut at different lengths, and each tip is bared of Teflon isolation for 100–200 μm. The final assembly is a step-down electrode in which each

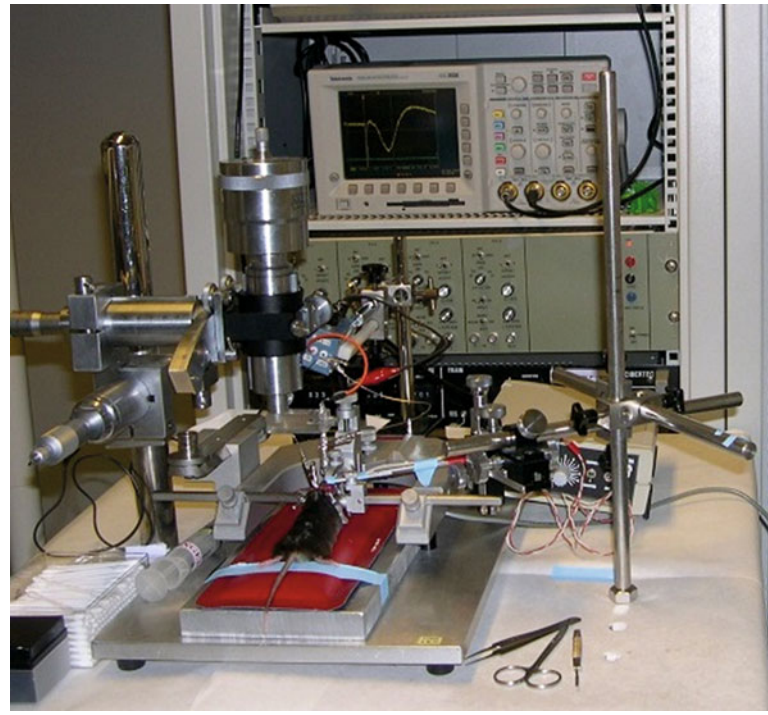

Fig. 2 A picture of the surgical theater for electrode implantation in mice

wire can record points slightly different in depth. Similar electrodes can be made with 25 μm, Teflon-coated, tungsten wire (Advent Research). In this case, it is possible to put together more than four electrodes.

4. Bipolar electrodes for EMG recordings are made with seven-stranded, Teflon-coated, stainless steel wire introduced inside a 21-gauge hypodermic syringe needle. For small animals, Teflon-coated, annealed stainless steel wire of 50 μs (A-M Systems) introduced inside a 25-gauge hypodermic syringe needle is used. Teflon isolation has to be removed from both ends. The tip to be inserted should be free of coating for ≈ 100–500 μm, depending on the size of the muscle, and should be bent to make a hook electrode.

2.2 Electrode Implantation during Surgery

Surgical procedures for implanting electrodes in experimental animals require a specific, clean surgery room (Fig. 2). The room will have all the equipment and material needed during the surgery in order to minimize the time the animal is maintained under anesthesia. In accordance with current animal care legislation, during surgery all the animals have to have their vital constants monitored. In particular, the level of anesthesia and the body temperature have to be continuously measured.

1. Prior to the surgery, it is highly recommended to prepare the surgical theater and the equipment to be used. All surgical instruments have to be sterilized using a cycle of dry heat of 150 °C for 60 min.
2. Stimulation and recording electrodes have to be implanted in the area with the highest density of somas or axons to be activated. This information should be collected prior to surgery from published reports and in the corresponding stereotaxic atlas.
3. Animals are anesthetized following the national and international regulations relating to research animals. Different protocols are followed for large (such as rabbits) or for small (mice and rats) animals.
4. Rabbits are anesthetized with a mixture of the hypnotic drug ketamine (Ketamidor®, 25 mg/kg) and the sedative drug xylazine (Rompun®, 3 mg/kg) delivered by intramuscular injection. For prevention of secretions, atropine sulfate (0.1 mg/kg) is injected with the same procedure. When the proper level of anesthesia is reached, the frontal, occipital, and parietal zones of the head are shaved using an electric shaver. The margin of the right ear and a small circular area on the anterior left leg are also shaved. After shaving, an antiseptic solution (Dermosil®, Schering-Plough Corp., Kenilworth, NJ, USA) is applied to prevent infections. Then, the marginal vein of the right ear is cannulated using a 24-gauge intravenous catheter (Abbocath®) connected to an adjustable flow probe. The infusion flow is maintained at 25 mL/h and comprises 100 mL of physiological serum with a concentration of 10 mg/mL ketamine and 3 mg/mL xylazine. Heart rate and oxygen saturation have to be monitored constantly with the pulse oximeter fixed to the shaved leg. The rabbit's temperature has to be monitored and controlled with the temperature control system coupled to an anal thermometric probe and to a thermal pad beneath the animal. The body temperature of rabbits should be kept within physiological values (39.0 ± 0.5 °C).
5. Mice and rats are anesthetized with 0.8–1.5 % isoflurane, supplied from a calibrated Fluotec 5 (Ohmeda-Fluotec) vaporizer, at a flow rate of 1–4 L/min oxygen (AstraZeneca, Madrid, Spain), and delivered via a mouse or rat anesthesia mask (David Kopf Instruments). Heart rate and oxygen saturation have to be monitored constantly with the pulse oximeter clamped to the right foot. The animal's temperature has to be monitored and controlled with the temperature control system coupled to an anal thermometric probe and to a thermal pad beneath the animal.

6. Each species (mouse, rat, or rabbit) is placed in the specific stereotaxic frame (David Kopf Instruments) and the animal's head immobilized. Mice and rats are fixed with the corresponding ear bars and head holders. Rabbits are immobilized with the help of a buccal support under the incisor teeth and two lateral brackets clamping both zygomatic arch bones.
7. A transparent gel is applied on both corneas (Methocel® 2 %, CIBA vision) to prevent ocular damage by desiccation.
8. A medial fronto-occipital incision of the head skin and subcutaneous tissues, a retraction of temporal muscles, and the removal of the periosteum with the help of a scalpel and a palette knife are performed to achieve the correct exposure of cranial bones. The skin is held away from the surgical area with the help of four bulldog serrefine clamps (one at each corner). The exposed area is cleaned with Ringer solution at 38 °C, and any bleeding is stopped with bone wax (Ethicon®, Johnson & Johnson Intl.).
9. The head has to be placed in the stereotaxic device in a perfectly horizontal position. This position is checked with the help of a needle attached to a second stereotaxic manipulator arm. These two manipulator arms will help to determine the location of *Bregma* and *Lambda* points and to adjust the final head position. The sagittal plane should have a difference of zero between right and left sides. The difference between *Bregma* and *Lambda* depth has to be zero in the case of mice and rats and ≈ 1.5 mm in rabbits. The distance between the two points at the scalp is ≈ 18 mm in rabbits and ≈ 4 mm in mice.
10. Bone perforations for the subsequent electrode and screw (used as ground and anchoring) implantations are performed with a dental drill (NE 120, NSK Dental-Spain, Madrid, Spain). Prior to introducing the electrodes, the dura mater has to be carefully removed with a needle bent at its tip.
11. Since the stereotaxic atlas has some inaccuracy, the final placement of stimulating and recording electrodes will be decided during the surgery and after checking their functional effects on the implanted sites. To test the stimulating electrode, a train of pulses (100 Hz for 50 ms) is recommended, trying to identify any movement produced if the implanted site is a motor structure (e.g., the oculomotor nucleus or the motor cortex). In some other cases, the effects of stimulation can be seen through the recording electrode (e.g., effects of stimulating Schaffer collaterals through a recording electrode placed in the dendrites of hippocampal CA1 pyramidal cells). But in most cases, and with an anesthetized animal, the stimulation of many brain areas does not produce any noticeable movement, and implanted electrodes have to be placed following only stereotaxic coordinates.

12. The final position of a chronically implanted recording electrode can be checked before it is fixed to the cranium with dental cement. With the help of the stimulating electrode, the position of the recording electrode can be checked while it is still attached to the stereotaxic arm. In this way, the depth of the recording electrode can be slightly adjusted. The profile and shapes of evoked field potentials can be compared with already published depth profiles collected from acute animals. Thus, it will be possible to implant the recording electrode in the most interesting recording site (soma, dendrites, specific layer, periphery, etc.).
13. Once all recording and stimulating electrodes have been implanted in the animal, they have to be soldered to multiple pin connectors. To these connectors are also soldered the silver wire attached to the stainless steel self-tapping screws acting as a ground. Combinations of four- and six-pin female connectors are extensively used for small animals (mice and rats) and nine-pin female connectors (DB-9) for rabbits. Any hole in the socket has to be covered (with dental cement or bone wax) before or after the soldering to prevent unwanted contacts between soldered wires and/or its obstruction with animal fluids.
14. All the soldering has to be protected with some isolating substance (nail polish is very effective as soldering isolation).
15. For electrophysiological recordings with glass micropipettes, an adequate window of 2–6 mm should be drilled in the scalp above the recording area. On occasions, and in order to avoid the electrode's displacement though key (or vital or difficult-to-cross) structures, the window is placed in some other part of the bone, and the pipette (or metallic electrode) is introduced at a known angle. A metal rod should be placed in one corner of the recording window to be used as a stereotaxic zero during recording sessions. The stereotaxic coordinates of the implanted metal references have to be calculated in relation to *Bregma*. The rod and the window perimeter are surrounded with dental cement. Slots made in the rod facilitate its attachment to the skull with the dental cement.
16. Screws and the sockets are attached to cranial bones with fast-acting glue and all the implanted devices are fixed to the skull by covering them with dental cement.
17. Once the whole assembly is finished, the rostral and caudal sides of the incision made in the scalp are sutured using a silk thread (2/0, cat. no 18020–20, Fine Science Tools Inc.) using single plain stitches with the aim of facilitating the animal's recovery process. In addition, eye drops containing gentamicin and dexamethasone (Gentadexa®) should be applied to the

sutured incision, as well as a topical ointment (Blastoestimulina®) for the regrowth of fibroblasts.

18. For rabbits, and to prevent infections, animals are injected with 0.5 mL of penicillin (Penilevel®, benzylpenicillin sodium power 25,000 IU/mL, ERN laboratories, Barcelona, Spain).
19. During the recovery period, the animal is kept in a comfortable box with some heat provided from a heat lamp. Once the animal starts to move normally and it recovers its physiological constants, it is returned to its home cage.

2.3 Electrophysiological Recordings

2.3.1 Stimulation

1. For stimulation, cathodal pulses will be used to depolarize the neuronal area adjacent to the active electrode by producing an outward current through the neuronal membrane. The stimulating pulses are square and short in duration (50 μs) to avoid the generation of significant artifacts in the recording system (see Note 2).
2. Brain stimulation in alert behaving animals needs to be carried out with special care. A stimulus around 0.1 mA activates all the neuronal elements within a radius of 1 mm; the sphere can extend to 2 mm if the stimulus reaches 1 mA. Pulses of intensity higher than 1 mA should not be used unless the anatomical organization of the stimulated zone and of its surroundings is solidly known (see Note 3).

2.3.2 Recording

1. Metallic electrodes might be the best choice when many areas have to be recorded at the same time. They also allow long periods of recording (days, months). The area of recording can be just the wire section, or some isolating material (no more than 300 μm) can be carefully removed. Such electrodes are recommended for recording evoked field potentials rather than unitary activity for two main reasons: (i) they cannot be moved once implanted, and the growth of glial elements will prevent them from recording action potentials; and (ii) their signal/noise ratio is lower than for glass micropipettes, making it difficult to isolate individual neurons during recording sessions.
2. To avoid damage to the tip of a glass micropipette introduced into the brain, a section of the dura mater has first to be removed. After 2 weeks, some granulated tissues grow on the surface of the brain in contact with the open window, making the penetration of the pipette into the brain difficult. This tissue formation can be prevented by cleaning the recording window daily with sterile Ringer solution and covering it with a sterile sheet of flexible, inert silicone elastomer (e.g., Silastic®, Dow Corning, Midland, MI, USA). Some antibiotic and steroid drops should be added to the window to prevent inflammation of the underlying nerve tissue. Finally, the window is closed with a piece of sterile gauze and some bone wax.

3. Two hook electrodes for EMG recordings are implanted in the same muscle (e.g., the orbicularis oculi muscle) since the differential recording will give a better signal/noise ratio.

2.3.3 Evoked Field Potentials

An intracerebral structure can be located by recording field potentials evoked in it by the electrical stimulation of afferent pathways. The ionic current is propagated homogeneously in the extracellular space if the medium is also homogeneous. However, the extracellular space is rough and limited by membranes of differing resistance to the ionic current. This can alter field potential shapes. To identify a brain structure or fascicle by extracellular recordings, the following points have to be taken into account: (i) its approximate situation in the nervous system, (ii) its composition (myelinic or non-myelinic in the case of the axons, presence of specific ionic channels, etc.), and (iii) its anatomical and morphological limits (presence of other fascicles, dendrites orientation, size of the somas, etc.).

1. Identification of a fascicle. The electrical stimulation of an axon produces an action potential that is propagated in both directions. A recording electrode close to this axon detects a positive wave when the action potential is approaching it, a negative wave when it is exactly below it, and, finally, a second positive wave when it is moving away. This recorded positive-negative-positive wave is similar to the second derivative of the action potential recorded inside the axon. The recorded extracellular potential has an amplitude approximately 1/10 that of the intracellular potential. A practical reference is that the extracellular potential decays approximately 5 μV per μm as the recording electrode moves away from the axon. If instead of one axon there are many of them, the potential will have the same shape if all the activated axons have the same conduction velocity. If conduction velocities are different, the potentials will be linearly and algebraically added, and in consequence, the shape will be considerably modified. The diameter and myelinization of the axon also have a crucial role in the shape of the evoked potential (see Note 4).
2. Identification of a nucleus whose neurons have a common projection (closed field, see Note 5). The best way to proceed is to obtain a field potential depth profile, in steps of 100–200 μm, and to interpret the results together with a detailed study of the anatomical organization of the nucleus. For example, antidromic field potentials can be recorded across the abducens nucleus when evoked by the electrical stimulation of the ipsilateral sixth cranial nerve (Fig. 3). For a cat, the stimulating electrode should be placed 10 mm from the recording nucleus. As the recording electrode approaches the center of the nucleus, the negativity of the recorded field potential increases

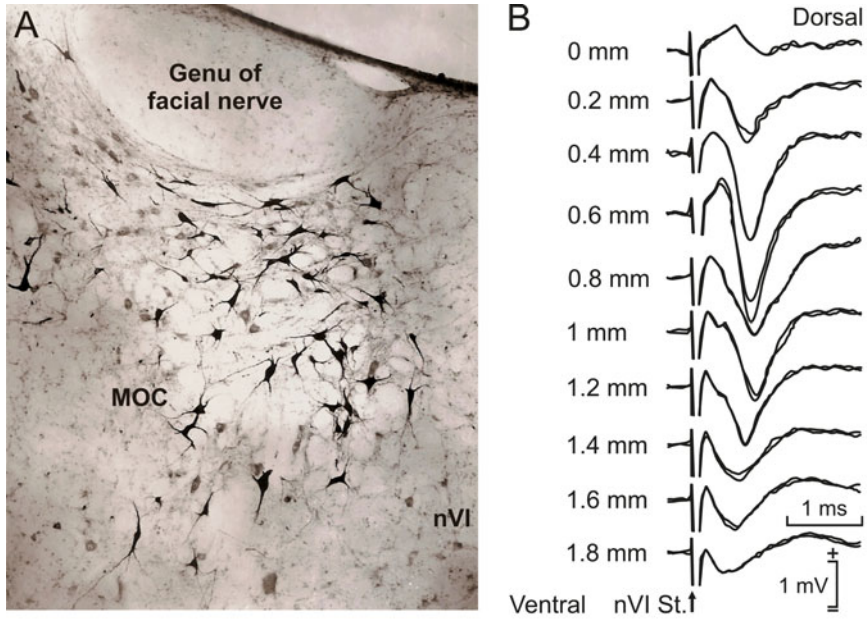

Fig. 3 Location of lateral rectus motoneurons in the cat abducens nucleus (**a**) and depth-profile representation of antidromic field potentials recorded in the same nucleus and animal (**b**). Abducens motoneurons were labeled with horseradish peroxidase injected in the ipsilateral lateral rectus muscle. Antidromic field potentials were evoked by electrical stimulation of the sixth cranial nerve (nVI St.)

due to the higher density of neuronal somas. The simultaneous depolarization of all these somas produces a greater negativity in the extracellular space. In the outer portion of the nucleus, a positive wave is recorded in simultaneity with the negative one, although with lower amplitude. This positive wave represents the outward current through the peripheral dendrites caused by the inward current entering motoneuron somas. The different amplitudes of field potentials recorded at the periphery and the center of a closed field are due to the fact that dendrites occupy all the periphery of the nucleus—i.e., a bigger space than that occupied by the somas. Figure 4 shows another example of the antidromic field potential recorded in the cerebellar fastigial, interpositus, and dentate nuclei after the stimulation of the contralateral restiform body, and oculomotor and red nuclei. The shape of the field potential profile confirms that neurons in the interpositus neurons project massively to the contralateral red nucleus and that the neurons in the fastigial nucleus project exclusively through the restiform body.

2.3.4 Neuronal Identification

Once the nucleus to be recorded is located, the unitary activity of single neurons of this structure can be recorded and identified. To identify the recorded neuron, it has to be antidromically activated

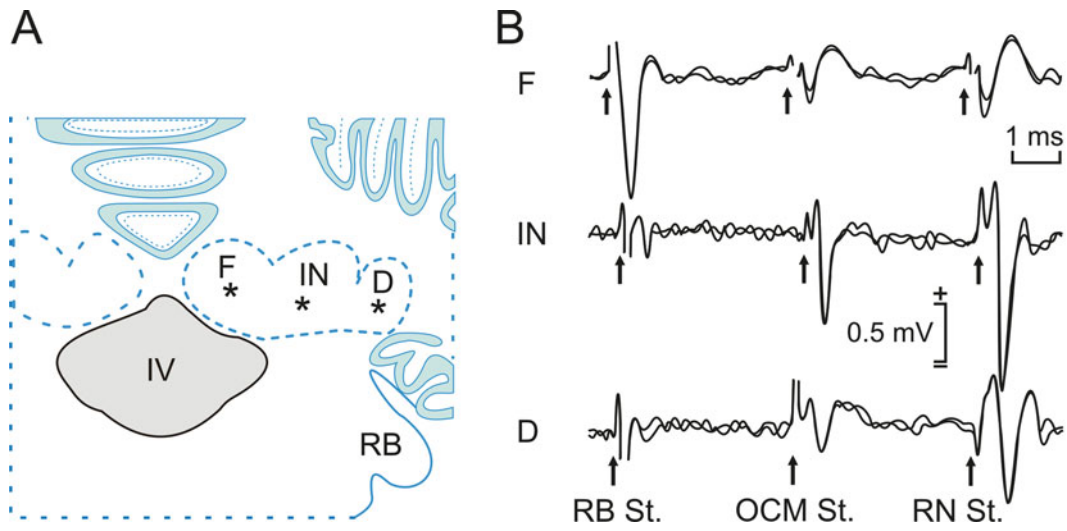

Fig. 4 Examples of antidromic field potentials recorded in a behaving cat. (**a**) A diagram of the recording sites. (**b**) Antidromic field potentials recorded in fastigial (*F*), interpositus (*IN*), and dentate (*D*) cerebellar nuclei. These field potentials were evoked in behaving cats by electrical stimulation of the contralateral restiform body (*RB*), oculomotor nucleus (*OCM*), and red nucleus (*RN*). Other abbreviations: *IV* fourth ventricle, *St.* stimulation

from its projection site, and it has to be checked that the recorded neuron coincides with the activated one. The antidromic activation of a single neuron inside a nucleus involves the production of an action potential in its axon (due to an electrical stimulation) and the recording of an action potential evoked in its soma. The stimulating electrode has to be bipolar to minimize the area stimulated and to avoid the production of artifacts in the recording area. A cathodal stimulus of 50 μs of duration and with an intensity lower than 0.1 mA should be enough if both electrodes (stimulating and recording) are in the right place. The stimulus should be applied at 1 Hz in order to prevent any accumulative effect. Figure 5a, b shows the antidromic activation of a red nucleus neuron from the ipsilateral facial nucleus. Some recordings are superimposed to show the stability of the antidromic activation. The shape of the potentials evoked antidromically can be positive-negative-positive if the recording is made proximal to the axon initial segment and negative-positive if the recording is proximal to the soma or to the main dendrites. Moreover, the shape depends on the macroscopic organization of the surrounding extracellular space. The amplitude of the recorded action potential depends on the characteristics of the electrode and the recording system, as well as on the distance to the plasmatic membrane of the activated neuron (see Note 6).

1. The threshold stimulus is the one that produces an antidromic action potential in 50 % of cases. The antidromic potential usually has smaller amplitude and longer duration than the spontaneously (or orthodromically) generated potential.

During the antidromic stimulus, it is easy to produce a delay in the invasion of the soma (or inflection in the IS/SD [initial segment/somatodendritic compartments] space) (Fig. 5c). The explanation is that the potential that goes from the initial segment to the soma has to discharge the considerable capacitance of the plasmatic membrane covering the neuronal body from the small current generated in the initial segment. This process needs time, and it can be observed as an inflection in the potential recorded extracellularly. During certain situations (high-frequency stimulation, neuronal lesion, etc.), the antidromic action potential could be unable to invade the somatic compartment (Fig. 5d).

2. To determine whether the unitary recording corresponds to a soma or to a passing axon. The action potential recorded in a soma has a different shape to the one recorded at the axonal level. Moreover, a somatic potential can be recorded around 50 μm away, while the distance can be considerably reduced when the recording corresponds to an axon. Finally, an inflection in the IS/SD space can be found in somatic recordings but never in axon recordings.
3. To check whether a particular activation is antidromic. Usually, an antidromic action potential is produced with a variation of <0.1 ms in its latency of activation, showing great stability in the velocity of propagation of this action potential through the axon (see Note 7). Frequently, the latency for the antidromic action potential is lower than the latency for the synaptic action potentials evoked by the stimulating electrode. The antidromic activation may be maintained after high-frequency stimulation (see Note 8).
4. To identify a unitary recording, it is crucial to determine whether the neuron whose electrical activity is being recorded is the one activated antidromically. In this case, the best procedure is to use the collision test. The electrical stimulus applied to an axon to evoke an antidromic action potential is triggered by a spontaneous action potential. If the stimulus is applied to the axon well after the spontaneous action potential, the two potentials (spontaneous and antidromic) do not coincide in time across the axon, and the antidromic action potential can reach the soma, where it is recorded (Fig. 5e). If the electrical stimulation is applied to the axon time in advance, the antidromic action potential can coincide in its way across the axon with the orthodromic potential, and the two activities will collide. In this case, the propagation of both potentials across the axon will stop, and no antidromic action potential will be recorded in the soma. The minimum interval (I) for this to occur is $I(s) = 2T(s) + \mathrm{PR}(s)$, where T is the conduction time

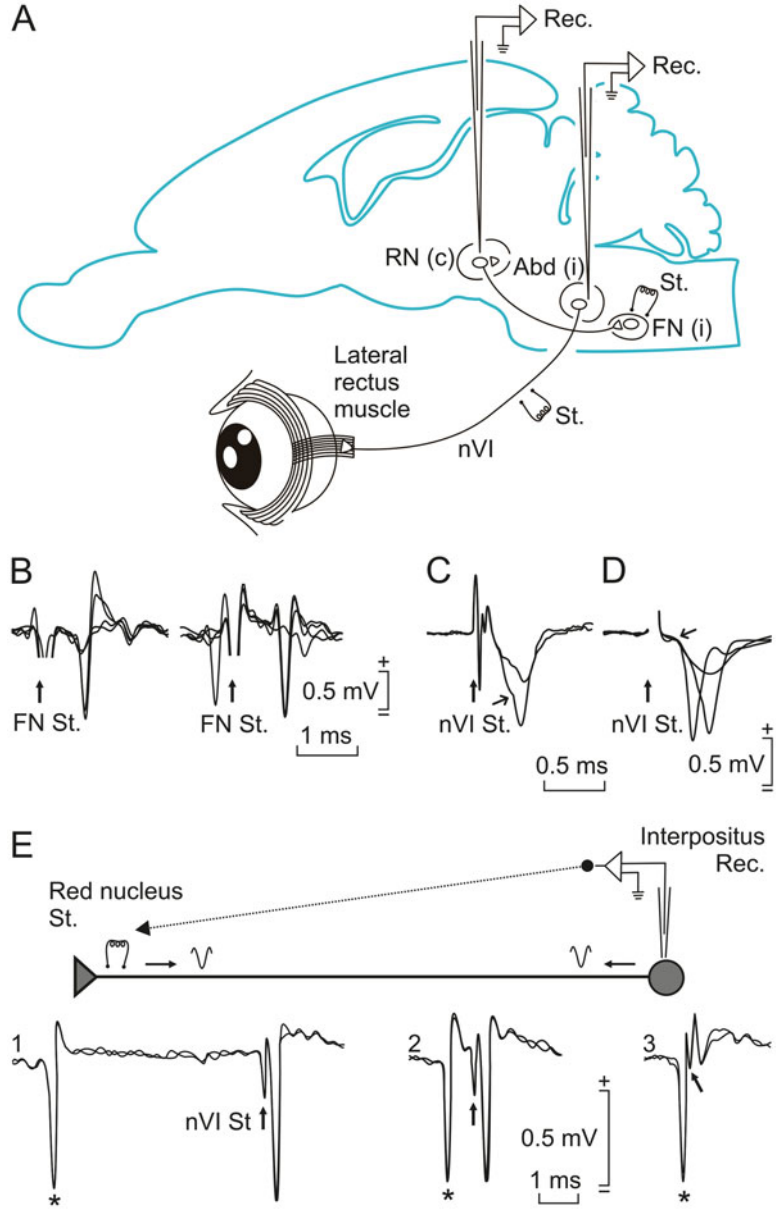

Fig. 5 Examples of antidromic identification of recorded motoneurons in a behaving rabbit. (**a**) A diagram of the stimulating (*St.*) and recording (*Rec.*) sites. (**b**) Example of the antidromic activation of a facial motoneuron at threshold intensity (*left*) and of a spontaneous collision test (*right*). (**c**, **d**) Antidromic activation of abducens motoneurons at high frequency, evoking delayed invasions of the initial segment/somatodendritic compartment (**c**) or the initial segment compartment (**d**). (**e**) Use of the collision test for the antidromic identification of a cerebellar interpositus neuron projecting to the contralateral red nucleus

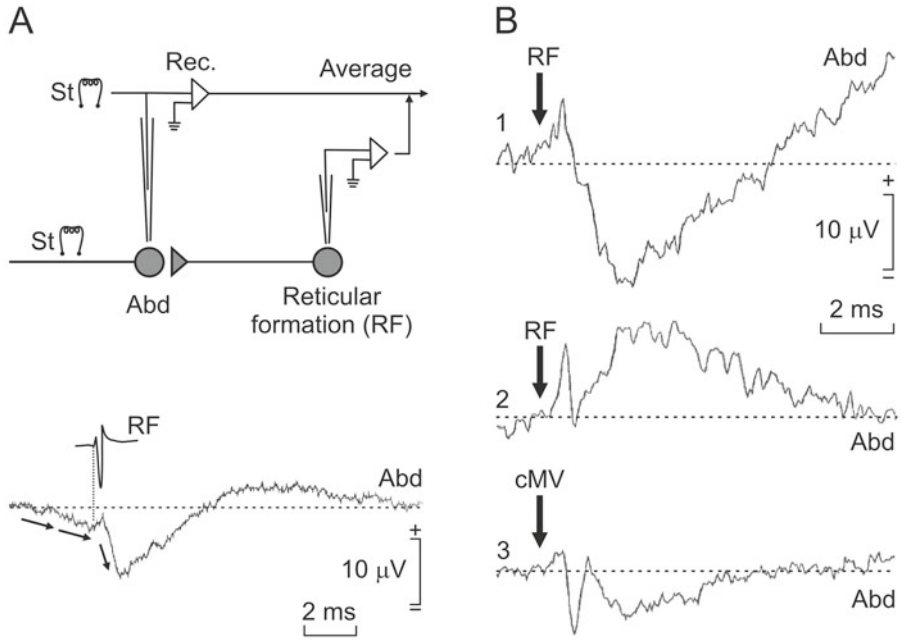

Fig. 6 Examples of spike-triggered average recordings. (**a**) A diagram of the experimental design and an example of a postsynaptic field potential recorded in the abducens (*Abd*) nucleus and triggered by action potentials recorded in the ipsilateral rostral reticular formation (*RF*). (**b**) Extracellular field potentials recorded in the Abd nucleus and triggered by action potentials recorded in the ipsilateral (*1*) and contralateral (*2*) RFs and in the contralateral (*3*) medial vestibular (*cMV*) nucleus

through the axon and PR is the refractory period of the same axon. In practice the refractory period changes between 0.8 ms and 4 ms, and the approximate values can be taken as those corresponding to the minimum interval (see Note 9).

2.3.5 Synaptic Effects

With the help of the different electrophysiological techniques described here, the synaptic effects (excitatory and/or inhibitory) of a neuron on its target (muscular fiber and other neurons) can be examined in an alert behaving animal. These synaptic effects can be studied through spike-triggered average techniques or by analyzing the experimentally evoked field postsynaptic potentials.

1. The action potential of the neuron can be used as a trigger of the extracellular electrical activity in the area where axons make synapses with their target. This activity should be recorded from 2 ms before to 8 ms after the presentation of the action potential. The recording tools have to be set at a very high resolution in terms of time and voltage. Fig. 6a shows an average obtained from 3000 stimulus presentations with a digital resolution of 20 μV and 5 μs. These recorded signals are usually very small; therefore, the acquisition resolution must be very high.

2. In this type of recording, two effects can be easily identified:
   (i) The action potential arrival evoked by the neuron used as a trigger. This potential should be positive-negative-positive (if the axon of the neuron acting as a trigger continues to other targets) or positive-negative (if the axon of the neuron acting as a trigger ends in the recording target).
   (ii) The beginning and the shape of the synaptic potential. The beginning of the extracellular synaptic potential has to take place ≈ 0.3 ms after the action potential arrival. The polarity of the potential will be positive if the synapse is inhibitory and negative if it is excitatory.
3. In general, the averaged synaptic potentials have a duration of 2–6 ms, due to the currents generated while postsynaptic membrane channels are open. The shape of the averaged potentials tends to simulate the first or second derivative of the recorded intracellular synaptic potentials. The amplitude of the averaged potential depends on a number of factors: number of activated cells, neuronal density around the recording electrode, density of the synaptic buttons, concentration and kinetics of the postsynaptic ionic channels, ions displaced through their channel, etc.
4. The spike-triggered average technique requires a solid anatomical and structural knowledge. For example, it is important to know whether the synaptic contacts are in the dendrites or in the soma of the neurons. Information regarding the approximate number of neurons activated by the trigger is also useful for the proper interpretation of the evoked synaptic potential (see Note 10). Figure 6b shows three examples of recordings carried out in the abducens nucleus triggered by three different neuronal types with excitatory (neurons 1 and 3) or inhibitory (neuron 2) effects. Differences in amplitude of the recorded potentials are due to different projection areas, to their density, of them, and to the number of innervated neurons.
5. Field postsynaptic potentials can be recorded in certain neuronal areas after stimulating a fascicle of axons projecting to it. If the recording electrode is big enough, it will act as an electric microscope, recording the effects of several postsynaptic potentials in different synapses. The algebraic addition of all these postsynaptic potentials will produce the field postsynaptic potential. The shape (positive or negative), latencies, amplitudes, etc. will follow the same principles as the postsynaptic unitary activity, depending on: (i) type of synapse (excitatory or inhibitory), (ii) neuron structure (dendrites or somas), and (iii) type of recording (intracellular or extracellular) (Fig. 7).

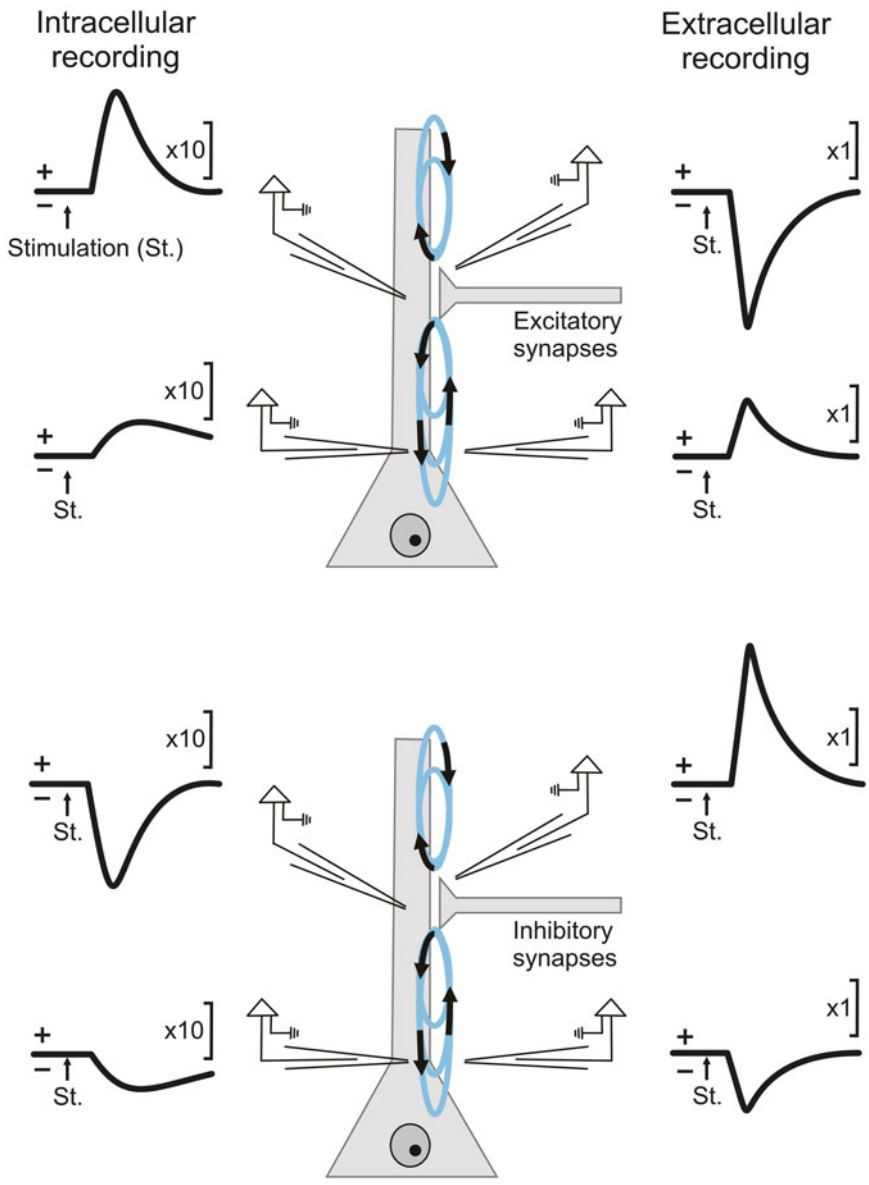

Fig. 7 Differences in amplitude and profiles of excitatory (*top*) or inhibitory (*bottom*) synaptic field potentials recorded intracellularly (*left*) or extracellularly (*right*) depending on the location of the synapse and of the recording electrode

6. Field postsynaptic potentials are easy to record in alert behaving animals, and changes in their amplitudes or slopes can be followed during successive recording sessions. Before recording these changes in chronically implanted animals, it is convenient to carry out a depth-profile analysis of field potentials recorded around the selected synapses in acute animals. The aim is to accurately identify the characteristics of the evoked field potentials. This will facilitate the proper identification of the recorded field potentials in the chronic preparation. Figure 8 shows a

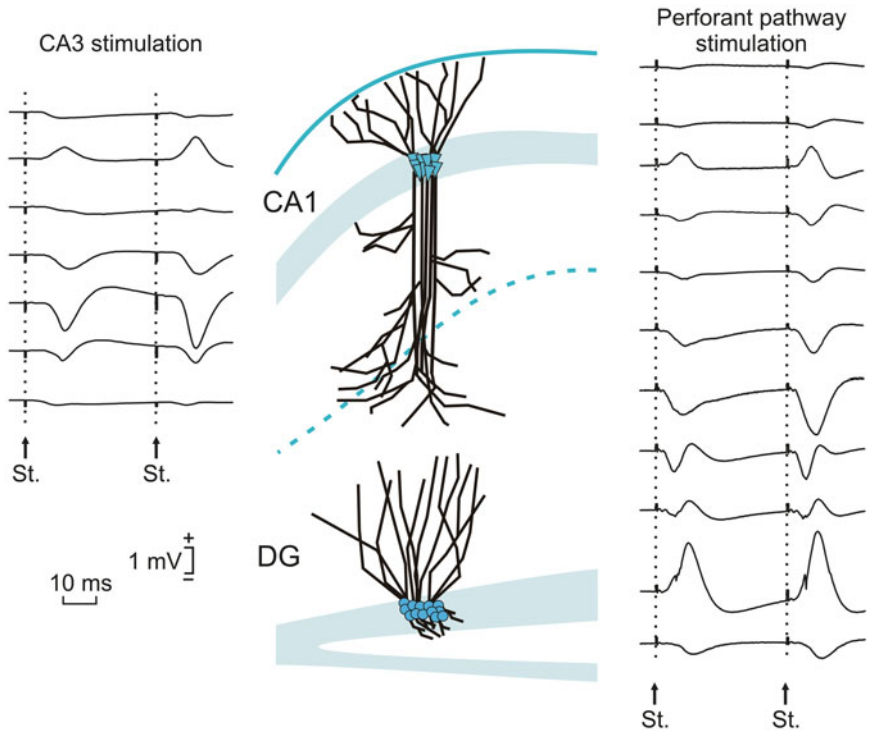

Fig. 8 Examples of depth profiles evoked in the hippocampus of a behaving mouse by electrical stimulation (*St.*) of the ipsilateral CA3 area (i.e., Schaffer collaterals) or the perforant pathway (*see* Ref. [10] for details)

field potential depth profile carried out through the different hippocampal layers from the CA1 area to the dentate gyrus. Interestingly, the recorded synaptic effects can be distinguished in the evoked postsynaptic potentials depending on whether the stimulation was done in the Schaffer collaterals or in the perforant pathway. Simultaneously, the short-term synaptic effects can be studied by presenting a pair of pulses. Depending upon the selected synapse, the effects of the second stimulus will be larger, smaller, or zero in relation to the effects of the first pulse. For depth-profile analysis, recordings should be carried out in steps of 100 μm. The differences along layers have to be interpreted depending on: (i) type of synapse (excitatory or inhibitory), (ii) neuron structure (dendrites or somas), and (iii) type of recording (intracellular or extracellular).

2.3.6 Relationships between Neural Activities and Behavior

The relevance of this approach is that neural activities can be correlated with some sensorial stimulation, motor responses, the performance of complex behavioral tasks, and, finally, the acquisition of new motor and cognitive abilities.

1. In the peristimulus time histogram (PSTH) procedure, the same signal used as sensorial stimulus or a particular moment of a motor response acts as a trigger of the recorded neural activity. Previously, the action potentials should be transformed

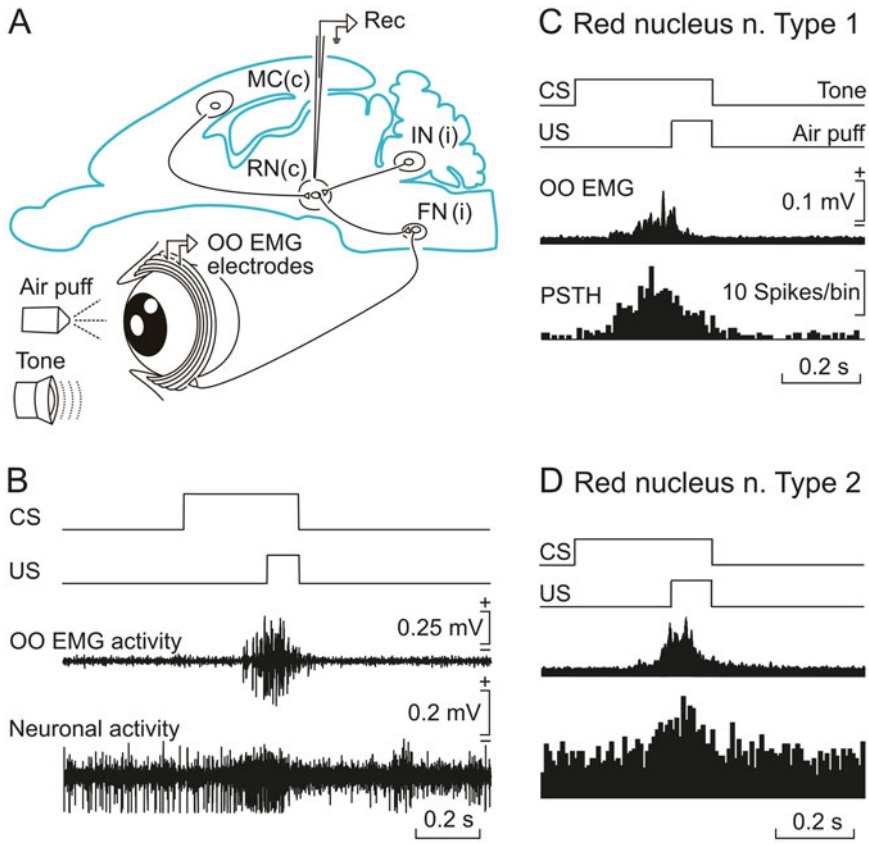

Fig. 9 Unitary recordings carried out in the red nucleus of a behaving rabbit during a classical eyeblink conditioning. (**a**) Experimental setup. (**b**) Representative recordings of the EMG activity of the orbicularis oculi (*OO*) muscle and of a red nucleus neuron following paired conditioned stimulus (*CS*) and unconditioned stimulus (*US*) presentations. (**c**, **d**) Two different types of neuron recorded in the red nucleus during classical eyeblink conditioning of a well-trained rabbit (*see* Ref. [8] for details)

into square pulses of a given duration (e.g., 1–2 ms). These pulses are accumulated during a given period around the trigger stimulus. For this analysis, the bin size has to be stated as well as the number of times that the test is applied. The obtained responses are considered as the number of action potentials accumulated in each temporal bin (ms). This PSTH procedure can also be applied to experimentally acquired motor responses (Fig. 9).

2. The multi-unitary spike-sorting analysis allows discriminating different action potentials from different neurons recorded simultaneously through the same recording electrode. Before correlating the recorded action potentials with sensory, motor, or complex behavioral signals, some mathematical analyses are needed to separate firing activities collected from each neuron.

3. A direct way to test synaptic properties is to study the input-output curves at different interstimulus intervals. For example, in the synapses between hippocampal CA3 and CA1 areas, the Schaffer collaterals are stimulated with paired pulses (40 ms of interstimulus interval) at increasing intensities (0.02–0.2 mA). Another test is to determine the effect of paired pulses presented at different (10, 20, 40, 100, 200, and 500 ms) interstimulus intervals when using intensities corresponding to 40 and 60 % of the amount necessary to evoke a saturating response. The pair of pulses is repeated five times with time intervals longer than 30 s, to avoid as much as possible interference with slower short-term potentiation (augmentation) or depression processes. To avoid any cumulative effects, intensities and intervals are presented at random. For the range of intensities suggested here, no population spikes should be observed in the collected recordings.
4. Long-term potentiation (LTP) is an experimental approach used to test functional synaptic properties. First, fEPSPs are collected for 15 min to establish a baseline. Pulse intensity is set at 35–45 % of the amount necessary to evoke a maximum field potential response (usually 0.05–0.25 mA)—that is, well below the threshold for evoking a population spike if records are carried out in the hippocampal circuit. After baseline recordings, high-frequency stimulation (HFS) sessions are presented, consisting of five 200 Hz, 100 ms trains of pulses at a rate of 1/s. This protocol is presented six times, at intervals of 1 min. Thus, a total of 600 pulses are presented during an HFS session (see Note 11). After each HFS session, the same stimulus is presented every 20 s for 30 min during the first LTP session and for 15 min on the following days.
5. These approaches can be used for correlating neuronal activity with learned responses in control animals but also in genetically manipulated ones. A very popular learning paradigm is the classical eyeblink conditioning using trace or delay paradigms (Fig. 10a, b). This classical conditioning task can be easily used in many species, such as mice, rats, or rabbits. For example, for trace conditioning in mice, a tone (20 ms, 2.4 kHz, 85 dB) is presented as conditioned stimulus (CS). The unconditioned stimulus (US) consists of a 500 μs, 3× threshold, square, cathodal pulse applied in the trigeminal nerve, producing the closure of eyelids. The US starts 500 ms after the end of the CS, and the pairing of the two stimuli evokes conditioned eyelid responses that can be recorded in the EMG activity of the orbicularis oculi muscle (Fig. 10c). A conditioning session consists of 60 CS-US presentations and lasts ≈ 30 min. A total of two habituation, ten conditioning, and five extinction sessions are usually performed for each animal.

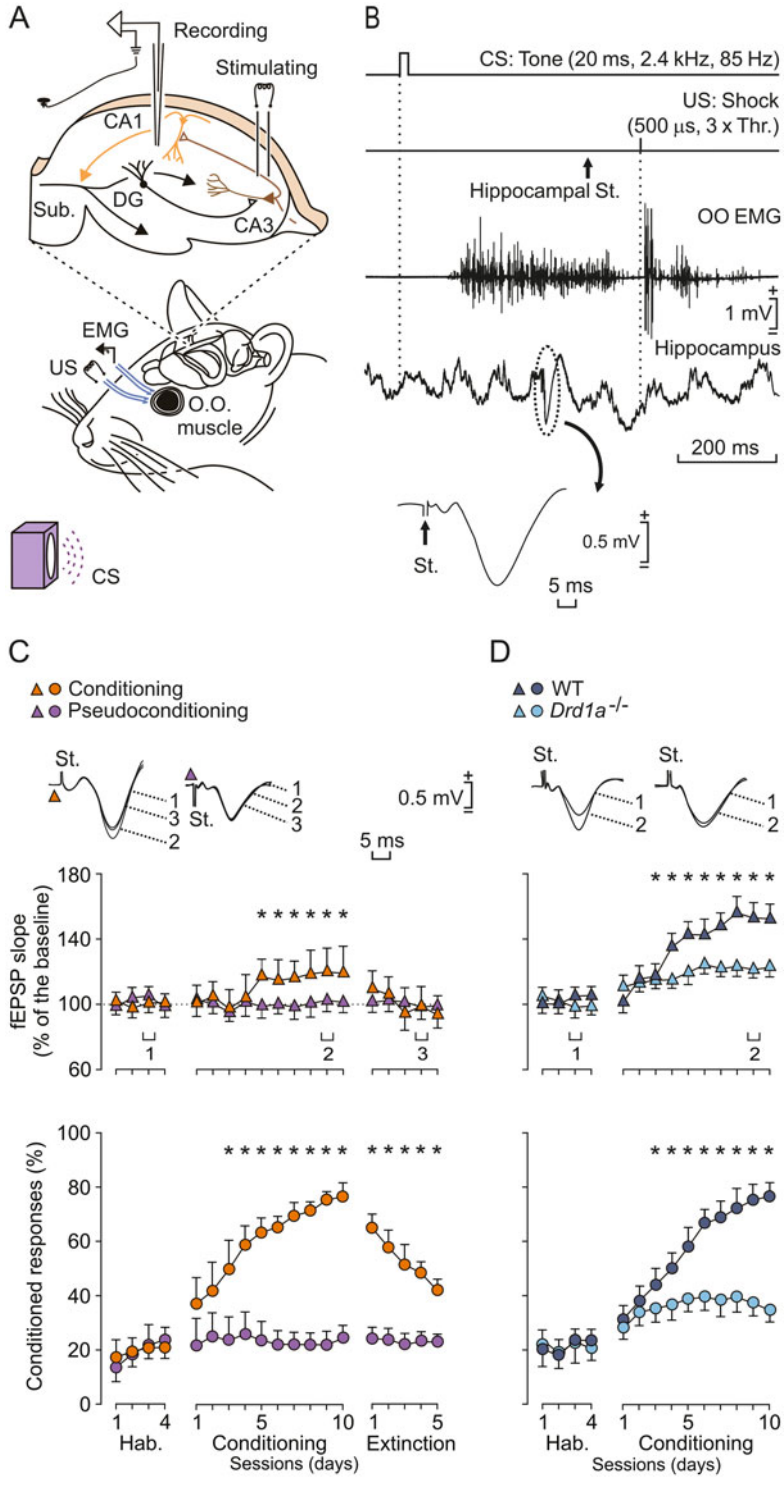

Fig. 10 Example of learning-dependent changes in synaptic strength evoked by classical eyeblink conditioning of alert mice. (**a**) Experimental diagram with indication of conditioned stimulus (*CS*) and unconditioned stimulus (*US*) presentations. (**b**) From *top to bottom* are illustrated conditioning paradigm, the EMG recording of the orbicularis oculi (*OO*) muscle, and the extracellular activity of the contralateral hippocampal CA1 area.

For habituation and extinction sessions, only the CS is presented. In the same sessions, the local field potential is recorded in some neuronal structures (e.g., the CA1 area of the hippocampus). During the stimulus interval, the fEPSP evoked by stimulating the axons making synapses with the CA1 area (e.g., the Schaffer collaterals) can be recorded. The amplitude and/or slope of the field-evoked postsynaptic potentials can be correlated with the number of conditioned responses through the experimental sessions.

6. Recording of the fEPSPs during paired-pulse stimulation, LTP tests, and learning tasks can be used to check functional changes produced after receptor and/or ion channel manipulation in mouse or rat experimental models (Fig. 10d).
7. The amount of data that can be obtained with electrophysiological techniques is huge, mainly because multiple recordings can be made simultaneously in different brain areas during different behaviors (innate and acquired). Therefore, this field also requires a thorough training in data analysis and in representation procedures (Fig. 11).

3 Notes

1. Enameled silver wire of 200 μm in diameter is the best option for stimulating electrodes in chronic preparation of large mammals (rabbits and cats). Although silver is toxic in the long term, no damage is seen during the experimental period. The advantage over stainless steel wire is that the latter is too rigid and can act as a knife in the brain during the animal's movements, including breathing. For small mammals (mice and rats), it is better to use Teflon-coated tungsten wire (25–50 μm). Other wires such as Teflon-coated platinum-iridium or chrome-nickel (25 μm) can also be used but are more expensive.
2. If the artifact persists, grounding of the animal and of the recording system has to be checked. As a general condition, all the electrical equipment and the animal preparation have to be carefully connected to the ground system. A simple procedure to prevent polarization of stimulating electrodes is to use very short-lasting (100 μs) positive-negative pulses.

Fig. 10 (continued) A field excitatory postsynaptic potential (*fEPSP*) was evoked in the CA1 area by electrical stimulation (*St.*) of ipsilateral Schaffer collaterals. (**c**) Evolution of fEPSP slopes (*top*) and of the percentage of conditioned responses (*bottom*) across habituation (*hab.*), conditioning, and extinction sessions of conditioned (*red triangles* and *dots*) and pseudoconditioned (*blue triangles* and *dots*) mice. (**d**) Differences in fEPSP slopes (*top*) and in the percentage of conditioned responses between wild-type (*dark blue triangles* and *circles*) and knockout (for dopamine D1 receptors; *light blue triangles* and *circles*) mice (see details in Refs. [1, 6])

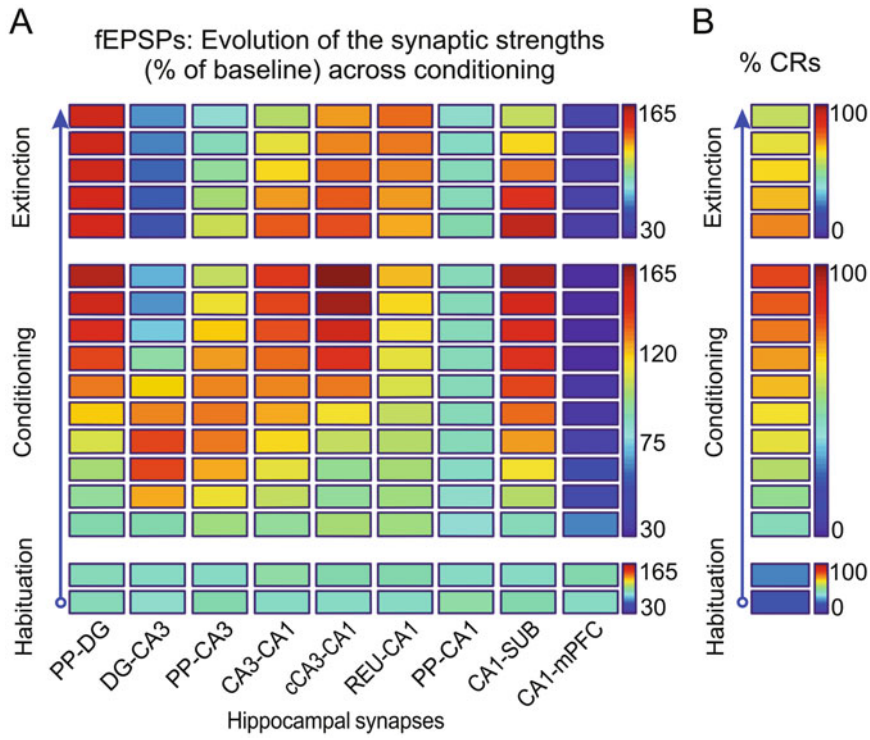

Fig. 11 Example of changes in functional capabilities of different hippocampal synapses across a classical eyeblink conditioning. (**a**) Changes in learning-dependent synaptic strength of the nine selected synapses. (**b**) Evolution of the percentage of conditioned eyelid responses. The corresponding color code is illustrated at the right of (**a**) and (**b**) (see Ref. [10] for details)

3. The same stimulus will activate a myelinated axon faster than a dysmyelinated one. Moreover, applying an excessive current during a repeated stimulation can polarize the electrode and even make an electrolytic lesion in the surrounding tissue. It is always better to use short-lasting pulses of a relatively high intensity than long-lasting ones of a lower intensity.
4. In general, the stimulation of a central pathway or a peripheral nerve usually produces a complex potential composed of positive and negative waves. For a proper interpretation of the collected field potential, it is always necessary to have a good understanding of the stimulated neural circuits. It is always helpful to implant the recording electrode as far as possible from the stimulating electrode. This simple procedure can help to record potentials at longer latencies, making it easier to discriminate the different components of the recorded field potential.
5. In 1947, Lorente de Nó termed a closed field to be when the electrical current flow goes from the center to the periphery of a nerve structure and vice versa, but no electrical activity can be

recorded outside this structure. This means that sources and sinks have a certain symmetric relationship so that currents and potentials are nearly all confined to some local region. Good examples of closed fields are brainstem motor nuclei.

6. As already indicated for field potentials, the potential recorded from a single neuron can also decay with distance, following the gradient of approximately 5 μV per μm as the recording electrode moves away from the neuron. The shape of action potentials recorded in the extracellular space corresponds approximately to the second derivative of the action potential recorded intracellularly. The intensity of the electrical stimulation and the exact site for the recording have to be accurately established to activate and to record a single neuron. Action potentials from different neurons can be added linearly and algebraically, a fact that cannot be easily interpreted from the electrophysiological point of view.
7. The velocity of an antidromic activation (V) is calculated from the antidromic activation (AA) latency, subtracting the time it takes to produce the action potential at the stimulation site (top), that is around 0.2 ms. Therefore, the conduction time though a given axon (T) is $T(s) = \mathrm{AA}(s) - \mathrm{top}(s)$. When the distance ($d$) between the stimulation and the recording sites is known, it will be $V\,(m/s) = d(m)/T(s)$.
8. The maximum frequency that can be applied to a neuron for an antidromic activation depends on its minimum interval, that is, the minimum time between two consecutive stimuli to induce two successive action potentials (Fig. 6b). The minimum interval is different between neurons and ranges from 0.8 to 4 ms for large neurons. These intervals represent frequencies between 200 and 1250 Hz. At these frequencies, it is usually not possible to evoke a synaptic activation. Even when the synaptic activation is accomplished, the action potential generated appears with a large variability (more than 0.2 ms), as opposed to the great stability found in the antidromic activation latency (less than 0.1 ms).
9. The collision test is applied online to identify a recorded neuron. New tools have been created to facilitate this identification, although the collision test remains one of the most accurate and, especially, fast tests to apply. Nevertheless, there is no point in taking too much time in identifying the neuron because this can be lost in the process.
10. The spike-triggered average technique should be used only with dense projections and with neurons densely assembled in the nucleus. The effect of a projection on distal dendrites, when the number of neurons is scant, or if neurons are dispersed in the recording site, is difficult to study with this technique; that is, the collected extracellular potential would be in the same range as the system (both recording and analysis) noise.

11. In order to prevent evoking large population spikes and/or the appearance of local seizures, the stimulus intensity during high-frequency stimulation should be set at the same value as that used for generating baseline recordings. Any animal showing an afterdischarge or a motor seizure following the high-frequency stimulation protocol should be eliminated from the study. These effects can be checked by online electroencephalographic recordings and by visual observation of the stimulated animal.

Acknowledgments

This work was supported by the grants BFU2011-29286 from the Spanish Ministry of Economy and Innovation and by the Excellence Program of the *Junta de Andalucía*. We are grateful to the technicians who have collaborated in the past few years to improve the electrophysiological in vivo recording and stimulating techniques used in our laboratory: José Antonio Santos-Naharro, María Esteban-Masferrer, Noelia Rodríguez-García, José María González-Martín, and María Sánchez-Enciso.

References

1. Gruart A, Muñoz MD, Delgado-García JM (2006) Involvement of the CA3-CA1 synapse in the acquisition of associative learning in behaving mice. J Neurosci 26:1077–1087
2. Madroñal N, Gruart A, Delgado-García JM (2009) Differing presynaptic contribution to LTP and to associative learning in alert behaving mice. Front Behav Neurosci 29:3. doi:10.3389/neuro.08.0072009
3. Valenzuela-Harrington M, Gruart A, Delgado-García JM (2007) Contribution of NMDA receptor NR2B subunit to synaptic plasticity during associative learning in behaving rats. Eur J Neurosci 25:830–836
4. Gruart A, Sciarretta C, Valenzuela-Harrington M, Delgado-Garcia JM, Minichiello L (2007) Mutation at the TrkB-PLCγ-docking site affects hippocampal LTP and associative learning in conscious mice. Learn Mem 14:54–62
5. Fontinha BM, Delgado-García JM, Madroñal N, Sebastião AM, Gruart A (2009) Adenosine A_{2A} receptor modulation of hippocampal CA3-CA1 synapse plasticity during associative learning in behaving mice. Neuropsychopharmacology 34:1865–1874
6. Ortiz O, Delgado-García JM, Espadas I, Bahí A, Trullas R, Dreyer JL, Gruart A, Moratalla R (2010) Associative learning and CA3-CA1 synaptic plasticity are impaired in D_1R Null, *Drd1a–/–* mice and in hippocampal siRNA silenced *Drd1a* mice. J Neurosci 30: 12288–12300
7. Trigo JA, Gruart A, Delgado-García JM (1999) Discharge profiles of abducens, accessory abducens and orbicularis oculi motoneurons during reflex and conditioned blinks in alert cats. J Neurophysiol 81:1666–1684
8. Pacheco-Calderón R, Carretero-Guillén A, Delgado-García JM, Gruart A (2012) Red nucleus neurons actively contribute to the acquisition of classically conditioned eyelid responses in rabbits. J Neurosci 32: 12129–12143
9. Leal-Campanario R, Delgado-García JN, Gruart A (2013) The rostral medial prefrontal cortex regulates the expression of conditioned eyelid responses in behaving rabbits. J Neurosci 33:4378–4386
10. Gruart A, Sánchez-Campusano R, Fernández-Guizán A, Delgado-García JM (2015) A differential and timed contribution of identified hippocampal synapses to associative learning in mice. Cereb Cortex. 25(9):2542–2555. doi:10.1093/cercor/bhu054

Chapter 24

Voltammetry in Behaving Animals

Kendra D. Bunner and George V. Rebec

Abstract

Fast-scan cyclic voltammetry (FSCV) is an electrochemical technique that provides rapid and reliable detection of key brain neurotransmitters (e.g., dopamine and other monoamines) with minimal tissue disruption. The technique can be applied to behaving animals, allowing for real-time monitoring of neurotransmitter release and uptake across a variety of behavioral situations. Changes in current due to the oxidation and reduction (redox reaction) of chemicals at the surface of the working electrode are recorded and later converted to concentration. Although the high spatial and temporal resolution of FSCV offers unprecedented access to the neurochemistry of brain function during behavior, a basic understanding of electrochemistry, instrumentation, and electrode performance is required to ensure accurate data analysis and interpretation. In this chapter, we introduce the basic concepts and methodology of FSCV and outline key experimental procedures.

Key words Fast-scan cyclic voltammetry (FSCV), Electrochemical methods, In vivo monitoring, Carbon fiber electrodes, Dopamine transients, Redox reaction, Cyclic voltammogram, Background subtraction

1 Introduction

Electrochemistry is remarkably good at detecting easily oxidized substances. When these substances include such widely studied neurotransmitters as dopamine (DA), norepinephrine (NE), and serotonin (5-HT), it is not surprising that electrochemistry has become a valuable tool in neuroscience. Fast-scan cyclic voltammetry (FSCV) is an especially useful electrochemistry technique because it can record fluctuations in the release and removal of DA as well as other monoamines with excellent selectivity in real time, in freely behaving animals, and with electrodes thinner than a human hair. Although microdialysis (*see* Chap. 27) is not restricted to measuring oxidizable substances, it operates on a time scale of minutes rather than milliseconds. This limits microdialysis to the measurement of basal or resting levels of a neurotransmitter. The short-lived or phasic neurochemical events associated with a specific stimulus or behavioral response would be missed. In contrast, the sub-second operation of

Rafael Luján and Francisco Ciruela (eds.), *Receptor and Ion Channel Detection in the Brain: Methods and Protocols*, Neuromethods, vol. 110, DOI 10.1007/978-1-4939-3064-7_24,

FSCV permits characterization of real-time neuronal signaling [1] and how it changes with behavior [2–4]. In fact, FSCV has revolutionized the way they think about the role of DA and other neurotransmitters in behavior.

Fast fluctuations in extracellular DA lasting from 0.2 to several seconds and ranging in concentration from 10 nM to >1 μM are known as DA transients. Their study has led to improved understanding of the role of DA in motivated behavior, such as novelty seeking [2], craving of natural or drug rewards [4–7], and social interaction [3, 8]. FSCV also has been used to study DA changes in neurodegenerative diseases [9–12].

The electrodes used for FSCV are small-diameter (typically 5–10 μm) carbon fibers, known as working electrodes. Their small size minimizes tissue damage and thus creates less diffusional distortion in the recording dynamics of a neurochemical event [13]. The small size also allows for electrode placement close to neurotransmitter release sites [14], giving FSCV the unique ability to evaluate the extracellular dynamics of neurotransmission, including the kinetics of neurotransmitter removal, which, in the case of DA, is mediated by the DA transporter [15]. The first use of FSCV with a carbon fiber electrode measured evoked DA release in anesthetized rats [16]. A decade later, DA release was measured during behavior [2, 17]. Continued technological advances have now led to the use of chronically implanted electrodes, which allows researchers to track longitudinal changes in neurotransmitter dynamics over the course of disease progression or learning paradigms [18, 19]. With this latest technology, one can record for days, weeks, or months from the same target region.

Because voltammetry depends on a redox reaction, the vast amount of substances in the brain that can oxidize creates a problem for identifying the substance being detected. FSCV solves this problem by relying on both oxidation and reduction reactions detected by the working electrode in response to the application of a "sweeping" potential. The sweep involves applying a triangular waveform that ramps up to an initial oxidizing potential (anodic scan) and then back to a final reduction potential (cathodic scan). Current at the carbon fiber electrode is continuously measured against the applied sweeping potential. This information (current vs. potential), known as a cyclic voltammogram, provides qualitative identification of the oxidized substance.

In this chapter, we discuss the application of FSCV to freely behaving rodents. Although our focus is on the detection of DA, it should be noted that this technique can be used to study other monoamines [20, 21] as well as nitric oxide [22], hydrogen peroxide [23], pH [24], and even ascorbate [25]. We discuss the materials and methodology of FSCV, including the underlying electrochemistry, software, system setup, electrode construction, stereotaxic surgery, and experimental parameters.

2 Materials

2.1 Electrochemistry and Instrumentation and Software

1. TarHeel CV: TH-1 Electroanalysis Software (ESA Biosciences, Inc., Chelmsford, MA, USA)
2. Computer-controlled interface boards (National Instruments, Austin, TX, USA)
3. Potentiostat: EI-400 (Cypress Systems, Lawrence, KS, USA)

2.2 2.4 Electrical Stimulation

1. Constant-current stimulator: NeuroLog NL800 (Digitimer, Hertfordshire, UK)

2.3 Electrode Construction

1. Carbon fiber: T650 (6.0 μm diameter, Cytec Engineering Materials, West Paterson, NJ, USA)
2. Capillary glass tubes: (1.0 mm diameter, A-M Systems, Inc., Carlsborg, WA, USA)
3. Pipette puller: PF-2 (Narishige, Tokyo, Japan)
4. Bismuth alloy (RotoMetals, Inc., San Leandro, CA)
5. Epoxy: 5 min epoxy (Devcon, Danvers, MA, USA)
6. Silica tubing: 1068150381 (Polymicro Technologies, Phoenix, AZ, USA)
7. Silver epoxy: 8331-14G (MG Chemicals, Ontario, Canada)
8. Connector pins: 23 K7802 (Newark Electronics, Chicago, IL, USA)
9. Silver wire (at least 90 % silver)
10. Concentrated hydrochloric acid (37 % HCL): 258148 (Sigma-Aldrich)

2.4 Surgery

1. Anesthetic:

   For rats: Ketamine HCL (Fort Dodge Animal Health, Fort Dodge, Iowa, USA), xylazine (Lloyd List No. 4821, Shenandoah, Iowa, USA)

   For mice: Chloropent (chloral hydrate (42.6 mg/mL) and sodium pentobarbital (9.8 mg/mL)). Store chloropent at 4 °C for no longer than 3 months after compounding
2. Stereotaxic frame: Rat/mouse stereotaxic (Stoelting Co., Wood Dale, IL, USA)
3. Guide cannula: Locally construction (Indiana University, Bloomington, IN, USA). Also commercially available: MD-2251 (Bioanalytical Systems, West Lafayette, IN, USA)
4. Anchor screws: O-80 × 1/8 (stainless steel, 1.25 mm) (Plastic One, Roanoke, VA, USA)

5. Dental cement: 675571/2 (Grip Cement) (DENTSPLY Caulk, Milford, DE, USA)
6. Stimulating electrode: MS303-2 (stainless steel, 0.2 mm, bipolar) (Plastic One, Roanoke, VA, USA)

2.5 Experiment

1. Video recorder
2. Swivel: SwivElectra 4-TBC-9-S (Crist Instrument Co. Inc., Hagerstown, MD, USA)

2.6 Electrode Calibration

1. Dopamine HCL (Sigma H-8592)
2. Flow injection apparatus: Rheodyne 6 port, 2 position switching valve, 18 gage tubing, and syringe pump
3. Tris–HCl buffer solution: 12.0 mM Tris–HCl, 140 mM NaCl, 3.25 mM KCl, 1.20 mM CaCl, 1.25 mM NaH2PO4, 1.20 mM MgCl2, 2.00 mM Na2SO4, pH7.40. Store at room temperature

2.7 Data Analysis

1. Software: TH-1 Electroanalysis Software (ESA Biosciences, Inc., Chelmsford, MA, USA)
2. Computer-controlled interface boards (National Instruments, Austin, TX)

2.8 Histology/ Electrode Placement Verification

1. Stainless steel wire electrode (0.5 mm diameter)
2. Current lesion maker: Grass Medical Instruments DCLM5A 115 V D.C. Constant Current Lesion Maker (Quincy, Mass, USA)
3. 10% formalin buffer solution: Formaldehyde (stock 37 %), sodium phosphate dibasic (87.5 mM); distilled H_2O
4. 30 % sucrose, 10 % formalin solution: 300 g sucrose, 100 mL formaldehyde (37 %), 600 mL H_2O. Refrigerate
5. Crystal violet stain: 5 g cresyl echt violet stain (must be echt), 1000 mL distilled H_2O, 3 mL glacial acetic acid, pH = 3.5–3.9. Store at room temperature
6. Potassium ferricyanide solution: 150 mM potassium ferricyanide in 10 % HCl. Make up fresh

3 Methods

3.1 Electrochemistry

Oxidation and reduction of the analyte or substance being detected are accomplished by applying a triangular waveform (Fig. 1a). For DA, this redox reaction converts DA to the DA-o-quinone by oxidation of the two hydroxyl groups of the catechol, leaving two electrons recorded at the electrode surface as faradaic current. These changes in current are later converted to concentration (Sect. 3.8). Initially, the carbon fiber electrode is held at a

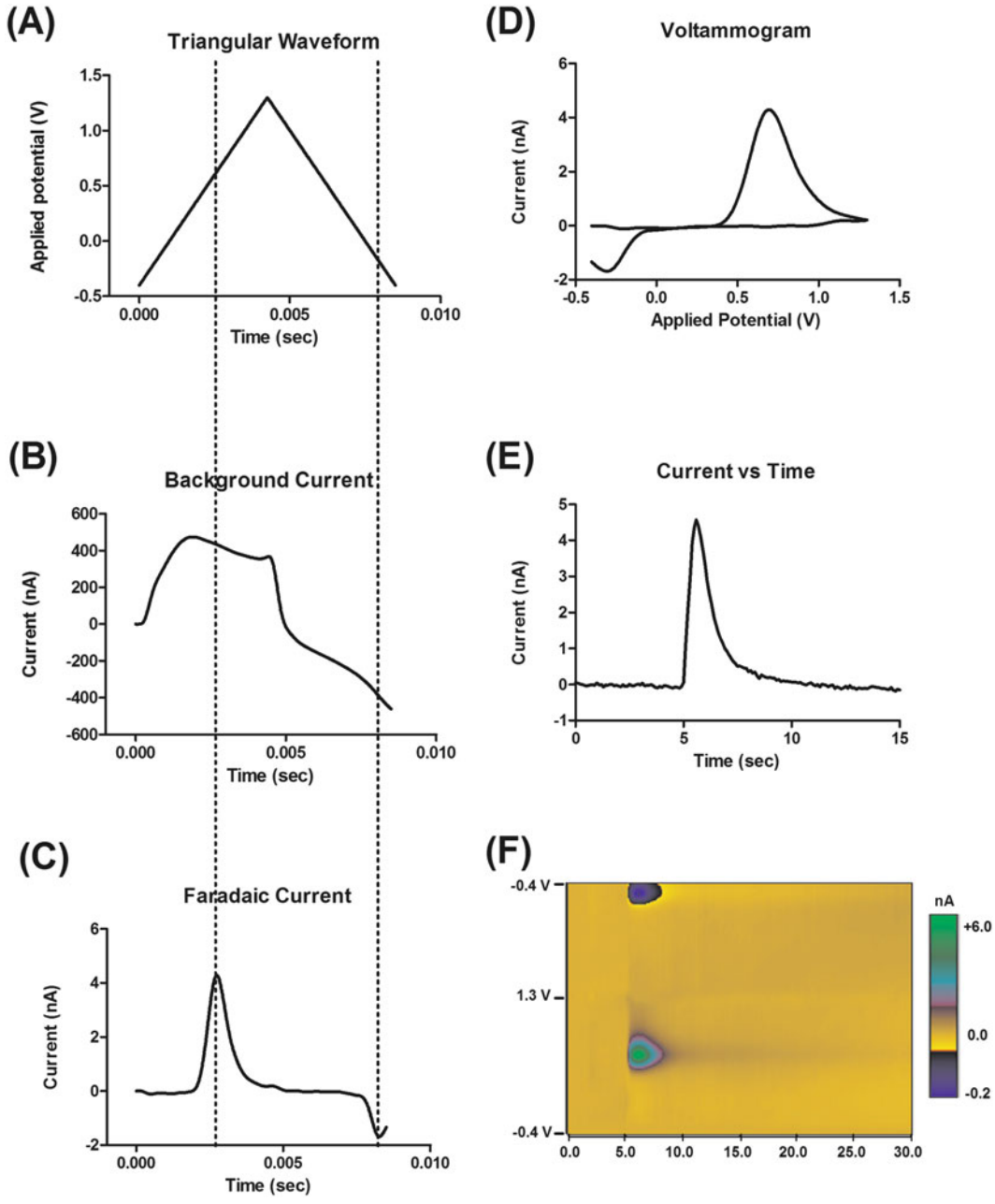

Fig. 1 Voltammetric information. A triangular waveform (**a**) is applied to a carbon fiber microelectrode. The applied waveform produces a background current (**b**). This background current, which includes the current for the analyte, in this case DA, can be over 100 times greater than the DA current. To measure DA, the background current before an event that triggers DA release is subtracted from the background current after the event. This reveals the faradaic current of the analyte (**c**). The background-subtracted signal can be plotted against the applied potential to give a cyclic voltammogram (**d**). The cyclic voltammogram provides confirmation of the analyte. The current plotted against time reveals the temporal profile of the analyte (**e**). A color plot (**f**) allows multiple cyclic voltammograms to be examined by plotting the applied voltage, current, and time in 2D. The vertical dashed lines indicate the oxidation (*left*) and reduction (*right*) points for DA

nonoxidizing (negative) potential and then periodically driven to an oxidizing potential and back again by the triangular waveform (Fig. 1a). The electrode is typically held at the negative potential of −0.4 V vs. an Ag/AgCl reference electrode and then ramped up to +1.3 V and back at a scan rate of 400 V/s, so that the entire scan is less than 10 ms. Scans are then typically repeated every 100 ms, to give a sampling rate of 10 Hz.

The high scanning rate produces a relatively large capacitance current due to the charging of the carbon fiber electrode. This capacitance current plus the faradaic current from redox processes of the carbon itself results in a large background current (Fig. 1b) that can be 100 times greater than the DA faradaic current (Fig. 1c). Fortunately, this background current is relatively stable throughout the experiment due to the properties of the carbon fiber electrode. Thus, the background current prior to a stimulation or behavioral event can be subtracted to determine the chemical change in the extracellular solution near the electrode (Fig. 1c).

The background-subtracted current collected during the scan yields a voltammogram (current vs. applied potential; Fig. 1d). In the case of DA, the cyclic voltammogram provides information on the DA oxidation and on the reduction of DA-o-quinone. When measured against an Ag/AgCl reference electrode, DA has an oxidation of +0.6 to +0.7 V and a reduction of −0.2 V. The position of the peaks provides information on the redox potential of the analyte and the separation of the peaks provides information on the electron transfer kinetics of the redox reactions [26]. Simply put, the voltammogram can be considered a DA "fingerprint" in that it differs from the voltammogram associated with other electrochemically active compounds, including 5-HT, 5-HT, and DA metabolites, pH, nitric oxide, and ascorbate [2, 20]. One exception is NE, which has the same voltammogram as DA; therefore, it is best, whenever possible, to confirm the identity of an electrochemical signal by pharmacological or other means (*see* **Note 1**).

3.2 Instrumentation and Software

Recording phasic fluctuations in DA, known as DA transients, requires low-noise instrumentation capable of measuring currents at the subnanoampere level. The use of high-pass filters and, in some cases, specialized treatment of working electrodes (*see* **Notes 2** and **3**) has improved the signal-to-noise ratio for DA detection [27].

TH-1 Electroanalysis Software (*TarHeel CV*), commercialized by ESA Biosciences, Chelmsford, MA, USA, is used in conjunction with computer-controlled interface boards (National Instruments, Austin, TX). This software generates the triangular waveform for FSCV as well as the stimulating biphasic waveform used to evoke neurotransmitter release by electrical stimulation. With this software, waveform generation, stimulation generation, and electrochemical

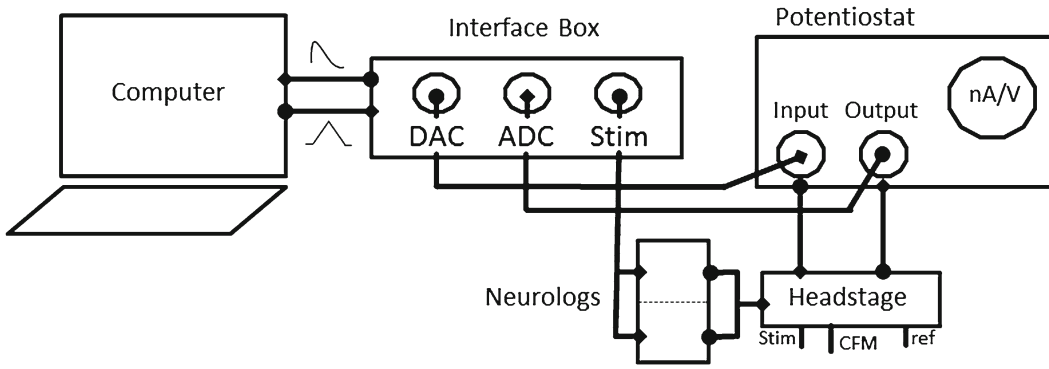

Fig. 2 *TarHeel CV* software controls the timing of the experiments and outputs the applied triangular waveform from a digital-to-analog converter, a component on the interface box. The generated waveform from the computer is sent to the digital-to-analog converter (*DAC*) on the interface box. The interface box is then connected to the potentiostat, which applies the generated waveform to the carbon fiber electrode via a headstage. Current generated by the analyte's redox reaction at the carbon fiber electrode is converted to voltage (100 nA/V) by a current-to-voltage converter, where it is sent back to the potentiostat, amplified (2–10×), and low-pass filtered (2 kHz). From the potentiostat, the voltage is sent back to the interface box analog-to-digital (*ADC*) converter and then back to the personal computer where the output voltages are digitized and stored in computer memory for later data analysis. *TarHeel CV* displays the information as a color plot, current vs. time trace, and cyclic voltammogram (*see* Fig. 1). The stimulation waveform is also generated by the *TarHeel* software and sent to the interface box. The computer-generated stimulation parameters are sent from the interface box to a separate stimulation generator (NeuroLogs; see Note 5), which sends the stimulation to the stimulating electrode. The headstage connects the working carbon fiber electrode, reference electrode, and stimulating electrode. Connections between the potentiostat and headstage are made through a tether connected to an electrical swivel

data acquisition can be carried out on a personal computer with the multifunction input/output card (Fig. 2).

The software outputs these generated waveforms to a digital-to-analog converter in an interface box (Fig. 2). The interface box is connected to a potentiostat, which applies the generated waveform to the carbon fiber electrode via a headstage (Fig. 2). The current generated by the redox reaction of the analyte at the carbon fiber is converted to voltage (100 nA/V) by a current-to-voltage converter, where it is sent back to the potentiostat, amplified (2 to 10×), and low-pass filtered (2 kHz). From the potentiostat, the voltage is sent back to the analog-to-digital converter in the interface box and then back to the personal computer where information can be displayed as a color plot, current vs. time trace, and cyclic voltammogram.

TarHeel CV allows customization of the applied potential: waveform shape, number of points, scan rate, voltages, frequency, electrical stimulation pulses, and timing between voltammetric sweeps can all be adjusted for optimization of the analyte. For DA, a triangular waveform of 1000 points at a scan rate of 400 V/s at 10 Hz is typically used. A digital oscilloscope

depiction shows the applied waveform (Fig. 1a) and non-background-subtracted current (Fig. 1b). This allows oxidation current at a specific potential as well as the background current of the electrode to be shown in real time, prior to and during data collection. Other data parameters that can be set include the gain (nA/V) of the signal as well as durations and repetition of data collection (single or sequential files).

Data can be presented as a cyclic voltammogram, current vs. time plot, and color plot (Fig. 1) and can be written to text files for use in other programs such as graph pad prism or sigma plot. *TarHeel CV* has an analysis component that allows one file at a time to be analyzed, with the user setting the background parameters (current vs. time plot and color plot background usually averages 10 consecutive scans, and cyclic voltammogram background typically averages 5 consecutive scans). The instrumentation does not filter the electrochemical signal as it is collected, which allows the data to be smoothed and/or filtered as appropriate in the analysis component.

Although *TarHeel CV* is commercially available and commonly used for FSCV, new software is emerging as experiments increase in complexity. Recently, the Wightman group has developed High-Definition Cyclic Voltammetry (HDCV) software [28], which aims to accommodate recent and future advances in FSCV. Similar to *TarHeel CV*, HDCV includes data acquisition and analysis programs.

3.3 Selecting a Waveform

There are two basic applied waveforms used in in vivo FSCV: traditional and extended. The traditional waveform applies a potential of −0.4 to +1.0 V and back. The extended waveform represents an expansion of the anodic and/or cathodic potentials from −0.6 to +1.4 V and back to enhance sensitivity to DA [29]. With the traditional waveform, the electrode is held at a nonoxidizing potential of −0.4 V between scans; this promotes adsorption of DA to the carbon surface-enhancing sensitivity [20]. When the holding potential of −0.4 V is increased to more negative values, the sensitivity of the electrode increases even further, but at the expense of the temporal resolution [29]. An increase in the anodic potential from 1.0 to 1.4 V also increases DA sensitivity but decreases selectivity due to potential interference with other oxidizable compounds. Thus, the extended waveform is useful for situations in which the concentration of endogenous DA is expected to be low. The decreased time resolution of a fully extended waveform (−0.6 to +1.4 V) compared to the traditional waveform makes the extended waveform less suitable for kinetic measurements of DA transients. Therefore, the most commonly used waveform in behaving animals is an extended waveform with the potential of −0.4 to +1.3 V and back. This extended waveform yields close to the same sensitivity as the

−0.6 to +1.4 V waveform but with better time resolution and selectivity [5, 30].

3.4 Electrical Stimulation

Electrical stimulation of DA neurons evokes a reliable and reproducible DA response. For behavioral experiments [4, 31, 32], electrical stimulation is useful for two reasons: (1) to ensure optimal placement of the carbon fiber in a DA-rich target region and (2) to confirm that DA is the source of the voltammetric signal recorded during the behavioral task by providing a DA template. Evoking DA release prior to and after the experiment also establishes the properties of the carbon fiber electrode as well as the recording site integrity did not change throughout the course of the experiment [26, 33].

Electrical stimulation trains can be generated using *TarHeel CV* software (*see* **Note 4**), which sends information from the digital-to-analog converter card to an optically isolated constant-current stimulator (NeuroLogs; *see* **Note 5**). Typically, a square biphasic current waveform is used for the stimulation. For in vivo experiments, electrical simulations range from 4 to 24 pulses, applied at 10–60 Hz at a current of 125 μA. The larger stimulation trains (24 pulses, 60 Hz, 0.4 s) produce larger and more reproducible signals, whereas smaller trains are more in line with physiological parameters (4 pulses, 10–20 Hz, 0.4 s–0.2 s). When larger stimulation trains are used, ample time must be allotted to allow for renewal of the readily releasable DA pool. Application of 24 pulses, 60 Hz, at 125 μA requires approximately 2 min between stimulations.

3.5 Electrode Construction

Carbon fiber microelectrodes are locally constructed.

3.5.1 Acute Carbon Fiber Microelectrodes

1. Individual T650 carbon fibers (6.0 μm diameter) are inspected and debris removed; the carbon fiber is aspirated into a 1.0 or 1.2 mm diameter borosilicate glass capillary tube (diameter depends on micromanipulator used). The carbon fiber should be extending on both ends of the tube.
2. The carbon-filled capillary tube is pulled using a vertical micropipette puller (Narishige, Tokyo, Japan). The magnet and heat settings should ensure that the pulled glass tappers and forms a tight seal around the carbon fiber.
3. Under a light microscope (~400× magnifications), a sharp scalpel is used to trim the carbon fiber to a length of 75–150 μm from the glass/carbon fiber seal. The electrode should be inspected under the microscope for visible cracks or abnormalities in the fiber or glass seal.
4. On the non-tapered end of the electrode, insert a small piece of bismuth followed by a small-diameter stainless steel wire. Melt the bismuth and push the stainless steel wire so that the

bismuth makes an electrical connection between the back end of the carbon fiber and the wire.

5. Using the *TarHeel* software, check the signal-to-noise ratio and stability of the electrode by placing the electrode in 150 mM NaOH solution and apply the selected waveform (usually −0.4 to 1.3 V; Sect. 3.3) at 60 Hz for >5 min followed by 10 Hz for at least another 5 min (i.e., "cycle" the electrode). Collect a recording to determine electrode drift and noise level. If the electrode is noisy (>0.3 nA) and/or does not stabilize, discard it.

3.5.2 Chronic Carbon Fiber Microelectrodes

1. Using a straight razor, cut silica tubing to the length needed to reach the recording site. The ideal cut will leave silica tubing with a straight edge, not slanted or jagged.
2. Place cut silica tubing in a petri dish with isopropanol and carbon fibers. Using cotton swabs, gently thread the carbon fiber through the tubing till the carbon fiber is extending on both sides. Make sure the carbon fiber is long enough to grab; there should be at least 1.0 cm protruding from both sides of the silica tubing.
3. Place beads of epoxy on the carbon fiber near one of the edges of the cut silica tubing and pull the other side of the carbon fiber till the epoxy forms a convex seal and let dry. Make sure that there is no epoxy coating the remaining carbon fiber.
4. Using a scalpel blade or sharp microscissors, cut the carbon fiber 75–150 μm from the silica tubing epoxy seal.
5. On the back end of the electrode (non-epoxied side), place a dab of Ag^{2+} epoxy on the carbon fiber near silica tube and attach a connector pin. Leave the electrode to dry overnight, and test in the same way as acute electrodes.

3.5.3 Ag/AgCl Reference Electrode

1. A piece of silver wire is cut (~10 mm for rats; ~3 mm for mice) and inserted into the socket of a connector pin and fixed with epoxy.
2. Once epoxy is dried, the silver wire is connected to the negative terminal of a current generator lesion maker and the positive voltage source is connected to a stainless steel wire. The stainless steel wire is then immersed in a concentrated solution of hydrochloric acid and the lesion maker is turned on.
3. The silver wire is then dipped into the hydrochloric acid for about 30 s until its surface becomes dark gray (bubbles should appear as gas is evolved during this process).

3.6 Stereotaxic Surgery

3.6.1 Acute Electrode Implantation in Rats

1. Anesthetize the rat with an intraperitoneal injection of ketamine (80 mg/kg) and xylazine (10 mg/kg; *see* **Note 6**). Shave the head and place the rat in a stereotaxic frame. Expose the skull by making a longitudinal incision along the midline of

the scalp. Clear fascia and blood to expose the anatomical markers bregma and lambda.

2. Drill holes for the guide cannula and stimulating and reference electrodes. Drill two to three additional holes for anchoring screws. The guide cannula and stimulating electrode holes are placed ipsilaterally, while the reference electrode and two of the screw holes are placed contralaterally. Position the stimulating electrode hole either over DA cell body regions (substantia nigra compacta or ventral tegmental area; 1.0 mm lateral and 5.2 mm posterior from bregma, ~8.5 mm ventral from brain surface) or over the ascending fibers in the MFB (1.4 mm lateral, 4.6 mm posterior, ~8.5 mm ventral from brain surface). Position the guide cannula above the target area (e.g., dorsal striatum 1.3 mm lateral and 1.3 mm anterior from bregma). Place the reference electrode on the contralateral side opposite the guide cannula leaving room for the anchoring screws.
3. Remove the dura mater and position the guide cannula, reference electrodes, and anchor screws, securing them with dental cement, but leaving the stimulating electrode hole exposed.
4. Separate tips of the stimulating electrode by 1.0 mm. Cut or file the electrode to uniform length. Thoroughly clear dura mater from the stimulating electrode hole and lower the electrode stereotaxically so that the tips of the electrode are orientated in the coronal plane. The electrode is lowered to about 1–2 mm above the target region (e.g., MFB).
5. Place a micromanipulator containing the carbon fiber electrode in the guide cannula. Lower the carbon fiber electrode to the DA target region.
6. Connect the stimulating electrode to the stimulator and attach the carbon fiber and reference electrodes to the headstage. Turn on the voltammetric waveform and cycle the carbon fiber for several minutes allowing it to stabilize. Stimulate DA release (24 pulses, 60 Hz, 125 μA) while DA is monitored at the carbon fiber electrode. The stimulating electrode is then lowered in 0.2 mm increments until DA efflux is detected following the stimulation. Then, the stimulating electrode is further lowered by 0.1 mm increments until DA release is optimized.
7. Apply dental cement to the exposed part of the skull, carefully covering the stimulating electrode up to its lower half of its plastic hub. The micromanipulator and carbon fiber are then removed and the guide cannula is capped. The animal is allowed to recover before experimental use.

3.6.2 Chronic Electrode Implantation in Rats

Surgery for chronically implanted electrodes is very similar to the surgery involving acute electrodes.

1. Anesthetize the rat, place the rat in the stereotaxic frame, drill the holes, and remove the dura mater as described above in the acute electrode implantation surgery (Sect. 3.6.1).
2. Secure the reference electrode and anchoring screws with dental cement leaving the stimulating electrode and working carbon fiber electrode hole exposed.
3. Sterotaxically lower the chronic electrode to the dopamine target region (e.g., caudate–putamen). Note that a guided cannula is not used for chronic electrodes.
4. Sterotaxically lower the stimulating electrode as described above (Sect 3.6.1). Make sure to lower the stimulating electrode till you get a maximal DA response.
5. Secure the rest of the exposed skull, screw, and electrodes with dental cement.
6. Place the rat back in its home cage until fully recovered.

3.6.3 Acute Electrode Implantation in Mice

Because mice are smaller than rats, some minor surgical modifications are recommended.

1. Anesthetize the mouse with an intraperitoneal injection of chloropent (0.10 mL/25 g; *see* **Note 6**). Shave the head (Nair can also be used to remove hair) and place the mouse in a stereotaxic frame. Expose the skull by making a longitudinal incision along the midline of the scalp. Clear the fascia and blood to expose the anatomical markers bregma and lambda.
2. Drill holes for the guide cannula and stimulating and reference electrodes. Drill two additional holes for anchoring screws. The guided cannula and stimulating holes are placed on the ipsilateral side, while the reference electrode and two screw holes contralaterally. Position the stimulating electrode hole either over DA cell body regions (substantia nigra/ventral tegmental area) or the ascending fibers in the MFB (1.0 mm lateral, 1.58 mm posterior, ~ 5.0 mm ventral from the top of brain). Position the guide cannula above the target area (e.g., dorsal striatum; 1.9 mm lateral and 0.5 mm anterior from bregma) and place the reference electrode on the contralateral side opposite the guide cannula leaving room for the anchoring screws.
3. Remove the dura mater and position the guide cannula, reference electrodes, and anchor screws, securing them with dental cement, but leaving the stimulating electrode hole exposed.
4. Separate the tips of the stimulating electrode by 1.0 mm and cut or file the electrode to uniform length. Thoroughly clear dura mater from the stimulating electrode hole and lower the electrode stereotaxically so that the tips of the electrode are orientated in the coronal plane. The stimulating electrode is lowered about 0.5–1 mm above the target region (e.g., MFB).

5. Place the micromanipulator containing the carbon fiber microelectrode into the guide cannula. Then, lower the carbon fiber microelectrode to the DA target region.
6. Connect the stimulating electrode to the stimulator and attach the carbon fiber and reference electrode to the headstage. Turn on the voltammetric waveform and cycle the carbon fiber for several minutes allowing it to stabilize. Stimulate DA release (24 pulses, 60 Hz, 125 μA) after the carbon fiber microelectrode has stabilized, and monitor DA at the carbon fiber electrode. The stimulating electrode is then lowered in 0.1 mm increments until DA efflux is detected following the stimulation. Then, the stimulating electrode is further lowered till DA release is optimized.
7. Apply dental cement to the exposed part of the skull, carefully covering the stimulating electrode to its lower half of its plastic hub. The micromanipulator and carbon fiber are then removed and the guided cannula is capped. The animal is allowed to recover before experimental use.

3.6.4 Chronic Electrode Implantation in Mice

Depending on experimental design, chronically implanted electrodes might be more suitable. The surgery is similar to the surgery involving acute electrode placement.

1. Anesthetize the mouse, place the mouse in the stereotaxic frame, drill the holes, and remove the dura mater as described above in the acute electrode implantation surgery (Sect. 3.6.3).
2. Secure the reference electrode and anchoring screws with dental cement leaving the stimulating electrode and working carbon fiber electrode hole exposed.
3. Sterotaxically lower the chronic electrode to the dopamine target region (e.g., dorsal striatum). Note that a guided cannula is not used for chronic electrodes.
4. Sterotaxically lower the stimulating electrode as described above (Sect. 3.6.1). Make sure to lower the stimulating electrode till you get a maximal DA response.
5. Secure the rest of the exposed skull, screw, and electrodes with dental cement.
6. Place the mouse back in its home cage until fully recovered.

3.7 Experiment Design

When developing a voltammetric experiment, one must evaluate which type of electrode to use (chronic or acute), waveform selection, electrical stimulation parameters, and duration of the experiment. If the purpose of the study is to track longitudinal changes in neurotransmitter dynamics over the course of a disease progression or learning paradigm, one may wish to use chronic electrodes. Chronic electrodes stability and sensitivity have been characterized

out to 4 months [18]. The density of dopaminergic cells in the recording region determines which waveform should be utilized. Determining if the stimulation should be physiological in nature and occur frequently influences the stimulation parameters used. When conducting an experiment, one should always keep in mind the question one is trying to answer.

3.7.1 Basic Procedure

1. On the day of the experiment, clean all connectors and check acute recording electrode.
2. Plug in the rat or mouse by connecting the working, reference, and stimulating electrode (located on the headstage) to the tether and connect the tether to the swivel (*see* **Note 7**).
3. If using an acute electrode, lower it slowly into the brain just dorsal of the target region and allow to stabilize (~10 min). Monitor its output display on the oscilloscope. If the electrode breaks during lowering, a sudden change in the shape of the background current will occur on the oscilloscope. Remove the electrode and replace it with a new one.
4. Apply an electrical stimulation (24 pulses, 60 Hz, 125 μA) to the stimulating electrode while DA is monitored at the carbon fiber electrode. Lower the recording electrode in small increments until evoked DA is optimized. The behavioral reaction to the stimulation is usually a head turn to the ipsilateral side or slight forward movement.
5. Before recording, allow the animal to habituate for roughly 30 min. This allows the acute electrode to equilibrate as well as allows habituation. Electrode should be stabilized so that there is minimal drift in the background current. This equilibration can take longer in chronic electrodes (*see* **Note 8**).
6. Synchronize the start of the electrochemical recording with the behavioral recording in order to get precise correlation of the neurochemistry and behavior.

3.8 Electrode Calibration

Immediately following the final data collection, the working electrode is removed and placed in a flow cell containing 12 mM Tris–HCl buffer solution. The flow cell is equipped with an injection loop which contains a known concentration of DA. A triangular waveform is applied to the working electrode while the buffer solution is continuously pumped through the flow cell at a rate of 3 mL/min. As the buffer solution continuously flows, the known concentration of DA (we used 1.0 μM DA) is injected into the flow cell allowing for a recorded change in current that corresponds to a known concentration of DA. This provides a calibration factor and allows the conversion from the recorded change in current to a change in DA concentration (*see* **Note 9**).

3.9 Data Analysis

Data analysis is carried out using the analysis component of the *TarHeel* software (described in Sect. 3.2). This software allows confirmation of DA. For every recording session, the chemical signature (voltammogram) of behaviorally evoked DA release is statistically compared to an electrically evoked DA template. The electrically evoked DA template is taken from electrically stimulated DA signal in the same animal, preferably with the electrode in the same location. The statistical comparison can be least squares analysis of normalized signals or principle component regression analysis. Once DA signals are confirmed, their current can be converted to concentration using the post-calibration factor (Sect. 3.8) and statistically compared to other animals and groups.

3.10 Histology/ Electrode Placement Verification

Since one cannot see the electrode as it is lowered into the brain, confirmation of the recording site following the experiment is important.

1. Administer a double surgical dose of anesthesia and lower a stainless steel electrode to the same depth as the carbon fiber electrode (*see* **Note 10**).
2. Make an electrolytic lesion by delivering a current (100 μA, 5 s) using a current lesion maker.
3. Transcranially perfuse the animal with saline till blood is removed and then switch to the fixative solution (10 % formalin buffer solution).
4. Remove the brain and store it in the fixative solution with potassium ferricyanide for 2 days and then transfer the brain to 30 % sucrose, 10 % formalin solution.
5. Once tissue is adequately fixed, freeze the tissue using dry ice and section tissue on a microtome or cryostat (60 μm coronal sections).
6. Mount the sections to slides and stain with crystal violet to aid in visualization of anatomical structures.

4 Notes

1. NE has a cyclic voltammogram indistinguishable from that for DA. In most cases, however, NE interference can be excluded. To distinguish DA from NE: (1) The anatomy should support the presence of the detected analyte; the electrode should be in a DA-rich region having little to no NE present. (2) The physiology should be consistent with release. The stimulation of the DA pathway should result in DA release. (3) Pharmacology should support DA; the use of a selective uptake blocker (e.g., GBR 12.921) or a DA agonist (e.g., quinpirole) or antagonist (e.g., eticlopride) should affect the signal accordingly.

2. The electrode can be soaked in isopropanol for 10 min prior to use. Pretreating the electrode with isopropanol has been shown to clean and improve the signal-to-noise ratio [34].
3. Nafion-coated carbon fibers increase the selectivity of the electrochemical detection of cationic substances such as DA by creating fixed anionic sites on the electrode. Thus, Nafion-coated electrodes are negatively charged and therefore decrease signal contribution from anionic substances such as ascorbate [35]. Nafion coating also seems to improve the biocompatibility of the electrode surface and decrease fouling of the electrode during an experiment [36].
4. While electrical stimulation trains are generated and the timing of stimulation can be done by using *TarHeel CV*, this software does allow electrical stimulation to be externally triggered by events such as lever presses for intracranial self-stimulation [37].
5. To apply biphasic stimulation, two stimulators are needed. One stimulator provides current in the positive direction; the other stimulator provides current in the negative direction. It is important that the current being applied in the positive direction is equal to that being applied in the negative direction. To accomplish this, a potentiometer can be used to divide the input from the computer.
6. Rats and mice can also be anesthetized with isoflurane in oxygen (4 % induction, 1.5 % maintenance).
7. When connecting an animal to the tether, it is important to avoid breaking an electrode or loosening the headstage. If using a rat, connections to the working electrode, stimulating electrode, and reference electrode can be done while the animal is in its home cage. Mice tend to be more jumpy. To prevent breaking the electrode during implantation and to allow for easier attachment of the connectors to the headstage, the mouse can be given a forth to a half of the surgical dose of anesthetic. If chronic electrodes are used, the mouse can be placed in a small chamber containing isoflurane for brief anesthetization to allow the animal to be connected easily.
8. For reasons not entirely understood, the electrode takes longer to stabilize when the extended waveform is used. This could be due to adaptations at the carbon surface. Robinson and Wightman [33] suggest applying a waveform of 60 Hz for 10–15 min followed by a waveform at 10 Hz for 5 min after the electrode is lowered into brain tissue and prior to optimizing the electrode placement for recording.
9. Electrode calibration can occur prior to and/or after the experiment, with post-calibration being the more conservative out of the two.

10. The working electrode can also be removed and an insulated stainless steel wire with exposed tip can be stereotaxically lowered to the same location as the carbon fiber. The lesion can then be made with the stainless steel wire. Although the lesion can be made directly with the carbon fiber [2], this makes the electrode unusable for post-calibration. Therefore, electrode calibration needs to be performed either prior to the experiment or a standardized curve can be used to determine the calibration factor. The standardized curve is constructed by plotting the background current of multiple electrodes (x-axis) against the current generated by a known concentration of DA (y-axis). The background current of the electrode is then plotted on this curve to determine the calibration factor.

References

1. Garris PA, Rebec GV (2002) Modeling fast dopamine neurotransmission in the nucleus accumbens during behavior. Behav Brain Res 137:47–63
2. Rebec GV, Christensen JRC, Guerra C et al (1997) Regional and temporal differences in real time dopamine efflux in the nucleus accumbens during free-choice novelty. Brain Res 776:61–67
3. Robinson DL, Phillips PEM, Budygin EA et al (2001) Sub-second changes in accumbal dopamine during sexual behavior in male rats. Neuroreport 12:2549–2552
4. Cheer JF, Wassum KM, Sombers LA et al (2007) Phasic dopamine release evoked by abused substances requires cannabinoid receptor activation. J Neurosci 27:791–795
5. Cheer JF, Wassum KM, Heien ML et al (2004) Cannabinoids enhance subsecond dopamine release in the nucleus accumbens of awake rats. J Neurosci 24:4393–4400
6. Stuber GD, Roitman MF, Phillips PE et al (2005) Rapid dopamine signaling in the nucleus accumbens during contingent and noncontingent cocaine administration. Neuropsychopharmacology 30:853–863
7. Brown HD, McCutcheon JE, Cone JJ et al (2011) Primary food reward and reward-predictive stimuli evoke different patterns of phasic dopamine signaling throughout the striatum. Eur J Neurosci 34:1997–2006
8. Robinson DL, Heien ML, Wightman RM (2002) Frequency of dopamine concentration transients increases in dorsal and ventral striatum of male rats during introduction of conspecifics. J Neurosci 22:10477–10486
9. Johnson MA, Rajan V, Miller CE et al (2006) Dopamine release is severely compromised in the R6/2 mouse model of Huntington's disease. J Neurochem 97:737–746
10. Ortiz AN, Kurth BJ, Osterhaus GL et al (2011) Impaired dopamine release and uptake in R6/1 Huntington's disease model mice. Neurosci Lett 492:11–14. doi:10.1016/j.neuet.2011.01.036
11. Bergstrom BP, Garris PA (2003) 'Passive stabilization' of striatal extracellular dopamine across the lesion spectrum encompassing the presymptomatic phase of Parkinson's disease: a Voltammetric study in the 6-OHDA-lesioned rat. J Neurochem 87:1224–1236
12. Zhang L, Le W, Xie W et al (2012) Age-related changes in dopamine signaling in Nurr1 deficient mice as a model of Parkinson's disease. Neurobiol Aging 33:1001.e7–1001.e16. doi:10.1016/j.neurobiolaging.2011.03.022
13. Wightman RM, Amatorh C, Engstrom RC et al (1988) Real-time characterization of dopamine overflow and uptake in the rat striatum. Neuroscience 25:513–523
14. Allen C, Peters JL, Sesack SR, Michael AC (2001) Micro-electrodes closely approach intact nerve terminals in vivo, while larger devices do not: a study using electrochemistry and electron microscopy. In: O'Connor WJ, Lowry JP, O'Connor JJ, O'Neill RD (eds) 9th international conference on in vivo methods. University College Dublin, Dublin, pp 89–90
15. Wu Q, Reith ME, Wightman RM et al (2001) Determination of release and uptake parameters from electrically evoked dopamine dynamics measured by real-time voltammetry. J Neurosci Methods 112:119–133
16. Millar J, Stamford JA, Kruk ZL, Wightman RM (1985) Electrochemical, pharmacological and electrophysiological evidence of rapid

dopamine release and removal in the rat caudate nucleus following electrical stimulation of the median forebrain bundle. Eur J Pharmacol 109:341–348

17. Garris PA, Christensen JRC, Rebec GV, Wightman RM (1997) Real-time measurement of electrically evoked extracellular dopamine in the striatum of freely moving rats. J Neurochem 68:152–161
18. Clark JJ, Sandber SG, Wanat MJ et al (2010) Chronic microsensors for longitudinal, subsecond dopamine detection in behaving animals. Nat Methods 7:126–129
19. Hart AS, Clark JJ, Phillips PEM (2015) Dynamic shaping of dopamine signals during probabilistic Pavlovian conditioning. Neurobiol Learn Mem 117:84–92
20. Baur JE, Kristensen EW, May LJ, Wiedemann DJ, Wightman RM (1988) Fast-scan voltammetry of biogenic amines. Anal Chem 60: 1268–1272
21. Bunin MA, Prioleau C, Mailman RB, Wightman RM (1998) Release and uptake rates of 5-hydroxytryptamine in the dorsal raphe and substantia nigra reticulata of the rat brain. J Neurochem 70:1077–1087
22. Iravani MM, Millar J, Kruk ZL (1998) Differential release of dopamine by nitric oxide in subregions of rat caudate putamen slices. J Neurochem 71:1969–1977
23. Sanford AL, Morton SW, Whitehouse KL et al (2011) Voltammetric detection of hydrogen peroxide at carbon fiber microelectrodes. Anal Chem 82:5205–5210
24. Runnels PL, Joseph JD, Logman MJ, Wightman RM (1999) Effect of pH and surface functionalities on the cyclic voltammetric responses of carbon-fiber microelectrodes. Anal Chem 71:2782–2789
25. Rebec GV (2007) From interferant anion to neuromodulator: Ascorbate oxidizes its way to respectability. In: Michael AC, Borland LM (eds) Electrochemical methods for neuroscience. Pennsylvania, Pittsburgh, pp 149–166
26. Phillip PEM, Robinson DL, Stuber GD et al (2003) Real-time measurements of phasic changes in extracellular dopamine concentration in freely moving rats by fast-scan cyclic voltammetry. In: Wang JQ (ed) Methods in molecular medicine, vol 79. Drugs of Abuse: Neurological Reviews and Protocols, Totowa
27. Cahill PS, Walker QD, Finnegan JM et al (1996) Microelectrodes for the measurement of catecholamines in biological systems. Anal Chem 68:3180–3186
28. Bucher ES, Brooks K, Verber MD et al (2013) A flexible software platform for fast-scan cyclic voltammetry data acquisition and analysis. Anal Chem 85. doi:10.1021/ac402263x
29. Heien ML, Phillips PE, Stuber GD, Seipel AT, Wightman RM (2003) Overoxidation of carbon-fiber microelectrodes enhances dopamine adsorption and increases sensitivity. Analyst 128:1413–1419
30. Heien MLAV, Khan AS, Ariansen JL et al (2005) Real-time measurements of dopamine fluctuations after cocaine in the brain behaving rats. Proc Natl Acad Sci U S A 102:10023–10028. doi:10.1073/pnas.0504657102
31. Budygin EA, Phillips PEM, Robinson DL et al (2001) Effect of acute ethanol on striatal dopamine neurotransmission in ambulatory rats. J Pharmacol Exp Ther 297:27–34
32. Daberkow DP, Brown HD, Bunner KD et al (2013) Amphetamine paradoxically augments exocytotic dopamine release and phasic dopamine signals. J Neurosci 33:452–463. doi:10.1523/JNEUROSCI.2136-12.2013
33. Robinson DL, Wightman RM (2007) Rapid dopamine release in freely moving rats. In: Michael AC, Borland LM (eds) Electrochemical methods for neuroscience. Pennsylvania, Pittsburgh, pp 17–34
34. Bath BD, Michael DJ, Trafton BJ et al (2000) Subsecond adsorption and desorption of dopamine at carbon-fiber microelectrodes. Anal Chem 72:5994–6002
35. Gerhardt GA, Oke AF, Nagy G et al (1984) Nafion-coated electrodes with high selectivity for CNS electrochemistry. Bran Res 290: 390–395
36. Turner RFB, Harrison DJ, Rojotte RV (1991) Preliminary in vivo biocompatibility studies on perfluorosulphonic acid polymer membranes for biosensor applications. Biomaterials 12:361–368
37. Cheer JF, Heien MLAV, Garris PA et al (2005) Simultaneous dopamine and single-unit recordings reveal accumbens GABAergic responses: Implications for intracranial self-stimulation. Proc Natl Acad Sci U S A 102:19150–19155

Chapter 25

In Vivo Brain Microdialysis of Monoamines

Jorge E. Ortega, J. Javier Meana, and Luis F. Callado

Abstract

Microdialysis is an in vivo neurochemical monitoring technique that measures changes in the extracellular compartment of selected brain regions. These changes are monitored through a microdialysis probe implanted into the brain tissue using standard stereotaxic techniques. The microdialysis probe consists of a semipermeable dialysis membrane that surrounds two silica capillary tubes that allow fluids flow into and out of the part of the probe containing the membrane. Dialysate samples contain detectable amounts of different substances including endogenous monoamine neurotransmitters. Microdialysis perfusates are applied to a chromatography column with electrochemical detection that separates the different monoamines according to their size, charge, and lipophilicity. In this chapter, we describe in detail the microdialysis methodology currently used in our laboratory to measure in vivo extracellular levels of monoamines in different brain regions.

Key words Microdialysis, Neurochemistry, Neurotransmitter release, Monoamines, Interstitial space fluid, HPLC, Electrochemical detection

1 Introduction

Microdialysis is an in vivo bioanalytical sampling technique for continuous monitoring of chemical changes in the extracellular compartment of the brain. It supposes a technical improvement derived from the previous push-pull technique. Microdialysis is based on sampling endogenous substances from the extracellular space through a probe that mimics the function of a blood vessel. The microdialysis probe is a specially designed cannula with a semipermeable membrane at its tip. The probe is constantly perfused with an artificial cerebrospinal fluid at a low flow rate. This perfusion solution contains essential ions to maintain ionic balance in the tissue. The microdialysis probe is implanted into the brain tissue of the anesthetized animal using standard stereotaxic techniques. After recovery, the endogenous substances in the area where the probe is implanted are filtered by diffusion from the extracellular fluid to the perfusion solution. Conventional microdialysis membranes allow only the diffusion of molecules of low

Rafael Luján and Francisco Ciruela (eds.), *Receptor and Ion Channel Detection in the Brain: Methods and Protocols*, Neuromethods, vol. 110, DOI 10.1007/978-1-4939-3064-7_25,

molecular weight. Perfusates are collected from the outlet of the microdialysis probe and then analyzed. Additionally, exogenous compounds and drugs can be infused locally in the same brain area through the probe.

The analysis of the perfusates is mainly performed by using HPLC techniques. These analytical techniques must have a high sensitivity and the feasibility of working using very small volumes. Moreover, for most substances the equilibrium between interstitium and the perfusion solution is incomplete. As a result, microdialysis probes need to be calibrated. The recovery is defined as the ratio between the concentration of a particular substance in the outflow solution and the concentration of the same substance in the solution outside the probe. The recovery is affected by several factors as the perfusion flow rate, the diffusion coefficients, the temperature, the dialysis membrane area, the substance concentration and interaction with the membrane, and the composition of the perfusion solution. When adequate calibration methods are used, individual coefficients of variation for microdialysis measurements range around 20 % depending on the analyzed substance.

The brain microdialysis technique presents several advantages compared to other neurochemical in vivo methods:

- There is no direct contact between the perfusion solution and the brain tissue because of the presence of the microdialysis membrane. This fact minimizes the appearance of obstructions or infections and reduces tissue damage in the brain area where the probe is implanted.
- The microdialysis membrane makes impossible the diffusion to the perfusion solution of molecules with a high molecular weight as enzymes that could degrade the endogenous substances to be analyzed.
- The sizes of the interchange area and the perfused area can be modified by changing the size of the probe. This feasibility enables to adapt the technique to the different sizes of the brain regions studied.
- The microdialysis probe is implanted into the brain tissue of an anesthetized animal. However, perfusates may be obtained from both anesthetized and freely moving animals. This second option allows performing experiments in better physiological conditions and during longer periods. Additionally, microdialysis technique can be combined in these animals with behavioral experiments.
- The microdialysis probe gives the option of local administration by reversal dialysis of drugs in the brain area studied. This possibility lets us avoid pharmacokinetic problems. Moreover, we can dissociate the local effects of a drug in the brain area studied from the systemic effects of the drug. This feasibility is

especially important because after implanting several probes in different brain regions, we can separately analyze the effects of a drug in somadendritic and terminal areas, as well as their interactions.

In contrast, brain microdialysis technique presents also some controversial aspects that must be mentioned:

- It is still not clear if the extracellular levels of neurotransmitters observed with this technique really reflect the synaptic or even extrasynaptic levels of those substances. Therefore, microdialysis probe has to be calibrated after use. Additionally, it is known that microdialysis probe constantly drains substances from the brain tissue. This effect changes the diffusion profile and makes it less step, thereby reducing with time substance transport into the probe.
- The implantation of the microdialysis probe induces tissue damage and causes severe disturbance in local glucose metabolism and blood flow. As a consequence, at the start of the monitoring, neurotransmitter levels are too high, despite that they normalize after 1–2 h to obtain stable baseline levels. Furthermore, a few days after probe implantation, a glial reaction appears in the brain tissue surrounding the dialysis membrane. The result is a coating of the membrane with inflammatory cells and connective tissue that makes difficult the diffusion of substances through it. Consequently, the reliability of long-standing microdialysis becomes questionable.
- Brain microdialysis presents a limited temporal and spatial resolution when compared with other techniques as electrophysiology. In this way, the size of the probe limits the brain structures that can be monitored. Moreover, the samples obtained must be accumulated during long periods (usually between 5 and 40 min) in order to obtain enough volume for detection methods. Thus, it is difficult, for example, to obtain good temporal resolution for a drug effect.

Finally, despite the present chapter is focused in brain microdialysis, probes can be also inserted into another organs and tissues as muscles, lung, fat, or blood vessels.

2 Materials

2.1 Material to Manufacture Microdialysis Probes

- Polyethene tubing (0.28 mm ID × 0.61 mm OD) (Portex Limited, Hythe, Kent, UK)
- 27G stainless steel tubing (0.2 mm ID × 0.4 mm OD) (A-M Systems Inc; Carlsborg, WA, USA)
- 25G stainless steel tubing (0.3 mm ID × 0.5 mm OD) (A-M Systems Inc; Carlsborg, WA, USA)

- Silica capillary (Polymicro Technologies Inc., Phoenix, AZ, USA)
- Microdialysis cuprophan membrane (cutoff: 6000 Da) of 0.25 mm diameter (Idemsa, Segovia, Spain)
- Loctite Super Glue Gel (Loctite España S.A., Madrid, Spain)
- 2-component epoxy adhesive (Araldite®, Ciba-Geigy, Basel, Switzerland)
- Dental cement TAB 2000 (Kerr®, Scafati, Italy)
- Plastic of low melting point
- Drill
- Jeweler's pliers
- Nail file or sandpaper
- Plasticine®
- Dissecting microscope

2.2 Material for Microdialysis Probe Calibration

- CMA 130 in vitro stand (CMA, Harvard Apparatus, Holliston, MA, USA).
- Syringe pump for low pulse-free flow rates. Pumps of one or two independent syringes are commercially available. Flow rate range (0.1–20 μL) (CMA, Harvard Apparatus, Holliston, MA, USA).
- Refrigerated fraction collector (optional). Manual fraction collection can also be performed (CMA, Harvard Apparatus, Holliston, MA, USA).
- Tubing and tubing adaptors (Microbiotech se/AB, Stockholm, Sweden).
- Noradrenaline bitartrate, dopamine hydrochloride, and serotonin hydrochloride (Sigma-Aldrich).
- Artificial cerebrospinal fluid (aCSF).
  - NaCl
  - KCl
  - $CaCl_2$
  - $MgCl_2$
  - K_2HPO_4 (1 mM)

2.3 Small Animal Stereotaxic Surgery

2.3.1 Stereotaxic Equipment

The stereotaxic frame (David Kopf Instruments, Tujunga, CA, USA) is an easy-to-use instrument that facilitates the proper alignment of small animals for the stereotaxic placement of cannulas. The instrument consists of a rugged "U" frame with one/two arms where a probe holder can be fixed. Using a stereotaxic atlas (*see* **Note 1**), it can be used to determinate stereotaxic coordinates for the target brain region. For that purpose, manipulator X, Y, Z

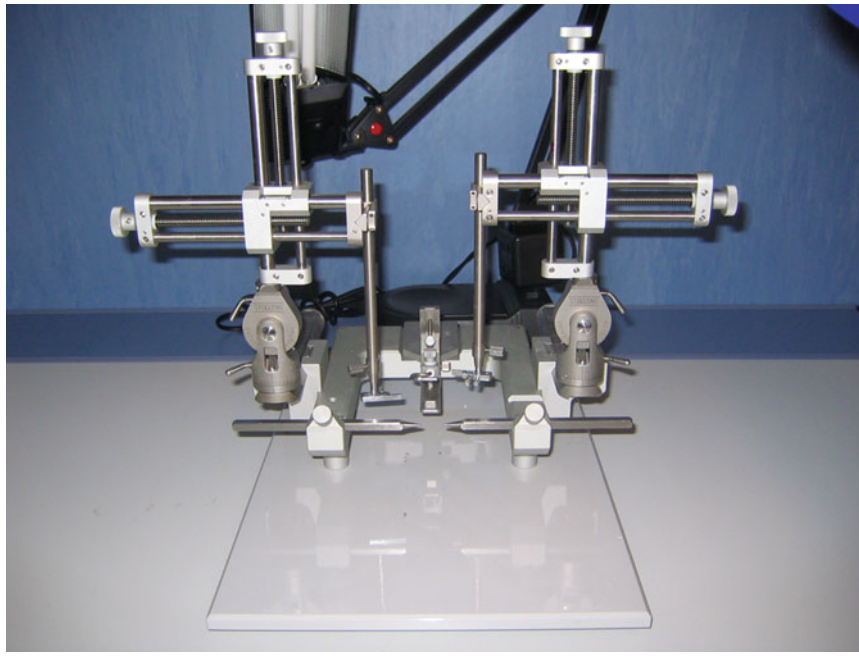

Fig. 1 Photography of a David Kopf® stereotaxic instrument adapted for microdialysis probe implantation

adjustment is used (metric scale 80 mm travel, calibrated 0.1 mm vernier scale). Equipments are versatile, and several standard accessories are available for use in the most appropriate conditions. For standard conditions in microdialysis of small animals, the following options are recommended (*see* Fig. 1):

- Animal adaptor (for rats, model 920 traditional or model 929-B for gas anesthesia, and for mouse, model 926 traditional or model 923-B for gas anesthesia). In addition, model anesthesia mask for rats and mice is also compatible with the model 920 (model 906 rat anesthesia mask) and 926 (model 907 mouse anesthesia mask).
- Ear bars (model 957 is recommended for rat and model 822 for mouse).
- CMA Probe Shaft Clip, which holds the shaft of the probe (CMA, Harvard apparatus, Holliston, MA, USA).

2.3.2 Surgical Instruments

- Isoflurane vapor stick system with small induction box (Harvard Apparatus, Holliston, MA, USA).
- Shaver.
- Homeothermic blanket.
- Scalpel handle and blades.
- Stainless steel hemostats [4].

- Cauterizer.
- Skin marker.
- Drill.
- Micro drill trephine (1.8 mm shaft diameter, 44 mm overall length).
- Micro drill stainless steel burrs (0.7 tip diameter, 44 mm overall length).
- Bone screws and screwdriver.
- Syringe with artificial cerebrospinal fluid.
- Dental cement TAB 2000 (Kerr®, Scafati, Italy).
- Gauze, suture, and needles.

2.3.3 Microdialysis Equipment for Freely Moving Animals

Setting up a system to effectively perform microdialysis requires some planning. There are different companies that supply microdialysis equipment. CMA, Harvard Apparatus (Holliston, MA, USA), BASi (West Lafayette, IN, USA), and Microbiotech/se AB (Stockholm, Sweden) are three of them. Although there are some differences between the equipments, all of them are based in similar principles. Here we will describe the minimal equipment required for performing microdialysis experiments.

- A plastic bowl with food and water containers for housing animals.
- Artificial cerebrospinal fluid (aCSF).
- Syringe pump for low pulse-free flow rates. Pumps containing one or two independent syringes are commercially available. Flow rate range (0.1–20 μL).
- Syringe selector (optional).
- Liquid switch for manual switching between up to three perfusion lines (syringes) and a microdialysis probe. This makes it possible to change between different solutions instantaneously without any risk of introducing air bubbles into the microdialysis probe.
- System for freely moving animals (swivel and balancing arm).
- Tubing and tubing adaptors.
- Plastic collars.
- Refrigerated fraction collector (optional). Manual fraction collection can also be performed.

2.3.4 Chromatography Equipment

HPLC apparatus (Hewlett-Packard Ltd., Waldbronn, Germany) with amperometric detection (Antec® Leyden, Holland):

- Hewlett-Packard model 1200 degasser
- Hewlett-Packard model 1200 pump

- Hewlett-Packard model 1200 injector
- Stationary phase (C18 column) (ALF-205, 150 × 2.1 mm, 3 μm; Antec® Leyden, Holland)
- Mobile phase (all reactive must be HPLC grade)
- Phosphoric acid
- EDTA
- Sodium chloride
- Sodium octyl sulfate
- pH = 6
- Methanol
- DECADE II™ electrochemical detector with VT-03 cell
- Interface for DECADE II and Hewlett-Packard HPLC system communication (HP ChemStation plus, Hewlett-Packard Ltd., Waldbronn, Germany)
- Computer with ChemStation (HP ChemStation plus, Hewlett-Packard Ltd., Waldbronn, Germany)
- pH meter
- Milli-Q water purification system (Merck Millipore, Darmstadt, Germany)
- Glass filter holder for HPLC (Merck Millipore, Darmstadt, Germany)
- Filters durapore of 0.45 μm (Merck Millipore, Darmstadt, Germany)

3 Methods

3.1 Construction of Concentric Probes

Numerous microdialysis probes have been developed and commercialized for intracerebral use in research. Several variants of concentric or linear, flexible, or rigid probes with their corresponding guide cannulas are commercially available. The main advantage of commercial probes is that they have standardized in vitro recovery. However, they are more expensive than the handmade ones. Construction of probes is relatively easy, and after refined manufacturing the reproducibility can be as good as using the commercial ones. Different designs have been employed, but at the present, probes of a concentric shape are the most used in experimental brain research. The basic structure of a microdialysis probe is a permeable membrane on the tip of two concentric silica tubes protected by stainless steel tubing.

Here we will describe the handmade construction of a rigid concentric probe (Fig. 2):

1. Cut 27G stainless steel tubing at 0.7 cm length using a drill.
2. Cut 25G stainless steel tubing at 2 cm length using a drill.

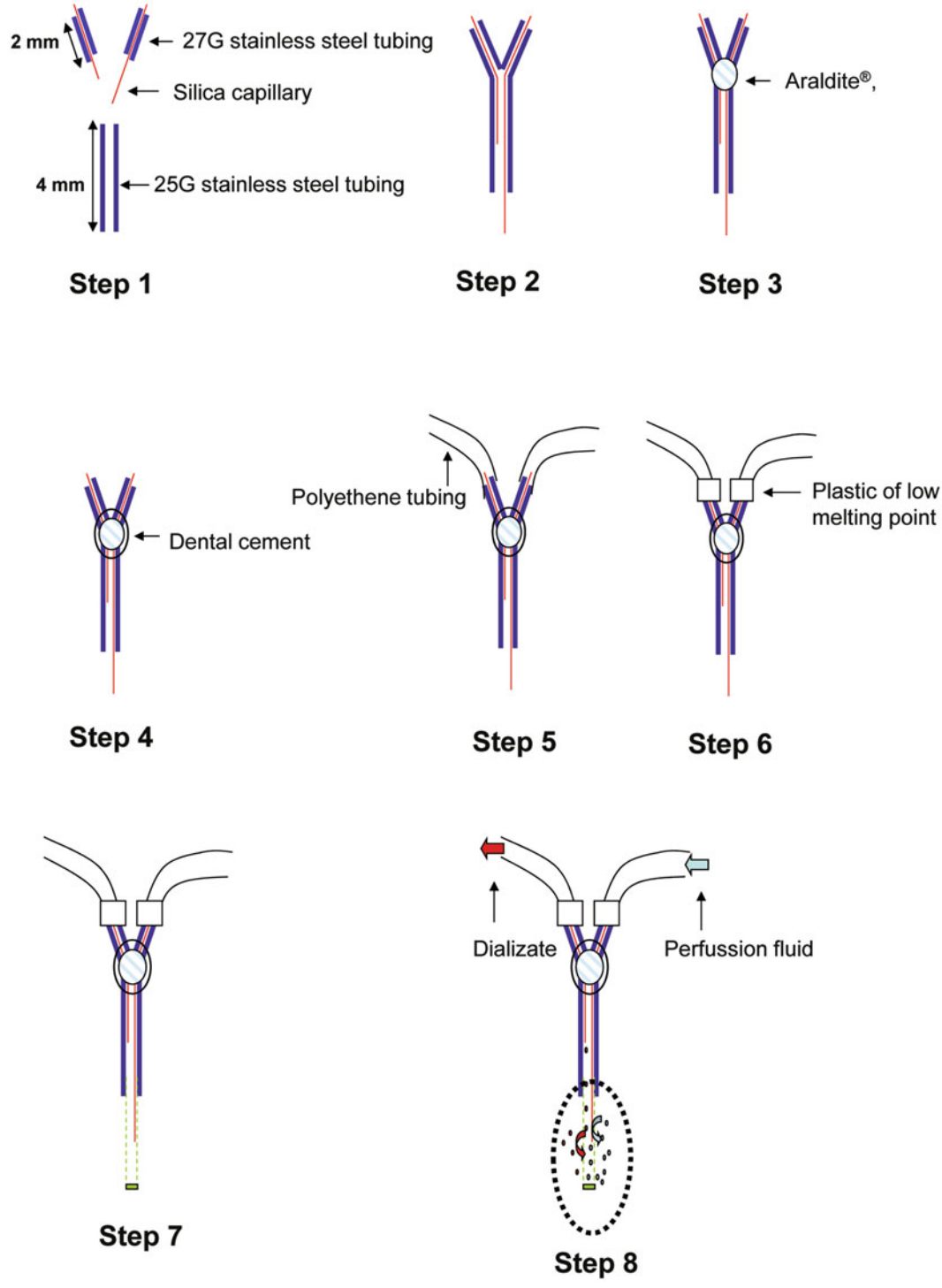

Fig. 2 Schematic representation of the construction of a concentric probe

3. Using a scalpel blade cut a length of 8 cm silica capillary to be used as inlet tube. It must be adapted to the minimum length needed for the area of probe implantation.
4. Using a scalpel blade, cut a length of 2 cm silica capillary to be used as outlet tubing.
5. Introduce the inlet silica capillary through 27G stainless steel tubing.
6. Introduce the outlet silica capillary through other 27G stainless steel tubing.
7. Introduce inlet silica capillary/27G stainless steel tubing and outlet silica capillary/27G stainless steel tubing through 2 cm 25G stainless steel tubing.
8. Place the three components as a "Y"-shaped frame over Plasticine® as a support. In order to identify the inflow and outflow tubing, it is recommended to pull inside at least 1.5 cm of outlet silica capillary and let 0.5 cm length visible.
9. Seal the junction of the main tubing and the two short ones applying a drop of the 2-component epoxy adhesive Araldite. It is important that the three steel tubes remain closely attached. The resin has to be completely dry before the next step (minimum 12 h period).
10. When the Araldite resin is hard, cover with a drop of dental cement and marks with a pen marker the inlet tubing. Afterward, cut the 0.5 cm excess silica tubing of the outlet side of 27G stainless steel tubing.
11. Attach polyethene tubing to the inlet and outlet cannulas. The length should be as short as possible since increasing length will increase the dead volume.
12. In order to increase the resistance, seal the polythene tubing and the stainless steel tubing with plastic of low melting point.
13. Cut the inlet silica tubing at the bottom end with a scalpel blade to let the size needed.
14. At this point, the probe can be stored in dry conditions until the day of stereotaxic surgery. Before operation, dialysis membrane is mounted under a dissecting microscope. Using fine scissors cut the membrane at the size required, and put the membrane over the silica inlet. Pull membrane until the steel tubing and introduce it 2–3 mm (leave 1 mm between the end of the silica tubing and the bottom part of the membrane). After that, add a drop of glue gel at the bottom part of the steel tubing touching the top part of the dialysis membrane. Finally, seal the open end of the membrane with another small drop of glue gel.

3.2 Stereotaxic Surgery

Good surgical techniques, appropriate anesthesia, proper instrumentation, and competent pre- and postoperative care are all essential for the welfare of the experimental animal and the success of the research project (*see* **Note 2**). Stereotaxic surgery for brain microdialysis is a minimally invasive form of surgical intervention that uses a three-dimensional coordinate system to place one or more probes inside the brain [1]. After implantation, probes are rightly cemented to the skull to prevent the access of the animal to the skull in order to avoid any damage when the animal recovers from anesthesia. Surgery, if carefully performed, exerts only minimal influence on the periprobe tissue.

1. Anesthetize the animal (*see* **Note 3**) in the induction chamber at 2.5–3 % isoflurane dose.
2. Place the animal over a thermal blanket, and position it in the stereotaxic frame with the corresponding adapters according to the animal and the type of anesthetic used. First, fix one of the ear bars to the stereotaxic device and introduce it in the ear of the animal. After that, place an ear bar in the other ear and fix it again. The head of the animal should pivot up and down but not from side to side. Finally, attach carefully the animal with the anesthesia mask, and reduce the dose of isoflurane in the vaporizer to 1.5 %.
3. Shave the head of the animal in the area of the incision.
4. Expose the skull by a single midline incision using a scalpel. The size of the incision depends on the brain area(s) where the probe(s) will be placed. Access to the skull is facilitated by the use of stainless steel hemostats.
5. Withdraw the fold of the skin and scrape the skull for cleaning of fascia. The skull should be dry. If some blood capillaries bleed, use a cauterizer to stop bleeding.
6. The head of the animal has to be adjusted as specified in the corresponding stereotaxic atlas. For that, the nose bar dorsoventral adjustment must be used. Flat-skull position is optimal when the heights of the lambda and bregma are equal. In rats, it is achieved when the incisor bar was lowered 3.3 ± 0.4 mm below horizontal zero.
7. When the animal is correctly placed, probe is clamped to the arm of the stereotaxic device with the CMA clip holder. Using the probe as a guide, the lambda and/or bregma coordinates should be defined. Lambda is defined as the point of intersection of the sagittal and lambdoid sutures. Bregma is the point of intersection of the sagittal suture with the curve of best fit along the coronal suture. Anteroposterior and lateral coordinates for both sutures will be used as a reference.

8. Calculate the target coordinates using the stereotaxic atlas.
9. Moving the anteroposterior and lateral manipulators, place the probe in the skull over the target brain region. A skin marker can be used in order to mark the exact coordinate before moving away the probe.
10. Perform a hole over the mark with a micro drill trephine taking care to leave the dura membrane intact.
11. Repeat points 8, 9, and 10 if a second probe is going to be implanted.
12. Drill two holes with a micro drill stainless steel burrs on the skull of the animal, and mount one screw in each one. The screws serve as an attachment of the dental cement that it will be used to immobilize the probe(s).
13. At this point the probe(s) has to be located in the target area by using previously selected coordinates (*see* **Note 4**). After that, place the microdialysis membrane in contact with the dura surface using dorsoventral coordinate manipulator. Use a hypodermic needle to make an incision in the area of contact. If bleeding, use gauze in order to keep dry the skull. Take dorsoventral reference at this moment and calculate the final coordinate.
14. Implant the probe slowly in the brain to prevent tissue damage. In order to increase the resistance of the microdialysis probe and to throw out retained air bubbles, it is recommended to pump artificial cerebrospinal fluid simultaneously during the insertion.
15. Repeat steps 13 and 14 if a second probe is going to be implanted.
16. Once located in the target area, dry the surface of the skull again to facilitate the adherence of dental cement to the skull.
17. Add dental cement to cover the surface of the skull, especially including the probes and the screw areas.
18. When dental cement is totally hard, release stainless steel hemostats and release the probe from the clamp.
19. Suture if necessary.
20. Apply further cement to preserve the integrity of the probe during the microdialysis experiments. It is also recommended the use of a modified pipette tip to protect the integrity of the probe.
21. Finally, check that the probe works, and seal the polyethylene tubing burning the top side with a lighter.
22. Let the animal recover from surgery during approximately 20–24 h in individual cages at controlled room temperature.

3.3 Microdialysis Procedure

3.3.1 In Vitro Microdialysis

The basic principles of microdialysis can be explained by the Fick's law of passive diffusion (*see* **Note 5**). One particular substance will cross the membrane from the surrounding environment into the inside of the probe if the substance concentration is higher than that present in the perfusion fluid. In these conditions, the flow rate of the perfusate removes continuously substances, and maximal concentration gradient is generated by the constantly perfused fluid. In addition, molecules can move in both directions. This allows the study of the delivery/administration of any particular substance to the sampled area.

Probe recovery is the integral parameter of microdialysis probe efficiency. The recovery designates the quota of molecules moved and retained in the perfusion solution relative to the external conditions. On the other hand, the efficiency of delivery to the external microenvironment is called reverse recovery (*see* **Note 6**).

1. Prepare modified cerebrospinal fluid (CSF).
   - 148 mM NaCl
   - 2.7 mM KCl
   - 1.2 mM $CaCl_2$
   - 0.85 mM $MgCl_2$
   - pH 7.4 (adjusted with K_2HPO4 1 mM)
2. Prepare 1, 3, and 5 nM of noradrenaline (NA), dopamine (DA), and serotonin (5-HT) standard solutions in CSF.
3. Place one Eppendorf vial of 1.5 mL with each standard solution in the CMA 130 in vitro stand.
4. Place one probe in each solution clamped with probe clip.
5. Pre-charge syringes with CSF.
6. Configure pump at 1 μL/min.
7. Connect the pump to the inlet of each probe using tubing and tubing adaptors, and then connect the outlet of the probe to the vial container.
8. Perfuse CSF through the system during 30 min.
9. Collect three samples of 35 min in vials containing 5 μL of $HClO_4$ 0.1 M. Monoamines are not stable in these solutions and break down rapidly. Adding a few microliters of concentrated acid to each collected fraction can prevent this effect.
10. Analyze samples using the selected analytical method. Care must be taken that the added preservative is not interfering with the chromatographic analysis.

3.3.2 In Vivo Microdialysis

Microdialysis offers a unique opportunity to monitor the chemistry of the brain microenvironment that surrounds the microdialysis membrane, without the removal of biological fluids (*see* **Note 7**) [2, 3]. This fact allows a minimal disturbance of the brain

physiological functions. Some substances as monoamines are characterized by a long distance diffusion in the brain between the release sites and their respective postsynaptic receptor or transporter proteins. This concept is known as volume transmission and supports the use of microdialysis probes to the evaluation of neurochemical circuits. After stereotaxic surgery, microdialysis probes are implanted in the area of interest. Constant flow rate of a physiological solution is perfused by a microdialysis pump through the inner tube to its distal end, reaching the exposed semipermeable membrane which is located in the brain area of study. Substances with a low molecular weight diffuse from the outside to the inside of the probe according to the concentration gradient. The membrane excludes molecules that present a molecular size higher than the diameter of the pore. Various materials are available with different weigh cutoff for probe construction (*see* **Note 8**). Thus, only small hydrophilic molecules can penetrate to the inside of the probe (*see* **Note 9**).

Samples must be collected per fractions to be able to detect the compounds of interest [4, 5]:

1. Prepare modified cerebrospinal fluid (CSF).
2. Pre-charge syringes with CSF.
3. Place the animal in CMA 120 plastic bowl for microdialysis.
4. Place a plastic collar on the neck of the animal.
5. Configure pump at 1 μL/min and connect it to the switch and swivel positioned in line using tubing and tubing adaptors. The swivel is mounted on the balancing arm allowing free movement of the animal. The swivel brace holds a wire with a collar connector and two holders for plastic vials. The wire attached to the animal collar turns the swivel and supports the tubing, aiding animal comfort and avoiding physical damage of the probes.
6. Perfuse CSF through the system before connecting the probes during 5–10 min depending on the dead volume of the tubing and connectors.
7. Connect implanted microdialysis probes at a low flow rate of 1 μL/min. It must be constant along the experiment. Attach inflow to the inlet tubing of the probe, and allow some time to assure proper flow.
8. Attach outlet tubing to the outlet of the probe.
9. An equilibration period of 1–2 h at the selected flow is needed before starting sample collection.
10. After this period for stabilization, collect samples at regular time periods in vials. The initial three to six samples are commonly used to establish the basal concentrations.

11. Perform experimental manipulation. Collect samples adding 5 μL of concentrated acid ($HClO_4$ 0.1 M) to each collected fraction, and store them refrigerated until analysis.
12. Analyze samples using the selected analytical method. At the end of the experiments, sacrifice animal by an overdose of anesthetic (2–3 times higher than the anesthetic dose previously used, *see* **Note 3**) and dissect brain for the visual verification of the correct implantation of the microdialysis probes.

3.4 Chromatographic Analysis

Detection of extracellular levels of neurotransmitters remains an analytical and technical challenge due, in large part, to the low levels of neurotransmitters collected (i.e., fmol amounts) and the small microdialysis sample volume (10–40 μL). These facts have traditionally been large impediments for microdialysis use. Nowadays, there is a growing interest for collecting smaller fractions as this results in a better temporal resolution of the microdialysis experiments. In addition, microdialysis samples are complex mixtures containing high concentrations of inorganic salts and other small molecules that require chromatographic separation for the measurement of individual neurotransmitters. For many decades, the most popular separation method for classical neurotransmitters has been carried out using high performance liquid chromatography (HPLC) techniques with electrochemical detection (ECD). In amperometric detection, only small percentages of the monoamines are oxidized because of the relatively small working electrode surface area. All together, the low levels of the neurotransmitters in some brain areas, the small sample volume, and the need for more sensitive detectors do not actually allow the design of some research projects in which the required detection is more demanding (*see* **Notes 10** and **11**).

Regardless of the equipment used, optimization of chromatographic separation is essential to detect very small amounts of monoamines in the dialysates which need to be differentiated from other unidentified peaks that usually appear in higher amounts (*see* **Note 12**).

3.4.1 Chromatographic Conditions for Separation of Noradrenaline and Dopamine

One of the most typically used chromatographic methods for measuring monoamines in microdialysis samples is the reverse-phase ion-pair chromatography on C-18 column. Although different conditions can be performed, the following is the method currently performed in our laboratory.

NA and DA concentrations are measured immediately after collection of the samples by HPLC coupled to an electrochemical detector in the same running. Samples are collected every 35 min, and NA concentrations analyzed by HPLC apparatus with amperometric detection at an oxidizing potential of 0.300 mV. The mobile phase is filtered, degassed (Hewlett-Packard model 1200 degasser),

and delivered at a flow rate of 0.2 mL/min by a Hewlett-Packard model 1200 pump through the column. Usually, 35 µL of sample + 5µL of $HClO_4$ 0.1 M is injected (injection volume 30 µL) and NA and DA analyzed in a run time of 15 min (*see* **Note 13**).

A calibration curve has to be performed each day of the experiment (*see* **Note 14**).

Mobile phase:

- 50 mM phosphoric acid
- 0.1 mM EDTA
- 8 mM sodium chloride
- 500 mg L^{-1} sodium octyl sulfate
- pH = 6
- 16 % methanol

Preparation of mobile phase (2 L):

1. Dissolve 0.074 g of EDTA in 10 mL of Milli-Q water
2. Dissolve 0.94 g of NaCl and 6.8 mL of phosphoric acid in 1500 mL of Milli-Q water, and shake the solution.
3. Add EDTA solution.
4. Adjust to pH = 6 with NaOH 6N.
5. Add 1 g of octyl sulfate to solution.
6. Add 320 mL of methanol.
7. Add water to reach 2 L volume.
8. Filter mobile phase through a filter of 0.45 µm.

Chromatographic column

C18 column (ALF-205 150 × 2.1 mm, 3 µm; Antec® Leyden, Holland).

Oven temperature 35 °C.

In these conditions retention time for NA is 4 and 9 min for DA and the detection limit is 0.1 nM.

3.4.2 Chromatographic Conditions for Separation of Serotonin

Very similar conditions are used for serotonin detection. The same column and oven temperature, same equipment, and same detector parameters as for NA and DA quantification are used. The injection of 35 µL of volume is also performed from vials containing 35 µL of sample + 5 µL of $HClO_4$ 0.1 M. The mobile phase was the only modification performed in the method (50 mM phosphoric acid, 0.1 mM EDTA, 8 mM sodium chloride, 500 mg L^{-1} sodium octyl sulfate, pH = 6 and 27 % methanol).

In these conditions retention time for serotonin is 10 min and the detection limits is 0.1 nM.

4 Notes

1. For rat surgery the most used atlas is "The Rat Brain in Stereotaxic Coordinates." [6]. It is based on the flat-skull position. The coordinates were developed from the study of adult male Wistar rats with weights ranging from 250 to 350 g. It offers a choice of the bregma, lambda, or midpoint of the interaural line as the reference points. The atlas represents the areas of the brain from the olfactory bulb to the middle of the medulla oblongata, displayed in three levels. It is also used for male and female Sprague-Dawley rats at the same weight range.
   For mouse surgery the most used atlas is "The Mouse Brain in Stereotaxic Coordinates" [7]. It is a coronal atlas of C57BL/J6 mice (weight range 26–30 g). The use of the C57BL/J6 strain was chosen because it is one of the most widely used strains and is of intermediate size. Some adjustments for using this atlas with other strains can be calculated from Wahlsten et al. [8]. If necessary, pilot studies should be conducted to validate or adjust the coordinates.
2. Surgery in field conditions should be performed in an environment as clean as possible, with sterile instruments, sterile surgical gloves, and aseptic technique. All persons performing surgical techniques should have demonstrated ability in the surgical procedures required. The suite in which aseptic surgery is performed should consist of the following separate areas:
   - Support area which would include an area for storing instruments, packs, supplies, and for washing and sterilizing instruments.
   - Animal preparation area.
   - Operating room.
   - Recovery area adequate for postoperative support of animals.

   It is not recommended to perform surgery in an animal housing room.
3. Anesthetics: gas anesthetics have the advantage of requiring minimal detoxification by the body, as they are exhaled through the lungs, and the level of anesthesia can be easily and rapidly controlled. However, their use requires specialized equipment for administration. In contrast, injected anesthetics have been traditionally used. However when the level of anesthesia is higher than expected, it may be accompanied by respiratory depression and bradycardia which may progress to heart block. Some of the most commonly used anesthetics are pentobarbital (30–40 mg/kg i.p. in mouse and 40 mg/kg i.p. in rat), thiopental (30–40 mg/kg i.p. in mouse and 20–40 mg/kg i.p. in

rat), and ketamine/xylazine (200/10 mg/kg i.p. in mouse and 90/5 mg/kg i.p. in rat).

4. For stereotaxic surgery, a guide cannula can also be implanted above the region of interest. Before the experiment, the probe is inserted in the guide cannula.
5. Accordingly, the diffusion rate depends on the following factors:
   - Flow rate of the perfusion solution.
   - Diffusion resistance of the tissue matrix.
   - Physical characteristics of the molecule (shape, oil/water partition coefficient, charge).
   - Molecule concentration.
   - Dialysis membrane: pore size and probe length and diameter.
   - Temperature and pH nearby the microdialysis probe.
   - Composition of the perfusion fluid.
6. The efficiency of the probe can be measured in terms of absolute recovery or relative recovery. Absolute recovery refers to the total quantity of the substance transferred during a defined period of time. The second one refers to the concentration of the molecule retained inside the probe in relation to the extracellular concentration, expressed as percentage. These parameters can be evaluated in vitro to estimate the efficiency of a particular probe for a particular substance. Absolute and relative recoveries correlate positively and negatively with the perfusion flow rate, respectively. Larger dialysis membrane surface and higher temperatures increase the recovery. The optimal flow rates for brain microdialysis of monoamines are between 0.3 and 1.5 μL/min. Under these conditions in vitro recoveries reach until 15–25 % depending on the dialyzed substance.
7. In vivo microdialysis plus automated dosing, blood sampling, and behavior parameters. For microdialysis experiments, a no liquid swivel-based system can also be used. Unlike the swivel, the Raturn (BASi, West Lafayette, IN, USA) is a movement responsive caging system. Rather than the swivel turning, the cage itself interactively responds to animal movements to keep tubing and/or wires from twisting. The Raturn does not cause, or force, the animal to move and allow the possibility of adding other physiological parameter measurements in the animal controlled by a single notebook computer. The system is optimized for the following options:
   Blood sampling collection: the company has developed a robotic system that can collect serial blood samples from awake freely moving animals. One of the developed bowls for housing the

animals permits the collection of feces and urine, while microdialysis and blood samples are collected, and thus, pharmacokinetics/pharmacodynamics (PK/PD) experiments can be performed in the same animal.
Automated dosing: the system uses an infusion pump that allows programming single, multiple or continuous administration of drugs by different routes of administration (intravenous, gastric, intraperitoneal or duodenal).
Behavioral monitoring: the system allows monitoring frequency of turning behavior events and their duration.

8. The tubular membranes are widely used in perfusion cartridges of kidney dialyzers. All microdialysis probes use a polymeric dialysis membrane: cuprophane, cutoff 6000 Da; polycarbonate, cutoff 20,000 Da; polyamide, cutoff 20,000 Da; polysulfones, cutoff 15,000–35,000 Da; polyacrylonitrile (PAN), cutoff 30,000 Da; and polyarylethersulfone (PAES), cutoff 10,000 Da.
9. In vivo recovery of a substance is also influenced by many physiological variables as active transport across membranes into cells, presence of specific enzymes, or extent of tissue vascularization and blood flow. All these factors could limit the quantity of the substance recovered, and thus, it is necessary to perform pilot tests in order to evaluate the in vivo recovery and the availability of analytical procedures sensitive enough for ensuring the viability of the proposed experiment.
10. The concentration of monoamines in the extracellular space is very low because they are quickly removed by their respective reuptake transporters. With such low baseline extracellular levels, small changes are most likely within the range of background noise making their detection very difficult. To overcome this drawback, a low concentration of a serotonin uptake inhibitor (1 μM citalopram for serotonin measurements) or a noradrenaline uptake inhibitor (1 μM desipramine for noradrenaline and dopamine measurement) is usually added to the LCR. The monoamine concentration in the extracellular fluid responds to the equilibrium between release and reuptake processes. Thus, with the addition of an uptake blocker, the release component is magnified.
11. In the last years, HPLC methods coupled to LC/MS or LC/MS/MS have been used for the quantification of neurotransmitter concentrations. However, the high ionic strength for microdialysis samples generates high background noise resulting in considerable reductions in sensitivity. Recently, the development of modern electrochemical microflow cells designed for microdialysis and the use of more appropriate columns has increased the sensitivity of the HPLC-ECD techniques.

In addition, ultra high performance liquid chromatography (UHPLC) coupled to electrochemical detectors has been characterized for more efficient separation of monoamines in a short period of time. The use of a smaller column diameter results in more signal and overall in a better detection limit. Standard HPLC technique coupled to low diameter column and microflow cell amperometric detection is also possible and can avoid replacement of laboratory technical equipment.

12. Different analytical testing is required for the validation of the method:
    Accuracy : expresses the closeness agreement between the value found and the value that is accepted as either a conventional true value or an accepted reference value. It may often be expressed as the recovery by the assay of known, added amounts of analyte.

    Precision, defined by *repeatability*, the variation experienced by a single analyst on a single instrument. Repeatability does not distinguish between variation from the instrument or system alone and from the sample preparation process. Intermediate precision: refers to variations within a laboratory in different days, with different instruments, or by a different analyst.
    Specificity: specificity is the ability to assess unequivocally the requested analyte in the presence of components that may be expected to be present such as other neurotransmitters and metabolites.
    Detection limit: it represents the lowest amount of analyte that can be detected (but not necessarily quantified as an exact value). It is generally estimated from a determination of signal-to-noise 3:1.
    Quantify limit: the lowest amount of analyte in a sample that can be quantitatively determined with suitable precision and accuracy. Estimated by a signal-to-noise 10:1
    Linearity: it evaluates the analytical procedure's ability to obtain response that is directly proportional to concentration (amount) of analyte in the sample
    Range: the interval between the upper and lower concentrations of analyte in the sample for which it has been demonstrated that the analytical procedure has a suitable level of precision, accuracy, and linearity.

13. Changes in the mobile phase composition are often needed in order to optimize the precision and specificity of chromatographic conditions. For this purpose retention times and the order of elution of the different substances can be altered. The most usual strategies are
    - the increase of ion-pair reagents, such as octyl sulfate, and increased selectively retention of amines, whereas acid and neutral metabolites are not affected.

– The increase of the pH decreases the retention time of acid metabolites and has little effect on the monoamines.

– The increase on the modifier methanol decreases retention times of all sample components.

14. In chromatographic analyses, calibration curves are generated by analyzing standard analyte solutions of known concentration and measuring the resulting chromatographic peak area. The resulting plot is then used to determine the concentration of unknown sample solutions containing the same analyte. This is done measuring the unknown peak area (y) and using the equation for the line to solve for the concentration of the unknown (x). Although referred to as a curve, it is usually a linear plot with a well-defined slope and y intercept.

Acknowledgments

This work was supported by the Basque Government (IT616-13 and S-PE12UN033), the University of the Basque Country (UFI 11/35), Ministry of Economy and Competitiveness (SAF2009-08460; SAF2013-48586-R), and the Instituto de Salud Carlos III, Centro de Investigación Biomédica en Red de Salud Mental, CIBERSAM, Spain.

References

1. Zapata A, Chefer VI, Shippenberg TS (2009) Microdialysis in rodents. Curr Protoc Neurosci Chapter 7:Unit7.2.
2. Muller M (2013) Microdialysis in Drug Development. Springer, New York, NYWesterink BHC, Cremers TIFH (2007) Handbook of Microdialysis. Methods, Applications and Clinical Aspects. Elsevier, Amsterdam.
3. Westerink BHC, Cremers TIFH (2007) Handbook of Microdialysis. Methods, Applications and Clinical Aspects. Elsevier, Amsterdam.
4. Ortega JE, Fernández-Pastor B, Callado LF, Meana JJ (2010) In vivo potentiation of reboxetine and citalopram effect on extracellular noradrenaline in rat brain by the α2-adrenoceptor antagonist RS79948. Eur Neuropsychopharmacol 20: 813--822.
5. Ortega JE, Gonzalez-Lira V, Horrillo I, Herrera-Marschitz M, Callado LF, Meana JJ (2013) Additive effect of rimonabant and citalopram on extracellular serotonin levels monitored with in vivo microdialysis in rat brain. Eur J Pharmacol 709: 13--19.
6. Paxinos G, Watson C (1986) The Rat Brain in Stereotaxic Coordinates, second ed. Academic Press, Orlando, USA.
7. Franklin K, Paxinos G (2001) The mouse brain in stereotaxic coordinates. San Diego: Academic Press.
8. Wahlsten D, Hudspeth WJ and Bernhardt K (1975) Implications of genetic variation in mouse brain structure for electrode placement by stereotaxic surgery. J Comp Neurol 162: 519–-531.

Chapter 26

Calcium Transients in Single Dendrites and Spines of Pyramidal Neurons In Vitro

Rhiannon M. Meredith and Martine R. Groen

Abstract

Calcium levels within dendrites and spines rapidly change during synaptic activity and in response to action potential backpropagation following somatic firing. These calcium transients can be measured and quantified by a combination of whole-cell patch-clamp electrophysiology and two-photon calcium imaging methods using membrane-impermeable calcium-dependent indicator dyes. Such methods have been applied both in vivo in the intact brain and in vitro in acute brain slice preparations and neuronal cultures. Here, we describe a dual dye technique, using a calcium-dependent indicator in combination with a morphological calcium-independent marker dye, to measure action potential backpropagation in dendrites and spines. Calcium transients can be correlated with simultaneous electrical recordings made from the cell soma or dendrites to investigate, for example, modulation of both membrane voltage and intracellular calcium signals simultaneously at different spatial locations in the neuron or modulation by pharmacological ligands. We highlight the key advantages of this technique but also note the limitations and caveats of making dynamic measurements in small structures of living neurons.

Key words Calcium, Dendrite, Spine, Backpropagation, Action potential

1 Introduction

Calcium signalling in neurons underlies many important physiological processes, including synaptic plasticity [1], neuronal excitability [2], dendrite and spine growth [3, 4] and activation of gene expression [5]. To understand the role calcium plays in such processes, calcium-dependent indicator dyes have played a significant role as a tool to measure and quantify the dynamics of calcium signalling in relevant spatial and temporal domains.

Here, we present detailed methods and relevant examples to illustrate the use of calcium-dependent indicators in combination with whole-cell patch-clamp electrophysiology to determine the extent of backpropagation of action potentials into the dendritic tree of a neuron and the adjacent dendritic spines (Fig. 1) [6, 7]. In this context, the indicator provides an indirect readout of the

Rafael Luján and Francisco Ciruela (eds.), *Receptor and Ion Channel Detection in the Brain: Methods and Protocols*, Neuromethods, vol. 110, DOI 10.1007/978-1-4939-3064-7_26,

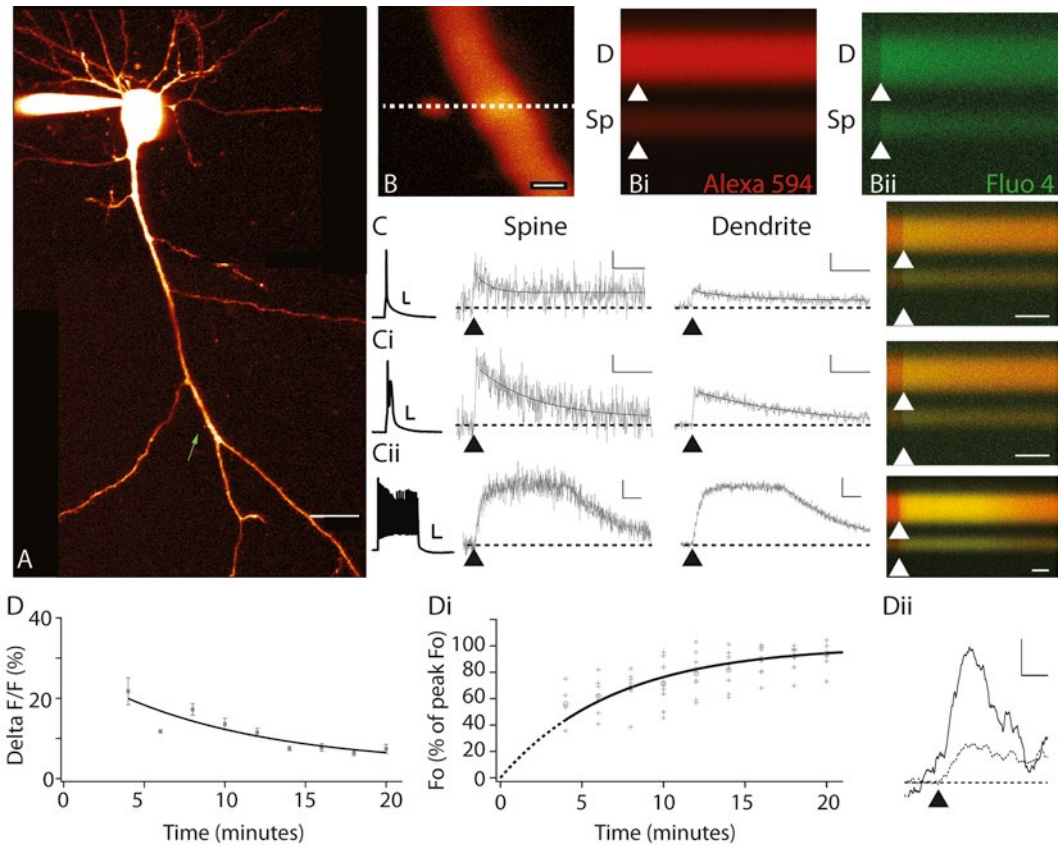

Fig. 1 Use of calcium indicators to measure AP-dependent backpropagation into dendrites and spines. (**a**) Whole-cell patch-clamp technique used to fill single neuron with morphological marker dye Alexa 594 and calcium-dependent indicator, Fluo-4. Scale bar 20 μm. *Green arrow* indicates apical dendrite region of interest (*ROI*) and spine. (**b**) Dendrite and spine ROI. *White line* indicates xt line scan. Scale bar 1 μm. (**b**i, **b**ii) xt line scans of dendrite and spine simultaneously for Alexa 594 (*red*) and Fluo-4 (*green*) signals following BAP after 80 ms (indicated by *arrowhead*). (**c**) Quantification of calcium transients following single BAP (*left*) in spine and dendrite ROI (*middle*) with corresponding xt line scan of 500 ms duration. Scale bars from *left* to *right*: 20 mV, 2 ms; 5 % $\Delta F/R$, 200 ms; line scan scale bar 100 ms. (**c**i) Respective calcium transients for same ROIs in (**c**) but following 2 APs during 20 ms stimulation. Scale bars as (**c**). (**c**ii) Respective calcium transients for same ROIs in (**c**) following 1 s AP train stimulation. Scale bars from *left* to *right*: 20 mV, 20 ms; 10 % $\Delta F/R$, 200 ms; line scan scale bar 200 ms. (**d**) *Left panel*, $\Delta F/F$ using OGB1 indicator for dendrite ROI of cortical pyramidal neuron of BAP repeated every 2 min. (**d**i) Baseline fluorescence measurement in dendrite ROI at corresponding time points following breakthrough of whole-cell patch at cell soma ($n = 8$ cells). (**d**ii) Respective fluorescence transient examples from time points at 6 and 18 min, respectively, in one example dendrite following soma breakthrough to reveal change in dendritic calcium transient in response to single BAP. Scale bars 5 % $\Delta F/R$, 50 ms. *Arrowhead* indicates AP induction at cell soma

change in membrane excitability caused by the action potential/s backpropagating along the dendritic tree, but one which is correlated to the level of neuronal activation. One clear advantage of these indicators is their ability to diffuse into thin dendrites and dendritic spines and provide readout signals in a replicable pattern

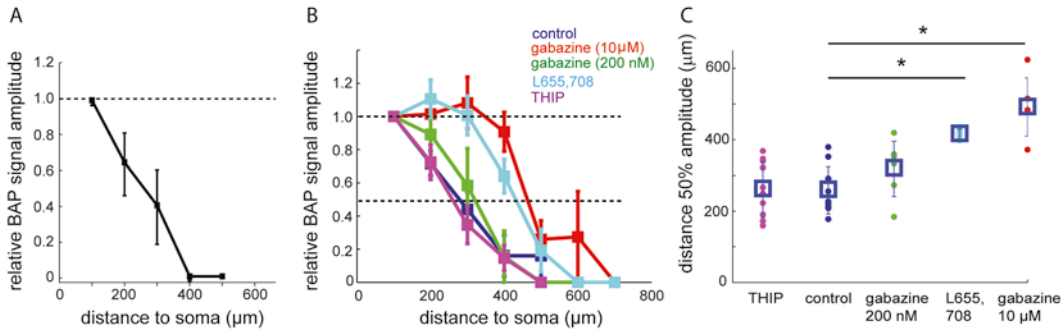

Fig. 2 Modulation of calcium transients along distance gradient and by selective pharmacological blockade. (**a**) Example ΔF/R for different distance measures from the cell soma along CA1 pyramidal dendrites in control ACSF conditions (Adapted from Sterratt et al. [8]). (**b**) Modulation of distance-dependent backpropagation along CA1 pyramidal dendrites in control ACSF (*blue*) and in response to separate application of different GABA(A) receptor antagonists: gabazine (10 μm, *red*), gabazine (200 nM, *green*), alpha5-subunit preferential antagonist L655,708 (100 nM, *light blue*) and delta-subunit preferential antagonist (4,5,6,7-tetrahydroisoxazolo[5,4-c] pyridin-3-ol) (THIP, 10 μm, *purple*). (**c**) Corresponding distance at which amplitude of calcium dye transient in response to backpropagation signal decreased by 50 % relative to signal taken at 100 μm from cell soma. Colour coding as in (**b**) (Adapted from Groen et al. [9])

from locations that are not accessible to recording pipettes to directly measure electrical changes in the membrane. In addition, one can measure calcium transients at multiple locations simultaneously. We demonstrate the modulation of backpropagating somatic action potential (BAP)-induced calcium transients along the apical dendrite, which decrement with increasing distance from the cell soma due to electrotonic filtering properties (Fig. 2, [9–12]). Furthermore, the relative change in this gradient measured along the dendrite can be modified by pharmacological blockade, as illustrated by the use of specific antagonists for the GABA(A) receptor and two of its subunits (Fig. 2b, c).

Calcium transients within a neuron are shaped by many factors including the source of calcium ions, the buffering capacity of endogenous proteins or loaded indicator dyes and both the diffusion within and extrusion mechanisms across the cell membrane [13, 14]. These regulatory properties raise a number of important technical caveats to take into consideration when performing experiments and interpreting results and are essential for further quantification of individual calcium transients [13, 15]. Therefore, technical considerations such as indicator dye properties and concentration levels diffused into the region of interest for imaging are discussed within the Notes section in this guide.

The techniques described here were performed in vitro in acute brain slice preparations of rodent prefrontal cortex and hippocampus, combining patch-clamp electrophysiology with multiphoton imaging. This protocol can be adapted for use in other

acute neuronal slice preparations, including adult human brain [16] and in cultured neurons [17].

2 Materials

2.1 Acute Brain Slice Preparation

1. Extracellular solution (final concentration in mM): 125NaCl, 3 KCl, 1.2 NaH_2PO_4, 2 $CaCl_2$, 1 $MgSO_4$, 10 glucose and 26 $NaHCO_3$. Stock solution (10×) containing NaCl, KCl and NaH_2PO_4 can be made in advance and stored at 4 °C for a week. $CaCl_2$, $MgSO_4$, glucose and $NaHCO_3$ need to be added on the day of recording.
2. Slicing solution (**Note 1**) (final concentration in mM): 110 choline chloride, 11.6 Na-ascorbate, 3.10 Na-pyruvate, 2.50 KCL, 1.25 NaH_2PO_4, 7 $MgCl_2$, 0.50 $CaCl_2$, 10 glucose, 26 $NaHCO_3$. Stock solution (10×) containing choline chloride, Na-ascorbate, Na-pyruvate, KCL, NaH_2PO_4, $MgCl_2$ and $CaCl_2$ can be made in advance and stored in the fridge for up to a month. Glucose and $NaHCO_3$ need to be added on the day of the recording.
3. Carbogen supply (5 % CO_2 and 95 % O_2 mixture)

2.2 Acute Brain Slicing

1. Large scissors or guillotine for rodent decapitation
2. Slice chamber which allows the storage of individual slices, containing carbogen-perfused extracellular solution
3. Waterbath to be heated up to 35 °C
4. Vibratome (e.g. LEICA VT1000S)

2.3 Preparation for Patching

1. Intracellular solution (in mM): 148 K-gluconate, 1 KCl, 10 HEPES, 4 Mg-ATP, 4 K_2 phosphocreatine, 0.4 GTP and 0.2% biocytin, pH adjusted to 7.3 with KOH. Choice of intracellular solution can vary, but ensure it does not contain a calcium chelator, e.g. ethylene glycol tetraacetic acid (EGTA) often added to specific intracellular solutions for cultured neurons.
2. Micropipette puller (i.e. Sutter Instruments P1000).
3. Calcium dye, excited at 830 nm: Fluo-4 pentapotassium salt (200 μM, Figs. 1a–c and 2) or Oregon Green BAPTA-1 hexapotassium salt (OGB1, 100 μM, Fig. 1d) excited at 810 nm. Fluo-4 and OGB1 dye aliquots can be stored in advance in the dark at −20 °C in individual vials of 5 mM dissolved in 2 μL intracellular solution.
4. Morphological marker dye, excited at 830 nm: Alexa 594 hydrazide cell impermeable sodium salt (80 μM). Alexa 594 aliquots can be stored in advance in the dark at −20 °C in individual vials of 2 mM dissolved in 2 μL intracellular solution.

2.4 Patch-Clamp Electrophysiology and Simultaneous Calcium Imaging

1. Combined two-photon imaging and electrophysiology rig which includes:
   - Electrophysiology set-up
   - DIC illumination or equivalent to visualise cells and direct targeted patching
   - Tunable laser which can emit 810–830 nm light (i.e. Ti:sapphire laser)
   - High-magnification water immersion objective (i.e. 63×) with high NA
   - Two PMTs to collect the emission light
   - Appropriate filters and dichroic mirrors to split the emission light from Alexa 594 and Fluo-4 dyes

3 Methods

3.1 Acute Brain Slice Preparation

1. Freshly prepare extracellular (1000 mL) and slicing solutions (500 mL) (**Note 1**).
2. Bubble both solutions with carbogen for at least 20 min.
3. Check osmolarity of solutions (295–305 mOsm).
4. Put 250 mL of slicing solution in freezer, for the next experiment.
5. Take 250 mL previously frozen slicing solution, and mix with the fresh slicing solution, using a kitchen mixer to make a smooth ice-cold solution. Split this solution in two parts, one to chill the brain immediately after decapitation and one for use in slicing the brain using the vibratome.

3.2 Acute Brain Slicing

1. Decapitate rodent and quickly remove the brain in ice-cold slicing solution.
2. Using a sharp razor knife, make a clean cut to the brain to make a flat section for gluing to the vibratome chuck. The location and orientation of this cut depend on the region investigated (**Note 2**).
3. Glue the brain to the vibratome chuck, and quickly submerge it in the slicing chamber filled with ice-cold choline solution, perfused with carbogen. Speed is required in **steps 1** until **3**, to minimise cell damage.
4. Use the vibratome to make brain slices of 300 or 350 μm thickness.
5. Transport the slices using a pipette into a slice chamber containing extracellular solution constantly bubbled with carbogen and heated to 32 °C using a water bath.
6. After making the final slice, leave the slice chamber in the heating bath for a further 10 min, and then transfer to room temperature for a recovery period of 1 h.

For a video of the slicing process, see similar methods demonstrated in [18].

3.3 Preparation for Patching

1. Pull glass pipettes using a vertical or horizontal puller (e.g. Sutter Instruments P1000) with a 4–6 MΩ resistance. Store the pipettes in a closed box to prevent clogging with dust.
2. Thaw premade intracellular solution and mix with dyes (*see* **Notes 3** and **4**).
3. Filter intracellular solution using a microfilter tip, and store the filtered solution on ice to prevent degradation of GTP and ATP.
4. Perfuse the recording chamber of the electrophysiology set-up with carbogen-saturated extracellular solution, ensuring a constant temperature of 32 °C.

3.4 Whole-Cell Patch-Clamp Recording of a Neuron

1. Place an acute slice in the recording chamber, ensuring the dendrites are intact and in the right orientation (**Note 2**).
2. Fill the pipette with the intracellular solution ensuring all air bubbles are removed. In case of non-filamented glass pipettes, tip filling the pipette with non-dye-containing intracellular solution and backfilling the pipette with solution containing the relevant dyes can help to achieve this.
3. Using visualisation from DIC microscopy, select and patch a neuron of interest. Aim for a low and stable series resistance (<20 MΩ) during the recording, to ensure sufficient and fast dye diffusion (*see* **Note 5**) and accurate electrophysiological recordings.
4. For mature CA1 pyramidal neurons, wait for 20 min in whole-cell recording configuration, to ensure a sufficient and stable dye concentration in the dendrites while monitoring cell health (holding current, series resistance, input resistance) (*see* **Note 5**, Fig. 1a, d).

3.5 Calcium Imaging of Dendrite and Spines

1. Select a region of interest for line scans including dendrite, adjacent background area and (optional) spine (Fig. 1a, *see* **Note 6**).
2. Excite the indicator dyes with an appropriate wavelength (830 nm in case of Alexa 594 and Fluo-4 combined) for two-photon imaging.
3. Collect the emitted fluorescence using photomultiplier tubes (PMTs) with the appropriate dichroic mirrors and filters (Fig. 1b).
4. Repeat the scanning for different stimulation conditions and different regions of interest (examples illustrated for dendrite with spine and different dendritic regions in Figs. 1b, c and 2a,

respectively), ensuring that there is no movement or photobleaching (**Note 8**). Per scanned region, make a single xy scan after completion of (xt) line scans to mark the scanned location.

5. At the end of the imaging, make a detailed z-stack (including stitching of overlapping z-stacks if the cell's dendritic tree is too large for a single point of view) to determine the exact location of the scanned region (Fig. 1a).

3.6 Calcium Fluorescence Analyses

1. Calculate the $\Delta F/R$ ratio according to [13]

$$\Delta F/R = \frac{F - F_{baseline}}{R - R_{baseline}} \quad (1)$$

where F is the fluorescence intensity from the calcium dye (Fluo-4) and R is the fluorescence of the voltage and calcium insensitive red dye (Alexa 594). By correcting for the fluorescence in the red channel, one can exclude the differences in amplitudes due to differences in effective power at the imaging location between different samples (*see* **Note 4**). In addition, it can control for movements, as the red dye intensity should not change significantly between successive line scans during the recording. If this is the case, the recording should be excluded from further analysis.

2. Calculate the calcium dynamics by fitting one of the following functions:

$$\Delta F/R = Ae^{-t/\tau_{decay}} \quad (2a)$$

$$\Delta F/R = A(e^{-t/\tau_{decay}} - e^{-t/\tau_{rise}}) \quad (2b)$$

where τ_{decay} and τ_{rise} are, respectively, the rise and decay time constants of a single (Eq. 2a) and double exponential (Eq. 2b) (Fig. 1c). Note that this fitting is only applicable for short signals such as backpropagation of single or bursts of action potentials and does not capture the signal dynamics of a plateau as observed following a tetanic train of action potentials (Fig. 1cii).

This technique can be used to analyse calcium dynamics in both dendrites and spines (Fig. 1b, c), at different locations in the dendritic tree (Fig. 2a) or under different types of GABAergic inhibition (Fig. 2b, c).

4 Notes

1. Choice of slicing solution
   Calcium imaging in dendrites can be carried out in neurons from all developmental ages. However, the choice of slicing medium for optimal cell and dendrite health in the slice preparation depends on animal age and brain region. This protocol uses choline solution, shown to work with adult neurons of the hippocampus and cortex, but others have used sucrose [19] or a solution containing a relatively high magnesium concentration with respect to calcium (7 mM Mg^{2+}, 0.5 Ca^{2+} in standard extracellular solution, *see* Sect. 2.1) for different ages and regions. When looking at the brain slice surface under DIC, the slice should contain numerous healthy cells.
2. Orientation of the slice
   For accurate dendritic calcium imaging, an intact dendritic tree is essential. Standard DIC methods, used to guide patching, show only cell bodies and the initial part of the apical dendrite. In addition, only the most superficial cell body layers are visible. However, the dendritic tree spreads hundreds of micrometres into the slice and is often cut during the slice preparation. Therefore, it is important to ensure a proper cutting orientation, which maximises the intact dendritic tree available for the neurons of interest. Optimal dendritic recordings are made when the cell body is located within the third cell body layer below the surface (approximately 50–100 μm depth), and the dendrite of interest is pointing into the acute slice, ensuring that it is not cut.
3. Selection of dyes and interference with normal cell function
   The mechanism behind calcium indicator dye fluorescence is a conformational change of the molecule upon binding to calcium. The rate of binding and release of the calcium molecule is dye specific. It is therefore very important to select a dye with fast enough kinetics to capture the process investigated and with appropriate binding affinity and concentration for the signal being measured [20]. For example, many interneurons fire at significantly higher rates than pyramidal neurons and have higher endogenous calcium-binding ratios [21]. Therefore, a dye used for pyramidal neurons might not be suited for use in specific interneurons. More recently, different varieties of genetically encoded calcium indicators (GECIs) have been developed. This allows expression of calcium dyes in a genetic subset of neurons. Note that if using this strategy, one should ensure sparse expression, to visualise isolated dendrites and spines [22].

   Since dye fluorescence is based on the binding of calcium to the dye molecule, this will interfere with endogenous buffering

processes, normal cell function and synaptic plasticity [23]. Therefore, if one is also interested in the result of the calcium changes, one should select a dye with low affinity to keep a sufficient amount of unbound calcium for activation of other intracellular functions. Alternatively, replicate the stimulation protocol in separate cells with indicator dyes to measure calcium transients and without indicators present to measure synaptic plasticity [23].

4. Use of a second, calcium- and voltage-insensitive dye as an internal reference
   When a change in calcium signal is detected, this could either be a valid signal or movement of the dendrite/spine out of focus. When using an additional, calcium- and voltage-insensitive dye such as Alexa 594, a movement-induced change will also be detected in the second dye. Such a recording should then be discarded.

   Another advantage of using the morphological marker dye fluorescence of Alexa 594 as a reference is the change in effective power in different regions of the dendrites: Deeper dendrites will have weaker calcium fluorescence than shallower neighbours due to a difference in the excitation laser power. The signal amplitude of the marker dye will scale down with power equally with the green channel, allowing the amplitude of the ratio to be compared between branches.

5. Dye diffusion
   Both the amplitude and dynamics of the calcium fluorescence are dependent on the dye concentration at the region of interest imaged (Fig. 1d). It is therefore essential to wait until dye concentration in the dendrite of interest has stabilised. For adult pyramidal cell apical dendrites, the minimum waiting time is 20 min. The required waiting time is dependent on the distance from soma, dendrite diameter, dye and cell type. It is therefore best to determine the required waiting time for your research question, by recording the calcium fluorescence induced by a fixed number of induced action potentials, at fixed intervals after the start of whole-cell configurations (e.g. $t = 5$ min, $t = 10$ min, $t = 15$ min, $t = 20$ min, etc.), until baseline (F0), delta F signal amplitude and dynamics are stable (Fig. 1di, dii).

6. Line scan selection
   Due to selection of a small region of interest, line scans allow the user to scan at higher temporal resolution than full-frame imaging. Temporal frequency of scanning is dependent on the biological signals and process investigated (*see* **Note 3**). In the examples given here, the line is scanned bidirectionally at 1 or 8 kHz for 0.5–1 s durations. Modern two-photon microscopes

allow a manual line scan selection, optimising the scan time spent on dendrites, background and spines. By zooming in to a small dendritic region, one can increase the number of points per ROI and therefore the signal to noise.

7. Movement
   This method requires a high level of stability of the preparation. If movement is present during the recording, the region of interest will shift, and signals cannot be reliably detected. Movement could arise from vibrations from the building or chiller unit of the laser, which can be minimised by the use of an air-table. In addition, equipment cables should always be without tension as they can transmit vibration to the rig. The slice preparation should be stabilised from perfusion-induced movement by placing a metal harp with nylon strings on top of the slice. Ensure the harp is correctly aligned so as not to put pressure or overlap the dendrites of interest and should preferably only touch adjacent regions not under investigation.
8. Photobleaching and phototoxicity
   When dyes are excited by excessive levels of laser power, their fluorescence will decrease over time, a process called photobleaching. To enable discrimination of a true decrease in the calcium transient from that due to photobleaching, one should minimise bleaching by using minimal laser power for excitation and reducing the time the dye is exposed to the laser.

   In addition excessively high laser power can cause damage to the dendrite and spine, by locally heating up the scanned region (phototoxicity). Dendrites will often start to swell and bleb if this occurs. Again, reducing the laser power and/or the exposure time can prevent this damage.

References

1. Sjostrom PJ, Nelson SB (2002) Spike timing, calcium signals and synaptic plasticity. Curr Opin Neurobiol 12(3):305–314
2. Kennedy MB (1989) Regulation of neuronal function by calcium. Trends Neurosci 12(11): 417–420
3. Sin WC et al (2002) Dendrite growth increased by visual activity requires NMDA receptor and Rho GTPases. Nature 419(6906):475–480
4. Engert F, Bonhoeffer T (1999) Dendritic spine changes associated with hippocampal long-term synaptic plasticity. Nature 399(6731):66–70
5. Bengtson CP, Bading H (2012) Nuclear calcium signaling. Adv Exp Med Biol 970:377–405
6. Spruston N et al (1995) Activity-dependent action potential invasion and calcium influx into hippocampal CA1 dendrites. Science 268(5208):297–300
7. Gasparini S et al (2007) Associative pairing enhances action potential back-propagation in radial oblique branches of CA1 pyramidal neurons. J Physiol 580(Pt.3):787–800
8. Sterratt DC et al (2012) Spine calcium transients induced by synaptically-evoked action potentials can predict synapse location and establish synaptic democracy. PLoS Comput Biol 8(6):e1002545
9. Groen MR et al (2014) Development of dendritic tonic GABAergic inhibition regulates excitability and plasticity in CA1 pyramidal neurons. J Neurophysiol 112(2):287–299
10. Koester HJ, Sakmann B (2000) Calcium dynamics associated with action potentials in

single nerve terminals of pyramidal cells in layer 2/3 of the young rat neocortex. J Physiol 529(Pt 3):625–646
11. Waters J, Helmchen F (2004) Boosting of action potential backpropagation by neocortical network activity in vivo. J Neurosci 24(49): 11127–11136
12. Rall W (1962) Theory of physiological properties of dendrites. Ann N Y Acad Sci 96:1071–1092
13. Sabatini BL, Oertner TG, Svoboda K (2002) The life cycle of Ca(2+) ions in dendritic spines. Neuron 33(3):439–452
14. Helmchen F, Imoto K, Sakmann B (1996) Ca2+ buffering and action potential-evoked Ca2+ signaling in dendrites of pyramidal neurons. Biophys J 70(2):1069–1081
15. Maravall M et al (2000) Estimating intracellular calcium concentrations and buffering without wavelength ratioing. Biophys J 78(5): 2655–2667
16. Verhoog MB et al (2013) Mechanisms underlying the rules for associative plasticity at adult human neocortical synapses. J Neurosci 33 (43):17197–17208
17. Larkum ME, Rioult MG, Luscher HR (1996) Propagation of action potentials in the dendrites of neurons from rat spinal cord slice cultures. J Neurophysiol 75(1):154–170
18. Dawitz J et al (2011) Functional calcium imaging in developing cortical networks. J Vis Exp (56):3550. doi:10.3791/3550
19. Kuenzi FM et al (2000) Reduced long-term potentiation in hippocampal slices prepared using sucrose-based artificial cerebrospinal fluid. J Neurosci Methods 100(1–2):117–122
20. Grienberger C, Konnerth A (2012) Imaging calcium in neurons. Neuron 73(5):862–885
21. Kaiser KM, Zilberter Y, Sakmann B (2001) Back-propagating action potentials mediate calcium signalling in dendrites of bitufted interneurons in layer 2/3 of rat somatosensory cortex. J Physiol 535(Pt 1):17–31
22. Chen TW et al (2013) Ultrasensitive fluorescent proteins for imaging neuronal activity. Nature 499(7458):295–300
23. Nevian T, Sakmann B (2006) Spine Ca2+ signaling in spike-timing-dependent plasticity. J Neurosci 26(43):11001–11013

Chapter 27

Dynamic Recording of Membrane Potential from Hippocampal Neurons by Using a FRET-Based Voltage Biosensor

Víctor Fernández-Dueñas, Xavier Morató, Thomas Knöpfel, and Francisco Ciruela

Abstract

Fluorescence-based biosensors for membrane voltage (mV) allow dynamic optical recording of neuronal activity. Interestingly, the development of genetically encoded voltage indicators constitute a good alternative to classical voltage-sensitive dyes, thus allowing overcoming some of the inherent problems (e.g., optical noise, etc.) associated with these organic compounds. Here, we show the use of a genetically encoded voltage-sensitive fluorescent protein (VSFP), namely the VSFP2.32, which contains a mCerulean and Citrine tandem engaging in a constitutive fluorescent resonance energy transfer (FRET) process. By expressing VSFP2.32 in hippocampal cultured neurons, we were able to monitor mV alterations in single neurons by recording VSFP2.32 conformation-mediated FRET changes in a real-time mode.

Key words FRET, Voltage indicators, Neuronal membrane potential

1 Introduction

The precise analysis of neuronal network dynamics within the active brain requires simultaneous recording of multiple neuron activities with a sharp spatiotemporal resolution. Interestingly, molecular probes (i.e., biosensors) that convert biophysical and/or biochemical cellular events into measurable alterations in light intensity have been successfully developed (for review, *see* [1]). Since biosensors allow a compelling and less invasive option to monitor cellular functions in living single cells, tissues, and entire organisms, they have became an outperform option in front of other classical approaches (e.g., electrode-based techniques). Indeed, biosensors in general and fluorescence-based biosensors in particular have great advantages compared to other transduction methods and are by far the most often applied approach [2]. In such way, the main advantage of fluorescence-based biosensors

Rafael Luján and Francisco Ciruela (eds.), *Receptor and Ion Channel Detection in the Brain: Methods and Protocols*, Neuromethods, vol. 110, DOI 10.1007/978-1-4939-3064-7_27,

consists of the ability to assess repetitive analysis and to gauge continuous monitoring (i.e., real time) of the analyte [2]. For instance, optical imaging based on voltage-sensitive dyes offers enough spatiotemporal resolution to fulfill the necessary electrophysiological requirements [3, 4]. Indeed, there are several other advantages of using fluorescent-based biosensors: (1) moderately low costs in design and synthesis, (2) high solubility in water, and (3) genetic refinement likelihood. Importantly, the development of genetically encoded fluorescence-based biosensors was doable thanks to the concomitant expansion of the multi-color palette of fluorescent proteins (FPs) [5]. Hence, the strategy most commonly used to produce a FP-based biosensor involves the molecular fusion of the transducer protein to a pair of FPs that are suitable for engaging in a fluorescent resonance energy transfer (FRET) process [6]. In such way, the FRET efficacy between FPs may serve as readout of the transducer protein structural state. Indeed, the analyte-mediated conformational modifications promote opposing changes in donor and acceptor FPs signal; thus, the ratiometric measurement of FP intensities provides a measure of analyte concentration that is independent of FP concentration, excitation light intensity, and absorption in the optical path [6]. Interestingly, another often alternative approach consists of fusing a conformation-sensitive green fluorescent protein (GFP)-based reporter to a transducer protein, which undergoes conformational rearrangements upon analyte detection [6]. Accordingly, a circularly permuted FP (cpFP) is fused to the sensor protein, which upon analyte detection is able to convey small conformational changes through the FP interface, thus inducing chromophore quenching [6].

Fluorescence-based biosensors for membrane voltage (mV) have been largely explored in order to enable optical imaging of neuronal circuits [7]. Initially, classical voltage-sensitive dyes (i.e., low-molecular-weight organic compounds) were extensively used, and more recently genetically encoded voltage indicators were developed, thus becoming a good alternative surpassing several inherent limitations of classical voltage-sensitive dyes [7]. Here, we report the use of a voltage-sensitive fluorescent protein (VSFP), which exploits the voltage-dependent conformational changes of a voltage-sensor domain coupled to a FRET compatible FP pair. Indeed, the voltage sensor domain of *Ciona intestinalis* voltage sensor-containing phosphatase (Ci-VSP) [8], a natural monomeric protein, fused to a tandem of FRET-compatible FPs (Fig. 1a), was in fact the first effective genetically encoded voltage indicator [9]. This family of voltage biosensors was named as VSFP2s, and the variant VSFP2.3 was the first FRET-based genetically encoded voltage biosensor that enabled optical imaging of spontaneous action and synaptic potentials in neurons [10, 11]. Overall, in the present chapter we describe the use of a new VSFP2.3 variant, the VSFP2.32, as an optical voltage reporter from targeted primary hippocampal neurons in culture.

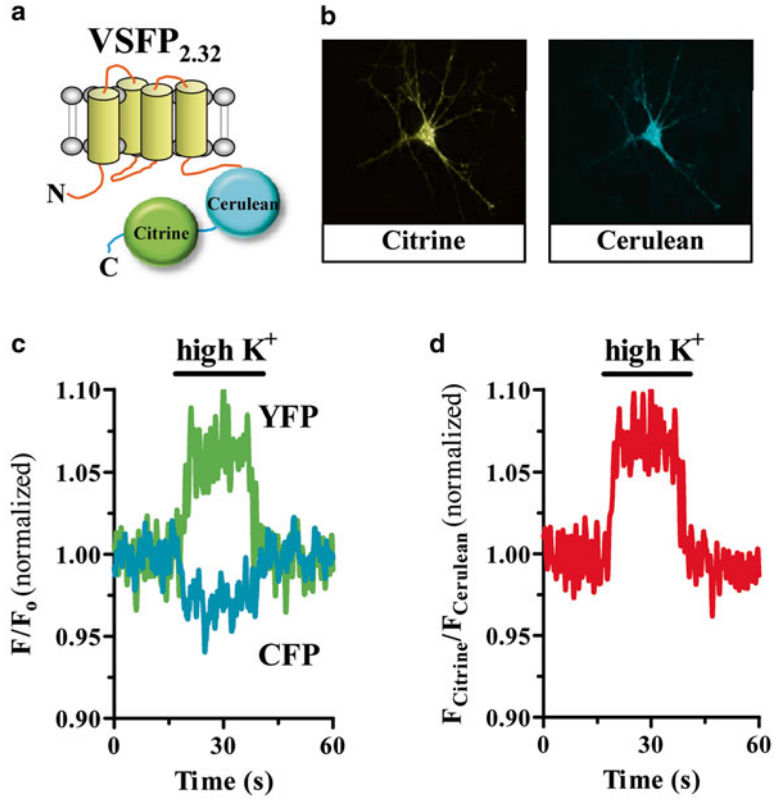

Fig. 1 (**a**) Schematic representation of the FRET-based voltage biosensor VSFP 2.32. (**b**) Expression of VSFP 2.32 in primary neuronal cultures. mCerulean and Citrine were visualized at 480 nm (mCerulean) and 535 nm (Citrine) upon excitation at 430 and 515 nm, respectively, using an inverted microscope. Scale bar: 10 μm. (**c**, **d**) Time-resolved changes in mCerulean and Citrine fluorescence emission signals in single cells transfected with VSFP 2.32. The emission intensities of mCerulean (*blue trace*), Citrine (*yellow trace*), and the ratio $F_{Citrine}/F_{mCerulean}$ (*red trace*) in low K^+ solution were recorded simultaneously. Shown are the changes induced by rapid superfusion with high K^+ solution. Traces are representative of five separate experiments

2 Materials

2.1 Animals

1. Sprague-Dawley rats (Charles River Laboratories, L'Arbresle, France) (*see* **Note 1**).

2.2 Buffers and Reagents

1. HBSS, Hank's Balanced Salt Solution (Gibco, Gran Island, NY, USA).
2. Trypsin (Sigma-Aldrich, St. Louis, MO, USA).
3. Poly-D-lysine (Sigma-Aldrich).
4. Plating media: Minimum essential medium (Invitrogen, Carlsbad, CA, USA) supplemented with 10 % horse serum, 1 mM pyruvic acid, and 0.59 % glucose.

5. Maintenance media: Neurobasal medium (GIBCO) supplemented with penicillin (100 U/mL) and streptomycin (100 μg/mL) (Biowest), 0.59 % glucose, and B27 1× (B27-Supplement GIBCO 50×).
6. Cytosine arabinoside (AraC) (Sigma-Aldrich).
7. 2× HBS (HEPES buffered saline, pH = 7.2): 274 mM NaCl, 10 mM KCl, 1.5 mM Na2HPO4, 11 mM Dextrose, 42 mM HEPES.
8. TE (Tris-EDTA pH7.3): 5 mL 1 M Tris-HCl (pH = 7.5), 2 mL 250 mM EDTA (pH = 8.0) in a final volume of 500 mL of H_2O
9. Kyanurenic acid (Sigma-Aldrich).
10. Low potassium (low-K^+) solution: 145 mM NaCl, 5 mM KCl, 2 mM $CaCl_2$, 1 mM $MgCl_2$, 5 mM HEPES; pH7.4.
11. High-potassium (high-K^+) solution: 125 mM NaCl, 25 mM KCl, 2 mM $CaCl_2$, 1 mM $MgCl_2$, 5 mM HEPES; pH7.4.

2.3 Instrumentation, Equipment, and Software

1. Inverted Axio Observer microscope (Axio Observer D1; Zeiss, Oberkochen, Germany) equipped with a 63× oil immersion objective.
2. Polychrome V (TILL Photonics, Gräfelfing, Germany).
3. Octaflow (ALA Scientific Instruments, Westbury, NY, USA).
4. Avalanche photodiodes (TILL Photonics).
5. Digidata 1440A analog/digital converter (Molecular Devices, Sunnyvale, CA, USA).
6. pCLAMP software (Molecular Devices).
7. GraphPad Prism software (GraphPad Software, La Jolla, CA, USA).
8. Attofluor holder (Life Technologies, Carlsbad, CA, USA).

3 Methods

3.1 Preparation of Primary Hippocampal Neuronal Cultures

1. Dissect hippocampi from 0- to 2-day-old rats and keep in ice-cold HBSS.
2. Incubate in 1.25 % trypsin for 10 min at 37 °C and keep back to ice-cold HBSS medium.
3. Dissociate hippocampi mechanically with a flame polished Pasteur pipette until a homogeneous cell suspension is obtained (*see* **Note 2**).
4. Plate neuronal cells (250,000 cells) onto poly-D-lysine-coated (0.1 mg/mL) 18 mm diameter round glass or plastic coverslips in plating medium (*see* **Notes 3** and **4**) with a 1 mL final volume/well.

5. Keep neurons at 5 % CO_2, 37 °C and 95 % humidity.
6. Substitute plating medium for maintenance medium after 4–14 h.
7. Add AraC (5 μM) at day in vitro 3 (DIV3) (*see* **Note 5**).
8. Transfect hippocampal primary cultures at DIV7.

3.2 Transfection of the Voltage Biosensor in Primary Hippocampal Neuronal Cultures

1. Dilute 4 μg of plasmid DNA encoding the VSFP2.32 construct (Fig. 1a) in 1× TE (pH = 7.3) to a final volume of 22.5 μL and vortex gently (*see* **Note 6**).
2. Add 2.5 μL of 2.5 M $CaCl_2$ in 10 mM HEPES pH 7.2 to the DNA/TE solution and gently mix with the pipette (*see* **Note 7**).
3. Add the DNA/$CaCl_2$/TE solution drop wise to 25 μL of 2× HBS (pH = 7.2) and allow the precipitate to develop at room temperature, for 30 min, and protected from light, vortex every 5 min.
4. Transfer coverslips with hippocampal primary cells to a new 12-well plate containing 200 μL of its original conditioned maintenance medium plus 50 μL of kynurenic acid (10 mM) (*see* **Note 8**) and maintain plates in the incubator until the DNA/$CaCl_2$/TE/HBS precipitate is ready.
5. Add 50 μL of the DNA/CaCl2/TE/HBS precipitate, dropwise, to each well with the coverslips and move the plate slowly to distribute the precipitate homogenously in all the well surface, without swirling (300 μL final volume/in the well plate).
6. Incubate the cultures with the precipitate for 4–8 h into the incubator.
7. Wash cells replacing the precipitate-containing medium for a mix of pre-warmed neurobasal medium plus kynurenic acid (10 mM) and leave the plate 30 min in the incubator (*see* **Note 9**).
8. Transfer each coverslip back to the original 12-well plate containing the original conditioned medium (800 μL) and add 250 μL of new fresh maintenance medium.
9. Return the cells to the 37 °C/5 % CO_2 incubator and allow neurons to express the voltage biosensor until DIV14.

3.3 FRET Assay in Hippocampal Neurons Expressing the Voltage Biosensor

1. Wash coverslips once with low K^+ solution containing 1 g/L glucose (*see* **Note 10**).
2. Mount coverslips in the Attofluor holder and place on the inverted Axio Observer microscope equipped with a 63× oil immersion objective and the dual-emission photometry system.
3. Switch on the Polychrome at the corresponding donor excitation (mCerulean, 430 ± 10 nm) or acceptor excitation wavelengths (Citrine, 515 ± 10 nm) (beam splitter dichroic long-pass

(DCLP) of 460 nm) to capture an image of the cell upon study (Fig. 1b) (*see* **Note 11**).

4. Change the Polychrome mode from image acquisition protocol to FRET illumination protocol (*see* **Note 12**).
5. The emission fluorescent signals of donor (Citrine emission: 535 ± 15 nm; F_{535}) and acceptor (mCerulean emission: 480 ± 20 nm; F_{480}) (beam splitter DCLP of 505 nm) are detected by photodiodes and digitized using a analog/digital converter. FRET is monitored as the emission ratio of Citrine to mCerulean (F_{535}/F_{480}).
6. Start superfusion of low K^+ solution using the Octaflow system and initiate FRET signals recordings.
7. After 30 s, exchange the superfusion valve to the one containing the high-K^+ solution (*see* **Note 13**).
8. After 20 s, the valve is exchanged again to perfuse the low K^+ solution for 30 s.
9. The recorded F_{535}/F_{480} ratio is corrected by the corresponding spillover of mCerulean emission into the 535-nm channel (the bleedthrough of Citrine into the 480-nm channel is negligible) and by the cross-talk due to the direct excitation of Citrine by light at 436 nm to give the corrected FRET ratio F^*_{535}/F^*_{480}.
10. Digitized fluorescent signals are analyzed by means of pCLAMP and GraphPad Prism software, respectively (Fig. 1c, d).

4 Notes

1. In our protocol animals are housed and tested in compliance with the guidelines described in the Guide for the Care and Use of Laboratory Animals [12] and following the European Community, law 86/609/CCE, FELASA, and ARRIVE guidelines. Thus, animals are housed in standard cages with ad libitum access to food and water and maintained under controlled standard conditions (12 h dark/light cycle starting at 7:30 AM, 22 °C temperature and 66 % humidity). Our Committee on Animal Use and Care might also approve the protocol.
2. Three decreasing tip diameters are made by snapping the original tapered end (1.5 mm) and then fire polishing. These are then sigmacoated (Sigmacote; Sigma-Aldrich) and autoclaved.
3. This concentration of cells is recommended for 12-well plates, but it has to be optimized for different culturing conditions.
4. It is recommended to pre-warm the 12-well plate containing the coverslips and plating medium before adding cells.

5. AraC is used for limiting glial division, at a concentration (5 μM) that avoids neuronal toxicity. Of note, in embrionary cultures AraC addition is not required, since glia presence is lower.
6. This amount of DNA is the needed per well for a 12-well culture plate (3.8 cm^2). High purity DNA may be used, for instance, obtained with a MAXIprep Genomed Kit.
7. Pipetting up and down up to ten times is recommended to ensure correct mixing.
8. The inclusion of inhibitors of glutamate receptors reduces transfection toxicity. Kynurenic acid is a nonselective NMDA and AMPA/kainate receptor antagonist. These receptors are highly expressed in hippocampal neurons, making them extremely sensitive to excitotoxicity.
9. For each coverslip 400 μL of neurobasal medium are mixed with 100 μL of kynurenic acid. Of note, kynurenic acid is used to remove the excess DNA/CaCl2/TE/HBS precipitate and to avoid neurotoxicity.
10. Low K^+ solution is stored at 4 °C before use and glucose is added before the experiment.
11. Images are useful not only to monitor correct voltage biosensor expression but also for next FRET recordings in order to analyze cells with comparable mCerulean and Citrine fluorescence levels
12. In the FRET illumination protocol, the Polychrome is switched on at donor excitation wavelength (mCerulean, 430 ± 10 nm) with an illumination time set to 10 ms at 10 Hz.
13. The solution exchange of the perfusion system is 10–20 ms.

Acknowledgements

This work was supported by Ministerio de Economía y Competitividad/ Instituto de Salud Carlos III (SAF2014-55700-P, PCIN-2013-019-C03-03 and PIE14/00034), Institució Catalana de Recerca i Estudis Avançats (ICREA Academia 2010), and Agentschap voor Innovatie door Wetenschap en Technologie (SBO-140028) to FC. Also, F.C., X.M. and V.F.-D. belong to the "Neuropharmacology and Pain" accredited research group (Generalitat de Catalunya, 2014 SGR 1251). We thank E. Castaño and B. Torrejón from the Scientific and Technical Services (SCT) group at the Bellvitge Campus of the University of Barcelona for their technical assistance.

References

1. Mutoh H, Knöpfel T (2013) Probing neuronal activities with genetically encoded optical indicators: from a historical to a forward-looking perspective. Pflugers Arch 465:361–371. doi:10.1007/s00424-012-1202-z
2. Borisov SM, Wolfbeis OS (2008) Optical biosensors. Chem Rev 108:423–461. doi:10.1021/cr068105t
3. Grinvald A, Hildesheim R (2004) VSDI: a new era in functional imaging of cortical dynamics. Nat Rev Neurosci 5:874–885. doi:10.1038/nrn1536
4. Knöpfel T, Díez-García J, Akemann W (2006) Optical probing of neuronal circuit dynamics: genetically encoded versus classical fluorescent sensors. Trends Neurosci 29:160–166. doi:10.1016/j.tins.2006.01.004
5. Day RN, Davidson MW (2009) The fluorescent protein palette: tools for cellular imaging. Chem Soc Rev 38:2887–2921. doi:10.1039/b901966a
6. Knöpfel T (2012) Genetically encoded optical indicators for the analysis of neuronal circuits. Nat Rev Neurosci 13:687–700. doi:10.1038/nrn3293
7. Mutoh H, Akemann W, Knöpfel T (2012) Genetically engineered fluorescent voltage reporters. ACS Chem Neurosci 3:585–592. doi:10.1021/cn300041b
8. Murata Y, Iwasaki H, Sasaki M et al (2005) Phosphoinositide phosphatase activity coupled to an intrinsic voltage sensor. Nature 435:1239–1243. doi:10.1038/nature03650
9. Perron A, Akemann W, Mutoh H, Knöpfel T (2012) Genetically encoded probes for optical imaging of brain electrical activity. Prog Brain Res 196:63–77. doi:10.1016/B978-0-444-59426-6.00004-5
10. Lundby A, Mutoh H, Dimitrov D et al (2008) Engineering of a genetically encodable fluorescent voltage sensor exploiting fast Ci-VSP voltage-sensing movements. PLoS One 3:e2514. doi:10.1371/journal.pone.0002514
11. Akemann W, Mutoh H, Perron A et al (2010) Imaging brain electric signals with genetically targeted voltage-sensitive fluorescent proteins. Nat Methods 7:643–649. doi:10.1038/nmeth.1479
12. Clark JD, Gebhart GF, Gonder JC et al (1997) Special report: the 1996 guide for the care and use of laboratory animals. ILAR J 38:41–48

Chapter 28

Determination of GPCR-Mediated cAMP Accumulation in Rat Striatal Synaptosomes

Jaume Taura, Víctor Fernández-Dueñas, and Francisco Ciruela

Abstract

G protein-coupled receptors (GPCRs) constitute the largest family of plasma membrane receptors, thus representing the more investigated drug targets in the design of new therapeutic strategies. In this family of receptors, the binding of an agonist typically triggers the activation of heterotrimeric G proteins, which in turn control the propagation of secondary messenger molecules, such as cAMP, which play a key role in important physiological processes. Accordingly, determining GPCR-mediated cAMP accumulation in native tissue (i.e., synaptosomes) constitutes an important step in the pharmacological characterization of these receptors. Here, we describe the methodology used to assess GPCR-mediated cAMP accumulation in rat striatal synaptosomes.

Key words cAMP, G protein-coupled receptor, LANCE, Striatum, Membranes

1 Introduction

G protein-coupled receptors (GPCRs), also known as seven-transmembrane domain (i.e., 7TM) receptors, constitute the largest family of plasma membrane receptors that sense molecules outside the cell and activate intracellular signal transduction pathways triggering cellular responses [1]. The GPCR-mediated signal transduction begins when an extracellular ligand "agonist" binds and switches the receptor from an inactive state to an active state conformation (Fig. 1). The activated receptor catalyzes the exchange of GDP for GTP within the α subunit of the heterotrimeric protein G ($G_{\alpha\beta\gamma}$), which in turn engages conformational and/or dissociational events between the G_{α} and dimeric $G_{\beta\gamma}$subunits (Fig. 1) [2]. Importantly, both the GTP-bound G_{α} protein subunit and the $G_{\beta\gamma}$ protein dimer can then trigger or inhibit effector enzymes (e.g., adenylyl cyclases, etc.) and ion channels (e.g., G protein-activated inwardly rectifying K^+ channels) that modulate diverse signaling pathways [3]. Adenylyl cyclase (AC) is a 12 TM glycoprotein that catalyzes ATP to form cAMP with the help of Mg^{2+} or Mn^{2+}.

Rafael Luján and Francisco Ciruela (eds.), *Receptor and Ion Channel Detection in the Brain: Methods and Protocols*, Neuromethods, vol. 110, DOI 10.1007/978-1-4939-3064-7_28,

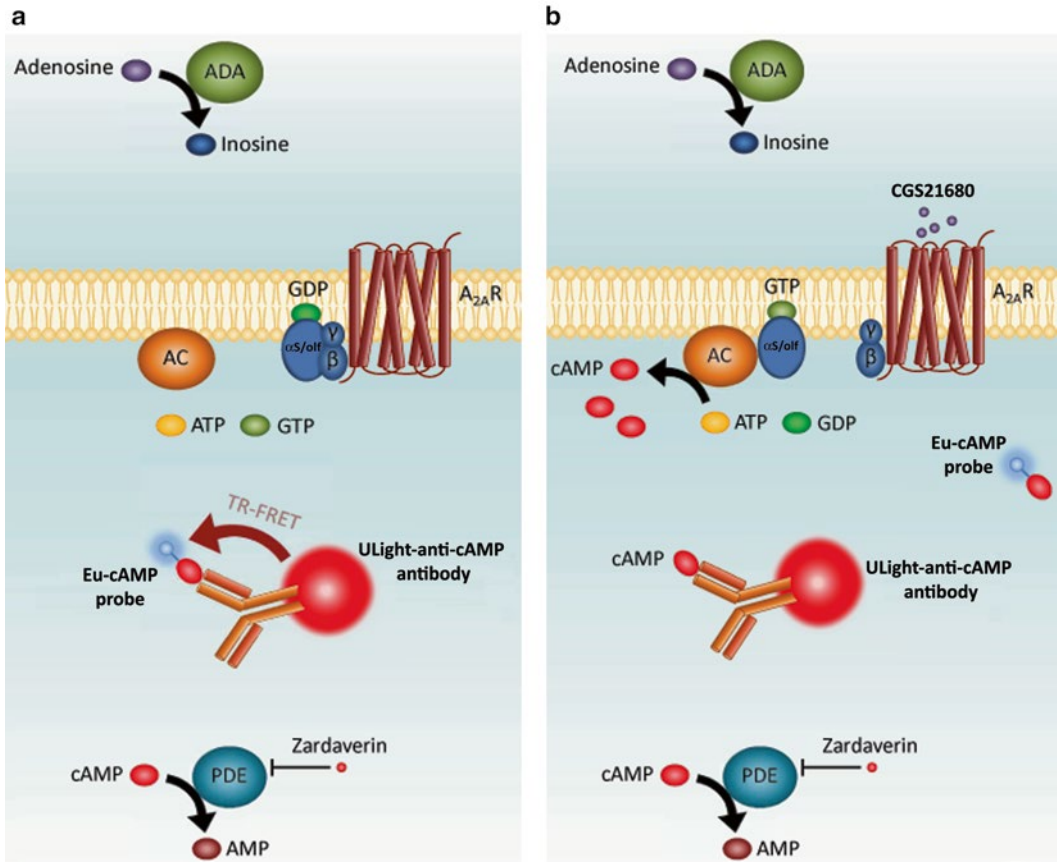

Fig. 1 Schematic representation of $A_{2A}R$ activation and cAMP determination. (**a**) Upon resting conditions, that means in the absence of any $A_{2A}R$ agonist, the receptor remains inactive and the protein $G_{\alpha S/olf}$ has the GDP bound (i.e., inactive state), thus the adenylyl cyclase (*AC*) stays inactive. Consequently, the concentration of cAMP is down and the Eu-cAMP probe remains bound to the ULight-anti-cAMP antibody, thus providing maximal TR-FRET signal. (**b**) Once the $A_{2A}R$ is challenged (i.e., 500 nM CGS21680), the receptor switches the $G_{\alpha S/olf}$ protein into an active state (i.e., GTP bound), which promote AC activation. As a consequence, cAMP is generated and competes with the Eu-cAMP probe for the ULight-anti-cAMP antibody, thus reducing the TR-FRET signal. Cells are preincubated with adenosine deaminase (*ADA*), to remove the endogenous adenosine and thus to avoid basal $A_{2A}R$ activation; zardaverine, to inhibit phosphodiesterase (*PDE*) and allowing cAMP accumulation; guanosine triphosphate (*GTP*), required for the $G_{\alpha S/olf}$ protein activation; and adenosine triphosphate (*ATP*), needed for the cAMP synthesis by AC

Interestingly, adenosine A_{2A} receptor ($A_{2A}R$) is a GPCR that stimulates AC through the activation of a $G_{\alpha S/olf}$ protein subunit, thus triggering the generation of cAMP (Fig. 1) [4]. Importantly, the cAMP generated, allosterically activates protein kinase A (PKA), which in turns triggers the stimulation of intracellular signaling cascades through selective phosphorylation events (for review *see* [5]). Finally, cAMP-mediated signal transduction can be terminated by cAMP phosphodiesterase (PDE), an enzyme that degrades cAMP into 5′-AMP (Fig. 1), thus inactivating PKA.

$A_{2A}R$ is highly enriched in the striatum and constitutes a well-known modulator of dopamine neurotransmission [6]. Indeed, challenging of striatal $A_{2A}R$ can putatively stimulate AC (subtype V; AC V), with the concomitant activation of the cAMP-PKA signaling pathway and the induction of certain genes (i.e., *c-fos* and *preproenkephalin*) through the CREB transcription factor and the MAPK/ERK pathway [6]. In addition, the $A_{2A}R$-mediated PKA activation can induce phosphorylation of DARPP-32 [7] and AMPA receptors [8], which play a key role in the initial steps of glutamatergic synaptic plasticity [9]. Interestingly, under basal conditions, the stimulation of striatal $A_{2A}R$ and cAMP-PKA signaling pathway activation is in fine equilibrium with the $G_{\alpha i}$ protein-coupled dopamine D_2 receptor (D_2R) activity, which tonically inhibits AC [6]. In fact, a functional and molecular antagonistic interaction between $A_{2A}R$ and D_2R in the striatum has been extensively described [10]. Indeed, characterizing the functional interplay between $A_{2A}R$ and D_2R in the striatum constitutes one of the major challenges for understanding the adenosine-dopamine interaction in this brain area both in normal and in pathological conditions. Accordingly, assessing changes on cAMP generation by these kinds of receptors is a major target in biomedicine. In the present chapter we describe the methodology used to assess $A_{2A}R$-mediated cAMP accumulation in striatal synaptosomes.

2 Materials

2.1 Animals

1. Sprague-Dawley rats (Charles River Laboratories, L'Arbresle, France).

2.2 Buffers and Reagents

1. *Ice-cold lysis buffer*: 10 mM Tris-HCl, 1 mM EDTA, 300 mM KCl; pH7.4.
2. *Tris-EDTA buffer*: 10 mM Tris-HCl, 1 mM EDTA; pH7.4.
3. *Membrane suspension buffer*: 50 mM Tris-HCl (pH7.4), 10 mM $MgCl_2$; pH 7.4.
4. *Stimulation buffer*: HBSS 1×, 5 mM Hepes (pH7.4), 10 mM $MgCl_2$, 0.1 % BSA
5. Hank's Balanced Salt Solution, HBSS (Gibco, Gran Island, NY, USA).
6. *Reagents*: adenosine deaminase (ADA) from calf intestine 10 mg (1 mL) (2000 U/mL) (Roche Diagnostics GmbH, Mannheim, Germany); bovine serum albumin (BSA) (Sigma-Aldrich, St. Louis, MO, USA).
7. *Drugs*: forskolin and CGS21680 (Abcam Biochemicals, Cambridge, UK); adenosine 5′-triphosphate (ATP) sodium salt hydrate, and guanosine 5′-triphosphate (GTP) sodium salt hydrate (Sigma-Aldrich); zardaverine (Tocris Bioscience, Bristol, UK).

8. BCA Protein Assay Kit (Pierce Biotechnology, Rockford, IL, USA).
9. LANCE *Ultra*cAMP kit (PerkinElmer, Waltham, MA, USA)

2.3 Instrumentation, Equipment and Software

1. Polytron: VDI 12 Adaptable Homogenizer (VWR, Radnor, PA, USA)
2. Heraeus Fresco 21 centrifuge (Thermo Fisher Scientific, Rockford, IL, USA).
3. Ultracentrifuge with a swing SW-32-out bucket rotor (Beckman Coulter, Roissy, France).
4. Clear flat-bottom immuno sterile 96-well plates (Thermo Fisher Scientific).
5. Eppendorf ThermoMixer C (ThermoFisher Scientific).
6. White 384-well plate (Greiner Bio-One GmbH, Frickenhausen, Germany).
7. POLARstar microplate reader (BMG Labtech, Durham, NC, USA).
8. GraphPad Prism software (GraphPad Software, La Jolla, CA, USA).

3 Methods

3.1 Preparation of Striatal Synaptosomes

1. Sacrifice rats weighting 200–250 g by decapitation and carefully dissect each striatum (*see* **Note 1**).
2. Add 2 mL of ice-cold lysis buffer to each striatum and homogenize in ice with the polytron for three periods of 10 s each (*see* **Notes 2** and **3**).
3. Spin the homogenate for 10 min at 1000×*g* at 4 °C.
4. Recover the supernatant and centrifuge for 30 min at 12,000×*g* at 4 °C.
5. Discard the supernatant and wash the pellet with 1 mL of ice-cold Tris-EDTA buffer.
6. Centrifuge for 30 min at 12,000×*g* at 4 °C and resuspend the pellet in 15 mL of Tris-EDTA buffer containing 10 % sucrose (wt/vol).
7. Layer the obtained striatal membrane solution onto 15 mL of Tris-EDTA buffer with 35 % sucrose (wt/vol) (*see* **Note 4**).
8. Centrifuge the preparation for 2 h at 100,000×*g* at 4 °C in a swing SW-32-out bucket rotor.
9. Collect the purified striatal synaptosomal fraction from the 10–35 % interface (*see* **Note 5**).

10. Add 30 mL of ice-cold membrane suspension buffer to the collected striatal synaptosomal fraction.
11. Centrifuge the sample for 30 min at 40,000×*g* at 4 °C and resuspend in 500 μL of membrane suspension buffer.
12. Determine the protein content of the purified synaptosomal fraction (e.g., Bradford assay).
13. Use the fresh obtained synaptosomes immediately. Alternately, they can be frozen down in liquid nitrogen and stored at −80 °C until use.

3.2 TR-FRET-Based cAMP Determination

A general scheme of the cAMP determination procedure is provided in Fig. 1.

1. Resuspend 41 μg of striatal synaptosomes (*see* **Note 6**) in 390 μL of ice-cold stimulation buffer containing 0.5 U/mL ADA and incubate in an Eppendorf thermomixer for 20 min at 700 rpm at 20 °C.
2. Add 10 μL of 40× mix working solution (*see* **Note 7**) to the striatal synaptosomal extract in order to achieve the indicated final concentration of zardaverine (i.e., 10 μM), GTP (i.e., 10 μM), and ATP (i.e., 150 μM). Incubate in the Eppendorf thermomixer for 10 min at 700 rpm at 20 °C.
3. Split the striatal synaptosomes according to the number of experimental conditions to be tested. For instance, three aliquots of 97.5 μL (10 μg) of membranes each should be prepared for the experiments described here.
4. Add 2.5 μL of stimulation buffer to the control condition (i.e., unstimulated synaptosomes) and 2.5 μL of the corresponding 40× ligand working solution into the respective stimulated synaptosomal condition, thus reaching a final concentration of 1 μM forskolin and 0.5 μM CGS21680 (*see* **Note 8**). Incubate in an Eppendorf thermomixer for 30 min at 700 rpm at 20 °C.
5. Following LANCE Ultra cAMP Kit manufacturer instructions, load 10 μL (1 μg) of the unstimulated/stimulated synaptosomal extract into each well of a white 384-well plate. Triplicates are recommended (*see* **Note 9**).
6. Prepare a 4× Eu-cAMP tracer working solution by making a 1:50 dilution of the Eu-cAMP tracer stock in the cAMP detection buffer provided by the manufacturer. Then, add 5 μL 4× Eu-cAMP tracer working solution into each sample well.
7. Prepare a 4× ULight-anti-cAMP working solution by making a 1:150 dilution of the ULight-anti-cAMP stock in the cAMP detection buffer provided by the manufacturer. Then, add 5 μL 4× ULight-anti-cAMP working solution for each well.
8. Incubate the plate for 60 min in dark at 20 °C.

9. Both fluorescence intensities, Eu-cAMP (donor) at 620 nm and ULight (acceptor) at 665 nm, are measured by using a POLARstar OMEGA reader with the proper setups (*see* **Note 10**).

3.3 Data Analysis

The specific TR-FRET signal is determined by calculating the Delta F (%), which represents the relative energy transfer rate for each sample (Fig. 2).

1. Calculate the TR-FRET ratio (665/620) and multiply by 10^4 as indicated by the manufacturer.
2. Obtain the Delta F (%) by subtracting the ratio of the negative control (*see* **Note 11**).
3. Adjust the Delta F (%) values of the cAMP standards dilutions to a sigmoidal dose-response using the GraphPad software (*see* **Note 12**) (Fig. 2).

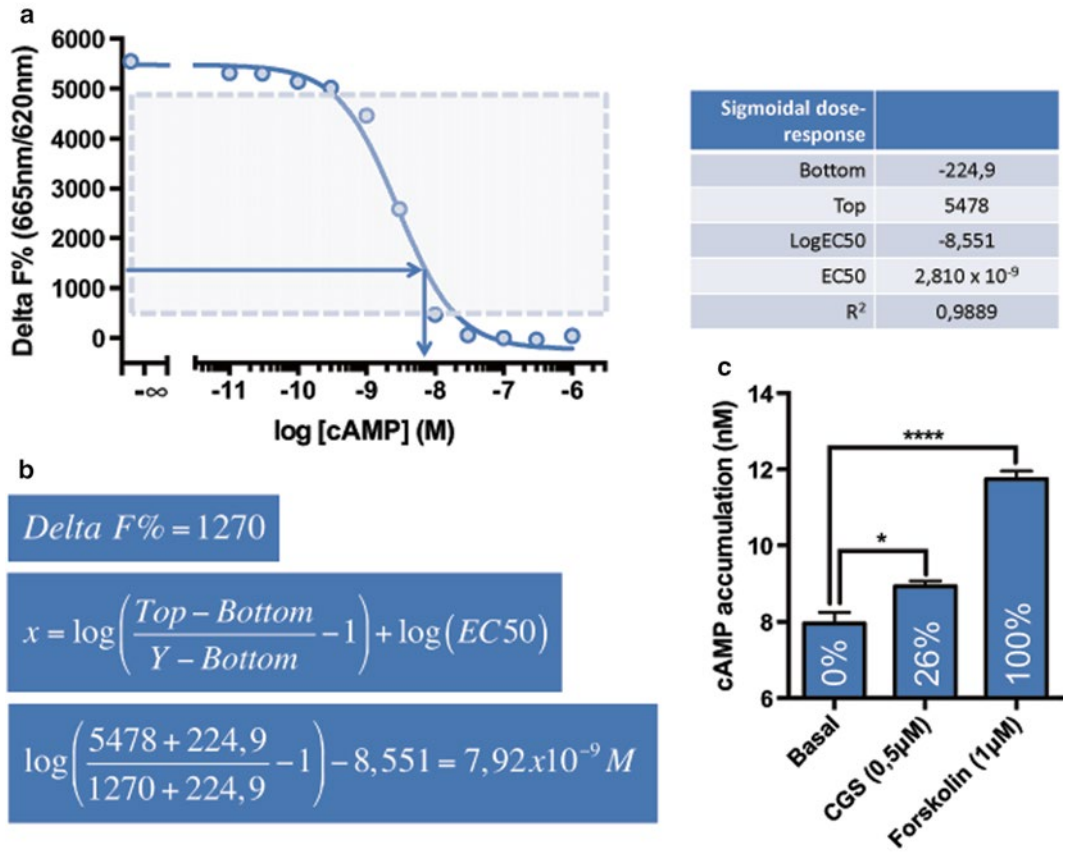

Fig. 2 Example of data analysis and cAMP determination. (**a**) Representative cAMP standard curve using the cAMP standard solutions provided by the manufacturer, which range from 10 pM to 1 μM. The Delta F% obtained for these standards is adjusted to a sigmoidal dose-response curve; thus bottom, top, and EC_{50} values are obtained (*right panel*). (**b**) Scheme of cAMP calculation. (**c**) Representative example of an $A_{2A}R$-mediated cAMP accumulation experiment performed in striatal synaptosomes (Adapted from Villar-Menéndez et al. [12])

4. Use the previously obtained bottom, top, and EC_{50} values to transform the sample data Delta F (%) values into a cAMP concentration (M) following the formula (*see* Fig. 2):

$$Y = \text{Bottom} + \frac{\text{Top} - \text{Bottom}}{1 + 10^{(x - \text{LogEC50})}}$$

5. Once all samples are expressed into cAMP concentration, data is graphed and analyzed by ordinary one-way ANOVA (Tukey's multiple comparisons test) using GraphPad Prism software.

4 Notes

1. Animals are housed and tested in compliance with the guidelines described in the Guide for the Care and Use of Laboratory Animals [11] and following the European Community, law 86/609/CCE, FELASA, and ARRIVE guidelines. Moreover, the experiments are approved by the regional animal ethics committee. Thus, animals are housed in standard cages with ad libitum access to food and water and maintained under controlled standard conditions (12 h dark/light cycle starting at 7:30 AM, 22 °C temperature, and 66 % humidity).
2. An initial manual homogenization of the sample can be performed by means of a glass Dounce homogenizer. Thus, both the tissue grinder tube and pestle should be pre-chilled in a beaker of ice before homogenization.
3. Polytron is usually set at position six. It is recommended to perform homogenization in an ice bath to preclude sample warming.
4. The generation of the sucrose step gradient is a critical issue. Accordingly, it is recommended to use a 10 mL standard glass/plastic pipette with a 9–10 cm long metal cannula (18–20 gauge) attached at the end tip. Alternately, the metal cannula could be adapted and connected to a peristaltic pump. Nevertheless, the delivery of sucrose into the centrifuge tube should be done at a very slow flow (<1 mL/min).
5. Collecting the purified striatal synaptosomes at the 10–35 % sucrose interface is also a critical step, thus avoid any contamination from the 35 % sucrose phase.
6. The membrane concentration necessary for the assay should be optimized in each case according to the brain area and GPCR under study. For instance, in the case of striatal synaptosomes and the $A_{2A}R$, we found suitable 1 μg of protein per each 384 well (20 μL final volume).

7. A 40× mix working solution containing 400 μM zardaverine, 400 μM GTP and 6 mM ATP in stimulation buffer should be prepared. Consequently, the 40× mix working solution is added into the sample following a 1:40 dilution.
8. A 40× ligand working solution containing either 40 μM forskolin or 20 μM CGS in stimulation buffer should be prepared. Consequently, the 40× ligand working solution is added into the sample following a 1:40 dilution.

   Prepare the 2× cAMP standard serial dilutions in stimulation buffer from an original 50 μM cAMP standard stock solution supplied by the manufacturer. Load 10 μL of each cAMP standard dilution in each 384 well and add tracers (i.e., 4× ULight-anti-cAMP and 4× Eu-cAMP) as for the other samples tested (i.e., treated/untreated striatal synaptosomal membranes). The cAMP standard values will allow the generation of the standard cAMP curve necessary to calculate the cAMP concentrations of the samples tested (Fig. 2) (*see* Sect. 3.3).
9. As described, for a white 384-well plate, a final volume of 20 μL per well must be obtained.
10. The POLARstar OMEGA reader should be configured for LANCE reading, this is, using the excitation filter (337 nm) and the emission filters (620 ± 8.5 nm and 665 ± 10 nm), the integration delay is set to 60 μs, and the integration time to 400 μs.
11. A negative control condition should be included by incubating a well only with the donor (Eu-cAMP) under the same experimental conditions.
12. Check the goodness of fit; R square, to be at least 0.95.

Acknowledgements

This work was supported by Ministerio de Economía y Competitividad/Instituto de Salud Carlos III (SAF2014-55700-P, PCIN-2013-019-C03-03, and PIE14/00034), Institució Catalana de Recerca i Estudis Avançats (ICREA Academia-2010), and Agentschap voor Innovatie door Wetenschap en Technologie (SBO-140028) to FC. Also, F.C., J.T., and V.F.-D. belong to the "Neuropharmacology and Pain" accredited research group (Generalitat de Catalunya, 2014 SGR 1251). We thank E. Castaño and B. Torrejón from the Scientific and Technical Services (SCT) group at the Bellvitge Campus of the University of Barcelona for their technical assistance.

References

1. Lohse MJ, Hein P, Hoffmann C et al (2008) Kinetics of G-protein-coupled receptor signals in intact cells. Br J Pharmacol 153(Suppl 1):S125–S132. doi:10.1038/sj.bjp.0707656
2. Bourne HR (1997) How receptors talk to trimeric G proteins. Curr Opin Cell Biol 9:134–142
3. Wettschureck N, Offermanns S (2005) Mammalian G proteins and their cell type specific functions. Physiol Rev 85:1159–1204. doi:10.1152/physrev.00003.2005
4. Kull B, Svenningsson P, Fredholm BB (2000) Adenosine A(2A) receptors are colocalized with and activate g(olf) in rat striatum. Mol Pharmacol 58:771–777
5. Ferré S, Ciruela F, Woods A et al (2003) Glutamate mGluR5/adenosine A2A/dopamine D2 receptor interactions in the striatum. Implications for drug therapy in neuropsychiatric disorders and drug abuse. Curr Med Chem Nerv Syst Agents 3:1–26
6. Ferre S, Ciruela F, Quiroz C et al (2007) Adenosine receptor heteromers and their integrative role in striatal function. Sci World J 7:74–85. doi:10.1100/tsw.2007.211
7. Kull B, Ferre S, Arslan G et al (1999) Reciprocal interactions between adenosine A2A and dopamine D2 receptors in Chinese hamster ovary cells co-transfected with the two receptors. Biochem Pharmacol 58:1035–1045
8. Håkansson K, Galdi S, Hendrick J et al (2006) Regulation of phosphorylation of the GluR1 AMPA receptor by dopamine D2 receptors. J Neurochem 96:482–488. doi:10.1111/j.1471-4159.2005.03558.x
9. Song I, Huganir RL (2002) Regulation of AMPA receptors during synaptic plasticity. Trends Neurosci 25:578–588
10. Ferre S, Quiroz C, Woods AS et al (2008) An update on adenosine A2A-dopamine D2 receptor interactions: implications for the function of G protein-coupled receptors. Curr Pharm Des 14:1468–1474
11. Clark JD, Gebhart GF, Gonder JC et al (1997) Special report: the 1996 guide for the care and use of laboratory animals. ILAR J 38:41–48
12. Villar-Menéndez I, Nuñez F, Díaz-Sánchez S et al (2014) Striatal adenosine A2A receptor expression is controlled by S-adenosyl-L-methionine-mediated methylation. Purinergic Signal 10:523–528. doi:10.1007/s11302-014-9417-4

Chapter 29

GPCR-Mediated MAPK/ERK Cascade Activation in Mouse Striatal Slices

Maricel Gómez-Soler, Víctor Fernández-Dueñas, and Francisco Ciruela

Abstract

G protein-coupled receptors (GPCRs) represent the largest family of plasma membrane receptors. GPCRs are involved in a large variety of physiological and also pathological processes in the central nervous system; thus, the understanding of their intracellular signaling pathways in the brain is a main goal in biomedical sciences. Several straightforward methods exist to measure the functionality of these receptors in vitro. However, measuring GPCR activity in native tissue is still a challenge, which is mainly due to the cross talk occurring in vivo between different signaling pathways. The extracellular signal-regulated kinase (ERK) pathway is a basic signaling route for many GPCRs. Accordingly, determining GPCR-mediated ERK activation has become a popular and straightforward way to measure receptor signaling. Here, we describe the methodology used to assess GPCR-mediated ERK phosphorylation in brain slices from adult mice.

Key words ERK phosphorylation, G protein-coupled receptor, Brain slices, Adenosine A_{2A} receptor

1 Introduction

The mitogen-activated protein kinase (MAPK) or extracellular signal-regulated kinase (ERK) is part of a signal transduction cascade highly conserved among eukaryotes. It is involved in the control of numerous cellular processes, including cell growth, differentiation, and neuronal plasticity [1, 2]. This signaling module consists of three enzymes, which are activated in a sequential phosphorylation cascade (Fig. 1a). First, the upstream kinase (MAPK/ERK kinase kinase, MEKK or Raf) phosphorylates and activates MAPK/ERK kinase (MEK). And subsequently, MEK triggers the activation of MAPK/ERK by phosphorylating a threonine (Thr) and a tyrosine (Tyr) residue within the activation loop. Interestingly, MAPK/ERK activation (i.e., phosphorylation) has been involved in the control of synaptic plasticity in the adult brain (for review, *see* [2]). Indeed, several studies have demonstrated that some forms of synaptic plasticity are ERK activation dependent. For instance, several forms of long-term potentiation (LTP) in the dentate gyrus,

Rafael Luján and Francisco Ciruela (eds.), *Receptor and Ion Channel Detection in the Brain: Methods and Protocols*, Neuromethods, vol. 110, DOI 10.1007/978-1-4939-3064-7_29,

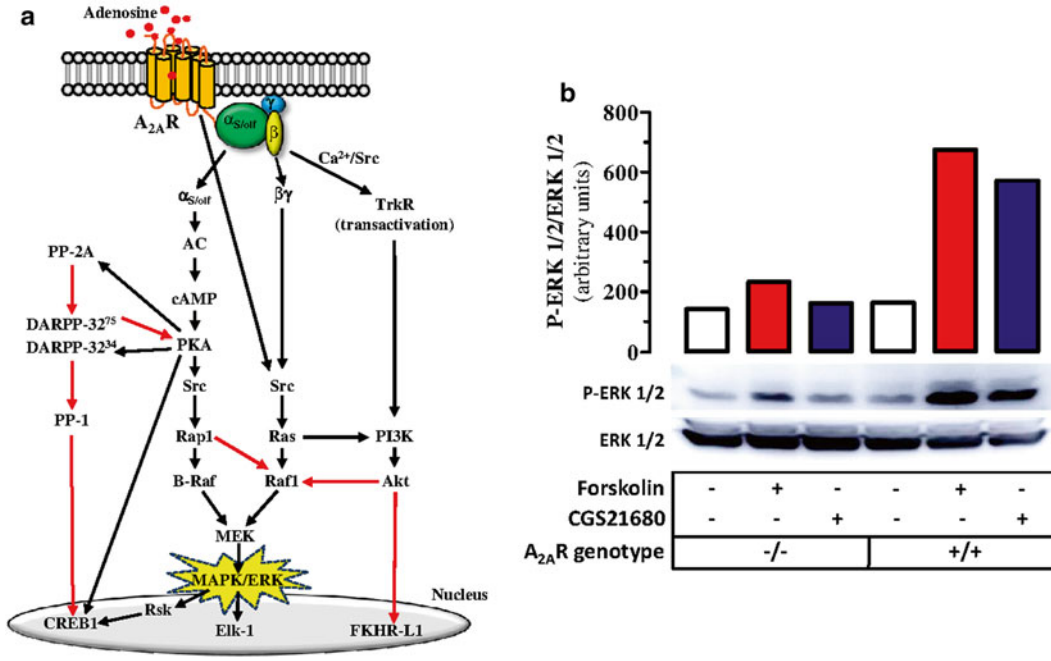

Fig. 1 $A_{2A}R$-mediated MAPK/ERK pathway activation in striatal brain slices from mouse. (**a**) $A_{2A}R$ signal transduction mechanisms in the striatum. *Black* and *red arrows* denote stimulatory and inhibitory effects, respectively. *AC* adenylyl cyclase, *Akt* serine-threonine kinase also known as protein kinase B, *CREB* cAMP response element-binding protein, *DARPP-32* dopamine and cAMP-regulated phosphoprotein, 32 kDa, *Elk-1* member of the ternary complex factor family of transcription factors, *FKHR-L1* transcription factor of the Forkhead family, *MAPK* mitogen-activated protein kinase, *MEK* MAPK kinase, *PI3K* phosphatidylinositol 3-kinase, *PKA* protein kinase A, *PP-1* and *PP-2A* protein phosphatases 1 and 2A, respectively, *Raf-1* and *B-Raf* members of the Raf family of MAPK kinase kinases, *Ras* and *Rap1* members of the small GTPase protein superfamily, *Rsk* Ribosomal S6 kinases, *Src* member of the Src family of non-receptor tyrosine kinases, *TrkR* neurotrophin receptor. (**b**) $A_{2A}R$-mediated MAPK/ERK pathway activation in mouse brain striatal slices. Brain striatal slices were obtained from adult mouse (+/+) and $A_{2A}R$-deficient mouse (–/–) and treated with vehicle (*white bars*), forskolin 1 μM (*red bars*), and the $A_{2A}R$ agonist CGS21680 500 nM (*blue bars*)

the N-methyl-D-aspartate (NMDA) receptor-independent forms of LTP in the CA1 area of the hippocampus, or LTP occurring in the amygdala, are associated with fear-dependent learning (for review, *see* [3]). Overall, it is well accepted that ERK activation is a common feature to many forms of synaptic plasticity in the forebrain.

In the brain, many G protein-coupled receptors (GPCRs) are able to activate the MAPK/ERK cascade. For instance, adenosine A_{2A} receptors (A_{2A}Rs), like other $G_{\alpha S}$ protein-coupled receptors, can trigger MAPK/ERK phosphorylation upon agonist challenge. Thus, $A_{2A}R$ stimulation prompts protein $G_{\alpha S/olf}$ activation, which in turn stimulates adenylyl cyclase (AC) [4] (Fig. 1a). $A_{2A}R$-mediated AC stimulation generates cAMP, which then activates a cAMP-dependent protein kinase (PKA), thus regulating the phosphorylation

status of some target proteins. Interestingly, in the striatum, some of the PKA-targeted proteins are (1) DARPP-32 (dopamine- and cAMP-regulated phosphoprotein of 32 kDa), which is highly expressed in the GABAergic efferent neurons; (2) CREB (cAMP response element binding); (3) PP-2A (protein phosphatase 2A); and (4) Src (non-receptor tyrosine kinase protein) (Fig. 1a). Of note, activation of striatal $A_{2A}R$ promotes DARPP-32 phosphorylation at Thr-34 and dephosphorylation at Thr-75, thus providing a mechanism of amplification of the PKA signal transduction pathway (for review, *see* [5]) (Fig. 1a). Indeed, activated PKA diffuses into the nucleus and phosphorylates CREB, thus inducing cellular gene expression (for review, *see* [5]) (Fig. 1a). Consequently, $A_{2A}R$-mediated PKA activation in GABAergic striatopallidal neurons can potentially produce a sustained increase in the transcription of some CREB-modulated genes by a mechanism involving increased CREB phosphorylation and decreased CREB dephosphorylation (through phospho-Thr-34-DARPP-32-mediated inhibition of PP-1 activity) (for review, *see* [5]) (Fig. 1a).

On the other hand, cAMP-mediated PKA activation also produces the stimulation of a GTPase of the Ras family throughout Src phosphorylation (Fig. 1a). In this manner, PKA activates Rap1, which in turn leads to the sequential phosphorylation of the Raf isoforms B-Raf, MEK, and ERK 1/2 (Fig. 1a) [6]. Interestingly, Rap1 can also bind and inactivate Raf1 (by blocking Ras binding to Raf-1 [6]). Thus, the predominant Raf isoform seems to be the main determinant of the final effect of cAMP on MAPK/ERK cascade activation. Accordingly, a predominance of B-Raf or Raf1 will produce a cAMP-induced increase or decrease of MAPK/ERK activation, respectively [7]. Of note, in the striatum, there is a predominant expression of B-Raf versus Raf1, thus suggesting that $A_{2A}R$-mediated AC stimulation will mostly lead to MAPK/ERK cascade activation [8] (Fig. 1a). Interestingly, this striatal Ras-dependent activation of MAPK/ERK cascade seems to require protein $G_{\beta\gamma}$ subunits and activation of Src (Fig. 1a) [7]. In addition, a cross talk between the MAPK/ERK cascade and the Akt signaling pathways has been demonstrated. Thus, an inhibition of the MAPK/ERK signaling by Akt-induced phosphorylation of Raf-1 [9] and a stimulation of PI3K by Ras have been described [10] (Fig. 1a). Hence, the balance between Akt and MAPK/ERK signaling seems to be linked to the agonist type, cellular background, and/or stage of differentiation [9]. Finally, it is also important to mention that striatal $A_{2A}R$ stimulation may also promote PI3K activation by transactivation of Trk neurotrophin receptors by a Ca^{2+}- and Src-dependent mechanism [11] (Fig. 1a), thus resulting in a potential signaling conflict due to the existing Akt and MAPK/ERK signaling balance.

Overall, in the striatum, depending on the cellular type, the $A_{2A}R$-mediated MAPK activation can be dependent on or independent of cAMP accumulation and PKA activation and, therefore, on the initial activation of AC pathway. Nevertheless, the quantification of the activation of this signaling pathway in this brain area represents a major challenge to study the effects of several drugs on target receptors, such as the adenosine $A_{2A}R$. In the present chapter, we describe the methodology used to assess $A_{2A}R$-mediated ERK phosphorylation in striatal slices from adult mice.

2 Materials

2.1 Animals

1. CD-1 wild-type (WT) and adenosine A_{2A} receptor ($A_{2A}R$)-deficient (KO-$A_{2A}R$) mice [1] weighing 20–25 g (*see* **Note 1**).

2.2 Buffers and Reagents

1. *Krebs/ HCO_3^- buffer* (*see* **Note 2**): For 1 L of Krebs stock solution: NaCl 124 mM (7.246 g), KCl 4 mM (0.298 g), KH_2PO_4 1.25 mM (0.17 g), $MgSO_4$ 1.5 mM (0.370 g) in Milli-Q water; adjust pH to 7.4. Before the experiment, take 500 mL of the Krebs stock solution, and add $NaHCO_3$ 26 mM (1.0921 g), glucose 10 mM (0.9008 g), and $CaCl_2$ 1.5 mM (750 μL of 1 M $CaCl_2$ solution). Oxygenate the Krebs HCO_3^-buffer with carbogen (O_2, 95 %; CO_2, 5 %) during 10 min before use. Check pH to 7.4. Keep two separate aliquots, one at 32 °C and the other at 4 °C.
2. *ERK homogenization buffer* (*see* **Note 3**): For 10 mL of ERK homogenization buffer: orthovanadate 1 mM (1.8 mg), Tris-HCl 50 mM (78 mg), sodium pyrophosphate 25 mM (111.5 mg), NaCl 50 mM (29 mg), sodium fluoride 50 mM (20.9 mg), zinc chloride 5 mM (6.8 mg), DTT 2 mM (3 mg); adjust pH to 7.5 and add 0.5 % protease inhibitor cocktail set III (Millipore, Temecula, CA, USA) and 10 % phosphatase inhibitor cocktail 1 (Sigma-Aldrich, St. Louis, MO, USA).
3. *SDS-PAGE sample buffer*: Tris-HCl 62.5 mM, pH 6.8, containing 40 % glycerol, 2 % SDS, and 0.5 % bromophenol blue.
4. *Tris-buffered saline (TBS)*: For 1 L TBS 10× stock solution: Tris base 500 mM (60.6 g), NaCl 1.5 M (87.6 g) in Milli-Q water; adjust pH to 7.6.
5. *TBS-tween (TBS-T)*: Prepare 1 L TBS 1× and add 250 μL of Tween 20 (Sigma-Aldrich).
6. *Western blotblocking solution*: TBS-T 1× with 5 % (w/v) of nonfat dry milk.
7. *Primary antibody dilution buffer*: TBS-T 1× containing 5 % (w/v) of bovine serum albumin (BSA) (Sigma-Aldrich).

8. *Primary antibodies*: mouse anti-phospho-ERK 1/2 antibody and rabbit anti-ERK 1/2 antibody (Sigma-Aldrich).
9. *Secondary antibodies*: HRP-conjugated goat anti-mouse IgG and anti-rabbit IgG (Thermo Fisher Scientific, Rockford, USA).
10. *Drugs*: Forskolin and CGS21680 (Abcam Biochemicals, Cambridge, UK).

2.3 Instrumentation, Equipment, and Software

1. Vibrating microtome VT 1200S (Leica, Wetzlar, Germany).
2. Eppendorf ThermoMixer C (Thermo Fisher Scientific).
3. Trans-Blot Turbo Transfer System (Bio-Rad, Hercules, CA, USA).
4. Mini-PROTEAN Tetra Cell (Bio-Rad).
5. Amersham Imager 600 (GE Healthcare Life Sciences).
6. ImageJ software (NIH, Bethesda, MA, USA).
7. GraphPad Prism software (GraphPad Software, La Jolla, CA, USA).

3 Methods

3.1 Brain Slice Preparation and Receptor Ligand Incubation

1. Sacrifice animals by cervical dislocation followed by decapitation (*see* **Note 4**).
2. Remove rapidly the brain and chill it during 5–10 min in ice-cold, carbogen-saturated Krebs/HCO_3^- buffer.
3. Apply a small drop of instant glue (i.e., Loctite Super Glue-3) in the center of the vibrating microtome cutting stage.
4. Cut out the cerebellum to form a flat base in the posterior part of the brain. Remove the excess of buffer on a wet piece of filter paper and glue the brain into the cutting stage by its posterior part (*see* **Note 5**). Avoid the brain from drying by adding a few drops of Krebs HCO_3^-buffer with a Pasteur pipette on the top of the brain before placing the cutting stage in the vibrating microtome slicing chamber.
5. Obtain 300–400 μm slices by setting the vibrating microtome amplitude at 1.50 mm and an advancing speed of 0.5 mm/s. The vibrating microtome slicing chamber should be continuously chilled with ice.
6. Dissect the region of interest (i.e., striatum) from the brain slice with the help of a paintbrush (size 1 or 2) and a scalpel.
7. Using a plastic Pasteur pipette, transfer the slices into the mesh-bottomed chambers immersed in ice-cold carbogen-saturated Krebs/HCO_3^- buffer, and allow equilibrating during 5–10 min.

8. Using a plastic Pasteur pipette, transfer slices to an Eppendorf with 1 mL of oxygenated Krebs HCO_3^-buffer at 32 °C (*see* **Note 6**).
9. Add adenosine deaminase (ADA) (Roche Diagnostics GmbH, Mannheim, Germany) to a final concentration of 0.5 U/mL to remove endogenous adenosine interfering with the adenosine receptor upon study.
10. Place the tubes into the Eppendorf ThermoMixer set with a carbogen-saturated atmosphere at 32 °C, and incubate for 2 h at 300 rpm.
11. Incubate for another 2 h without shaking.
12. Remove the solution from the slices, add 0.5 mL of carbogen-saturated Krebs/HCO_3^- buffer, and incubate for further 15–30 min without shaking.
13. Prepare the receptor ligands in carbogen-saturated Krebs/HCO_3^- buffer at 2× final concentration.
14. Gently add 0.5 mL of the indicated 2× ligand solution onto the slices (*see* **Note 7**), and incubate in the Eppendorf ThermoMixer, holding a carbogen-saturated atmosphere at 32 °C, and incubate for another 5–10 min without shaking (*see* **Note 8**).
15. Aspirate the incubation solution and quickly freeze down the slices on dry ice. Samples can be stored at –20 °C until usage.

3.2 Western Blot Determination of ERK Phosphorylation

1. Add 30 µL (per slice) of ice-cold ERK homogenization buffer.
2. Incubate for 5–10 min at 4 °C.
3. Disaggregate the slices by pipetting up and down 3–5 times using a P200 pipette.
4. Mix the samples with an equal volume of SDS-PAGE sample buffer.
5. Heat the samples at 95–100 °C for 5 min.
6. Run on a 10 % SDS polyacrylamide resolving gel.
7. Electro-transfer proteins to a nitrocellulose membrane (i.e., polyvinylidene difluoride membrane; GE Healthcare Life Sciences, UK).
8. After transfer, wash the nitrocellulose membrane with TBS for 5 min at room temperature.
9. Incubate membrane with the Western blot blocking solution for 1 h at room temperature.
10. Wash three times (5 min each) with TBS-T.
11. Incubate the membrane with mouse anti-phospho-ERK 1/2 antibody (1:1000) or rabbit anti-ERK 1/2 antibody (1:30,000) with gentle agitation, overnight at 4 °C.

12. Wash three times (10 min each) with TBS-T.
13. Incubate the membrane with the appropriate secondary antibody for 1 h at room temperature.
14. Wash three times (10 min each) with TBS-T.
15. Detect bound immunoglobulins using a chemiluminescence substrate (i.e., Pierce ECL Western Blotting Substrate, Thermo Fisher Scientific).
16. Quantify the intensity of the Western blot bands using the ImageJ software [12].
17. The level of phosphorylated ERK 1/2 isoforms is normalized for differences in loading using the total ERK protein band intensities.
18. Statistical differences between the different groups are analyzed by GraphPad Prism software.

4 Notes

1. Animals are housed and tested in compliance with the guidelines described in the Guide for the Care and Use of Laboratory Animals [13] and following the European Community, law 86/609/CCE, FELASA, and ARRIVE guidelines. Thus, animals are housed in standard cages with ad libitum access to food and water and maintained under controlled standard conditions (12 h dark/light cycle starting at 7:30 AM, 22 °C temperature, and 66 % humidity). Our Committee on Animal Use and Care might also approve the protocol.
2. This is an oxygenated artificial cerebrospinal fluid to maintain the brain slices. The stock solution can be stored at 4 °C for several days.
3. This is a Tris-HCl buffer adapted for brain tissue. It is recommended to prepare fresh homogenization buffer every time.
4. Do not use anesthesia to avoid unwanted influences of anesthetics in ERK phosphorylation. Also, it is important to prepare all the materials and to make sure it is at 4 °C before the experiment starts.
5. In our case, since the region of study was the striatum, the anterior part of the brain was exposed to the razor blade.
6. In our case, we put two slices of striatum per condition.
7. In our experiment, we used a final concentration of forskolin 1 μM and CGS 21680 500 nM (Fig. 1).
8. In previous experiments in HEK 293 T cells, we have observed maximal phosphorylation of ERK 1/2 with 5 min. incubation [14].

Acknowledgments

This work was supported by Ministerio de Economía y Competitividad/ Instituto de Salud Carlos III (SAF2014-55700-P, PCIN-2013-019-C03-03 and PIE14/00034), Institució Catalana de Recerca i Estudis Avançats (ICREA Academia-2010), and Agentschap voor Innovatie door Wetenschap en Technologie (SBO-140028) to FC. Also, F.C., M.G.-S., and V.F.-D. belong to the "Neuropharmacology and Pain" accredited research group (Generalitat de Catalunya, 2014 SGR 1251). We thank E. Castaño and B. Torrejón from the Scientific and Technical Services (SCT) group at the Bellvitge Campus of the University of Barcelona for their technical assistance.

References

1. Zhang W, Liu HT (2002) MAPK signal pathways in the regulation of cell proliferation in mammalian cells. Cell Res 12:9–18
2. Thomas GM, Huganir RL (2004) MAPK cascade signalling and synaptic plasticity. Nat Rev 5:173–183
3. Adams JP, Sweatt JD (2002) Molecular psychology: roles for the ERK MAP kinase cascade in memory. Annu Rev Pharmacol Toxicol 42: 135–163
4. Kull B, Svenningsson P, Fredholm BB (2000) Adenosine A(2A) receptors are colocalized with and activate g(olf) in rat striatum. Mol Pharmacol 58:771–777
5. Ferré S, Ciruela F, Woods A et al (2003) Glutamate mGluR5/adenosine A2A/dopamine D2 receptor interactions in the striatum. Implications for drug therapy in neuro-psychiatric disorders and drug abuse. Curr Med Chem Nerv Syst Agents 3:1–26
6. Vossler MR, Yao H, York RD et al (1997) cAMP activates MAP kinase and Elk-1 through a B-Raf- and Rap1-dependent pathway. Cell 89:73–82
7. Schmitt JM, Stork PJS (2002) Galpha and Gbeta gamma require distinct Src-dependent pathways to activate Rap1 and Ras. J Biol Chem 277:43024–43032
8. Morice C, Nothias F, König S et al (1999) Raf-1 and B-Raf proteins have similar regional distributions but differential subcellular localization in adult rat brain. Eur J Neurosci 11:1995–2006
9. Moelling K, Schad K, Bosse M et al (2002) Regulation of Raf-Akt cross-talk. J Biol Chem 277:31099–31106
10. Rodriguez-Viciana P, Warne PH, Dhand R et al (1994) Phosphatidylinositol-3-OH kinase as a direct target of Ras. Nature 370: 527–532
11. Lee FS, Chao MV (2001) Activation of Trk neurotrophin receptors in the absence of neurotrophins. Proc Natl Acad Sci U S A 98: 3555–3560
12. Schneider CA, Rasband WS, Eliceiri KW (2012) NIH Image to ImageJ: 25 years of image analysis. Nat Methods 9:671–675
13. Clark JD, Gebhart GF, Gonder JC et al (1997) Special report: the 1996 guide for the care and use of laboratory animals. ILAR J 38:41–48
14. Fernández-Dueñas V, Gómez-Soler M, López-Cano M et al (2014) Uncovering caffeine's adenosine A2A receptor inverse agonism in experimental parkinsonism. ACS Chem Biol 9:2496–2501

Subject Index

Rafael Luján and Francisco Ciruela (eds.), *Receptor and Ion Channel Detection in the Brain: Methods and Protocols*, Neuromethods, vol. 110, DOI 10.1007/978-1-4939-3064-7, © Springer Science+Business Media New York 2016

G

H

I

L

M

N

P

Q

R

S

T

V

W